Design of Robust Slow-Speed Ships for Sustainable Operation

Alaa Balkees

School of Engineering - Marine Technology

Newcastle University

This dissertation is submitted for the degree of

Doctor of Philosophy

October 2019

School of Engineering

Armstrong Building

Newcastle University

NE1 7RU

United Kingdom

Abstract

Multi-objective optimisation that considers the energy efficiency and economic success is an important aspect of ship design and operation. Both the hydrodynamic and economic performance characteristics need to be addressed in the early stages of the design, and secured during the life span of a ship. Because of the conflicting nature of these two objectives, there are various trade-offs at stake in the goal for making ships more efficient and greener to comply with IMO regulations while reducing the building and operating costs and increasing the profitability at the same time for all stakeholders especially owners and operators.

In attempt to reduce the amount of greenhouse gas emissions from ships, and hence to achieve a lower EEDI value, this research approaches the problem of improving the energy efficiency of ships. That is achieved by optimising the hull design over a speed range through parametric modification to reduce resistance and required power, and also through adopting slow steaming concept.

Moreover, the research aims to determine the best practice to reduce the annual cost of running a ship and to increase the annual revenue as well as to make the ship a more profitable investment over her life span. The profit per tonne.mile and the net present value NPV are estimated in the economic analysis to be used as indicators to compare alternative designs for different routes and market conditions scenarios. To achieve this aim, the main operational and economic aspects such as the fluctuations in the fright rates and fuel prices in the shipping market are covered in the economic analysis. In addition, the acquiring price and salvage value are included in order to obtain solid comparisons.

An optimisation framework using a VBA macro code has been developed based on the concept of Pareto optimality to assess decision making, and to determine robust designs as well as operational profiles based on results from the hydrodynamic model, environmental impact model, and the economic model. The optimisation process is carried out for a Panamax tanker case study using 5 parameters and a set of constraints for the hull parameters and speed.

The outcome from the optimisation framework is a set of Pareto optimal solutions where weight factors are appointed to give the flexibility when addressing the importance of each individual function. The solutions are presented graphically to form what is known as Pareto front which determines the design space and the trade-offs between the different competing objective

functions. This optimisation framework could assist decision making where it is possible to choose a robust design or designs that offer a near-optimum performance regardless any fluctuations in the market and or the operation profile, and eliminate any significant sub-optimal designs.

Key Words:

Ship design, hydrodynamic performance, slow steaming, energy efficiency, economic performance, fuel cost, multi-objective optimisation, Pareto front.

Acknowledgements

I would like to thank a number of people who made the experience of working as a research student an enjoyable and personally rewarding one.

Many Thanks to my supervisors, Dr. Zhiqiang Hu and Professor Richard Birmingham who have provided academic support and friendly encouragement through this journey. I also would like to express my gratitude to my previous supervisors Dr. Peter Wright and Dr. Michael Woodward who provided considerable guidance and support at the beginning of my research work.

I also would like to express my gratitude to the staff in the School of Marine Science and Technology for being kind and supportive through the tough years since I started my studies in Newcastle University. I am grateful to Professor Mehmet Atlar for his guidance when it was needed. I would like to acknowledge the help of Mr. Ian Applegarth for extending my knowledge of using AVEVA software.

My thanks extend to my colleagues and officemates who provided a constructive and joyful place of study in Newcastle. Last but not least, I would like to thank my family who without them I would not complete this challenge successfully, my friends back home in Syria for their continuous support, and my friends in Newcastle for all their encouragement, support, and love.

Alaa Balkees

Newcastle October 2019

Table of Contents

List of Tables

List of Figures

Chapter 1. Introduction

1.1 Introduction

This introductory chapter is dedicated to provide a brief overview of the research thesis on optimising the hull design and the operational profile aiming to improve the energy efficiency and to increase the profitability of running a vessel as well. This chapter initially states the motivations behind this study, describing the problems associated with greenhouse gases and environmental damage caused by international shipping, and addressing the challenges to all stakeholders to face and solve this issue in a cost-effective manner. Then, the aims of the research are outlined together with the main objectives that must be achieved on the way in order to reach these aims and goals. Following this, the thesis structure is presented highlighting the outline and contribution of each individual chapter.

1.2 Motivation for the Research

Ship design and optimisation are becoming more challenging due to the contrary implications of the necessity to build greener ships to cut emissions from shipping activities, the rising fuel prices, and the need to meet the owner requirements such as speed and capacity. In other words, several technological challenges have to be met and reconciled with the economics of the ship operation in order to help owners and charterers to operate their fleet efficiently and secure an appropriate profitability. More important, that assists them to reduce the environmental impact because the shipping industry is under pressure to take its share of responsibility for tackling global warming in the future.

Climate change is a serious environmental threat facing the world today, and indeed it is a challenge to everyone cares about the future of our globe. The maritime activities in 2007 were responsible for about 3.3% of the total world carbon dioxide emissions as it was estimated to have emitted more than 1.0 billion of CO_2 according to the Second IMO GHG Study (2009). Figure 1.1 presents a detailed comparison for CO_2 emissions from shipping against other contributors to the global total emissions. However, even the maritime shipping is responsible for less than 4% of the world's total GHG, and it is considered as the most productive mode of transportation but the international community still addresses it as a major source of emissions

such as $[CO_2, NO_x, SO_2, PM]$ (Ballou *et al.*, 2008). Different emissions scenarios were demonstrated in both the Second and Third IMO GHG Studies presenting possible ways in which emissions could develop in the future. Those scenarios were built on feasible social and economic factors, energy and policy circumstances and potential trends in the shipping market. The resulting CO_2 figures show that across all scenarios the average emissions growth in 2020 amounts to 7% of 2012 emissions, and the average increase in emissions for 2030 is 29% and 95% for 2050 (Buhaug *et al.*, 2009; *Third IMO GHG Study*, 2014)

Generally speaking, in the absence of introducing more strict regulations and significant market-driven efficiency improvements, maritime emissions are expected to gradually increase in the period up to 2050. The main cause of the emissions increase is the predicted rise in transport demand in the shipping market which will lead to introducing more ships into the market, or increasing the number of days at sea, or increasing ship speed. Hence, emissions are likely to increase to higher levels as a result of the increase in fuel consumption assuming that fossil fuels will remain dominant. This noteworthy contribution to global emissions puts international and domestic shipping under increasing pressure to reduce its carbon and other emissions footprint from the combustion of petroleum-based fuels such as distillate or residual diesel fuels.

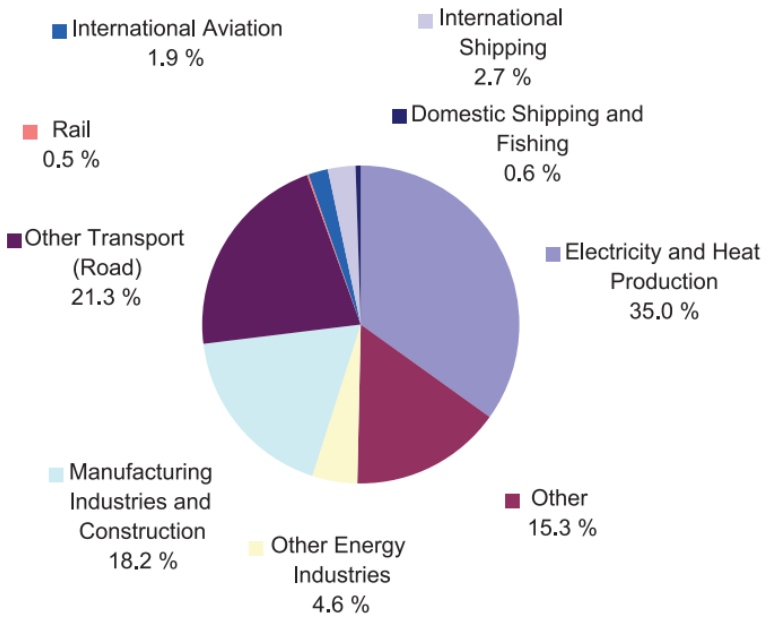

Figure 1.1 CO_2 Emissions from shipping compared with global total emissions

The Marine Environment Protection Committee (MEPC) at its 59th session (August 2009) in London and previous sessions since 2000 brought to light the importance of developing an effective tool to measure the energy efficiency for ships in order to improve the overall efficiency of each individual ship. One of the most crucial measures developed by IMO is the Energy Efficiency Design Index (EEDI) which is a regulatory measure for CO_2 output of new ships. Basically, the EEDI is the main benchmark set by the IMO to monitor marine CO_2 emissions from the international fleet. EEDI represents a ship's performance from environment point of view and its performance which is expressed by the transport work capacity. Theoretically, EEDI is defined as a ratio between a ship's impact to the environment and the benefit to society as shown in Eq (1.1). It is a function of: installed power, cargo carried, and ship speed. The attained Energy Efficiency Design Index for new ships is measured in grams CO_2 emitted per capacity.nmile.

EEDI formula was adopted by MEPC.1/Circ.681 in August 2009, and has become a mandatory benchmark for new ships over 400 gross tonnage (GT) on international voyages along with other measures such as the Ship Energy Efficiency Management Plan (SEEMP) for all existing and new ships. The main purpose of the SEEMP as an operational management tool is to establish a robust approach to monitor and manage a ship and fleet efficiency performance continuously, and to improve the energy efficiency in a cost effective way. It assists the responsible person or company in managing and improving the day-to-day environmental performance (IMO, 2017).

$$Basic\ EEDI\ concept = \frac{Environmental\ cost}{Benifit\ for\ society} \tag{1.1}$$

A significant amount of work and research has been done to construct a greener and more fuel-efficient fleet by national and international organisations, design offices, shipyards, engine manufactures, shipping companies, and even private bodies that concern about the danger of air pollution. This level of growing interest in mitigating shipping emissions and reducing fuel consumption in the past few decades is linearly related to the fuel price (Wijnolst and Wergeland, 2009). For example, fuel oil prices increased significantly between 1970 and 1980 up to 10 times the prices in the previous years, leading to ships with high fuel consumption to be laid up. As fuel oil prices fell between 1985 and 2000, energy efficiency of ships and development research had received just a little attention by the maritime industry. However, fuel oil prices started to increase again after 2000 and, hence, the fuel cost has become a matter

of concern for ships' operators even though after 2008 recession as there was a short period when oil price decreased (Bialystocki and Konovessis, 2016).

A combination of the economic recession in 2008, rising fuel prices, decreasing demand in the shipping market, and growing awareness in the shipping industry about climate change emissions has encouraged ship owners and operators to adopt "slow steaming". Reducing the operating speed affects the total fuel consumption because of the cube law between speed and power. Slow steaming is widely adopted by ships' operators to achieve the required EEDI value as slow steaming is an effective tool to reduce fuel consumption and hence reducing emissions, and it is a useful way to lower transport costs on the other hand.

Sailing slower reduced the tone-mile supply in the shipping market in the last decade, and hence created an artificial balance in the marketplace (Faber *et al.*, 2012). In 2011, the excess ton-mile capacity in the tankers and bulk carriers market was around 25 to 30%. Devanney (2011b) suggested that absorbing all this extra capacity would be achieved by sailing at an average speed of about 11 knots as slow steaming is a flexible mechanism for a short-term solution to control cost and capacity for the tankers and bulk carriers fleet. Psaraftis *et al.* (2012) have reviewed different motivations for adopting slow steaming such:

- Reducing bunker bill when fuel prices are high and volatile;
- Reducing fuel consumption and hence fuel cost due to the obligation to use more expensive fuel;
- Increasing the profit by optimising the ship operational profile as that might reduce some expenses related to port charges for example for night departures and arrivals;
- Absorbing the market overcapacity and the resulted low fright rates.

However, in order to meet the above goals and achieve a balance between all the desirable but incompatible trade-offs in the shipping industry, significant effort and work on the technical, operational, financial, and management sectors should be done to reduce fuel consumption and to keep running a ship a profitable investment. First of all, reducing the lifetime ownership costs requires a significant effort towards each stage of the vessel's life starting with design, build, through-life maintenance and ending with scrapping. Secondly, increasing the day-to-day profit requires reducing energy consumption and operating the vessel efficiently on a daily basis and within a long-term strategy to increase the productivity (in terms of tonne.mile) for a given market condition and, hence, to increase the revenue.

The most common practice by naval architects when it comes to reduce the energy consumption is to focus only on reducing the hull resistance to reduce the required power and hence cut the fuel bill. However, such practice might actually lead to increase the initial production cost and the through-life maintenance cost which might lead to a loss or making just a small profit.

Finally, running a greener ship with low emissions during the lifetime at an effective-cost manner involves designing an efficient hull with efficient machinery, installing emissions mitigating technology, optimising the operational profile of the ship, and adopting measures related to the logistical chain for the whole fleet and the maritime policies. These competing aspects of production and maintenance costs and operating costs on the other hand need to be addressed carefully during the early design stages. Multi-objective optimization techniques can effectively assist designers and decision makers to search the trade spaces for robust solutions that are beyond simple design convergence and to eliminate any significant sub-optimal designs (Dylan W. Temple and Matthew Collette, 2012).

1.3 Aims and Objectives

The principal aims of this research thesis are to explore the potential of the slow steaming concept and hull optimization on ships with an effort to improve the hydrodynamic performance, reduce the environmental impact, and to improve the whole economic performance.

These aims are achieved by developing a framework consisting of a number of models that take into account the hydrodynamic performance, energy efficiency, and the economic performance through a ship's life span. The developed framework deals with complex and conflicting multi-objective problems starting at the early design stage of a ship through her entire operating life and ending with the scrapping stage. The framework will help in choosing a robust deign(s) which are able to operate efficiently and response to any changes in the unstable maritime market, to comply at the same time with the international regulations regarding the environmental impact, and to generate the most for shipowners and charterers.

The aforementioned research study, which leads to the achievement of the aim of the thesis, has been conducted to meet the following specific objectives of the research study presented in this thesis:

1. To produce the base hull of the oil tanker ship in AVEVA Marine.

2. To utilize design of experiments techniques DOE to create the design space that consists of 4 design variables, and then to carry out the systematic parametric distortion process to generate new hulls.

3. To build the hydrodynamic model to examine the hydrodynamic performance and energy saving potential across a range of speeds for both the laden and the ballast conditions. Also, to compare the performance of the alternative designs with the base hull's performance using different hydrodynamic characteristics.

4. To build the environmental impact model to investigate the greenhouse footprint of the ships by estimating CO_2 emissions and calculating EEDI value which is used as a benchmark.

5. To examine the influence of varying the operating speed as a key factor and hull parameters as well on the attained EEDI to the reference EEDI ratio. Achieving lower EEDI values to meet the strict future IMO requirements is an important issue in the deign process.

6. That can be achieved once the fuel consumption is calculated using power requirements' results from the hydrodynamic model. EEDI values are analysed to examine if the generated hulls meet the EEDI reference value addressed by IMO. is a key factor in any hydrodynamic optimisation model as the power is a function of the speed to the cubic power, so any small reduction in speed leads to a significant reduction if fuel consumption. Therefore,

7. To conduct a comprehensive economic study to evaluate the economic feasibility of building and running a vessel. That includes building an economic model that covers the key criteria and factors that ship charterers and operators should take into account to maximize their profit during a ship's lifetime while considering the market conditions.

8. To analyse the economic performance of the base ship and the alternative ships for two selected maritime routes and four scenarios of different combinations of fuel prices and fright rates. The impact of speed reduction to be investigated for the different scenarios to determine the potential to maximize the economic performance taking into account all the fluctuations in the shipping market.

9. To construct a multi-objective optimisation framework based on the concept of Pareto optimality to determine robust designs as well as operational profiles utilizing the three previous models. To develop a VBA macro code to carry out the optimisation process for the case study in order to determine a robust design or designs that offer a near-optimum performance regardless any fluctuations and eliminate any significant sub-optimal designs.

1.4 Research Contribution and Novelty

It is the intent of this research to focus on selecting an optimised hull which has a higher efficiency when operating over a selected wide range of speeds that allow for improving the economic performance regardless the shipping market conditions, compared to ones that have been optimised for a single design speed and particular market conditions and neglecting the secondary factors and parameters that might affect the final decision. This concept is novel, as constructing a robust framework to optimise the hull design and the operation of a ship while satisfying several objective functions simultaneously using an optimisation model as it has been presented in this thesis, to the best of the author's knowledge, is not presented in other research studies.

More parameters and factors are taken into account to build the three models that the optimisation framework is composed of. The knowledge accumulated through the models' chapters and then used to design and establish the multi-objective optimisation tool which is used to estimate, calculate, and optimise the objective functions more accurately compared with previous studies that looked into the parametric optimisation coupled with emissions mitigation and/or profit maximization. The results obtained from the optimisation framework demonstrate a novel approach to solve multi-objectives optimisation problem in the marine industry in a fluctuating market. Moreover, the thesis provides an effective tool that gives the user the ability to assess accurately the contrary implications of changing hull parameters at the design speed on the ship performance over her life span as well as the impact of speed optimisation on the ship emissions and the financial performance. This robust and straightforward tool can be considered a major contribution as it enables investigating the hydrodynamic performance, energy consumption, and economic performance individually and simultaneously, and gaining a better understanding of the trade-offs between the different competing objective functions in

order to achieve a greener and more efficient fleet. Such contribution to the literature justifies the novelty of the methodology proposed in this thesis.

1.5 Layout of the Thesis

This section provides a synopsis of the thesis construction which is presented in seven chapters and associated appendices as following:

1.5.1 Chapter 1 – Introduction

This chapter provides a broad understanding of the research work to the readers including the motivations behind conducting this research into hydrodynamic optimisation and slow steaming adoption, and its implications on economic performance. This introductory chapter also includes the aims and objectives of the study as well as the layout of the thesis.

1.5.2 Chapter 2 – Literature Review

The main objectives of this chapter is to review the natural environment conditions in which a vessel operates, to present the contribution of the maritime shipping to the global warming and climate change, and to cover the main and important aspects of the economics of ships with focusing on the key criteria that affect decisions making when it comes to design and build a new ship, and also on all the considerations that ship charterers and operators should take into account to maximize their profits.

1.5.3 Chapter 3 – Hull Form Hydrodynamic Optimization Based on Parametric Modelling

In Chapter Three, the hull optimization concept is described along with discussing the main elements including geometry manipulation tool, performance evaluator, and an optimization method. A bare-hull of a 54,000 DWT Tanker ship is chosen as a case study for this project. Four hull parameters have been chosen for the parametric analysis in addition to the operating speed. A set of regression formulas to estimate the required power per displacement are developed for a set of speed ranges. Taguchi statistical and experimental technique has been used to search for the most favourable form(s) and insensitive designs depending on the common naval architecture knowledge and skills, and on a trial and error procedure.

1.5.4 Chapter 4 – Environmental Impact Model

The environmental model which is built upon the EEDI formula is discussed in this chapter. A set of regression equations are obtained to estimate the attained EEDI to EEDI reference ratio $(EEDI_A/EEDI_{Ref})$ which is chosen as the objective function (response parameter) in the environmental model. It is used as an indicator while exploring the design space to choose alternative designs that demonstrate a better energy efficiency performance in order to meet the IMO requirements.

1.5.5 Chapter 5 – Ship Economical Model

An economic model is developed in this chapter to evaluate the economic performance in order to determine the sensitivity of a ship performance and profitability to changes in the market conditions. In specific, this model evaluates the impact of speed optimisation on fuel consumption and emissions reduction as well as shipping economics and the benefits for owners and charterers, and it also evaluates the cost of adopting this measure. The economic model is conducted for the base hull and other alternative designs for a set of eight different scenarios in order to investigate the implications of changes in the previously-mentioned elements and factors of a ship finance.

1.5.6 Chapter 6 – Multi-objective Optimisation

This chapter focuses on how to improve, simultaneously, the design and the operational profile of ships by balancing the conflicting performance indicators which have been addressed in the previous chapters. An optimisation framework has been developed based on the concept of Pareto optimality to assist decision making and to determine robust designs as well as operational profiles. VBA macro code is developed to carry out the optimisation process for the case study using 5 parameters and a set of constraints for the hull parameters and speed. The objective functions which are considered in this multi-criterion problem consist of the hydrodynamic performance (P_D/Dis), environmental impact ($EEDI_A/EEDI_{Ref}$), and economic performance (Net Present Value and Profit per tonne.mile).

1.5.7 Chapter 7 – Conclusions and recommendations for future work

Chapter Seven wraps together all the main findings of the thesis, and it summarises the main conclusions from this research study. This is followed by recommendations for future research on the subject.

A flow chart of the optimisation process is presented in Figure 1.2 showing the main steps as following:

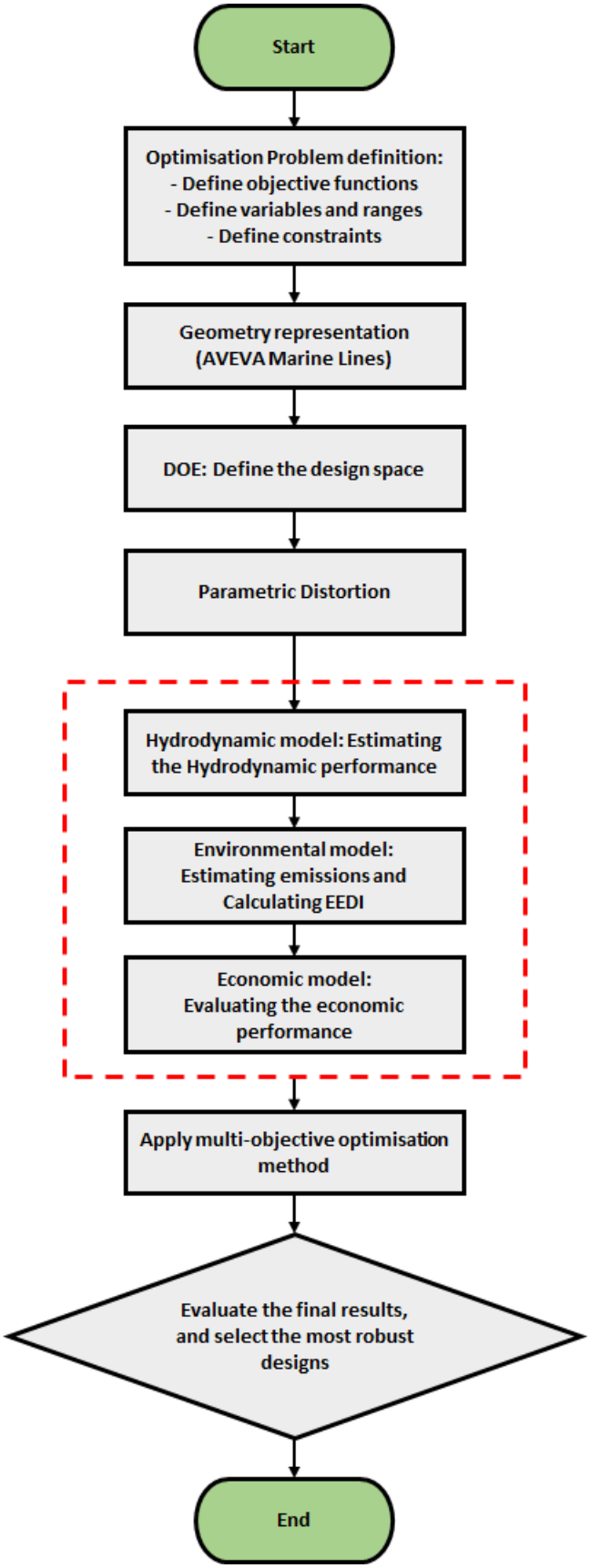

Figure 1.2 Flowchart of the design optimization process

Chapter 2. Literature Review

2.1 Introduction

As explained in Chapter 1, the motivation for committing to undertake this PhD research study was recognising the necessity to introduce more efficient and greener ships with a good energy management practice with a particular focus on the economic performance in a fluctuating shipping market. Therefore, multi-objective optimisation that considers the energy efficiency and economic success is an important aspect of ship design and operation. Both the hydrodynamic and economic performance characteristics need to be addressed in the early stages of the design, and secured during the life span of a ship. Because of the conflicting nature of these two objectives, there are various trade-offs at stake in the goal for making ships more efficient and greener to comply with IMO regulations while reducing the building and operating costs and increasing the profitability at the same time for all stakeholders especially owners and operators.

Within the framework of this motivation, the main objectives of this chapter is to review the natural environment conditions in which a vessel operates, to present the contribution of the maritime shipping to the global warming and climate change, and to cover the main and important aspects of the economics of ships with focusing on the key criteria that affect decisions making when it comes to design and build a new ship, and also on all the considerations that ship charterers and operators should take into account to maximize their profits.

2.2 Ship Resistance Estimation

2.2.1 General Considerations

When a ship is traveling in the seaway at speed V, the power required to drive her is mainly a function of her parameters, speed, and the shape of the hull which is subject to the forces and moments imposed by the surrounding environment. Understanding the nature of the ship resistance and the characteristics of the flow around the hull and propeller helps in improving

the ship performance and efficiency, and it is essential in order to improve the operating profile of the ship and choosing a suitable propeller and subsequently the main engine.

2.2.2 Hull Resistance

Over the past 100 years, a significant effort has gone to develop and improve methods that can be used to evaluate a ship's resistance. The total resistance of a ship with clean hull moving in calm weather conditions is referred to as calm water resistance or trial conditions resistance. It is imperative to determine the hydrodynamic components of the ship resistance and to understand the physics of their behavior and nature. It is common to breakdown the total resistance depending on the forces acting on the hull or depending on the energy dissipation (Molland *et al.*, 2011). Although the resistance components are generated in different ways, they still coexist and interact to some degree. However, by physical measurements, it is possible to determine the final breakdown of the total resistance R_T which consists of the pressure, frictional, viscous and wave resistance components as shown in Figure 2.1. The following equation shows the hydrodynamic breakdown of the total resistance:

$$R_T = R_F + R_W + R_{VP} \tag{2.1}$$

Where:

R_T: The total resistance;

R_F: The frictional resistance;

R_W: The wave resistance;

R_{VP}: The viscous pressure resistance.

A typical decomposition of the calm water resistance of a VLCC ship as an example is given as follows (OCIMF, 2011b):

- 72% frictional resistance,
- 20% viscous pressure resistance,
- 8% wave resistance.

Most resistance calculations use dimensionless coefficients $C = R/K$ to describe the ship resistance (MAN B&W, 2001). The term K is called the reference force and it is calculated as:

$$K = ½\rho V^2 A_S \tag{2.2}$$

Where:

ρ: Water density,

V: Model speed,

A_S: The hull's wetted area.

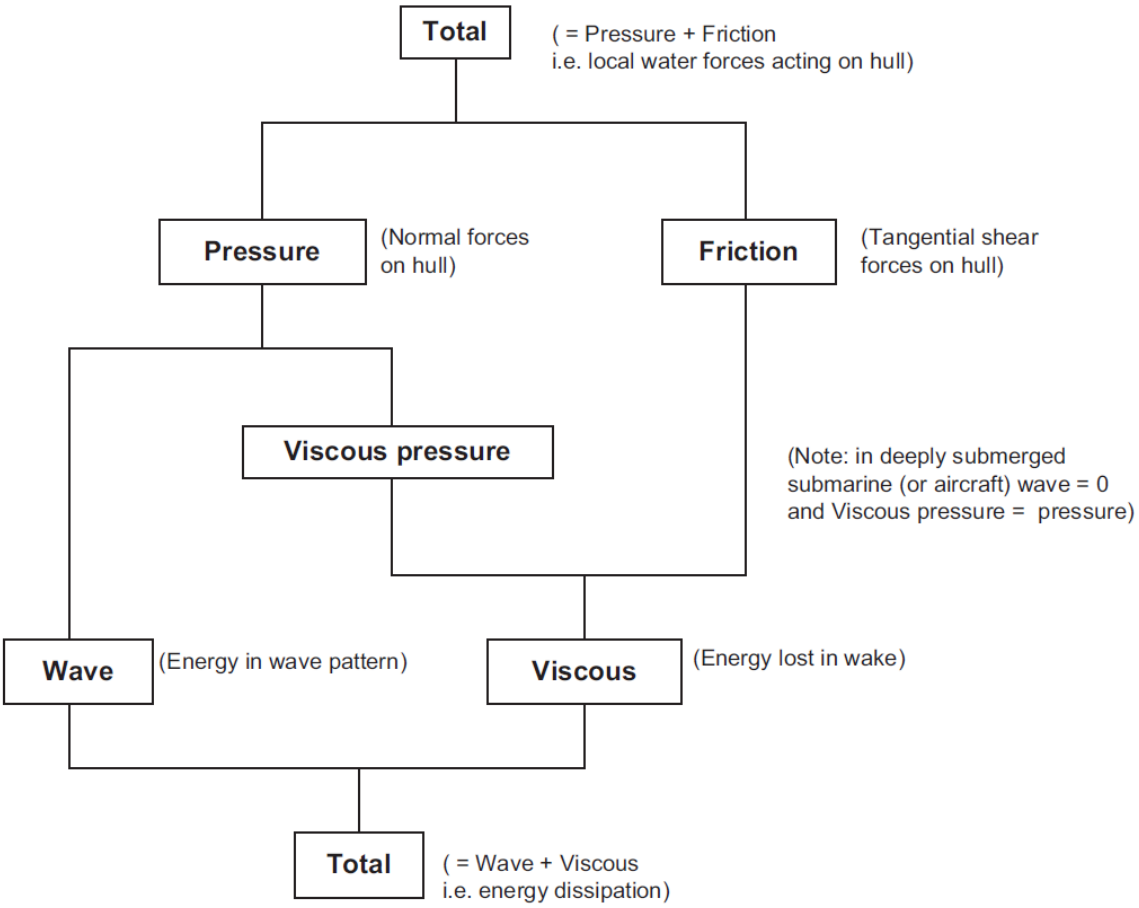

Figure 2.1 Basic resistance components

Several studies and methods, on the basis of different tank tests experiments and the results for the models' hulls, have been established to calculate all the main dimensionless resistance coefficients (C_F, C_W, C_P, C_R), and thus the pertaining total resistance R. Froude (1868) was one of the first pioneers to determine the ship's resistance and calculate it quite accurately by carrying out a series of experimental and theoretical investigations of ship models. His experiments on ship models showed that models of similar geometric forms would behave similarly within a flowing fluid. Froude (1868) also noticed that these geo-symmetric forms would dynamically behave in the same way to the full-sized ship if they operate at speeds that create the same wave patterns and thus forces. These speeds would be in proportion to the square roots of the length, and they are called the corresponding speeds. That led Froude to say

that if we could determine the resistance for the model, then we could scale it up and calculate the ship's resistance. According to Froude's method, the total resistance coefficient C_T is determined as a sum of the frictional resistance coefficient C_F and the residual resistance coefficient C_R which takes into account the wave and pressure resistance sum. Consequently, a ship's total resistance coefficient can be found using the towing tank results for a small-scaled model as following:

$$C_{TS} = C_{FS} + (C_{TM} - C_{FM}) \tag{2.3}$$

Where:

C_{TS}: Total resistance coefficient for the ship;

C_{FS}: Frictional resistance coefficient for the ship;

C_{TM}: Total resistance coefficient for the model;

C_{FM}: Frictional resistance coefficient for the model;

One of the primary methods to calculate the frictional resistance was approved and adopted by the International Towing Tank Conference (ITTC, 1957) with some modifications, and it is known as the ITTC 1957 model-ship correlation line. Hughes (1954) introduced this method in the 1950s based on the flow analysis in two dimensions where the results of the resistance test need to be extrapolated from models to ships. In fact, Hughes' approach is also based on Froude's law where the total resistance is the sum of the residual resistance which is calculated depending on the experiments depend on Froude number and the friction resistance which is calculated depending on experimental tests run at speeds where Reynolds number Re is applied. This approach is summarised as follows:

$$C_T = (1 + \mathrm{k})C_F + C_w \tag{2.4}$$

Where:

$(1 + \mathrm{k})$: The form factor that takes into account the hull form, and can be derived from model tests at low Froude's numbers and low speeds where the wave resistance coefficients C_w tends to zero and can be neglected:

$$(1 + \mathrm{k}) = C_T/C_F \tag{2.5}$$

C_T, C_F, C_w: Coefficients of total resistance, friction resistance, and wave resistance respectively.

When extrapolating model results to the full-scale ship on the basis of Froude's law, then the wave resistance coefficients are equal for the model and the ship. Therefore:

$$C_{TS} = C_{Tm} - (1 + \mathrm{k})(C_{FM} - C_{FS}) \tag{2.6}$$

The form factor $(1 + \mathrm{k})$ can also be determined using Prohaska (1966) method from slow speed data. This method, in fact, is an extension of Hughes' method but applies more data points to the correlation line that improves the scaling technique between the model and the ship. Prohaska's method was modified later in 1978 and recommended by ITTC, and it is still used till now by naval architects to estimate the total resistance as follows:

$$C_T = (1 + \mathrm{k})C_F + A.Fr^n \tag{2.7}$$

Where k, n, and A can be derived from a least-squares approximation of the low-speed experiments ($Fr = 0.1{\sim}0.2$).

While different methods have been suggested in addressing the total resistance, it is common when calculating the required engine power based on the total resistance to consider the total resistance coefficients as made up of five coefficients as in Watson (1998) method:

$$C_{TS} = (1 + \mathrm{k})C_{FS} + C_R + C_{App} + \Delta C + C_{Air} \tag{2.8}$$

Where:

C_R: The residuary resistance coefficient which takes into account mainly the wave-making resistance, and it is governed by Froude's number.

C_{App}: The appendages resistance coefficient.

ΔC: The roughness allowance.

C_{Air}: The air resistance coefficient.

In this thesis, a method proposed by Holtrop and Mennen (1982) and Holtrop (1984) is used to predict the resistance of the case study as it is one of the widely used techniques to determine a ship resistance and estimate the required propulsive power at the initial stage of designing a ship. A regression analysis of random test experiments on 334 models and full-scale data for displacement and semi-displacement vessels at Netherlands Ship Model Basin was carried out

to develop a numerical representation of ship's resistance and her propulsion properties. However, Holtrop and Mennen algorithm is limited to be suitable for particular ranges of hull parameters and different ship types as shown in Table 2.1 (Holtrop, 1977; AVEVA MARINE, 2011):

Table 2.1. Parameters ranges for different ship types

Type of ship	Fn	C_P		L/B		B/T	
	max.	min.	max.	min.	max.	min.	max.
Tankers, Bulkcarriers	0.24	0.73	0.85	5.10	7.10	2.40	3.20
General cargo	0.30	0.58	0.72	5.30	8.00	2.40	4.00
Fishing Vessels, Tugs	0.38	0.55	0.65	3.90	6.30	2.10	3.00
Containerships, Frigates	0.45	0.55	0.67	6.00	9.50	3.00	4.00
Various	0.30	0.56	0.75	6.00	7.30		

In the numerical representation based on the regression analysis, the total resistance R_{Total} of a ship has been subdivided into components, and each component has been expressed as a function of the hull form characteristics and the ship's speed as follows:

$$R_{Total} = R_F(1 + k_1) + R_{APP} + R_W + R_B + R_{TR} + R_A \tag{2.9}$$

Where:

R_F: Frictional resistance as calculated according to the ITTC 1957 friction formula,

$1 + k_1$: Form factor describing the viscous resistance of the hull form in relation to the frictional resistance,

R_{APP}: Appendages resistance,

R_W: Wave-making and wave-braking resistance,

R_B: Bulbous bow additional pressure resistance near the water surface,

R_{TR}: Additional pressure resistance of the immersed transom stern,

R_A: Model-ship correlation resistance which takes into account the full-scale roughness.

2.3 Sea Trials and In-Service Conditions

A sea trial, as a part of the contractual settlement between the builder and ship owner, is the last testing phase of a ship's performance including speed capability, manoeuvrability, construction, and safety features. The primary purpose of carrying out these trials is to make sure that the design specifications have been met along with the International Maritime Organisation criteria regarding speed, manoeuvring performance, and general seakeeping (IMO, 1993). Moreover, the final verification of the attained EEDI value is carried out for ships depending on the results and information gathered under the sea trials condition (MEPC - IMO, 2012). It is essential to make sure that these trials take place in an open, deep, and calm water in order to reduce the impact of the wind, current, and tides. That will help in minimising the required corrections since it is almost impossible to perform these trials under such ideal conditions.

At the early stages of ship design, it is very important to pre-determine the ship behaviour at sea, resistance, and the required power in order to ensure that the final design including the hull, propeller, and engine will operate adequately to fulfil the contract specifications (mainly the service speed). The cost penalty of a 0.3 knots deviation in speed, between the corrected trial speed and the contracted service speed, is around USD 100,000, and this fine increases by USD 100,000 for each additional 0.1 knots (Haakenstad, 2012). In fact, the consequences of speed loss for ship owners is the increased journey time, and, as a result, a loss of ship's productivity which impacts the revenue and the final profit of their ships as an investment.

In practice, it is required to evaluate and analysis the ship performance and calculate the hull resistance at conditions of her normal operation other than those accrued during the sea trials. These conditions are referred to as in-service conditions which take into account the influence of forces and moments imposed on the ship by wind, waves, and surface currents and also the effect of the hull fouling which plays a significant role in increasing the hull resistance and reducing the service speed in a seaway. Therefore, some key corrections should be designed to indicate the impact on speed, propeller and hull efficiency, propulsive power, and consequently the fuel consumption.

To provide a ship with sufficient power to overcome the speed loss in the seaway, it is common at the design stage to increase the engine power by a constant percentage (15-30 %) over the trial power. This increase in the engine power is referred to as sea-margin or service-margin. Szelangiewicz and Żelazny (2007) showed that the additional power margin varies, and it is

calculated depending on the ship type, size, service speed, voyage route and the weather parameters the ship will face in her day-to-day operation. Guldhammer and Harvald (1974) suggested average values for the sea margin for different shipping routes to maintain the operation schedule as shown in Table 2.2. It must be noticed that any additional increase in the propulsive power may provide only a slight increase in the ship's speed. That is because the extra power will lead to a higher wave resistance for a particular hull optimised at the design speed (MAN B&W, 2001). That could be explained, for a given hull design, as the ship speed boundary is imposed by the wave wall where any increase in the propulsive power will be converted into wave energy rather than an increase in the speed as shown in Figure 2.2.

Table 2.2. Average percentage for Sea Margin allowance for different shipping routes

	Summer	**Winter**
North-Atlantic Eastwards	15%	20%
North-Atlantic Westwards	20%	30%
Pacific	15%	30%
South-Atlantic and Australian routes	12%	28%
East-Asiatic route	15%	20%

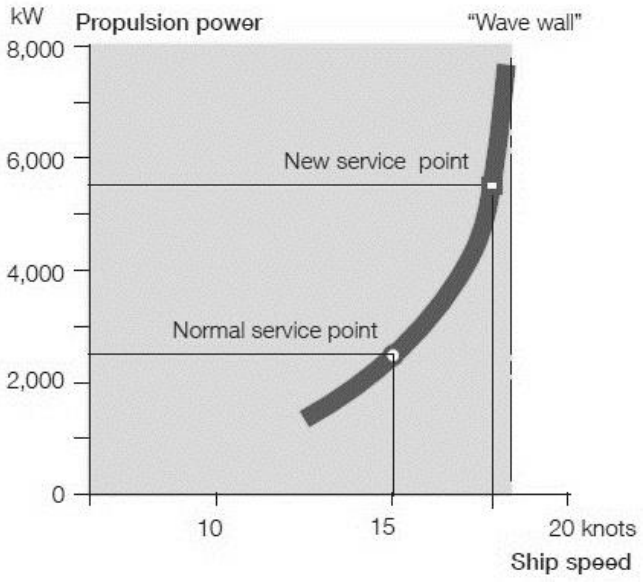

Figure 2.2. Power and Speed relationship

International Organization for Standardization ISO (2015) states the procedures and guidelines to conduct the speed and power trials based on the experience, recommendations and analysing real data from previous sea trials. Moreover, these standards contain resistance correction methods, to be used by shipyards, to take into consideration the added resistance due to currents,

wind and waves mainly, and the effect of water temperature and density, the water depth, and the deviations in trim and displacement. Most of the traditional correction methods are empirical to some extent, and they involve manual interpolation curves (Bertram, 2012). Such methods can be found in (Bose *et al.*, 2005) and (Van Den Boom *et al.*, 2008). However, the resistance corrections are out of the scope of this thesis, and an acceptable sea-margin will be added to the estimated propulsive power to ensure that the selected engine has sufficient power to propel the ship at the design speed.

2.4 Added Resistance and Speed Loss

2.4.1 Added Resistance due to the wind

The increase in resistance due to wind can be as much as 10% of total resistance for ships, with a big cross-sectional area above the waterline, in head winds. This added resistance due to wind occur in two ways: direct aerodynamic resistance by the wind on the ship body which is a friction force, and indirect power demand to maintain the ship course against the drift because of side winds (Hochkirch and Bertram, 2010). The air resistance magnitude depends on the size and shape of both the above-water hull and the superstructure and on the speed as well. Therefore, improvements of the superstructure such as rounding sharp corners are necessary to reduce the air drag especially for big ships with a boxed-shape superstructure. The wind resistance coefficient is defined by running model tests in wind tunnels or by using previous data from similar vessels as such databases are available for shipyards. Much work has been performed in the study of the added resistance due to the wind. Bertram and Schneekluth (1998) provide simple and easy design approaches to estimate the wind resistance with empirical formulas such as Jensen (1994) method for cargo ships as in Eq (2.10):

$$R_{AA} = C_{AA} \frac{\rho_{air}}{2} \cdot (V + V_{wind})^2 \cdot A_F \tag{2.10}$$

Where:

C_{AA}: The wind resistance coefficient. $C_{AA} = (0.8 \div 1.0)$ for cargo ships,

ρ_{air}: The air density. $\rho_{air} = 1.25\ Kg/m^3$,

V, V_{wind}: Ship speed and wind speed, respectively,

A_F: The ship frontal projected area above sea level.

Data from wind tunnel tests on small models was analysed at the Institute of Naval Architecture (IS) by Blendermann (1996) in order to determine the wind loads on ships using a set of tables and diagrams for data stems from experiments in a uniform flow. He also provided an empirical formula to calculate the wind forces on various ship types, floating docks and other objects. Blendermann (1996) formula to estimate the wind resistance gives more accurate results and further details for side forces, yaw and roll moments, and it is given as following (Bertram and Schneekluth, 1998):

$$R_{AA} = \frac{\rho_{air}}{2} u^2 \cdot A_L \cdot CD_l \cdot \frac{cos\varepsilon}{1 - \frac{\delta}{2}\left(1 - \frac{CD_l}{CD_t}\right) \cdot sin^2 2\varepsilon} \tag{2.11}$$

Where:

u: The apparent wind velocity,

A_L: The lateral-plane area,

ε: The apparent wind angle ($\varepsilon = 0^o$ in head wind),

δ: The cross-force parameter,

$CD_l \; and \; CD_t$: Non-Dimensionless drag coefficients in beam wind and head wind.

2.4.2 Added Resistance due to waves in a seaway

There has been an increasing interest in calculating the added resistance in waves at service conditions which is more severe comparing with the speed-trials conditions in calm weather (Beaufort 2) and the model test conditions. The loss of speed because of rough weather is referred to as involuntary loss, and it occurs because the ship's excessive motion response caused by wind and waves, and because of the loss in the propulsive efficiency (Trodden, 2014). There is a handful of empirical methods and corrections proposed in the literature, and most of them are based on physical assumptions and sea-state statistics. Being hard to predict and measure the sea-state parameters on different routes, and because of the inaccuracy involved in the seakeeping statistics, powerful computational simulations are being used to determine ships performance in a seaway and to optimise the voyage profile in order to minimise the delay due to weather and to keep the operating costs low.

A simple design formula, based on statistical analysis of full-scale data for tankers and container ships, is given by Townsin and Kwon (1983) for the speed loss due to added resistance in wind and waves as following (Bertram and Schneekluth, 1998):

$$\Delta V = C_{\mu} \cdot C_{ship} \cdot V \tag{2.12}$$

Where:

ΔV: Speed loss in a seaway due to wind and waves,

V: Service speed,

C_{μ}: A factor considers the predominant direction of wind and waves μ^{o}, and it depends on the Beaufort number BN.

C_{ship}: A factor takes into account the ship type:

In addition, several methods have been provided by the International Organization for Standardization ISO (2002, 2015) to assist calculating the added resistance for different ship sizes and types, and different wave lengths and directions. For example, Faltinsen's formula is restricted to short waves $(\lambda/L < 0.5)$, and applicable for wave directions in the $(\beta = 90^{o} - 270^{o})$ range. Another method is Maruo's method which is based on a slender ship approximation. It is applicable for all wave directions and wave length, and it gives good predictions for fine and medium ship forms. It provides good results and shows good agreement with the experimental results especially in the intermediate range of Froude's number $(Fn = 0.18 - 0.23)$ (Zakaria and Baree, 2008).

2.4.3 Added Resistance due to surface currents

Due to the actions of surface currents generated by tides and/or winds, there is relatively a high level of turbulence on a ship's course which influences the body forces and, hence, the powering performance of the ship. These forces acting on the body depend on the current direction and speed. It is important to take into account the effect of the surface currents and tides in the manoeuvring calculations to maintain the ship's course and her speed (Trodden, 2014). In fact, the tidal currents do not flow at a constant speed or direction as they frequently vary according to the state of the tides. However, in practice and during speed trials, it is assumed that the currents are constant in speed and direction (Haakenstad, 2012).

2.4.4 Added Resistance due to roughness and fouling

According to paint suppliers, every 25 μm increase in the average hull roughness will cause about 2-3% increase in the required power to maintain a ship's speed or a speed loss of about 1% (MAN B&W, 2001). Technically, during a normal daily operation of a ship, hull's paint and coating film will break down, and hence the erosion starts and fouling covers the hull and propeller surface. Throughout the lifetime of a ship, the frictional resistance will be greater, and the average increase in the total resistance may be up to 25-50% with a drastic reduction in the ship's speed. To take into account the roughness effect on the resistance, it is recommended to increase the friction resistance coefficient determined from the model tests by a particular allowance called the roughness allowance coefficient ΔC_F. Different methods were proposed to estimate ΔC_F such as Bowden–Davison equation which was originally recommended to be used for the power performance prediction by The International Towing Tank Conference (ITTC, 1979), and it is as follows:

$$\Delta C_F = \left[105\left(\frac{ks}{L}\right)^{1/3} - 0.64\right] \times 10^{-3} \tag{2.13}$$

Where (ks/L) is the roughness criterion. In fact the surface roughness ks is not constant but it is a function of the ship size and determined based on experience. However, for the approximate purpose the surface roughness can be taken as $ks = (100 - 150) \times 10^{-6}$ m (Molland *et al.*, 2011).

In addition, there are different methods to calculate ΔC_F and they were derived basing on data from various model basins and shipyards. Bertram (2012) showed some recommended values for ΔC_F in conjunction with the ITTC 1957 friction coefficients as a function of the ship length as in Table 2.3:

Table 2.3. Recommended values for ΔC_F

L_{BP} (m)	ΔC_F
50-150	0.00035-0.0004
150-210	0.0002
210-260	0.0001
260-300	0
300-350	-0.0001
350-400	-0.00025

2.5 Hull-propeller Interaction

Ship propulsion performance is a measure of the energy consumption and an indicator of a ship efficiency during her lifetime at any scenario and condition. From an economic and environmental point of view, shipping industry needs to improve the hydrodynamic performance of a ship and to optimise the overall operation profile in order to make ships more profitable and decrease the carbon footprint. Hence, a significant amount of research and development has been done in an effort to search for potentials to increase the overall propulsive efficiency and to meet the recent international requirements to make the shipping industry greener.

Having the basic knowledge and ability to estimate the required propulsive power for a robust and steady operation is fundamental in the early design stages as it ensures a ship is fitted with the right powering system, and to attain greater efficiency in her day-to-day service. Figure 2.3 shows a simple sketch of the overall concept of the powering system (Pedersen and Larsen, 2009; Molland *et al.*, 2011). The energy of the fuel, mainly crude oil, is converted into thrust to overcome the total drag and propel the ship at the required speed. Fuel consumption and the amount of emissions for a particular ship depend on:

- Fuel quality and engine efficiency: low-quality and dirty marine fuels and incomplete combustion inside the main engine lead to emitting a relatively high mass of pollutants including CO_2, NOX, CO, SOX, and other particulars.
- The overall efficiency of the propulsion system.
- The operating speed as the fuel consumption increases as a third power function of the speed.

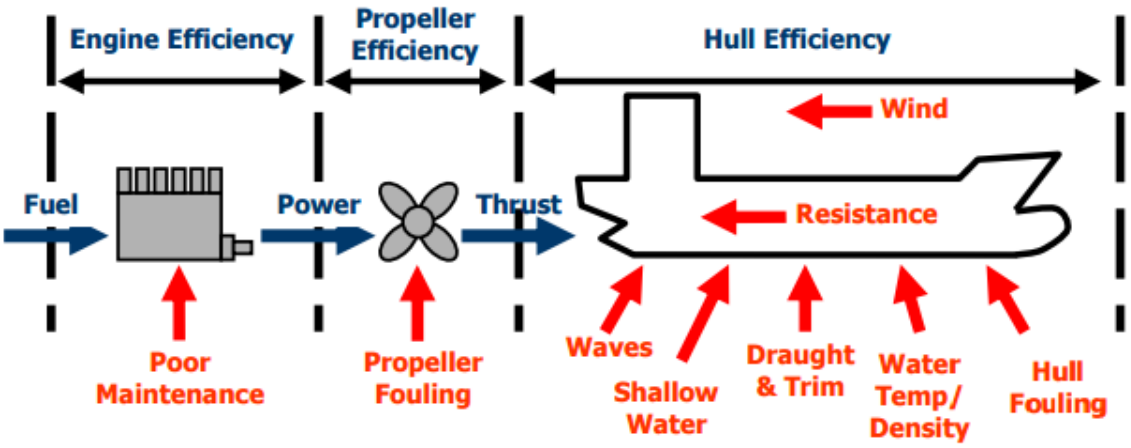

Figure 2.3. Energy Conversion

The total propulsion efficiency (η_D) depends mainly on the propulsion device efficiency and also on the interaction between it and the hull. It is determined as the ratio between the effective power P_E (the power required to tow the ship) and the delivered power P_D to the propulsion unit (Molland *et al.*, 2011). However, a breakdown of the total propulsion system efficiency [The propeller quasi-propulsive coefficient QPC] can be shown as in Eq (2.14). Moreover, because of the inherent inefficiencies in the transmission system (shafting and gearing losses), the total installed power of the prime engine will exceed the required power delivered to the propeller. The ratio between the delivered power to the propeller and the power delivered by the main engine is the transmission efficiency η_T.

$$\eta_D = \frac{P_E}{P_D} = \eta_H \cdot \eta_O \cdot \eta_R \tag{2.14}$$

Where:

η_O: The open water efficiency of the propeller. It describes the propeller performance in open water with a homogenous wake field where there is no hull (Molland *et al.*, 2009). A typical value for (η_O) for conventional propellers is taken as 0.65.

η_R: The relative rotative efficiency. It is defined as a ratio between the delivered power to the propeller to produce the same thrust in the open water condition and in the wake behind the ship. (η_R) value depends on the propeller parameters and the hull design, and typically it ranges between 0.95 and 1.05.

η_T: The transmission efficiency. It is an indicator of the power generated in the main engine and lost in the transmission through the shaft to the propeller. A typical value for (η_T) is 0.95 for a geared drive installation and 0.98 for a direct drive installation (Kristensen, 2012).

η_H: The hull efficiency. It is defined as the ratio between the effective power and the thrust power P_E/P_T. It is a function of the wake fraction (w) and the thrust deduction (t), and it lies typically between 1.10 and 1.25 (Harvald, 1983; 1992):

$$\eta_H = \frac{P_E}{P_T} = \frac{R_T \cdot V}{T \cdot V_A} = \frac{1-t}{1-w} \tag{2.15}$$

Where:

V, V_A: The ship's speed and the velocity of the water arriving to propeller, respectively,

R_T: Total towing resistance,

T: Thrust force,

w: Taylor wake fraction,

$$w = \frac{V - V_A}{V} \tag{2.16}$$

t: Thrust deduction fraction which is the ratio between the loss of thrust ($T - R_T$) and the thrust T required to propel the ship and to overcome the resistance R_T:

$$t = \frac{T - R_T}{T} \tag{2.17}$$

The interaction between the hull and the propulsive device is very complex, and it is determined by three main components which are wake fraction, thrust deduction and the relative rotative efficiency. The nature of this interaction is dominated by the propeller-hull clearance, the shape of the aft end hull and the finesses of the waterline endings (Molland *et al.*, 2009). It is obvious that the best practise is to minimise t and maximise w in order to optimise the hull efficiency and consequently the propulsion efficiency η_D.

Holtrop and Mennen (1982) and Holtrop (1984) method is used in this study to obtain accurate estimations for (w, t). It is a complex method based on analysing data obtained from 334 model tests. The regression analyses produced imperial formulas to calculate the wake fraction and thrust deduction for a single-screw ship. These formulas were extended over a sequence of advanced studies, and they include new coefficients. Wake fraction and thrust deduction fraction are estimated as in Eq (2.18) and (2.19):

$$\begin{aligned} w = {} & c_9 c_{20} C_V \frac{L}{T_A}\left(0.050776 + 0.93405 c_{11} \frac{C_V}{(1 - C_{P1})}\right) \\ & + 0.27915 c_{20} \sqrt{\frac{B}{L(1 - C_{P1})}} + c_{19} c_{20} \end{aligned} \tag{2.18}$$

$$t = \frac{0.25014 (B/L)^{0.28956} \left(\sqrt{BT}/D\right)^{0.2624}}{(1 - C_P + 0.0225 LCB)^{0.01762}} + 0.0015 C_{stern} \tag{2.19}$$

Recently, Kristensen (2012) calculated the wake fraction and thrust deduction fraction using Harvald's formulas for a sample of 26 single screw tankers and bulk carriers in the trial

conditions. These values have been compared with model tests values measured in full load and ballast conditions. The results show that the wake fraction obtained from model tests is marginally lower than the calculated wake fraction using Harvald's method. Moreover, it is noticed that the measured thrust deduction fraction is, in general, less that the calculated values. Subsequently some corrections have been addressed in Kristensen's study in order to achieve more accurate values for w and t to match the model test values. The difference between the measured and calculated values were plotted as a function on the length-displacement ratio $M = L/\nabla^{1/3}$. The results show that for lowest length-displacement ratios the difference has the highest values. However, the correction formulas which obtained from the analysis of the plotted comparisons for takers and bulkers as following:

$$w_{corrected} = w_{Harvald} + 0.08M$$
$$t_{corrected} = t_{Harvald} - 0.26 + 0.04M \quad (2.20)$$

2.6 Ship Power Prediction

In this study, the aim is to evaluate the ship performance by comparing the fuel efficiency of the power plant at different speeds and different operation scenarios. The power requirements have to be, relatively, accurately estimated in the early design stages. That helps in determining the necessary bunker storage, and it provides adequate details to minimise the installed power, and hence to reduce the capital cost and/or improve the fuel economy.

However, the power estimation process has to be done repeatedly within the design loops. Therefore, empirical approaches are employed for a quick and simple estimate as they require a few design parameters (Bertram, 2012). These methods can be categorised into three groups, and they will be discussed briefly:

- Regression analysis for data of many ships, e.g. Holtrop–Mennen, Hollenbach, Lap–Keller,
- Systematic series, e.g. Taylor–Gertler, Series-60, SSPA,
- Estimate from parent ship, e.g. Admiralty Coefficient method, Arye's method, Circle C method, or similar formulae.

Holtrop and Mennen method is employed in this research to carry out the resistance and power calculations, and the procedures follow the overall mechanisms of any method are introduced in (Molland *et al.*, 2011).

2.6.1 Regression analysis Methods

These methods are addressed as resistance-based methods. Using the resistance estimation methods and propulsion factors previously derived, the amount of power required at any speed to propel a ship through the water to reach the final destination is calculated. A typical mechanism of estimating the ship power starts with estimating the total calm water resistance, and the process ends by calculating the total installed power (P_I) (Molland *et al.*, 2011).

First of all, the effective (towing) power (P_E) is the power necessary to move the ship through the water at speed V. In other words, it is the power necessary to tow a ship at speed V, and it is usually determined by carrying out model tests and measuring the force resisting the movement of the model. The towing power then needs to be scaled up to determine the full-scale ship resistance and the effective power as in Eq (2.21):

$$P_E = R_T \times V \tag{2.21}$$

As a matter of fact, the propeller is the least efficient component of a ship's drive train because of the losses in converting the rotational motion of the propeller into linear thrust. Studies show that recent well-designed propellers have an efficiency of 70-75% at the design speed. Therefore, the power produced by the propeller's thrust P_T is smaller than the delivered power to the propeller by the shaft (J. Falls and Mayer, 2012). The thrust power is given as a multiple of the propeller thrust T and the speed past propeller (speed of advance) V_a:

$$P_T = T \times V_a \tag{2.22}$$

The power delivered to the propulsion unit at the tail-shaft and required to propel the ship at her design speed is called the delivered power P_D. The ratio between the effective power and the delivered power is referred to as the Quasi-propulsive coefficient QPC or η_D as mentioned before. It is made up of the open water propeller efficiency, the relative rotative efficiency and the hull efficiency. That depends, in particular, on the flow conditions around the propeller and the propeller efficiency itself. An approximate value of η_D can be calculated using Emerson's formula (Watson, 1998):

$$\eta_D = K - \frac{N\sqrt{L}}{10000} \tag{2.23}$$

where N is the propeller RPM, and K is a constant and it is about 0.84 for single-screw ships. Remarkably, a great advantage in the propulsive efficiency can be gained by adopting as low revs/min as possible. For instance, a gain of about 7.6% can be obtained by today's slower revving engines (80 rpm) comparing with a 110 rpm engine for a 300 m ship.

So far, considering the transmission and gearing allowance and the sea margin allowance too, the calculated power is the power produced by the ship's prime mover's power, i.e. Brake Horsepower P_I.

$$P_I = \frac{P_E}{\eta_D} \times SCF \times \frac{1}{\eta_T} + margins \tag{2.24}$$

where SCF is the model-ship correlation factor applied to the delivered power.

Finally, it is worth mentioning that diesel engines manufacturers recommend limiting the service power to a fraction of the total continuous power capability of the engine in order to reduce the engine's maintenance and improve its life efficiency. The maximum capacity of the diesel engine power is called Maximum Continuous Power (P_{bc}, MCR), and the most recommended limit for the service power is about $(85 - 90\%)$ and it is known as derating (Watson, 1998).

2.6.2 Systematic Series Method – Series 60

Most of the systimatical series approaches are outdated and not broadly used as they often underestimate the actual resistance of the modern hulls (Bertram, 2012). Series 60 method was developed by Todd in the United States in the 1950s, and it is based on the results of 45 models in a towing tank with variations of five basic forms (Todd, 1953; Todd *et al.*, 1957). The series covers the following range of hull parameters and speeds (Molland *et al.*, 2011):

Fr	$0.06 - 0.27$
C_B	0.6−0.8
B/T	2.5−3.5
L/B	5.5−8.5
LCB	(−2.5%)−(+3.5%)

The results of such tests are expressed in design charts from which naval architects, by interpolation where necessary, can select some forms suitable for a particular problem, and then determine their relative resistance and propulsive qualities. That helps to make an informed choice of the best combination of parameters to give the minimum power within the other limitations of the design conditions. However, instead of using Todd's charts, Lackenby and Milton (1972) proposed a new presentation for Series 60 method using both Sochoenherr and Froude lines. A circular notation is used to represent non-dimensional power coefficient © as in Eq (2.25) [in imperial units] and Eq (2.26) [in metric units]:

$$© = \frac{579.8 \cdot P_E}{\Delta^{2/3} \cdot V^3} \tag{2.25}$$

where $(P_E: kW, \Delta: tonnes, V: knots)$

$$© = \frac{427 \cdot P_E}{\Delta^{2/3} \cdot V^3} \tag{2.26}$$

where $(P_E: hp, \Delta: tonnes, V: knots)$

2.6.3 Estimation from Parent Ships - Admiralty Coefficient Method

The Admiralty coefficient method is one of the oldest and simplest approaches for the power prediction. Although, it is a crude method and its results are not sufficiently accurate, but it is still fairly useful when there are not enough details about the hydrodynamic performance of the ship or when there is no model experiments data.

The Admiralty coefficient A_C is constant for a given hull, and it gives the approximate relations between any corresponding power supplied by the engine, ship speed and displacement Δ. This method is limitted where there is only a relatively samll variation in the speed and dispalcement from the parent hull. The accepted variance is 8% fro the speed and 10% for the dispacement. Thus, the constant A_C is defined as follows (Molland *et al.*, 2011):

$$A_C = \frac{\Delta^{⅔} \cdot V^3}{P} \tag{2.27}$$

Values of A_C vary for different ship types as a function of dimensions and speed, and the higher values indicate more efficient hulls (Barbahan, 2008). Figure 2.4 shows the influence of fouling and weather on the Admiralty cofficient as it is plotted against a base of time for fouling effects,

and against Beaufort number for weather effects (Molland *et al.*, 2011). Shipping companies often use this criterion as an comprehensive measure of the effects of changes in the engine efficiency, weatehr and fouling.

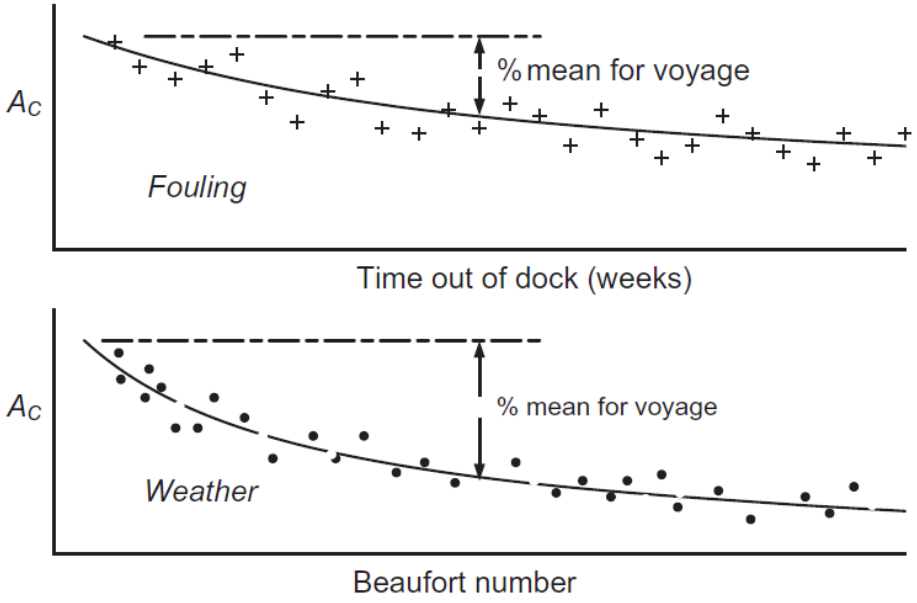

Figure 2.4. Influence of fouling and weather on Admiralty coefficient (Molland et al.*, 2011)*

2.6.4 CFD Tools

As mentioned before, over the past decades there was a significant number of studies and proposals aiming to improve the accuracy of estimating the ship resistance and power requirements for many variations in hull shapes and over a broad range of speeds and different scenarios. However, from about the start of 1980s, there was an increasing role of the numerical methods and the potential future of the computational fluid dynamics in the shipbuilding and naval architecture sectors.

Numerical methods have become increasingly important and have proven a substantial ability in estimating the ship resistance. They are faster and cheaper than model tests, and they provide adequate understanding of the flow details. On the other hand, using numerical modelling requires a huge amount of time and computing power as it needs parallelisation of a large number of processors. Moreover, while physical model tests demonstrate all flow physics and characteristics, CFD methods can only model the physics and theories we know about the flow and its interaction with the objects. Therefore, the accuracy of the CFD is still insufficient in many aspects, and it needs a lot of improvements especially in resistance and the power requirements prediction.

Design offices at ship yards tend to employ CFD methods, model tests and full-scale speed trials to generate high quality and reliable figures and database to assess the power characteristics. In the design process, CFD is used for pre-selection of potential modifications and improvements and to gain comprehensive understanding of the flow physics before carrying out the expensive traditional towing tank tests.

Computational Fluid Dynamics (CFD) tools have been widely used to simulate different aspects such:

- the motion response of a ship in a seaway,
- the flow direction and characteristics around ship's hull,
- the flow over superstructures and appendeges,
- the derivation of viscous resisatnce and free-surface waves,
- the friction resistance,
- the hull and propeller interaction and behaviours.

The art of the latest effective CFD tools is being able to overcome some challenges to ship designers and naval architects such as the interaction between developing the boundary layer of the hull and generating free gravity waves because of the hull shape (Wilson *et al.*, 2007; Molland *et al.*, 2011). The CFD methods for the marine applications are used for inviscid flows and for viscous flows which are well described in (Bertram and Schneekluth, 1998; Molland *et al.*, 2011; Bertram, 2012).

As Navier-Stokes solvers which use viscous CFD codes become more robust and efficient to use, Date and Turnock (2000) applied Reynolds-Averaged Navier–Stokes (RANS) solver to develop the resistance correlation line and pridect the friction values for a plate and at a range of speeds. Their work demonstarted a reasonable performance of the CFD tools as the produced formula was very close to Schoenherr friction line. The Reynolds averaged Navier–Stokes equation has been utilized by (Choi *et al.*, 2010) to predict the speed performance of eight commercial ships including four large-sized container carriers, two LNG carriers, one VLCC, and one bulk carrier. Their CFD model is built to investigate the wake characteristics on the propeller plane, wave characteristics around the model ship, and the limiting streamlines on the hull. To evaluate the accuracy of the computational results, a series of model tests were conducted and the results were compared. For instance, the resistance characteristics' results present a relatively high correlation between the CFD outcome and the model tests' ones as the

variation is between $[0\,,5.7\%]$. Also, the study shows that the difference between the computational and the experimental predictions for the propeller relative rotative efficiency stands between $[-3.19\%\,,2.27\%]$ and $[-8.99\%\,,0.17\%]$ for the delivered power. That indicates that in the initial design stages, computational predictions can be confidently employed considering the need to enhance the accuracy for greater precision

2.7 The Contribution of Shipping Activities to Global Warming

The maritime activities in 2007 were responsible for about 3.3% of the total world carbon dioxide emissions as it was estimated to have emitted more than 1.0 billion of CO_2 according to the Second IMO GHG Study (2009). Emissions from shipping is slightly more if the analysis takes into account the other greenhouse gases such as (CH_4, N_2O, O_3) bearing in mind that carbon dioxide accounts for the vast majority of emissions from ships, roughly 97%. This significant contribution to global emissions puts international and domestic shipping under increasing pressure to reduce its carbon and other emissions footprint from the combustion of petroleum-based fuels such as distillate or residual diesel fuels. The maritime shipping is relatively clean compared to other transportation methods and considered as one of the lowest contributors of GHGs. For example, per tonne-mile, it emits less than half as much CO_2 as rail transport, one-third that of road transport, and surprisingly less than 1% of what air transport emits per work unit (Bodansky, 2016).

Figure 2.5 presents a detailed comparison for CO_2 emissions from shipping against other contributors to the global total emissions. However, even the maritime shipping is responsible for less than 4% of the world's total GHG and it is considered as the most productive but the international community still addresses it as a major source of emissions such as $[CO_2, NO_x, SO_2, PM]$ (Ballou *et al.*, 2008).

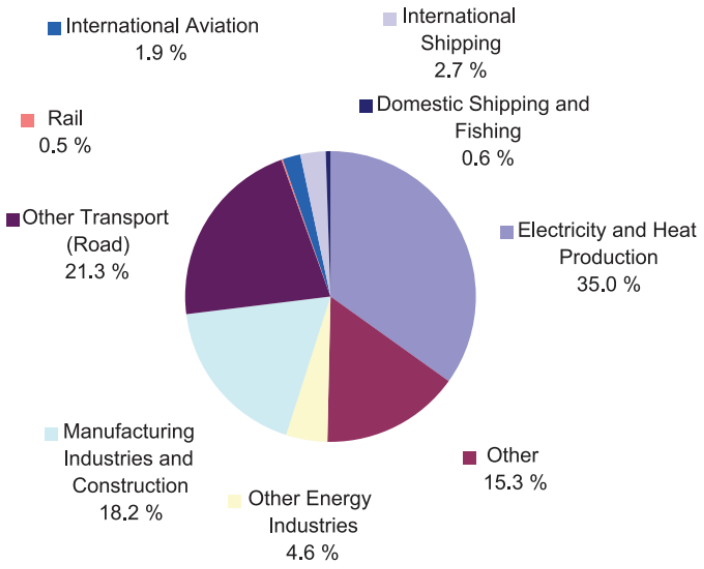

Figure 2.5 Emissions of CO_2 from shipping compared with global total emissions

Table 2.4 shows the full-time series comparison of shipping CO_2 emissions with global total CO_2 between 2007 and 2012 as estimated by the *Third IMO GHG Study* (2014) where the figures are marginally different from the ones used in the Second IMO GHG Study by (Buhaug *et al.*, 2009). CO_2 emissions from international shipping are estimated to be 796 million tonnes in 2012, and that accounts for approximately 2.2% of global CO_2. That is a significant drop in the emissions from the international shipping comparing with the estimated numbers from 2007. Taking into account all GHGs emissions combining $[CO_2, CH_4,$ and $N_2O]$, the Third GHG study estimates that for the year 2012, total shipping emissions were approximately 961 million tonnes and 816 million tonnes from the international shipping (2.1% of the global emissions).

Table 2.4 Shipping CO_2 emissions compared with global CO_2 (Values in million tonnes CO_2)

Year	Global CO_2	Total shipping	% of global	International shipping	% of global
2007	31,409	1,100	3.5%	885	2.8%
2008	32,204	1,135	3.5%	921	2.9%
2009	32,047	978	3.1%	855	2.7%
2010	33,612	915	2.7%	771	2.3%
2011	34,723	1,022	2.9%	850	2.4%
2012	35,640	938	2.6%	796	2.2%
Average	33,273	1,015	3.1%	846	2.6%

2.7.1 Estimating Fuel Consumption and Shipping Emissions

Regulating air emissions from shipping needs an effective policy strategy based on robust and accurate estimation in terms of type, quantification, and location. That will help to place the most suitable and appropriate approach to mitigate emissions (Miola and Ciuffo, 2011). Basically, estimating emissions from ships accurately is based on a correct and detailed estimation and statistics of number of vessels, number of operating days, global maritime routes, the fuel consumption and the quality of the combustion process in the engines and boilers. The Third IMO GHG Study (2014) has estimated the average annual fuel consumption over the period 2007-2012 for the international shipping ranged between 201 million and 272 million tonnes per year depending on the used method to estimate fuel consumption whether it is top-down or bottom-up method, respectively. These two approaches have been broadly used in several studies concerning the evaluation of emissions from maritime shipping such as:

- Top-down approach: (Corbett and Fischbeck, 1997; Corbett *et al.*, 1999; Skjølsvik *et al.*, 2000; Cariou and Cheaitou, 2012).
- Bottom-up approach: (Wang and Corbett, 2007; Wang *et al.*, 2007; Jalkanen *et al.*, 2009; Olesen *et al.*, 2009; Schrooten *et al.*, 2009; Miola *et al.*, 2010; Paxian *et al.*, 2010; Tzannatos, 2010; Wang *et al.*, 2010; Anderson and Bows, 2011).

The top-down method used in IMO studies and other studies is based on estimating the fuel consumption and emissions from ships without considering individual ships' characteristics. Total emissions are calculated using the data and statistics derived from fuel delivery reports and figures about the fuel allocated to international and all other voyages. Different emissions factors are applied to different fuel types and engine types and sizes. Basically, the used data on marine bunker sales in IMO studies is available from International Energy Agency (IEA) for 2007-2011 and is divided into international, domestic and fishing sales. Moreover, further historical IEA statistics were used to review the data for any misallocation in the statistics.

The bottom-up method is based on summing the fuel consumed by individual ships engaged in the international voyages as part of the global fleet. Two main data sources have been combined and used in IMO studies to estimate the fuel consumption for individual ships. They are the global fleet technical data from HS Fairplay and the observations for Automatic Identification System (AIS) on-board ships. Miola and Ciuffo (2011) address the required technical information and operational data to carry out the estimation calculations as following: ship's

type and category, ship's dimensions, deadweight, gross tonnage, sea and weather conditions, journey routes, design speed and operating speeds, engine(s) power and age, engines' specific fuel consumption, fuel types, emissions factors, engine load and running hours.

It is worth mentioning that both methods show a level of uncertainty, and that can be seen by comparing $\boldsymbol{CO_2}$ emissions results from different resources and studies. The uncertainty in the bottom-up method arises because there is no accurate statistics about the number of the sailing days of each ship per year (as a result of incomplete coverage of ships' activities) and because of the discrepancy in the number of ships in service observed in the ISA data and logged as in service in the IHSF database. On the other hand, the most important sources of uncertainty in the top-down method are the contradiction data between global imports and exports of bunker oil and distillate, the potential inaccuracy in allocating fuels between the different shipping sectors such as international and domestic.

2.7.2 Emissions Factors EFs

Generally speaking, measuring greenhouse gases can be done by continuous monitoring and recording of the emissions at the source or alternatively by estimating the amount emitted using the amount of fuel used and applying relevant conversion factors such as emission factors and calorific values. Defining these conversion factors is based on the results from different methodological and thermodynamic approaches, technical information, and assumptions and key data collected from different sources (Hill *et al.*, 2016). To enable organisations and individuals to estimate shipping emissions in a detailed and accurate manners, a set of data should be available and designed to provide these emission factors for different fuel types, engine types, and operational and loading conditions. Exhaust gas from marine engines mainly contains nitrogen, oxygen, carbon dioxide and water vapour, with small amounts of carbon monoxide, oxides of sulphur and nitrogen, non-combusted hydrocarbons, and particular materials (Murphy *et al.*, 2013). A technical report by David Cooper (2002) reviewed the outcomes of several studies been carried out by engine manufacturers, research institutions and classification societies to calculate emission factors (g/kWh) for emissions released by diesel engines. His report reviewed studies since 1990 which can be divided into two categories: studies where emission measurements have been carried out on-board ships in operation, and studies that compiled data from other reports and used them for emissions inventories. The emission factors presented in the report are for main (ME) and auxiliary (AE) engines. They vary between the operating modes in the sea and during manoeuvring and are determined

according to the engine type and fuel type. However, the emission factors presented in Cooper's report are valid for engines built before 2000, and because of the modifications on engines and the improvements in monitoring emissions and collecting data from ship's journeys, these factors might not be applicable for modern engines. Therefore, IMO, climate change and environmental panels, and engine manufactures provide continuous updates and guidebooks as a source of emission factors which are considered as a reference adopted by research bodies and environment organisations for emission estimation at international levels. However, emissions estimation can be carried out at different levels of complexity. Three methods with increasing complexity are adopted in the 2006 IPCC (Intergovernmental Panel on Climate Change (2006)) Guidelines for National Greenhouse Gas Inventories (Trozzi, 2010). These methods are expressed in three tires as following:

- Tier One method: a simple method where default emission factors are used, and they represent average conditions. The emission factors information is not available on an industry / country basis. This method applies a basic and simple relation between activity data and emission factors.
- Tier Two method: A more advanced method where the default emission factors from Tier One are replaced by emission factors based on country basis, and they are developed using information on technical data, process conditions and characteristics, fuel types, etc.
- Tier Three method: it is regarded as the most detailed method. This approach is used when there is a need to determine the location of emissions from ships for example or to estimate the emissions from specific segments. It uses the latest and most sophisticated approaches and technologies in monitoring the emissions disaggregated by activities and sources.

Emissions factors used in the bottom-up emissions inventories (2007-2012) in the *Third IMO GHG Study* (2014) were developed for different GHGs and pollutants, and were used together with fuel consumption figures to estimate emissions. The Third IMO GHG Study considered several emissions such as Carbon dioxide (CO_2), Nitrogen oxides (NO_X), Sulphur oxides (SO_X), and Particulate matter (PM), etc.

Those combustion EFs vary by different variables which were been taken into account in the bottom-up method to estimate emissions. Basically, HFO fuel with 2.7% sulphur content is used as the baseline for the emissions factors. A correction methodology is used to calculate

the actual emissions factors by converting energy-based baseline emissions factors in $[kg\ pollutant\ /kWh\ ]$ to fuel-based emissions factors in $[kg\ pollutant\ /Kg\ fuel\ consumed]$, and then adjust the actual values for the specific fuel used by the engine and for different engine load conditions. The main variables are:

- Fuel type: HFO, MDO, MGO, LNG,
- The fuel sulphur content,
- Engine type: main, auxiliary, boilers,
- Engine rating: SSD (slow-speed diesel engine), MSD (medium-speed diesel engine), HSD (medium-speed diesel engine),
- Engine load and the combustion process completion,
- Type of service: Duty cycle in which they operate (direct-drive propulsion or auxiliary).

For example, the baseline emissions factors for CO_2 for main and auxiliary engines at slow, medium, and high speeds are as following (based on MEPC 63/23, annex 8):

It should be noted that the carbon content of any fuel type is constant when looking on the basis of kg CO_2 per tone fuel. It is not affected by engine type and size, duty cycle, the sulphur content or any other parameters mentioned before.

Table 2.5 presents the average emissions factors for three different fuel types (HFO, MDO, and LNG). These values are applied for pre-2000 engines (Tier 0) and assume 70% load factors. EFs are used in the *Third IMO GHG Study* (2014) to estimate the shipping emissions using the bottom-up method. All emissions factors are measured in mass of emissions per same unit of fuel; i.e. (g/g fuel). The main disadvantage of the top-down approach when using the emissions factors is that they are not machinery-type-specific. It means that it does not take into account the variation in engine types as the used fuel statistics are combined for fuel consumption in all engine types including main and auxiliary engines and boilers.

Table 2.5 Emissions factors for top-down emissions from combustion of fuels

Emissions substance	Marine HFO emissions factor (g/g fuel)	Marine MDO emissions factor (g/g fuel)	Marine LNG emissions factor (g/g fuel)
CO_2	3.11400	3.20600	2.75000
CH_4	0.00006	0.00006	0.05120
N_2O	0.00016	0.00015	0.00011

NO_x	0.09300	0.08725	0.00783
CO	0.00277	0.00277	0.00783
$NMVOC$	0.00308	0.00308	0.00301

It is worth mentioning that emissions factors are typically derived by using data from emissions testing results. However, the emissions factors used in both the Second IMO GHG Study 2009 and the Third IMO GHG Study 2014 do not correlate with each other for some values. Observations showed that the differences are basically because the emissions factors used in the Second IMO GHG Study do not differentiate for several engine types, engine tier (0, I, II) or duty cycle (propulsion, auxiliary) while the Third GHG IMO Study includes all of these differentiations and it takes into account engine load in adjusting emissions factors. Even though the initial emissions calculations in my study were completed using emissions factors from the Second IMO GHG Study but corrections were made using the most updated values from the Third IMO GHG Study 2014 as they are significantly more detailed as well.

2.7.3 Fuel Consumption and Engine Loads

In the recent years, and because of the rising fuel prices and the pressure on shipping companies to reduce the environmental footprint of air pollution, fuel efficiency of ships has become a major topic for engines manufactures, shipping companies, national and international organisations, and even private bodies that concern about the danger of air pollutants. Therefore, there is an increasing interest in designing a greener and energy-efficient fleet. This level of growing interest in reducing fuel consumption is linearly related to the fuel price (Wijnolst and Wergeland, 2009). For example, fuel oil price increased significantly between 1970 and 1980 up to 10 times the prices in the previous years, forcing ships with high fuel consumption to be laid up. As fuel oil prices fell between 1985 and 2000, energy efficiency of ships and development research had received just a little attention by the maritime industry. However, fuel oil prices started to increase again after 2000 and, hence, the fuel cost has become a matter of concern for ships operators even though there was a short period after 2008 recession when oil price decreased (Bialystocki and Konovessis, 2016). Therefore, a significant amount of work on both the technical and operational sectors has been done to reduce fuel consumption by designing high efficient engines, introducing technical innovation and developments to the propulsion system, optimising hulls, and optimising the operational profiles, etc. In general, ship owners look for vessels that operate efficiently and consume less bunker per carrying

capacity, resulting in reducing the environmental foot print of ships and especially greenhouse gases GHG.

Several studies have estimated the total emissions on the base of the actual power consumption per mile for the different stages of the entire journey. A comprehensive and robust study should consider the fuel consumption of different ship types and sizes, engine types, propulsion arrangements, and different maritime routes. An example of such robust and comprehensive studies is a project called (ACCESS) funded by the European Commission within the Seventh Framework Programme (2007-2013). The project was carried out to estimate the shipping emissions in the Arctic and to investigate the influence of the shipping activities on the Arctic climate change in past, present, and in future. A software called ICEROUTE has been developed, based on an existing program ETA (Estimated Time of Arrival), at HSVA (The Hamburg ship Model Basin) to assess the potential impacts of international shipping on Arctic climate by calculating the fuel consumption as a function of actual power consumption, ship's speed, ship's type, ice condition, ice routes, etc. Moreover, the input data for the software includes environmental data like sea state, wind speed and current speed as well as ice parameters like thickness and concentration strength, and also required power and thrust data and all available ship characteristics and voyage details. The calculations included in this report cover data from the past (1960-2000), the present (2000-2010) and future scenarios for different ship types and mainly bulk carrier, oil carrier, and LNG carrier (ACCESS: Arctic Climate Change - Economy and Society, 2014). Figure 2.6 shows a flowchart of the calculation steps for ICEROUTE and ETA programs where the travelling time is determined based on ship speed for each leg of the journey, and the fuel consumption is calculated using the information of the specific engine data. The final outcome of the programs are the exhaust emissions from the consumed fuel during the journey.

Moreover, ICEROUTE software takes into account the increase in fuel consumption as a result of longer journey because of delays due to hard sailing in ice, and also as a result of the increase in resistance resulting from navigating in ice areas which leads to more fuel consumption. Generally speaking, the total fuel consumption rate depends on secondary factors in addition to the primary ones like vessel type and size, engine age and efficiency, technological innovations, etc. These secondary factors include wind and current directions, ice conditions, hull fouling, operating trim, etc. The primary and secondary factors are utilized to investigate the fuel consumption profile of the vessel using an appropriate method such as:

- Numerical methods to calculate and predict fuel consumption and demand.
- Actual field measurements of vessel's fuel consumption rates.
- Using fuel expenses per trip or per year to assess the ship fuel efficiency.

It is common to use the brake specific fuel consumption (BSFC) as an indicator for ship's fuel efficiency, and it is used to compare the efficiency of reciprocating engines. It is measured in grams per joule $[g/J]$ or grams per kilowatts-hour $[g/kWh]$, and it is simply calculated by dividing the fuel consumption rate (r) by the power produced at the shaft of the engine (P) as in Eq (2.28). The actual fuel consumption is then calculated at the actual power of the vessel at any load, and the actual mass of consumed fuels depends on the engine efficiency, and fuel used in the engine, and also it varies by the fuel's heating value.

$$BSFC = r/P \tag{2.28}$$

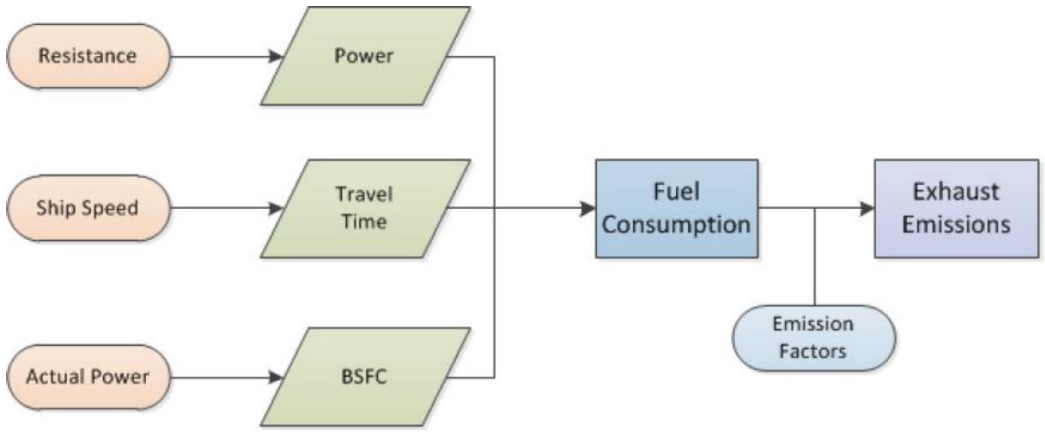

Figure 2.6 Calculations of fuel consumption and exhaust emissions

Generally speaking there are three primary sources of GHGs emissions and other relevant substances on-board ships:

- Main engine(s): Emissions from the main propulsion engine(s) are a function of the engine build year, engine rated power output, and load factor (% MCR) (*Third IMO GHG Study*, 2014).
- Auxiliary engines: As for the main engine, emissions from auxiliary engines vary as a function of its manufacturing specifications (the engine build year, engine maximum power) and operational modes which influence the required output from each individual auxiliary engine during the journey.

- Boilers: Emissions from boilers vary as a function of the vessel class (type and size) and her operation mode. Boilers, for most vessels, are typically small and mainly used to provide the main engines with hot water to keep them warm during off-work hours when a ship is at anchor or at berth and to supply hot water to the crew. During open-ocean operations, these small boilers do not operate as the waste heat recovery systems provides hot water by using the waste heat from the main engine. However, for specific ship types like tankers for example, large boilers are used as a part of the steaming and heating system that supplies steam to the cargo pumps and cargo tanks.

Optimizing a marine diesel engines requires balancing fuel economy and engine emissions. Typically, diesel engines are designed and optimized to work within a specific optimized load range where working outside the optimum load range will cause higher emissions or higher specific fuel oil consumption per power unit ($g\ fuel/kWh$) or both simultaneously. However, it is possible to adjust the engine and the combustion process by controlling the valve timing and fuel injection by changing the electronic engine control unit programming. For instance, this can be achieved with modern engines using MDO and fitted with smart control units but more adjusting and tuning effort is required by the engine manufacturer for older engines with mechanical controlling system (camshaft). Operating at slower speeds requires reducing engine load, and hence some modification work is needed to adjust the optimum default working load range to a lower range (engine derating) where diesel engines become more efficient in the low load range. Moreover, depending on the intended operational profile and load range (high, part, and low) of the ship main engine, there are different methods available for SFOC optimisation. The main engine tuning methods are (MAN Diesel & Turbo, 2010):

- Installing an Exhaust Gas Bypass (EGB),
- Variable Turbine Area or Turbine Geometry,
- Engine Control Tuning (only for ME/ME-C).

Figure 2.7 shows the changes in the specific fuel oil consumption of a large two-stroke engine (MAN 6S80ME-C8.2) during three different load factor operations as the solid black line represents the standard tuning, the solid blue line shows a part load optimization operation, and the broken blue line shows a low load operation where the engine is more efficient at low loads in terms of fuel consumed per unit time to produce one unit kW. Table 2.6 illustrates the specific fuel oil consumption SFOC data (or so-called Brake specific fuel consumption BSFC) for marine diesel engines used in the calculations in the Third IMO GHG Study 2014. While

Table 2.7 shows the baseline values of specific fuel oil consumption for gas turbines, boilers and auxiliary engines. Basically, marine main engines are SSD and MSD while auxiliary engines are MSD and HSD.

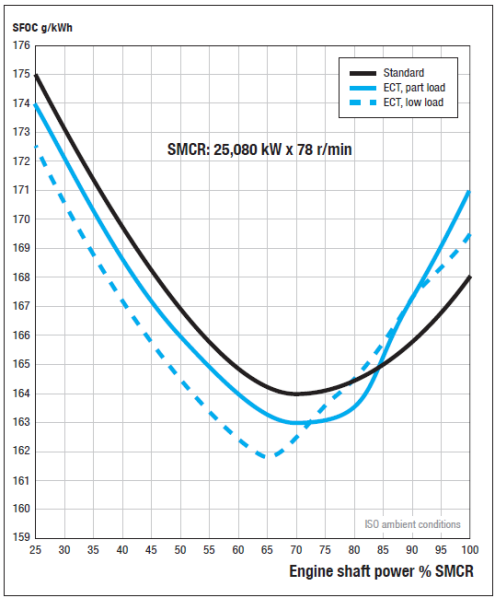

Figure 2.7 Impact of engine control tuning on SFOC – source: (MAN Diesel & Turbo, 2010)

Clearly, the engine load affects fuel consumption and the emissions. Therefore, to increase the engine's performance and minimize fuel consumption, it is very critical to operate diesel engines within the optimum load range which is for most diesel engines between 70% and 85% or alternatively at the new optimized range that can be achieved by using one or more of the engine tuning methods. Studies assume a non-linear dependency function to calculate the changes of SFOC as a function of engine load over the whole engine load (0-100%). Jalkanen *et al.* (2012) has used a parabolic function of engine load in the Ship Traffic Emissions Assessment Model (STEAM2) to evaluate the exhaust emissions of marine traffic. Using regression analysis, a second degree polynomial equation for the specific fuel oil consumption as a function of the load factor was derived from a comprehensive SFOC measurements data from a medium sized four-stoke Wärtsilä engine as shown in Eq (2.29). This formula was applied to all diesel engines for simplicity to estimate SFOC at different load factors. The SFOC base value is constant for each individual engine. It is influenced by engine stoke type, engine power, and building year as modern engines are more efficient as a result of the new technical developments.

$$SFOC_{(load)} = SFOC_{(base)} \times (0.455 \times load^2 - 0.71 \times load + 1.28)\ [g/kWh] \quad (2.29)$$

Table 2.6 Specific fuel oil consumption of marine diesel engines (g/kWh)

Speed	Slow-speed diesel (SSD)	Medium-speed diesel (MSD)	High-speed diesel (HSD)
Before 1983	205	215	225
1984-2000	185	195	205
Post 2001	175	185	195

Table 2.7 Specific fuel oil consumption of gas turbines, boilers and auxiliary engines (g/kWh)

Engine type	HFO	MDO/MGO	HSD
Gas Turbine	305	300	225
Steam boiler	305	300	205
Axuiliary engine	225	225	195

A statistical analysis carried out by Bialystocki and Konovessis (2016) on 418 noon reports of a Pure Car and Truck carrier case ship in order to determine the influence of some major factors on ship's fuel consumption such as draft, displacement, weather force and direction, and also hull and propeller roughness. An algorithm to predict the fuel consumption and speed curve is developed to assist ship owners and operators in managing upcoming trips' profiles aiming to save fuel and control environmental footprint of air pollution. Considering a ship operating 280 days/year, and assuming a 50 ton/day fuel consumption, the study estimates that a 5% error in fuel estimation could easily accumulate to 280,000 USD/year in fuel cost of 400 USD/ton. Therefore, fuel consumption calculations should be accurate because any small deviation in the fuel consumption calculations is reflected significantly in the operational cost and decision making. The fuel consumption estimating algorithm applies three corrections for the collected data before generating the initial speed-fuel consumption cure. The corrections take into account the ground speed for the complete steaming time and whole journey, the fuel consumption at the departure and arrival drafts which is interpolated using the fuel consumption at the design draft and corrected using the Admiralty coefficient, and finally the corrections take into account the change in speed due to currents which affect the ground speed depending on its directions.

2.7.4 Emission Estimation Procedures

In the absence of extensive empirical and robust data regarding shipping emissions, a number of models have been developed to estimate emissions. Studies that calculate the emissions

emitted by all vessels over all trips during a year use a set data collected for a representative sample of ships for specific maritime routes and trips and over different periods over the year. Then the total emission inventory is calculated by scaling up the results from the vessels sample to give the total for all ships operating in a specific area or sailing on a specific route or for a specific type and size of ships. For the purpose of accurate estimate of the emissions, the fuel consumption for each phase of a ship's trip should be known. That includes the cruising, manoeuvring, and hoteling phases. Furthermore, in practise it is common to divide vessel operating modes into five modes according to the operating speed and engine load. They are defined in Table 2.8 as used in the Third IMO GHG Study.

Table 2.8 Vessel operating modes

Speed	Mode
Less than 1 knot	At berth
1÷3 knots	Anchored
Greater than 3 knots and less than 20% MCR	Manoeuvering
Between 20% MCR and 65% MCR	Slow steaming
Above 65% MCR	Normal crusing

Studies that estimate greenhouse gas emissions from commercial vessels use a simple methodology by summing the emissions on a trip by trip basis. This methodology is quoted as "Tier Three" in the EMEP/EEA air pollutant emission inventory guidebook, and is applied in Trozzi (2010) study. It is expressed as in Eq (2.30) for a single trip:

$$E_{Trip} = E_{Hotelling} + E_{Manouvering} + E_{Crusing} \tag{2.30}$$

Then the emissions of pollutant (i) can be calculated for a complete trip as following if fuel consumptions is known for each phase:

$$E_{Trip,i,j,m} = \sum_{p} \left(FC_{j,m,p} \times EF_{i,j,m,p} \right) \tag{2.31}$$

where:

E_{Trip}: Emission over a complete trip (tonnes),

FC: Fuel consumption (tonnes),

EF: Emission factor (kg/tonnes),

i: Pollutant,

j: Engine type (slow-, medium-, and high-speed diesel, gas turbine and steam turbine),

m: Fuel type (bunker fuel oil, marine diesel oil / marine gas oil (MDO/MGO), gasoline),

p: Trip phase (cruise, hotelling, manoeuvring).

If fuel consumption information is not available, then Eq (2.32) is used to calculate the emissions per trip based a detailed knowledge of the installed power for main and auxiliary engines, load factors, and also time spent for each phase of the trip.

$$E_{Trip,i,j,m} = \sum_{p} \left[T_p \times \sum_{e} \left(P_e \times LF_e \times EF_{e,i,j,m,p} \right) \right] \quad (2.32)$$

where:

E_{Trip}: Emission over a complete trip (tonnes),

EF: Emission factor (kg/kW),

LF: Engine load factor (%),

P: Engine nominal power (kW),

T: Time (hours),

e: Engine category (main, auxiliary),

i: Pollutant (NO_X, NMVOC, PM),

m: Fuel type (bunker fuel oil, marine diesel oil / marine gas oil (MDO/MGO), gasoline),

p: Trip phase (cruise, hoteling, manoeuvring).

Psaraftis and Kontovas (2008) has developed a web-based tool to calculate three types of ships' emissions (CO_2, SO_2 and NO_X) for a wide range of ships types and sizes operating at different routes and scenarios. The emissions calculation tool is based on analysing world fleet data collected from Hellenic Chamber of Shipping (HCS) database and from individual shipping companies for different ship types, routes and bunkers. The output of the web tool algorithm is the emissions per tonne-km. That helps in carrying out a "cause and effect" examination for an individual ship to search for an optimum and robust design and operation profile. It also helps in evaluating the environmental efficiency of ships and their impact on the environment, and

determining measures to mitigate emissions at sea and port depending on the scenario. The main input for the emissions model built within the web tool is the fuel consumption rather that the engine horsepower as the bunker consumption data was the main parameter provided by ships' operators and companies. However, when the fuel consumption information is not available, it can be computed indirectly as proportional to the consumed total power (kWh).

The model algorithm of the web tool was developed by the National Technical University of Athens (Laboratory for Maritime Transport), and it calculates CO_2 emissions per tonne-km as in Eq (2.33):

$$CO_2 = 3.17 \times [(GT + gt)/L + F/V + f/v]/W \quad (2.33)$$

For uniformity and comparability purposes, the model assumes a ship operates between ports A and B carrying a cargo payload of W (tonnes) for a distance L (km) at speed V (km/day) from A to B and at speed v (km/day) from B to A. All ships are assumed to be 100% loaded at the laden leg and they are on ballast at the return leg of the journey. The time spent for loading the cargo at port A and discharging at port B is (T, t (days)) respectively. Fuel consumption is assumed to be known as following in (tonnes per day): G at loading port, F for the laden leg, g at discharging port, and f for the ballast journey. When speed is different from the design speed, the cube law is applied and the fuel consumption is proportional to the cube of the speed. One shortage in (Psaraftis and Kontovas, 2008) study is that it excludes triangular or multi calls journeys, and hence no such routes have been examined as the calculations become more involved but, anyway, the philosophy remains similar to some extension. Running the model for the Lloyds-Fairplay fleet database after breaking down by ship type and size showed, as expected, that faster ships emit more than slower per tonne-km and in absolute levels as in the case of container ships. Similarly, emissions per tonne-km is higher for smaller ships than larger ships as can be seen in Figure 2.8 for crude oil tankers - 2007 fleet.

It is worth mentioning that when evaluating the calculations for different approaches applied to estimate maritime emissions, it is common to find that there is considerable difference in the results and, hence, in the sensitivity of the parameters considered in individual approaches. A technical paper by Dolphin and Melcer (2008) estimated the theoretical stack emissions of four pollutants ($CO_2, NO_x, SO_2, Hydrocarbon$) from a tanker ship with a15,000 kW slow-speed diesel engine and two 3,000 kW high speed auxiliary engines. Two estimating models used by the maritime industry are compared. The first model is presented by the US Environmental

Protection Agency (EPA), and the second one is developed by the European Commission (Entec). Both models use data from Lloyds Register Engineering Service to generate the required emission factors.

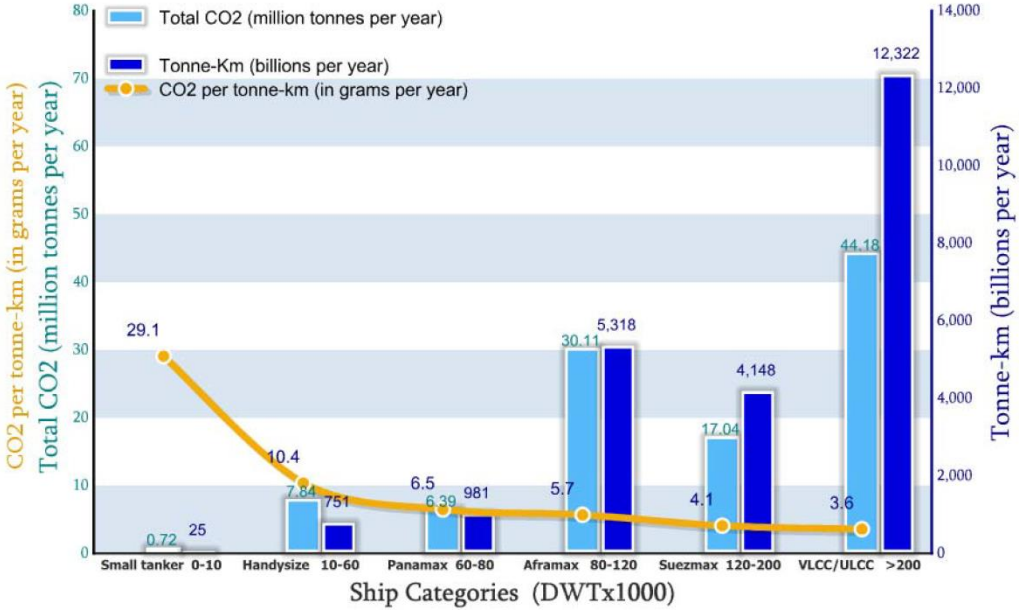

Figure 2.8 CO_2 Emissions statistics for bulk carriers

The Entec approach to calculate emissions depends primarily on the type of the fuel and the engine as it has been concluded that emissions are dictated by engine more than by ship type and class. This model is built using empirical data more than statistical data. The emissions factors $(g/kW\ hr)$ are derived for the main engine(s) and the auxiliary engines and broken into two main groups: At sea and in port/ manoeuvring. Emissions are calculated as following:

$$Emissions\ (kg/hr) = \frac{Engine\ Power\ (kW) \times Emission\ Factor\ (g/kW\ hr)}{1000} \qquad (2.34)$$

Comparing the two models' results shows that the NO_x values in the EPA method and the Entec method are equivalent while CO_2 and SO_2 values appear to be higher consistently in the EPA model. Finally, Hydrocarbon values from the Entec model are at least six times higher comparing with EPA model's values. The two methods' results show that each model will yield different amounts of pollution proportional to the ship activity. However, for uniformity and comparability purposes within this study, a simple and consistent model based on IMO study and EEDI calculations will be utilized to calculate fuel consumption and hence greenhouse gas emissions from the new designs generated by AVEVA for different routes and operating speed.

2.8 Review of Maritime Economics

In today's marine world there is an increasing effort and focus on balancing the economic and environmental performance of maritime shipping. There are various trade-offs at stake in the goal for making ships greener and more environmentally friendly and for reducing the building and operating cost and increasing the profitability for all stakeholders especially owners and operators.

First of all, reducing the lifetime ownership costs requires a significant effort towards each stage of the vessel's life starting with design, build, through-life maintenance and ending with scrapping. Secondly, increasing the day-to-day profit requires reducing energy consumption and operating the vessel efficiently on a daily basis and within a long-term strategy to increase the productivity (in terms of tonne.mile) for a given market condition, and hence to increase the revenue. The most common practice by naval architects when it comes to reducing the energy consumption is to focus only on reducing the hull resistance to reduce the required power, and hence to cut the fuel bill. However, such practice might actually lead to increase the initial production cost and the through-life maintenance cost which might lead to a loss or a small profit. Finally, running a greener ship with low emissions during the lifetime at an effective-cost manner involves designing an efficient hull with efficient machinery, installing emissions mitigating technology, optimising operational profile of the ship, and adopting measures related to the logistical chain for the whole fleet and the maritime policies. These competing aspects of production and maintenance costs and operating costs on the other hand need to be addressed carefully during the early design stages. Multi-objective optimization techniques can effectively assist designers and decision makers to search the trade spaces for robust solutions that are beyond simple design convergence and to eliminate any significant sub-optimal designs (Dylan W. Temple and Matthew Collette, 2012).

The focus in the maritime world is on developing robust designs where there are possibilities to meet all the criteria and requirements with benefits to all stakeholders, and ensuring that it is achievable at a cost-effective manner. According to the Second IMO GHG Study (2009), CO_2 emissions in 2050 are estimated to increase by 150-250 % if no action is taken with assuming that the world trade will be triple (business as usual scenario). Other studies such as (Eyring *et al.*, 2010) and (OECD, 2010) reported same growth prospects, and they concluded that substantial annual greenhouse gas reductions should be taken across all shipping sectors. Chang (2012) concluded that there is a close relation between the international economic growth GDP,

marine energy consumption, and GHG emissions from international shipping fleet. The empirical results of co-integration and Granger causality tests showed that economic growth and increased marine energy consumption are the main cause for the rapidly increase in greenhouse gas emissions in the short-term and the long-term as well. In the short term, the relation between shipping GHG emissions and economic growth is very close. Therefore, implementing emissions mitigating policies and measures in the shipping sector might affect this growth negatively. However, over the long term, this relation does not cause a significant trouble to the economic growth. On the other hand, these policies to reduce emissions need to give more attention to the technical and operational measures which are related to the energy efficiency saving and optimizing hull design as well as the main engines operation.

The above facts put pressure on stakeholders in the maritime sector to cut the shipping carbon footprint during all stages from building down to scrapping through operating and maintenance. In addition to the pressure from IMO and other organisations and national authorities regarding emissions, the shipping market has been facing some difficult times due to unexpected and sudden changes in the market, crisis, and depressions as a result of over-supply in the fleet during boom periods (Stopford, 2009). Therefore, all efforts and research are addressed towards determining the best practice and optimum measures to make the marine sector a profitable business despite the regular uncertainty and instability in the market.

One more challenge for ships operators is the additional cost that might be applied for some routes and ship sectors regarding emissions like CO_2 tax or allowance which may increase the transport cost per unit shipped. In such cases, charterers might prefer bigger ships to increase the total quantity of goods unites to reduce the net transportation cost per unit. Moreover, a bigger vessel is cheaper to build and also to buy in terms of cost per capacity unit (tonne or TEU). For instance, a 300,000 DWT VLCC is estimated to cost mUS$ 100 in 2009 carries 3 times the cargo an 110,000 DWT Aframax which is estimated to cost mUS$ 52 (Faber *et al.*, 2009).

However, this economy of scale advantage (bigger is cheaper) that arises with increasing the ship size might not be a possible option as it depends on some different parameters and constraints that control the size of the ship. Basically the main factors are: trade route geographical limitations, port and berth restrictions, port infrastructure limitations, building cost, operating cost, cargo availability, and market conditions.

It is essential to consider the current and forecast market conditions when it comes to deciding the ship size because, based of historical trends and experience, the economy of scale has not always had a positive impact on the ship efficiency in the market. One example is the Ultra Large Crude Carriers ULCC which are the largest tankers range from 320,000 DWT to 546,650 DWT. This class of ships was built to carry crude oil to US and Europe from the Middle East Gulf, and the ULCC fleet peaked in 1982 and 1983 (116 ships) as the oil trading boomed during that time. However, just two ships are left in service in the commercial tanker market. The main reason behind the failure in the ULCC sector is the changes in the oil trading market. The oil prices were very volatile and there were more traders in the market who would not be willing to take the risk by shipping 3-5 million barrels of oil as the value of the cargo might change significantly. Therefore, there was a preference for smaller carriers as in today's market as traders tend to favour Suezmaxes instead of VLCCS to limit the risk and the profit losses in case the oil prices drop (Faber *et al.*, 2009). Based on the above facts, selecting the optimum ship size is more complicated than it looks based on the economy of scale advantages as the shipping market conditions play a significant role.

A study by Psaraftis and Kontovas (2010) focused on a central key point in the maritime trade and logistics which is the importance of trade-offs that should be made when making a decision among several environmental, economic, and logistic issues when it comes to adopt any combination of measures to reduce the CO_2 footprint of a ship and the whole fleet simultaneously. They evaluate the trade-offs between reducing ship emissions and cutting the operational costs and the associated logistics. Moreover, they discuss the different available measures to cut emissions including technical, operational and market-based measures, and the conflict that might occur between the adopted measures which may lead to negative consequences on the ship economy. For instance, sailing at a lower speed is an effective way to reduce the fuel bill but, from the supply chain point of view, any speed reduction might require more ships and causes side effects on the operational profiles of some types of ships such as container ships. Therefore, depending on the assumed scenario, there might be an increase in the total costs as in-transit inventory might increase significantly as well as other operational costs.

However, slow steaming might be used as an input in fleet optimisation model as an efficient way to absorb the oversupply in the market and reduce the fuel costs as in the case around 2007-2008 when the market started to experience high supply of shipping tonnage, high fuel oil

prices, and low freight rates. When it is necessary to maintain constant throughput within a particular period of time from the original port to the discharging destination, then more slow steaming ships will be deployed on the rout. That will serve to deliver the same amount of cargo and keep the felt productivity constant $[ton.miles/year]$ unlike what other studies propose the need to order and build extra ships assuming that there will be a gap between supply and demand. The existing oversupply creates a need to reduce speed to ease the problem and to avoid forcing more ships to lay-up during economic recession periods which result in a significant fall in the volume of cargo transported internationally. This practice, as estimated by (Faber *et al.*, 2010), would reduce emissions from bulkers, tankers and container vessels by about 30%, relative to the situation in 2007, in the coming years by using the current oversupply tonnage in circulation to reduce sailing speed.

In the next sections, the main and important aspects of the economics of ships are covered. The focus is on the key criteria that affect decisions making when it comes to design and build a new ship, and also on all the considerations that ship charterers and operators should take into account to maximize their profits during a ship's lifetime while considering the market conditions. In other words, that includes the potentials to maximize the economic performance of a ship within the life span taking into account all the fluctuations in the shipping market such as newbuilding prices, fuel prices, fright rates, the interaction between supply and demand, and interest rates etc.

The basic factors that are likely to influence the economic performance of a ship and related to the design and operational profile are outlined. The cost and revenue structure of a ship is discussed and summarised. Then, different methods in the literature for optimising the economic performance are presented showing the impact of several technical and operational measures on the characteristics of the economic performance. Different methods to estimate the construction cost and newbuilding prices are presented focusing on the different factors that affect the newbuilding market and purchasing and selling decisions. Moreover, a set of economic criteria that are often used to assess a business or investment are discussed. Some of these criteria and more are used later in evaluating the economic performance of all ships and in order to determine the sensitivity of a ship performance and profitability to changes in the market conditions.

2.9 The Cost and Revenue Structure of Shipping Industry

All shipping companies face a challenging environment of booms, recessions and depressions where shipowners and operators aim to increase the revenue received from chartering and operating the ship as well as to reduce the cost of running the ship in the best possible way to secure a reasonable profit. The three key variables that shape a vessel finance are (Stopford, 2009):

- The method of financing the business,
- The cost for running the ship,
- The cash and revenue received from operating and/or chartering the ship.

Although the economic structure of the shipping industry is a complex and fluctuating system, costs can be divided into operating costs (OPEX), periodic maintenance cost, voyage costs, cargo-handling costs, and capital cost of the ship and repayments. Elements of these costs and their average share of the total cost can be found in (Branch, 1988a; Stopford, 2009; Anaxagorou *et al.*, 2015). Stopford (2009) covers all the above items of the cost structure in his book (Maritime Economics) where he extensively addresses all the aspects and features of the cost equation.

In practice, running a successful shipping operation is not just a matter of optimizing and minimizing costs, it also involves generating as much revenue as possible out of a vessel during the life span through the succession of booms, recessions and depressions that characterize the shipping market. Wise decisions and future plans are vital during prosperous periods as it is the perfect time to take advantage of such opportunities to increase the revenue earned and boost the profit. However, the challenge for shipping companies is to keep control of the business during recession periods when the completion in the market is high. The surplus capacity is forced out of the system, and winners are those who manage to stay in business and keep the fleet running and generate enough revenue to cover all costs and to survive till next boom.

The revenue for shipping companies might be steady and secure as in a long-time charter or irregular revenue on the spot market and day-by-day business (Stopford, 2009). However, a ship revenue depends on cargo capacity, operating speed, port time, off-hire time, and freight rates. Calculating a ship’s freight revenue starts with determining how much cargo a ship can transport and how many trips can be completed within a particular period at a specific speed. Then a price or freight rate should be established by the shipowner or charterer per cargo

transported in terms of tons or ton-miles etc. In more technical terms, a ship revenue per dwt can be addressed as the product of its productivity and the freight rate per ton mile and divided by the deadweight as in Eq (2.35):

$$R_{tm} = \frac{P_{tm} \cdot FR_{tm}}{DWT_{tm}} \tag{2.35}$$

where:

R: the revenue per dwt per annum,

P: the ship productivity measured in ton miles per annum,

FR: the freight rate per ton mile of cargo transported for a specific route,

DWT: the ship deadweight,

t: the time period,

m: ship type.

A ship's productivity is expressed in tonne.mile of cargo shipped per annum, and it is used to assess a ship's efficiency for the purpose of comparison with other ships' operating performance in terms of cargo capacity, speed, and flexibility. It is determined as in Eq (2.36) by the distance travelled in a day, the number of loaded days in a year, and the level of travelling with full deadweight:

$$P_{tm} = 24 \cdot S_{tm} \cdot LD_{tm} \cdot DWU_{tm} \tag{2.36}$$

where:

S: the average operating speed per hour,

LD: the number of loaded days at sea per annum,

DWU: the average deadweight utilization.

The challenge for shipowners and operators is to turn their fleet into a profitable business and to create sufficient financial strength and strong cashflow during boom periods which helps them to survive during depression times while waiting till next shipping boom. Profit is a measure for the financial returns gained from a business. It is calculated as the difference between the total revenue generated by operating the ship during a particular accounting period and the total costs incurred during the period of generating that revenue. It is essential for shipowners and investors to estimate at early stages how much profit their business will be making taking into account the market forecast and how much depreciation is deducted from

the cashflow cycle annually. In the next section, a review of different studies and methods to optimise ships economic performance at different scenarios is presented.

2.10 Optimizing Ship Economic Performance

Building and running a ship are driven predominantly by the economic rate of return on the owner's investment and the charterer's expenses over a specified period of time (Molland *et al.*, 2009). However, predicting streams of income and costs in order to optimize a ship finance over her lifetime is accompanied with different kinds of uncertainties and varying variables (Psaraftis *et al.*, 2012). Both the income and expenditures depend mainly on the way the ship is utilized over the entire lifetime. As mentioned earlier, a ship's productivity, freight revenue and profit are functions of different factors some related to the ship such as size, deadweight utilization, speed, and voyage routing while others are the market conditions.

Different methods have been proposed to optimise the economic performance of a ship as well as the environmental impact. For a variety of reasons, speed reduction has recently become very popular as a measure to reduce costs, and it is commonly adopted by ships' operators to face the increase in fuel prices and low freight rates in depressed markets as happened after mid-2008 (Psaraftis *et al.*, 2012).

Some studies have suggested that newbuilding ships' owners should consider installing less powerful engines and operating at slower speeds as has been recommended by a spokesman from Germanischer Lloyd GL (Justin Stares - Lloyd's list, 2008a). However, experts and several energy efficiency reports have a different opinion regarding low-powered ships and the disadvantages of such decision as in (Janet Porter - Lloyd's list, 2009). The risk behind reducing the installing power is that the ship will lose the flexibility to operate over a wide range of speeds as the shipping market is fluctuating constantly during the lifetime of a ship. In the scope of optimising a ship's operational and economic performance, same criticism regarding lowering the installed power inspired by the EEDI formula was addressed by Devanney and Beach (2010) who believe lowering the installed power does not in practice result in greenhouse gas mitigation especially when ships operate far from the optimum engine design load.

The introduction of speed reduction measure in the shipping market has the potential to offer balancing the supply-demand chain during recession periods with high level of cargo space availability alongside reducing GHG emissions from international shipping. Such trends in the

shipping market would result in absorbing the fleet capacity which has advantages and disadvantages depending on the demand and supply status of any segment or maritime route. Reducing the fleet supply and shrinking the fleet overall capacity result in increasing the fright rates and hence leads to a higher revenue which may overcome the extra operating costs due to more expensive fuel. Such scenarios happened in the early 1970s where slow steaming and other drastic measures were adopted by many tanker ships' owners because of the overcapacity in the tankers tonnage as a result of over newbuilding orders. In the last few years, fleet overcapacity has been observed in the containerships segment where fleet growth and tonnage supply exceeded the market demand and resulted in low freight rates. As a result, ship owners had to reduce the operating speed to shrink the gap between and supply and demand and hence to balance the market (Psaraftis *et al.*, 2012).

Optimising an individual ship's or fleet's operational profile and economic performance is a complex process involves a wide spectrum of decision variables. Since it is hard to predict the future trends in the tonnage demand, it is not easy to guess the consequence of the wide adopt of slow steaming as it has several consequences related to shortage of the total fleet annual capacity, slowing down sea transport, and right-on-time arriving principle which affects the logistics chain. As shipping speed and arriving time are important issues for shippers, producers, and consumers, a ship might be left laid-up in a competitive market full with more efficient ships with high technologies and offer faster service at a lower cost. Moreover, in a competitive transportation market there might be more cost-effective alternatives for maritime shipping. In such cases, customers may consider shifting to other transport means to carry their goods and products such as rail, road, air, or pipeline transport (IMO MEPC 57/4/5, 2007).

Devanney (2010) investigated the impact of fuel prices on the spot rates for VLCC and the relation between fuel prices and the optimal speed. He explained the motivations behind optimum steaming speed as a function of spot rate and bunker fuel oil price. The owner should lay-up the ship if rates are low where operating the ship would be a loss. As rates improve, the owner would be in a position where he operates at a very reduced speed. Once rates further improve, the owner would speed up as the additional revenue balances the additional fuel cost. However, Devanney (2010) stated that the amount of the speed increase responding to the sport rates is critically dependent on bunker fuel prices as ship operators attempt to maximise the revenue and minimise costs. These fluctuations in sport rates, bunker prices, and service speeds would shape and control the market in terms of ton-mile supply.

Psaraftis and Kontovas (2013) take one step further in analysing Devanney (2010) speed optimisation problem by re-formatting the objective function. For a given ship and route, the optimal speed is determined by the ratio of the bunker price and the spot rate ($\rho = p/s$). To figure out the degree of change in speed as a function of variations of the ratio (ρ) (meaning bunker price and spot rate) and the fuel consumption curve exponent (n), the ratio of two optimal speeds (v_{01}/v_{02}) is calculated for several values of the ratio (ρ_1/ρ_2) and (n). According to this model, ships with high exponent (n) such as containerships would have a tendency to reduce the service speed proportionally less than tanker ships and bulkers for the same variations in ratio (ρ).

Anderson and Bows (2011) apply an energy consumption equation along with a profit-maximizing equation to evaluate whether speed reduction can be a potentially cost-effective measure for CO_2 mitigation. They investigate the impact of speed reduction on the total cost, and also define the relation between changes in fuel price and the optimal operating speed by linking fundamental and simplified equations related to speed, energy usage, and cost. Moreover, they explore the impacts of some policies such as a fuel tax and a speed reduction mandate on CO_2 emissions. It was found that a fuel tax of about \$150/ton will force ships to reduce speed by around 20-30%. Moreover, applying a speed reduction mandate (maximum speed limit) in the container fleet for instance to achieve 20% CO_2 reduction will cost between \$30 and \$200 per ton CO_2 reduced.

Another interesting economic and emissions models are built by (Klanac *et al.*, 2010) to analyse the economic effects of speed reduction as well as the environmental impact for an AFRAMAX tanker ship taking into account the extra ships needed to transport the same amount of cargo. In the economic model, the optimum speed is seen from the ship owner and the time charterer's point of view as the benefit from speed optimisation is shared equally between the ship owner and charterer. The study claims that according to some records from AIS data [www.marinetraffic.com] and marine news of AFRAMAX tankers, those tankers are not sailing at the optimum and most profitable speed but at a higher speed than the optimum speed calculated by their economic model. They predict that for a daily charter rate of \$21,500, the service speed should be 11.8 knots rather than the recorded average speed of 12.6 knots. However, the reasons behind this difference could be the assumptions made by (Klanac *et al.*, 2010) to simplify economic model and to reduce the overall optimisation work. Mainly,

additional investments for new slow-steaming ships to transport the same amount of cargo per year is neglected as well as the influence of duration of the journey.

Most of speed optimisation studies assume that ships are sailing at the same speed in the laden and ballast legs, and same fuel consumption functions are used which may lead to having unreliable results and conclusion. Psaraftis and Kontovas (2009) consider emissions and profit in a logistical context and investigates a simple voyage scenario for a fleet of N identical ships sailing at a known speed V_1 for the laden leg and returning at a speed V_2. Results show that speed reduction for both legs remains profitable if the fuel price and inventory value of the cargo are no more than specific thresholds. Also, the results show that by slowing down, total emissions would always be reduced even though more ships are added to the fleet. An interesting scenario that was investigated is the mandatory speed reduction in Sulphur Emissions Controlled Areas (SECAs) in order to cut SOX emissions. Such behaviour would force ship operators to increase their speeds outside the SECAs if they are keen to keep the total transit time the same. Hence, the total fuel consumption will increase as well as the total cost and emissions.

Another study by Gkonis and Psaraftis (2012) focuses on determining optimal operational speeds for different tanker carriers types on both route legs. The optimisation tool runs the model for different scenarios and combinations of the speeds on both legs. For a single VLCC tanker ship, Figure 2.9 shows how optimal speeds for the loaded and ballast legs may vary as a function of bunker price and freight rate over reference trade routes. It can be seen that optimal ballast speeds are higher that optimal laden speeds by 1-1.5 knots. Gkonis and Psaraftis (2012) state one exception where the laden speed might be higher which is the case when the cargo inventory costs are accounted for in the optimisation model. Since the most profitable speed may be different for the ballast leg and the full leg, it is beneficial to separately analyse each voyage trip within the feasible range of speeds as has been done in (Ronen, 1982) where three models to determine the optimal speed are presented.

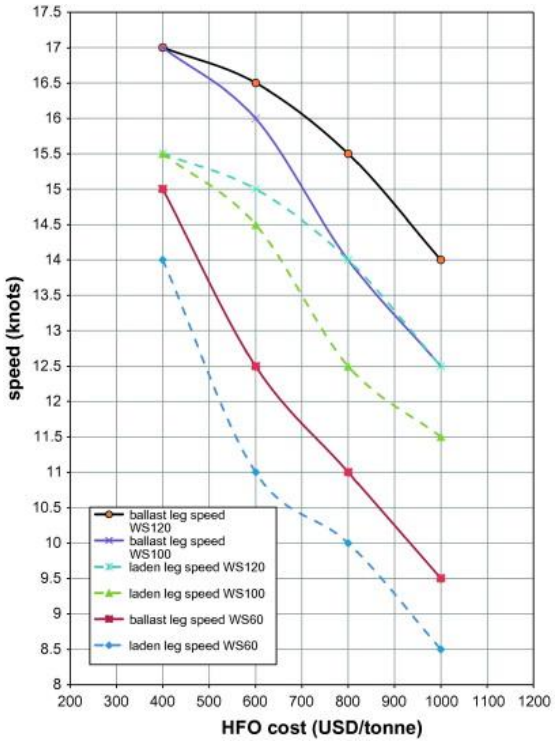

Figure 2.9 Optimal VLCC laden and ballast speeds as functions of fuel price and spot rate- Gkonis and Psaraftis (2012)

Reviewing the rich literature of speed models that mentioned above and others reviewed by (Psaraftis and Kontovas, 2013), the key points that are used to address and differentiate those models and studies can be summarised as following:

- Optimisation criterion,
- Ship type,
- Who is the decision maker?,
- Is bunker price an explicit input?,
- Is freight rate an input?,
- Fuel consumption function,
- Optimising speeds in various trip legs,
- Logistical context,
- Fleet size,
- Extra ships on the route,
- Including inventory costs,
- Port time and charges included in the model or not.

2.11 Newbuilding Market and Construction Cost

In an industry as complex and volatile as shipping, it is crucial to have the right ship at the right time as that guarantees significant success and rewards. For shipowners, it is vital to understand the market, track movements, assess the supply and demand waves, and to make wise predictions for the near and far future before starting a new investment. According to (Stopford, 2009), the shipping industry can be divided into four closely related markets which are: Newbuilding market, freight market, sale and purchase market, and demolition market. Those four markets depend on each other and on the global economy in general. When the global economy is in its booming conditions, the demand for goods and services is increasing as a result of such growth. That will create a high demand for international transportation means which will deliver and distribute these good globally. The newbuilding market is driven by supply and demand. The factors that determine it from the demand side are freight rates, expectations, the price of modern second-hand vessels, financial liquidity of the buyers, and the availability of credit. While from the shipyard supply side, the key issues are the size of the order-book, the number of available berths, and the production costs (Stopford, 2009).

Gaining accurate and real data about building costs from shipyards is difficult and near impossible as such data is confidential and all information regarding cost details especially during building stages is kept between the shipowner and the shipyard. Since real information about the building costs is limited in the literature, different simple and classic mathematical methods have been presented aiming to provide a tool to predict the ship building cost at the early design stages. Such studies can be found in (Bertram and Schneekluth, 1998; Watson, 1998; Rigo, 2001; Lamb and Society of Naval Architects and Marine Engineers (U.S.), 2003).

Generally speaking, the main cost driving parameters are: length, breadth, depth, deadweight, special equipment, speed, and power. The hull size and shape have a significant impact on the building cost, and it is essential for the shipowner to choose the right capacity for the new ship that can compete and operate efficiently. There have been recent trends to increase the storage capacity for tankers as this might improve the productivity in terms of cost per tonne.mile. However, that might not be the case among all ship sizes and classes or even some maritime routes as it depends on the service of the ship and the market demand.

A robust and simple parametric method of preliminary prediction of the ship building costs is built by (Michalski, 2004b). This developed method is a top-down method, and it is based on

some historical and statistical collected data related to the main and secondary ship parameters, building costs, and available information regarding the cost structure. It has been assumed that costs of each individual cost group are related to the weight of a respective group.

Another study by (Robert, 2008) presents a simple model consists of regression equations for estimating newbuilding costs. The regression formulas in (Robert, 2008) study are extracted by analysing a large set of shipyards deliveries reports from Lloyd's Shipping Economist in years 2003-2007. All data is adjusted using the producer price index (PPI) to allow for adjustments for inflation. The newbuilding cost function is modelled as a first-order function of the PPI and third-order function of the deadweight tonnage. These formulas indicate that there is an average increase in the total newbuilding cost of $2.6 million for every 1% increase in the PPI. Moreover, every increase in 1000 tons deadweight will result in increasing the cost of around $1.8 million.

A practical bottom-top cost estimation software is developed by (Ross, 2004) based on data collected at different phases and during design and construction such as initial and detailed drawings and tables, materials and equipment bills, historical vendor and subcontractor costs, labour costs, and existing quotes. The software is divided into two integrated and linked models, one focuses on the engineering side of the process and the second one focuses on the cost side. A more robust and detailed software is developed by (Ross, 2005) integrating weight estimation with building cost estimation into a single process.

However, the selection of an appropriate method for the construction cost estimation at any stage of the design and building process depends on the data availability and the level of details at each stages that best suited the relevant approach. These approaches vary from simple sheets formed in a shipyard by some old-timer experienced engineers to a very complex and detailed software counting every little bits and pieces (Shetelig, 2013).

2.12 Economic Criteria and Financial Analysis

Any economic optimisation model has one or more criteria used as an objective function to evaluate an investment such ships, and to assess the performance of individual ships or the entire fleet of a company. Moreover, these criteria are used to measure and analyse the sensitivity against fluctuations in the market conditions such as supply-demand balance when

a ship is ordered and also when she is at work, freight rates and bunker prices and changes in the operating profile such as speed and routing and scheduling.

To design a ship that has the most optimum characteristics (size, capacity, speed, etc.) for the job and the best profitable portfolio, it is essential to evaluate the influence of different design features on the initial cost in depth. However, the initial cost paid in cash or by loan is only a part of the overall picture of such massive investment. Therefore, shipowners should make it clear for shipbuilders and naval architect to consider the cost of running and maintaining the ship during the whole lifetime as the optimum design is not only the cheapest to build but also the cheapest to operate with a high competitive advantage, and hence the most profitable design (Branch, 1988b).

Different methods are common in the shipping economy to compute a ship or a fleet finance and evaluate a ship profitability during the entire lifetime. That depends on the nature and the preference of the shipping company and stakeholders. (Buxton, 1987; Stopford, 2009; Psaraftis *et al.*, 2012) discuss the key financial criteria that should be considered in the economic optimisation practice to gain a better understand of individual characteristics of ships and hence to identify the most effective ship design that meets the performance requirements. The main three criteria and measures of merit used to evaluate alternatives investments are Net Present Value (NPV), Required Freight Rate (RFR), and Internal Rate of Return (IRR). Details about those criteria can be found in the literature such as(Buxton, 1987). The net present value is used in the economic model to assess the ships performance.

The Net Present Value is the difference between the present value of cash inflows and the present value of cash outflows, and it is used to analyse the profitability of a project. When the acquisition cost of a ship is known as well as the required rate of return of the capital (or discount rate), annual income from freight transported, and the annual expenditures, then the general definition of NPV for freight earning ships is given as in Eq (2.37). All annual cash-flows are discounted back to the present, so the present value (worth) (PW) of each item is calculated using an accepted rate (10% per annum for example).

$$NPV = \sum_{t=0}^{N} \frac{Annual\ Cashflow}{(1+i)^t} - Intial\ investment \tag{2.37}$$

Where $N$is the lifetime of the ship in years, and i: the shipowner's cost of capital i.e. discount rate per annum (assumed constant).

According to the NPV criterion, the best alternatives for an investment like a ship or a combination of ships are the ones that yield the maximum possible NPV. The main advantages of the NPV method are its simplicity and that it takes into account all the revenue and cost flows and produces a single figure that makes the comparison of alternative options a simple issue. However, on the negative side, the apparent simplicity of this criterion is misleading because of the uncertainties associated with predicting all the revenue flow and cost stream. That would be the case especially for a ship trading on the spot market where the income and cost flows are subject to the changes and fluctuations in the market. Therefore, the NPV method is most appropriate to be used when evaluating vessels built for a long-term time charter.

2.13 Conclusions

This Chapter has reviewed the background in terms of the ship performance in her day-to-day operation. It started with a brief review of the different components of the total resistance that is produced by external forces and moments. The chapter outlines the hydrodynamic performance in different sea conditions including trial condition and more realistic in-service conditions. That was followed by an outline of the available estimation tools and methods to predict the resistance in calm water and the added resistance as well. Then different empirical and experimental methods to estimate the required propulsion power and engine maximum power are discussed taking into account the sea margin and all the energy losses. The nature of the resistance and the hull-propeller interaction phenomenon was demonstrated in the light of sailing at different speeds. Those estimation methods indicate how propulsion efficiency and hence the required power vary as a function of the operating speed.

A broad review of the contribution of the maritime shipping to the global warming and climate change was presented providing some background on the greenhouse gas emissions from domestic and international shipping. That was followed by describing some methods to estimate fuel consumption and emissions on-board ships during different journey phases including cruising, manoeuvring, and hoteling.

Moreover, this chapter outlined the basic factors likely to influence the economic performance of a ship and related to the design and operational profile. Different economic criteria and performance indicators were discussed, and some selected as an objective function of the economic model.

Chapter 3. Hull Form Hydrodynamic Optimisation Based on Parametric Modelling

3.1 Introduction

There has always been a growing interest in the hydrodynamic optimization to improve ships performance in service. Different methods have been proposed to develop the process of ship design that accounts, simultaneously, for several characteristics such as ship motions, loads, lightship, resistance, seakeeping, and propulsion. As a result, that will lead to a robust design and will increase the ship's total efficiency. However, disregarding any of the design requirements will, without any doubt, lead to an unacceptable design from the hydrodynamic point of view or economic perspective.

A typical optimization model includes basic components and steps which are, as shown in Figure 3.1,: selecting appropriate objective functions, optimization scheme, geometrical representation of the hull surface and choosing the appropriate design variables and constraints, selecting a numerical method to evaluate the objective function (Percival *et al.*, 2001). Two options are available to perform the optimization process: for a single-point design or for a multi-point design. For example: carrying out the optimization model for a single speed or for a range of speeds. Also, there are a single objective function model or multi-objective function model. The literature has addressed the hull optimization problem and the inherent basic issues in different ways, and they are covered later in this chapter and later chapters.

In this chapter, the hull optimization concept is introduced by describing its main elements including geometry manipulation tool, performance evaluator, and an optimization method. Then in Section 3.3, different methods for hull representation and modification are presented along with some examples highlighting the advantages and shortcomings of each approach. That includes point manipulation or vortex control method, perturbation surfaces generated by geometric modification functions such as the B-spline definition and Bezier patch, and the

parametric modeling method. AVEVA Marine 12.1 has been adopted in this thesis to generate the base body and as a tool for the hull parametric scaling and distortion, and also to perform basic and complex naval architectural analyses and evaluations such as the hydrostatics calculations and power estimations. Section 3.4 summarises the main features and applications of AVEVA Marine including: Lines, Surface & Compartment, and Hydrostatics and Hydrodynamics Calculations. The descriptive part of AVEVA Marine in this section is mostly taken from the Help file (AVEVA MARINE, 2011) as it illustrates the main specifications, components, empirical techniques, and modules of the design programme.

The main hull parameters of a 54,000 DWT tanker ship which is chosen as a case study are given in Section 3.5. Four hull parameters have been chosen for the parametric analysis in addition to the operating speed. In order to determine the effect of the hull parameters on the hydrodynamic performance, the distortion process is done in three stages where the performance sensitivity is investigated when parameters change individually and simultaneously.

The results are presented and discussed in Section 3.6 where the general hydrodynamic performance of the generated hulls and the powering characteristics are compared with those of the initial design. A set of regression formulas to estimate the required power per displacement are developed for a set of speed ranges using Minitab17 and the Regression Tool built in Excel.

Those results are analysed in order to search for the most favourable form(s) depending on the common naval architect knowledge and skills, and on a trial and error procedure. So, initially the main aim is to select the most robust shapes of the underwater hull that perform efficiently with minimum resistance across a wide range of speeds and when the operating conditions change frequently.

3.2 Hull Form Optimization Concept

Different hull optimization methods have been developed and presented in the naval architecture field in the last decades dedicated to improve ships' hull hydrodynamic performance. That involves (Brizzolara, 2004):

- Different parametric modeling approaches for the variation of the hull shape,

- Different numerical codes and methods to predict and evaluate the objective functions such as resistance and ship motions,
- Different optimization algorithms to search for optimal solutions.

Li and Zhao (2012) have developed an innovative hullform design technique for low carbon shipping. This optimization technique, as any typical hullform optimization tool, combines three main elements which are geometry manipulation tool, computational fluid dynamics CFD evaluator, and an optimization method as shown in Figure 3.1.

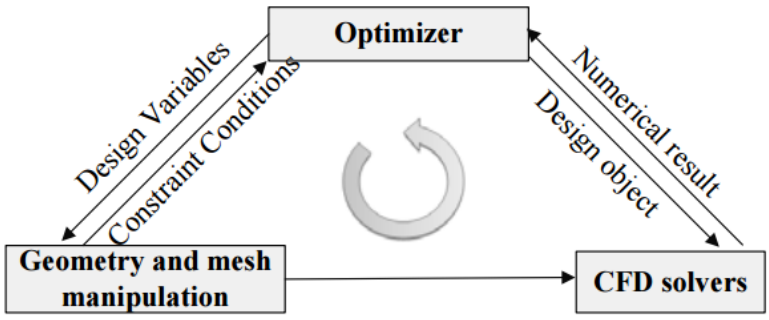

Figure 3.1. Hullform Design Optimization Environment

Fundamentally, a geometry modelling and modification tool provides the required connection and link between design parameters and the distortion of the hull form. A solid and effective geometry and grid manipulator plays a vital role in the optimization process as the modelling and modification procedures affect the flexibility of the optimizer to explore the constrained design space. However, achieving that flexibility requires minimizing the number of the design variables needed for the geometry variation which leads to minimizing the number of objective function evaluations. Moreover, an efficient geometry and grid modifier is necessary when it comes to implement various geometrical constraints within the optimization environment, and it is helpful to produce a variation of hull forms which allows for free-form design (Li and Zhao, 2012).

The second element of the optimization environment is the numerical solvers which are used for analysing and evaluating the objective functions and the functional constraints. The success of the optimization study depends on the accuracy of the CFD solvers in dealing with the objective functions.

Finally, the last component of the design optimization environment is the optimizer, i.e. the optimization method which is used to determine the optimal solution(s) within the design space.

Li and Zhao (2012) have addressed that selecting an effective and robust optimization algorithm plays an important role in improving the optimization process efficiency, and in reducing the time needed to explore the design space. The optimization algorithm is used to minimize and/or maximize chosen objective functions taking into account a set of assumed constraints. The most familiar optimization algorithm is the gradient-based technique. The main advantages of this algorithm are that it shows a high convergence performance and fast computational properties especially when a relatively small set of design variables are chosen. However, current algorithms which rely on gradient based methods have some limitations as they assume a continuous objective function, and they are not efficient when it comes to converging some specific shapes as spherical shapes (Alvarez *et al.*, 2009). Therefore, these algorithms might be trapped when searching for local solutions, and might be inefficient in solving problems with nonlinear constraints and non-convex feasible design spaces.

Recently, there has been an increasing interest in developing non-gradient based optimization algorithms and adopting global optimization algorithms which have several advantages comparing with local optimization algorithms. The main advantage of using non-gradient based algorithms is that they are robust and can be used for more complex optimization problems and works for several surface shapes. However, that requires more computation time and power which also depends on the number on the design variables. Moreover, the global optimization algorithms are easy to compute and design, and they can deal with continuous and non-continuous objective functions.

3.3 Parametric Geometry Modelling

For hull form optimization problems, there is always a need for a geometry modification algorithm. In the recent years, there has been an increasing interest in introducing the concept of the computer-aided parametric modification of hull forms to the naval architects community. In the past, it was common to use a limited number of local and global parameters to define hull forms, and to optimize the hull performance by changing these parameters depending on the results available from towing tank tests of typical systematic series of hulls.

The parametric representation of the hull surface is an essential component of any typical automated optimization problem in the naval architecture. Moreover, the intention of using geometry modification tools is to generate a series of underwater hull forms, and then test them to choose the one(s) that can lead to a better performance and meet the optimization process

goals like maximizing the wave cancellation effects along the hull length and reducing the resistance. Several attempts that deal with this issue can be found in the literature. The parametric geometry definition module should be capable of defining a series of hull forms characterized by several global and local form parameters (Brizzolara, 2004).

Various hull form modeling and manipulation methods are introduced in the literature such as point manipulation or vortex control method, perturbation surfaces generated by geometric modification functions such as the B-spline definition and Bezier patch, and the parametric modeling method (Chun, 2010).

Chun (2010) adopted a user-friendly parametric modification tool to modify the hull geometry of the KRISO container ship ($LBP = 230m, B = 32.2m, T = 10.8m$), and to generate a series of hull forms. In his developed approach, the original geometry is deformed by changing a selection of basic design parameters. These chosen parameters are varied systematically one by one while keeping all the others constant. B-spline surfaces are used to represent the initial hull surface and to generate a grid for the CFD solver. A modified geometry (H_{new}) can be obtained as in Eq (3.1) by superimposing the parametric modification function on the initial hull (H_{old}):

$$H_{new}(x, y, z) = H_{old}(x, y, z) + r(x) \cdot s(y) \cdot t(z) \tag{3.1}$$

The three functions (r, s, t) are the parametric modification functions, and they are polynomial functions defined along the three directions (x, y, z), respectively.

The parameters for the hull optimization process in Chun's study are: sectional area curve, section shape, and bulb shape. Different techniques are used to modify the initial shapes. For instance, three polynomial functions defined in (x, y, z) directions are used to modify the section shape into U-shaped section or V-shaped section. In this case, the modified grid point is obtained by using the perturbation in the (y) direction by using the three modification functions (r, s, t) as in Eq (3.2). Finally, the parametric modification functions will be parametrically distorted by varying the shape parameters such as the horizontal movement of the waterline within the minimum and maximum limits.

$$y_{new} = y_{old} + r^{(4)}(x) \cdot s^{(5)}(y) \cdot t^{(3)}(z) \tag{3.2}$$

Vertex control method is adopted by (Jinfeng, 2012) for the geometry parameterization using B-spline surfaces. This method has been proved to be versatile for shape optimization. Ragab

(2001) used it to optimize a submarine shape for minimum wave resistance subject to constraints on displacement, depth, and surface area. He assumes that the submerged body has a plane of symmetry. On half of the body there are $(m+1)(n+1)$ control points, and each individual control point is defined by two indices (i,j) where $(i=0,1,\dots,m)$ and $(j=0,1,\dots,n)$. Figure 3.2 shows the case for $m=8$ and $n=14$ after combining these two indices into one-dimensional index $k=(m+1)j+i+1$. The stream-wise coordinates x_{ij} of the control points vary only along index j while their offsets y_{ij} and depths z_{ij} vary with i and j together. Then when it comes to modify the shape, the stream-wise positions x_k of the control points are kept fixed while the offsets y_k and depths z_k are varied, and they are used as design variables. In a later stage, the B-spline surface patches are transformed to the flow solver to represent the body, and adjoint formulations for the determination of the objective functions' gradients are derived, and then used to solve the optimisation problem.

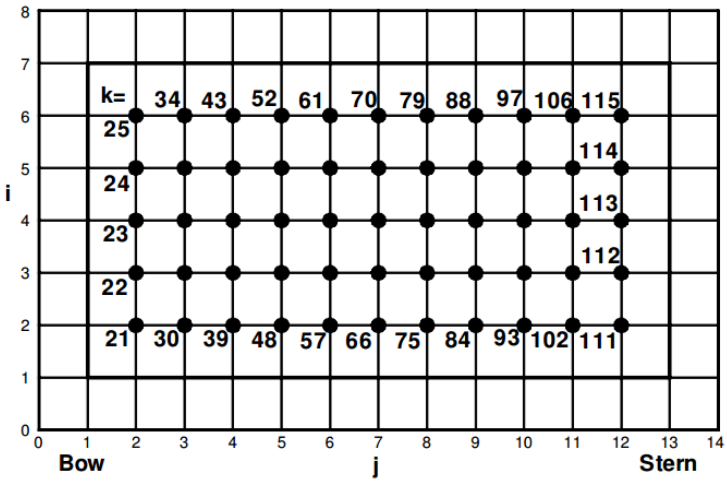

Figure 3.2 Indices of bi-cubic B-spline control points for a submarine configuration (Ragab, 2001)

A more direct geometrical modification approach has been used by Peri *et al.* (2001) in their study of a numerical shape optimization of a tanker ship hull. The adopted modification method acts directly on the control points of Bezier surface patches. To modify the shape of the hull, a perturbation surface has been used. That has resulted in a sharp reduction of the number of design variables required to represent the hull and for the optimization method. That makes it possible to minimize the number of evaluations of the gradient of the objective function. However, this approach requires utilizing a group of non-intuitive continuity and fairing constraints in order to control the nature of the modifying surface, and other design constraints, as fixed displacement, need to be included in the objective function. Figure 3.3 shows a sketch

representing the modification of the original hull geometry (top left) as it has been perturbed by adding a perturbation surface (Bezier surface) to obtain the modified geometry (bottom right).

The Bezier frame can have a different number of vertical and horizontal control points where the patch is controlled by a Bezier frame of $m \times n$ nodes. That makes this approach very flexible and efficient in modifying hull shapes and obtaining different hull shapes. Other advantages of this approach are that the smoothness is guaranteed and the required computational effort for the geometric modelling and the CFD solver is minimized as the number of design variables is kept small. The new modified geometry H_{mod} can be obtained easily by superimposing the patch on the y offsets of the original hull form H^o as in Eq (3.3). The y positions of each individual control point form the design variables where we search for the optimum values.

$$Y_{H_{mod}} = Y_{H^o}(u, v) + Y_B(u, v) \tag{3.3}$$

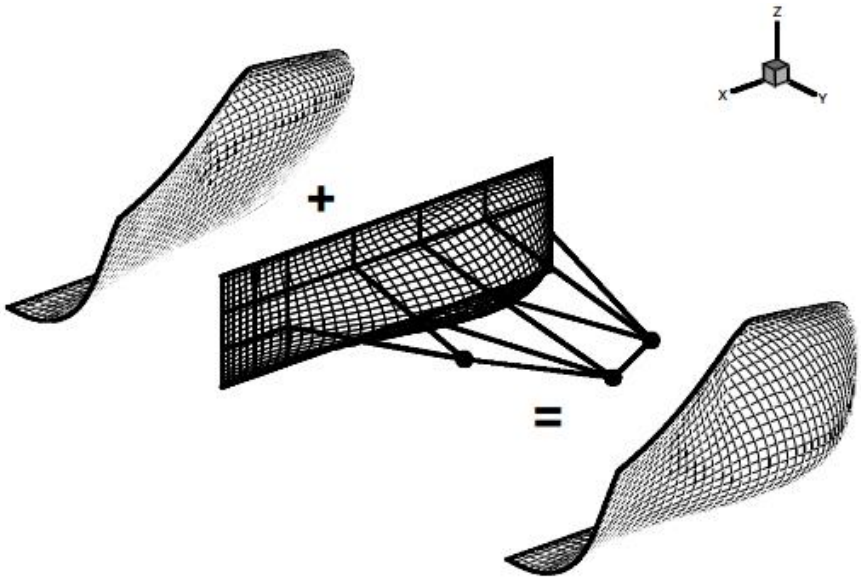

Figure 3.3 Perturbation Surface (Peri et al., 2001)

Jinfeng (2012) used an integrated tool to carry out a geometric modeling and hydrodynamic optimization for the hull form of a standard U.S. Navy ship DTMB5415 $[L_{BP}(m) = 142, B(m) = 19.06, T(m) = 6.15, Dis(m^3) = 8424.4]$. The developed genetic algorithm is capable of exploring the design space, evaluating the parametric modification of the hull form and the hydrodynamic performance, and improving the hull shape. For the parametric modelling of the ship hull, TU Berlin's FRIENSHIP Modeler has been used. This modeler is

based on B-spline curves and surfaces in determining the hull form. SHIPFLOW CFD codes have been developed to calculate the objective function. Also, calm water resistance has been chosen as a measure of merit. The displacement and LCB are considered as inequality constraints. Results from Jinfeng's resistance optimisation model show a significant reduction in the wave resistance coefficient of 24.30%.

3.4 Hull Form Generation and Distortion in AVEVA Marine

3.4.1 Overview

Parametric modeling techniques, as a whole, are based on expressing the hull shapes in terms of the chosen and preferred characteristics and properties. The modelling structure allows to use these properties as an input for the geometric modeller i.e. the CAD software. Then, the input is used to produce the shape geometry that is represented mathematically by points, lines, and surfaces. Also, the parametric modification tool is used to scale/distort the original hull shape by modifying a selection of standard design parameters chosen depending on a good naval architecture's knowledge and practice. That will generate a set of subsequent hull forms starting from a basic hull form built of a flexible set of basic curves which are defined in terms of the main design parameters from which the basic curves are laid out.

For the purpose of producing the basic hull form and then scaling or distorting it to generate new forms, AVEVA Marine 12.1 software has been adopted in the thesis. Version 12.1 of AVEVA Marine was launched in the second half of 2011. AVEVA Initial Design, as a part of the integrated CAD/CAM shipbuilding system, is a tool to create an initial ship hullform and her internal arrangement. Moreover, it consists of a number of functional modules which are based on a combination of mathematical methods and empirical techniques. These methods and techniques are used to preform basic and complex naval architectural analyses and evaluations such as the hydrostatics calculations and power estimations. It is worth

The company has added several completely-new modules offering a powerful detailed design features and applications. That covers the entire design course and building process for all types of ships from hull design to parts manufacture and block assembly. In general, features of the AVEVA Initial Design include (AVEVA MARINE, 2011; Wright *et al.*, 2012):

- Parametric generation of new hullforms and modification of existing vessels,

- Modelling of compartments, thruster openings and appendages,
- Output of lines plans and loftbooks,
- Calculation of hydrostatics, intact and damage stability inc. water on deck and probabilistic,
- Calculation of hydrodynamics, powering, manoeuvring and seakeeping.

The Geometry modeller in AVEVA Initial Design contains three separate but integrated systems which are:

- Lines: The Lines program can be used for refinement and fairing of the design. It can be used for fairing directly from offset data.
- Surface: Surface allows the user to rapidly and very accurately model surface features required for production, such as lateral thrust units, anchor pockets, shaft bossings, etc.
- Compartment: Compartment is an extension of Surface which allows the user to accurately model the major internal surfaces and compartmentation from the production hull definition for use in Hydrostatics.

Having adopted AVEVA Marine to generate and distort the base hull and to carry out the powering calculations, Holtrop and Mennen method buit within AVEVA gurantees a great degree of accuracy for the optianed results. Some major world's top shipbuidling yards such as Hyundai Heavy Industries and Daewoo Shipbuilding and Marine Engineering (DSME) have adopted AVEVA marine as a tool for 3D design and for obtaining accurate production information. For the purpose of confirming the accuarcy of the results obtained from AVEVA for the case study, a number of cases have been tested to validate the useage of AVEVA for the resistance and power estimation using Hottrop and Mennen. The power requirements of several commercial ships collectd from Clarkson Research Services and Seaweb are estimated using Holtrop and Mennen method where the main ship parameters and design speed are used as an input for the calculations. Moreover, other estimation methods built within the the Hydrostatics & Hydrodynamics module such as Guldhammer and Harvald, and Series 60 are used to carry out the calculations. The results obtained from AVEVA agree very well with the power data for the commercial ships. However, some of the power results show a 10% difference which could be a result of special design and energy requirements for some ships studied. Generally speaking, the results have shown very good levels of accuracy for the

hydrodynamic calculations, and hence the adopted software is demonstrated to be an efficient tool for the resistance and power estimations.

3.4.2 AVEVA Initial Design Lines

There are two methods for creating a design within Lines: by importing or by digitising offset data for a set of sections and various control curves. The appropriate method to use will depend on the type of ship and the data that exists for any particular project. Various different files can be imported to create the initial definition. Boundary curves are created from simple 2D and 3D input files. Knuckle curves are created from 3D files. The initial section definition can be provided in the form of a Britfair file, a Design file or an HFD file.

In this project, Lines system has been used to produce the initial hullform for the case study rather than using Britfair editor to create the initial sections definition. Each method has several advantages and disadvantages regarding the flexibility and simplicity to create and manipulate the design, the accuracy and fairness of the surfaces, and also the required time to generate a design. In comparison, the Britfair editor enables the user to, quickly and easily, create and edit section data. This data can then be used in a number of other AVEVA Initial Design applications which are able to import Britfair files. For example, the Surface & Compartment application can import a Britfair file, and use it to automatically generate an approximate hullform. This is very important in the early stages of the design, allowing compartmentation to begin and variations to be quickly tested. Even after compartmentation has begun, the design can be updated by replacing this approximate hullform with a faired version. On the other hand, even though the Lines system requires more effort to create a Lines design than a Britfair design, there are advantages in that the volume calculations will be more accurate as the hullform is a free form surface as opposed to a facetted one. Furthermore, the Lines design gives a wider range of hullform distortion tools. Also, in Lines it is possible to monitor the various hydrostatic properties of a hullform as the hullform is being developed. This means that it is not necessary to wait until the hullform is imported into Calc module before obtaining the hydrostatic properties of a hullform.

One main advantage in using Lines over Britfair appears when the end purpose of the hullform requires to be accurate or even highly production faired. That could be achieved efficiently if the base model is created using Lines. When the base Lines design contains sufficient curves and those curves are sufficiently fair, then if this design is transformed, the resulting design

should be close to being fair. In practise, when a Lines design is transformed to the Surface module, it is necessary to regenerate the hullform surface. The regenerated surface is based only on the base curves in the design. Therefore, any direct manipulation of the surface that has been carried out on the original model will be lost. However, if the curves of the base model are sufficiently fair, then any required direct surface manipulation to bring the hullform up to production fairness will be minimal.

Lines is a sophisticated hullform design system which enables naval architects to define and fair a hullform by means of a series of orthogonal and 3D space curves. Lines is capable of defining virtually any form of marine vessel including multi-hulls chinned and asymmetrical hulls. Lines uses 2-D and 3D-space curves to define a hullform, of which the mathematical basis is B-Splines.

The input to the system is generally via an offset file, digitisation of a preliminary lines plan. Once inserted, the hullform and its appendages can be developed by the progressive refinement of frame, Waterline, Buttock, 3-D angle curves and stem/stem profiles, which between them provide a complete three-dimensional wire frame definition of the hullform. Fairness can be checked by viewing these curves in the traditional manner, supplemented with several special features to assist in measuring fairness. The rapid development of hullforms is also aided by features such as 3-D curves, contracted fairing, special Waterline endings and hull distortion techniques, including sectional area curve transformations and parallel mid-body insertion. Once defined, comprehensive lofting information including lines plans and loft books can be obtained for model or full scale production.

It is worth mentioning after creating the initial definition of the design, it is important to review the design and refine, fair, and modify some sections and curves which is referred to as fairing the design. The ultimate fairness of the ship design is a subjective decision and the same judgement must be made when using Lines. The principal means for measuring the fairness of a curve in Lines is showing the inverse of the radius curvature at points on the B-spline as already described. The Lines approach to fairing is based very much on the traditional methods used in lofting and design offices. The batons are replaced by the B-Spline and weights are applied by specifying conditions (KNOTS) at selected points. Both 2D and 3D curves can be faired using this method. Either the full curve can be faired or a region can be specified whereby the curve outside the specified region will not be changed. The region can be specified by giving lower and upper X, Y or Z values or by picking two positions on the curve with the cursor.

Various techniques can be applied in the fairing process. That includes: removing and replacing points, offsetting points, moving points, inserting points, offsetting the vertices of the b-spline, inserting and removing knots, and the automatic fairing. The automatic fairing algorithm (based on Eck and Hadenfeld method) can be used to fair the current curve easily by clicking the Auto Fair button. When automatic fairing takes place, vertices are moved such that energy in the curve is reduced. As a result, the size and irregularity of curvature tufts will also be reduced.

Improving the fairness of an individual curve can be achieved by removing the unnecessary data points. Excessive data points often lead to unwanted undulations in the curve, particularly if they are close together. Also, the effort required for editing is reduced if there are fewer data points to deal with, and the design as a whole becomes easier to manage. 'Thinning out' the data points defining a curve is thus a good first step in the process of manipulation and fairing. Often, quite a large proportion of the data points defining a curve can be removed, to produce a substantially improved curvature distribution without straying significantly from the original point positions. In the example below (Figure 3.4), the set of active data points has been reduced from 38 to 10. The curvature distribution is much improved, though the curve remains perceptibly very close to all of the original data points (for clarity, the active data points are shown highlighted).

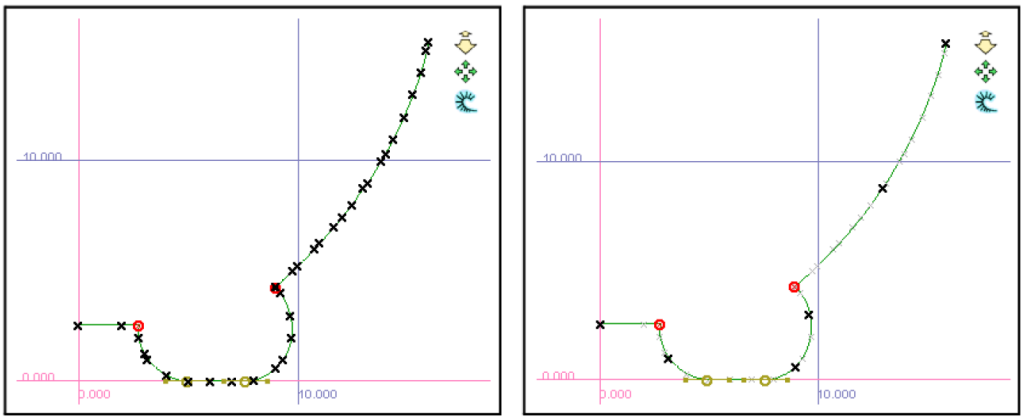

Figure 3.4 Curve points prior and after thinning

Finally, when a ship is been faired to an acceptable level, the design can be patched to allow the vessel to be described by a surface. A surface is the eventual output of the hull design and fairing process. With Lines, this surface is based upon a set of curves that describe its shape. There are methods of generating a surface. The recommended method is to use the Patch and Curve Editor (PACE) to semi-automatically generate the surface and then interactively assess

and manipulate it. This surface can then be released for use in other AVEVA Marine modules such as Surface/Compartment, Structural Design and Hull.

3.4.3 Distorting the Basis Hullform

For the purpose of carrying out the parametric analysis, a systematic set of new hulls by is generated by changing a set of selected variables. A design can be distorted or scaled up or down from within Lines. Lines can be utilized to distort either geometrically or by linear scaling existing hulls to generate new vessels. Hull scaling option is used to scale a patch by entering the new values required for length, beam, and draught. That will result in the model being scaled independently (by the Scale Factor) in each direction. The hull distortion option enables the variation of the block coefficient, longitudinal centre of buoyancy and lengths of the parallel midbody in the fore and aft bodies. It starts by producing a Sectional Area Curve (SAC) and subsequently modifying it by using a systematic geometric distortion method such as:

- One minus Prismatic Coefficient (1 - Cp).
- The Lackenby Method.
- Or, interactively by the user.

The 1-cp method allows only the vessel's CB to be varied, while the Lackenby method allows C_B, LCB, Parallel Midbody Forward (PBF) or Parallel Midbody Aft (PBA) to be modified. Lackenby method was developed by Lackenby (1950) after the well-known One Minus Prismatic $(1 - C_P)$ method to avoid some major disadvantages of the later method as it has no control over the extent of the parallel middle body in the distorted form and the uncontrolled change in the longitudinal distribution of the added or removed displacement in the case of a given change in the form fullness. In Lackenby method, the fore and aft body are transformed separately as a function of the desired changes in the prismatic function of the two bodies in the case when the parent and the new hulls have different values for the prismatic coefficient and the LCB position. Lackenby approach is an easy and simple method to distort the sectional area curve SAC and design waterlines independently. That helps in giving designers the option to preserve the ship length and to change the form fullness, location of centroid, and the length and location of the parallel meddle body for each SAC.

When the SAC is modified, Lines allows the design to be distorted so that it matches the new desired SAC. Moreover, if Lackenby is selected, then several options are enabled which control

how the Sectional Area Curve is altered. Fix Perpendiculars ensures that the sectional areas aft the perpendiculars will not be changed. Fix Overhangs ensures that the sectional areas aft of the AP and forward of the FP are not changed.

The advantages of using the Lines module are that distorting the hull forms is achieved easily and in a highly-concerted manner, and it allows to carry out a considerable set of changes by varying a few selected form parameters.

Once the design has been distorted/scaled, then there is a need to smoothen and improve the quality of the surface before releasing the design to the Surface & Compartment module. Distorting a design requires modifying the original SAC and making changes to the original patches as well. However, if the SAC is modified or changes are made to the patches, then the stored curves can be transposed to match the new SAC and the patch boundary networks remain connected after the transposition. This is achieved via the Rebuild Options that offer the ability to preserve or change certain characteristics of the existing surface such as: boundary network, patch settings, and patch geometry.

In general, users should always seek as much improvement in surface quality as possible by iteratively rebuilding the surface whilst changing the boundary curve network and global patch options. That can be achieved via the Patch and Curve Editor (PACE). Figure 3.5 shows the distorted design after rebuilding and smoothening have been applied.

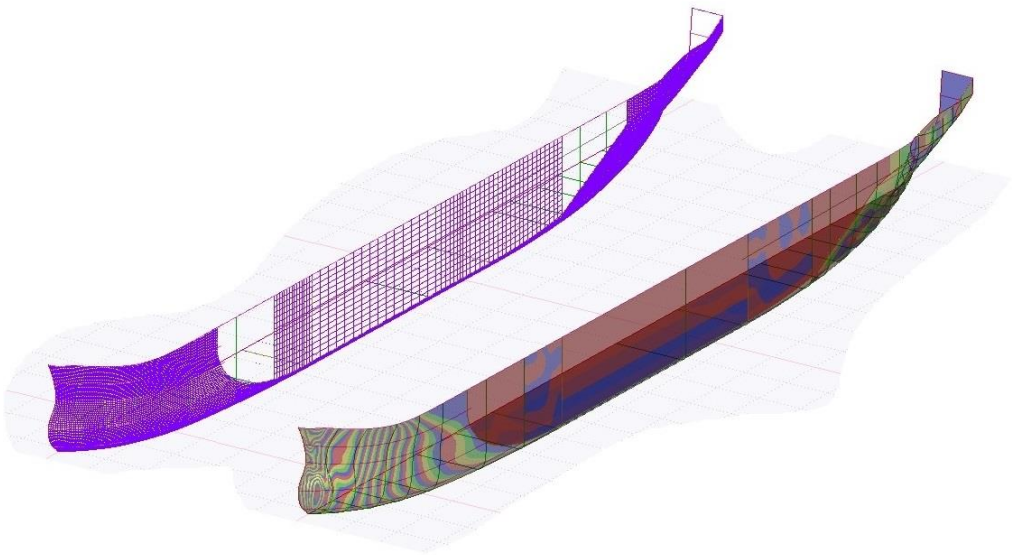

Figure 3.5 Rebuilding and Smoothening the Surface using PACE

3.4.4 AVEVA Initial Design Surface & Compartment Modules

AVEVA Initial Design Geometry Surface is a part of the AVEVA Marine integrated hull geometry modelling software. Its main purpose is for the surface modelling of production features such as appendages connected to the hull, submarine hulls, semi-submersibles, special internal arrangements and other complex multi-surface geometries not adequately defined by simply using points or curves. The Surface module provides ship designers with the ability to define a product model of the outer surfaces of the main hull and its appendages. The hullform is represented as a connected set of non-uniform rational B-Spline (NURBS) patches. Facilities are included for intersection and clipping of appendages and/or special geometries, blending, filleting and visualisation. The Compartment module has been designed specially to facilitate the quick definition of transverse bulkheads, longitudinal bulkheads, decks and compartments.

The internal surface definition gives full topology, with bulkheads and decks of flat or complex shape, and automatic calculation of any intersections with the hullform. Bulkheads have the option of vertical or horizontal corrugation and stools, while decks can be quickly constructed with sheer and/or camber. Any internal surface can be constrained either interactively or by using a drag drop facility. Compartments are constructed, bounded by bulkheads, decks and the hullform. More complex shapes can be produced by merging compartments by addition or subtraction. All internal structures can be topologically defined and therefore easily regenerated at the users' request.

3.4.5 AVEVA Initial Design Hydrostatics & Hydrodynamics Module

The Hydrostatics & Hydrodynamics module is an efficient platform designed to assist naval architects and ship designers to perform hydrostatics and hydrodynamics calculations upon any floating object and for a wide range of hullforms. It offers a comprehensive toolkit of simple and sophisticated naval architectural assessment practises and methods to be used during design stages and on-board. The main list of calculations include: hydrostatics calculations, loading and ballasting conditions, tank calibrations, damage stability assessment, intact and damage stability, trim, seakeeping, critical KGs, longitudinal strength, freeboard, Inclining Experiment, tonnage and launching, manoeuvring, powering, ship's motions, and more options covering other calculations and important evaluation methods (AVEVA MARINE, 2011; Wright *et al.*, 2012).

The geometry definition of the hull needs to be released to the Hydrostatics & Hydrodynamics Module. Then the user is bale to define the ship's general data and preferable geometry units, any number of loading conditions, water conditions including depth and speed, propeller data, etc. Moreover, the user can later decide which methods to be used to carry out the required calculations and evaluations. For the resistance and powering estimation, the bare hull is first determined at model scale using one of fifteen empirical methods such as Holtrop and Mennen, Guldhammer and Harvald, and Series 60.

Using 1978 ITTC Performance Prediction Method, the bare hull resistance for the ship is then derived as Hydro module determines a suitable form factor for the design and also the ship-model correlation allowance. However, the user is bale to alter these auto-determined values if desired. Moreover, Hydro module provides five empirical methods for the calculations of the propulsion factors. The user is able to use pre-defined values for the wake fraction, thrust deduction and relative rotative efficiency or to choose one of the built-in methods such as Holtrop and Mennen and Series 60. More options are offered to the user regarding the powering and propulsion calculations. That includes selecting the propeller series, its characteristics and its likely open water performance. Also, additional performance corrections can be defined for controllable pitch and noise reduced propellers for the purpose of optimising the propeller design and performance against cavitation.

The output is available in both graphical and tabular formats in a way that design offices, ship's owners, classification societies, and other authorities can use them to evaluate the new design and approve it. The main output of Calc Module that is used in this study includes mainly the Hydrostatics Particulars, Righting Lever values, Resistance Calculations, and Powering Calculations.

3.5 The Reference Vessel and Basis Hull Details

In order to demonstrate the potential resistance reduction and energy saving that can be achieved by adopting the slow steaming concept and hull optimization process, a bare-hull of a 54,000 DWT Tanker ship is chosen as a case study for this project. The ship particulars and details are provided privately by AVEVA to be used for this project. As this design has not been used before, the hull design has been edited a few times, and several modifications have been made to amend some missing patches and disconnected surfaces. Table 3.1 shows the main particulars of the ship. The ship has not been actually built yet, and even no hydrodynamic

studies have been carried out on her bare body. As a result, there is no sufficient data about the hull regarding resistance, propulsion test, wake measurements, powering tests, and other main operating information.

Table 3.1 Main Ship's Particulars

Length Overall	L_{OA}	210.215 m
Length Between Perpendiculars	L_{BP}	202.500 m
Breadth	B	32.250 m
Design Draught	T	12.180 m
Longitudinal Center of Buoyancy	LCB	2.49%L fwd=106.30 m
Longitudinal Center of Floatation	LCF	0.27%L fwd
Block Coefficient	C_B	0.8254
Prismatic Coefficient	C_P	0.827
Midship Section Coefficient	C_m	1.000
Waterplane Area Coefficient	C_{wp}	0.891
Wetted Surface Area Coefficient	A_S,	6.098
Half Angle of Intrance	½Φ	44.5°
Design Speed	V	15 knots
Froude Number	Fn	0.173

Figure 3.6 and Figure 3.7 show a drawing of the body plan and profile view of the initial hull, respectively while Figure 3.8 shows an isometric view of the surface shape rending of the bare hull.

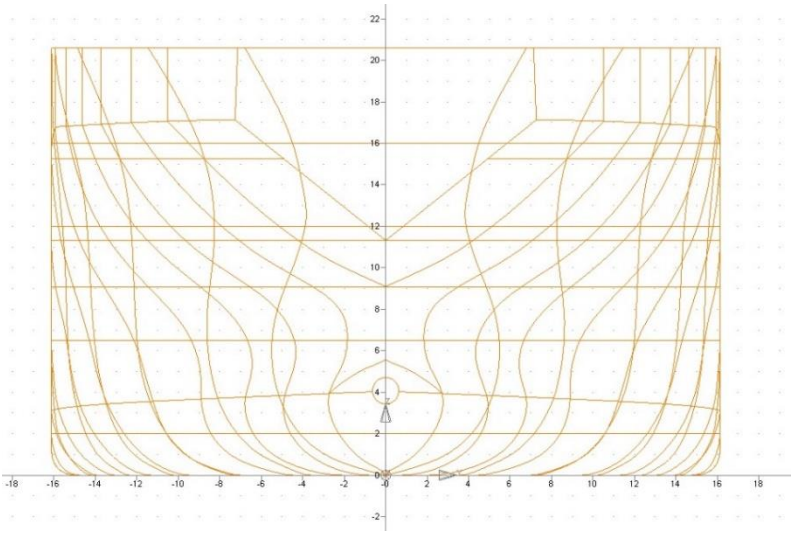

Figure 3.6 Body Plan of the Initial Hull

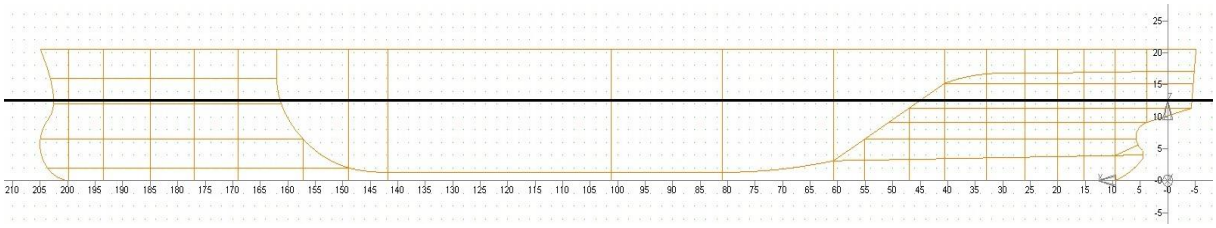

Figure 3.7 Profile View of the Initial Hull

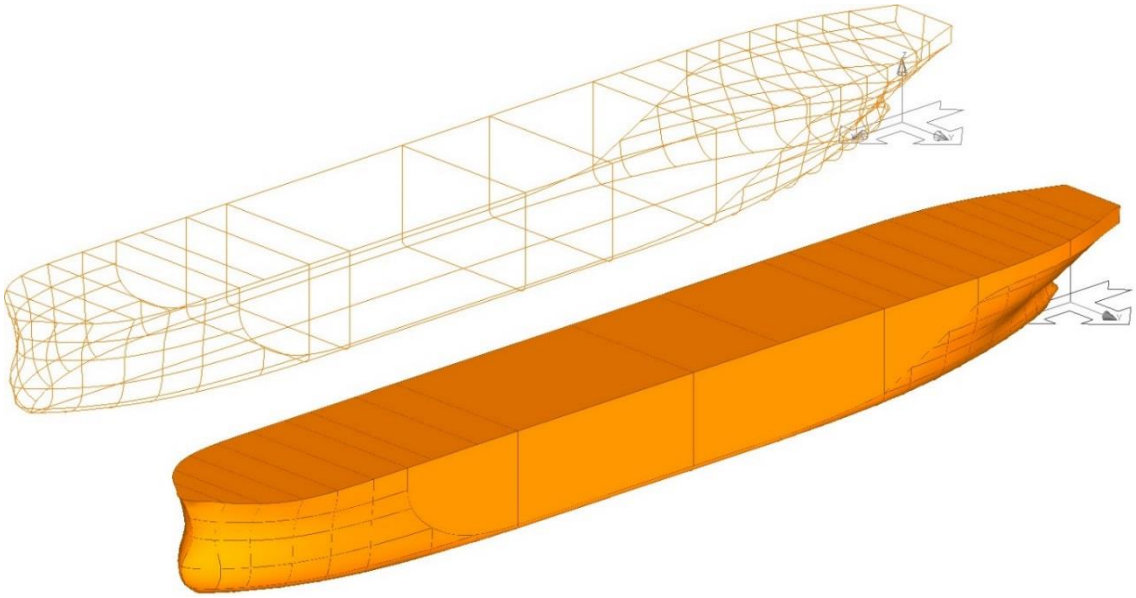

Figure 3.8 Surface Shape of the Initial Hull

As has been mentioned before, the main aim of this study is to identify and solve several design challenges and concerns facing existing and future designs to select the most robust and appropriate design for the case study. A series of new hull forms has been generated by modifying the main hull parameters and form coefficients. These parameters and coefficients are addressed as the controllable design variables. They are divided as primary and secondary variables as following:

- Primary design variables: Hull length, L
  Breadth to draught ratio, B/T
- Secondary design variables: Block coefficient, C_B
  Logitudinal centre of buoyancy, LCB

The design space for the parametric analysis problem is expressed as a percentage change from the basic hull for both the primary and secondary variables. To keep the case study relatively simple and the analysis process more focused and effective, the variables' upper and lower bounds are selected relatively within a small array as shown in Table 3.2:

Table 3.2 Design Space for the case study problem

Variable	Parent Value	Lower Limit	Upper Limit
Length L_{BP}	202.500 m	-10%	+10%
Breadth to Draught Ratio B/T	2.648	-10%	+10%
Longitudinal Center of Buoyancy LCB	106.558 m 2.49%L fwd	-1% L	+1% L
Block Coefficient C_B	0.8254	-6%	+6%

The parametric analysis is divided into three stages in order to cover different hull shapes, characteristics, and capacity. That helps to investigate how the controllable variables affect the ship performance when they are varied individually and also in different schemes/scenarios. However, the three stages of the parametric distortion process can be summarised as following:

3.5.1 Stage One

In this stage, the chosen primary and secondary design variables are varied individually within the upper and lower limits. The aim is to investigate the impacts of changing the variables while maintaining the displacement constant. In order to change the length L while the displacement is fixed, the midship section area is altered in inverse ratio to the length. Also the breadth to draught ratio B/T stills constant as well as the other form parameters and coefficients such as the block coefficient C_B. In this case the new main hull form dimensions can be derived from the basis dimensions (L, B, T) as shown in Eq (3.4):

$$\begin{aligned} L_{new} &= (1 + \delta L) \cdot L \\ B_{new} &= B/\sqrt{(1 + \delta L)} \\ T_{new} &= T/\sqrt{(1 + \delta L)} \end{aligned} \tag{3.4}$$

The length is changed from the parent value within the range $[182.25 \div 222.75]m$ and the step is 2%. The associated changes in the breadth and draught are in the range $[30.75 \div 34.0]m$ and $[11.613 \div 12.839]m$ respectively. The geometry scaling and modification technique for the hull offsets is very basic as the waterlines and offsets of corresponding stations can be found by multiplying the basis offsets by a constant expansion or contraction factors as following:

- Station spacing design = Basis station spacing × δL
- Waterline spacing design = Waterline spacing basis × δT
- Offsets design = Offsets basis × δB

Similarly, the displacement is maintained constant with a fixed length while varying the second design variable, i.e. the breadth to draught ratio B/T, by a factor of δx as in Eq (3.5). Since L is constant, and (B,T) varies, the waterlines and offsets of corresponding stations can be modified in the same way described above. The B/T ratio varies within $[\pm 10\%]$ range from the parent value 2.648, and the changing step is $\delta x = 2\%$. In this case, the length and the displacement are constant. The resulted ranges for the breadth and draught are $[30.595 \div 33.824]m$ and $[11.613 \div 12.839]m$ respectively.

$$B_{new} = B \cdot \sqrt{(1+\delta x)}$$
$$T_{new} = T/\sqrt{(1+\delta x)} \tag{3.5}$$

Stage one of the geometry modification plan also includes deriving a series of alternative designs with the same main dimensions but with different values for C_B or LCB. That is done by changing the location of stations at which the offsets are given. In such way, the shape of the sections remain the same as in the original hull but they are moved forward or aft in some manner, and the curve of sectional area changes in the desired manner. For this purpose, Lackenby method 1950 is used within AVEVA Lines module.

The upper and lower limits of the block coefficient and the longitudinal centre of buoyancy within the design space are defined based on the classic and recommended values of conventional tanker ships (Bertram and Schneekluth, 1998; Watson, 1998). For the chosen case study, the selected ranges are $C_B = [0.776 \div 0.875]$ with a varying step 2%, and $LCB = [104.533 \div 108.583]\ m$ but the varying step is a percentage of the length $(0.2\%L)$.

The ship's main dimensions $[L, B, T]$ are kept constant while changing the secondary design variables $[C_B, LCB]$ individually. Moreover, when changing the block coefficient, the longitudinal centre of buoyancy is not constant, and it varies within a very small range $[\pm 0.08\%]$ as changing the form fullness using Lackenby method distorts the longitudinal distribution of mass. Since the hull main dimensions are constant, the displacement will vary from the original value $(67301\ \text{tonnes})$ at the same percentage as the changes in the block coefficient in the range $[63258.5 \div 71333.0]\ tonnes$. On the other hand, varying the longitudinal centre of buoyancy while keeping $[L, B, T]$ constant leads to a small change in the block coefficient around $[0.24\%]$ as a result of distorting the hull form and shifting the sections. As a consequence, the hull fullness will change and the displacement will change slightly from the original value $(67301\ \text{tonnes})$ within a very small range $[\pm 2\%]$.

Varying the primary and secondary design variables individually results in generating **36** new hull forms in Stage One. That helps in having a clear understanding of the impact of changes in main parameters on the resistance components, seakeeping characteristics, propulsion performance, fuel consumption, and the profit as well at different operating scenarios such as loading conditions, weather conditions, and ship's speed.

3.5.2 Stage Two

Analyzing Stage One's results presented in Section 3.6.1 show that the primary variables $[L,\ B/T]$ have a significant impact on the objective functions and mainly on the total resistance and delivered power all over the speed range. Therefore, in Stage Two of the parametric analysis study, more investigation has been done to obtain a sufficient insight of their influence on the ship's hydrodynamic performance. Since the performance characteristics are dominated by the primary variables, then the secondary design variables will not be taken into more consideration at this stage as their combined influence is not considered to be sufficiently significant comparing with the primary variables impact but will be looked at in the Third Stage of the analysis.

The primary controllable design variables $[L,\ B/T]$ vary simultaneously within the design space: L $[\pm 10\%]$ & B/T $[\pm 10\%]$. The new design variables become:

$$\begin{aligned} L_{new} &= (1 + \delta L) \cdot L \\ (B/T)_{new} &= (1 + \delta x) \cdot (B/T) \end{aligned} \tag{3.6}$$

For each new value of the length, there will be 11 new generated hulls as a function of changes in the breadth to draught ratio as shown in the matrix below. Therefore, Stage Two includes (10x11=**110)** new hull forms geometrically distorted using AVEVA Lines Module.

$$\begin{bmatrix} L \\ 2\% \\ 4\% \\ 6\% \\ 8\% \\ 10\% \\ -2\% \\ -4\% \\ -6\% \\ -8\% \\ -10\% \end{bmatrix} \rightarrow \begin{bmatrix} & & & & & B/T & & & & & \\ 10\% & 8\% & 6\% & 4\% & 2\% & 0\% & -2\% & -4\% & -6\% & -8\% & -10\% \end{bmatrix}$$

As the block coefficient is kept constant, then the ship displacement will be a function of the changes in the length and breadth to draught ratio, i.e. $\delta\Delta = f(\delta L, \delta B/T)$. Moreover, since the breadth and the draft vary in reverse when changing the breadth to draught ratio as in Eq (3.7), then the displacement varies linearly as a function of changes in the length even when B/T varies.

$$B_{new} = B \cdot \sqrt{(1+\delta x)}$$
$$T_{new} = T/\sqrt{(1+\delta x)} \tag{3.7}$$

3.5.3 Stage Three

The aim of Stage Three of the parametric analysis is to expand the exploration of the design space defined by the primary and secondary variables and for a range of speeds. That helps in selecting a design or several alternatives which are more robust with respect to a set of hydrodynamic and economic criteria at a wide range of speed and at any operating condition.

Varying the design variables all together using all their levels as shown in Table 3.2 will result in generating $(11 \times 11 \times 11 \times 7 = 9317)$ new hull forms. Taking into account that the speed varies in the range $[5 \div 17]$ knots, then Holtrop and Mennen method will be used in the resistance calculations for 121121 times which means time consuming to analysis this great mass of data. Therefore, there is a critical necessary need to reduce the number of the required runs to generate new hulls in order to reduce time and cost required at the early stages of design.

Design of experiments techniques DOE are employed in Stage Three as they allow to search the full design space, efficiently, by selecting a small set of designs using full factorial designs and/or designs from orthogonal arrays as used in (Taguchi Method). That includes varying and testing different levels of each of the control and noise factors, and analysing their effect on the response function with minimum number of tests.

It is up to the experiment designer to set appropriate levels for each design factor, and also to choose the most viable size of the experiment runs array. In practical engineering experiments, running extra tests is very time consuming and expensive, so a small orthogonal array can be used to reduce the number of the runs. A thorough explanation of Taguchi approach for robust design can be found in the literature (Taguchi and Wu, 1985; Ross, 1988; Bendell, 1989; Logothetis and Wynn, 1989; Taguchi and Phadke, 1989; Barker, 1990; Lochner and Matar, 1990; Peace, 1993; Taguchi, 1993; Fowlkes and Creveling, 1995; Ross, 1996; Garzon *et al.*,

2000; Wu and Wu, 2000; Mori, 2011). Moreover, Section 3.6.4 presents a review of Taguchi's Quality Loss Function and the Signal-to-Noise Ratio that are used in the search for a robust design that has minimum sensitivity to variations in the design parameters.

In this study, a three full factorial central composite design (CCD) is used for Stage Three experimental plan as in Table 3.3 which indicates the controllable design factors and their levels. Hence, a traditional full factorial design 3^4 is used and it has 81 runs (degrees of freedom) which indicates that all possible factors combinations are taken into account. Appendix A (tables A.1 and, A.2) shows the runs' combinations (generated using Minitab 17) for the design factors and their levels as $[1, 2, 3]$ refer to the lower, centre, and upper level for each factor, respectively. The type of the central composite design (CCD) used for this analysis is known as face centred (CCF) where it has a centre point and the star points are at the centre of each face of the factorial space.

However, even it was decided to choose a full factorial design for this case study, other options are available to use fractional factorial designs suggested by Dr. Taguchi as can be seen in (Taguchi and Wu, 1985; Ross, 1988; Taguchi and Phadke, 1989; Barker, 1990; Lochner and Matar, 1990; Peace, 1993; Taguchi, 1993; Fowlkes and Creveling, 1995; Ross, 1996; Wu and Wu, 2000; Mori, 2011). In the case of having 4 design factors and the number of levels is 3 levels, the L_9 (3^{4-2}) orthogonal array is the most common option in the engineering quality experiments as it allows to search the design space with the minimum number or experimental runs.

Table 3.3 Design Control Factors and Their Levels

Variable	Level 1	Level 2	Level 3
Length L_{BP}	-8%	1%	+10%
Breadth to Draught Ratio B/T	-10%	-1%	+8%
Block Coefficient C_B	-6%	-1%	+4%
Longitudinal Center of Buoyancy LCB	-1.1%L	-0.1%L	+0.9%L

Varying the design variables in such systematic way does not preserve the initial displacement of the original ship as the modification method involves varying the main hull parameters and the form coefficients. The maximum and minimum percentage changes for the displacement are around $[\pm 14.0\%]$. Moreover, the lightship and the carrying capacity DWT of the ship will change while the ship's parameters and the displacement vary. Hence, carrying out this

parametric modification does not only have an impact on the hydrodynamic performance but also on the ship's environmental footprint and her economic performance as will be seen in the next chapters.

3.6 Hydrodynamic Performance Model's Results

In this section, the results from hydrodynamic model are presented. They are the first set of input in addition to EEDI and economic performance results for the multi-objective optimisation framework that is discussed in Chapter 6. The hydrodynamic performance of the generated hulls and the powering characteristics are compared with those of the initial design. Then, the results are analysed in order to determine the most favourable form(s) depending on the common naval architect knowledge and skills, and on a trial and error procedure. Initially, the main aim is to select the most robust shapes of the underwater hull that perform efficiently with minimum resistance and required power across a wide range of speeds and with the operating conditions change frequently. Therefore, the laden and ballast conditions have been taken into account for the resistance calculations and required propulsive power.

The resistance components and the total resistance have been estimated using Holtrop and Mennen method 1984 built within AVEVA Marine package. The hydrodynamic performance is defined and assessed by a set of particulars, parameters and coefficients. They are:

- The total resistance coefficient (C_T),
- Quasi-propulsive coefficient (η_D, QPC),
- Hull efficiency (η_H),
- Wake fraction and thrust deduction factor (w, t),
- Delivered power (P_D),
- Effective power (P_E).

In the most general case, the objective functions and the evaluation criteria can be assumed as the percentage of the deviation from the original hull values which are taken as a reference value. For example Eq (3.8) shows the objective function $R(V_i)$ expressed as a percentage of the original hull resistance:

$$\Delta R_{\%}(V_i) = \frac{R(V_i) - R_{ref}(V_i)}{R_{ref}(V_i)} \tag{3.8}$$

3.6.1 Stage One Results

Figure 3.9 shows the percentage change in the total resistance coefficient C_T for the first group of the new hulls generated for Stage One. The length parameter is varied while keeping the other design variables constant as in Eq (3.4). The displacement is kept constant, and the main hull parameters vary accordingly. The plot shows the $C_T\%$ curves just for a selected set of speeds for illustration. It is obvious that changing the ship's speed has a small effect on the total resistance coefficient in this case. For the design speed 15 $knots$, C_T decreases by more than [10 %] when increasing the length by [10 %], and it increases by about [9 %] when the length decreases by [10 %]. However, the total resistance coefficient sensitivity decreases dramatically for small speeds which is obvious in Figure 3.9. The change in C_T for speeds less than 12 $knots$ for each individual hull is almost constant. For instance, for the same hull [+10 % L], the drop in the total resistance coefficient is somehow constant [+5 %] for slow speeds. In other words, at high speeds the impact of changing the hull parameters on the resistance coefficient is more significant than the impact at lower speeds. Table 3.4 shows the changes in C_T at speeds [15, 10, 7] $knots$.

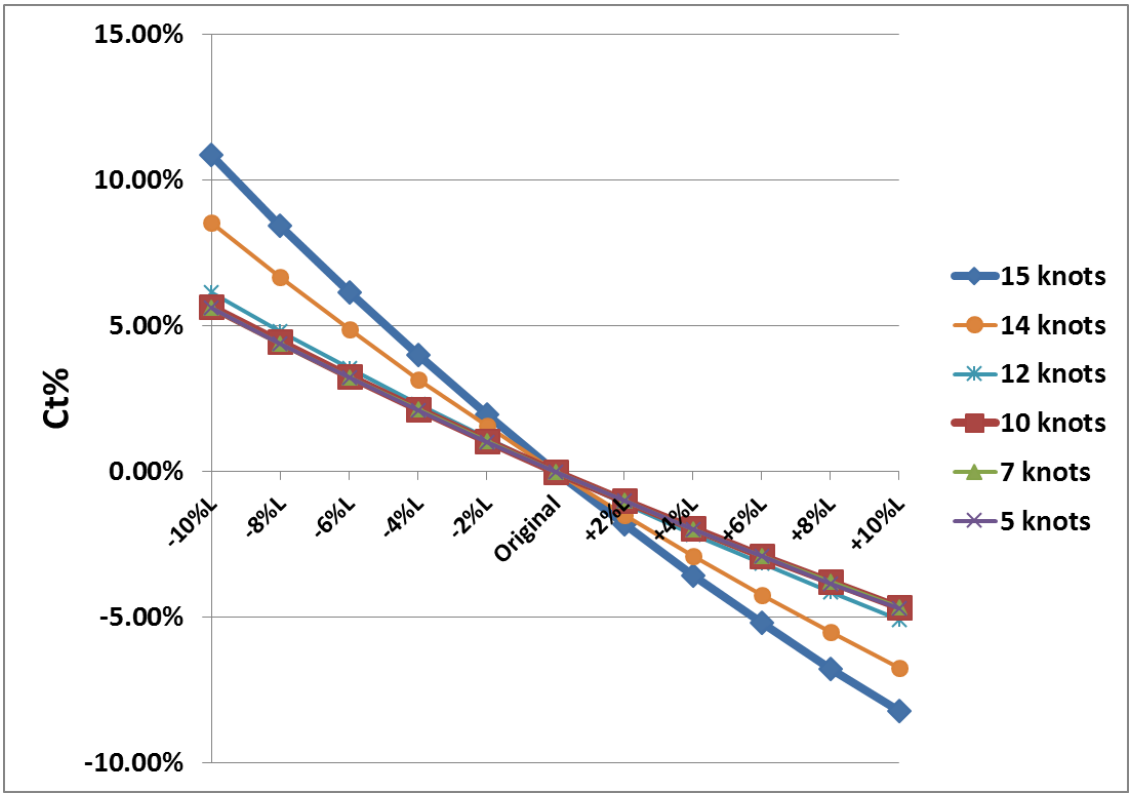

Figure 3.9 Changes in the total resistance coefficient for First Group – Stage One

Table 3.4 Changes in the total resistance coefficient at different speeds

Hull	15 kn	10 kn	7 kn
-10%L	10.85%	5.65%	5.64%
-8%L	8.43%	4.45%	4.39%
-6%L	6.16%	3.24%	3.22%
-4%L	3.99%	2.12%	2.13%
-2%L	1.96%	1.04%	1.05%
Original	0.00%	0.00%	0.00%
+2%L	-1.81%	-1.00%	-1.01%
+4%L	-3.56%	-1.95%	-1.97%
+6%L	-5.20%	-2.91%	-2.90%
+8%L	-6.76%	-3.78%	-3.78%
+10%L	-8.22%	-4.66%	-4.67%

Next, the effect of the hull geometry distortion on the resistance components is invistigated. Mainly, the friction resistance and the residual-wave resistance will be looked at. The contribution of frictional and residual resistance depends on how much of the hull is below the waterline and the hull speed which influences the dynamic pressure on the body. Figure 3.10 shows the percentage contribution of the resistance components for the basic hull at different speeds. For slow speeds, the frictional resistance represents a considerable part of the total resistance $(70 - 90\%)$, and it drops at higher speeds. While the residual resistance increases significantly when speed increases above 12 knots. These trends are the same for all other hulls. Therefore, for slow ships like tankers and bulk carriers with big wetted area, more attention should be imposed to avoid the energy loss because of the hull friction.

Table 3.5 shows a comparison of the resistance components for three hulls which have same displacement and block coefficient. They are the basic hull, +10%L hull, and -10%L hull. The total resistance at all speeds for designs with long hulls are lower than the basic hull and short hulls.

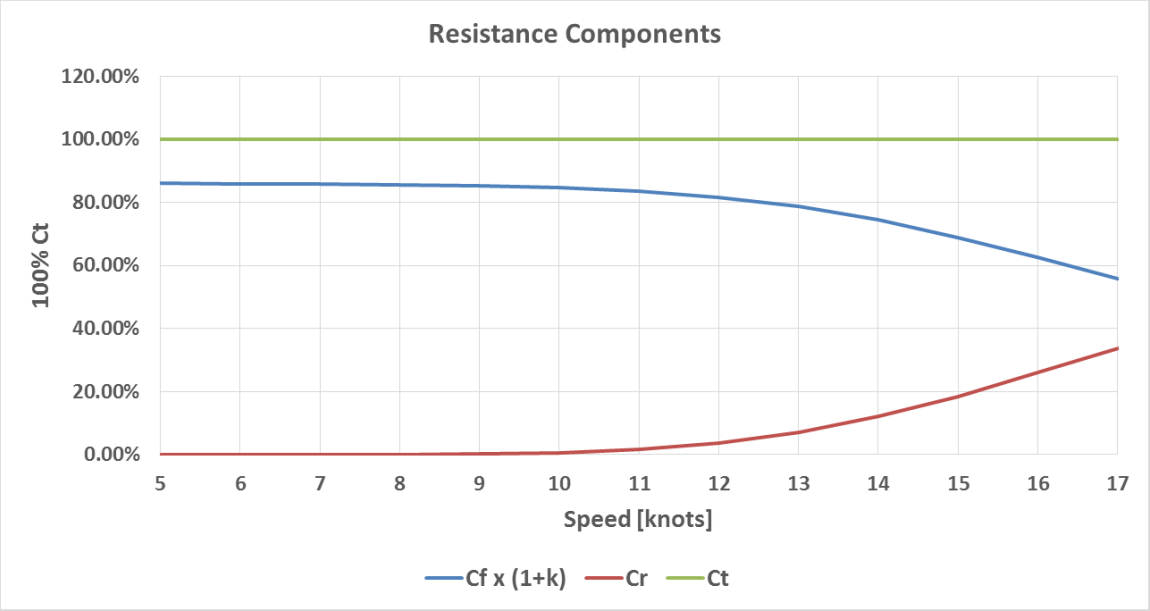

Figure 3.10 Friction Resistance and Wave Resistance Contribution of the Total Resistance

Table 3.5 Comparison of the Resistance Components for some Hulls

	Basic Hull			**+10%L Hull**			**-10%L Hull**		
Speed [knots]	R_F **[kN]**	R_r **[kN]**	R_T **[kN]**	R_F **[kN]**	R_r **[kN]**	R_T **[kN]**	R_F **[kN]**	R_r **[kN]**	R_T **[kN]**
5	76.16	0.00	88.35	76.16	0.00	88.01	76.49	0.00	88.97
6	107.05	0.00	124.61	107.09	0.00	124.15	107.51	0.00	125.48
7	142.89	0.00	166.79	142.95	0.00	166.18	143.46	0.00	167.91
8	183.47	0.09	214.78	183.59	0.09	214.02	184.20	0.08	216.22
9	228.87	0.55	268.94	228.88	0.58	267.86	229.63	0.53	270.58
10	278.72	2.19	329.70	278.99	2.01	328.40	279.84	2.22	331.96
11	333.44	6.80	399.27	333.41	6.24	397.01	334.49	7.43	402.31
12	392.48	18.15	480.88	392.67	15.88	476.81	393.75	20.69	486.31
13	455.99	41.69	580.12	456.48	35.10	571.69	457.69	49.68	591.71
14	524.00	85.41	705.03	524.36	69.90	687.17	525.95	105.75	729.52
15	596.60	160.33	866.69	597.11	127.28	831.05	598.48	204.59	915.35
16	673.19	278.89	1076.96	673.87	216.31	1011.55	675.58	365.88	1169.23
17	754.82	455.82	1351.62	755.36	346.43	1238.79	757.01	612.78	1514.01

Understanding the impact of the parametric distortion on the hydrodynamic and power requirements in depth needs to look to other hydrodynamic features more than the resistance coefficients. Figure 3.11 shows the results at the design speed 15 $knots$ for the first group of new hulls generated in Stage One. The new designs are compared with the basic hull over a

speed range $[5 \div 17]\ knots$ in order to explore the impact of slow steaming concept on the ship performance. Figure 3.12 & Figure 3.13 show same comparisons at different speeds $[10\ and\ 7]\ knots$, respectively.

The figures show that the hull efficiency η_H decreases when ship's length increases; bearing in mind that both the breadth and draught decrease as well to keep the displacement constant. This drop in the hull efficiency happens across all speeds, and it is in the range $[0.4 \div 0.5\ \%]$ for each $2.0\ \%$ increase in the hull length while it is vice versa for each $2.0\ \%$ decrease in the length. This penalty in the hull efficiency along the horizontal axis (increasing the ship's length) is because of the decrease in the wake fraction w which is a function of the breadth- length ratio B/L which has a significant influence on the wake of the vessel as the wake fraction tends to be smaller when this ratio increases.

The total efficiency of the propulsion system η_D is a function of the propeller open water efficiency η_O, relative rotative efficiency η_R, and the hull efficiency as in Eq (2.14). Results show that η_R is almost constant for all hulls ($\eta_R = 1.019$) while η_O varies slightly depending on the propeller parameters (diameter and pitch) and the rate of revolution. Hulls with deeper draughts can benefit of being capable of accepting propellers with larger diameter. Therefore, Stage One – First Group hulls with longer hulls will be fitted with smaller propellers as the draught is scaled down to keep the displacement constant.

The total efficiency is in a linear relation with the hull efficiency and propeller open water efficiency. Therefore, increasing the first design variable L while keeping the other variables constant $(B/T\ , C_B, LCB)$ results in a reduction in the efficiency of about $1.6\ \%$ for an $10\ \%$ increase in the hull length while reducing the breadth and draught by about $\left(1/\sqrt{1 + 10\%} = 4.65\ \%\right)$ to keep the displacement constant. Changes in the total efficiency can be seen in Figure 3.11 & Figure 3.12 & Figure 3.13 for speeds $[15, 10\ and\ 7]\ knots$ respectively.

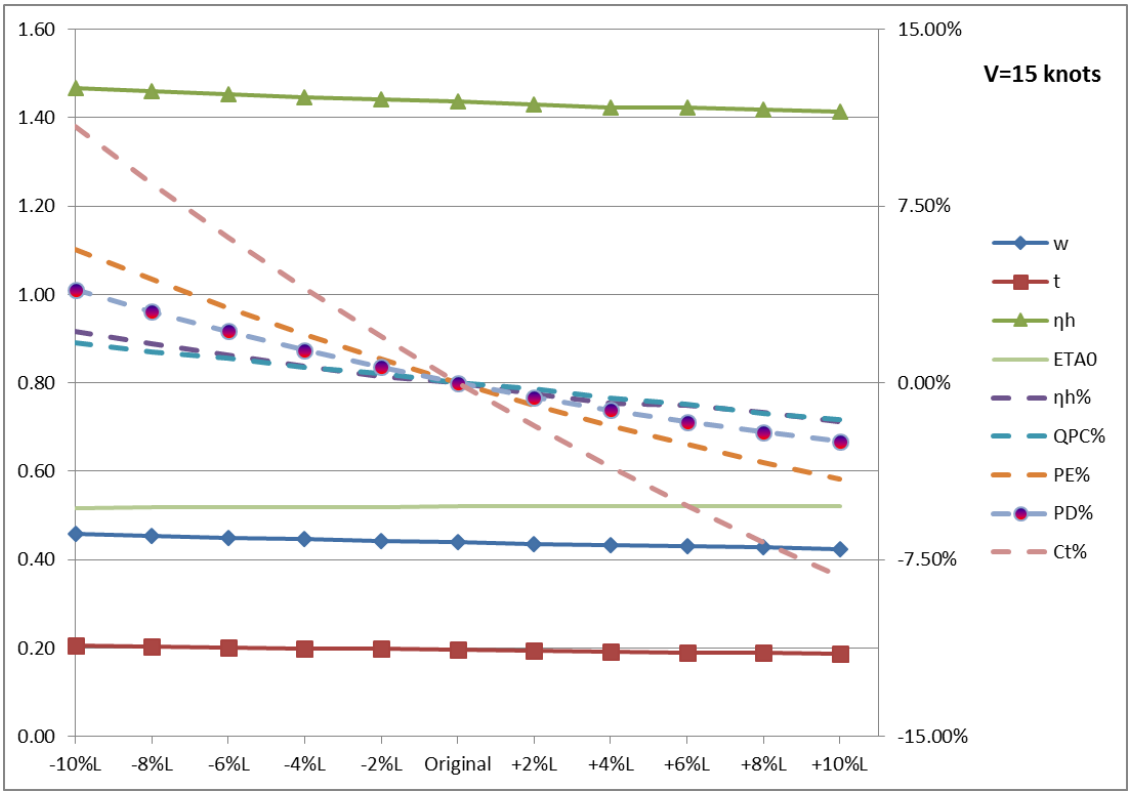

Figure 3.11 Hydrodynamic Performance for First Group – Stage One at 15 knots

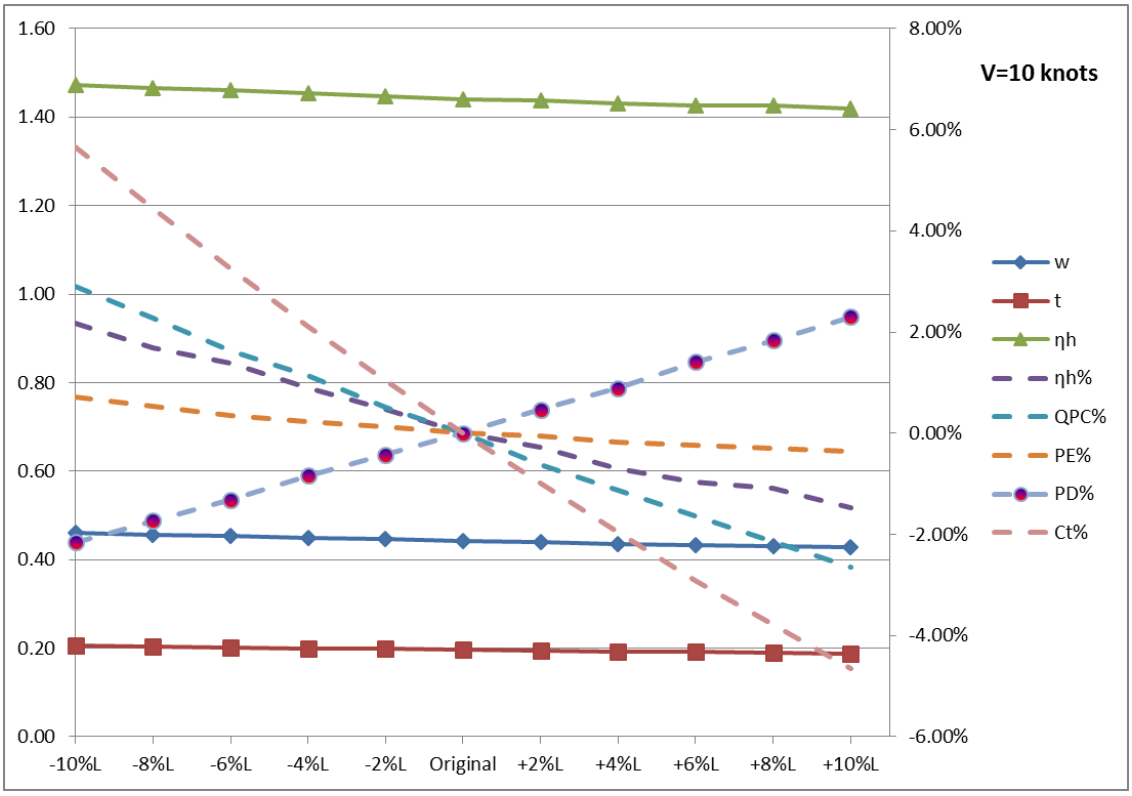

Figure 3.12 Hydrodynamic Performance for First Group – Stage One at 10 knots

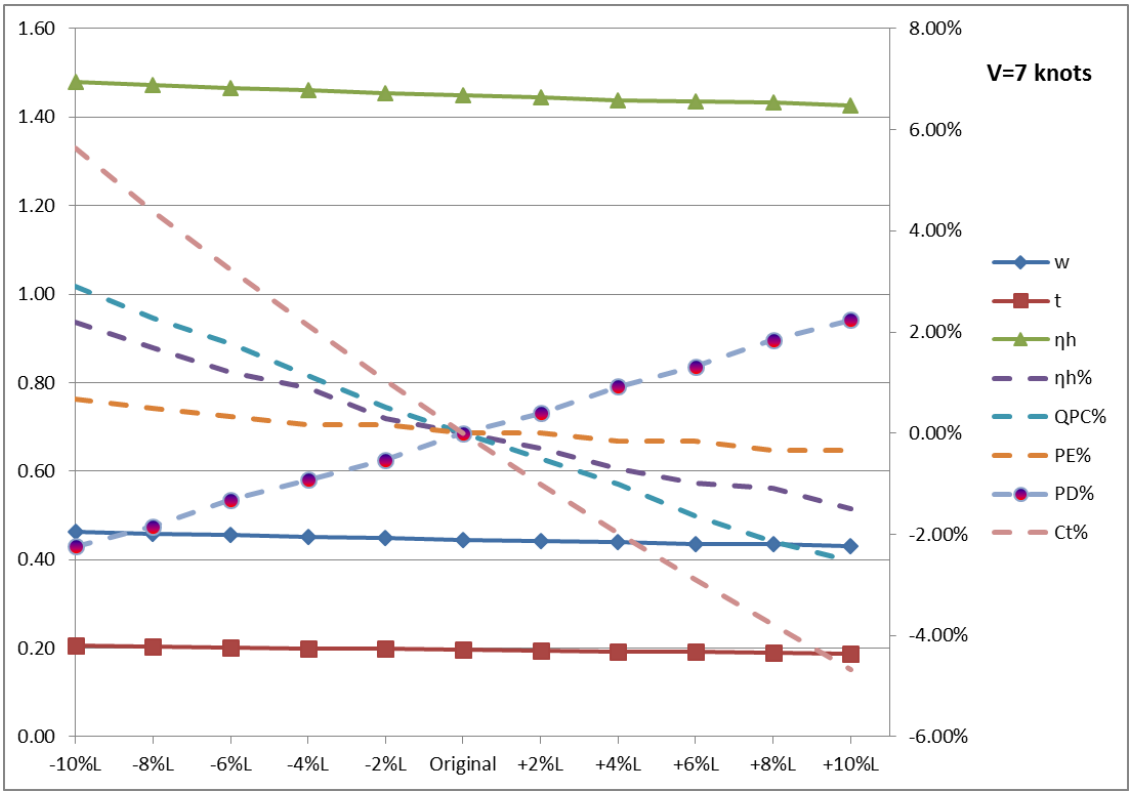

Figure 3.13 Hydrodynamic Performance for First Group – Stage One at 7 knots

It is vital to evaluate the influence of the main parameters on the power needed to be delivered to the propulsion unit P_D to propel the ship at any desired speed V. Figure 3.11 & Figure 3.12 & Figure 3.13 show that changing the hull length while keeping the breadth to depth ratio and the displacement constant, i.e. the hull is much slender comparing with the basic hull, has a significant impact on the required power. Basically, the delivered power is a function of the speed, resistance coefficient, wetted area, and the total efficiency $[P_D \sim f(C_T, S, V^3, 1/\eta_D)]$. Therefore, changing the main parameters does not have a specific trend on the required power.

The curves in Figure 3.14 represent the changes in the delivered power P_D for hulls from first group of Stage One over all speeds range. It is obvious that a significant saving in the power can be gained at speeds above 13 knots for ships with hulls longer than the basic hull $[+2 \div +10\%\ L]$. For speeds less than 13 knots, these hulls show a moderate increase in the required power. For the other half of the ships with shorter hulls $[-2 \div -10\%\ L]$, the impact on P_D is the opposite. A significant penalty occurs at high speeds above 13 knots as the required power increases significantly, while it tends to decrease for low speeds.

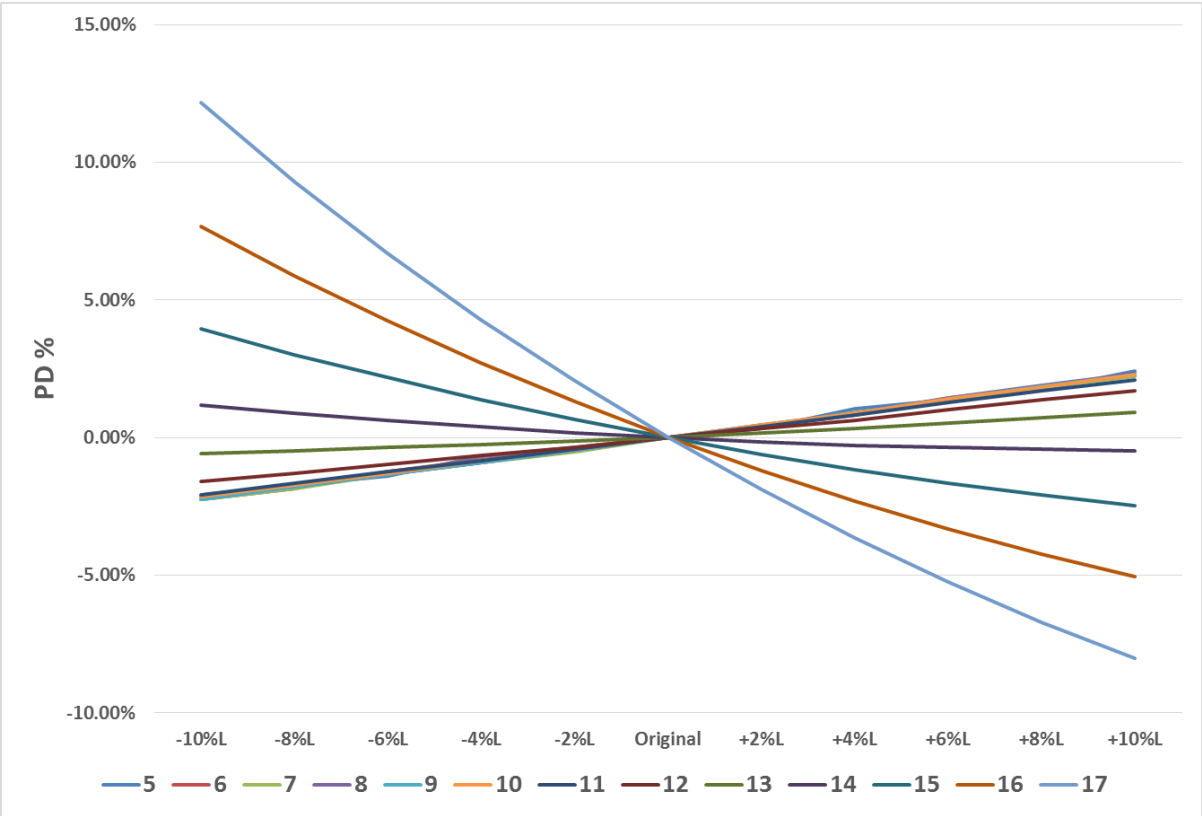

Figure 3.14 Changes in the delivered power at speeds range for First Group – Stage One

To illustrate the influence of varying hull parameters and speed on the required power, more examination is needed for the overlapping impact between the relevant factors. Taking $[+10\%\ L]$ hull as an example, it is obvious that it is more efficient at high speeds comparing with the basic hull and vice versa at slow speeds. Even though the total resistance coefficient decreases for slender hulls because of the improvements in the flow around the immersed hull, the wetted surface area increases. That is mainly because the wetted surface area is a function of the hull length and other hull parameters as can be seen in Mumford´s formula Eq (3.9) (Watson, 1998). The hull's wetted area increases by 4.5 % from $10103\ m^2$ to $10559\ m^2$ for the $[+10\%\ L]$ hull.

$$S = 1.025 \cdot LBP \cdot (C_B \cdot B + 1.7 \cdot T) \tag{3.9}$$

At the design speed, P_D decreases from $8785\ Kw$ for the original hull to $8567\ kW$ for the $[+10\%\ L]$ hull, and that is about -2.48% saving in power. This saving occurs because the hull resistance decreases as the reduction in the resistance coefficient is greater that the increase in the wetted surface and the loss in the total efficiency. At slow speeds the $[+10\%\ L]$ hull demonstrates an increase in the required power as the reduction in the resistance coefficient

does not compensate the increase in the wetted area and the loss in η_D. For instance, the delivered power at speed 10 knots increases by 2.3 %, and by 2.42 % at the slowest speed in the range; i.e. 5 knots.

Likewise, the other half of the generated hulls with full and shorter shapes demonstrate a moderate improvement in reducing the required power at a wide range of slow speeds (13 knots and less). The saving in the power as shown in Figure 3.14 is in the range $[-0.26 \div -2.25\ \%]$ for these hulls, and the maximum saving is for the shortest hull $[-10\%\ L]$. That is mainly because of the decrease in the wetted surface area and the increase in the hull efficiency η_D.

In conclusion, the overall variation in the delivered power at the tail-shaft from the reference power for the original hull at any speed depends on the changes in all factors $[P_D \sim f(C_T, S, V^3, 1/\eta_D)]$ simultaneously.

Similarly, AVEVA output for the second group of the generated hulls in Stage One is examined. In this set of hulls, the second primary variables i.e. the breadth to draught ratio B/T is varied while the other parameters are kept constant. That will result in maintaining the vessel's displacement as well. The B/T ratio varies within $[\pm 10\%]$ range from the parent value 2.648, and the changing step is $\delta x = 2\%$. The resulted ranges for the breadth and draught are $[30.595 \div 33.824]m$ and $[11.613 \div 12.839]m$, respectively. The results are shown in figures Figure 3.15 & Figure 3.16 & Figure 3.17 and Table 3.6 which in brief are as following:

- Varying the breadth to draft ratio B/T does not have a significant impact on the total resistance coefficient C_T. Within the design space, the maximum reduction in C_T is less than 1%, and it occurs for the $[-10\%\ B/T]$ hull as shown in Figure 3.15.
- Looking at the friction and residual components and the total resistance in Table 3.6, the results show that varying B/T does not have an important influence on the ship's resistance values. That is mainly because varying the breadth to draught ratio does not have a big impact on the wetted surface area and the body fullness while keeping the hull length constant. For instance, 10% increase in B/T causes less than 0.6% change in the wetted surface area which means the friction component of the total hull resistance remains almost constant.
- It can be seen that residual resistance; mainly wavemaking resistance, does not become important until the speed reaches high values.

- The rather minor reduction in the total resistance as a result of the B/T change can be of a high importance when its mutual impact on the ship performance with other modifications is considered.
- Figure 3.16 and Figure 3.17 show the hydrodynamic features of the second group hulls from stage one distortion process at two speeds (15 and 10 knots). The hull efficiency η_H, for all speeds, increases for hulls with greater breadth while decreases for slimmer bodies. That is because of the increase in the wake fraction w for greater values of B/T and B/L. The hull efficiency increases by 0.4 % for each 2.0 % increase in the breadth to draught ratio while it is vice versa for each 2.0 % decrease in the ratio. Moreover, the propeller open water efficiency η_O decreases in the case of hulls with bigger breadth and smaller draught while it increases for deeper bodies. For example, η_O for the basic hull is 0.521, while it is 0.547 for the $[-10\%\ B/T]$ hull. That equals 5 % gain the propeller open water efficiency.
- As mentioned before, the total efficiency of the propulsion system η_D is a function of the propeller open water efficiency η_O, relative rotative efficiency η_R, and the hull efficiency. Figure 3.16 and Figure 3.17 show that reducing the second variable B/T (slimmer and deeper hulls) while keeping the other design variables constant results in a high gain in the total efficiency of about 3.0 % for a 10 % reduction in the breadth to draught ratio. This gain in the total efficiency can be achieved at all speeds as the results show.
- Examining the delivered power P_D curves shows that deeper hulls with smaller breadth $[-2 \div -10\%\ B/T]$ can achieve a reasonable reduction in the required power. For instance, the reduction in the delivered power is around 4.5 % for the $[-10\%\ B/T]$ hull comparing with the original hull at the design speed and other speeds as well. That is mainly because of the higher efficiency η_D and the smaller wetted area. On the other hand, designs with wider and shallower hulls; while keeping the length and displacement constant; show an increase in the delivered power needed to propel the ship at any desired speed V.

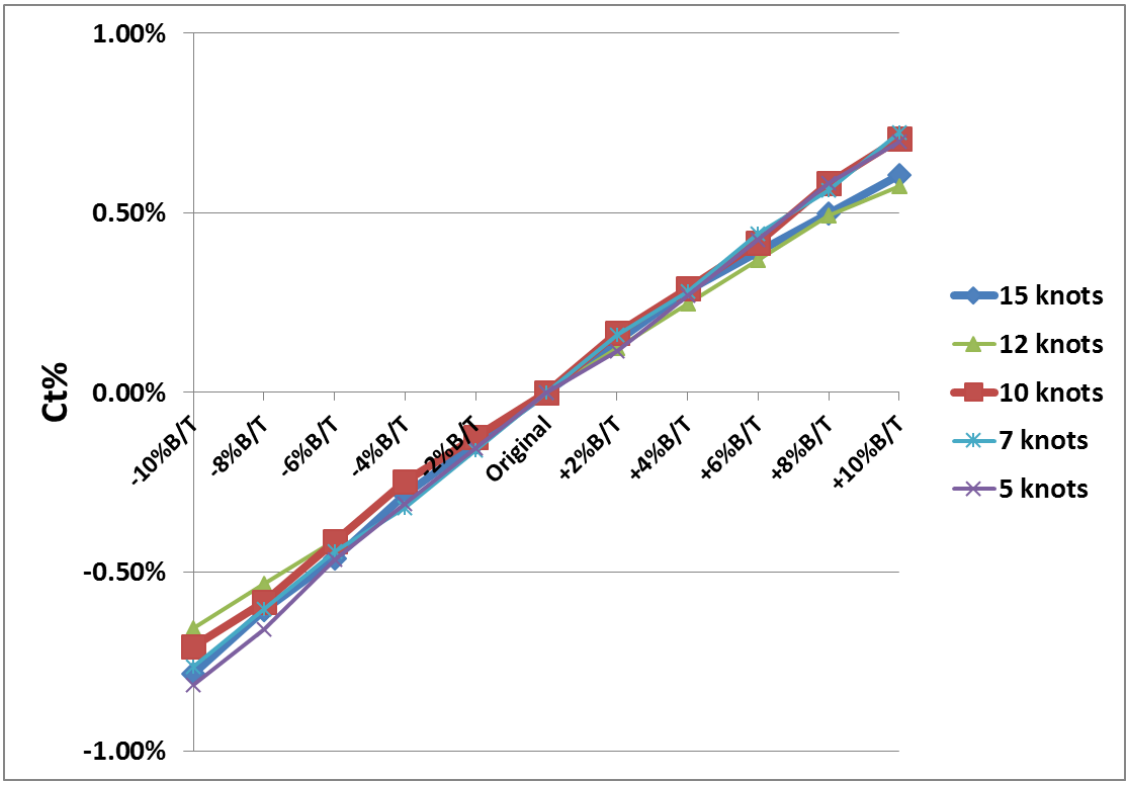

Figure 3.15 Changes in the total resistance coefficient for Second Group – Stage One

Table 3.6 Comparison of the Resistance Components for some Hulls (Second Group – Stage One)

	Basic Hull			+10%B/T Hull			-10%B/T Hull		
Speed [knots]	R_F [kN]	R_r [kN]	R_T [kN]	R_F [kN]	R_r [kN]	R_T [kN]	R_F [kN]	R_r [kN]	R_T [kN]
5	76.16	0.00	88.35	77.26	0.00	89.53	75.19	0.00	87.35
6	107.05	0.00	124.61	108.63	0.00	126.29	105.72	0.00	123.22
7	142.89	0.00	166.79	144.95	0.00	169.00	141.09	0.00	164.91
8	183.47	0.09	214.78	186.15	0.09	217.64	181.14	0.09	212.33
9	228.87	0.55	268.94	232.13	0.45	272.33	225.93	0.55	265.86
10	278.72	2.19	329.70	282.86	2.07	334.00	275.24	2.18	326.03
11	333.44	6.80	399.27	338.26	6.50	404.14	329.08	6.94	394.83
12	392.48	18.15	480.88	397.99	17.67	486.32	387.50	18.28	475.78
13	455.99	41.69	580.12	462.66	41.23	586.82	450.17	41.76	574.07
14	524.00	85.41	705.03	531.44	85.38	713.00	517.27	85.10	697.63
15	596.60	160.33	866.69	605.11	161.28	876.80	588.89	158.20	856.45
16	673.19	278.89	1076.96	683.18	283.01	1091.82	664.78	272.97	1062.18
17	754.82	455.82	1351.62	765.67	465.30	1372.80	745.35	443.50	1329.31

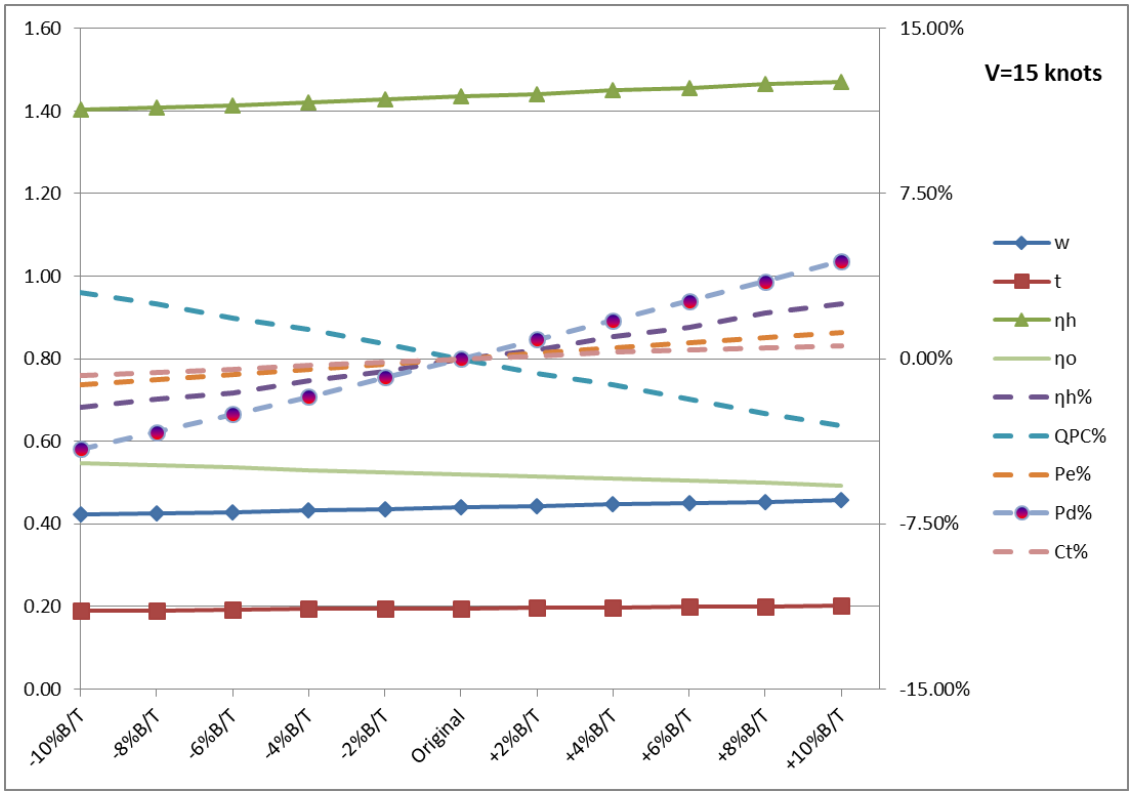

Figure 3.16 Hydrodynamic Performance for Second Group – Stage One at 15 knots

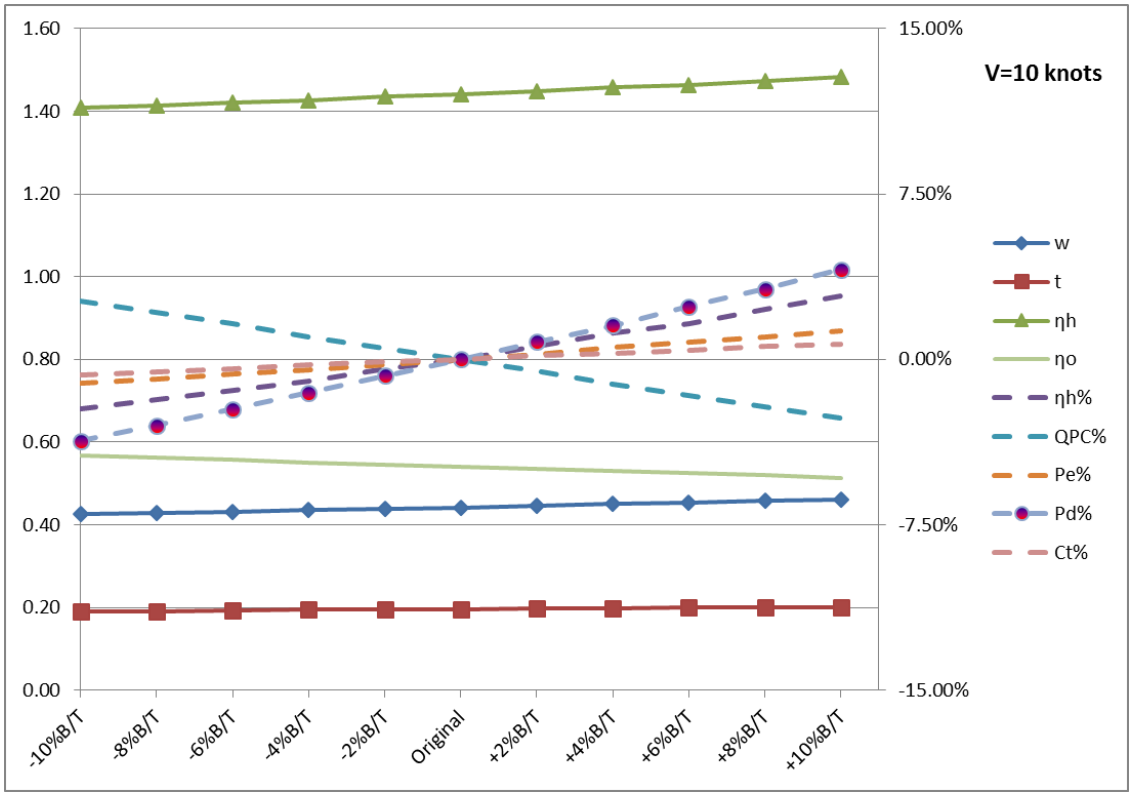

Figure 3.17 Hydrodynamic Performance for Second Group – Stage One at 10 knots

The third design variable in the parametric analysis is the block coefficient C_B. In order to understand the direct influence on the ship performance when the block coefficient is changed within the upper and lower bounds of the constrained design space, the process of the parametric distortion has kept the other design variables constant. Therefore the main hull parameters i.e. length, breadth, and draft are fixed. That implies the ship displacement will not be kept constant, and it changes at the same rate as the block coefficient changes. C_B varies within $[\pm 6\%]$ from the parent value 0.8254, and the changing step is $\delta x = 2\%$. Hence, C_B values vary in the range $[0.776 \div 0.875]$.

Based on hydrodynamic considerations, the block coefficient should decrease with an increasing speed and Froude number. The normal ship design practice has proved that this basic guideline leads to a considerable improve in ships' hydrodynamic performance. The direct influence on the hull hydrodynamic performance and the propulsion power at a wide range of speeds is summarised as following:

- Varying the block coefficient C_B has a significant impact on the total resistance coefficient C_T as shown in Figure 3.18. Designs with smaller fullness coefficient show a considerable reduction in C_T. For example, at the design speed (15 knots), the reduction for the $[-6\%\ C_B]$ hull reaches 10% while it is around 4% for speeds less than 10 knots. On the other hand, C_T values for hulls with greater fullness coefficient increase significantly especially at high speeds. At the design speed, the $[+6\%\ C_B]$ hull shows a significant increase in the resistance coefficient and it reaches 25%.
- Examining the friction and residual components and the total resistance in Table 3.7 shows that varying C_B has major impact on the resistance. First of all, any increase in the block coefficient increases the wetted surface area which leads to an increase in the friction resistance. The wetted surface area for the basic hull is $(10103\ m^2)$, and $(10505\ m^2)$ for the $[+6\%\ C_B]$ hull, and it is $(9730\ m^2)$ for the $[-6\%\ C_B]$ hull. Also, the water flow around the hull and waves generated along the hull act on the hull in a larger amplitude on designs with fuller bodies comparing with fine and slim bodies that benefit form a smoother water filed acting on the hull.
- The total resistance at the design speed for the basic hull is (866.69 kN), and it drops to (748.58 kN) for the $[-6\%\ C_B]$ hull, and that equals about 14% reduction. However, this 14% drop in the total resistance includes 43% drop in the residual resistance and 8% drop in the friction resistance which represents about 74% of the total resistance. Also,

at slow speeds up to 10 knots, the reduction in the total resistance is about 7%. On the other hand, hulls with greater C_B experience a significant increase in the resistance. It reaches 30% for the $[+6\%\ C_B]$ hull at the design speed (15 knots), 47% at speed 17 knots, and about 10% for speeds up to 10 knots. The increase in the friction resistance at the design speed is about 11% while it is 122% for the residual resistance.

- The hydrodynamic features for hulls from the third group - stage one are shown in Figure 3.19, Figure 3.20, and Figure 3.21 at speeds (15, 12, and 7 knots), respectively. The hull efficiency η_H, for all speeds, increases for hulls with greater block coefficient while decreases for slimmer bodies. That is because of the increase in the wake fraction w in the case of fuller bodies. Moreover, the propeller open water efficiency η_O decreases in the case of hulls with greater block coefficient while it increases for thinner bodies. For example, η_O for the basic hull is 0.521, while it is 0.574 for the $[-6\%\ C_B]$ hull at the design speed. That means 10 % gain in the propeller open water efficiency.
- The total efficiency QPC for hulls with greater block coefficient increases significantly at slow speeds as the hydrodynamic performance figures show. It increases by about 7% and 5% for the $[+6\%\ C_B]$ hull at speeds (7 and 12 knots), respectively, while it drops by 0.5% at the design speed.
- Since varying the block coefficient individually while keeping the other variables constant does not keep the displacement constant, then using the delivered power to compare the energy requirements for the new hulls with the reference hull is not efficient. Therefore, the (delivered power /displacement) curve is used to investigate the influence of the block coefficient on the ship performance. Results show that any increase in the block coefficient introduces a significant impact on the propulsion power requirements. At the design speed, for instance, P_D/Dis increases by about (5%, 12%, and 24%) for the $[+2\%, 4\%, and\ 6\%\ C_B]$ hulls respectively. For the $[-2\%, 4\%, and\ 6\%\ C_B]$, this ratio decreases by about (3%, 5%, and 6%) respectively at the design speed. These hulls follow the same trend for the 12 knots speed but the opposite trend for the 7 knots speed.

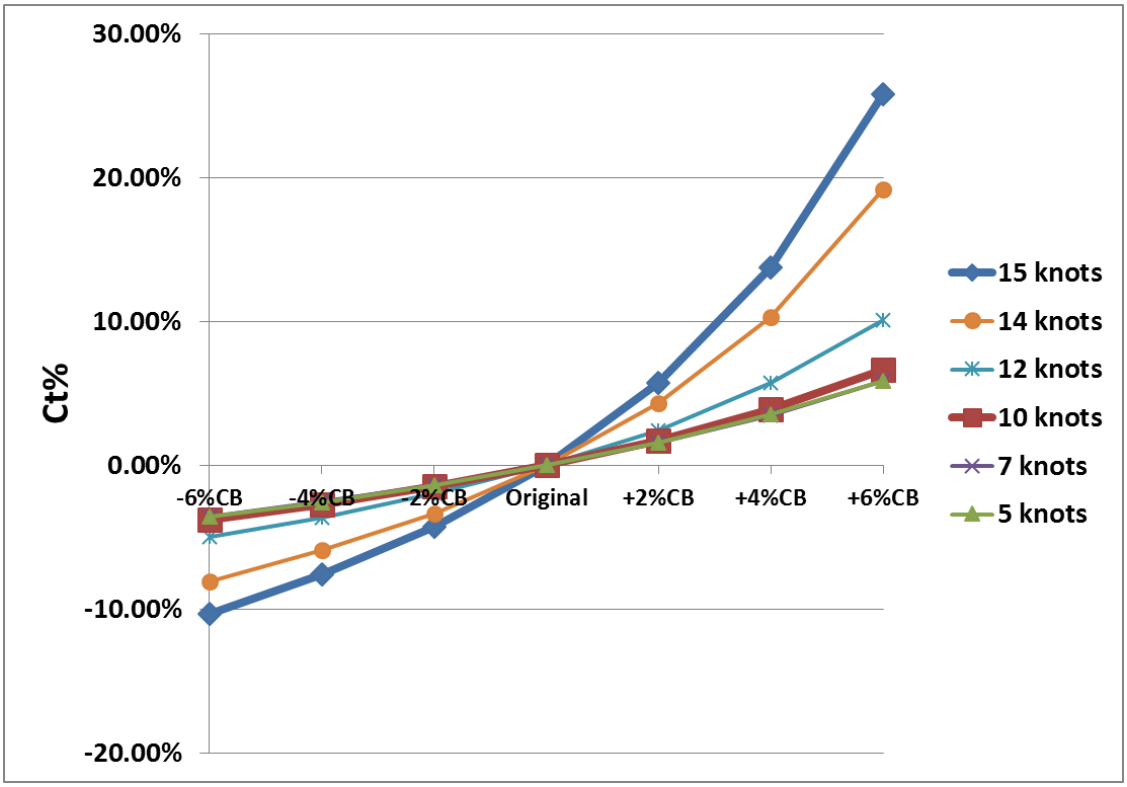

Figure 3.18 Changes in the total resistance coefficient for Third Group – Stage One

Table 3.7 Comparison of the Resistance Components for some Hulls (Third Group – Stage One)

	Basic Hull			+6%CB Hull			-6%CB Hull		
Speed [knots]	R_F **[kN]**	R_r **[kN]**	R_T **[kN]**	R_F **[kN]**	R_r **[kN]**	R_T **[kN]**	R_F **[kN]**	R_r **[kN]**	R_T **[kN]**
5	76.16	0.00	88.35	84.60	0.00	97.28	70.31	0.00	82.05
6	107.05	0.00	124.61	118.95	0.00	137.21	98.87	0.00	115.78
7	142.89	0.00	166.79	158.76	0.00	183.62	131.98	0.00	155.01
8	183.47	0.09	214.78	203.81	0.18	236.46	169.43	0.08	199.58
9	228.87	0.55	268.94	254.25	1.27	296.61	211.34	0.32	249.71
10	278.72	2.19	329.70	309.76	4.99	365.47	257.35	1.19	305.52
11	333.44	6.80	399.27	370.33	15.86	447.57	307.88	3.67	368.40
12	392.48	18.15	480.88	436.00	41.45	550.49	362.41	10.07	440.13
13	455.99	41.69	580.12	506.64	94.39	686.76	421.09	23.42	523.91
14	524.00	85.41	705.03	582.00	191.86	873.27	483.71	48.63	624.42
15	596.60	160.33	866.69	662.98	356.82	1133.93	550.82	92.05	748.58
16	673.19	278.89	1076.96	748.12	616.08	1494.06	621.64	161.49	903.41
17	754.82	455.82	1351.62	838.79	1001.04	1986.42	696.82	265.84	1098.43

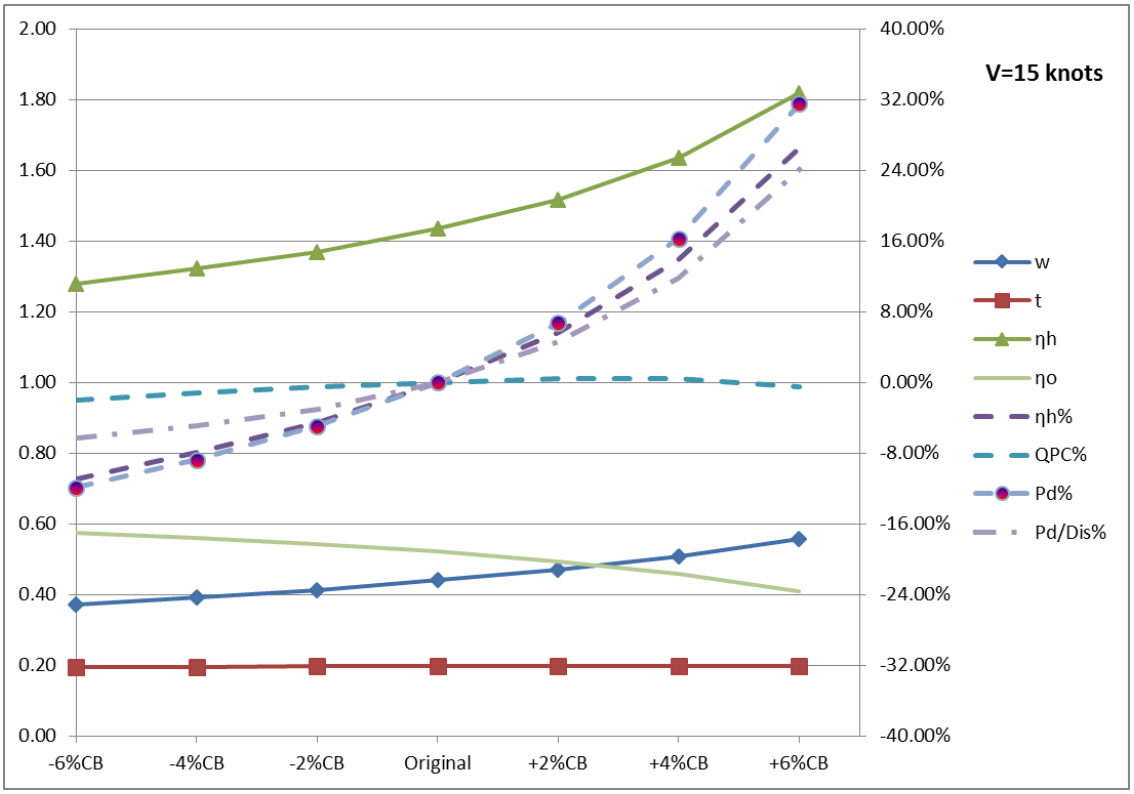

Figure 3.19 Hydrodynamic Performance for Third Group – Stage One at 15 knots

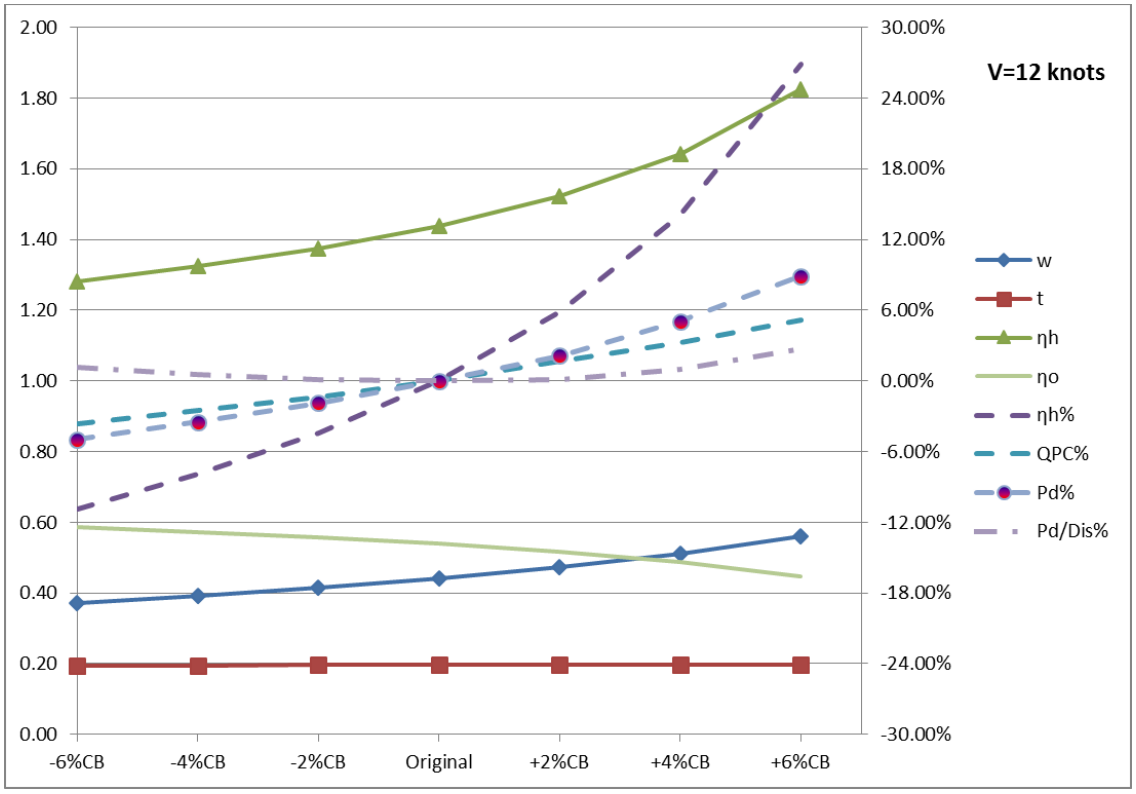

Figure 3.20 Hydrodynamic Performance for Third Group – Stage One at 12 knots

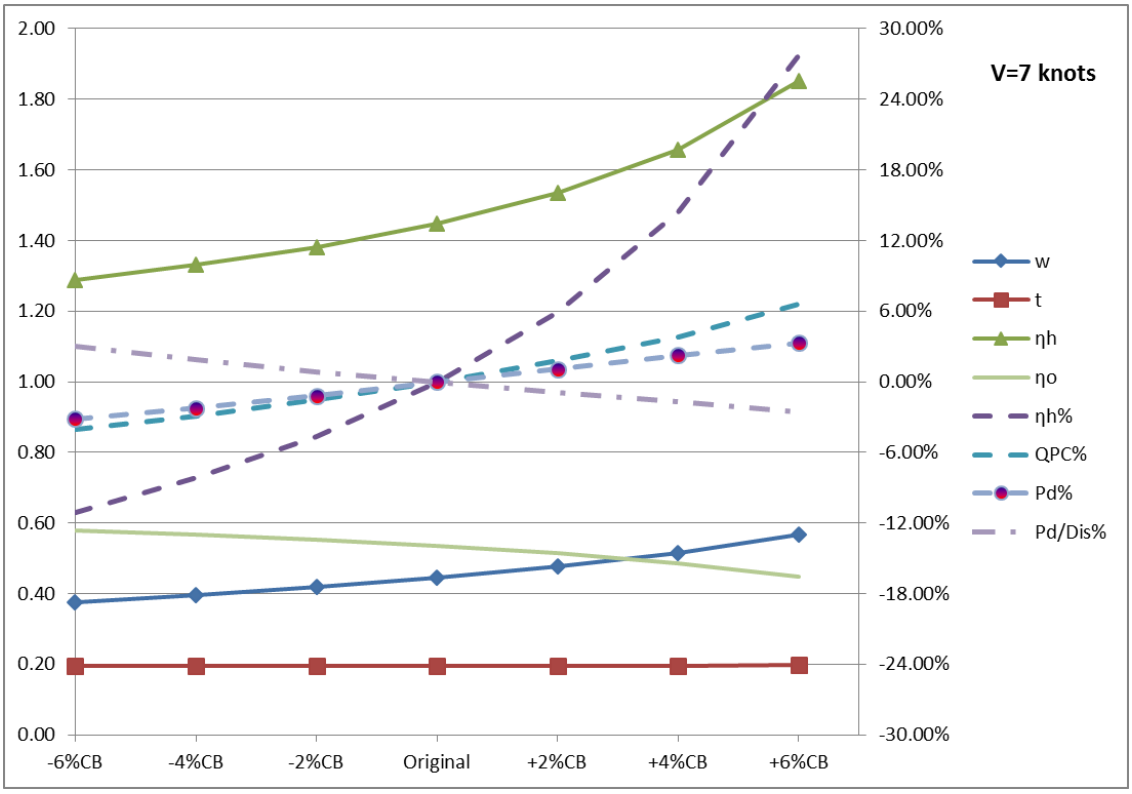

Figure 3.21 Hydrodynamic Performance for Third Group – Stage One at 7 knots

The final design variable, in the first stage of the parametric analysis, to discuss its influence on the hydrodynamic performance is the longitudinal centre of buoyancy LCB. The optimum position of LCB is governed by the need to achieve a satisfactory trim, and the demand for minimum power. However, it is certainly more accurate to think in terms of an optimum range rather than an optimum position. The range differs for ships with normal bows and bulbous bows, and for ships with single or twin-screw ships. The LCB optimum range depends mainly on Froude number and the block coefficient (Watson, 1998).

The lower and upper values of LCB are subjected to the recommendations regarding the optimum range for the LCB position. For the basic hull's block coefficient value in this case study, the chosen upper and lower limits to vary LCB are $[-1.0\%L]$ and $[+1.0\%L]$, and the step for the modified hulls is $0.2\%L$. Studies have shown that varying LCB while keeping other design parameters constant is not considered to have a significant impact on the hydrodynamic performance. Before discussing its impact, it is worth mentioning that the ship's displacement does not stay constant but it changes as a result of the hull geometry modification to achieve the desired position of LCB. However, the changes in the hull displacement for this case are very modest and do not exceed 0.2%. Therefore, it is assumed that the changes in the

displacement are negligible, and the displacement is kept constant while varying LCB. AVEVA results are summarised as following:

- Varying the longitudinal centre of buoyancy LCB has a minor impact on the total resistance coefficient C_T as shown in Figure 3.22. At high speeds, designs with more advanced position of LCB show a small increase in C_T while designs with a rearward LCB position show a small reduction in C_T. On the other hand, at speeds lower than 12 knots, the trends are the opposite but the changes are not significant and less than 0.5%.
- The greatest changes appear at higher speeds. For example, at the design speed (15 knots), the reduction in C_T for the $[-1\%L, LCB]$ hull is less than 1%, and the increase in C_T is about 1.5% for the $[+1\%L, LCB]$ hull.
- Table 3.8 shows a comparison of the friction and residual components and the total resistance of two hulls have different LCB values with the original hull. The hydrostatics particulars from AVEVA show that the wetted surface area is almost constant for these hulls as it is $(10103, 10107, 10101\, m^2)$ for the original, $[-1\%L, LCB]$ and $[+1\%L, LCB]$ hulls respectively. Therefore, the frictional component of the total resistance will slightly change and can be considered constant.
- The total resistance changes mainly as a result of the changes in the residual resistance that occur because of the alterations in the water flow behaviour in the boundary area, and the changes in the water pressure and waves amplitudes along the hull. The $[+1\%L, LCB]$ hull with advanced position of LCB experiences a noteworthy increase in the residual resistance (10.18%) at the design speed for example. That results in a moderate increase in the total resistance of about 1.56% (880.17-866.69 kN). On the contrary, the $[-1\%L, LCB]$ hull with rearward position of LCB shows a 7% reduction in the residual resistance at the design speed. That accounts for about 1% reduction in the total resistance (858.71-866.69 kN). Moreover, it is obvious that varying LCB has insignificant impact on the bare hull total resistance at slow speeds as the percentage change is less than 0.4%.
- Figure 3.23 and Figure 3.24 show examples of the hydrodynamic features for the hulls from the fourth group – stage one at two speeds (15, and 7 knots) respectively. The hull efficiency η_H, for all speeds, decrease for hulls with advanced LCB position while it increases for bodies with rearward LCB position. The open water efficiency for the propeller η_O is constant as all designs have the same optimum propeller. Consequently,

the total efficiency QPC for hulls with rearward LCB position increases up to 2.5% for the $[-1\%L, LCB]$ hull over all the speeds range, and decreases for hulls with advanced LCB position.

- Examining the delivered power curves shows that hulls with rearward LCB position achieve a reasonable reduction in the required power. The saving in the delivered power for $[-1\%L, LCB]$ hull, for instance, is in the range of (3.5% for high speeds ÷ 1.8% for slow speeds) comparing with the original hull. This saving in the power is a result of the improvement in the hull performance including the increase in the total efficiency and the drop in the bare hull resistance. On the other hand, the second group of hulls with advanced LCB position experience an increase in the required power that reaches 3.75% at the design speed.

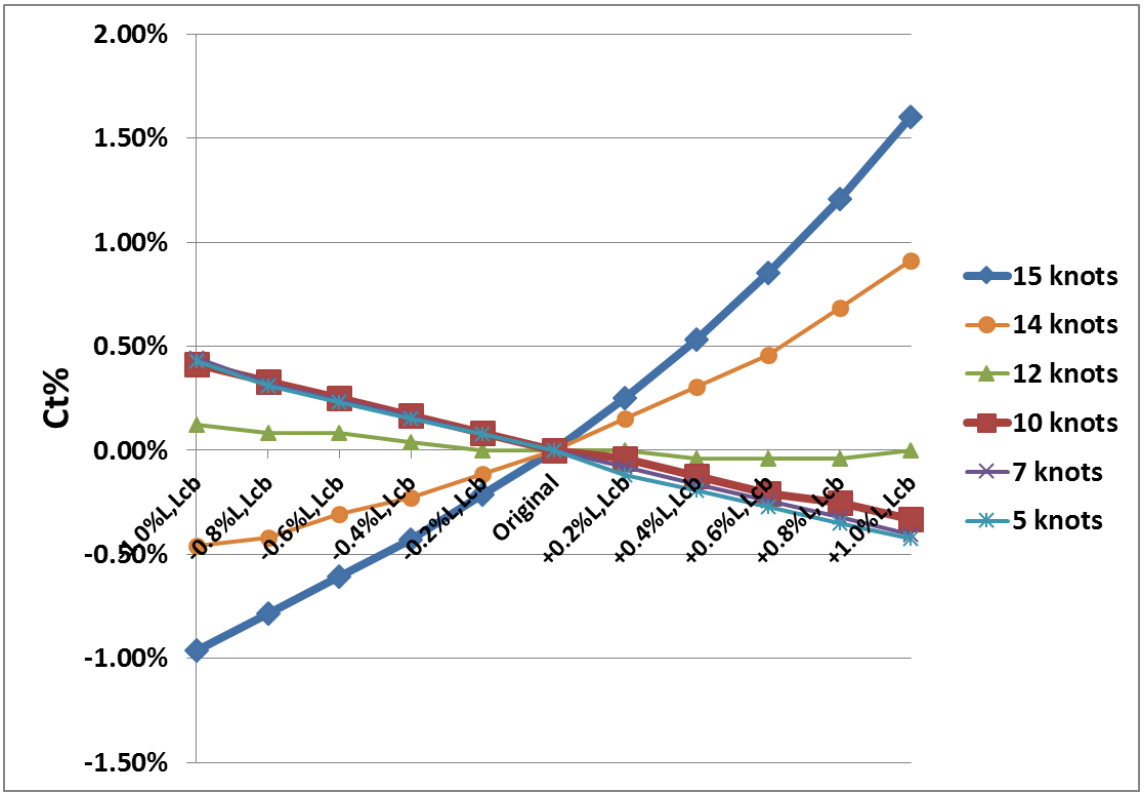

Figure 3.22 Changes in the total resistance coefficient for Fourth Group – Stage One

Table 3.8 Comparison of the Resistance Components for some Hulls (Fourth Group – Stage One)

	Basic Hull			+1.0%L, LCB Hull			-1.0%L, LCB Hull		
Speed [knots]	R_F **[kN]**	R_r **[kN]**	R_T **[kN]**	R_F **[kN]**	R_r **[kN]**	R_T **[kN]**	R_F **[kN]**	R_r **[kN]**	R_T **[kN]**
5	76.16	0.00	88.35	76.56	0.00	88.76	75.77	0.00	87.97
6	107.05	0.00	124.61	107.63	0.00	125.20	106.55	0.00	124.11
7	142.89	0.00	166.79	143.68	0.00	167.59	142.20	0.00	166.10
8	183.47	0.09	214.78	184.42	0.09	215.74	182.57	0.09	213.88
9	228.87	0.55	268.94	230.07	0.44	270.05	227.74	0.55	267.81
10	278.72	2.19	329.70	280.20	1.92	330.93	277.46	2.33	328.57
11	333.44	6.80	399.27	335.23	6.30	400.59	331.75	7.46	398.23
12	392.48	18.15	480.88	394.61	16.78	481.67	390.47	19.93	480.64
13	455.99	41.69	580.12	458.49	38.69	579.65	453.86	45.85	582.14
14	524.00	85.41	705.03	526.90	79.53	702.08	521.54	94.26	711.40
15	596.60	160.33	866.69	599.92	148.98	858.71	593.77	176.65	880.17
16	673.19	278.89	1076.96	676.96	259.34	1061.24	669.96	307.62	1102.46
17	754.82	455.82	1351.62	759.08	423.91	1324.03	751.18	502.90	1395.05

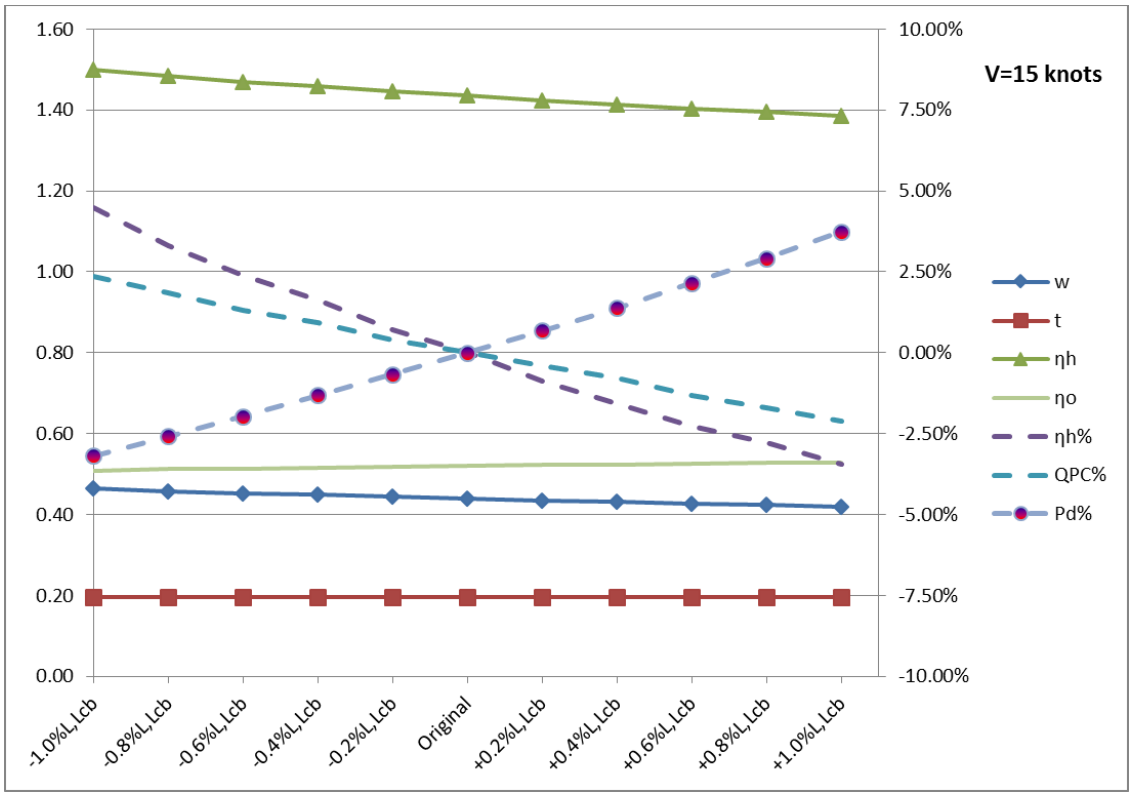

Figure 3.23 Hydrodynamic Performance for Fourth Group – Stage One at 15 knots

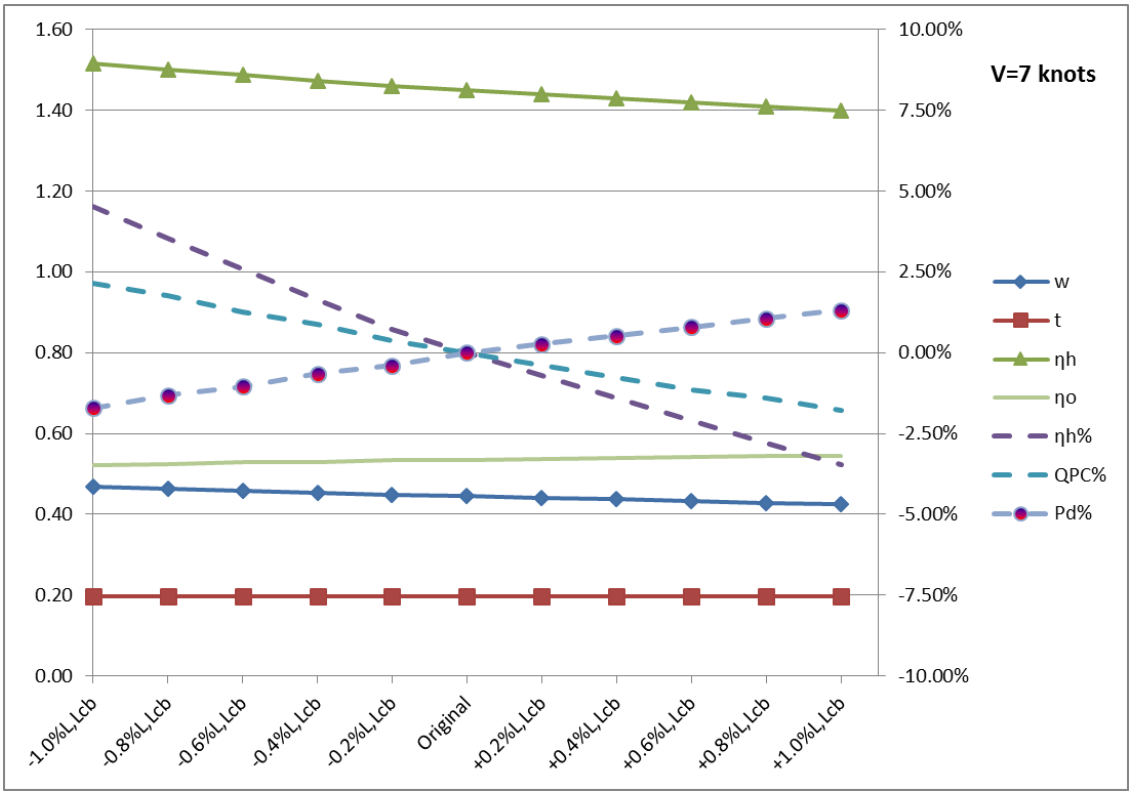

Figure 3.24 Hydrodynamic Performance for Fourth Group – Stage One at 7 knots

3.6.2 Stage Two Results

After considering the impact of the individual design parameters on the vessel's hydrodynamic performance, Stage Two of the parametric analysis investigates the combined impact of the two primary design parameters. The ship length and breadth/draft ratio $[L,\ B/T]$ will be varied simultaneously, therefore there are (10x11=110) new hull forms that are geometrically distorted using AVEVA Lines Module.

In Stage One, the influence of the four design variables on several hydrodynamic and power characteristics was invistigated to gain a better understanding of how to improve the hull performance by selecting the most optimum parameters based on their individual impact. However, the only objective function that is considered in Stage Two is the delivered power to displacement ratio as as the main focus is only on the final impact of these variables on the ship performance and profit. AVEVA results are presented graphically as a surface chart against both parameters at some selected speeds as shown in Figure 3.25, Figure 3.26, and Figure 3.28.

From the graphs below, it is obvious that both design parameters have a significant impact on the requuired power. Results show that the power needed at the tail-shaft per displacement unit

is reduced at all speeds for longer, deeper hulls with smaller beams. The maximum reduction in P_D/Dis is achieved by the $[+10\%L, -10\%\, B/T\,]$ hull. For example, at the design speed, the reduction in P_D/Dis is significant, and it is about 12% comparing with the reference design. At other speeds (12, 10, 7 knots), the saving in the required power per displacement unit is notable, and the results show that it reaches (7.15%, 6.36%, 6.34%), respectively.

On the other hand, from hydrodynamic point of view, the $[-10\%L, +10\%\, B/T\,]$ hull supports the finidngs from Stage One. Designs with shorter, wider and shallower hulls show an increase in the delivered power needed to propel the ship at any desired speed V taking into account the ship's displacement. For instance, P_D/Dis increases by more than 15% for the $[-10\%L, +10\%\, B/T\,]$ hull at the design speed, and by around 8% at the other selected speeds.

It is interesting to notice that $P_D/Dis\,\%$ and $P_D\%$ curves are very steep at high speeds and tend to be constant at slow speeds as can be seen in Figure 3.29 where the $[+10\%L, -10\%\, B/T\,]$ hull is used for illustration. Moreover, it is surprising to note that even the displacement is greater by 10%, the required power tends to be less comparing with the basic hull for speeds over 14 knots. That is a strong indicator that choosing the right parameters and operating speed can lead to a significant increase in the hull efficiency and a substantial reduction in the required power and fuel consumption.

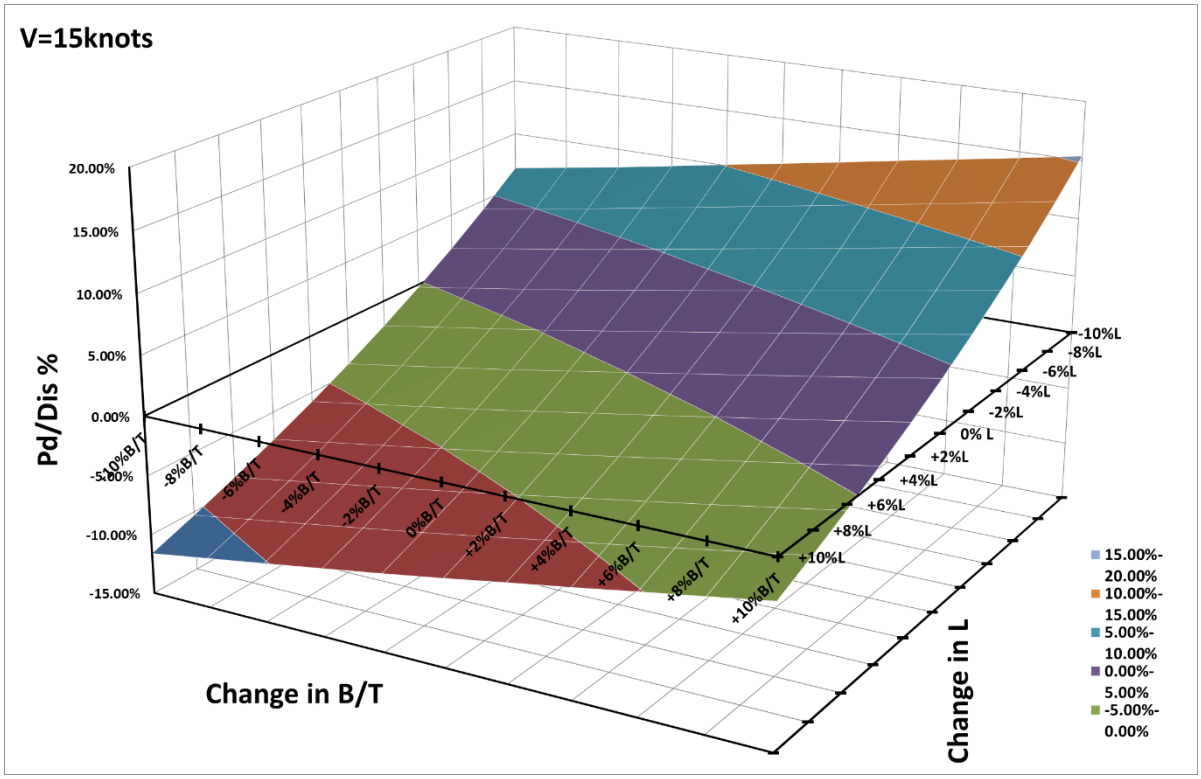

Figure 3.25 Change in Delivered Power to Displacement Ratio at 15 knots speed

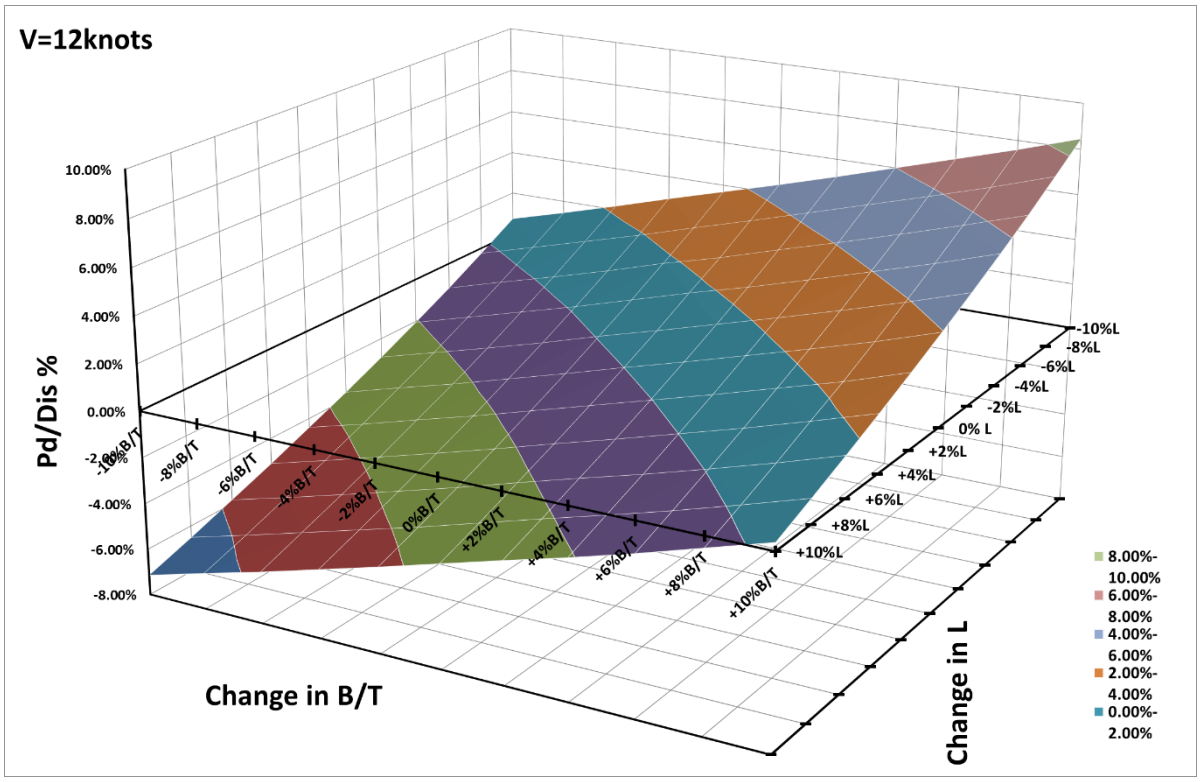

Figure 3.26 Change in Delivered Power to Displacement Ratio at 12 knots speed

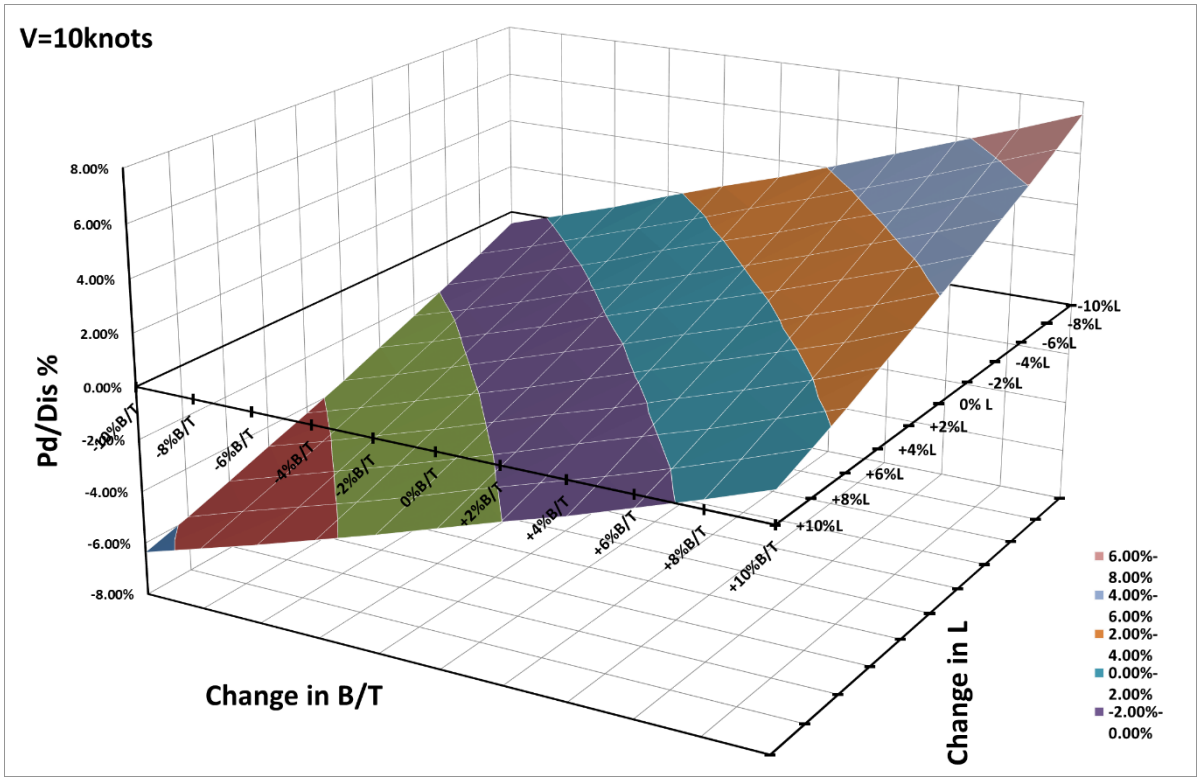

Figure 3.27 Change in Delivered Power to Displacement Ratio at 10 knots speed

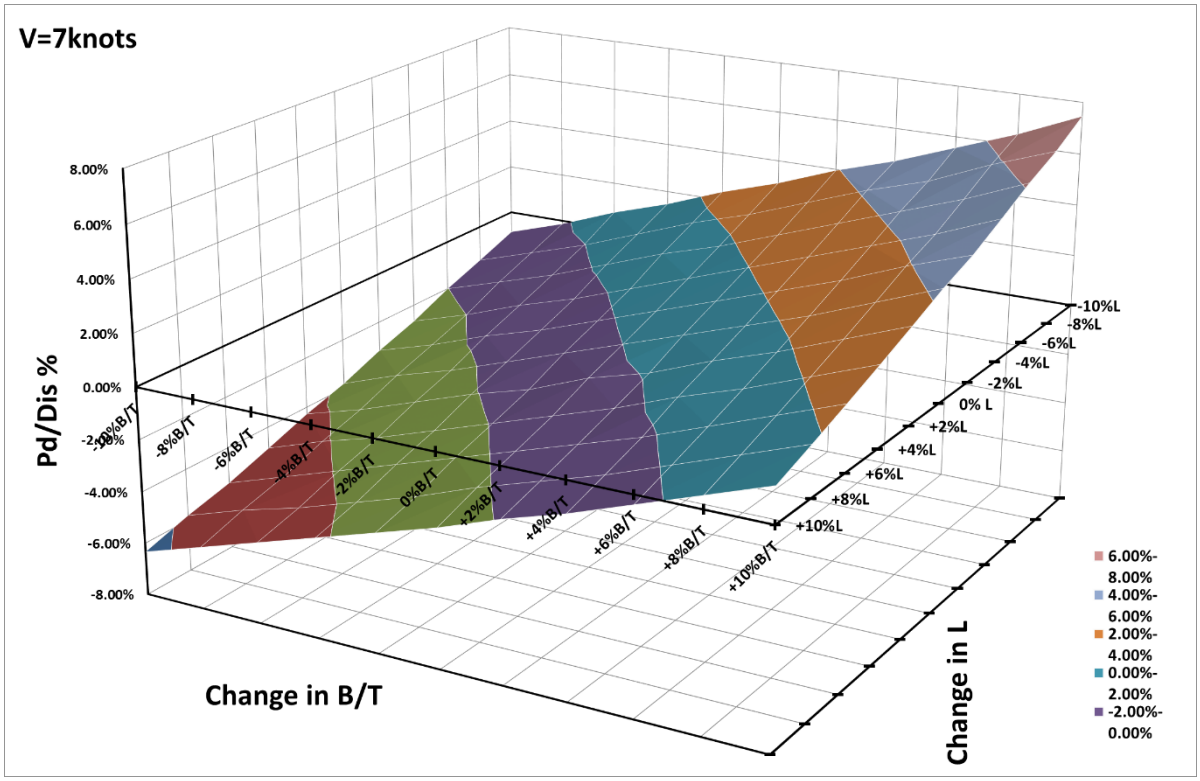

Figure 3.28 Change in Delivered Power to Displacement Ratio at 7 knots speed

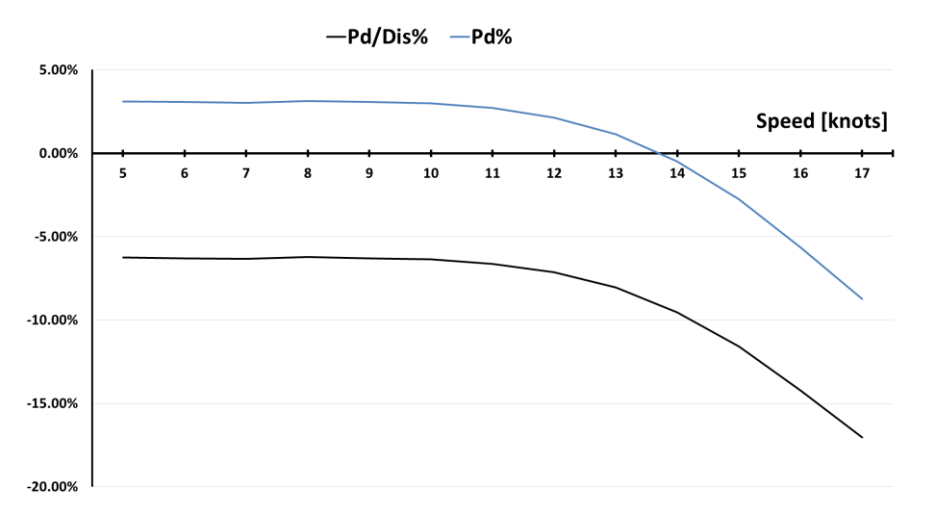

Figure 3.29 Changes in P_D/Dis and P_D for the hull [+10%L, -10%B/T]

3.6.3 Stage Three Results

In the final stage of the geometric distortion and parametric analysis process, the aim is to investigate the influence of changing the controllable primary and secondary design variables simultaneously on the hull performance over the speed range. Moreover, this research aims to explore the design space and choose alternative hull forms that demonstrate an equal or better hydrodynamic performance.

The required power quantities are selected to be minimized, and that will undoubtedly reduce the fuel consumption and greenhouse emissions. However, since the hull displacement varies among all hulls, and to keep the problem relatively simple and consistent among all the generated hulls, minimizing the delivered power to displacement ratio is used as the objective function (response parameter) considering the constraints set by the upper and lower bounds of the design variables.

In order to measure the variation in the response parameter, there is a need to address the response parameter using the control parameters based on the results from AVEVA as shown in Eq (3.10):

$$Y = f(X_i) = P_D/Dis$$
$$X_i = [L, B/T, C_B, LCB\%L, V] \quad (3.10)$$

where:

$Y = f(X_i)$: the response parameter which will be used as an indicator for the hydrodynamic performance for this stage [kW/ton].

X_i: the design parameters array for the optimisation problem including the hydrostatics particulars and the operating speed. The following symbols are used to indicate these variables:

Variable	**Symbol**
L	x_1
B/T	x_2
C_B	x_3
$LCB\%L$	x_4
V	x_5

Mimitab17 and the Regression Tool built in EXCEL are used to run the regression analysis, and they gave the same regression formulas as they both use the same statistical process for estimating the relationships among variables. However for the purpose of increasing the accuracy of the equations, data from all generated hulls was divided into 4 groups depending on the speed ranges from very slow to very high.

The following regression equations were obtained to estimate the delivered power to displacement ratio [kW/ton]:

5-8 knots	$Y = 0.00346373 - 1.27742 \cdot 10^{-5}x_1 + 0.00146963x_2 - 0.005831954x_3 + 0.0165634x_4 + 3.17065 \cdot 10^{-5}{x_5}^3$	(3.11)
9-12 knots	$Y = 0.004524085 - 5.986 \cdot 10^{-5}x_1 + 0.005500814x_2 - 0.01158857x_3 + 0.07644087x_4 + 3.25522 \cdot 10^{-5}{x_5}^3$	
13-15 knots	$Y = -0.13670687 - 34.98746 \cdot 10^{-5}x_1 + 0.014829589x_2 + 0.1494632x_3 + 0.38021522x_4 + 4.944 \cdot 10^{-5}{x_5}^3$	
16-17 knots	$Y = -0.7209819 - 141.022 \cdot 10^{-5}x_1 + 0.036967245x_2 + 0.86353241x_3 + 1.367961916x_4 + 8.4125 \cdot 10^{-5}{x_5}^3$	

In general, linear regression uses the ordinary least squares techniques that minimize the sum of the squared residuals. In other words minimizing the distance between the fitted regression line and all of the data points. To evaluate how accurate the model is in fitting the data, it is

necessary to check if the differences between the observed values and the model's predicted values are small and unbiased. Therefore, to measure how close the data are to the fitted regression line, some statistical indicators such as R-squared which is also known as the coefficient of determination is used. R-squared varies between 0% and 100%, and in general, the higher the R-squared, the better the model fits the data.

R-squared values for the obtained regression formulas in Eq (3.11) are 99.8%, 99.6%, 96.4%, and 89.5% respectively for the speed ranges. That is a strong evidence that each regression equation fits the data well to the fitted regression line. Moreover, these high values for R-squared show that there is a strong relationship between the model and the response parameter. However, a high R^2 does not necessarily indicate that the regression model has a good fit for the data observations. R-squared cannot determine whether the coefficient estimates and predictions are biased. That is why the residual and normality plots must be assessed. Therefore, the standardized residuals graphs are selected to assess the quality of the regression, test the normality of the data, examine the goodness-of-fit in regression, and to investigate the equality of variance.

Looking at the Histogram of the residuals in Figure 3.30, it can be sees that the residuals exhibit a relatively symmetric bell-shaped distribution especially for low speeds plots. These symmetric bell-shaped histograms which is moderately distributed around zero indicate that the variance is relatively normally distributed, and the normality of the distribution assumption is likely to be true.

Figure 3.31 shows the Residuals versus Fits plots for the four regression equations at different speed ranges. Residuals versus Fits plot is the most frequently created plot, and it is used in the regression analysis to verify the assumption that the residuals have a constant variance. In other words, it is used to identify non-linearity, unequal error variances, and outliers. Looking at the four corresponding plots shown in Figure 3.31 of the estimated delivered power to the displacement ratio, it can be seen that the residuals bounce randomly around the horizontal 0 line especially for the low speeds plots while it is relatively less obvious for high speeds plots. Moreover, most of the residuals stands in the random pattern of residuals which suggests that there are no outliers that lie at an abnormal distance from other residuals in the total data.

In order to test and reject the null hypothesis that any of the design variables has no effect on the response parameter, it is necessary to determine the P-values for each variable in the model.

A low P-value (< 0.05) indicates that the null hypothesis can be rejected. That means a variable that has a low P-value is likely to be a meaningful addition to the model since changes in its value are related to changes in the response variable. Looking at the regression analysis output summary in Table 3.9, it can be seen that the design variables of *Length, Breadth to Draft Ratio, Block Coefficient, Longitudinal Centre of Buoyancy, and Speed* are significant because their P-values are almost 0.000. That is a sufficient indicator to reject the null hypothesis, and to keep all the design parameters in the regression model.

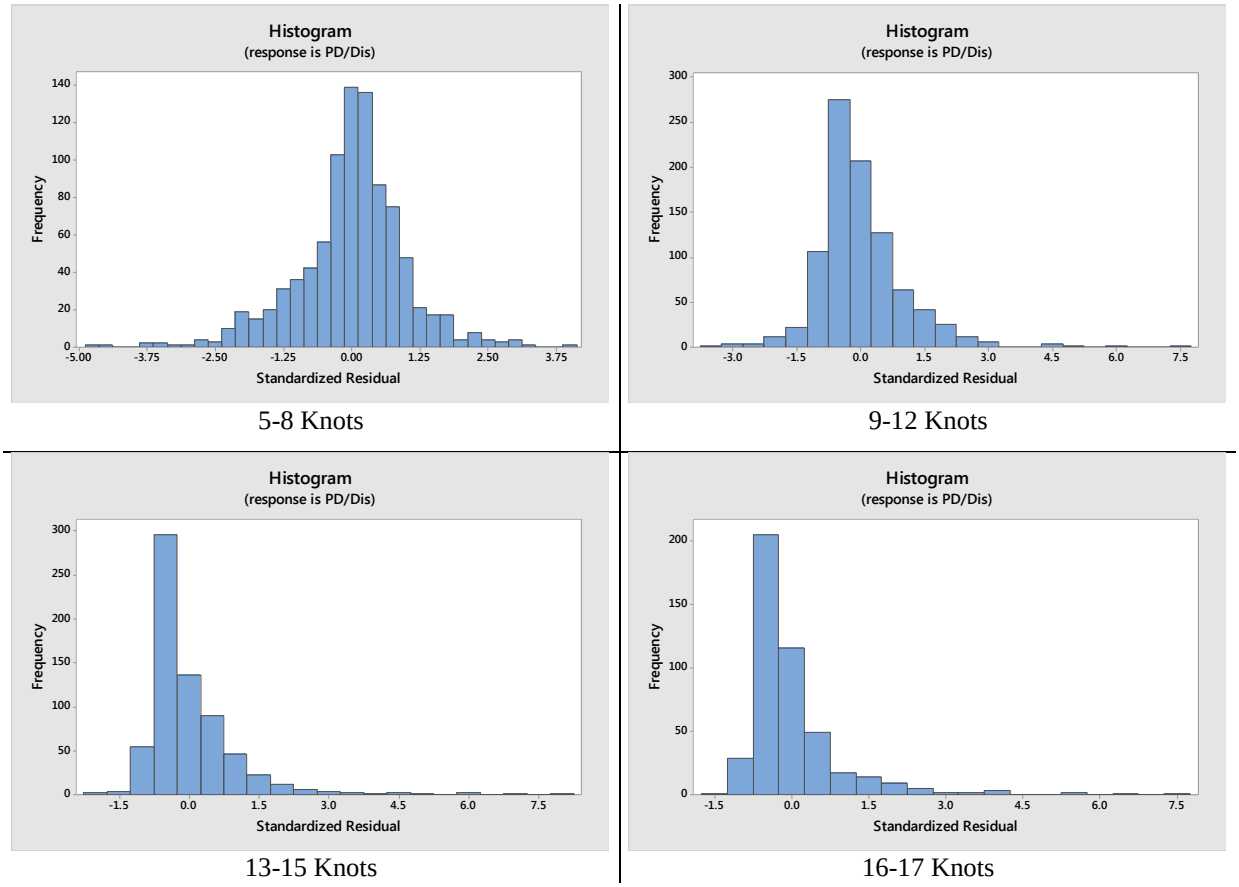

Figure 3.30 Histogram of the residuals

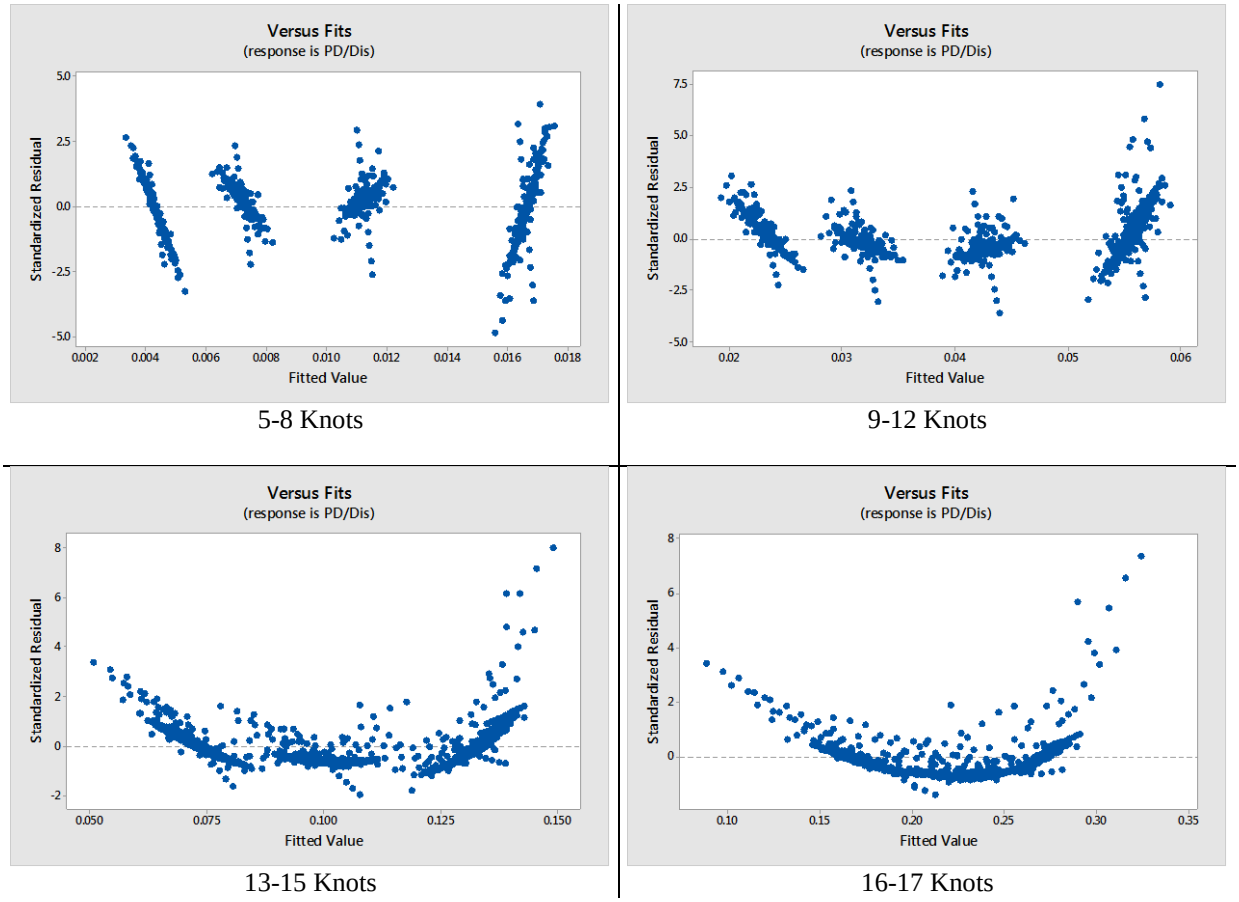

Figure 3.31 Residuals vs Fits Plots for P_D/Dis

Table 3.9 P-Values for the design variables - Regression Analysis Results

Term	5-8 Knots	9-12 Knots	13-15 Knots	16-17 Knots
Intercept	1.31E-33	2.35E-05	4.23E-52	3.37E-72
L	3.8E-122	1.5E-160	1.5E-100	1.11E-91
B/T	5.4E-206	4.3E-198	3.45E-38	5.7E-17
CB	7.25E-75	7.39E-24	4.25E-56	3.15E-89
LCB	2.72E-39	2.17E-53	1.74E-24	2.4E-20
V^3	0.00	0.00	0.00	5.1E-179

The previous stages have looked at the effect of one variable in the hydrodynamic model at a time on different aspects of the performance while keeping other variables constant. However, by using the regression formulas, it is possible now to isolate the influence of an individual variable or more, and simply include the variables we are interested in estimating how their changes is related to the change in the objective function.

The regression model can be used to describe the robust optimization concept by understanding how sensitive the response variable is to changes in the values of the design variables. That will help to gain a better 'cause and effect' understanding for this hydrodynamic model regarding the influence of the changes in the hull parameters and operating speed. That helps designers to make decisions in the early design stages. Basically, the lower the sensitivity on changes in variables, the more robust the design is. Therefore, the aim in in this study is to look for a design or a set of designs that are not sensitive to modest variations in the design variables. Also, examining the regression model will help in modifying the hullform geometry to achieve some improvements in the performance with respect to the energy requirements. On the other hand, in the process of searching for a robust design(s), designers should do it in such a way that other considerations such as building cost, environmental considerations, operating costs and profit are not compromised. Such comprehensive analysis and examination will be discussed in later chapters of this thesis.

To show the significance of the design variables on the performance indicator, the upper or the lower limit (whichever leads to a better performance) is used to calculate the percentage change in the delivered power to displacement ratio P_D/Dis with respect to the basic hull. The regression formulas in Eq (3.11) are used to estimate P_D/Dis at speed 8 knots for illustration. The P_D/Dis values at this speed are compared with the base hull value, and the percentage changes are calculated.

It is apparent from Figure 3.32 that the relative power to displacement ratio is very influenced by all the primary and secondary variables. For instance, reducing the second primary variable (B/T) by 10% while keeping the other three variables constant results in a significant reduction in P_D/Dis of 2.4%. Running the same analysis for the other three variables and also over the speed range show a notable reduction in P_D/Dis in all cases. These reductions in P_D/Dis due to changes in the design variables are a strong evidence that the decision to choose these variables for the parametric analysis was right. Also, using the full factorial design has produced an accurate representation for the hydrodynamic model, and it is sufficient to explore the design space.

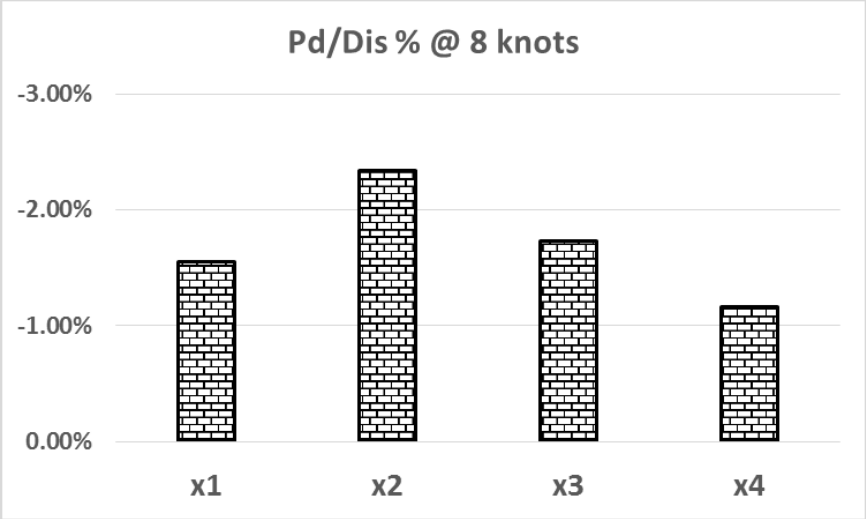

Figure 3.32 Contribution to P_D/Dis of each design variables

To examine the complex relationship between all the design variables and the response parameter, further evaluation and examination are needed for the generated hulls in Stage Three in order to find the best and most robust design parameters for the case study. That will be demonstrated in later chapters using a multi-objective optimisation model. However, based on the results from the previous sections, the suggestions to change the individual hull parameters to improve the hydrodynamic performance and to reduce P_D/Dis are shown in Table 3.10. It is worth mentioning that this table does not provide clear facts, and it could be misleading as there are some assumptions made earlier such as changing the parameters while keeping the displacement constant.

Table 3.10 Optimum trends for the control parameters

	L	**B/T**	**CB**	**LCB%L**
V=15 knots	Incraese	Decrease	Decrease	Decrease
V=13 knots	Decrease	Decrease	Decrease	Decrease
V=12 knots	Decrease	Decrease	Decrease	Decrease
V=10 knots	Decrease	Decrease	Incraese	Decrease
V=7 knots	Decrease	Decrease	Incraese	Decrease

3.6.4 Analysis of the Signal-to-Noise Ratio

Using AVEVA results from Stage Three, Taguchi statistical and experimental technique has been employed in optimising the hull form of four parameters and at different speeds in respect of the hydrodynamic performance at this stage of study. This approach is called Taguchi's

parameters design approach, and it helps in selecting the optimal combination of parameters and illustrates the optimal trends when selecting the parameters for a robust design. Hence, the parameter design approach seeks to find design conditions and parameters that make a design insensitive to variations in the operating conditions and noise factors which makes the design more robust.

In the previous stages of the parametric analysis, design of experiments techniques were employed in Taguchi's method to select the appropriate number of levels and quantities for the design factors. To test all the different combinations of the four design parameters at different speeds and to identify their effect on the response factor i.e. Delivered Power to Displacement ratio, Taguchi approach recommends using the signal to noise ratio S/N which is derived from the quadratic loss function. The S/N ratio is expressed in a decibel scale i.e. logarithmic function. The S/N ratio is calculated for each run of the experiment, and the preferred parameters are defined by analysing all the S/N ratios and choosing the levels with the highest S/N ratio. Therefore, the settings where the factor levels of the design parameters maximize the S/N ratios should be determined.

There are three standard types of S/N ratios regardless of the response type and the number of levels (Taguchi and Phadke, 1989):

- Smaller the better (for minimizing the system response):

$$S/N_{SB} = -10\ log\left(\frac{1}{n}\sum_{i=1}^{n} y_i^2\right) \tag{3.12}$$

- Nominal the better (for reducing variability around a target):

$$S/N_{NB} = 10\ log\left(\frac{\overline{y}}{S^2}\right) \tag{3.13}$$

- Larger the better (for maximising the system response):

$$S/N_{LB} = -10\ log\left(\frac{1}{n}\sum_{i=1}^{n} \frac{1}{y_i^2}\right) \tag{3.14}$$

Where:

y_i: the observed data

$\overline{y}$: the average of the observed data, $\overline{y} = \frac{1}{n}\sum_{i=1}^{n} y_i$

S: the standard deviation of the observed data, $S = \sqrt{\sum_{i=1}^{n} \frac{(y_i - \overline{y})^2}{n-1}}$

n: the number of observations.

The average (P_D/Dis) and the mean S/N ratio for each level of the control parameters (low, medium, and high) as shown in Table 3.3 are calculated using the equations above. The results are shown in Table 3.11 and Table 3.12 respectively. Moreover, Figure 3.33 and Figure 3.34 show, graphically, the control factors' effects on the average response parameter and S/N. However, Appendix B shows the average (P_D/Dis) and the mean S/N ratio for all the 81 hulls generated in Stage Three.

Results reveal that of the design parameters length and block coefficient have a greater effect on the average P_D/Dis and S/N than breadth to draught ratio and LCB. The third level for the length (L_3 – longer hull) is clearly a better choice to minimize P_D/Dis and maximize S/N comparing with the shorter hulls (L_1 & L_2). For the other design parameters, the preferred levels are:

- Breadth to draught ratio: (B/T_1) where the breadth to draught ratio is minimum.
- Bloch Coefficient: (CB_1) which states that fine and slim hulls are better for the hydrodynamic performance.
- Longitudinal centre of buoyancy: LCB%L_1 where the position of LCB moves aft.

Hence, based on AVEVA results using Holtrop and Mennen method, the P_D/Dis ratio has a tendency of decreasing when the hull is longer, the breadth to draught ratio is smaller, the block coefficient is smaller, and for backward centre of buoyancy position. However, as the results give just an indication to how the hydrodynamic performance can be improved, further analysis will be carried out in the next chapters to investigate the complex interactions between the design parameters at different speeds and the effect on other performance aspects. Moreover, the desired robust solution should consider the other features of the study like the economic performance and the environmental impact of the new designs but obviously there will be trades between the different performance indicators and parameters.

Table 3.11 Average response parameter for P_D/Dis

	L	B/T	CB	LCB%L
Level 1	0.077	0.068*	0.066*	0.068*
Level 2	0.071	0.072	0.069	0.071
Level 3	0.065*	0.074	0.080	0.075
max-min	0.012	0.006	0.014	0.007

Table 3.12 Mean signal-to- noise S/N ratio for P_D/Dis

	L	B/T	CB	LCB%L
Level 1	19.015	20.338*	20.948*	20.428*
Level 2	19.967	19.900	20.295	19.986
Level 3	20.865*	19.608	18.603	19.433
max-min	1.851	0.730	2.345	0.995

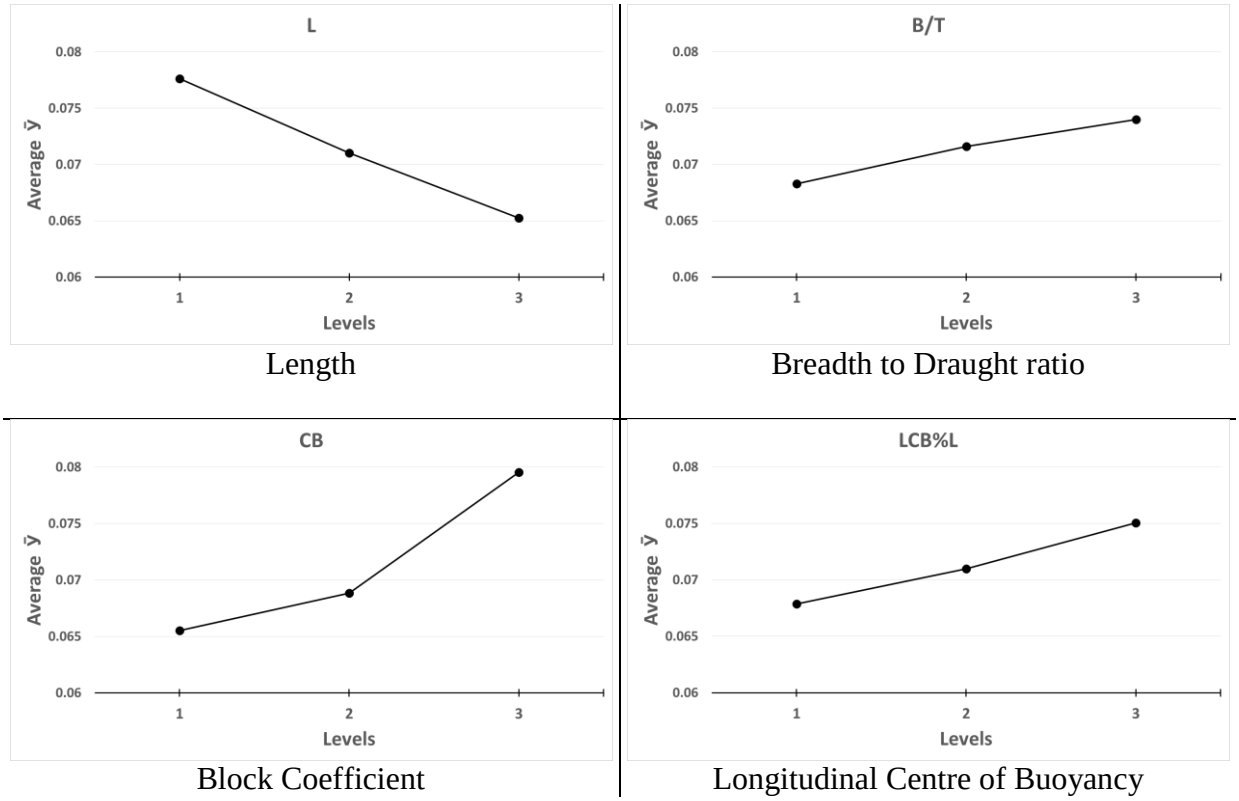

Length | Breadth to Draught ratio

Block Coefficient | Longitudinal Centre of Buoyancy

Figure 3.33 Control Factors Effects on Average P_D/Dis

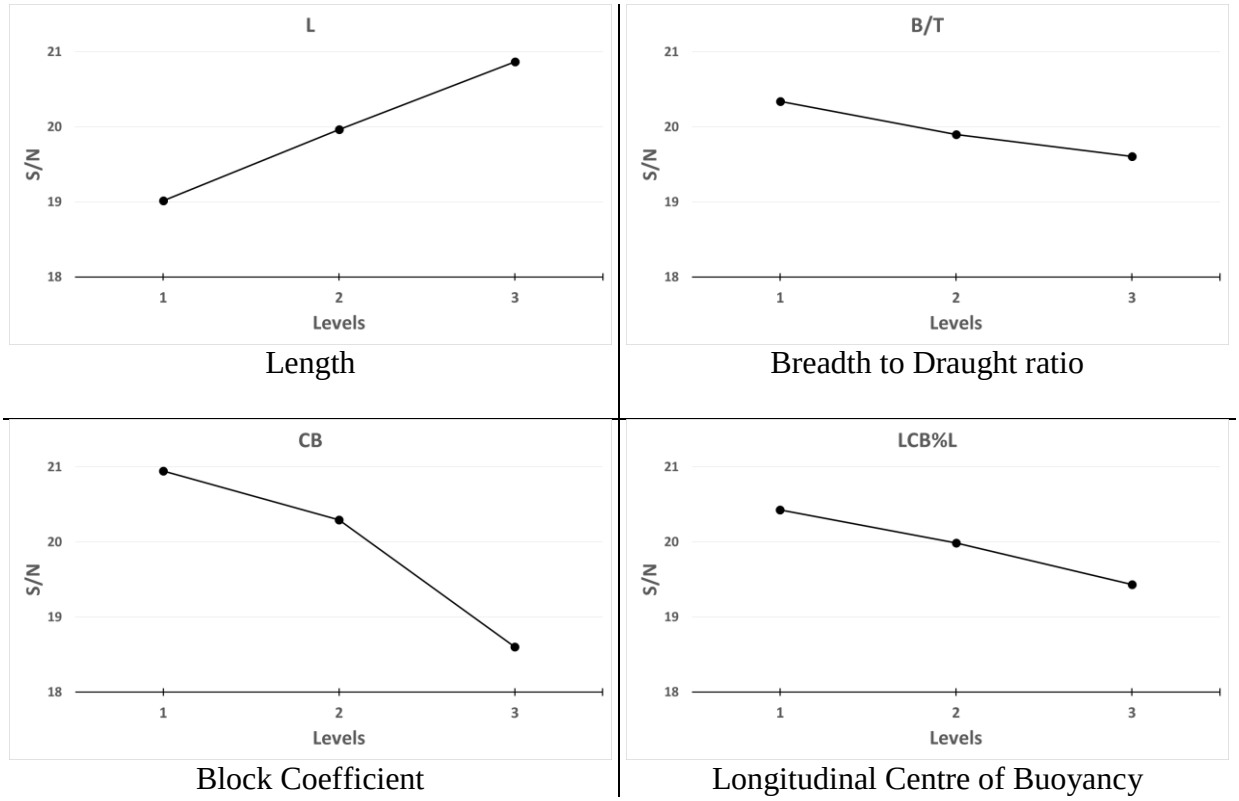

Length | Breadth to Draught ratio

Block Coefficient | Longitudinal Centre of Buoyancy

Figure 3.34 Control Factors Effects on S/N

3.7 Conclusion

This chapter has laid out the complexity of hull optimisation which accounts for ship resistance and propulsion. The main elements of a basic hull optimisation technique were presented.

AVEVA Initial Design Lines was used to build and modify lines and surfaces of a 54,000 DWT tanker ship. Length, breadth to draught ratio, block coefficient, and the longitudinal position of the centre of buoyancy are chosen for the parametric modification process to generate the new alternative hulls.

The hydrodynamic performance of the alternative hulls was compared with the base hull performance by calculating the percentage change in the resistance coefficients, efficiency, delivered power, etc. The results suggested that modifications in the hull parameters and optimising the sailing speed can improve the energy saving and required power by up to 15%. A significant reduction in the delivered power P_D can be gained at high speeds above 13 knots for ships with hulls longer and slimmer than the basic hull while keeping the displacement constant. Moreover, for a constant displacement, the P_D results show that a reasonable reduction of about 4.5% in the required power can be achieved across all the speed range for designs with

deeper hulls and smaller beam while keeping the length constant. Results show that any increase in the block coefficient introduces a significant increase in the required propulsion power per ton displacement which could reach 24% at the design speed for a 6% increase in C_B at the design speed. This undesirable impact on the required power as a result of increasing the block coefficient drops in value for slower speeds till it has a positive impact in reducing the required power at lower speeds. The results showed that moving the LCB position backward would lead to a reasonable reduction in the required power up to 3.5% for high speeds and 1.8% for the $[-1\%L, LCB]$ for instance.

AVEVA output from Stage Three hulls was used to obtain a set of regression formulas to estimate the delivered power to displacement ratio P_D/Dis as a function of speed and the design variables. The delivered power to displacement ratio was used as the objective function (response parameter) that needs to be minimised to improve the energy efficiency of the designs. The results were analysed to understand the direct influence of changes in the design parameters and the sensitivity of the hull performance to those changes. The signal to noise ratio analysis showed that longer hulls with a minimum breadth to draught ratio and a slim shape (low block coefficient) and a backward LCB have generally a better hydrodynamic performance. A closer look at the results from Stage Three revealed that some individual designs show a great energy saving potential such as design no.61 with long hull, low breadth to draught ratio, high block coefficient and backward LCB position which shows the best performance among all other alternative hulls at slow speeds up to speed 13 knots.

Chapter 4. Environmental Impact Model

4.1 Introduction

Climate change is a serious environmental threat facing the world today, and indeed it is a challenge to everyone cares about the future of our globe. The Kyoto Protocol is a milestone and an important step to fight the global warming by setting limits on total emissions by major economies and industrialised countries. It was adopted in Kyoto – Japan in 1997 and entered into force in 2005 as an international agreement linked to the United Nations Framework Convention on Climate Change (UNFCCC) where all the parties commit to reduce their GHG emissions to an average level over different periods against 1990 levels. This protocol was signed by 84 countries, and all participated parties and world's leading economise have agreed that strict policies should be adopted to save energy, reduce emissions, and act against forest loss and decreasing air quality. The main targets of Kyoto Protocol vary from nation to nation and from one industrial sector to another, and different mechanisms have been set up to achieve those targets.

Because of lack of reliable data about emissions from maritime and aviation activities, these two sectors were barely covered in the Kyoto Protocol Agenda 1997. Therefore, the Marine Environment Protection Committee (MEPC) has recognized the need of doing something to mitigate the emissions from shipping activities. The International Maritime Organisation IMO has responded to the Kyoto Protocol (Article 2.2) regarding reducing the greenhouse gas emissions but the action was considered insufficient by many bodies and individual countries. However, three studies addressing the greenhouse gas emissions from ships have been completed so far by the International Maritime Organisation IMO in 2000[1], 2009[2], and 2014[3] (Bodansky, 2016). Those studies tried to shed more light on the trends of the energy consumption and greenhouse gas emissions taking into account the current and prospective scenario of the maritime shipping activities. Different energy saving measures have been proposed and become a focusing point for many governments and organisations to build a robust scheme for a greener shipping industry.

[1] Study of Greenhouse Gas Emissions from Ships (London: IMO, 2000).
[2] Second IMO Greenhouse Gas Study 2009 (London: IMO, 2009).
[3] Third IMO Greenhouse Gas Study 2014: Executive Summary and Final Report (London: IMO, 2015).

IMO studies have reported that the shipping industry including the three main sectors (designing, building, and operating) is becoming more challenging and complicated due to the contrary implications of rising fuel prices, the need to reduce CO_2 as well as other emissions, and the need for new designs to meet the efficiency gains required by the IMO and other regulations required by state authorities. In other words, several technological challenges have to be met and reconciled with economics of ship operation in order to help owners and charters to operate their fleet efficiently and secure an appropriate profitability, and more important to reduce the environmental impact because the shipping industry is under pressure to take its share of responsibility for tackling global warming in the future.

Following this brief introduction, a number of technical and operational measures to reduce shipping emissions are introduced. Mainly, three schemes and measures promoted by IMO are discussed (EEDI, EEOI, and SEEMP). Then, speed optimisation as an efficient way to mitigate CO_2 emissions from ships is discussed. The environmental model which is built upon the emissions calculations and EEDI formula is discussed.

Assumptions regarding emission factors, energy consumption, engine loads, cargo capacity, etc. to calculate the reference EEDI and attained EEDI values for the environmental model are presented. Amedia method to estimate the lightship weight and hence to calculate the ship deadweight to be used in the EEDI formula is discussed. The model is conducted to calculate EEDI for the base and alternative hulls over the range speed using the hydrodynamic model results. EEDI Results from the three stages are presented; graphically and in tables, and compared with the base hull results at the design speed as well as at other speeds.

The attained EEDI to EEDI reference ratio $\left(EEDI_A/EEDI_{Ref}\right)$ is chosen as the objective function (response parameter) in the environmental model. It is used as an indicator while exploring the design space to choose alternative designs that demonstrate a better energy efficiency performance in order to meet the IMO requirements. As previously, Mimitab17 and the Regression Tool built in EXCEL are used to run the regression analysis. A set of regression equations are obtained to estimate the attained EEDI to EEDI reference ratio. Moreover, to gain a better 'cause and effect' understanding of the implications of changes in hull parameters and how the operating speed affects the $(\mathrm{EEDI_A}/\mathrm{EEDI_{Ref}})$ value, a sensitivity analysis will be carried out as has been done earlier in the hydrodynamic model.

4.2 Measures to Reduce Shipping Emissions

Recent studies show that international shipping contribution to the global CO_2 emissions is expected to increase significantly in the coming decades if no mitigation measures are taken. Therefore, worldwide cooperative efforts have been put in action to reduce emissions of greenhouse gasses and to ensure that shipping is cleaner and greener. The United Nations Framework Convention on Climate Change (UNFCCC) sets emissions targets, and has tasked the International Maritime Organisation (IMO) to establish a framework of legislations and measures that helps the prevention of air pollution from international shipping (Anink and Krikke, 2009). Since the late 1980s, IMO has given full consideration to control air pollution by ships through addressing a set of practical measures and guidance that leads designers, ships owners and operators to mitigate fleet's emissions through different options in hydrodynamics, engines and machinery, and also operation and management. Many of these measures to reduce ships emissions are cost-effective and can increase efficiency by 25% to 75% according to the Second IMO GHG Study 2009. Basically, the options to reduce shipping emissions can be categorised in four fundamental groups:

- Improving energy efficiency,
- Adopting renewable energy resources,
- Using cleaner types of fuels such as biofuels or natural gas as their total fuel-cycle emissions per unit of work is less,
- Adopting emission reduction technologies such as using chemical conversion options and capture-and-storage technologies.

In principle, improving energy efficiency is about energy management and reducing energy consumption on board by avoiding unnecessary operation of energy machines and optimising the ship systems. In other words, generating the same amount of power or achieving the same amount of work using less energy. Key areas of energy saving with their potential reductions of CO_2 are presented in Table 4.1, and some measures will be discussed in more details later in this chapter.

Table 4.1 Emissions reduction measures and potential reductions of CO_2 emissions. Source: Second IMO GHG Study 2009

Design (new ships)	**Saving of $CO_2/tonne.mile$**	**Combined**	**Combined**
Concept, speed and capacity	2% to 50%[+]	10% to 50%[+]	25% to 75%[+]
Hull and superstructure	2% to 20%		
Power and propulsion systems	5% to 15%		
Low-carbon fuels	5% to 15%[*]		
Renewable energy	1% to 10%		
Exhaust gas CO_2 emissions reduction	0		
Opeation (all ships)			
Fleet management, logistics and incentives	5% to 50%[+]	10% to 50%[+]	
Voyage optimization	1% to 10%		
Energy management	1% to 10%		
[+] Reductions at this level would require reductions of operational speed. [*] CO_2 equivalent, based on the use of LNG.			

The International Maritime Organisation IMO is the only body that have adopted a wide range of energy-efficiency measures that are applying to all countries and across all vessels classes and types. A series of baselines have been established to determine the amount of fuel each type of ships burns depending on her size and the cargo capacity. These baselines are also an indicator for the greenhouse gas emissions limits from ships. IMO regulations require that all new ships need to beat the 2007 representative emissions baseline by a specific amount which gets higher by time. For example, to comply with IMO regulations, all new ships built by 2025 need to be at least 30% more energy efficient than ships built in 2014 (IMO, 2017). On the other hand, IMO energy-efficiency requirements address that existing ships should adopt an operational measure that introduces a mechanism for a company and/or a ship that works to improve the total efficiency of a ship in a cost-effective manner and also improve the management system for shipping companies.

IMO, as the main regulatory body for shipping, aims to lead maritime industry and transport into a low-carbon future by building understanding and knowledge within the shipping market of potential saving in energy through technical and operational measures. Therefore, and for this purpose, three schemes and measure have been introduced by IMO under the banner of

MEPC and its associated Energy Efficiency working group as shown in Figure 4.1. These schemes are:

- Energy Efficiency Design Index (EEDI).
- Energy Efficiency Operational Indicator (EEOI).
- Ship Energy Efficiency Management Plan (SEEMP).

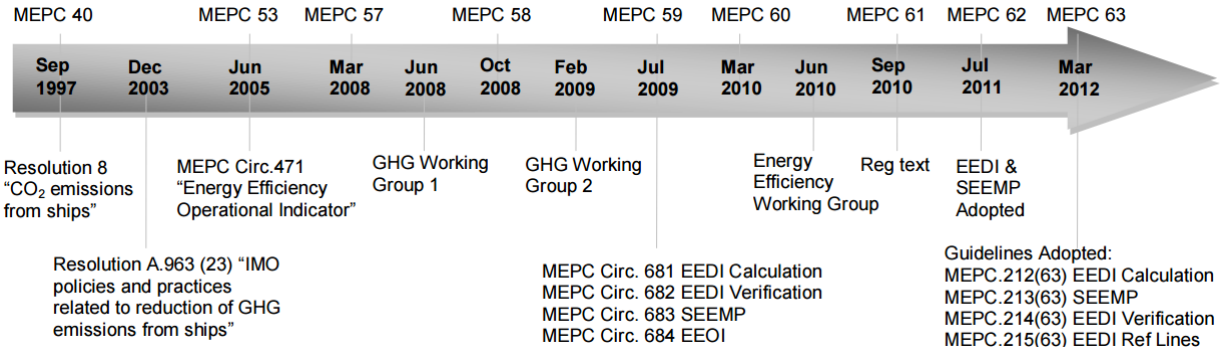

Figure 4.1 MEPC and Working Group Timeline. Source: (Lloyd's Register, 2012a)

4.2.1 Energy Efficiency Design Index (EEDI)

4.2.1.1 EEDI Concept

The Marine Environment Protection Committee (MEPC) at its 59th session (August 2009) in London and previous sessions since 2000 brought to light the importance of developing an effective tool to measure the energy efficiency for ships in order to improve the overall efficiency of each individual ship. One of the most crucial measures developed by IMO is the Energy Efficiency Design Index (EEDI) which is a regulatory measure for CO_2 output of new ships. For existing vessels, implementing the EEDI is irrelevant in most cases because IMO has made EEDI mandatory just for new ships which the building contract is placed on or after 1st January 2013. Therefore, EEDI is not suitable for existing ships as it was developed for the design of new ships and future emissions reduction goals. However, the most common case where EEDI becomes relevant for the existing fleet is when a ship undergoes a major conversion. In such extensive conversion process, it is regarded as a newly constructed vessel, and then the EEDI and the technical file will be under the process of verification by the flag administration.

Basically, the EEDI is the main benchmark set by the IMO to monitor marine CO_2 emissions from the international fleet. EEDI represents a ship's performance from environment point of view and its performance which expressed by the transport work capacity. Theoretically, EEDI is defined as a ratio between a ship's impact to the environment and the benefit to society as shown in Eq (4.1). The attained Energy Efficiency Design Index for new ships is measured in grams CO_2 emitted per capacity.nmile, and given by a formula which adopted by MEPC.1/Circ.681 in August 2009. Basically, EEDI is a function of: installed power, cargo carried, and ship speed. A simplified formula for the attained EEDI value is given in Eq (4.2) (Jon Rysst and Eirik Nyhus, 2009):

$$Basic\ EEDI\ concept = \frac{Environmental\ cost}{Benifit\ for\ society} \tag{4.1}$$

$$Attained\ EEDI = \frac{C_F \times SFC \times P}{Capacity \times V_{ref}} \tag{4.2}$$

Where:

C_F: carbon emission factor(s) [gCO_2/ton fuel],
SFC: specific fuel consumption(s) [g fuel/kWh],
P: the ship demand power [kW],
Capacity: it is specified as gross tonnage, deadweight, TEU, or number of passengers depending on ship type [DWT ton],
V_{ref}: the speed measured during speed trial (in calm weather) at maximum draught and 75% of maximum continuous rating [mile/h].

The interim guidelines on the method of calculation of the Energy Efficiency Design Index for new ships over 400 GT is published in the Marine Environment Protection Committee in its circulars 681 (MEPC.1/681 - 2009). However, different amendments have been applied to the EEDI equation after many discussions and suggestions took place during the previous years within IMO meetings, national and international conferences. The extended formula to calculate EEDI was stated in Resolution MEPC.212 (63) adopted in March 2012 as in Eq (4.3). A full explanation of the terms and factors detailed EEDI formula is in Appendix C. This formula takes into account special design features and innovations. That includes the use of energy recovery technologies, the use of low carbon fuels such as LNG, corrections to account

for specific design elements for ice classed ships and shuttle oil tankers for example, capacity correction, corrections indicating the ship performance in waves and the decrease in speed in bad weather conditions.

$$\frac{\left(\prod_{j=1}^{n} f_j\right)\left(\sum_{i=1}^{nME} P_{ME(i)} \cdot C_{FME(i)} \cdot SFC_{ME(i)}\right) + \left(P_{AE} \cdot C_{FAE} \cdot SFC_{AE}*\right) + \left(\left(\prod_{j=1}^{n} f_j \cdot \sum_{i=1}^{nPTI} P_{PTI(i)} - \sum_{i=1}^{neff} f_{eff(i)} \cdot P_{AEeff(i)}\right) C_{FAE} \cdot SFC_{AE}\right) - \left(\sum_{i=1}^{neff} f_{eff(i)} \cdot P_{eff(i)} \cdot C_{FME} \cdot SFC_{ME}**\right)}{f_i \cdot f_c \cdot Capacity \cdot f_w \cdot V_{ref}} \tag{4.3}$$

It is worth mentioning that there are some criticism against EEDI formulation as it is based purely upon the design of the target ship at her full laden draft condition in calm water and sailing at her design speed (OCIMF, 2011a). Hence, the EEDI formula is contradicting the basic hydrodynamic laws and the common operational conditions as it ignores the ballast leg, the day-to-day behaviour of the ship in the seaway condition, and also the related CO_2 emissions. One of the EEDI limitations is that it encourages to maximise cargo deadweight for a given deadweight and hence place pressure on ship owners to minimise lightship which has a very serious implications on the structure in terms of the fatigue life. Moreover, EEDI formula suggests reducing the engine installed power in order to reduce the attained EEDI and meet IMO regulations. That eventually sacrifice the safe performance of the vessel in rough sea. One last concern about the EEDI formula is that the minimum EEDI values ships should attain are derived using data from IHS Fairplay database which is a commercial database and its accuracy is not certain.

4.2.1.2 EEDI Reference Line:

To introduce the EEDI requirements to new ships, IMO has established a unique baseline curve for each type of ships which represents average index values for this defined group of ships. The EEDI reference line provides a fair basis for comparison between selected designs, and to encourage the development of more efficient and greener designs. The primary input database to generate EEDI reference lines are selected from the HIS Fairplay database (IHSF) after a filtering process where all data deviating more than two standard deviation from the generated regression line are removed (Vladimir *et al.*, 2017) .The reference line is formulated as in Eq (4.4) according to Regulation 20 of Annex VI of Chapter 4 IMO MARPOL 73/78 (IMO MEPC 203(62) 2011):

$$Reference\ EEDI\ value = a \times b^{-c} \quad (4.4)$$

where $(a, b, and\ c)$ are constant and are derived using regression analyses of a large number of data of attained EEDI values of the world fleet. They are determined depending on ship type as shown for some types in Table 4.2 (source: (IMO, 2016)). Some ship types like tankers and bulk carriers have high (c) values comparing with other types such as container ships and general cargo ships. This means that tankers and bulk carriers' EEDI is more dependent on the ship capacity i.e. DWT. For illustration, Figure 4.2 shows a typical EEDI reference line for tanker ships over 400 GT.

Table 4.2 Parameters $(a, b, and\ c)$ for determination of reference values

Ship Type	a	b	c
Bulk carriers	961.79	DWT of the ship	0.477
Gas carrier	1120.00	DWT of the ship	0.456
Tanker	1218.80	DWT of the ship	0.488
Container ship	174.22	DWT of the ship	0.201
General cargo ship	107.48	DWT of the ship	0.216

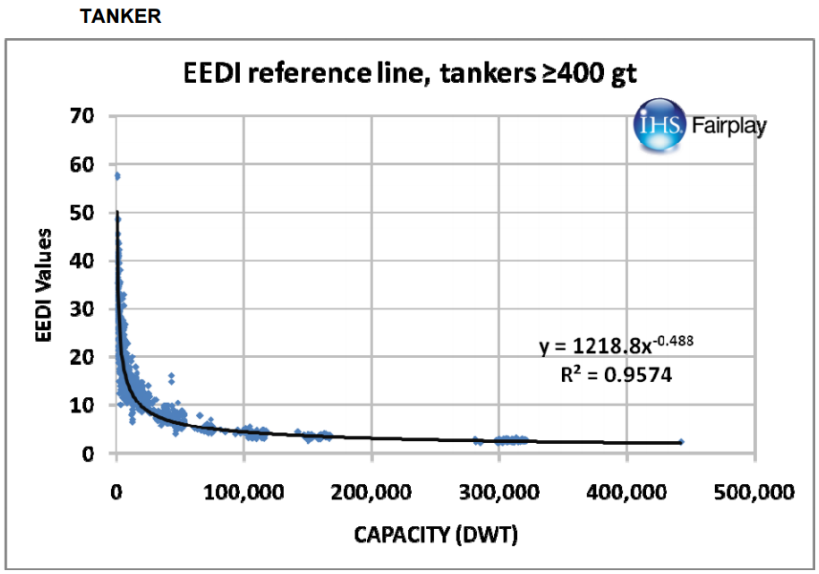

Figure 4.2 EEDI reference line for Tankers ≥ 400 GT (source: (IMO MEPC 68/6/4 (2011)))

4.2.1.3 Phases of the EEDI:

The EEDI provides a fair standardized indicator for new ships' energy efficiency. The attained EEDI for new ships as addressed by IMO should be less or equal the required level which is calculated as in Eq (4.5) according to Regulation 21 of Annex VI of Chapter 4 MARPOL 73/78:

$$Attained\ EEDI \leq Required\ EEDI = \left(1 - \frac{X}{100}\right) \times Reference\ line\ value \qquad (4.5)$$

Where X is a reduction factor which is defined in a set of time intervals comparing to the EEDI reference line as shown in Table 4.3 for the most common ship types (Tien Anh, 2016). As mentioned before, from 1st January 2013, all new designs are expected to meet the EEDI reference level after an initial two year phase zero, and furthermore, the EEDI requirements are going to be tightened continuously to keep pace with all the new innovation and development that influence ship's efficiency. Figure 4.3 shows how the reduction progression will gradually be implemented in four phases over the next years to reduce shipping CO_2 emissions. These targets vary by vessel class and by size. Each phase addresses more stringent requirements regarding energy efficiency that all new building must follow.

Table 4.3 Reduction factors (in %) for the EEDI relative to the EEDI reference line (source: (Papanikolaou, 2014))

Ship Type	Size	Phase 0 1 Jan 2013-31 Dec 2014	Phase 1 1 Jan 2015-31 Dec 2019	Phase 2 1 Jan 2020-31 Dec 2024	Phase 3 1 Jan 2025-onwards
Bulk carriers	20,000 DWT and above	0	10	20	30
	10,000-20,000 DWT	n/a	0-10*	0-20*	0-30*
Tanker	20,000 DWT and above	0	10	20	30
	4,000-20,000 DWT	n/a	0-10*	0-20*	0-30*
Container ship	15,000 DWT and above	0	10	20	30
	10,000-15,000 DWT	n/a	0-10*	0-20*	0-30*

n/a means that no required EEDI applies.

* Reduction factor to be linearly interpolated between the two values dependent upon ship size. The lower value of the reduction factor is to be applied to the smaller ship size.

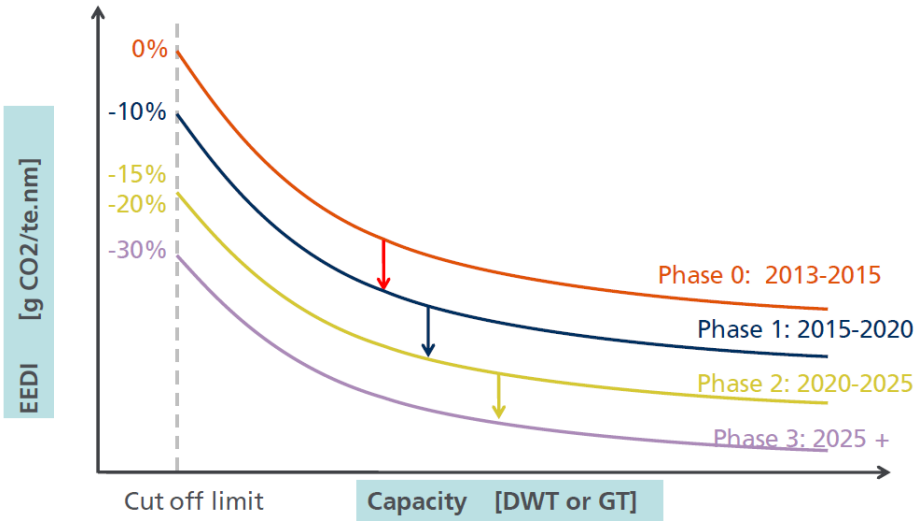

Figure 4.3 EEDI phases concept (source: (Lloyd's Register, 2012b))

4.2.2 Energy Efficiency Operational Indicator (EEOI)

The EEOI is the actual total carbon emissions of a ship in her real operation conditions in a given period of time per unit of work i.e. [tonnes.miles, TEU.miles, or person.miles] taking into account actual speeds, journey distance, capacity utilization, draughts, weather conditions, hull and machinery conditions, and other parameters. The guidelines for voluntary use of EEOI was approved by The Marine Environment Protection Committee (MEPC) at its 59th session in July 2009 [MEPC.1/Circ.684, 2009]. It represents the energy efficiency of a ship operating over a specific period like a whole journey or a period in question such a day. This indicator enables operators, ship owners, and shipping companies to monitor and measure the effect of any changes in the operation profile such as voyage planning and hull cleaning, or the introduction of any new technical measure such as a new propeller or a waste heat recovery system (DNV GL).

EEOI [g CO_2/tonne.mile] is defined in its most simple form as the ratio of CO_2 mass emitted per unit of transport work as in Eq (4.6). Eq (4.7) calculates the average EEOI when data for a number of voyages is obtained or for a particular period of time during the year (IMO, MEPC.1/Circ.684, 2009). The fuel consumption that used to calculate the emitted CO_2 mass is defined as all fuel consumed during a voyage or even a single day at sea and in port by the main and auxiliary engines and other equipment. EEOI, as a performance indicator, provides a basis to review both the current performance of a ship or a fleet and future trends over time. However, EEOI should be used with other performance indicators like EEDI and SEEMP as that provides

a better understanding of what is necessary to improve the energy performance for a single trip or over the ship life span.

$$EEOI = \frac{M_{CO_2}}{Transport\ work} = \frac{\sum_j FC_j \times C_{Fj}}{m_{cargo} \times D} \quad (4.6)$$

$$Average\ EEOI = \frac{\sum_i \sum_j \left(FC_{ij} \times C_{Fj}\right)}{\sum_i \left(m_{cargo,i} \times D_i\right)} \quad (4.7)$$

Where:

j: fuel type,

i: the voyage number,

FC_{ij}: the mass of consumed fuel j at voyage i,

C_{Fj}: the fuel mass to CO_2 mass conversion factor for fuel j as in Table 4.4. The carbon factors used for EEOI calculations should be harmonized with those in EEDI,

m_{cargo}: the cargo carried (tonnes) or work done (number of TEU or passengers) or gross tonnes for passenger ships,

D: the distance in nautical miles.

Table 4.4 Fuel mass to CO_2 mass conversion factors C_F - Source: *(IMO, MEPC.1/Circ.684, 2009)*

Type of fuel	**Carbon content**	$\boldsymbol{C_F\ (t-CO_2/t-fuel)}$
Diesel/Gas Oil	0.875	3.206
Light Fuel Oil (LFO)	0.86	3.151040
Heavy Fuel Oil (HFO)	0.85	3.1144
Liquified Petroleum Gas (LPG)	0.819 0.827	3.0 3.03
Liquified Natural Gas (LNG)	0.75	2.75

Using EEOI as a performance monitoring tool provides users with the ability to analysis the effect of different factors by carrying the following analysis (MEPC, 2009):

- Efficiency of ship including hull and propeller fouling, engine condition, etc.;
- Variation in speed;

- Delays in the journey and days at anchor, in port, and on manoeuvring;
- Relative utilization of cargo space;
- Weather and currents;
- Relative consumption of fuel at ballast leg;
- Port conditions;
- Errors in data collection and measurements.

Acomi and Acomi (2014) developed an Excel programme (.xls), and used a commercial software developed by TotemPlus Company to estimate the EEOI value before the voyage and then compare it with the real value calculated during the voyage on board based on the unpredictable factors that might appear and change during the voyage. A handy-size chemical/product tanker (38,000 DWT) has been used as a case study, and both the EEOI and the average EEOI are calculated. Results show that EEOI values vary accordingly with changes in the voyage parameters including the controllable and unpredictable ones. Analysing the results show that by reducing the average speed from 15 knots to 10 knots, the EEOI value decreased from 15.07 to 13.55.

A technical report by UCL Energy Institute (Sophia Parker *et al.*, 2015) examines the determinants of the EEOI by looking at the components that comprise the equation after decomposing it into sub-indices that reflect both the technical and operational (logistic) characteristics of the ship and the journey. The study has used a set of data of fuel consumption parameters and ship's transport work to construct a model that estimates the EEOI sub-indices.

The main logistic factors that influence the EEOI value are: average payload utilization, allocative utilization, operating speed, draught, and trim. These variables influence both EEOI equation's numerator and denominator in different ways. For instance, a ship's payload utilization affects both the transport work (productivity) and fuel consumption. Also, both the fuel consumption and the transport work achieved within a specific period of time are affected by the operational speed. This contradictory impact and combined contribution of the logistics variables on the EEOI makes interpretation of the index not completely clear and straightforward. Analysing results for different ship types and sizes show that there is no strong correlation between EEOI and any factor of the logistic factors. That is why it is important to consider any contributions for a particular combination of those factors. Moreover, results show that across different ship sizes, there is a relation between technical factors and efficiency

(EEDI) and EEOI but within one ship size class there is a wide dispersion of EEOI values. For instance, the annual EEOI values for large bulk carriers are between 5 and 20 ($gCO_2/t.km$) while for smaller bulk carriers, the variation in the annual EEOI is wider and it is between 5 and 40 ($gCO_2/t.km$). This variations in EEOI can be explained by DWT and the variations in the combination of the operational and logistics factors for all the type and sizes considered in the study. Generally speaking, high EEOI values occur as a result of poor payload utilization and low ratio of days laden to the total sailing days (allocative utilization). Moreover, within one ship class, the study results show that ship size influences the EEOI value as EEOI is monotonically decreasing with size.

4.2.3 Ship Energy Efficiency Management Plan (SEEMP)

The main purpose of the SEEMP as an operational management tool is to establish a robust approach to monitor and manage a ship and fleet efficiency performance continuously and to improve the energy efficiency in a cost effective way. It assists the responsible person or company in managing and improving the day-to-day environmental performance (IMO, 2017). SEEMP's guidelines were first regulated and agreed during MEPC 59 (2009). This operational management measure has become a mandatory tool and all existing and new ships (over 400 GT) on international voyages must have it on board. It entered into force in 1st January 2013 under MARPOL Annex VI after had been introduced on a voluntary basis for many years. The mandatory implementation of the EEDI for new ships and SEEMP for all ships was agreed for all ships at MEPC 62 in July 2011 to be, since the Kyoto Protocol 1997, the first legally binding climate change treaty in the maritime shipping sector

The SEEMP process is achieved through four critical stages which are as listed in IMO MEPC.1/CIrc.683. (17 August 2009)): planning, implementation, monitoring, and self-evaluation and improvement as shown in Figure 4.4. All key processes of SEEMP are summarized below:

- Planning: It is the most important stage of the SEEMP process. It determines the current status of ship energy efficiency and the expected technical and operational improvements of the ship energy usage.
- Implementation: After identifying the required measures by the ship and the company, the next stage is to establish a system of how to implement each energy improvement measure.

- Monitoring: A continuous assessment of the energy improvement scheme design for a ship or a fleet can only be fulfilled by monitoring each measures quantitatively. This can be carried out using an established system that might be adopted by the ship owner although it is preferable to carry it out by an international standard.
- Self-evaluation and improvement: It is the final stage of the SEEMP management cycle. The purpose of this phase is to evaluate each measure periodically over the planned period. Then, all the collected information should be analysed to provide meaningful feedback that can be used as an input in the next improvement cycle.

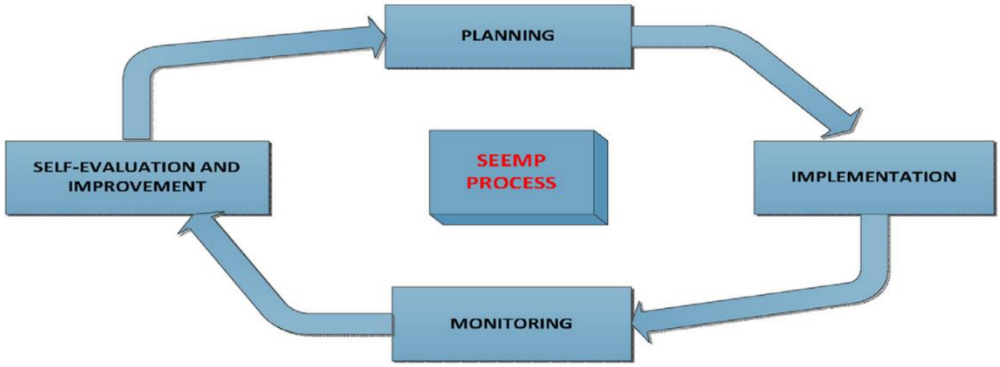

Figure 4.4 Ship Energy Efficiency Management Plan (SEEMP) process- Source (Tran, 2017).

Before heading to the next section to discuss the available technical and operational means to reduce energy consumption and improve energy saving, it is worth addressing the other regulations on the local, national and international levels which are addressed to cut the other emissions from shipping activities. The two main pollutants which are considered very harmful to humans are Nitrogen oxides (NO_x) and Sulphur oxides (SO_x), and they are very high on the IMO agenda. The regulations for the Prevention of Air Pollution from Ships (MARPOL Annex VI) to minimize these two non-greenhouse gases entered into force in 2005 and a revised Annex VI with significant tighten emissions limits was adopted in 2008 which entered into force in 2010.

MARPOL Annex VI sets limits on emissions from ship exhausts including a global cap by mass on the sulphur content of fuel oil and also provisions allowing for Sulphur Emission Control Areas (SO_x ECAs, SECAs) where either the sulphur content of fuel oil must not exceed a specific limit or some technologies must be installed to achieve equivalent SO_x emissions. The Baltic Sea and the North Sea are designated as SECAs in the Protocol. Also, limits on emissions of NO_x from diesel engines were set. The main key provisions can be summarised as following:

- A reduction in the global limit of sulphur content in fuel to 3.5% by mass effective from 1st January 2012, then to 0.5% effective from 1st January 2020.
- A reduction in sulphur limits for fuels in SECAs to 1% from the beginning of July 2010 and to 0.1% from 1st January 2015.
- Tiered reductions in NO_x emissions from marine engines where Tier III came into force in July 2010. It applies to all engines greater than 130 kW installed on ships constructed on or after 1/12016 or which undergo a major conversion on or after this date. Those emission limits are set for diesel engines depending on the rated engine speed which can be seen in the revised MARPOL Annex VI. Tier 0,I, and II limits are global while Tier III standards apply only in NO_x ECAs.

Due to the application from the start of 2015 of the 0.1% MARPOL limit in the SO_x ECAs in the North and Baltic Sea and English Channels, ship-sourced sulphur emissions have reduced considerably in these areas. More reduction will be achieved in the near future in the remaining EU seas with the implementation in 2020 of the 0.5% regional limits. Moreover, technical measures are implemented to cut air pollution from ships. That includes the adoption of cleaner fuels, adding closed-loop 'scrubbers' or other exhaust gas cleaning devices to ships (for SO_x), SCR systems (for NO_x), slow steaming, and wider use of alternative sources of energy including wind power and port-side electricity.

The EEDI has been selected as a criterion for ship's energy efficiency and her performance from an environmental point of view in this study. The main reason is that the SO_x and NO_x emissions are more related to the fuel quality and the diesel engines efficiency rather than the ship operational profile and speed which this study is investigating. Basically, the main causes for SO_x and NO_x in marine engines are the high presence of sulphur compound in the marine fuels, improper air and fuel ratio for combustion, bad quality of fuel used for engines, and heavy loads on the engine. Moreover, EEDI provides a robust way to measure and assess ship performance in terms of CO_2 emissions and her compliance with the international policies regarding emissions.

According to DNV GL, the Energy Efficiency Design Index EEDI is the most important key performance indicator in the shipping industry to benchmark vessels on the same market or within the same fleet. It is a simple and straightforward measure to state a ship's transport efficiency in terms of carbon emissions according to IMO requirements. In other words, it offers

a straightforward way to calculate a vessel's energy efficiency based on the fuel consumption, capacity and speed using a single formula. Therefore, using EEDI in this study as an objective function allows comparison of a ship's theoretical CO_2 emissions relative to peer vessels of a similar size and type. Moreover, using EEDI in the environmental model helps in investigating and measuring the implications of adopting slow steaming on the ships emissions and energy saving.

4.3 Methods for Energy Efficiency Improvements

To ensure that shipping and marine industry are cleaner and greener, and to help ships' owners and operators to comply with the international and national regulations regarding shipping emissions by improving the EEDI for new designs, IMO has provided guidance for the best practices and cost-efficient solutions for energy improvements. Adopting IMO energy improvement measures have led to a great saving in fuel consumption and significant reductions in emissions. IMO has estimated up to 180 million tonnes of CO_2 emissions reductions by 2020 and up to 390 million by 2030 by introducing EEDI for all new ships and SEEMP for all ships. That counts of $(9 \div 16\ \%)$ reductions by 2020 and $(17 \div 25\ \%)$ by 2030. On the other hand, by using more sophisticated technologies, the annual fuel cost saving is estimated to be between \$34 and 60 billion by 2020 and between \$85 and 150 billion by 2030 (MARPOL Annex VI, 2013).

The technical and operational measures that have been adopted by IMO to improve ships' efficiency and to optimize fuel consumption leading to EEDI reduction are summarised below. In addition, an interesting study has been done by ABS (2013) providing ship designers, owners, and operators with useful information and a detailed guidance regarding the status and the current state of energy efficiency measures and options in the marine sector. The (ABS, 2013) advisory study includes descriptions and explanations of key issues, effectiveness and limits of the technical and operational measures, and a comparison of the pros and cons of each measure. Another leading maritime organization in fighting the global warming from maritime activities is Lloyd's Register which has an important responsibility in addressing strict environmental standards and prescriptive requirements for the maritime industry, and continuously proposing new innovations to mitigate CO_2 footprint. Lloyd's Register within its Strategic Research plan has addressed several projects aimed to increase energy efficiency of ships. One promising example of improving energy efficiency is a Handysize Bulk Carrier

(35200 DWT) optimisation by Lloyd's Register in collaboration with Shanghai Bestway Marine Engineering Design Co. Ltd. By focusing on hull-propeller interaction, rudder-propeller integration, machinery optimization, hull weight optimisation, heat recovery systems, and using 2nd generation of antifouling paints, 12% reduction in steel weight, 20% saving in fuel consumption, and 18% reduction in EEDI have been achieved (Hirdaris and Cheng, 2012).

The options and practises that available for existing and new vessels are:

- Hull design optimization,
- Designing larger ships,
- Improving propulsion system,
- Renewable energy,
- Developing more efficient engines,
- Optimising operation speed,
- Low-carbon fuels,
- Hull maintenance,
- Waste heat recovery,
- Voyage optimization,
- Fleet management.

In a general sense, ship owners and operators have a board spectrum of viable technical and operational measures to choose from to reduce their emissions, and hence to comply with the regional and international regulations. However, it is obvious that the options available to existing ships are significantly fewer than for new buildings where new technologies can be fit from scratch (Lloyd's Register, 2012b). There are trade-offs linked to each measure, and it is crucial to investigate all the benefits and disadvantages of adopting any individual or a combination of the available measures. In other words, the application of one of the energy saving measures may reduce or even exclude or the impacts of other measures. Moreover, some technical or operational emissions reduction measures may possibly have ramifications related to the logistical supply chain, and vice versa (Psaraftis and Kontovas, 2009). The next section focuses on the effect of speed optimization and mainly slow steaming concept considering the benefits and challenges. It analyses both the environmental and economic impacts.

4.4 Speed Optimization

4.4.1 Slow Steaming measure

The EEDI requirements and the reduction phases in Table 4.3 aim to reduce shipping carbon footprint and increase the energy efficiency of new buildings against business-as-usual in a cost-effective manner. Several Studies indicate that speed optimization has a significant effect on the shipping busiiness in the short term and also in the medium and long terms. The reason is that it can help to increase the engine efficiency by optimising its load, and also reducing the total resistance by optimizing the hull hydrodynamic and aerodynamic loads. Speed optimization means looking for a speed(s) at which fuel conumption for a particular voyage per tonne mile is at the most practical and acceptable minimum level. However, the optimumu speed does not mean minimum speed. In fact, possible adverse consequences of sailing at esxtremely lower or higher speeds than the optimum one includes higher fuel consumption per journey, problems with the engine and the exhaust systems, and increased vibration in the propulsive system (IMO MEPC 63/23 Annex 9. (2012)).

However, these efficiency goals can be gained directly by reducing the service speed which is known as slow steaming. Slow steaming is a quick, easy, and effective practice to achieve energy savings, and it presents the largest opportunities for fuel savings and hence CO_2 emissions reduction for commercial vessels. The core insight is simple and straighforward as the propulsion power is a function of the speed to the power of three or even more for high speeds ($P \sim V^{3+}$). Therefore, a small drop in speed will casue a great saving in the required propulsion power and hence in fuel consumption (Lindstad *et al.*, 2011). That has been demonstrated in (Haakenstad, 2012) study where she has illustrated the relation between the required power P and speed V by transforming the speed-power equation as in Eq (4.8) and looking at the speed dependency of the total resistance coefficient C_T. It was found that the estimated C_T is proportional to the speed of the first, second or third power. Therefore, ship power is proportional to the service speed of the fourth, fifth, or sixth power. Table 4.5 shows the fuel consumption saving for an 8500 TEU container when sailing at slow speeds.

$$P = C_T \cdot const \cdot V^3 \tag{4.8}$$

Where $const = \frac{1}{2} \cdot \rho \cdot S$,

S: is the wetted surface area, and ρ: is the water density.

Table 4.5 Impact of Speed Reduction on Vessel Fuel Consumption

% Speed Reduction	Speed (knots)	Daily Main Engine Fuel Consumption (tons)	% Reduction in Fuel Consumption
0%	15.00	230	0%
10%	13.50	168	27%
20%	12.00	118	49%
30%	10.50	79	66%
40%	9.00	50	78%
50%	7.50	29	87%

Source: (Philippe Crist, 2009)

Slow steaming is not a new practice introduced to the shipping market in the last decade to reduce fuel costs. In fact, already in the early 1970's during the first oil crisis, in response to rapidly increasing bunker prices, the maritime sector and especially large and relatively high speed vessels adopted slow steaming to cut the operating cost (Philippe Crist, 2009). Once again, the rapid spike in bunker prices in the first half of 2008, and bearing in mind that fuel cost represents around 50-60 per cent of the total operational cost depending on the ship type, ship operators and charterers who are under economic pressure return to sail at lower speeds. That helps to cover the extra fuel cost and, hence, to maintain good levels of service and face the increasing costs for goods shipping. Studies have shown a considerable adoption of slow steaming among international fleet over the period 2007-2012. The slow steaming concept is more embraced by big ships rather than small ship size categories that often operate with a trivial change in the operating speed, and hence in the fuel consumption. The average reduction in design speed at sea over the period 2007-2012 according to the fleet activity report run by *The Third IMO GHG Study* (2014) was about 12% and the associated saving in the daily fuel consumption was about 27%. However, many ship type and size categories demonstrated a greater reduction in speed and, hence, a greater saving in fuel consumption. For instance, the daily fuel consumption in some oil tanker and container size categories was reduced by approximately 50% and 70%, respectively.

A model has been developed by Lindstad *et al.* (2011) to calculate costs and emissions as a function of speed for individual ship classes including bulk, container, and RoRo vessels. These three different ship types operate within different speed regimes, and hence the model demonstrates different responses in terms of emissions and costs resulting from reducing speed.

The results from (Lindstad *et al.*, 2011) model show that there is a significant potential for energy saving and reducing CO_2 emissions in shipping by purely operating at lower speeds. Based on fuel prices in the study, emissions reductions by around 19% can be achieved with a negative abatement cost (cost minimization), and by 28% free of charge (a zero abatement cost). The study has concluded that annual emissions from shipping can be reduced from 1122 million ton CO_2 to 804 million ton CO_2 at no cost. Chapter 5 reviews more studies which are motivated by the opportunity for cost saving and/or profit maximization by adopting slow steaming.

As said before, the EEDI value is very sensitive to the design speed. Therefore, a small reduction in the service speed will contribute to a significant reduction in the attained EEDI value. In the EEDI formula (Eq (4.3)), the service speed V_{ref} and the non-dimensional coefficient f_w which indicates the decrease of speed because of the weather condition are in the denominator. In this case, the lower the service speed and the higher the f_w coefficient, the lower the attained EEDI value because of the cube law between speed and power. Table 4.6 shows the influence of the service speed on the EEDI value for some tanker classes.

Table 4.6 Influence of service speed on the EEDI for Tankers (IMO MEPC 60/4/34, 2010)

Ship Class		**-2 knots**	**-1 knots**	**Standard**	**+1 knots**
Panamax	EEDI attained	4.33	5.16	5.95	6.82
	% Change	-27%	-13%	---	+15%
Aframax	EEDI attained	3.04	3.22	3.73	4.37
	% Change	-19%	-14%	---	+17%
Suezmax	EEDI attained	2.53	2.74	3.14	3.63
	% Change	-19%	-13%	---	+16%
VLCC	EEDI attained	2.10	2.24	2.53	2.87
	% Change	-17%	-1%	---	+14%

An important implication of practising slow steaming by the maritime fleet is stabilizing the supply and demand market. In 2011, the excess ton-mile capacity in the tankers and bulk carriers market was around 25 to 30%. Devanney (2011b) has suggested that absorbing all this extra capacity would be achieved by sailing at an average speed of about 11 knots as slow steaming is a flexible mechanism for a short-term solution to control cost and capacity for the tankers and bulk carriers fleet. However, some vessel sectors have not slowed down at all or

that much despite the massive increase in bunker costs. That is because they carry reefer or perishable products or carrying people commuting to their morning work.

The three-year (2011-2013) EU-project ULYSSES (Ultra Slow Ships) take the slow steaming concept further by investigating the possibility of achieving particular environmental targets by introducing the Ultra Slow Steaming into the tankers and bulk carriers sectors. The objectives of ULYSSES are to increase the world fleet efficiency to a point where greenhouse gas emissions are reduced by 30% before 2020 compared to 1990 levels and by 80% beyond 2050. These targets will be met by coupling ultra slow speeds with other measures and technologies to achieve the highest efficiency gains. The target speeds of ULYSSES project are (ULYSSES, 2011):

- Phase I - Existing vessel in 2020: ~10 knots
- Phase II - New vessel built in 2020: ~7.5 knots
- Phase III - New vessel built in 2050: ~5 knots.

Unfortunately the ULYSSES project website (http://ultraslowships.com/) is broken and not available, and there are no publications available regarding the final results or suggestions. Therefore, it is hard to validate the applicability of ultra slow speeds concept as it is a challenge to safely reduce the ship speed down to 5 knots for example and to foresee the economic impact on the overall supply chain.

4.4.2 Slow Steaming Challenges and Concerns

Shipping companies started adopting slow steaming around 2007/2008 as an effective way to trim operating costs and overcome the increasing fuel prices, oversupply of shipping tonnage, and declining freight rates. However, as the shipping market is periodic and repetitive, the question is for how long it will stay stable and whether slow steaming will be acceptable in case shipping market conditions have changed again. Another question that arises is whether ships that have been optimised and built to sail efficiently at slow speeds will be able to compete in a booming market with high demand and high fright rates or when bunker prices are low.

On the other side, even though slow steaming is a common operating feature to reduce energy consumption and CO_2 emissions but it may require the ship engine to operate at low loads conditions and outside its rated envelope. Operating at lower load factors which occurs with slow steaming leads to an increase in the specific fuel consumption SFC as the combustion

process becomes less optimal in diesel engines and hence the power produced per unit of fuel is less. However, even though a ship uses less fuel for the same journey when she goes at slower speeds but she consumes more fuel per power unit (1 kWh) generated by the engines because the fossil fuel combustion process is not optimal. Moreover, sub-optimal combustion that produces relatively less power is the main reason of producing proportionally higher amount of pollutants such as particulate matters (PM) and Nitrous Oxides (NO_x) that are linked to human health concerns, climate forcing effects, and harms to ozone layer (MAN B&W, 2001; Faber *et al.*, 2012).

Operating continuously in off-design conditions has several disadvantages that might occur to the main engine(s), the propulsion system units, and vessel's performance (Faber *et al.*, 2012). That includes:

- Lower combustion temperatures and pressures inside the engine,
- Inefficient heat recovery system,
- Increased lubrication oil demand,
- Loss of turbo charger efficiency, so less air flow to the engines,
- Fouling of the exhaust gas economizer,
- Possible increase in particulate matter (PM) emissions,
- Increasing carbon deposits,
- Loss of propeller efficiency,
- More maintenance may be required for auxiliary engines and boilers as these systems are working for longer hours to compensate the loss in the heat recovery and turbo charger systems,
- Increased fouling on the hull and propeller because of the reduced flow velocity,
- Increased level of vibration in the engine room because of operating in off-design conditions,
- At variable pitch, cavitation may occur on the pressure side of the propeller,
- Higher maintenance routine is needed, and reference should be made to the engine manufacturer's power/consumption curve and the ship's propeller curve to avoid operating outside their optimised profile.

A shipowner may decide to de-rate the main diesel engine to operate at less than its rated maximum capability in order to extend its life. This option is often endorsed when speed

reduction is taken on a long or permanent basis. Engine derating will result in improving the engine performance at the new operating speed, and hence better fuel saving. However, most bulk carriers and crude oil tankers operate in voyage charter frameworks where charter parties decide on ship speeds. Therefore, derating a ship engine will lead to changes in the charter contracts, and that should be agreed between the shipowner and the charter party as the shipowner is responsible for the conversion cost while the charter party will pay for the fuel cost.

Reducing the service speed leads to longer sailing time, and hence less journeys per year. Therefore, ships' operators need to take account of the coordinate arrival times at the port with the availability of the berths. However, several studies have reported that reducing the service speed of the world fleet may boost the shift in freight transport from maritime shipping to other modes such as land and air in order to maintain capacity. Alternatively, this adopted strategic reductions of service speed may result in more ships being needed in the market for a stable demand and supply level. Therefore, the actual effect on emissions for the whole fleet will be less than the third-power reduction for individual ships. It was estimated that the net effect on CO_2 emissions is approximately a second-power reduction (Buhaug *et al.*, 2009). In this case, a 10% speed reduction will equates to a 27% reduction in shaft power for induvial ships and only 19% in energy saving on a tonne-mile basis.

Ship safety is a serious concern for all parties involved in maritime transport when it comes to slow steaming especially when sailing in rough sea and against head or oblique waves as there will be a significant loss of safety. The bad weather effect will be in slowing the ship more, and hence with no additional power input, the ship might be left with no manoeuvring ability to a certain extent. Ships sailing at low engine loads have worse manoeuvrability especially when a ship is not equipped with additional steering devices such as bow tunnel thrusters (Szelangiewicz and Żelazny, 2012). Therefore, IMO in the EEDI guidelines has indicated that the potential energy savings via speed reduction and engine power to fulfil EEDI requirements should not lead to worsening the safety conditions of the ship. Equipping ships with a redundant power source for the propulsion system is one of the solutions that can be used even it is considered as extra cost and an economic constraint. Another potential safety problem is navigation when sailing in busy areas with large traffic such as English Channel where the passing ways are crossed especially during heavy shore-to-shore communication. With low engine power, avoiding collision between ships will be a problem. Also sailing at slow speed

in areas infested by pirates will be dangerous for both the ship and the crew as the slower a ship goes, the bigger the exposure to pirate attacks becomes (Claudepierre *et al.*, 2012). A draft EEDI regulation (22.4) states that "For each ship to which this regulation applies, the installed propulsion power shall not be less than the propulsion power needed to maintain the manoeuvrability of the ship under adverse conditions, as defined in the guidelines to be developed by the Organization."

4.4.3 Speed Limits

Currently, the average speed of the world fleet vary as a function of the state of the market as the circumstances in the shipping market are volatile all over the year and at different level for the ships sectors. In recent years, ships have practiced slow steaming voluntarily to face the current economic downturn and as a need to reduce the extra tonnage in the market and to cut fuel costs. Aside from the voluntary speed reduction, mandatory speed control has been proposed by the Clean Shipping Coalition (CSC) to the International Maritime Organization's Marine Environment Protection Committee (IMO MEPC – 61st session 2010) as an efficient and fast way to reduce greenhouse gas emissions from ships. In their proposal, they have looked to the potential of regulating slow steaming at different levels and its impact on emissions. The proposal has suggested that logical and effective regulations for enforcing mandatory speed limits globally can be achieved only by IMO.

The CE Delft report (Faber *et al.*, 2012) explores the technical constraints, the associated social costs and benefits, the long and short-term effects of implementing slow steaming, and the legal feasibility of regulating slow steaming by national and international bodies. For instance, a global scheme that limits ships' average speed by 85% of their average speed in 2007 would achieve a net savings by USD 178-617 billion in the period between 2010 and 2050 according to a report for Transport and Environment and Seas at Risk by CE Delft, the ICCT and Professor Mikis Tsimplis. While a speed restriction regime which limits the average speed in the European ports would either result in additional cost of USD 1 billion or a significant net benefits of up to USD 74 billion. These figures takes into account the extra costs of building additional ships and the significant benefits from reducing fuel expenditures. The net savings are sensitive to fuel price projections as higher fuel prices result in larger benefits that outweigh the costs by a larger amount, and also are sensitive to the used discount rate in the future scenarios although it does not change the trend of the net cost and benefits in most case.

The speed restrictions introduced by IMO or any sea state depend on ship size and type and can be either addressed for average speeds or top speed. However, a ship's average speed is easier to determine than the top speed as journey details such as trip total duration and distance, port entry and exit times, and ship's locations are available on the log book while monitoring the top speed can be done only by using (S-)AIS system data that provide the ship operator and the regulator the ability to monito the ship's speed over ground SOG (Faber *et al.*, 2012).

Some proposals have been made suggesting that setting a single speed limit for all ships regardless of type and size would be relatively easy to regulate, enforce, communicate, and monitor. Nevertheless, regulating a single speed limit would not be effective and efficient for ships that already sail at slow speeds. For example if the single speed limit is set at 15-16 knots, then it will have impact on high-speed vessels such as container ships but a small or neglected impact on tankers and bulk carriers unless the single speed limit is set at 10 knots which might not be practical for several ships types that might lose the competition in the market. In the case of some cargo types that can either be shipped in bulk or containerised for example, then shippers might prefer a fast containership than a slow bulk carrier. On the other hand, that create a flexible and vital market for shippers (Maggs, 2011).

Devanney (2011b) has claimed that introducing speed limits by IMO or any other national state as one of the mandatory measures to force ships to slow down is either ineffective or inefficient. It is ineffective in case ships slow down voluntarily and sail at speeds lower than the mandated speed in response to the rising fuel prices and low fright rates. If the speed limits set by the regulations are less than the voluntary speed, there will be a shortage in the fleet market and hence an artificial spot-rate boom in the short term. As a response, more ships will be built to balance the increasing demand, and these new ships will be underpowered as they are built with smaller engines and designed to sail at slower speeds which makes them unsafe for oceangoing journeys. Therefore, ships should be designed in a way that can operate efficiently over a range of speed in order to respond quickly to any changes in the demand shortage in the market and changes in fuel prices. In this case, ships would return to operate at normal and higher speeds when the economy recovers to balance the supply and demand market.

4.5 EEDI Calculations

The study is built upon robust design philosophy. It is where the overall energy balance is taken into account to deliver a greener design with optimum performance whilst remaining commercially viable. The aim is to achieve, through coupling slow steaming and hull optimization, the maximum increase in efficiency and maximum reduction in CO_2 emissions produced per tonne mile of cargo transported.

As a means of quantifying performance and efficiency of alternative deigns and investigating the influence of slow steaming on energy efficiency and ships' environmental footprint, EEDI is used as an initial indicator to compare the new hulls generated within the hydrodynamic model from the original Panamax tanker ship in Chapter 3. The attained EEDI value for each individual ship is calculated over the selected speeds range which reflects the possible operation profile. Then it has been tested against the EEDI reference baseline based on the ship capacity (deadweight) as in Eq (4.4). Moreover, EEDI reduction factors have been used to validate if the alternative designs meet the IMO future regulations regarding greenhouse gas emissions targets till year 2025.

Carrying out the EEDI calculations and estimating fuel consumption and CO_2 emissions aim to search for a robust design(s) that can operate efficiently at different speeds and is able to respond to any fluctuation in the market such as fuel prices and supply-demand conditions. Hence, in calculating the EEDI values, assessing the influence of speed reduction on energy saving and fuel consumption is essential and will be carried out.

The EEDI value will be fixed for the initial design at the service speed, and the simplified EEDI formula Eq (4.9) will be used for the environmental model taking into account the following assumptions suggested by IMO guidelines:

$$Attained\ EEDI = \frac{(C_{FME} \times SFC_{FME} \times P_{ME}) + (C_{FAE} \times SFC_{FAE} \times P_{AE})}{Capacity \times V_{ref}} \qquad (4.9)$$

where:

- C_{FME}: For HFO is 3.1144 $(t - CO_2/t - fuel)$.
- C_{FAE}: For Diesel Oil is 3.206 $(t - CO_2/t - fuel)$.
- SFC_{FME}: 165.0 (g/kWh) using data from MAN Engines catalogue (MAN Diesel & Turbo, 2013).

As long as speed reduction is not significant (up to 10-15%), then SFC_{FME} remains relatively constant. When speed reduction is more than 10%, the engine load decreases by a third power and the specific fuel consumption increases accordingly depending on the engine characteristics and age. For example, a 30% reduction in speed will result in decreasing the engine load to around 40% of MCR and SFC_{FME} increases by up to 10% (Cariou, 2011). The variation of the specific fuel consumption for both two-stroke and four-stroke engines has been analysed by (Kristenen and Psaraftis, 2015). It has been found that changes in the SFOC due to changes in engine loading can be estimated as a percentage deviation from the minimum value occurring at approximately 75% MCR for 2-stroke engines and at 80% MCR for 4-storke engines as in the following equations:

$$\begin{aligned} &\text{2-stroke engines:} && \text{SFOC deviation } \% = 0.0028 \cdot MCR^2 - 0.41 \cdot MCR + 15 \\ &\text{4-stroke engines:} && \text{SFOC deviation } \% = 0.0036 \cdot MCR^2 - 0.58 \cdot MCR + 23 \end{aligned} \quad (4.10)$$

However, this study assumes that engine tuning methods will be applied depending on the operating profile, and hence the specific fuel consumption is optimised for the loading range.

- SFC_{FAE}: 210.0 (g/kWh) as suggested by IMO for new 4-stroke engines.
- P_{ME}: is 75% of the rated installed power MCR as calculated using AVEVA in the next chapter.
- P_{AE}: the auxiliary engine(s) power is calculated as following:
  - For ships with a main engine power of 10000 kW or above, P_{AE} is defined as:

$$P_{AE(MCRME>1000kW)} = \left(0.025 \times \left(\sum_{i=1}^{nME} MCR_{MEi} + \frac{\sum_{i=1}^{nPTI} P_{PTI(i)}}{0.75}\right)\right) + 250$$

  - For ships with a main engine power below 10000 kW, P_{AE} is defined as:

$$P_{AE(MCRME<1000kW)} = 0.05 \times \left(\sum_{i=1}^{nME} MCR_{MEi} + \frac{\sum_{i=1}^{nPTI} P_{PTI(i)}}{0.75}\right)$$

- V_{ref}: Ship speed at 75% MCR in deep water assuming the weather is calm with no wind and no waves.

- $Capacity$: Deadweight is used as capacity for tanker ships. Basically, it is the difference in tonnes between the ship displacement at the summer load draught in water of relative density of 1025 kg/m^3 and the lightweight. Different methods are available in the literature to estimate the deadweight as will be discussed in the economic model in Chapter 5. Generally, the lightship weight has three main components including hull weight, equipment weight, and machinery weight as in Eq (4.11):

$$LW = W_H + W_E + W_M \tag{4.11}$$

Where:

W_H: The weight of the structural steel of the vessel hull, the superstructure, and the outfit steel. The hull weight estimation can be improved by considering some corrections such as

W_E: The weight of the equipment, outfit, deck machinery, etc.

W_M: The weight of all the engine room machinery.

To calculate the hull lightweight, an estimation method based on statistical analysis regression for data from existing ships by Jorge d' Almeida (2009) is used for this purpose, and hence to estimate the deadweight in the EEDI formula. Jorge d' Almeida (2009) regression formulas are given as following:

$$W_H = K1 \times L^{K2} \times B^{K3} \times D^{K4} \tag{4.12}$$

$$W_E = K5 \times (L \times B \times D)^{K6} \tag{4.13}$$

$$W_M = K7 \times {P_{MCR}}^{K8} \tag{4.14}$$

Where:

L, B, D: The length, breadth and depth of the ship.

$K1, K2, K3, K4, K5, K6$: Non-dimensional coefficients, and they are given for each vessel types as in Table 4.7.

P_{MCR}: The installed power in HP. $1\ kW = 1.34102209\ HP$

$K7, K8$: The machinery weight coefficients, and they vary depending on the main propulsion plant type as in Table 4.8.

Table 4.7 Hull and Equipment weight coefficients for d' Amedia method

Ship type	$K1$	$K2$	$K3$	$K4$	$K5$	$K6$
Oil tankers	0.0361	1.600	1.000	0.220	10.820	0.410
Bulk carriers	0.0328	1.600	1.000	0.220	6.1790	0.480
Container carriers	0.0293	1.760	0.712	0.374	0.1156	0.850
Gneral cargo	0.0313	1.675	0.850	0.280	0.5166	0.750

Table 4.8 Machinery weight coefficients for d' Amedia method

Propulsion Plant type	$K7$	$K8$
2-Stroke Diesel	2.410	0.620
4-Stroke Diesel	1.880	0.600
2 x (2-Stroke Diesel)	2.350	0.600
Steam Turbine	5.000	0.540

After carrying out the EEDI calculations for all alternative designs over the speed range, each individual EEDI value is then compared with the reference EEDI given as in Eq (4.15) for tanker ships.

$$Reference\ EEDI\ value = 1218.80 \times DWT^{-0.488} \tag{4.15}$$

For the purpose of assessing the energy efficiency, the %EEDI is used to compare hulls against the Reference EEDI for example as following:

$$\%EEDI\ (Ref) = (Attained\ EEDI / Reference\ EEDI) - 1 \tag{4.16}$$

Finally, it is important to validate weather the new generated hulls will meet the following IMO future regulations:

$$EEDI\ (January\ 2015) = 0.9 \times (1218.80 \times DWT^{-0.488})$$

$$EEDI\ (January\ 2020) = 0.8 \times (1218.80 \times DWT^{-0.488})$$

$$EEDI\ (January\ 2025) = 0.7 \times (1218.80 \times DWT^{-0.488})$$

4.6 EEDI model's Results

For each individual hull of the three stages generated in the parametric model, CO_2 emissions from the main engine(s) and the auxiliary engines are calculated based on the EEDI guidelines, as well as the ship deadweight using d' Almeida estimation method. The attained Energy Efficiency Design Index (EEDI) is then calculated within the environmental model at the design speed and also over the speeds range (5-17 knots). Analysing the model results helps to investigate the influence of the chosen design parameters and operating speed on the ships' energy efficiency and the environmental footprint from all the different hulls. These values are analysed in order to search for the most favourable parameters and speeds that minimize the fuel consumption and, hence, CO_2 emissions. It is also very vital to make sure that the desired designs comply with the IMO requirements representing by the reference EEDI values and also not to exceed the tight EEDI targets in the coming years.

It is worth mentioning again that the actual CO_2 emitted from ships is different from what is considered in the EEDI formula which considers only the fuel consumption in the main and auxiliary engines at the design speed, as well as in the laden leg and for calm water conditions. However, the economic model in the next chapter calculates the actual total fuel consumption during a roundtrip (laden and ballast leg, and in port) burned in the main and auxiliary engines and boilers. That helps the purpose in identifying more accurately the actual trends in fuel consumption and CO_2 emissions reductions and the operation cost as well.

Table 4.9 shows the estimated deadweight for the base ship and the corresponding EEDI reference value at the design speed. It also shows the EEDI targets for the future phases addressed by IMO. The attained EEDI values for the base ship (original hull) over the speed range are shown in Table 4.10 along with the percentage change from the EEDI value at the service speed (15 knots). Table 4.11 shows the percentage EEDI variation from the EEDI Reference value for the base hull as well as from the future EEDI reduction baselines. Those values are plotted in Figure 4.5 to illustrate the influence of the service speed on the attained EEDI values.

It is very obvious that the EEDI is predominantly sensitive to the operating speed, and that is because the propulsion power is a function of the cubic power of the speed or even more as suggested by many studies. As shown in Table 4.10 and Figure 4.5, reducing the speed by 1 knot reduces the EEDI by 18% from 5.68 to 4.65 at speed 14 knots, whereas increasing the

speed by 1 knot increases the EEDI by 25% from 5.68 to 7.10 at speed 16 knots. Table 4.11 shows that this oil tanker base ship complies with the current IMO regulations regarding CO_2 emissions for speeds equal to the service speed or less. However, when it comes to comply with the future tight phases' requirements, the base ship sailing at the service speed fails for all the three EEDI phases (2015, 2020, and 2025). The grey cells in Table 4.11 shows the speeds where the ship fails to meet the required EEDI minimum values as the difference is higher than zero. The results show that the base ship with a service speed of (15 knots) needs to reduce her speed at least by 1 knot to meet the required minimum EEDI for phase 1 and phase 2 and by 2 knots to avoid the EEDI penalty for phase 3 (January 2025).

Table 4.9 EEDI Reference and future phases

Base ship DWT	53902.12
EEDI Reference (Baseline)	5.98
Phase 0 (0%) – January 2013	5.98
Phase 1 (10%) – January 2015	5.39
Phase 2 (20%) - January 2020	4.79
Phase 3 (30%)- January 2025	4.19

Table 4.10 Attained EEDI for the Base Ship and EEDI Change with speed

Speed [knots]	5	6	7	8	9	10	11	12	13	14	**15**	16	17
Design Speeed Variation	-10 knot	-9 knot	-8 knot	-7 knot	-6 knot	-5 knot	-4 knot	-3 knot	-2 knot	-1 knot	---	+1 knot	+2 knot
Attained EEDI	1.83	1.82	1.91	2.07	2.29	2.57	2.91	3.34	3.91	4.66	**5.68**	7.10	9.04
% EEDI change	-68%	-68%	-66%	-64%	-60%	-55%	-49%	-41%	-31%	-18%	0%	25%	59%

Table 4.11 Difference between Attained EEDI and Future Phases for the Base Hull

Speed [knots]	5	6	7	8	9	10	11	12	13	14	**15**	16	17
Attained EEDI	1.83	1.82	1.91	2.07	2.29	2.57	2.91	3.34	3.91	4.66	5.68	7.10	9.04
% Diffrence from Reference EEDI	-69%	-70%	-68%	-65%	-62%	-57%	-51%	-44%	-35%	-22%	-5%	19%	51%
% Diffrence from Phase 1	-66%	-66%	-65%	-62%	-58%	-52%	-46%	-38%	-27%	-14%	6%	32%	68%
% Diffrence from Phase 2	-62%	-62%	-60%	-57%	-52%	-46%	-39%	-30%	-18%	-3%	19%	48%	89%
% Diffrence from Phase 3	-56%	-57%	-54%	-51%	-45%	-39%	-30%	-20%	-7%	11%	36%	69%	116%

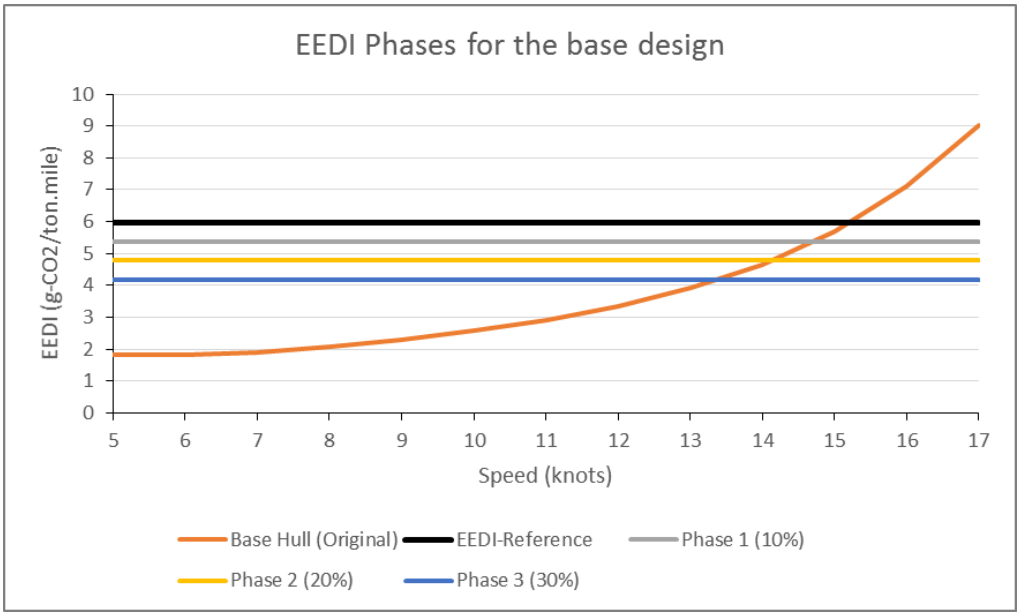

Figure 4.5 EEDI for the Base Hull

Figure 4.6 shows the attained EEDI obtained for the 36 hulls generated in Stage One at design speed (15 knots). The attained EEDI values are plotted against the EEDI reference line and also against the required EEDI for Phase 1 (January 2015). The black dotted lines represent the percentage difference between the attained EEDI and the EEDI reference. The results can be summarised as the following:

- All Group One hulls (Figure 4.6-a) have an attained EEDI at the design speed less than the EEDI reference baseline while none of those hulls meet the EEDI Phase 1 minimum requirements as the attained EEDI is greater than Phase 1 baseline. Varying the length while keeping the other design variables constant has a significant influence on the

EEDI. Taking the +10%L hull as an example, increasing the length by 10% and keeping the displacement constant results in achieving a -6.35% difference from the EEDI reference value while it is just -5.05% for the original hull. That is because for a constant displacement, when increasing the length and reducing the breadth and depth, the relative saving (decrease) in the required propulsive power is generally bigger than the relative loss (decrease) in the ship carrying capacity i.e. deadweight. This suggests that increasing the hull length will tend to improve the EEDI.

- Similarly to Group One hulls, all Group Two hulls (Figure 4.6-b) have an attained EEDI at the design speed less than the EEDI reference baseline. However, none of those hulls meet the EEDI Phase 1 minimum requirements as the attained EEDI is greater than Phase 1 baseline. Varying the B/T ratio while keeping the other design variables constant has also a significant influence on the EEDI. Taking the -10%B/T hull as an example, it can be seen that reducing B/T by 10% [smaller beam B and greater draft] while keeping the length and displacement constant results in achieving around -10% difference from the EEDI reference value vs -5.05% for the original hull. This suggests that increasing the draft and/or making the hull slimmer improves the EEDI.
- Examining Group Three hulls (Figure 4.6-c) shows that at the design speed, slim hulls with reduced block coefficient C_B have an attained EEDI less than the EEDI reference baseline while the attained EEDI for hulls with increased C_B is greater than the EEDI reference. That is, as discussed previously in the hydrodynamic model, because increasing the hull fullness coefficient increases the required propulsion power, and hence fuel consumption. Reducing the third design variable C_B while keeping the other variables constant results in improving the energy efficiency as can be seen for the $[-2\%, 4\%, 6\%\ C_B]$ hulls. Basically, as the block coefficient is reduced, the ship capacity is reduced as well as the required power. The results indicate that the changes in the required power are more significant than the changes in the cargo capacity. Taking the $-6\%\ C_B$ hull as an example, it can be noticed that the difference between the attained EEDI and the EEDI reference is around -13% i.e. it improves by around 8%. Moreover, it is the first hull so far that meets the EEDI requirements for Phase 1 at the design speed as well as the $-4\%\ C_B$ hull. Later in the economic model, it is vital to investigate if the gain in power efficiency would offset the loss in cargo capacity and hence revenue when the block coefficient is reduced.

- The final design variable to be discussed is the longitudinal centre of buoyancy LCB. It can be seen on (Figure 4.6-d) that all Group Four hulls have an attained EEDI smaller than the EEDI reference baseline at the design speed. Shifting the position of the longitudinal centre of buoyancy backwards certainly improves the energy performance of the ship. It can be seen that the percentage EEDI difference for the $[-1.0\%\ L, LCB]$ hull is more than -8% comparing with the -5.05% difference for the original hull.

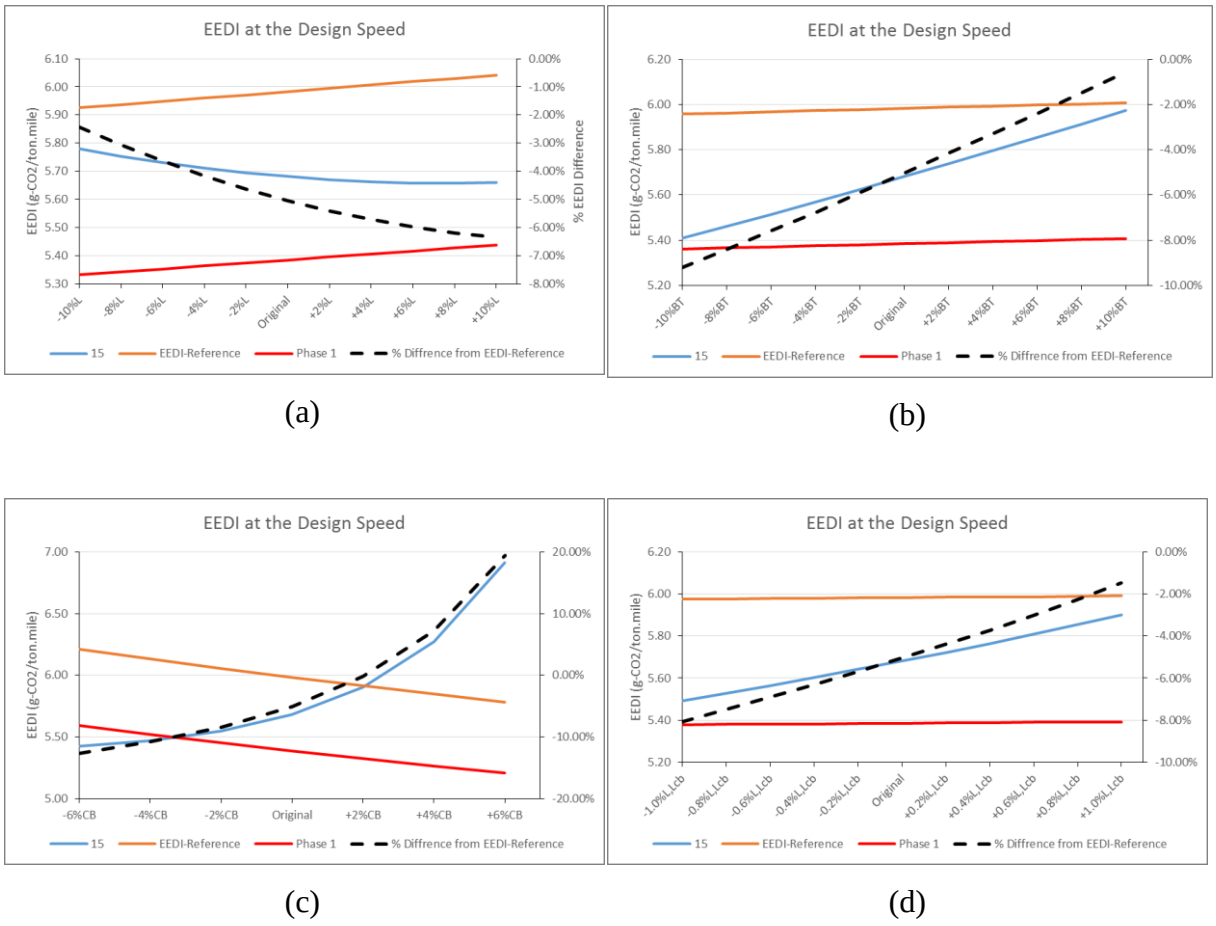

Figure 4.6 Attained EEDI at the deign speed for Stage One Hulls

In order to meet the IMO future targets regarding energy efficiency, the influence of slow steaming is investigated as one of the most effective measures adopted by ship operators to reduce energy consumption and emissions and achieve the required minimum EEDI targets. As the main diesel engine power output is more-or-less a cubic function of the speed, then a small drop in the speed can lead to a great energy saving and thus an important reduction in the EEDI value as can be seen in Appendix D1 (a, b, c, d). The results from the EEDI calculation model show that all the 39 hulls in Stage One meet Phase 3 (January 2025) at speed 13 knots and

below. At the 13 knots speed, the hull -10%B/T among all Stage One hulls archives the best performance in terms of energy efficiency level per capacity mile. The results show that the difference between the attained EEDI and Phase 3 target is (-10.40%) which looks very promising.

After discussing the influence of speed and the four individual design parameters on the ship energy performance, the interest lies in analysing the combined impact of the two primary design parameters (L, B/T) in Stage Two. Figure 4.7 and Table 4.12 show the %EEDI difference between the attained EEDI and the EEDI Reference at the design speed for the 110 generated hulls. While Appendix D2 shows the %EEDI difference figures at other speeds to illustrate the EEDI trends at other speeds.

It is obvious that both design parameters have a significant impact on the energy performance and the EEDI. This impact comes from the fact that the ship deadweight (cargo capacity) and the required engine power are functions of variations in the hull dimensions (L, B/T, D). The dark grey cells in Table 4.12 represent hulls that fail to meet the EEDI baseline requirements as the attained EEDI is greater than the EEDI reference. While cells highlighted in light grey represent hulls which are less efficient than the original hull (centre cell) in terms of CO_2 emitted per transport work unit ($gCO_2/t.nm$). The remaining cells represent hulls that are more efficient than the original hull as they have a smaller %EEDI at the design speed.

Generally speaking, designs with longer and deeper hulls and smaller beams show an improvement in the energy efficiency and reduction in CO_2 emissions per transport work done during a specific period (EEDI). The same trends for the attained EEDI i.e. (energy consumption or carbon emissions per transport capacity) can be seen among Stage Two hulls at other speeds as shown in Appendix D2 figures. Moreover, the potential fuel and emission savings under slow steaming are considerable as the attained EEDI is reduced significantly where IMO future targets regarding EEDI phases are met. For instance, by reducing the service speed by 3 knots from 15 knots to 12 knots, the attained EEDI for $[+10\%L, -10\%\ B/T]$ drops by around 39% from 5.03 to 3.09. Hence, the %EEDI difference from the reference EEDI drops from -12% to around -46% which demonstrates a significant benefit against the EEDI restrict requirements as can be seen in figures (b and c) in Appendix D2.

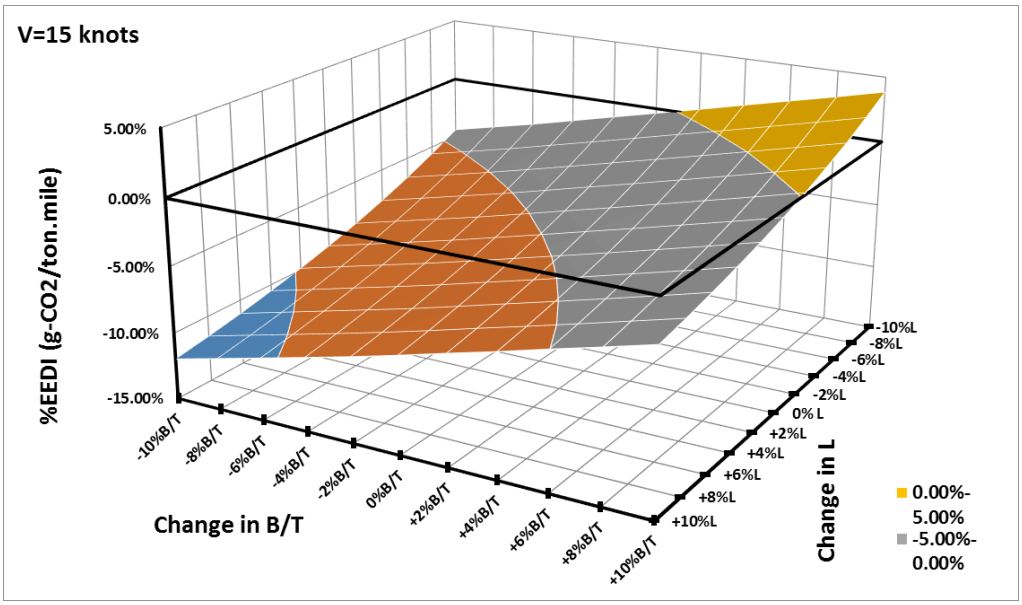

Figure 4.7 %EEDI Difference at the design speed for Stage Two Hulls

Table 4.12 %EEDI Difference at the design speed for Stage Two Hulls

	-10%L	-8%L	-6%L	-4%L	-2%L	0% L	+2%L	+4%L	+6%L	+8%L	+10%L
-10%B/T	-4.45%	-5.60%	-6.65%	-7.59%	-8.45%	-9.21%	-9.89%	-10.50%	-11.05%	-11.54%	-11.97%
-8%B/T	-3.67%	-4.83%	-5.86%	-6.80%	-7.65%	-8.41%	-9.08%	-9.69%	-10.23%	-10.72%	-11.15%
-6%B/T	-2.90%	-4.05%	-5.08%	-6.00%	-6.84%	-7.59%	-8.26%	-8.86%	-9.41%	-9.90%	-10.33%
-4%B/T	-2.07%	-3.21%	-4.26%	-5.20%	-6.03%	-6.78%	-7.45%	-8.06%	-8.59%	-9.07%	-9.50%
-2%B/T	-1.23%	-2.37%	-3.41%	-4.33%	-5.18%	-5.91%	-6.60%	-7.21%	-7.76%	-8.23%	-8.66%
0%B/T	-0.40%	-1.52%	-2.55%	-3.47%	-4.30%	**-5.05%**	-5.72%	-6.32%	-6.86%	-7.35%	-7.78%
+2%B/T	0.44%	-0.67%	-1.70%	-2.61%	-3.44%	-4.16%	-4.84%	-5.44%	-5.96%	-6.43%	-6.86%
+4%B/T	1.29%	0.18%	-0.84%	-1.73%	-2.55%	-3.29%	-3.95%	-4.53%	-5.06%	-5.54%	-5.96%
+6%B/T	2.13%	1.03%	0.03%	-0.85%	-1.66%	-2.39%	-3.05%	-3.62%	-4.15%	-4.62%	-5.02%
+8%B/T	2.97%	1.90%	0.92%	0.05%	-0.78%	-1.49%	-2.14%	-2.70%	-3.23%	-3.69%	-4.10%
+10%B/T	3.84%	2.78%	1.80%	0.94%	0.14%	-0.57%	-1.21%	-1.77%	-2.29%	-2.75%	-3.17%

Finally, this section discusses the combined influence of speed reduction and variations in the controllable primary and secondary design variable on the energy efficiency and attained EEDI. In order to evaluate the over-all influence of speed reduction and each combination of parameters variations, the %EEDI as in Eq (4.16) is selected as an indicator for alternative hulls vs. the base original hull. The attained EEDI for Stage Three hulls at selected speeds as well as

the EEDI reference and %EEDI are provided in Appendix D3. Cells highlighted in dark grey represents hulls that fail to meet EEDI Reference minimum requirements (2013 target) at the service speed (15 knots). Whereas cells highlighted in light grey represent hulls that meet the EEDI Reference target but less efficient than the basic hull in terms of energy efficiency level per capacity mile i.e. EEDI. It is found that the maximum reduction of (-18.20%) in EEDI is achieved for Hull 55 while Hull 27 demonstrates the poorest practice among all hulls as the increase in the EEDI is around (+31.22%). Table 4.13 and Table 4.14 show the design variables for both hulls. The results of Stage Three are consistent with those of the previous stages (Stage One and Tow) regarding the energy efficiency and EEDI trends with variations in design variables.

Table 4.13 Design Variables for Hull 55

Variable	Level	%Change	Value
Length L_{BP} [m]	3	+10%	222.750 m
Breadth to Draught Ratio B/T	1	-10%	2.383
Block Coefficient C_B	1	-6%	0.776
Longitudinal Center of Buoyancy LCB	1	-1.1%L	114.764

Table 4.14 Design Variables for Hull 27

Variable	Level	%Change	Value
Length L_{BP} [m]	1	-8%	186.300 m
Breadth to Draught Ratio B/T	3	+8%	2.860
Block Coefficient C_B	3	+4%	0.858
Longitudinal Center of Buoyancy LCB	3	+0.9%L	99.710

The attained EEDI to EEDI reference ratio $(EEDI_A/EEDI_{Ref})$ is chosen as the objective function (response parameter) in the environmental model. It is used as an indicator while exploring the design space to choose alternative designs that demonstrate a better energy efficiency performance in order to meet the IMO requirements. Eq (4.17) shows the response parameter as a function of the design variables and the ratio of the operating speed to the service speed V_S for the base design as addressed in the EEDI documents:

$$Z = f(X_i) = EEDI_A/EEDI_{Ref}$$
$$X_i = [L, B/T, C_B, LCB\%L, V, V/V_S] \quad (4.17)$$

where:

$Z = f(X_i)$: the response parameter which will be used as an indicator for the energy efficiency performance EEDI,

X_i: the design parameters array for the optimisation problem. The following symbols are used to indicate these variables:

Variable	**Symbol**
L	x_1
B/T	x_2
C_B	x_3
$LCB\%L$	x_4
V	x_5
V/V_S	x_6

As previously, Mimitab17 and the Regression Tool built in EXCEL are used to run the regression analysis, and they gave the same regression formulas as they both use the same statistical process for estimating the relationships among variables. However for the purpose of increasing the accuracy of the equations, the whole data of all generated hulls was divided into 4 groups depending on the speed ranges from very slow to very high. The following regression equations were obtained to estimate the attained EEDI to EEDI reference ratio $\left(EEDI_A/EEDI_{Ref}\right)$:

5-8 knots	$Z = 0.22513973 - 1.45112 \cdot 10^{-4}x_1 + 0.00424541x_2 + 0.1994372x_3 + 0.7117334x_4 + 7.01016 \cdot 10^{-3}{x_5}^2 - 1.167082x_6$	(4.18)
9-12 knots	$Z = 0.174603 - 1.5957 \cdot 10^{-4}x_1 + 0.0688386x_2 + 0.18141677x_3 + 1.004597x_4 + 6.58176 \cdot 10^{-3}{x_5}^2 - 1.18996x_6$	
13-15 knots	$Z = 1.87683 - 7.8 \cdot 10^{-4}x_1 + 0.125773x_2 + 1.459394x_3 + 2.919081x_4 + 23.769 \cdot 10^{-3}{x_5}^2 - 7.71747x_6$	
16-17 knots	$Z = 4.6377 - 41.3756 \cdot 10^{-4}x_1 + 0.220956x_2 + 4.734612x_3 + 7.091411x_4 + 46.402 \cdot 10^{-3}{x_5}^2 - 17.93971x_6$	

As the EEDI is a measure of the ship's energy efficiency per capacity mile, then it is possible to estimate the objective function $\left(EEDI_A/EEDI_{Ref}\right)$ as a function of the delivered power to displacement ratio (P_D/Dis) and the relative speed ratio as well as shown in Eq (4.19). The delivered power to displacement ratio can be estimated at any speed and for any alternative design using the regression formulas from the hydrodynamic model as a function of the design parameters as can be seen in Eq (3.11).

$$Z = 0.27103342 + 5.137083101\ P_D/Dis + 2.798783 \cdot 10^{-3}\ (V/V_S - 1) \qquad (4.19)$$

However, for the optimisation problem, regression formulas in Eq (4.18) will be used to calculate $\left(EEDI_A/EEDI_{Ref}\right)$ as they give a more accurate estimation for the objective function. In order to evaluate how accurate my model is in fitting the data on the regression lines, it is important to assess R-squared values. For the EEDI model, R-squared values obtained for those regression formulas are 95.6%, 99.4%, 95.3%, and 90.7% respectively for the speed ranges. That is a strong evidence that each regression equation fits the data well to the fitted regression line. Moreover, these high values for R-squared show that there is a strong relationship between the model and the response parameter. However, as previously, it is vital to assess the residual and normality plots to determine whether the coefficient estimates and predictions are biased. Therefore, the standardized residuals graphs are used to assess the quality of the regression, test the normality of the data, examine the goodness-of-fit in regression, and to investigate the equality of variance.

The Histogram of the residuals in Figure 4.8 exhibit a relatively symmetric bell-shaped distribution especially for low speeds plots. These symmetric bell-shaped histograms which are moderately distributed around zero indicate that the variance is relatively normally distributed, and the normality of the distribution assumption is likely to be true. Figure 4.9 shows the Residuals versus Fits plots for the regression equations in Eq (4.18). The four corresponding plots show that the majority of the residuals scatter randomly around the horizontal 0 line, and most of the residuals stand in a random pattern which suggests that there are no outliers that lie at an abnormal distance from other residuals in the total data.

Finally, to test and reject the null hypothesis that any of the design variables has no effect on the response parameter, the P-values for each variable in the model are assessed. The regression analysis output show that the design variables of Length, Breadth to Draft Ratio, Block

Coefficient, Longitudinal Centre of Buoyancy, and Speed are significant because they all have a P-values equals to 0.000. That is a sufficient indicator that all the design parameters in the regression model should be kept.

To gain a better 'cause and effect' understanding of how changes in hull parameters and how operating speed affects the $(\mathrm{EEDI_A}/\mathrm{EEDI_{Ref}})$ value, a sensitivity analysis is carried out as has been done earlier in the hydrodynamic model. To show the significance of the design variables, the upper or the lower limit (whichever leads to a better performance) is used to calculate the percentage change in $(\mathrm{EEDI_A}/\mathrm{EEDI_{Ref}})$ with respect to the basic hull. It is apparent from Figure 4.10 that the relative attained EEDI to the Reference EEDI ratio is influenced by all the primary and secondary variables at different levels. That is a strong evidence that the decision to choose these variables for the parametric analysis was right. Also using the full factorial design has produced an accurate representation for the hydrodynamic model and it is sufficient to explore the design space.

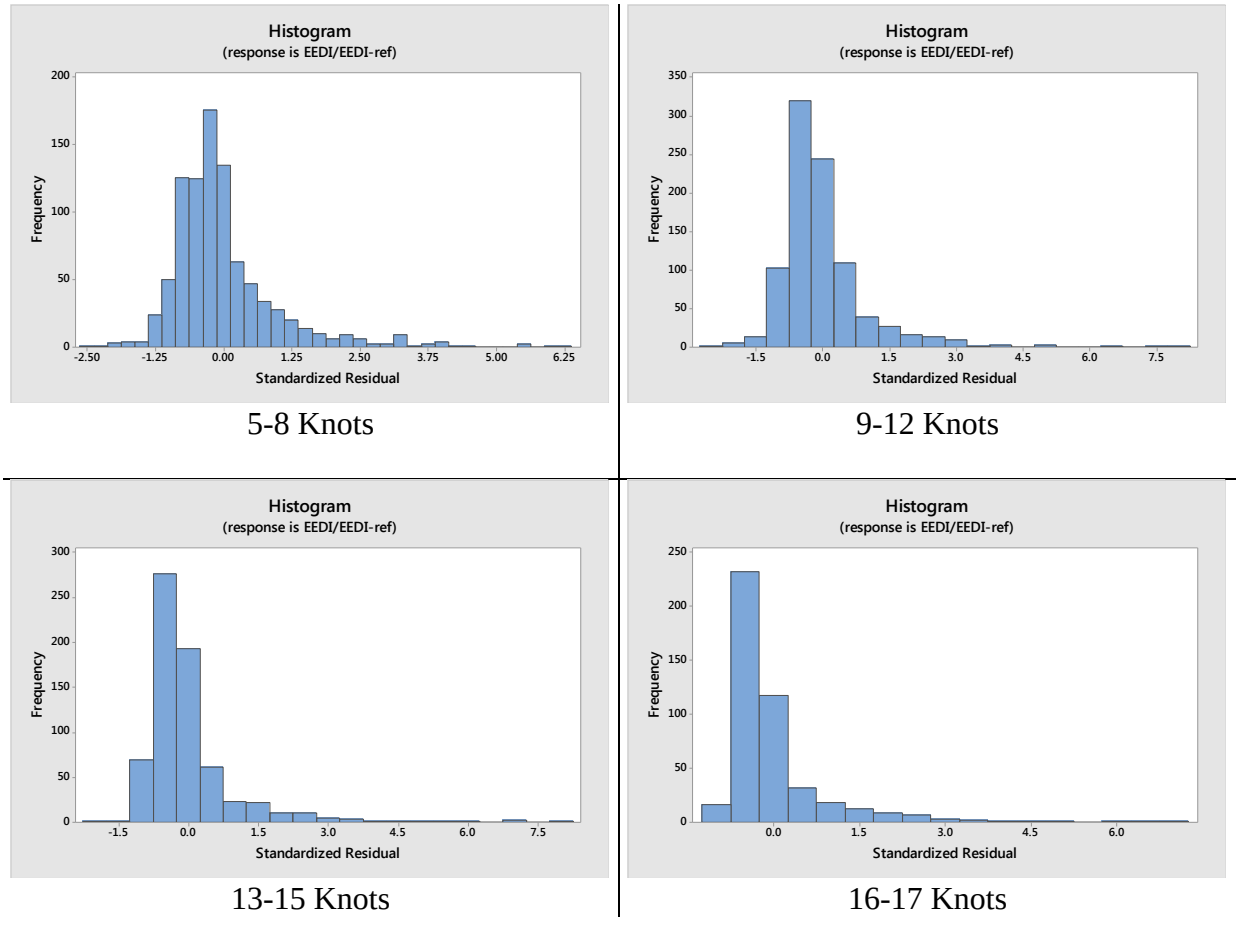

Figure 4.8 Histogram of the residuals

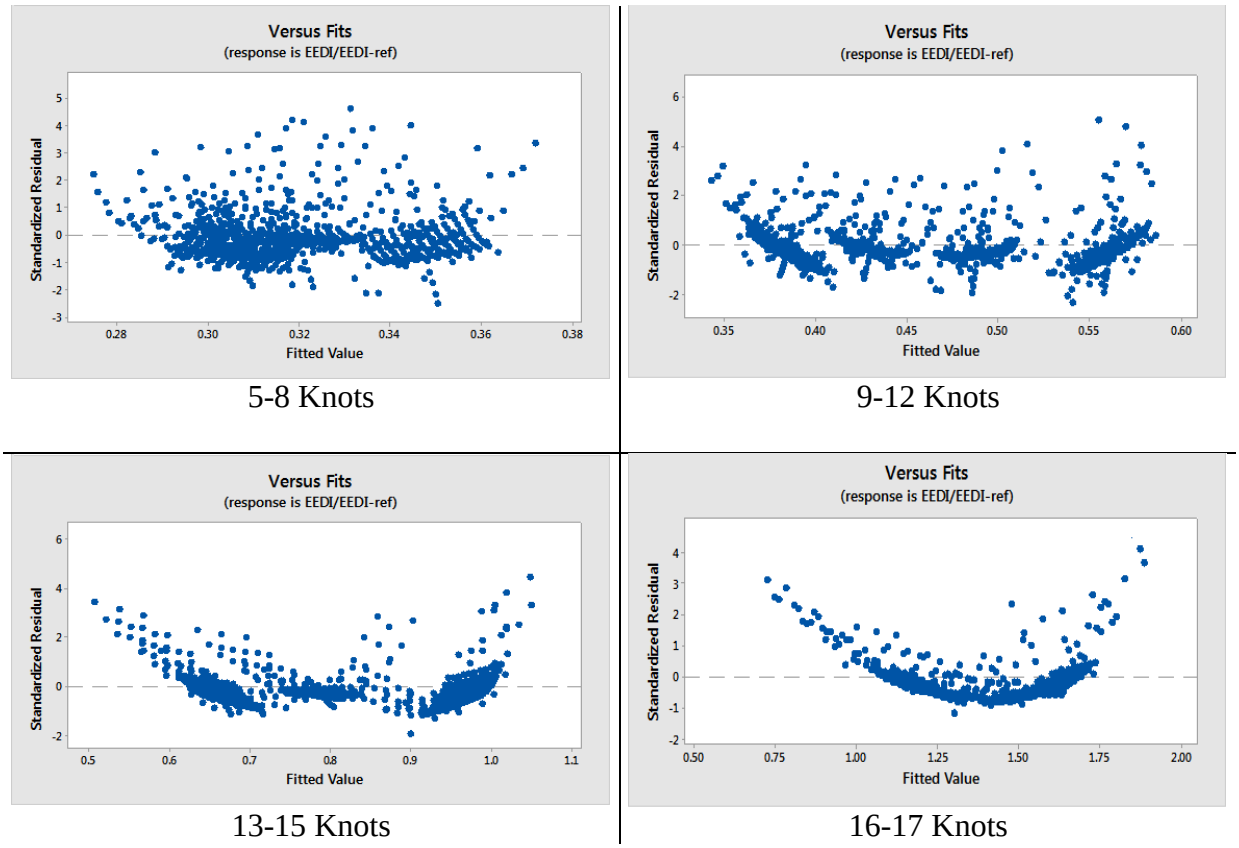

Figure 4.9 Residuals vs Fits Plots for $EEDI_A/EEDI_{Ref}$

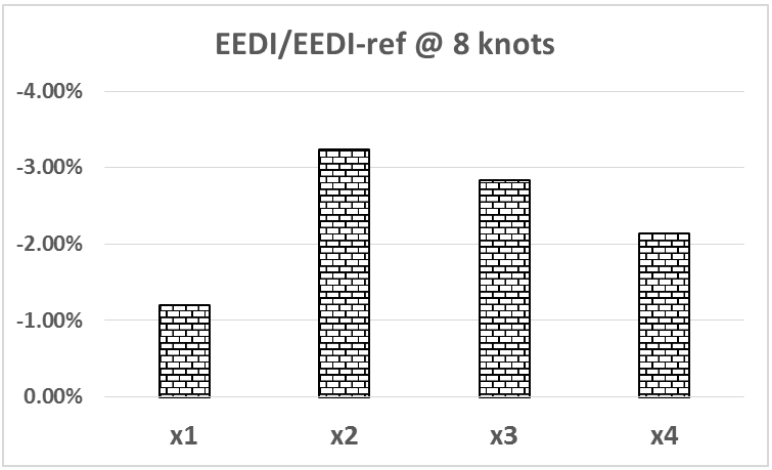

Figure 4.10 Contribution to $EEDI_A/EEDI_{Ref}$ of each design variables

The S/N ratio is calculated for each run of the experiment in order to search for the settings where the factor levels of the design parameters maximize the S/N ratios. The "smaller the better" equation is used as the aim is to minimise the system response ($\mathrm{EEDI_A/EEDI_{Ref}}$). The results of the average ($\mathrm{EEDI_A/EEDI_{Ref}}$) and the mean S/N ratio for each level of the control parameters (low, medium, and high) are shown in Table 4.15 and Table 4.16. Moreover,

Figure 4.11 and Figure 4.12 show, graphically, the control factors' effects on the average response parameter and S/N. In addition, Appendix D-4 shows the average $(\mathrm{EEDI_A}/\mathrm{EEDI_{Ref}})$ and the mean S/N ratio for all the 81 hulls generated in Stage Three.

Results reveal that of the design parameters, the block coefficient have a greater effect on the average $(\mathrm{EEDI_A}/\mathrm{EEDI_{Ref}})$ and S/N than the other three design parameters. The third level for the length (L_3 – longer hull) is clearly a better choice to minimize $(\mathrm{EEDI_A}/\mathrm{EEDI_{Ref}})$ and maximize S/N comparing with the shorter hulls (L_1 & L_2). For the other design parameters, the preferred levels are:

- Breadth to draught ratio: (B/T_1) where the breadth to draught ratio is minimum.
- Bloch Coefficient: (CB_1) which states that fine and slim hulls are better for the hydrodynamic performance.
- Longitudinal centre of buoyancy: LCB%L_1 where the positon of LCB moves aft.

Hence, based on the EEDI calculation and the environmental model, the $(\mathrm{EEDI_A}/\mathrm{EEDI_{Ref}})$ ratio has a tendency of decreasing when the hull is longer, the breadth to draught ratio is smaller, the block coefficient is smaller, and for backward centre of buoyancy. However, as the results give just an indication of how a ship can improve her energy performance and achieve a better EEDI value. Further investigation is necessary while carrying out the optimisation process to identify the complexity of the multi-objectives problem.

Table 4.15 Average response parameter for $EEDI_A/EEDI_{Ref}$

	L	**B/T**	**CB**	**LCB%L**
Level 1	0.657	0.610*	0.587*	0.611*
Level 2	0.637	0.639	0.619	0.635
Level 3	0.617*	0.662	0.704	0.665
max-min	0.040	0.052	0.117	0.055

Table 4.16 Mean signal-to- noise S/N ratio for $EEDI_A/EEDI_{Ref}$

	L	**B/T**	**CB**	**LCB%L**
Level 1	2.285	3.083*	3.615*	3.106*
Level 2	2.694	2.646	2.980	2.720
Level 3	3.085*	2.334	1.469	2.238
max-min	0.799	0.748	2.146	0.869

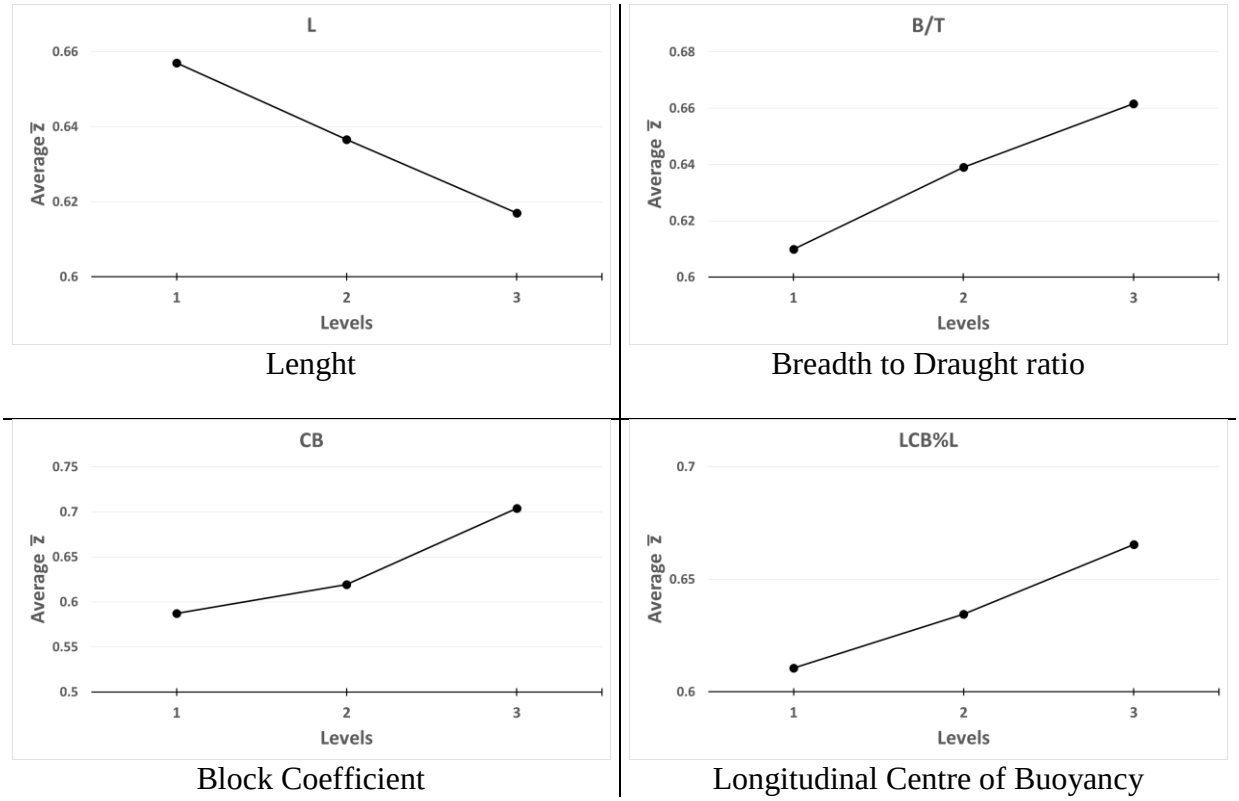

Lenght | Breadth to Draught ratio

Block Coefficient | Longitudinal Centre of Buoyancy

Figure 4.11 Control Factors Effects on Average $EEDI_A/EEDI_{Ref}$

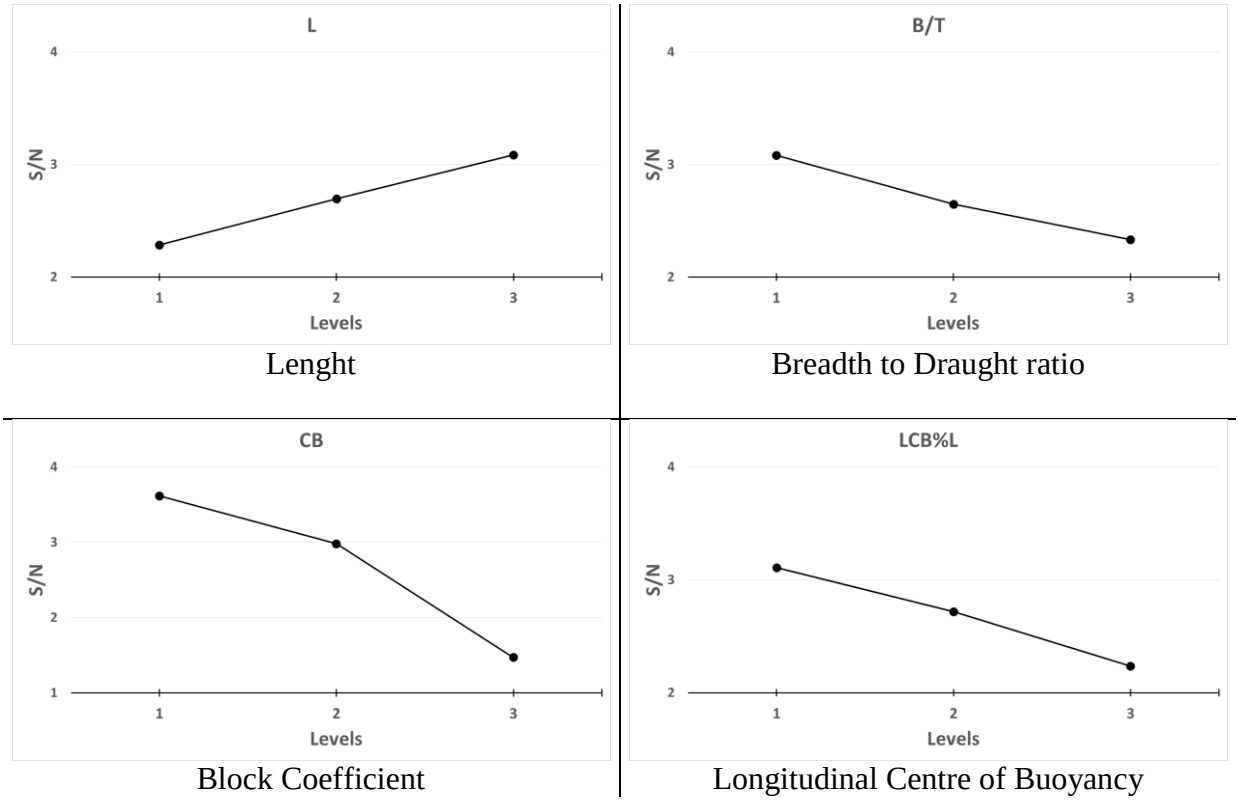

Lenght | Breadth to Draught ratio

Block Coefficient | Longitudinal Centre of Buoyancy

Figure 4.12 Control Factors Effects on S/N

4.7 Conclusion

Slow steaming concept and the implications of speed optimisation on the hydrodynamic performance and emissions mitigation were discussed in Chapter Four. An environmental model to estimate the change in EEDI value as a result of optimising hull parameters and sailing speed was developed. The model estimates energy consumption and a ship's productivity based on EEDI formula assumptions and other technical and operational assumptions.

The results of the attained EEDI values for the base ship over the speed range (5-17 knots) showed that the EEDI is predominantly sensitive to the operating speed. Reducing the speed by 1 knot from the design speed reduces the EEDI by 18%, whereas increasing the speed by 1 knot increases the EEDI by 25%. Moreover, the results showed that the base ship at her design speed fails to meet the required EEDI minimum values for the future reduction phases. Therefore, to comply with IMO regulations, the base ships needs to reduce the operating speed at least by 1 knot to meet the required minimum EEDI for phase 1 and phase 2 and by 2 knots to avoid the EEDI penalty for phase 3 (January 2025).

The model results suggest that a significant gain in energy saving on-board a ship can be achieved by optimising the hull design through parametric modification. All the four design variables (L, B/t, CB, LCB) have a significant influence on the EEDI value. However, analysing the individual influence of the design parameters has shown that none of the new generated hulls in Stage One would meet Phase I EEDI baseline at the design speed but hulls $-4\%\ C_B$ and $-6\%\ C_B$. The results obtained from the model indicated that the new designs in Stage One need to sail at speed 13 knots and below in order to meet Phase III (January 2025) EEDI targets.

Finally, the combined influence of speed reduction and variations in the controllable primary and secondary design variable on the energy efficiency and attained EEDI has been analysed using a set of derived regression formulas to estimate the attained EEDI to EEDI reference ratio $\left(EEDI_A/EEDI_{Ref}\right)$. It was found that the maximum reduction of (-18.20%) in EEDI is achieved for Hull 55 (L_3, B/T_1, C_{B1}, $LCB\%L_1$) while Hull 27 (L_1, B/T_3, C_{B3}, $LCB\%L_3$) demonstrates the poorest practice among all hulls as the increase in the EEDI is around (+31.22%). The signal to noise ratio analysis showed that longer hulls with a minimum breadth to draught ratio and a slim shape (low block coefficient) and a backward LCB have generally a better energy efficiency performance.

Chapter 5. Ship Economic Model

5.1 Introduction

Previously in Chapter 2, the main and important aspects of the economics of ships were presented focusing on the key criteria that affect decision making when it comes to design and build a new ship. Studies aiming to maximize the economic performance of a ship within the life span were discussed taking into account the fluctuations in the shipping market.

In this chapter, the economic model and methodology of the thesis are presented in Section 5.2 where the key factors and features that define the main aspects of a ship economy are discussed. Firstly, ballast conditions are determined as the economic model takes into account the whole journey including the laden leg which has been discussed before and also the ballast leg as tanker ships spend almost 40-60% of their time on ballast. AVEVA Hydrostatics and Hydrodynamics is used to obtain the power and efficiency data for the ballast condition at the chosen draughts and trim over the speed spectrum.

Then, two different tanker routes (2000 n.mile and 7000 n.mile) are chosen to carry out the calculations to estimate the voyage and annual revenue using the average freight rates from year 2012 using the Worldscale index. Low and high fright rates for both routes are determined to be used in the revenue calculations in order to investigate the market fluctuations on a ship financial performance and optimum operating speed.

Simplified approximation regression formulas are developed as a function of the deadweight to estimate the operating costs and also dry-docking costs for tanker ships using commercial data from OpCost annual report 2012. The operating costs formula is applicable across a wide range of deadweight tonnage $[10{,}000 - 320{,}000\ DWT]$, and it does not represent any specific ship trading in any specific route.

Costs occurred at ports are taken into account in the economic model as they represent a major component of the total voyage costs. Information regarding port tariffs and dues for different ports around the world are collected for the purpose of determining a straightforward way to estimate costs a tanker ship pays at both the lading and discharging ports. Tariff for Ports of

Jebel Ali and Port Rashid in Dubai is used for the economic model calculations as no detailed calculations are necessary. Moreover, a linear regression formula to calculate a ship gross tonnage GT is derived using collected data for 908 tanker ships from Seaweb website to be used in estimating the port costs while waiting at the berth.

Fuel cost per round trip and per annum is calculated by estimating fuel consumption by all consumers onboard (main and auxiliary engines and boilers) during journey phases (cruising, manoeuvring and hotelling). High and low fuel prices for both bunker and diesel fuels will be used in the calculations to determine the influence of oil prices on the optimum operating speed. In specific, this model evaluates the impact of speed optimisation on fuel consumption and emissions reductions as well as shipping economics and the benefits for owners and charterers and also the cost of adopting this measure. For example, the results from Lindstad *et al.* (2011) model demonstrate that there is considerable potential for reducing emissions by 19% with a negative abatement cost, and it is possible to achieve 28% emissions reduction at a zero abatement cost.

Finally, an approximation formula for estimating the newbuilding price is derived using real data of 218 crude oil and product tankers from Sea-web Ships database. The newbuilding price is estimated as a function of the ship deadweight and length, and the producer price index is included to allow for inflation adjustments. The scrapping value is also taken into account in the model as it is an important item in the balance sheet and the cashflow statement. The scrapping value per lightship ton varies from one year to another and from one country to another, therefore an average value for the scrapping steel is chosen to estimate the current value of the ship in the demolition market.

The economic model is conducted for the base hull and all the other alternative designs for a set of eight different scenarios in order to investigate the implications of changes in all the previous elements of the ship finance.

5.2 Economic Model and Methodology

5.2.1 Introduction

The proposed methodology in this study links the key factors and features that define the main aspects of a ship economy. The developed economic model calculates the annual profit by

estimating the operating cost, voyage cost, and revenue per trip. They are estimated using functions of the ship size and type, cargo carrying capacity, operating speed, energy consumption, fuel prices, freight rate, maritime route, and other market conditions. The model also estimates the newbuilding price based on examining data collected from previous years and using empirical methods where the average acquiring price can be estimated. The scrapping price is also taken into account in the model as it is an important part of the ship economy which is mostly ignored by studies optimising the economic performance of ships.

Different scenarios are examined in this chapter to analyse the sensitivity of the key cost and revenue sources to changes in a ship operational profile as well as fluctuations in the maritime transportation sector. In particular, the direct and indirect economic impact of slow steaming on a ship economy is examined in the light of different scenarios considering the key parameters in the tankers market and for different maritime routes. For each scenario, the model calculates and examines the additional costs and/or savings associated with slow steaming and other operational measures such as routing optimisation. The main parameters of the model are: ship parameters, cargo capacity, fuel prices, freight rates, ship speed, and cargo availability, i.e. supply and demand.

Most economic models assume that the ship owner bears the day-to-day costs (operating costs) and the charterer pays for the fuel cost when the ship is under a time chartering contract while on spot charter, the owner pays even the fuel costs. However, to generalise the optimisation problem in a way where it is not necessary to define what costs the ship owner is responsible for and what the ship charterer is paying for, the optimisation problem will typically be a cost minimisation and revenue maximisation.

The developed economic model takes into account a wide range of factors which play a fundamental role in increasing the total ship profit through her life span and in reducing the expenses. In this section the following elements are included:

- Operating cost: by analysing collected data for tanker ships from OpCost report and other resources, the daily operating cost can be estimated.
- Voyage cost: this model calculates the daily fuel consumption of the main and auxiliary engines and boilers in-service and in port for the laden and ballast legs.
- Fright rate: data for different routes and different ship sizes have been analysed for the last few years. This data is used to calculate the voyage revenue and the annual revenue.

These data has been collected from different shipping companies and shipbrokers reports.

- Port dues: all the expenses accrued in ports should be included in the economic model. Therefore data about the port dues and charges for cargo loading and unloading have been collected for the main ports in this study. A regression analysis was carried out to calculate the GT for a tanker ship.
- Acquiring price: A regression analysis has been carried out to estimate the acquiring price for a tanker ship. This regression analysis takes into account the following parameters for tanker ships built between 2000 and 2013: newbuilding prices, DWT, PPI, and L.

5.2.2 Ballast Loading Conditions

Tanker ships often travel fully or partly loaded on one leg of the route and on ballast on the return leg which means tanker ships spend half of the sea time on ballast. Therefore, it is very crucial to optimise the underwater hull to perform efficiently with minimum resistance across a wide range of speeds and for the both laden and ballast operating conditions. Moreover, the economic optimisation process should include the operational and routing profile of the journey. The ship performance in the laden and ballast conditions is under investigation within the economic model for a return journey between two ports A and B.

Previously, the hydrodynamic performance of the base hull and other alternative hulls has been analysed for the laden condition with a full capacity. However, since the ballast leg is of interest as well, the required power over the speed range and hence fuel consumption need to be determined when the ship is sailing at the ballast condition(s). The ballast condition is determined by the ship's draught and trim unlike the fully loaded condition where ships float on a level keel. Different considerations need to be met when determining the ship minimum allowed draft and the ballast trim to suit minimum powering.

Firstly, for tankers and bulk carriers, it is essential to have a sufficient forward draft to avoid or minimise slamming when sailing at ballast condition (Watson, 1998). The desired forward draught should not be less than $[0.035 \times L]$. Moreover, recent MARPOL requirements suggest a mean draught not less than $[T_{mid} = 2 + 0.02 \times L]$ with a trim not exceeding $[0.015 \times L]$ while using segregated ballast tanks. The second factor to consider is the propeller immersion as the stern draught should provide at least 0.3 m above the propeller tip. According to DNV

structure rules for ships with length above 100 metres (DNV -Det Norske Veritas, 2014), trim at any ship's condition should not exceed any of these three limits: trim by stern of 3% of the hull length, trim by bow of 1.5% of the hull length, or any trim that cannot maintain adequate propeller immersion where the ratio of the distance from propeller centreline to the waterline $[I]$ to the propeller diameter $[D]$ is not less than $[I/D = 0.25]$. Also, to demonstrate compliance with Lloyd's Register rules and regulations (Lloyd's Register, 2013), the bottom forward of a ship needs additional strengthening except when a minimum forward draught of $[0.045 \times L]$ can be achieved at any laden or ballast condition. In addition to the limits when determining the aft draught and stern trim, an adequate clearance for the propeller tip above the keel of 3% of the diameter should be considered when calculating the minimum shaft height.

Based on the above considerations, the base ship has to meet the following restrictions:

- Minimum draught at midship: 6.05 m
- Maximum trim by stern: 3.31 m
- Minimum distance from propeller centreline to the waterline: 1.83 m
- Minimum shaft height: 3.87 m
- Aft draught to maintain a full propeller emersion: 7.53 m

One ballast condition is used for AVEVA calculations as in Table 5.1 with a mean draught of 7 meter and trim of 1 meter to the stern:

Table 5.1 Ballast condition data for the base hull

Draught aft	8.000	metres
Draught fwd	6.000	metres
Displacement	37252	tonnes
Long. centre buoy.	2.968	metres
Wetted surface	7745	sq.metres
Block coeff. (Cb)	0.795	
Lpp/B	6.279	
B/T	4.607	
Effective power at 15 knots	4979	kW
Delivered power at 15 knots	5928	kW

It was found before that at low speeds, the frictional resistance represents about 70-90% of the ship total resistance, and it in turn depends on the size of the wetted area. Therefore, the required power to propel a ship, which is a function of the total resistance imposed on the hull, is determined as a function of the wetted area. By comparing the effective power from AVEVA results over the speed range (5-17 knots) in both loading conditions, it is found that the total power is proportional to the wetted surface area. With a good accuracy, it is assumed that over the speed range, the effective power ratio of both loading conditions is 0.745. Appendix E shows AVEVA output for the chosen ballast condition.

5.2.3 Worldscale and Tanker Maritime Routes

Freight rates in the tankers market are defined using a unified system of established payments applying to the carriage of crude oil and oil products by sea. This nominal freight scale is called Worldscale, and it is published annually in a book for more than 320,000 individual routes globally. This unique system provides a straightforward method to calculate the freight for transporting oil on many different routes based on a reference rate for a standard vessel of 75,000 tonnes capacity on a round trip voyage operating at speed 14.5 knots. The Worldscale index does not reflect the day-to-day changes in the market but it is used as the basis to calculate the spot rates for tanker ships. The transporting cost values in the book are known as Flat Worldscale 100 (WS100) while the real market levels of fright are expressed as a percentage of the Flat Worldscale. For example, in recent years the actual rates for a 280,000 DWT VLCC have varied anywhere between WS40 and WS300. In this way, calculations and negotiations become easier for shipowners and charterers (Dinwoodie and Morris, 2003; Stopford, 2009; Inkpen and Moffett, 2011).

Appendix F shows the main trade routes for the dirty tanker sector (TD) and the clean product sector (TC). Moreover, the Flat Rates values (WS100) for some popular routes in year 2012 are also presented. Details for those routes are collected from different reports and shipping services websites as shown in Appendix F.

Calculations are performed for two standard routes and for freight rates that vary between the low and high WS values as in Table 5.2. The economic model calculates the voyage revenue for all alternative ships, and then the annual revenue is calculated depending on number of voyages per year which depends on the operating speed for both laden and ballast legs. The selection of those two reference maritime routes was mainly based on different factors. First of

all, the availability of information for the trade routes regarding the distance between ports, the Flat Worldscale 100 (WS100) over years, detailed monthly freight rates where the lowest and highest rates can be defined and an average freight rates for the selected year can be estimated, etc. Moreover, the trade routes were refined to exclude the routes where there are return trips with backhaul cargo or there are more than one port stop as in this case the agreed fright rates between shippers and charterers vary immensely. The grounds to carry out the model calculations for those two trade routes are to select representative routes for the wide spectrum of the tanker market routes and ship sizes. Since, the case study vessel in this thesis has a deadweight of a 54,000 DWT, then in order to avoid the hassle of re-estimating and evaluating the flat Worldscale for some routes and in order to eliminate possible mistakes in doing so, the choice was to select two trade routes where the vessel size falls in a range not far from the case study vessel deadweight. The two most appropriate routes in this case are TD10 (1750 ÷2026 n.mile) for the short route and TC5 (6547 ÷ 7991 n.mile) for the long route.

Since slow steaming has become a normal behaviour in the tanker market, it is most likely to negotiate the freight rates between shippers and cargo owners when there is a delay in delivering the cargo or the opposite scenario when the cargo arrives earlier. Since the in-transit value for crude oil is low comparing with some finished products shipped in containers, most studies, for simplicity, assume that the fright rates are independent of the speed and hence neglect the effect of voyage duration on the revenue. However, some reports such as (Weber Tanker Report / Week 10 - March 2013) suggested a 0.5 point premium for each additional 0.5 knot increase and a 0.5 point discount is applied for each 0.5 knots decrease.

Table 5.2 Routes used in the economic model

	Route One - Short	**Route Two - Long**
Distance (nautical mile)	2000	7000
Low Freight Rate ($/ton)	9.00	26.00
High Freight Rate ($/ton)	15.00	40.00

5.2.4 Operating and Dry-Docking Costs

Results obtained from different studies and methods used to predict ship operating costs in early design stages show different levels of accuracy and lead to uncertainty at the decision making board. The reasons behind this matter are firstly insufficient data available to build a robust

method and, secondly, as these parametric, mathematical, or graphical methods (Gentle and Perkins, 1982; Buxton, 1987; Michalski, 2004a; Počuča, 2006; Jorge d' Almeida, 2009) use different source of data and depend on different design variables and parameters, there would be variations in the results. Another issue to be aware of is that some models and methods include fuel costs in the operating costs calculations which lead to some confusion when it comes to estimate the total costs of a voyage.

Therefore, for the purpose of this study, a generalised and simplified approximation formula to estimate the operating costs and dry-docking cost for tanker ships is developed using commercial data from (Moore Stephens LLP., 2013)[4]. A linear regression analysis is performed to obtain the approximation formulas using the deadweight as the only variable. The OpCost 2013 report is based on database for over than 2650 vessels including 26 vessel types such as 12 tanker, 5 bulk and 3 container ship types. Moreover, the report includes 12 cost categories including crew wages, stores, repairs & maintenance, insurance, registration, etc. Separately, data about dry-docking cots is included in the OpCost report as well. However, the dry-docking data does not take into account the age of the ship nor the location of the drydock. Under flag legislations and classification scarcities rules, all vessels should undergo regular intermediate surveys each two years (or 2.5 years) and a special survey with a dry docking every 5 years to maintain a ship in class for insurance purpose (Stopford, 2009). Dry-docking cost figures provided by Moore Stephens annual publications are assumed to be taken into account within a ship cash-flow calculations twice each 5 years. Therefore, the economic model divides the dry-docking cost over 2.5 years, and it is assumed that it increases by an annual rate of 3%. Comprehensive analysis of the factors that influence dry-docking costs for tanker ships can be found in a study carried out by Apostolidis *et al.* (2012) who built a cost model by analysing data collected over 4 years 2007-2011 from one of the biggest ship repair yards of the Persian Gulf.

The operating costs formula in Eq (5.1) is applicable across a wide range of deadweight tonnage$[10{,}000 - 320{,}000\ DWT]$, and it does not represent any specific ship trading in any specific route but it estimates the average daily operating costs for tankers in 2012 as a function of the deadweight. The operating costs are expected to increase by 3% in 2013 and 2014 according to Moore Stephens' report based on a survey targeted key players in the international

[4] Moore Stephens LLP is the eighth largest accounting and consulting firm in London, employing over 650 partners and staff and with turnover of £68 million.

shipping. Therefore, for further calculations in any year, some adjustments are needed to represent the actual expenses. Similarly, Eq (5.2) calculates the average dry-docking costs as a function of the ship size. Both equations have a high value of R-square (R^2) over 0.9 which means the accuracy is acceptable, and both equations are used in the economic model.

$$OPEX = 7620.5 + 0.0089 \cdot DWT \ \ [\$/day] \tag{5.1}$$

$$DryDocking\ costs = 916114 + 3.6785 \cdot DWT \ \ [\$/year] \tag{5.2}$$

5.2.5 Port Charges and Costs

Costs occurred at ports represent a major component of the voyage costs, and they are the fees paid for the use of facilities and services at port. These fees levied against the vessel and cargo vary considerably from one port to another, and they fall into port dues and service charges. Port dues include docking and wharfage charges, and the provision of the main port infrastructure and facilities. Different methods are applied to calculate port dues but mainly based on the weight or volume of the cargo, the net or registered tonnage of the vessel. On the other side, service charges cover the use of pilotage, towage and cargo handling services (Stopford, 2009).

As some ports calculate the charges depending on the ship Gross Tonnage (GT), a regression formula is used to determine the gross tonnage as a function of a ship's main particulars. The data used to generate the GT regression equation is collected from Seaweb website. It contains 908 tanker ships built between 1990 and 2014, and the deadweight range is between (30,000 and 100,000 tonnes). The GT regression linear formula (Eq (5.3)) has a high R-squared value of 0.9894 with a very good fit as shown in Figure 5.1.

$$GT = 0.294 \cdot (L \cdot B \cdot D) - 1304.1 \tag{5.3}$$

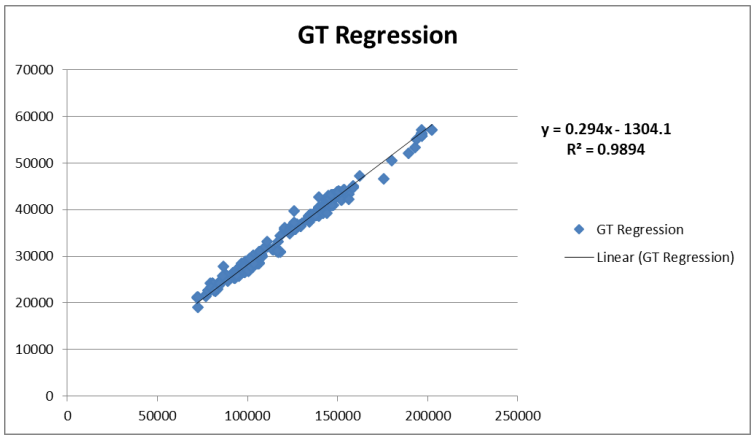

Figure 5.1 GT Regression fit line for tankers

Typically for tanker ships, port time varies depending on the size of the ship and on the speed of port services and the loading and discharging facilities. In this study, 2 days are allowed at each port as it is suggested by the Worldscale' estimate which allows 4 days at ports for a return journey.

In fact, each individual port has a different pricing policy depending on the ship size, time spent in the port, type of cargo, usage of port facilities, etc. Therefore, it is impossible to establish a general model or formula to estimate port costs as every port is different (Alderton, 2008). In this study, information about port tariff and charges in the recent years is collected from various port websites or by contacting port authorities in different countries asking for quotes regarding the case study ship in this thesis. Table 5.3 presents a good example of how port charges can vary for the same ship from one port to another and country to another. They are calculated using data collected online and from contacting ports authorities.

Table 5.3 Port Charges

Country/port	**Port charges US$**
Ports of Jebel Ali and Port Rashid in Dubai	64759
Port of Gdansk	36442
Sharjah port	76705
Rotterdam port	67088
Aruba Port	49412
New York port	92553
Yokohama port	38731
Chennai Port Trust in India	29195
APM Terminal - Poti Sea port in Georgia	82913

The most forward and simplest port costs calculation method for tanker ships among all the considered ports in this study is for Ports of Jebel Ali and Port Rashid in Dubai as other ports tariff calculation methods include several unnecessary items and details. Therefore, the economic model will use this Port Tariff for port dues and charges estimation. Calculating port costs for tankers is available at (http://www.dpworld.ae/en/home) and summarised as following:

- 308- PORT CHARGES FOR TANKERS:

  308.1 The Port charge per Vessel per 48 hour period or part thereof is levied for Port services, as hereinafter itemized. The charge will be AED 2.00 per gross Ton.

- 401- PORT HANDLING Charges are per Freight Ton:

  401.4 Bulk Materials - Liquids (Rates per Tonne) AED 3.00

- Currency convert rate is 1 AED = 0.2723 USD

5.2.6 Fuel Costs

As discussed previously, the total fuel bill depends on different factors such as bunker prices, engine power and efficiency, design and state of the hull, the operating speed of the ship. The main three fuel consumers are main engine(s), auxiliary engines and boilers. Most of previous studies in the literature that have investigated the effect of slow steaming and voyage optimisation on fuel consumption and cost reduction din not consider fuel consumption in the auxiliary engines and boilers at sea and in ports for cargo heating for example. The reason behind that is there is no historical data or accurate analysis and reports available to be used as a basis for the energy and fuel saving calculations.

Even though none of the studies in the literature has considered all fuel consumers onboard, some studies take a step further. Trozzi (2010) estimates air pollutant emissions from ships in cruising, manoeuvring and hotelling phases using data on fuel consumption in the both main and auxiliary engines for more than 100,000 ships. Calculations are based on average engines' loads during different ship activities. A report by (Hellenic Shipping News) calculating the Time-Charter Equivalents (TCE) for different tanker types estimates that fuel consumption for a 47,000 dwt tanker is around 5 and 12 IFO ton per day at port during loading and discharging days respectively and 4 MDO ton during time spent in ports. A cargo heating management tool

was developed by Teekay Shipping Ltd, and it estimates that fuel consumption for cargo heating is about 100 MT per voyage for an Aframax vessel. Armstrong (2013) shows that the average daily fuel consumption for cargo heating can be reduced from 8 MT/day to 5.5MT/day by optimising the energy use onboard the ship which leads to a significant saving in the voyage costs.

Fuel cost per round trip (C_{Fuel}) is divided into cost of heavy fuel C_{IFO} and cost of marine diesel fuel C_{MDO}. It is calculated within the economic model for all alternative designs and for all different operating conditions using Eq (5.4):

$$C_{Fuel} = C_{IFO} + C_{MDO} = P_{IFO} \cdot FC_{IFO} + P_{MDO} \cdot FC_{MDO} \quad (5.4)$$

where:

P_{IFO}, P_{MDO}: the fuel prices for IFO and MDO respectively [$\$/ton$],

FC_{IFO}, FC_{MDO}: fuel consumption per trip of both fuel types. Fuel consumption is calculated as the sum of fuel consumption at sea and in port using the specific fuel consumption and engine load and time spent in each phase of the trip as has been seen before when calculating emissions for the EEDI calculations.

Required main engine power is taken from AVEVA results, and the auxiliary engine power is calculated using EEDI guideline formula as suggested in (Buhaug *et al.*, 2009). The model assumes that, at port, two auxiliary engines are operating to provide electrical and accessory power (hotelling) (Energy and Environmental Analysis Inc and EPA, 2000). Most ships turn off main engines at port except tankers where steam is always required for cargo heating for pumping work. The required steam might be provided by boilers that use heavy fuel. Fuel consumption in boilers for small tankers is estimated to be about 5-15 tonnes per day (Buhaug *et al.*, 2009). In this study, an average of 10 tonnes per day is used to calculate fuel consumption at port.

Bunker prices vary dramatically as shown in Figure 5.2 for IFO 380 between 2006 and 2014, and they also vary from one country to another. In the economic model, two different fuels are used which are IFO 380 and Marine Diesel Oil for auxiliary engines. Table 5.4 presents the highest, lowest and average fuel prices in 2012 according to Fearnleys report (2012). Daily fuel prices can be found on http://www.bunkerindex.com/prices/indices.php.

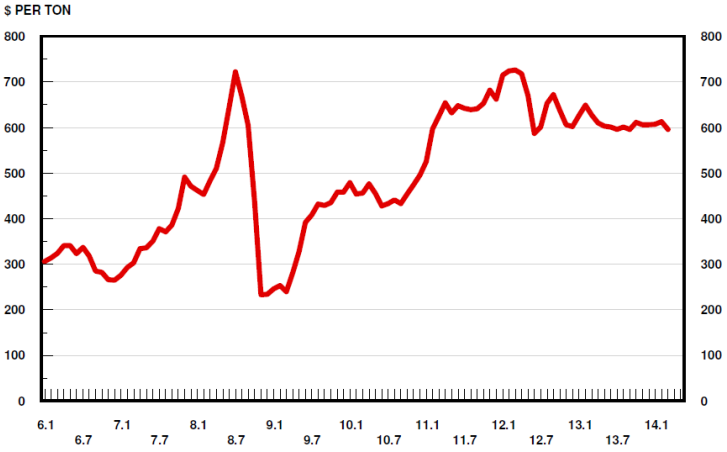

Figure 5.2 Monthly Average Bunker Price (2006-2014) – Source http://www.platou.com

Table 5.4 Fuel prices in 2012 ($/ton)

	High	**Low**	**Average**
380 CST	740	545	610
MDO	1028	813	937

Moreover, it is worth mentioning again that the actual CO_2 emitted from ships is different from what is considered in the EEDI formula which considers only the fuel consumption at the 75% MCR and design speed, as well as in the laden leg and calm water conditions. However, the economic model calculates the actual total fuel consumption during a roundtrip (laden and ballast leg, and in port) burned in the main and auxiliary engines and boilers. That helps in identifying more accurately the actual trends in fuel consumption and CO_2 emissions and the operation cost as well.

5.2.7 Capital Cost Estimation

Building costs do not represent the actual newbuilding market because the ratio between the values of materials and resources and labour wages on one side and the newbuilding prices on the other side vary depending on the market conditions (supply-demand) and on the future expectations (Gentle and Perkins, 1982). In practice, there is no simple and direct approach that is agreed universally to predict the cost of building and the cost for acquiring a new ship.

In fact, the market price of vessels is determined as a function of construction costs in shipyards and the dynamic conditions in the market demand for transport services. Results from (Xu *et al.*, 2011) study show a positive directional relation between fright rates and newbuilding prices, and therefore any new investment is encouraged by a strong fright market. However, a few

attempts to develop a more accurate price model are carried out in this study by including the fright rates as an extra variable. In this case, the model takes into account the fluctuations in the newbuilding market, second-hand ships market, the fright rates market from year to year, and hence represents the real newbuilding market. However, for consistency and simplicity in this study, fright rates or earnings are not included in the price model. Moreover, year 2012 is considered as the base year to carry out the calculations for all ships.

A simple model to estimate newbuilding prices for tanker ships has been developed in this study using data extracted from Sea-web Ships database (https://maritime.ihs.com/). The approximation formula for estimating the newbuilding price uses real data of 218 crude oil and product tankers built by different shipyards mainly in China, South Korea, and japan between 2000 and 2014. In some models in the literature, deadweight is used as the main and only ship parameter to estimate the building cost as in (Mulligan, 2008) study. However, different ship parameters have been tested in this study in the aim to determine the most dominant factors that influence the ship price and a sensitivity analysis has been run. The presented model calculates the newbuilding price as a function of the deadweight and length since they are the key factors influencing the required amount of steel and the labour costs. The length parameter is chosen as a key variable in the price equation because it is an expensive construction cost driving parameter compared with hull breadth and depth.

To take the inflation into account, the producer price index (PPI)[5] for heavy industry and capital equipment is included in the model equation. PPI values for heavy industry and capital equipment are available from US. Bureau of Labor Statistics [https://www.bls.gov/]. The base year index is 100 for 01-06-1980, and the PPI value is 163.0 for year 2012.

Eq (5.5) gives the acquiring price in millions of dollars for tanker ships with deadweight range between 20,000 and 115,000 dwt.

$$NB = -19.591 + 0.2745PPI + 2.2786 \times 10^{-2}L + 1.5011 \times 10^{-4}DWT \qquad (5.5)$$

The Regression Tool built in EXCEL is used to run the regression analysis. Results show that the obtained regression formula has a high R-squared value of 0.96 which indicates that the

[5] Producer Price Index (PPI): It measures price change from the perspective of the seller. It is a family of indexes that measures the average change in selling prices received by domestic producers of goods and services over time.

model fits the original data, and it is an evidence that there is a strong relationship between the model and the response parameter.

5.2.8 Scrapping Value

The scrapping market is different from the newbuilding and second-hand markets as it is common to value ships after a certain age at the scrap value rather than the market value which is driven by the supply and demand in the shipping market. Prices of ships at age of demolition are determined by negotiation between shipowners and scrap yards through brokers. The scrap prices depend on the availability of old ships for scrap and also on the demand for scrap metal in some countries as it provides a convenient source of raw materials for mini-mills (Stopford, 2009).

Estimating the scrapping value of a ship at the end of the life span depends on different factors such as the state of the ship and its suitability for scrapping. Moreover, it depends mainly on the state of the local steel market and current scrap price, and also on the availability and productivity of scrapping facilities. Therefore, the prices might vary considerably from ship to ship and year to year (Stopford, 2009). Several studies have analysed the interrelation between the four shipping markets including the demolition market in the aim of understanding the dynamic of the ship recycling market. For example, (Knapp *et al.*, 2008; Bijwaard and Knapp, 2009; Anyanwu, 2013) used historical data to derive regression formulas and to build empirical model to illustrate the linkage between market conditions and ship condition on one side and the profitability and probability of ships scrapping on the other side.

However, in practice, shipbreakers estimate the price they are willing to pay for a ship depending on the lightweight of the ship including steel scrap which provides most of the ship value especially flat panels and also non-ferrous items which might provide a significant revenue for scrapyards. According to market reports, the scrap prices of tankers during the last few years have varied between $300/lwt and $600/lwt. Table 5.5 shows the historical demolition prices for tankers for the last 15 years in the Indian market according to a report by (Athenian Shipbrokers S.A.) in March 2018. It can be seen that the recycling activities and prices are not steady and do not follow a certain trend over time because of the strong relation between the demolition market and the newbuilding market and the freight market which have fluctuating supply and demand.

Table 5.5 Historical Demolition Prices

2004	2005	2006	2007	2008	2009	2010	2011	2012	2013	2014	2015	2016	2017	2018
362	302	405	507	278	338	485	482	405	435	425	300	300	440	450

The economic model assumes an average life time of 25 years for tanker ships as has been suggested by different studies in the literature (Stuer-Lauridsen *et al.*, 2004; Stopford, 2009; Lun *et al.*, 2012). The future residual value of a ship at any stage of its life time cannot be estimated with any certainty as it is a function of three determinants which are the depreciation rate, the rate of inflation and the market cycle (Stopford, 2009).

The financial return from the scrapping deal might be of a significance importance in a company cash flow. Therefore, choosing the right time to sell is crucial. However, in this study since it is impossible to gain an accurate forecast for the demolition market, and to avoid the hassle of taking the inflation rate into account to calculate the present value in the economic performance equation, the average price per lightship ton (LTD) in 2012 is used in the economic performance model. Such data are analysed and published by shipping service companies such as (Athenian Shipbrokers S.A.; Clarkson Research Services; Hellenic Shipping News). The average price per lightship ton for tankers in 2012 was reported to be around $400/LDT in counties such as India, Pakistan and Bangladesh. The economic model uses this average price for the purpose of estimation the scrapping value of ships.

5.2.9 Scenarios and Assumptions

In practice, shipowners and charterers optimize their fleet operational profiles based on bunker prices and freight rates. Therefore, different scenarios are under investigation in this study in the aim to determine the optimum design(s) and operating profile that generate the maximum profit for a hip during the total life span. Those scenarios include combinations of fuel prices and freight rates as they are the key factors in determine the day-to-day cost and revenue.

All scenarios are run for different speeds to determine the implications of sailing at slower speeds. Moreover, the sailing speed at both the laden and ballast legs determines the number of journeys a ship makes per year, and hence the annual amount of cargo shipped between ports, and hence the annual revenue generated.

The main prominent scenarios that can be recognised in the fluctuating shipping market can be summarised as following:

- Low fuel prices, Low freights,
- Low fuel prices, High freights: Gains,
- High fuel prices, Low freights: Losses,
- High fuel prices, High freights.

Table 5.6 presents the combinations of high and low values for fuel prices and freight rates that are used in the above scenarios and in the economic model calculations:

Table 5.6 Fuel prices and freight rates values

		Freight Rate ($/ton cargo)	**380 CST ($/ton fuel)**	**MDO ($/ton fuel)**
Rout One 2000 n.mile	Scenario 1	9.00	500.00	700.00
	Scenario 2	15.00	500.00	700.00
	Scenario 3	9.00	800.00	1000.00
	Scenario 4	15.00	800.00	1000.00
Rout Two 7000 n.mile	Scenario 1	26.00	500.00	700.00
	Scenario 2	40.00	500.00	700.00
	Scenario 3	26.00	800.00	1000.00
	Scenario 4	40.00	800.00	1000.00

For uniformity and comparability purposes when calculating costs and revenue, the model assumes that the ship carries a cargo of full payload W from port A to port B for a distance L (miles), and sails at speed V_1 (knots) on the laden leg and at speed V_2 (knots) on the ballast leg. The deadweight utilization when estimating the cargo payload is assumed to be 96% for tankers as suggested by (Stopford, 2009) based on surveys. The port time for loading and discharging cargo is assumed to be 2 days at each of the return trip ports. Fuel consumption of the journey for each fuel type is the sum of the daily fuel consumption by each machinery onboard during any phase of the journey. The Off-hire duration per annum is assumed to be 25 days to account for any events when the ship is not operating and hence no revenue is generating.

Moreover, to eliminate the hassle of dealing with more than one individual decision maker to plan a ship operational and routing profile, and to simplify the optimisation process, it is assumed that the ship is operating in the voyage charter market where the shipowner pays all

the cost and he is responsible for running the ship and managing the voyage. In this case, a shipowner will select a design and operational specifications that maximise the annual profit (π_{pa}).

Commission at an average rate of 2.0% is deducted from the total freight revenue as suggested by (Clarkson Research Services Limited, 2014) for tanker ships.

In practice, the in-transit inventory is often ignored when the difference in the arriving time is just a matter of few days. However, when investigating the influence of ultra slow steaming on a ship's performance, then the in-transit inventory should be considered in the model and especially in the case of transporting valuable cargos where an interest rate is applied for cargo value as in (Devanney, 2011a) model where an interest rate of 5% is applied . However, for bulk carriers and tankers, most studies assume that freight rate is independent of ship speed as in (Smith *et al.*, 2011) model. After running some tests for this study to determine the influence of computing the in-transit inventory, it was concluded that the relative difference in the annual revenue calculations can be neglected and it does not affect or change the final decision.

For uniformly increasing cash flow cases, it is assumed that all income and expenditure are rising at $[e = 3\%]$ per annum during the ship life time, and are discounted at $[i = 10\%]$ rate when the present worth is calculated using the NPV method. Both escalation and discount rates can be combined to be used in the Series Present Worth type calculations and Capital Recovery calculations as suggested by (Buxton, 1987; Michalski, 2004a).

The economic model focuses mainly on the operating performance of tanker ships rather than how ships are financed and how shipping companies are committed to pay back the debt with interest. Therefore, and for simplicity purpose, it is assumed that the owner pays in cash to purchase the ship and in full by the time the ship is delivered and ready to operate and generate revenue. However, in case the ship is purchased with bank loans, then the cashflow calculations should consider the annual interest payments and depreciation. Assuming a 10% interest, then the annual payments would be in the range of a few millions of dollars as new-building cost is typically in the range of several tens of millions (Faber *et al.*, 2009).

5.3 Economic Model Results

5.3.1 Results for the Base Ship

Results for the base ship will be presented first to demonstrate how calculations are carried out aiming to determine the relationship between ship economic performance and the market conditions and speed as well. Later in this section, the effect of the main hull and machinery characteristics of other alternative designs on the economic performance are discussed.

First of all, the base ship characteristics and some main results of the economic model are shown below in Table 5.7:

Table 5.7 Base Ship Details

Length Between Perpendiculars	L_{BP}	202.50 m
Breadth	B	32.25 m
Design Draught	T	12.18 m
Depth	D	20.60 m
Displacement	Dis	67300.50 ton
Lightship	LW	13398.40 ton
Deadweight	DWT	53902.12 ton
Design Speed	V	15.00 knots
Delivered Power at service speed	P_D	8785.00 kW
Main Engine MRC	P_{ME}	11000.00 kW
Auxiliary Engine power at cruising phase	P_{AE}	525.02 kW
Gross Tonnage for Port costs calculations	GT	38247.98

Table 5.8 and Table 5.9 show the model results for the number of laden and ballast days per trip and number of trips per year over the speed range (5-17 knots) for Route ONE (2000 n.mile) and Two (7000 n.mile) respectively. It is assumed that the ship is sailing at a constant speed during the voyage for both laden and ballast legs, and the model assumes 25 off-hire days a year and 4 days at ports per trip:

Table 5.8 Trip Details for Route ONE

Speed [knots]	Laden days per trip	Ballast days per trip	Trip Duration	Trips per year
5	16.67	16.67	37.33	9.11
6	13.89	13.89	31.78	10.70
7	11.90	11.90	27.81	12.23
8	10.42	10.42	24.83	13.69
9	9.26	9.26	22.52	15.10
10	8.33	8.33	20.67	16.45
11	7.58	7.58	19.15	17.75
12	6.94	6.94	17.89	19.01
13	6.41	6.41	16.82	20.21
14	5.95	5.95	15.90	21.38
15	5.56	5.56	15.11	22.50
16	5.21	5.21	14.42	23.58
17	4.90	4.90	13.80	24.63

Table 5.9 Trips Details for Route TWO

Speed [knots]	Laden days per trip	Ballast days per trip	Trip Duration	Trips per year
5	58.33	58.33	120.67	2.82
6	48.61	48.61	101.22	3.36
7	41.67	41.67	87.33	3.89
8	36.46	36.46	76.92	4.42
9	32.41	32.41	68.81	4.94
10	29.17	29.17	62.33	5.45
11	26.52	26.52	57.03	5.96
12	24.31	24.31	52.61	6.46
13	22.44	22.44	48.87	6.96
14	20.83	20.83	45.67	7.45
15	19.44	19.44	42.89	7.93
16	18.23	18.23	40.46	8.40
17	17.16	17.16	38.31	8.87

Table 5.10 and Table 5.11 show fuel consumption in the main and auxiliary engines and boilers as it is calculated for the base ship during all voyage phases for Route ONE and Route Two, respectively. Total annual bunker fuel and MDO fuel consumptions are calculated in tonnes per year for comparison purpose among all alternative designs and conditions. It is apparent that annual MDO consumption does not vary much when sailing at slower or higher speeds as fuel consumption in auxiliary engines is not a function of the ship speed and the electricity required on board is relatively constant for a particular vessel. However, MDO consumption for the short route i.e. Route One is higher than for the long route i.e. Route Two. That is because of the extra number of trips and port stops per year for the short distance route as the ship spends more time at port where MDO consumption per hoteling day is higher than per sailing day. The MDO consumption increases with speed because of the extra port stops. It is in the range of 7% at speed 5 knots and 17% at speed 17 knots.

The total bunker fuel consumption per year in main engines and boilers, and hence CO_2 emissions, vary considerably between the short and long routes and as a function of speed. First of all, speed reduction is an effective way to reduce fuel consumption and the profit loss especially when the market conditions are not in boom. For instance, reducing the service speed by 5 knots would reduce the bunker consumption by around 70% and by 95% when speed is reduced by 66% down to 5 knots. However, the results for the base ship show that fuel saving per year is higher for long distance routes when a ship slows down in the range between [5-10 knots] while the annual bunker fuel saving is higher for the short distance route when sailing at higher speeds. For example, annual bunker fuel consumption at speed 7 knots for the short route is greater by around 20% than fuel consumption for the long distance route and it increases to 43% at speed 5 knots.

These findings are applicable for the base tanker ship presented in this case study, and it might vary for other ship types and sizes as the results depend on the hull particulars, main engine specific fuel consumption at sea and fuel consumption in port for cargo heating for tankers.

Table 5.10 Fuel Consumption (ton) per trip and per year for Route ONE

Speed [knots]	Bunker Cons per trip	MDO Cons per trip	Bunker Cons per year	MDO Cons per year
5	80.41	109.37	732.34	996.07
6	96.96	94.67	1037.38	1012.92

7	116.03	84.17	1418.65	1029.08
8	137.73	76.30	1885.69	1044.59
9	162.18	70.17	2448.69	1059.48
10	189.88	65.27	3123.83	1073.80
11	221.79	61.26	3937.39	1087.58
12	259.74	57.92	4936.61	1100.84
13	306.57	55.09	6196.77	1113.62
14	366.54	52.67	7835.68	1125.94
15	445.33	50.57	10019.85	1137.82
16	550.16	48.73	12974.93	1149.29
17	689.48	47.11	16982.39	1160.37

Table 5.11 Fuel Consumption (ton) per trip and per year for Route TWO

Speed [knots]	**Bunker Cons per trip**	**MDO Cons per trip**	**Bunker Cons per year**	**MDO Cons per year**
5	181.45	329.88	511.27	929.50
6	239.35	278.43	803.97	935.23
7	306.12	241.68	1191.77	940.88
8	382.05	214.11	1688.82	946.46
9	467.63	192.68	2310.45	951.97
10	564.58	175.52	3079.52	957.41
11	676.25	161.49	4031.62	962.77
12	809.08	149.80	5228.68	968.07
13	972.99	139.90	6769.04	973.31
14	1182.90	131.42	8806.99	978.48
15	1458.64	124.07	11563.34	983.58
16	1825.57	117.64	15341.54	988.62
17	2313.18	111.97	20527.44	993.60

5.3.2 Cost Results for Route One (2000 n.mile)

The developed economic model helps to evaluate the sensitivity of a ship's profit to market conditions across a range of assumed scenarios as in Table 5.6. The four scenarios represent combinations of the most influential key factors in the tanker market which are freight rate and fuel price. The model is run for the two selected routes (short and long). The calculations are

carried out for the eight scenarios, first, for the base ship over the speed range (5 knots to 17 knots) and the results are presented and plotted, and then discussed.

The economic model calculations' output for the base ship sailing at the design speed (15 knots) is presented in Table 5.12 for Route One (short trip) across the four selected scenarios. It shows the main cost and revenue items per trip and per year as well as the profit per trip and the annual profit. All figures are in million dollars.

Fuel cost for the base ship at the design speed which is ($5.8 m) and ($9.15 m) for scenarios (1&2) and (3&4) respectively dominates and represents around 48% and 60% for the low and high fuel price scenarios respectively of the total annual cost .While port charges including port dues and cargo handling costs represent 23.6% of the total annual cost. It should be noted that the capital cost is not taken into account as it is assumed in the model that the ship is bought by cash and there is no interest or regular debt repayments.

Table 5.12 Cost, revenue, and profit results for the base ship for the short route

	1 Low Freight Rate Low Fuel Price	2 High Freight Rate Low Fuel Price	3 Low Freight Rate High Fuel Price	4 High Freight Rate High Fuel Price
Capital cost	37.86	37.86	37.858	37.86
Annual Operating cost	2.96	2.96	2.960	2.96
Bunker cost per trip	0.22	0.22	0.36	0.36
MDO cost per trip	0.04	0.04	0.05	0.05
Total fuel cost per trip	0.26	0.258	0.41	0.41
Annual fuel cost	5.81	5.806	9.15	9.15
Port charges per trip	0.13	0.13	0.13	0.13
Annual Port Charges	2.84	2.84	2.84	2.84
Dry-Docking costs, once each 2.5 years	1.11	1.11	1.11	1.11
Dry-Docking costs per year	0.45	0.45	0.45	0.45
Total Annual Cost	**12.05**	**12.05**	**15.40**	**15.40**
Revenue per trip (Gross Freight) before commission	0.47	0.78	0.47	0.78
Revenue per trip (Net Freight) with commission	0.45	0.76	0.45	0.76
Annual Net Revenue	**10.22**	**17.03**	**10.22**	**17.03**

Annual (Revenue - Fuel cost)	4.41	11.22	1.06	7.87
Annual Profit / Loos	**-1.84**	**4.98**	**-5.18**	**1.63**
Scrapping Value in 2012	5.40	5.40	5.40	5.40
Adjusted Scrapping Value after 25 years	11.22	11.22	11.22	11.22

*All figures are in $ million

For the high freight rate scenarios, the revenue generated by the ship at the design speed is greater than the total annual cost, and apparently there is a positive profit made. However, at the design speed under Scenario One, the high fixed costs and low freight revenue lead to a negative profit i.e. a loss of around ($1.84 m) while the loss is the highest for Scenario Three where fuel prices are high and freight rates are low. In such cases, the shipowner or charterer has, first, to consider operating at a different speed where it is possible to reduce the loss till the market conditions change and there is an opportunity to maximize profit.

Running the model for other speeds shows the implications of adjusting operating speed in response to fluctuations in freight rates and fuel prices. Table 5.13 presents the influence of sailing at lower and higher speeds on the total annual profit across the four scenarios. It can be seen that the ship makes a loss at all speeds for Scenario One and Scenario Three as in both cases low freight rate is assumed. However, the lowest loss for Scenario One occurs in the range [9-12] knots and exactly at speed 11 knots as the loss is less by 83% comparing with the loss at the design speed [15 knots]. Whilst the highest loss for Scenario One (-$4.63 m) occurs at speed 17 knots as the fuel cost is the highest and the extra revenue generated by making more trips does not compensate the increase in the fuel and port costs. Similarly, the lowest loss for Scenario Three occurs at speed 8 knots where it is less by 72%, and the loss at speeds between 7 knots and 10 knots is the minimum.

The results show that the maximum profit in the case of high freight rates (Scenarios 2&4) occurs at higher speeds compared with the low freight rates scenarios. The ship generates the highest profit when fuel price is low at speed 13 knots and at 11 knots when bunker and MDO prices are high. It is very obvious that the economic performance of the ship in terms of annual profit is improved at speeds lower than the design speed. However, it is crucial to choose the optimum speed as going very slow might have an adverse effect on the ship profit as can be

seen across all scenarios where the loss might be at the highest levels or the profit at the lowest levels at very slow speeds as in Table 5.13.

Table 5.13 Annual Profit / Loss across all speeds for Rout One for the base ship [$ million]

Speed [knots]	1 Low Freight Rate Low Fuel Price	2 High Freight Rate Low Fuel Price	3 Low Freight Rate High Fuel Price	4 High Freight Rate High Fuel Price
5	-1.483	1.27	-2.00	0.76
6	-1.13	2.11	-1.74	1.50
7	-0.83	2.87	-1.56	2.14
8	-0.59	3.55	-1.47	2.67
9	-0.42	4.15	-1.47	3.10
10	-0.33	4.66	-1.59	3.40
11	-0.32	5.06	-1.82	3.55
12	-0.41	5.34	-2.23	3.53
13	-0.66	5.46	-2.85	3.27
14	-1.10	5.37	-3.79	2.68
15	-1.84	4.98	-5.18	1.63
16	-2.97	4.17	-7.20	-0.06
17	-4.63	2.82	-10.08	-2.62

* Highlighted cells show the highest profit for each scenario

For a better understanding of the influence of slow steaming on economic performance optimisation in shipping, Figure 5.3 shows the effect of sailing at different speeds on fuel cost and revenue per year and hence on the annual net profit for Scenario One. The three curves show the sensitivities and trends in fuel cost, revenue and profit over the speed range [5-17] knots as a percentage from the results at the design speed. The first observations is the linear relation between speed and revenue as the annual freight income increases with speed as more trips are made. Varying speed by 2 knots from 15 to 13 (around 13%) leads to a 10% reduction in revenue. One the other hand, the fuel cost follows a polynomial trendline of increasing power for high speeds. For example, by reducing speed by 13% (from 15 to 13 knots), fuel cost is reduced by 33% while increasing speed 13% (from 15 to 17 knots) leads to an enormous increase in the fuel bill of about 61% as the speed-fuel cost curve is of the power of 3.8. That is a strong indicator that by slowing down, the potential to cut shipping emissions is significant.

The profit curve in Figure 5.3 suggests that during depression periods in the shipping market as in this scenario (low freight rate and low fuel price), it is important for the shipowner or charterer to carefully determine the most optimum speed where costs are reduced and hence profit is increased or loss is minimised. As mentioned before, the optimum speed where the loss is minimum is 11 knots as the annual net saving is more than ($1.52 m). However, it is apparent that operating at any lower speeds than the design speed will be of a great benefit to the ship finance when freight rates are low.

The influence of speed on fuel cost, revenue and profit for all of the four scenarios is presented in Figure 5.4.

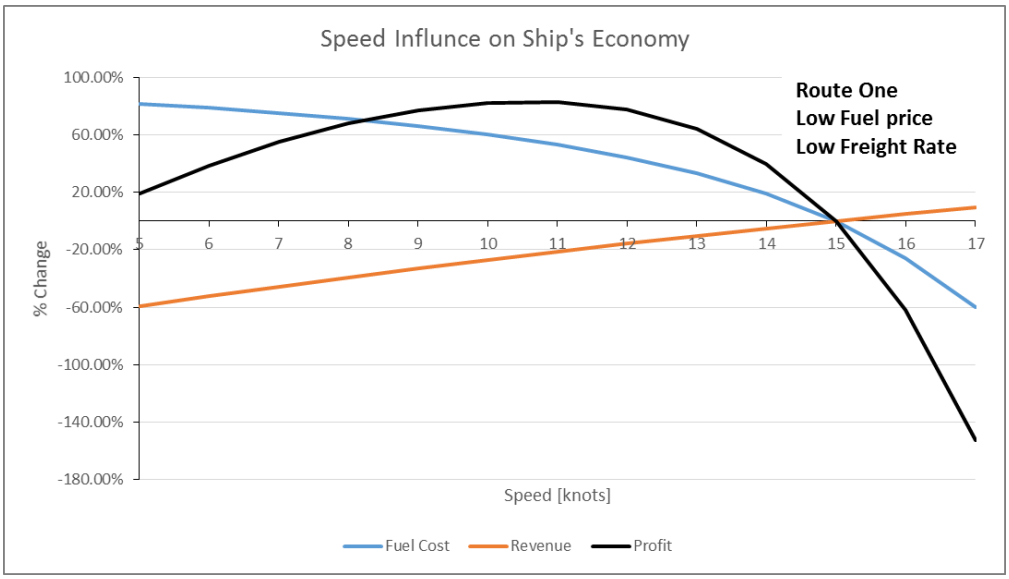

Figure 5.3 Influence of Speed on Fuel Cost, Revenue, and Profit for the Base Ship (Short Route and Scenario One)

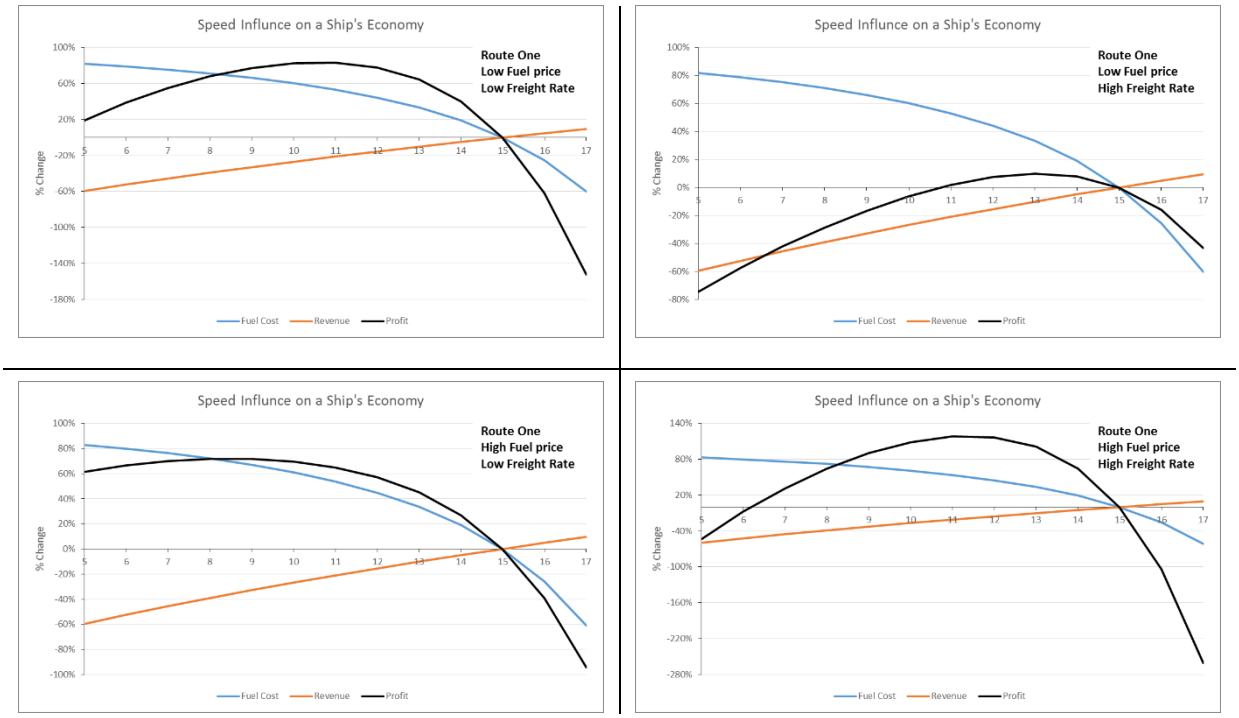

Figure 5.4 Influence of Speed on Fuel Cost, Revenue, and Profit for the Base Ship (Short Route)

More useful operational indicators, economic relations and financial characters are calculated by the developed economic model in the light of different operational and market scenarios and across different speeds. They can be employed to gain a better understanding of how to improve the operating management of an induvial ship or a fleet in order to maximise productivity and efficiency, and to meet the market demand. Moreover, those indicators give a thorough meaning of all cost, revenue and profit values while comparing alternative designs, routes, and operational practise such as optimising speed. The output of the economic model includes:

- Annual Productivity [tonne.mile/year],
- Revenue per DWT [$/tonne],
- Revenue per tonne.mile [$/tonne.mile],
- Fuel Consumption per tonne.mile [$/tonne.mile],
- Unit Cost per tonne transported [$/tonne],
- Profit per tonne.mile [$/tonne.mile].

However, Table 5.14 shows the profit per tonne.mile for the base ship in the four scenarios when sailing on the short distance route. It can be seen that the highest value of profit per tonne.mile might occur at speeds different from the ones where the maximum annual profit occurs as it is a function of the annual productivity and profit. Therefore, careful consideration

is vital when planning and optimising a journey as some economic indicators could provide different information and conclusion.

Table 5.14 Profit per tonne.mile for the base ship on Route One across all speeds

Speed [knots]	1 Low Freight Rate Low Fuel Price	2 High Freight Rate Low Fuel Price	3 Low Freight Rate High Fuel Price	4 High Freight Rate High Fuel Price
	* 10^-3 [$/tonne.mile]			
5	-1.57	1.35	-2.12	0.80
6	-1.02	1.91	-1.57	1.35
7	-0.65	2.27	-1.23	1.69
8	-0.42	2.51	-1.04	1.89
9	-0.27	2.66	-0.94	1.98
10	-0.19	2.73	-0.93	1.99
11	-0.17	2.75	-0.99	1.93
12	-0.21	2.72	-1.13	1.79
13	-0.31	2.61	-1.36	1.56
14	-0.50	2.43	-1.71	1.21
15	-0.79	2.14	-2.23	0.70
16	-1.22	1.71	-2.95	-0.03
17	-1.82	1.11	-3.95	-1.03

* Highlighted cells show the greatest profit per tonne.mile for each scenario

5.3.3 Cost Results for Route Two (7000 n.mile)

In the tanker market, there is enough flexibility over the way ship owners or charterers have to choose their preference when it comes to accept a deal in long-term charter market or spot charter market. They all aim to make a journey more profitable than other available options where a ship might make a loss. That depends on the demand for shipping services of a specific size and type on a particular maritime route. Therefore, the length of the maritime route plays an important role in determining the annual utilization of a ship and profit, and ships might do well on a specific journey rather than on another of a different distance and operating constraints. To illustrate this point, the economic model is run for the second case study as the base ship is operating on the long distance route (7000 n.mile), and the calculations are run for

the four scenarios to determine the economic performance. The results are presented in Table 5.15.

Based on the assumptions regarding fuel consumption during all voyage phases (laden, ballast, and hoteling) in the main and auxiliary engines and boilers, it is obvious from Table 5.12 and Table 5.15 that the trends in profits are the same. The ship makes a loss in Scenarios 1&3 where the fright rates are low despite the fuel prices are high or low. However, the loss made by sailing on the long route is less than the loss made on the short route. That is mainly, in this particular case, due to the high port charges occur because of the extra stops at ports even though the fuel cost is higher for the long route journey. It is worth mentioning that by assuming that the ship is operating between two destinations where port dues and cargo handling charges are lower comparing with the model assumptions, then the results might reveal different preferences for the shipowner as cost per trip on the short distance route will be reduced.

On the other hand, for the high freight rate and low fuel price scenario (2), the positive profit is greater for the long distance route case than the short distance route by ($0.146 m) as the total cost is less even though the revenue is less by more than one million USD ($1.03 m). The annual net freight revenue after commission and the annual cost in Scenario 4 are ($ 16.00 m) and ($ 14.64 m) respectively, and that leads to a positive profit of around ($ 1.36 m). The profit in Scenario 4 for both routes cases are almost equal, and hence the shipowner or the charterer needs to make a decision depending on what is available in the market. However, a voyage planning and routing optimisation are necessary as the next stop plays an important role in accepting or refusing the offered contract at the present.

From the environmental point of view, bunker fuel consumption per year is less by 13% for the short distance trip. Therefore, trade-offs are on the steak when it comes to the energy efficiency and economic performance as there is a great potential to reduce CO_2 emissions by optimising journey planning as well as slow steaming even though there might be a reduction in the profit generated.

Table 5.15 Cost, revenue, and profit results for the base ship for the long route

	1 Low Freight Rate Low Fuel Price	2 High Freight Rate Low Fuel Price	3 Low Freight Rate High Fuel Price	4 High Freight Rate High Fuel Price
Capital cost	37.86	37.86	37.86	37.86
Annual Operating cost	2.96	2.96	2.96	2.96
Bunker cost per trip	0.73	0.73	1.17	1.17
MDO cost per trip	0.09	0.09	0.12	0.12
Total fuel cost per trip	0.82	0.82	1.29	1.29
Annual fuel cost	6.47	6.47	10.23	10.23
Port charges per trip	0.13	0.13	0.13	0.13
Annual Port Charges	1.00	1.00	1.00	1.00
Dry-Docking costs, once each 2.5 years	1.11	1.11	1.11	1.11
Dry-Docking costs per year	0.45	0.45	0.45	0.45
Total Annual Cost	**10.88**	**10.88**	**14.64**	**14.64**
Revenue per trip (Gross Freight) before commission	1.35	2.07	1.35	2.07
Revenue per trip (Net Freight) with commission	1.31	2.02	1.31	2.02
Annual Net Revenue	**10.40**	**16.00**	**10.40**	**16.00**
Annual (Revenue - Fuel cost)	3.93	9.53	0.17	5.76
Annual Profit / Loos	**-0.48**	**5.12**	**-4.24**	**1.36**
Scrapping Value in 2012	5.36	5.36	5.36	5.36
Adjusted Scrapping Value after 25 years	11.22	11.22	11.22	11.22

*All figures are in $ million.

Running the model for other speeds (5-17 knots) reveals the significant implications of sailing at different speeds on the cost components, revenue, and annual profit in the case of different scenarios that represent the fluctuations in freight rates and fuel prices. The results are presented in Table 5.16 and Figure 5.5. They relatively have the same trends as the ones for the short route case in Table 5.13. Some differences can be highlighted. For example, a positive profit is made at speeds between 8 knots and 14 knots on Scenario One unlike the short route case where the ship makes a loss (negative profit) at all speeds (5-17 knots). Also, at the optimum speeds for both routes, the maximum profit is greater for the long journey across all scenarios.

However, those findings do not suggest that in the tanker market, a voyage is more profitable when operating on a long route or on a short route. Therefore, shipowners and charterers need to consider all the available options and they might, in some cases, prefer to wait till a more preferable contract is offered. Basically, the voyage and annual cashflow estimate provides ship owners and charterer with an approximate financial cost and return that can be expected from prospective contracts. This kind of information gives ship operators the ability to operate on the most profitable and suitable trips.

Table 5.16 Annual Profit / Loss across all speeds for Rout Two for the base ship [$ million]

Speed [knots]	1 Low Freight Rate Low Fuel Price	2 High Freight Rate Low Fuel Price	3 Low Freight Rate High Fuel Price	4 High Freight Rate High Fuel Price
5	-0.97	1.02	-1.40	0.59
6	-0.48	1.89	-1.00	1.37
7	-0.05	2.71	-0.69	2.07
8	0.33	3.45	-0.46	2.66
9	0.63	4.12	-0.35	3.14
10	0.85	4.70	-0.36	3.49
11	0.97	5.18	-0.53	3.69
12	0.96	5.53	-0.90	3.67
13	0.78	5.69	-1.55	3.37
14	0.33	5.59	-2.60	2.66
15	-0.48	5.12	-4.24	1.36
16	-1.81	4.13	-6.71	-0.77
17	-3.84	2.42	-10.30	-4.03

* Highlighted cells show the highest profit for each scenario

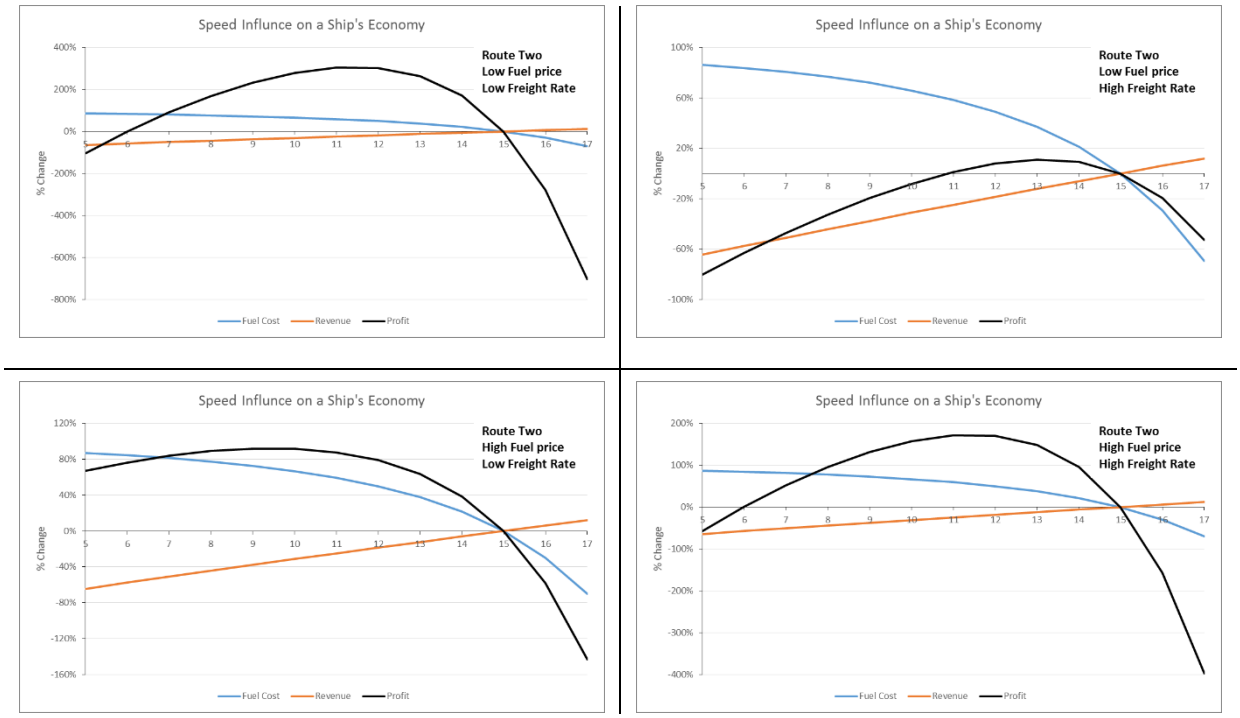

Figure 5.5 Influence of Speed on Fuel Cost, Revenue, and Profit for the Base Ship (Long Route)

5.3.4 NPV Results for the Base Ship

To evaluate the attractiveness of acquiring a new ship as an investment opportunity, and to analysis the economic performance of the base ship while sailing at the design speed across all the four scenarios of fuel prices and freight rates combinations, the Net Present Value NPV values over 25 years life span are calculated.

It is assumed that cash flow increases uniformly by year. The annual escalation rate for prices and services is assumed to be $(e = 3\%)$ including fuel prices and freight rates. However, all cash flow items are discounted at a rate of $(i = 10\%)$ per year. The 'time value' of cashflow is determined using the Present Worth factor PW to convert a future sum after N years into a present sum or by using the reciprocal of (PW) which is the Compound Amount factor (CA or FV) which is the multiplier to calculate the future sum of a present sum with interest as in Eq (5.6) and Eq (5.7):

$$PW = (1 + i)^{-N} \tag{5.6}$$

$$CA = (1 + i)^{N} \tag{5.7}$$

For the use in Series Present Worth type calculations, the discount and escalation rates can be combined to carry out the Discounted Cash Flow calculations (DCF). The effective discount rate in such cases is given as $\left(r = \frac{i-e}{1+e}\right)$, and the effective Sereies Present Worth factor SPW which is the multiplier to convert a number of regular payments over N years into a sum present is given in Eq (5.8) as suggested by (Buxton, 1987; Sullivan *et al.,* 2006). The Net Present Value is calculated using Eq (5.9) showing the components of the equation:

$$SPW = \frac{1 - \left(\frac{1+i}{1+e}\right)^{-N}}{\frac{i-e}{1+e}} \tag{5.8}$$

$$\begin{aligned} NPV = & -Intial\ Building\ cost \\ & + Present\ worth\ [anual\ net\ revenue - total\ annual\ cost\ ] \\ & + Discounted\ Salvage\ value \end{aligned} \tag{5.9}$$

Applying the NPV method on the base ship operating at the design speed for Route One and Scenario one, it results in a negative NPV as can be seen below taking into account that $(PW = 1/10.835, CA = 2.094, SPW = 11.87)$.

$$NPV = -37.858 + 121.28 - 143.066 + 1.036 = \mathbf{-58.609}\ (\$\ US\ million)$$

The negative net present value of the cash inflows and outflows during the whole ship lifespan indicates that running the ship in such market conditions is not a good investment for the shipowner nor the shipping company as the present value of the inflows is less than the present value of the outflows. In other words, the revenue earned is worth less today than the costs of the initial capital price and the running costs, therefore, it is not a profitable investment. In practise, investors should look for other alternatives with higher NPV of all options and operation conditions.

In order to have a positive NPV, costs need to be reduced and cash inflows should be increased. For example, if the freight rate has increased from 9 ($/ton cargo) to 13.35 ($/ton cargo) or greater, NPV would have a positive value. A positive NPV can also be achieved if all cost items including the initial price is reduced by 20% and all the income items are increased by 20%.

Similarly, NPV values are calculated for the base ship across the speed range (5-17 knots) and the four scenarios. The results are shown in Table 5.17 and Table 5.18 for Route One and Route

Two, respectively. Since the initial capital cost and the salvage value are constant for the same base ship and the annual operating cost as well, then NPV is a function of the fuel and port costs and the freight revenue. Therefore, NPV trends are exactly the same as what has been found when discussing the profit maximising options. In other words, optimum speeds where the base ship makes the maximum profit for each scenario and route are the ones where she has the most efficient economic performance in terms of the present value of the investment.

Examining NPV results in Table 5.17 and Table 5.18 shows that based on the profitability of a projected investment as a benchmark, operating at slower speeds on Route Two is a better option for the shipowner as it offers a superior value of the money over time for the majority of speeds. Moreover, it is a strong evidence that sailing at slower speeds for all fuel price and freight rate combinations is more profitable as NPV has fairly higher values to some degree. That means the shipowner will benefit from adopting slow steaming measure as the investment will have a better financial return.

In the next section, NPV analysis will be used to compare other alternative designs which have different capital costs, operating costs and revenues.

Table 5.17 Net Present Value for the Base Ship on Route One, NPV [$ million]

Speed [knots]	1 Low Freight Rate Low Fuel Price	2 High Freight Rate Low Fuel Price	3 Low Freight Rate High Fuel Price	4 High Freight Rate High Fuel Price
5	-54.43	-21.71	-60.59	-27.86
6	-50.19	-11.74	-57.49	-19.04
7	-46.64	-2.71	-55.36	-11.42
8	-43.84	5.36	-54.27	-5.08
9	-41.83	12.43	-54.32	-0.06
10	-40.69	18.43	-55.64	3.48
11	-40.56	23.23	-58.46	5.34
12	-41.73	26.57	-63.23	5.07
13	-44.62	28.02	-70.65	1.99
14	-49.92	26.90	-81.83	-5.01
15	-58.61	22.24	-98.34	-17.49
16	-72.03	12.72	-122.33	-37.58
17	-91.83	-3.32	-156.44	-67.93

* Highlighted cells show the highest NPV value for each scenario

Table 5.18 Net Present Value for the Base Ship on Route Two, NPV [$ million]

Speed [knots]	1 Low Freight Rate Low Fuel Price	2 High Freight Rate Low Fuel Price	3 Low Freight Rate High Fuel Price	4 High Freight Rate High Fuel Price
5	-48.36	-24.73	-53.49	-29.86
6	-42.52	-14.36	-48.72	-20.55
7	-37.36	-4.71	-44.95	-12.31
8	-32.93	4.13	-42.32	-5.25
9	-29.34	12.08	-40.96	0.47
10	-26.72	19.01	-41.10	4.64
11	-25.28	24.71	-43.07	6.92
12	-25.38	28.80	-47.45	6.74
13	-27.61	30.72	-55.18	3.15
14	-32.88	29.55	-67.72	-5.30
15	-42.49	23.98	-87.18	-20.71
16	-58.26	12.21	-116.41	-45.95
17	-82.46	-8.05	-159.10	-84.69

* Highlighted cells show the highest NPV value for each scenario

5.3.5 Newbuilding Cost Results for Alternative Designs

The economic model is run for all the 228 designs generated by AVEVA in the aim to determine how optimising the hull shape and parameters affects the acquiring price, the cost to run a ship during the whole life span, and the total revenue that is expected to be generated.

Figure 5.6 shows the sensitivity of the newbuilding prices corresponding to changes in the main key parameters for the 36 hulls generated in Stage One. The estimated newbuilding prices and their percentage change from the base ship price are plotted alongside the percentage change in the ship deadweight capacity. The results can be summarised as following:

- For Group One hulls with constant displacement (Figure 5.6-a), the newbuilding price NB increases linearly with the hull length while the deadweight, and hence, the cargo capacity decreases for longer hulls. Varying the length while keeping the other design variables constant has a moderate influence on the NB cost. Taking the +10%L hull as an example, increasing the length by 10% and keeping the displacement constant results

in increasing the NB cost by around ($0.3 m) which equals a +2.5% increase in the cost. This extra increase in capital cost occurs because of the increase in the amount of required steel and the labour costs to roll and fabricate the hull plates. On the other hand, for a constant displacement, by increasing the length and reducing the breadth and depth, there will be a loss (decrease) in the ship carrying capacity i.e. deadweight. For a 10% increase in length and 5.4% decrease in both beam and draught (constant B/T), lightweight increases by around 8% and deadweight decreases by 2%. This suggests that increasing the hull length while keeping the displacement constant will tend to increase the steel needed for construction and reduce the ship available carrying space. However, on the other hand, it has been found previously that increasing length increases the energy efficiency of the hull and reduces the fuel bill.

- Figure (Figure 5.6-b) for Group Two hulls shows how varying B/T ratio while keeping the length and displacement constant would affect the newbuilding price and deadweight. It can be seen that for higher B/T ratio values where breadth increases while draught decreases, the newbuilding cost decreases as well as deadweight. However, changes in NB cost and DWT are not significant which means that varying B/T has a minor influence on the construction cost and lightweight for a constant displacement and body fullness. For example, increasing B/T by 10% reduces the NB cost by less than 0.2% ($0.067 m) which means it can be assumed that the NB cost is not sensitive to changes in B/T ratio. Similarly, the influence of varying B/T ratio on deadweight is very small as figure (Figure 5.6-b) shows for all hulls where deadweight varies in the range ±0.85%.

- Examining Group Three hulls (Figure 5.6-c) shows that NB cost for slim hulls with reduced block coefficient C_B decreases at a higher level comparing with the previous two groups. By reducing the block coefficient by 6%, a shipowner can save up to $0.6 million in the capital cost. However, that comes at a loss in the ship productivity and freight revenue as deadweight decreases and hence the available cargo space is less. Deadweight of the $-6\%\, C_B$ hull decreases by 7.4% from 53902 to 49930 tons. Therefore, shipowners should carefully consider the trade-offs when making a decision regarding the optimum design from the cost point of view and capacity even though a bigger is better (economy of scale).

- The final design variable to be discussed is the longitudinal centre of buoyancy LCB. It can be seen on (Figure 5.6-d) that shifting the position of the longitudinal centre of buoyancy backwards or afterward has relatively no effect on the NB cost and slight effect on the deadweight. It has been found previously that the position of the longitudinal centre of buoyancy plays a vital role in improving the energy efficiency of the hull. The combined effect of LCB will be discusses later in the next chapter.

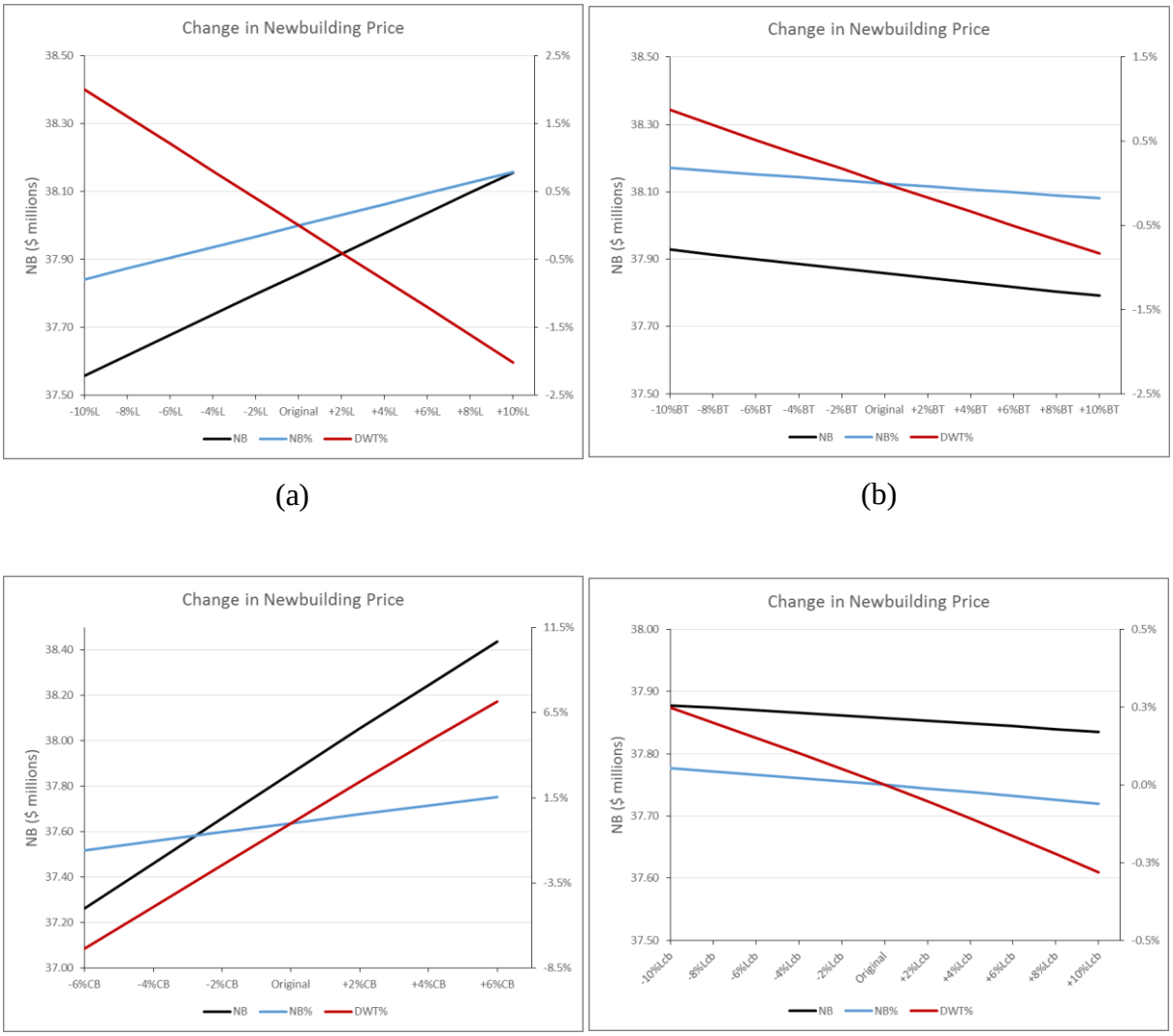

Figure 5.6 Newbuilding Price for Stage One Hulls

Once the individual driving parameters for the newbuilding cost and its sensitivity to a basic parametric optimisation are determined, the next stage is to examine the influence of different combinations of the four design parameters on the newbuilding cost. However, since the alternative designs have different lightweight and deadweight, then it does not sound rational

to compare the acquiring price of vessels with varying cargo carrying capacity. Therefore, newbuilding price to deadweight ratio (NB/DWT) is used as a response parameter for the hull parametric distortion.

The newbuilding cost per deadweight ratio (NB/DWT) and the S/N ratio are calculated for each run of the experiment in order to search for the settings where the factor levels of the design parameters maximize the S/N ratios. The "smaller the better" equation is used as the aim is to minimise the (NB/DWT). The results of the average (NB/DWT) and the mean S/N ratio for each level of the control parameters (low, medium, and high) are shown in Table 5.19 and Table 5.20. Moreover, Figure 5.7 and Figure 5.8 show, graphically, the control factors' effects on the average response parameter and S/N. In addition, Appendix G shows (NB/DWT) values in [$/dwt ton] and the mean S/N ratio for all the 81 hulls generated in Stage Three.

Results reveal that of the design parameters, length and block coefficient have a greater effect on the average (NB/DWT) and S/N than the other two design parameters. The third level for the length (L_3 – longer hull) is clearly a better choice to minimize (NB/DWT) and maximize S/N comparing with the shorter hulls (L_1 & L_2). For the other design parameters, the preferred levels are:

- Breadth to draught ratio: (B/T_1) where the breadth to draught ratio is minimum.
- Block Coefficient: (CB_3) which states that a full body is better as bigger-is-better when it comes to economy of scale as hulls with greater block coefficient have more cargo carrying capacity.
- Longitudinal centre of buoyancy: ($LCB\%L_1$) where the position of LCB moves aft even it has a minor effect on (NB/DWT).

Hence, based on the economic model results, the newbuilding cost per deadweight has a tendency of decreasing when the hull is longer, the breadth to draught ratio is smaller, the block coefficient is greater, and for backward centre of buoyancy. Those optimal control factor settings make the design more robust and resistant to variations from noise factors as S/N values are maximised (Taguchi design).

Table 5.19 Average response parameter for (NB/DWT) - [$/dwt ton]

	L	B/T	CB	LCB%L
Level 1	747.139	704.139*	743.604	708.287*
Level 2	706.260	708.631	706.954	708.534
Level 3	672.267*	712.896	675.108*	708.845
max-min	74.873	8.756	68.496	0.550

Table 5.20 Mean signal-to- noise S/N ratio for (NB/DWT)

	L	B/T	CB	LCB%L
Level 1	-57.461	-56.938*	-57.419	-56.990*
Level 2	-56.972	-56.994	-56.980	-56.992
Level 3	-56.544*	-57.046	-56.579*	-56.996
max-min	0.917	0.107	0.8394	0.007

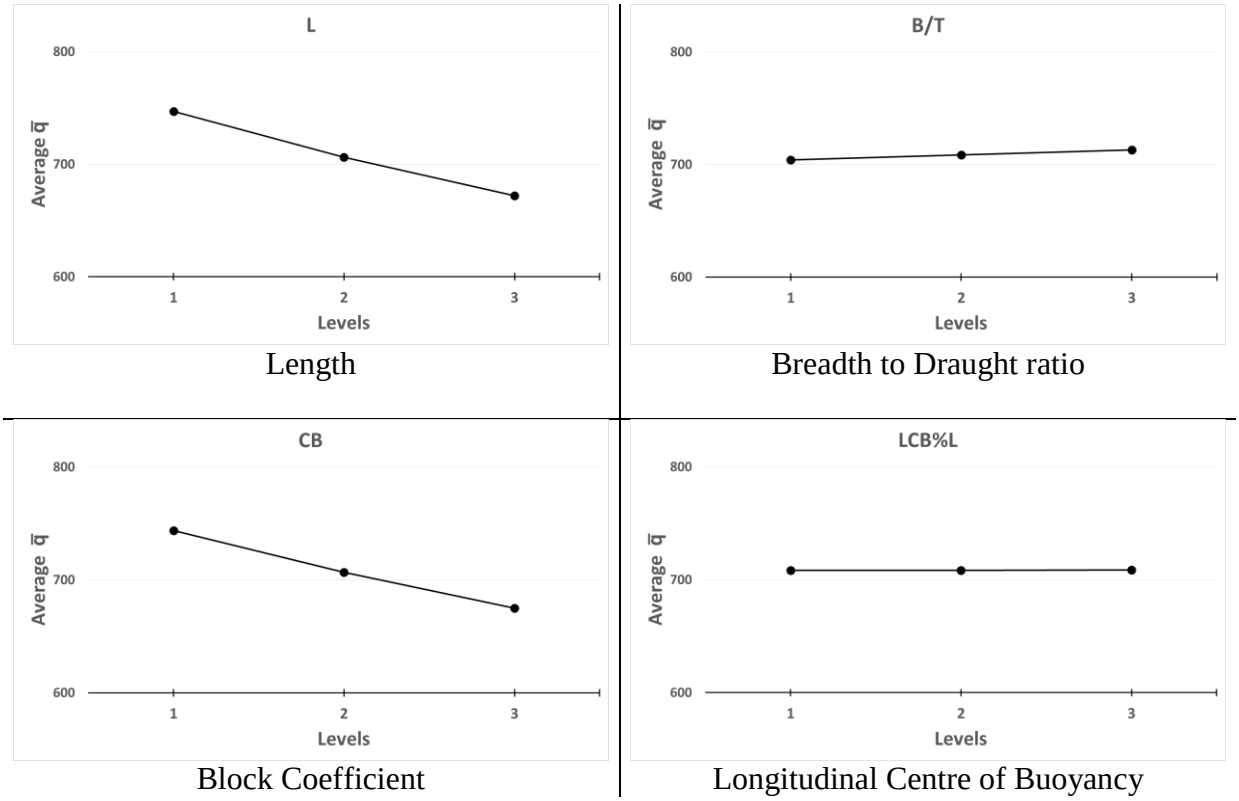

Length | Breadth to Draught ratio

Block Coefficient | Longitudinal Centre of Buoyancy

Figure 5.7 Control Factors Effects on Average (NB/DWT)

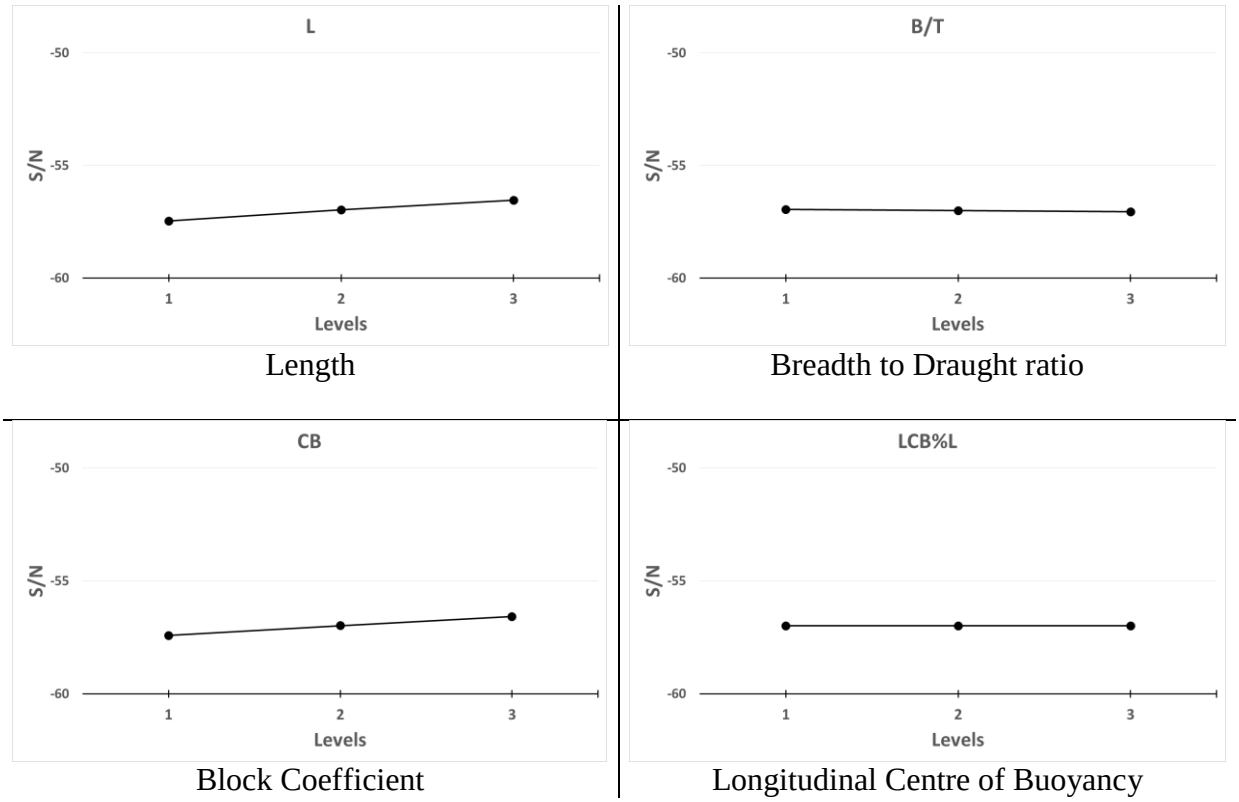

Length | Breadth to Draught ratio

Block Coefficient | Longitudinal Centre of Buoyancy

Figure 5.8 Control Factors Effects on S/N

5.3.6 Results for Alternative Designs

With regard to the investment potential and project profitability analysis of the case study vessel in the light of a fluctuating market and operating conditions, the overall economic performance of alternative designs across the four scenarios and for both the short and long routes is determined. The main criteria that are used to evaluate the economic performance of alternative vessels and for the comparison purpose to measure the likelihood to successfully investment are the annual profit per deadweight and the net present value NPV.

Before discussing the economic model results, it is worth mentioning that the calculations are carried out for 228 different hull where the economic performance (profit and NPV) is tested over 13 speeds (5-17 knots). Also, there are four different compensation scenarios of fuel prices and fright rates. Moreover, the economic performance of the ships is tested for two maritime routes (2000.0 and 70000.0 n.mile). That yield in having 23712 readings for the profit and NPV.

First of all, a quick look to the results reveals that the optimum speed range for all ships across the four scenarios is below the design speed. For example, Figure 5.9 presents, graphically, the annual profit per deadweight ton from the economic model for the short distance route assuming

a low fuel prices and low freight rates. Results for other scenarios for both routes are shown in Appendix H. It can be seen that profit per deadweight for all hulls regardless market conditions is improved for speeds between 10 and 13 knots. However, the optimum speed that maximises the economic performance varies among hulls and varies by journey distance and market conditions.

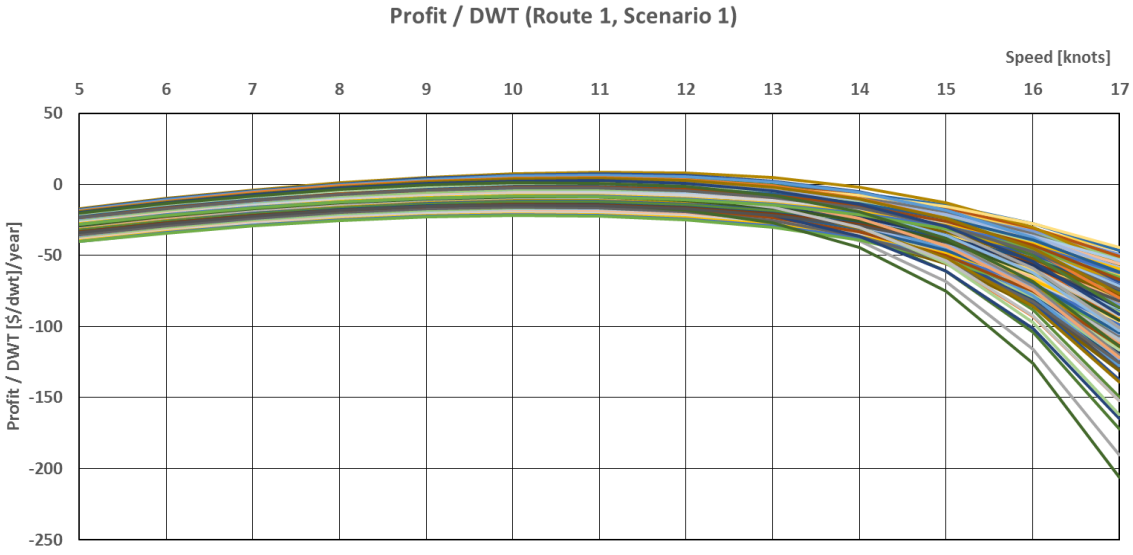

Figure 5.9 Profit per Deadweight (Route 1, Low Fuel Price and Low Freight Rates)

On the other hand, a quick analysis of the profit results for individual hulls shows that hull no. 61 as in Appendix A shows the best performance across all speeds and scenarios. Table 5.21 shows the main design parameters and characteristics of hull no.61 while and Table 5.22 and Table 5.23 present its economic performance compared with the base hull for the eight scenarios.

The economic model results reveal that, basically, designs with longer and narrower hulls and bigger cargo carrying capacity show a better performance even though the initial capital cost would be higher. Taking Hull no. 61 as an example, the initial newbuilding cost is higher by $1.7 million (+4.5%). That is mainly because of the increase in lightweight used in constructing the vessel. It can be seen from Table 5.21 that the new hull's lightweight is greater by around 10% and the deadweight by more than 15%. That enables the ship to carry around 8273.0 extra tons of cargo in each journey which generate additional freight revenue. It is worth mentioning that Hull no.61 has the lowest P_D/Dis value at the design speed among all alternative designs. That means it has the most favourite economic and hydrodynamic performance. A further

optimisation analysis will be carried out in the next chapter as this multi-objectives optimisation problem is examined.

Comparing the results for Hull no.61 presented in Table 5.22 and Table 5.23 with the base hull results presented earlier shows that the base hull makes a loss across all speeds for the short distance route in the case of low freight rates while Hull no.61 generates a reasonable profit when sailing at low speeds (8-13 knots) in the case of low freight rates and low fuel prices. However, in the case of Scenario Three which is the worst market conditions scenario, the loss per deadweight made by Hull no.61 is less by up to 55%. In the case of the long distance route, Hull no.61 performance is relatively superior as even in Scenario Three (High freight rates and fuel prices), it generates a satisfactory profit for speeds between 8 and 12 knots. The highest profit per deadweight for Scenario Three occurs at speed 10 knots and it is higher than the profit made by the base hull by 238.4%.

Analysing the net present values for Hull no.61 shows that, over the 25-year lifespan, it is not a profitable investment (negative NPV) for scenarios where freight rates are assumed to be low, and it is a profitable investment (positive NPV) for scenarios with high freight rates as in Table 5.23. The main reason behind the poor performance (negative NPV), besides the low revenue due to recession conditions in the shipping market, is the high building cost.

Table 5.21 Hull no.61 parameters

Variable	Value	Difference from Base Hull
Length L_{BP}	222.750 m	+10% (Level 3)
Breadth to Draught Ratio B/T	2.383	-10% (Level 1)
Breadth B	30.590 m	-5.13%
Draught T	12.839 m	+5.41%
Block Coefficient C_B	0.858	+4% (Level 3)
Longitudinal Center of Buoyancy LCB	114.764 m	-1.1%L (Level 1)
Deadweight DWT	62175.160 ton	+15.35%
Displacement	76950 ton	+14.34%
Lightweight	14774 ton	+10.27%
Newbuilding cost	$39.561 m	+4.5%

Table 5.22 Maximum profit per deadweight ton for Hull no.61

	Value	Speed	Difference from Base Hull
Route One: Scenario One	$8.67	@ 11 knots	+248.30%
Scenario Two	$118.26	@ 13 knots	+16.70%
Scenario Three	$-12.18	@9 knots	+55.40%
Scenario Four	$85.10	@12 knots	+29.40%
Route Two: Scenario One	$33.10	@12 knots	+83.50%
Scenario Two	$122.57	@14 knots	+16.10%
Scenario Three	$8.95	@10 knots	+238.40%
Scenario Four	$87.39	@12 knots	+27.80%

Table 5.23 Maximum NPV values for Hull no.61

	Value [$ millions]	Speed	Difference from Base Hull
Route One: Scenario One	-32.02	@ 11 knots	+21.10%
Scenario Two	48.87	@ 13 knots	+74.40%
Scenario Three	-47.41	@9 knots	+12.70%
Scenario Four	24.39	@12 knots	0357.10%
Route Two: Scenario One	-13.99	@12 knots	+44.60%
Scenario Two	52.044	@14 knots	+69.40%
Scenario Three	-31.18	@10 knots	+22.30%
Scenario Four	26.06	@12 knots	+276.50%

However, fluctuations in the shipping market are common as any economic cycle in other sectors when supply and demand are out of balance. Freight rates move up and down within time intervals which can be categorised in three groups: seasonal cycles, short cycles, and long cycles. Assuming that the ship's life is divided evenly between the four assumed scenarios, and by taking the average of the maximum NPV values for Hull no.61 over the four scenarios for both routes, then the results tell a different story as in Table 5.24. Operating for 25 years on both routes evenly and assuming that the ship is trading continuously during booms and recessions periods will promote a profitable investment as the project has a positive NPV value (3.265 m). Sailing on the long distance route (7000.0 n.mile) for the whole ship's life span proves to be a successful investment as the NPV value is over $8.0 million. Finally, a ship owner can turn the loss made by operating on Route One (2000.0 n.mile) with negative NPV ($-1.543 m) into a profit by seeking a better newbuilding contract, investing in some energy

saving technology that helps to reduce the bunker bill, reducing port days, route optimisation, etc. These conclusions might not be applicable for all maritime routes as the results found are for the assumptions made regarding the route freight rates, fuel prices, port charges, operating costs, and most importantly the initial newbuilding cost.

Table 5.24 Average NPV values for Hull no. 61

Variable	NPV [millions]
Average NPV for both routes	3.265
Average NPV for Route One	-1.543
Average NPV for Route Two	8.073

To again a better thorough understanding of how sensitive the economic performance is to changes in operating and market conditions, Hull no.61 is examined using Taguchi technique. Basically, Taguchi technique, which combines experimental design techniques and quality loss functions, is employed in determining the optimum design parameters settings which have the greatest influence on a product performance and quality. In this case, the main parameters that will be investigated at this stage are speed, route distance, fuel price, and freight rates. Those parameters affect voyage costs (mainly fuel cost), revenue, and net profit.

Experimental design is used to arrange the parameters in a full orthogonal arrays as the performance is tested for 2 levels for fuel prices (low and high), freight rates (low and high), and route distance (short and long), and 3 levels for the speed (11, 13 and 15 knots) as shown in Table 5.25. The average responses and S/N ratios are tabulated and plotted for each factor against each of its level. The results are summarised in Table 5.26, Table 5.27, Figure 5.10, and Figure 5.11. The results are examined to pick up the winning factors and levels that maximise the S/N ratios and the net present values NPV. The main aim is to determine a robust design(s) where it is vital to reduce the variation in performance when conditions change (noise variables). In other words, designers should seek a design which is insensitive to variations.

Analysing the results reveals that the fright rates has the largest impact on S/N and on the net present value of the project NPV. The fuel price is ranked as the second most influential factor on the project profitability (NPV) followed by speed and the route distance. The second level of freight rates is clearly the best choice for maximising NPV where the revenue generated is higher. Moreover, the best combination for other factors to maximise the net present value for the ship is the first level of fuel price (low), second level of distance (long), and first level of

speed (low speed; 11 knots). On the other hand, from Table 5.27, it is found that speed (13 knots), short distance route, and low fuel price are the best matching to maximise the signal to noise ratio and they yield nearly equal S/N in addition to the high freight rates. Those settings are the optimal market and operational parameter settings to reduce variability in the response parameter and minimize the effects of the noise factors.

Table 5.25 Runs layout

Run no.	Speed	Distance	Fuel	Freight Rates	Response NPV
1	11	Short	Low	Low	-32.02
2	11	Short	Low	High	41.57
3	11	Short	High	Low	-50.16
4	11	Short	High	High	23.43
5	11	Long	Low	Low	-14.80
6	11	Long	Low	High	42.86
7	11	Long	High	Low	-32.86
8	11	Long	High	High	24.80
9	13	Short	Low	Low	-34.92
10	13	Short	Low	High	48.87
11	13	Short	High	Low	-61.42
12	13	Short	High	High	22.36
13	13	Long	Low	Low	-15.42
14	13	Long	Low	High	51.87
15	13	Long	High	Low	-43.54
16	13	Long	High	High	23.74
17	15	Short	Low	Low	-48.02
18	15	Short	Low	High	45.24
19	15	Short	High	Low	-88.55
20	15	Short	High	High	4.71
21	15	Long	Low	Low	-28.86
22	15	Long	Low	High	47.81
23	15	Long	High	Low	-74.50
24	15	Long	High	High	2.17

Table 5.26 Average Response Parameter for (NPV) – [$ m]

	Speed	Distance	Fuel Price	Freight Rate
Level 1	0.352*	-10.743	8.682*	-43.756
Level 2	-1.060	-1.393*	-20.818	31.620*
Level 3	-17.500			
max-min	17.852	9.350	29.499	75.375
Rank	3	4	2	1

Table 5.27 Mean signal-to- noise S/N ratio

	Speed	Distance	Fuel Price	Freight Rate
Level 1	29.769	30.8692*	30.898*	31.687*
Level 2	30.720*	28.300	28.272	27.480
Level 3	28.266			
max-min	2.453	2.570	2.625	4.205
Rank	4	3	2	1

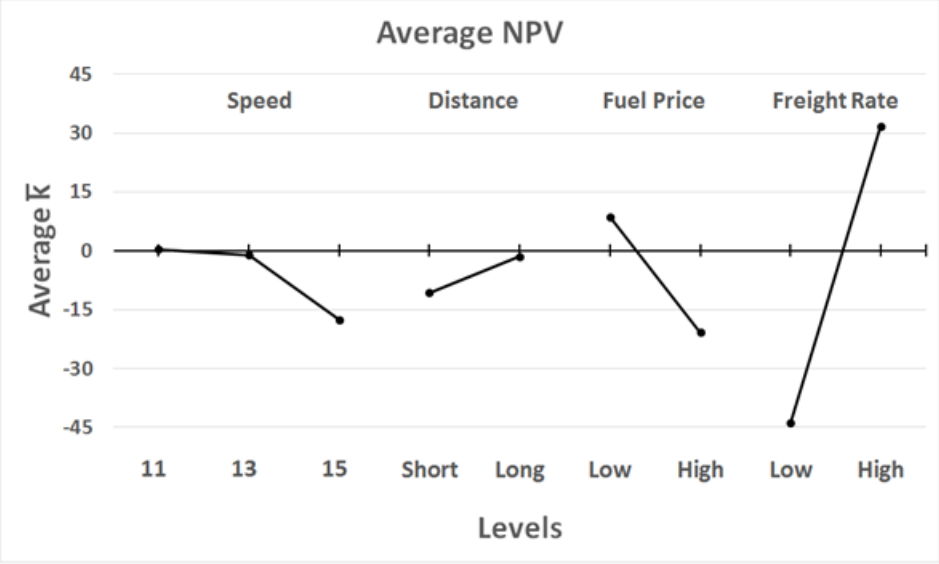

Figure 5.10 Factor effects on S/N for Hull no.61

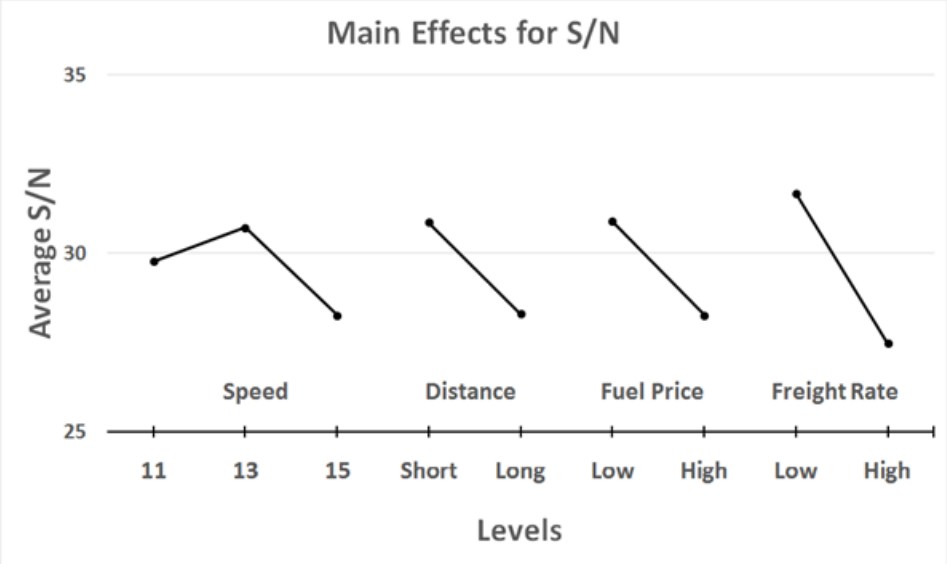

Figure 5.11 Factor effects on average NPV for Hull no.61

5.4 Conclusions

An economic model was built to estimate the capital cost and the main cash flow elements. That includes bunker cost for both laden and ballast trips and in port, operating cost, port costs, freight revenue, and commissions.

Simplified approximation regression formulas were developed as a function of the deadweight to estimate the operating costs and also dry-docking costs for tanker ships using commercial data from OpCost annual report. Tariff for ports of Jebel Ali and Port Rashid in Dubai was used for the economic model calculations. Moreover, a linear regression formula to calculate a ship gross tonnage GT was derived using collected data for tanker ships to be used in estimating the port costs while waiting at the berth. More importantly, an approximation formula to estimate the newbuilding acquiring price was derived using real data from Sea-web Ships database. The newbuilding price is estimated as a function of the ship deadweight and length, and the producer price index is included to allow for inflation adjustments. Finally, the scrapping value was also taken into account in the model, and an average value for the scrapping steel is chosen to estimate the current value of the ship in the demolition market.

The economic model was conducted for two maritime routes (2000 n.mile and 7000 n.mile), and for different fuel prices and freight rates combinations. The study examined the influence of speed reduction and hull optimisation on maximising the annual profit and economic

performance as measured by profit by deadweight and Net present value in light of fluctuating market conditions.

The first set of results for the base hull has showed that the MDO consumption does not vary much as a function of speed since the electricity consumption on board is relatively constant for a particular vessel. However, the annual MDO consumption varies in the range of (7% at speed 5 knots and 17% at speed 17 knots) between the short and long routes since the number of port stops per year varies. On the other hand, reducing the service speed by 5 knots would reduce the bunker fuel consumption significantly by around 70%. However, the results showed that the annual fuel saving and CO_2 emissions for the base ship is higher for the long distance route than the short distance route. This saving was found to be up to 43% at speed 5 knots.

The model results showed that by operating at slower speeds, the base ship would cut the huge loss at the design speed occurs for scenario one and scenario three as in both scenarios low rates were assumed. The annual loss is reduced by 83% for scenario one when sailing at speed 11 knots compared with the loss at the design speed, and by 72% for scenario three at speed 8 knots. On the other hand, the ship generates a greater profit at higher speeds for the high fright rate scenarios (Scenarios 2&4). The results showed that the optimum operating speeds are 13 knots for Scenario Two with low fuel price, and 11 knots for Scenario Four with high fuel price.

Some interesting findings from the study showed that sailing on the long distance route would benefit the ship and reduce the loss in the case of low fright rate scenarios when high port dues and cargo handling charges are assumed. That is mainly because of the reduction in the number of port visits per year. On the other hand, the results showed that the bunker fuel consumption per year at the design speed for the short distance trip is less by 13%. Therefore it is crucial to investigate the trade-offs linked to both the economic performance and the environmental performance.

The findings obtained from running the model for other speeds (5-17 knots) highlighted the importance of speed and routing optimisation on the revenue and cost items. For instance, a positive profit is generated for Scenario One (low freight rate and low fuel price) at speeds between 8 knots and 14 knots while a negative profit occurred when operating at the design speed and speeds in the range (5-7) and (16-17) knots. NPV results showed that at the design speed, the base ship has a negative net present value across all the scenarios expect Scenario Two where fright rates are high and fuel prices are low. However, reducing the speed by a few

knots would offer a superior value of the investment over time for both routes; i.e. the short and long ones.

The economic model was conducted for the base hull and all other alternative designs to highlight the sensitivity of newbuilding prices, operating cost, and revenue to the design parameters and speed. The results revealed that length and block coefficient have the greatest effect on the newbuilding price to deadweight ratio NB/DWT. Hull no. 61 (L_3, B/T_1, CB_3, $LCB\%L_1$) has showed the best performance across all speeds and scenarios. Moreover, the results for both routes and across the four scenarios showed that profit per deadweight for all alternative hulls regardless market conditions has been improved for low speeds between 10 and 13 knots.

Chapter 6. Multi-objective Optimisation

6.1 Introduction

This chapter focuses on how to improve, simultaneously, the design and the operational profile of the tanker ship case study by balancing the conflicting performance indicators which have been addressed in previous chapters. Within this chapter, a brief explanation of optimisation is introduced covering single and multi-objective optimisation problems in engineering, economy, and other disciplines. Some examples are presented showing the complexity of some optimisation cases in the marine sector and the challenges that naval architects and shipowners face.

An optimisation framework has been developed based on the concept of Pareto optimality to assess decision making and to determine robust designs as well as operational profiles based on results from the hydrodynamic model, environmental impact model, and the economic model. The objective functions that the optimisation model is handling are: hydrodynamic performance (P_D/Dis), environmental impact ($EEDI_A$/$EEDI_{Ref}$), and economic performance (Net Present Value and Profit per tonne.mile). A detailed methodology is presented in Section 6.7, and a flow chart of the optimisation process has been presented in Figure 1.2 showing the main steps.

The outcome from the optimisation model is a set of Pareto optimal solutions. Those solutions are presented graphically to form what is known as Pareto front which determines the design space and the trade-off between the different competing objective functions. Because of the variations in the system parameters which are likely to influence the total performance, it is required not only to allocate the optimum and best designs but also robust designs whose performance is steady and robust.

6.2 Optimisation

Optimisation is defined as the science of selecting the best and most optimum solutions for problems defined mostly with mathematical models. Optimisation techniques involve studying the optimality criteria of a particular defined problem, determining mathematical methods to

search for solutions, computing these methods using experimentation data under trial conditions and of real life problems (Fletcher, 1987).

The applicability of the optimisation techniques is widespread, and it covers problems in engineering, science, economics, math, etc. Those problems might be of a one-objective nature where the goal is to minimise or maximise a single function by varying a set of design variables. However, in the marine field, naval architects deal mostly with problems that are more complex than classical optimisation problems with a single unimodal objective or goal.

Most of the design and operating problems in the marine world involve optimising multiple contradictory objectives and solving conflicting problems. These multi-objective problems face naval architects, shipyards, shipowners and other stalk holders during the lifetime of a ship. Optimising a design based on only one of the performance criteria while overlooking others may produce a design that has unfavourable trends or unacceptable values in other criteria. Therefore, it is essential to balance all features of the design equally or weight them based on the importance of the objective functions and the design aspects.

On the other hand, most of multi-objective functions in engineering designs have more than one single optimum point. Because of the complexity of objective functions and applying several constraints, they feature several local minima (Birk, 2009). Therefore, in order to determine the best of all designs which is defined as (global optimum), changing the design conditions and restarting the optimisation process with different initial designs or applying global optimisation algorithms could increase the chance to find the global optimum design. However, that comes as a price as it is time consuming and the computational cost will be higher (Birk *et al.*, 2004). A short summary explaining the main components and aspects of optimisation methods, and the different available and common mathematical methods in the engineering sector.

6.3 Multi-Objective Optimisation

Multi-objective optimisation is an area of multi criteria decision making where more than one objective function of a design are to be optimised simultaneously. Such multi-objective problems involve trade-offs where a designer or a decision-maker has to diminish or lose one property, quality or quantity of a design, project, product, investment, etc. in return for gains in one or more other aspects. In other words, in a multi-objective problem, there are always

advantages and disadvantages of any change in the factors and parameters that define the system. For instance, in cars manufacturing industry, multi-objective optimisation problems involve maximising performance while minimising fuel consumption and emissions, and maximising comfort and luxury of the car whilst minimising cost.

Engineering design problems have a complex nature as they often consist of a number of conflicting objectives. Therefore, it would be challenging to allocate a single solution or design that simultaneously optimizes all individual objectives. In that case, there might be infinite number of solutions where each of them is addressed as a non-dominated solution or Pareto optimal. Generally speaking, a solution for a multi-objective functions problem is called Pareto optimal if none of the design objective functions can be improved without violating any of the other objectives' values in the light of the selected constraints. Employing different optimisation techniques and solution philosophies might produce a different set of solutions that are acceptable from different point of views and satisfy the different objectives in a different way.

Basically, those conflicting objectives can be dealt with individually. That will result in designs that meet the requirements addressed for one objective function and might not be an optimum design in the light of other objectives. Those designs or solutions are defined as sub-optimal designs that favourite one criteria or more than others. Multi objectives can be arranged in many ways to form one single objective function. Then, an optimisation method is applied in order to find one optimal design. The resulted optimal design depends on how the multiple objectives are combined to form one single objective function. Moreover, that depends on the importance of each individual objective function as weight factors can be addressed to the objective functions to form the formulation of the single objective function (the scalar preference function). Assigning different weight factors values to the objective functions would produce different optimal designs (Andersson, 2001).

In other words and from a practical point of view, the chosen weights represent the priorities of the problem criteria. For a single preferred solution of a multi-objective optimisation problem for applications to one-off products such as building a new ship, the designers are in charge to determine the order of the objectives on the priority scale which could be cost, time, environmental impact, benefit to the society, geographical limitations, regional and international regulations, etc. Those decisions to define the best single possible solution/design

are mainly based on knowledge and experience of the designers and also on the desired preferences of the owners. In practice, when there are several comparable solutions for a problem, it is common to choose the cheapest. However, considering the design and building of a new vessel, it should not only be cheap but have a long life and good performance, safe, profitable, and suitable for the mission. Therefore, it is very crucial for the designers and decision-makers to trade-off characteristics against each other, and to assess which characteristics contribute the most to the overall value and of the design.

The use of multi-objective optimisation methods in engineering has been gaining wide attention for years especially with the rapid growth of computational capabilities. The use of numerical optimisation is the core part of any engineering design process. Numerical optimisation and analytical methods enable users to examine complex relationships between variables, and they provide an efficient tool to improve designs and allocate the optimum solutions.

A multi-objective design problem can be expressed as following by Eq (6.1):

$$min\ f(X) = [f_1(X), f_2(X), \dots, f_k(X)] \tag{6.1}$$

$$s.t.\ X \in S$$

$$X = (x_1, x_2, \dots, x_n)^T$$

Where:

$f_1(X), f_2(X), \dots, f_k(X)$: are the $[k \geq 2]$ objective functions of the optimisation problem that need to be minimised. When an objective function is to be maximised, it is equivalent to minimise its negative.

$(x_1, x_2, \dots, x_n)$: are the n optimisation problem parameters,

$S \in R^n$: is the parameters space or the feasible set.

For a general and simple multi-objective design problem, $f(X)$ is often assumed to be non-linear and multimodal function having several modes or maxima where it is much more difficult to solve than linear functions. The parameters space S might be shaped by linear or non-linear constraints depending on the design problem, and the design parameters might be continuous or discrete variables (Andersson, 2001).

The ideal solution $f^*(X)$ will consist of the individual minima of all objective functions. In this case, the utopian solution will be defined as $f^*(X) = [f_1^*(X), f_2^*(X), \dots, f_k^*(X)]$. In reality, it is rarely feasible to obtain $f^*(X)$ solution that minimises objective functions all together at once.

Since there is no single feasible solution in the parameters space that minimises all objective functions at once, therefore, attention is paid to determine what is called Pareto optimal solutions. In theory, an X^1 solution is said to be a Pareto optimal that dominates another solution X^2 if the following two conditions are true:

$$\begin{aligned} &f_i(X^1) \leq f_i(X^2) \text{ for all indices } i \in \{1, 2, \dots, k\} \text{ and} \\ &f_j(X^1) \leq f_j(X^2) \text{ for at least one index } j \in \{1, 2, \dots, k\}. \end{aligned} \tag{6.2}$$

The set of Pareto optimal solutions form what is often called Pareto front $\mathcal{P}$ as shown in Figure 6.1 for an optimisation problem with two design parameters (x_1, x_2) and two objective functions (f_1, f_2). In this simplified figure, $Y \in R^n$ is the attribute space for all obtainable solutions while ∂Y is the boundary of space Y. Pareto optimal front $\mathcal{P}$ is a subset of ∂Y, and it contains all non-dominated solutions.

The overall objective function $f(X)$ can be formulated in several ways as the objective functions $f_1(X), f_2(X), \dots, f_k(X)$ can be aggregated in any way. In this case, the solutions can be allocated in different points on the Pareto front. However, designers and decision makers can choose their final design or solution at any position along Pareto optimal front depending on the importance of the design objectives and how the overall objective function has been formulated as it will be described later.

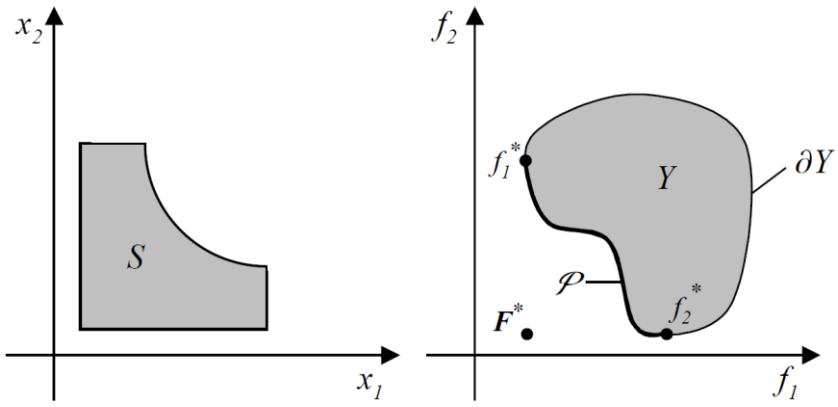

Figure 6.1 Parameters and attribute spaces of the design problem (Andersson, 2000)

6.4 Optimisation Methods

Several optimization algorithms have been introduced in the literature providing a descent direction for optimization process.

Different criteria could be used to categorise the optimisation methods into groups. Andersson (2000) in his paper has carried out a survey of optimisation methods in engineering design. In the survey, the optimisation methods are divided into derivative and non-derivative methods. Since objective functions of engineering design problems contain a mixture of analytical calculations, numerical simulations, sophisticated computational systems, and catalogue selections, then calculating the derivatives of all the objective functions is not an easy straightforward practice. However, the latter group of methods are more applicable for general design problems in the engineering sector and in a boarder set of area. Another advantages of the non-derivative methods are that calculating the optimum does not require any derivatives of the objective function, and they are more likely to allocate a global optima rather than be stuck on local optima (Goldberg and Holland, 1988) On the other hand, the disadvantages of the non-derivative methods include the need to conduct the optimisation process several times with different conditions to find the actual global optima. They require more computational work which makes the process more time consuming and expensive but with the increasing capacities of computational power, such problem can be overcome.

A brief description will be presented for one derivative method which is the Gradient Method, and then some non-derivative methods will be discussed.

6.4.1 Gradient Method

Gradient Method is a simple optimisation method to solve problems of the form $[min\, f(X)]$ where X is the *n*-vector: $X = (x_1, x_2, \dots, x_n)^T \in R^n$. It is known as the steepest descent method, and it is a first-order iterative algorithm that does not require second derivative to search for a local minimum. Two main parameters define this method which are the direction of the search and the step size to move from the current point towards the next one. The idea of this method is based on the observation that a function $f(X)$ decreases faster if the search moves in the neighbourhood of a point in the direction of the negative gradient of $f(X)$ i.e. $(-\nabla f)$.

The method can be described as starting with an arbitrary point $X^{(0)}$, and then for each iteration $j \geq 0$ it moves at direction $\boldsymbol{d^j}$ by step $\boldsymbol{t^j}$ to the next point $X^{(j+1)}$ as in Eq (6.3):

$$X^{(j+1)} = X^{(j)} + t^j \cdot d^j \tag{6.3}$$

Where $d^j = -\nabla f\left(X^{(j)}\right)$.

The gradient of the objective function ∇f at the current point which defines the search directions is given as in Eq (6.4):

$$\nabla f(X) = \begin{bmatrix} \frac{\partial f}{\partial x_1} \\ \frac{\partial f}{\partial x_2} \\ \vdots \\ \vdots \\ \frac{\partial f}{\partial x_n} \end{bmatrix} \tag{6.4}$$

Once the direction of the steepest descent is evaluated in the search process for a stationary point within the constrained space, then choosing the step size $\boldsymbol{t^k}$ for the k^{th} iterative search should be in a manner to reduce the objective function value. The process is repeated again by evaluating the steepest direction at the new point $X^{(j+1)}$ until convergence criterion is achieved or the stopping condition has been reached. It is important to note that the value of the step size t^j is allowed to change at every iteration. Therefore, when the algorithm does not produce well-scaled search direction, then a different strategy should be used to choose/guess a different step size in the search direction within the design space. More details along with examples for using Gradient method are presented and discussed in (Kim, 2009) thesis for the hydrodynamic optimisation of the design of a ship hull form.

6.4.2 Genetic Algorithm

A genetic algorithm is an algorithm that imitates the same mechanisms of natural selection which is the central concept of evolution in the course of generations. Genetic algorithms are widely used in optimisation problems to find the best solutions. Generally speaking, genetic algorithms are a stochastic search technique, and they are a part of the broader class of evolutionary algorithms. These algorithms which are classed as non-gradient methods have

grown in popularity since early 70's after two main researches were published by a German researcher and pioneer in the fields of evolutionary computation and artificial evolution (Rechenberg, 1973) and by an American scientist of electrical engineering and computer science (Holland, 1975).

Genetic algorithms are modelled based on bio-inspired processes such as mutation, crossover, mutation, and selection. In a genetic algorithm, each optimisation parameter is represented by a gene using binary as strings of 0s and 1s or any other encoding. The corresponding genes for all optimisation parameters form an individual candidate solution which has a set of properties that can be mutated and altered. The evolution starts from a population consists of random individuals. Then, within a population of candidate solutions, the fittest are selected to reproduce. A crossover is used to combine genes from different solutions to generate a new offspring which are inserted into the population and the process it repeated again. This iterative process to find a solution follows a number of steps which are run it a loop till the value of the objective function is being solved and the conditions are met. The steps of this evolutionary algorithm can be summarised as following which are presented in many studies such as (Davis, 1991; Holland, 1992; Whitley, 1994; Konak *et al.*, 2006):

1. Initialization: A number of candidate solutions with random values is generated,
2. Evaluation: A fitness function allows to evaluate each candidate. The evaluation tells how good this solution solves the problem,
3. The following steps are run until a stop criterion is met:
    i. Selection: Pick the solutions/individuals for the next iteration
    ii. Recombination: Combine the solutions picked
    iii. Mutation: Randomly change the newly generated solutions
    iv. Evaluation: Apply the fitness function, back to step 2.
    v. If the stop criterion is not met, re-start with the selection step.

6.4.3 Particle Swarm Optimisation (PSO)

Particle Swarm Optimisation is relatively a new and modern method of optimisation that has been widely and successfully applied to many problems in order to search for global optimum solutions. It is another biologically inspired optimisation algorithm by social behaviour of bird flocking or fish schooling, and it was first presented by (Kennedy and Eberhart) in 1995 for simulating social behaviour.

PSO technique shares several similarities with Evolutionary Algorithms EAs such as Genetic Algorithms GAs which are inspired by the theory of evolution by natural selection. Both PSO and GA techniques start with a population of randomly generated solutions, both use fitness values to evaluate the population, and the population is repetitively updated and the search is runs with random techniques. However, PSO technique has no evolution operators as in GA such as crossover and mutation (Clerc, 2006; Gazi and Passino, 2011).

This method might sound complicated but it is really a simple technique built upon the idea of how swarms conform a cooperative way to find food. Each individual member in the swarms keeps changing the search pattern within the search space according to the learning experiences of its own and other members (information sharing mechanism) (Wang *et al.*, 2018). Basically, the PSO algorithm starts with a population of random candidate solutions (particles), and then searches for optima by updating generations. The potential solutions fly through the problem space according to a simple mathematical formula over the particle's current position and velocity. The movements of each individual particle are influenced by its local best-known position (local optimum solution) and also guided towards the best-known positions in the search space. The positons of best solutions are updated while other particles allocate better positions. The process is repeated till a satisfactory solution is discovered even though it is not guaranteed. Different schemes have been introduced to formalise the PSO algorithm and to reposition the particles as well as update the velocity of each particle as in (Lin and Feng, 2007; Kim, 2009; Hernández-Domínguez *et al.*, 2012; Wang *et al.*, 2018).

6.4.4 Simulated Annealing SA

Simulated annealing is an effective method in searching for global optima in the presence of a multiple local optima. It is used to solve unconstrained and bound-constrained problems (Teukolsky *et al.*, 1992). This method is one of the physics inspired algorithms, and it was first developed in the early 80's by Kirkpatrick (Kirkpatrick *et al.*, 1983). The term Annealing refers to the natural analogy phenomena of heating a material or metals and then slowly cooling it down to increase the size of its crystals. That will minimizes the system energy, and thus decrease its defects (Du and Swamy, 2016).

Simulated annealing method uses the objective function of the optimisation problem instead of the energy of a material. Implementation of Simulated annealing algorithm is simple and straightforward. It starts with a random initial design. Then the algorithm picks a random design

in the neighbourhood of the current design. The objective function of the selected design i.e. the new generated design is calculated as well as the change of the objective function value. The change is calculated as a measure of the energy change within the system ΔE.

The algorithm accepts all new points that lower the objective as the aim is to minimise the objective function. Therefore, if the new design improves the objective function i.e. $(\Delta E < 0)$, then it replaces the previous design, and the procedures are repeated. The process is scheduled to systematically decrease the temperature and searching for new solutions which decrease the system energy further. As temperature drops, the algorithm reduces searching range to converge to a minimum. However, if the new design increases the objective value $(\Delta E > 0)$, the SA algorithm still accepts it with a certain probability. By doing so, the algorithm would avoid being trapped in the searching loop for local minima, and thus that increases the chance to explore the design space globally for more possible solutions.

The algorithm generates a random number in the range of (0 to 1), and if it is less than P, then the new design replaces the current one. Within the SA algorithm, T is a control variable in the same units as the problem objective function. As the annealing process runs, the temperature drops according to cooling scheme. The temperature variable allows the algorithm, with some frequency, to accept solutions which are worse than the current solution. This characteristic of simulated annealing helps it to jump out of any local optimums which the process might get stuck in. The simulated annealing begins with high values of the temperature, and at the end of the search, the temperature cools down and hence the probability of accepting worse designs. The search terminates by converging to an optimal solution.

6.4.5 The Complex method

It is an efficient method to find the maximum of a general non-linear function with a set of variables within a constrained space developed first by (Box, 1965), and improved later by (Guin, 1968) to increase the chance of reaching the optimum solution. This method is based on the Simplex method of (Spendley *et al.*, 1962) as Box (1965) modified it so it can recognize constraints. In the Complex technique, the word complex refers to geometric shape made of at least $k \geq n+1$ points where n is the number of the design variables (Swann, 1969). The k points are identified as vertices of the complex, and typically the complex consists the double number of the optimisation variable i.e. $k=2*n$.

To simplify the method, it can be explained using a two-dimensional space (*n=2*) and it is assumed that the complex has four vertices (*k=4*). The starting points are randomly generated without violating the constraints. Each of the *k* points can expressed as an intermediate point allocates anywhere between the upper and lower variable limits (Holland, 1975). The centroid $\bar{x}$ is calculated using Eq (6.5) where x^l and x^h represent the points with minimal and maximal function values.

$$\bar{x} = \frac{1}{n-1}\sum_{i=1}^{n} x^i \quad , \quad x^i \neq x^l \tag{6.5}$$

The objective is to minimize an objective function $f(x)$. The Complex method algorithm replaces the worst point of the design space by a new and better point. The new point x^r is obtained by reflecting the worst point through the centroid $\bar{x}$ of the remaining points in the complex as in Eq (6.6). The reflection coefficient β is assumed to be equal to 1.3 according to Box.

$$x^r = \bar{x} + \beta(\bar{x} - x^l) \tag{6.6}$$

The worst point corresponds to the maximum value of the design function vector. The objective function is evaluated at the new point, and if it is better than the objective function value at the worst point x^l, then the worst point is disregarded. The worst point is replaced by the new point which becomes part of the complex and it moves towards the centroid of the remaining points. This process starts over by reflecting the point that is worst in the new generated complex. This procedure is repeated until the new points stop repeating the worst point. Obtaining the same result after several consecutive attempts indicates that the complex has converged on the centroid (Swann, 1969). Figure 6.2 shows a visualised example of the progress of the Complex method with two dimensions and the optimum is located in the middle.

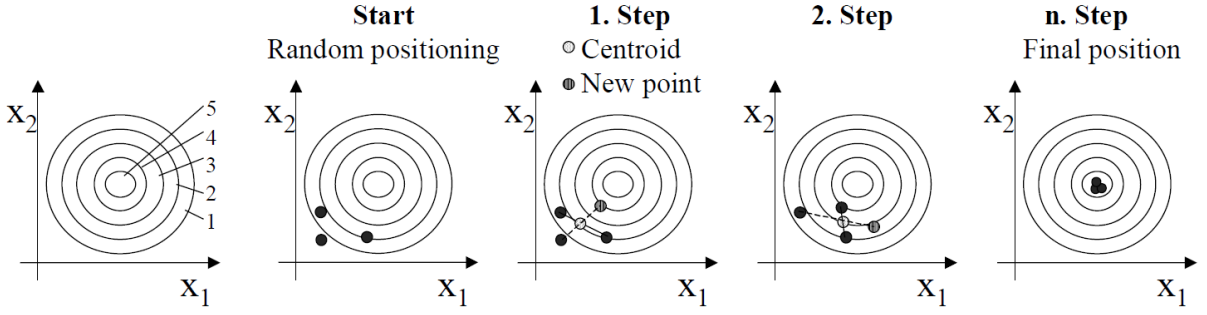

Figure 6.2 The progress of the Complex method,

6.4.6 Tabu Search TS

Tabu Search method was developed by Glover in 1986 and, and it was formalised and presented through a series of papers in the late 80s and early 90s (Glover, 1989; Glover, 1990). The method has proved itself by now to be one of the most successful meta-heuristic to obtain non-dominated solutions. The method guides a local heuristic search to explore the design solution space beyond local optimality. A distinguishing feature of Tabu search is its use of adaptive memory and some associated problem-solving strategies. Flexible memory cycles are used to guide and control the search procedures. The process of TS explores all feasible solutions in the design space by a scheduled sequence of moves as it explores promising areas to hold good solutions while, rapidly, eliminates unpromising areas that are classified as Tabu.

Connor and Tilley (1998) have used this method in developing an efficient algorithm to optimise fluid power circuits. Also, Pacheco and Martí (2006) have used it for an interesting two-objective problem of routing school buses aiming to minimize the number of buses, and minimize the longest time of a journey a student would have. However, generally speaking, the main algorithm steps to carry out Tabu Search can be summarised as following (Glover *et al.*, 1993; Glover and Marti, 2006; Cui *et al.*, 2017):

- Local search procedure
- Neighborhood structure
- Aspiration conditions
- Form of Tabu moves
- Addition of a Tabu move
- Maximum size of Tabu list
- Stopping rule

Tabu Search can be applied to both discrete and continuous solution spaces but there are a few disadvantages such as too many parameters to be determined, the number of iterations could be very large, and global optimum may not be found, depends on parameter settings.

Finally, for any design optimisation problem, different methods are available on the top of the table to be chosen to be used to search for solution(s). More than one optimisation method might be used for complex problems, and they might result in different solutions and that provide more understanding of the problem objective functions. However, that depends on the problem

complexity and on the nature of the objective functions. A wide set of studies and books have provided comprehensive comparison of different types of non-derivative methods such as (Fletcher, 1987; Borup and Parkinson, 1992; Jansson, 1994; Hajela, 1999; Mongeau *et al.*, 2000; Zitzler *et al.*, 2004; Spillers and MacBain, 2009; Deb and Deb, 2014).

In the next section, a light is set on several approaches that are used to formulate single objective function that is needed to solve multi-criteria problems.

6.5 Formulating the Total Objective Function

There are different ways to perform multi-objective optimisation when there are conflicting objectives and goals that a design has to meet especially in the real engineering design problems. A multi-criteria problem that consists of a vector-valued objective function of the form $f(X) = [f_1(X), f_2(X), \dots, f_k(X)]$ to be minimised must be interpreted in an alternative formulation in order to be solved within the equality and/or inequality constraints.

In the literature, different methods are clustered in four different classes depending on the level of intervention from the decision maker in expressing his preferences regarding the problem objectives as well as the stage of addressing the preferences through the optimisation procedures. Reference to multi-criteria optimisation can be found in (Hwang *et al.*, 1980; Osyczka, 1984; Osiadacz, 1989; Arora *et al.*, 1995; Andersson, 2000; Xiujuan and Zhongke, 2004; Deb, 2005; Spillers and MacBain, 2009; Eschenauer *et al.*, 2012; Deb and Deb, 2014)

These four types of methods can be summarised as following:

- No articulation of preference information: No preference information are used in this type of methods. Min-max method is one of the popular approaches in this group.
- Priori aggregation of preference information: In this type of methods, the objective functions are aggregated in one objective function before conducting the optimisation process. The weighted-sum method is an example of this type and it results with one optimal solution.
- Progressive articulation of preference information: The decision maker makes his or her preferences information regarding the multi-criteria optimisation problem after conducting the optimisation problem. That is because of the complexity of the problem where the decision maker does not have enough information.

- Posteriori articulation of preference information: This type of methods provide the decision maker with a set of Pareto optimal solutions, and hence those solutions are independent from the decision maker preferences. Since there will be too many solutions to choose from, screening methods can be applied to cluster optimal solutions.

A considerable number of methods to formulate the objective function of multi-objective optimisation problems can be assigned to these four groups. However, the philosophy behind each method is out of the concern of this study, and can be found in the above reference and more in (Parsons and Scott, 2004). Parsons and Scott (2004) have applied different methods to solve a multi conflicting criteria problem in marine design consists of six parameters, three objective functions and 14-16 constraints. An optimisation model was developed for a family of bulk carries with the aim to minimise light ship weight, minimise transportation cost and maximise annual cargo by changing length, beam, draft, depth, block coefficient and speed.

For a classical multi-objective optimisation problem of the form as in Eq (6.7), the most common methods to formulate a single objective function or in other words to transform the objective function vector into a scalar function can be summarised as following:

$$min\ f(X) = [f_1(X), f_2(X), \dots, f_k(X)] \tag{6.7}$$

$$s.t.\ X \in S$$

$$X = (x_1, x_2, \dots, x_n)^T$$

where $f^*(X) = [f_1^*(X), f_2^*(X), \dots, f_k^*(X)]$ is the ideal and optimum function vector.

6.5.1 The weighted sum optimum

One of the most common-used and earliest approaches to obtain a single solution where the scalar objective function is the weighted sum of the problem individual objectives. The substitute preference function $P[f_k(X)]$ replaces $f(X)$, and it has the form as following:

$$P[f_k(X)] = w_1 \cdot f_1 + \cdots + w_k \cdot f_k \tag{6.8}$$

where $w_1, \dots, w_k$ are non-negative weights and are often normalised to total one. Varying these weights results in obtaining different solutions and all are efficient points. Because the

objectives might have different units and scales, they are often normalised, and then the scalar function $P[f_k(X)]$ has the form:

$$P[f_k(X)] = w_1 \cdot f_1/f_1^* + \cdots + w_k \cdot f_k/f_k^* \tag{6.9}$$

where $f_k^*(X)$ is the k-th optimal function value obtained by individually optimising $f_k(X)$.

6.5.2 The min-max optimum

The min-max formulation is based on transforming the original multi-function problem into a single objective problem of the form as in Eq (6.10). The maximum of absolute distance of objective function values from ideal values f_i^* is minimised to obtain a single solution.

$$P[f_k(X)] = \max_{i=1..k}\{w_i \cdot |f_i - f_i^*|/|f_i^*|\} \tag{6.10}$$

The min-max method can be defined in up to six different ways as been presented by (Schittkowski, 2003).

6.5.3 Global criterion optima

The scalar function that needs to be minimised in the global criterion method is the sum of relative distances of individual objectives $f_i(X)$ from their known optimum values f_i^*. The normalised scalar function to be minimised is given as following:

$$P[f_k(X)] = w_1 \cdot (f_1 - f_1^*)/|f_1^*| + \cdots + w_k \cdot (f_k - f_k^*)/|f_k^*| \tag{6.11}$$

6.5.4 Global criterion optima in the L_2-norm

This method formulates the objective functions in one single scalar function which is the sum of squared distances of individual objectives $f_i(X)$ from their known optimum values f_i^*which are obtained by minimising $f_i(X)$ individually. The scalar function to be minimised is given as in Eq (6.12):

$$P[f_k(X)] = w_1 \cdot ((f_1 - f_1^*)/f_1^*)^2 + \cdots + w_k \cdot ((f_k - f_k^*)/f_k^*)^2 \tag{6.12}$$

6.5.5 The nearest to the utopian optimum

This method formulates a multi-criteria optimisation problem into the minimisation of the distance from the utopian solution to the Pareto set. The distance is given as in the following formula:

$$P[f_k(X)] = [w_1 \cdot ((f_1 - f_1^*)/f_1^*)^2 + \cdots + w_k \cdot ((f_k - f_k^*)/f_k^*)^2]^{1/2} \qquad (6.13)$$

6.5.6 Trade-off method

In this method, the user selects one objective to be minimised while other objectives are considered as constraints with respect to individual minima. The choice of the objective function depends on its importance in the overall design problem.

6.5.7 Method of distance functions

The scalar function to be minimised in this method is the sum of absolute values of the difference of objective functions from goals predetermined by the user as in Eq (6.14). Determining the goals $[y_1, \ldots, y_k]$ are based on previous knowledge about the optimum solutions.

$$P[f_k(X)] = w_1 \cdot |f_1 - y_1| + \cdots + w_k \cdot |f_k - y_k| \qquad (6.14)$$

6.6 Plotting the entire Pareto front

When dealing with multi-objective optimisation problems, generating and demonstrating the entire Pareto front is one of the desirable techniques that helps the design team to analyse the entire Pareto front before determining the most preferred point i.e design solution.

In most of the optimisation problems especially in the engineering sector, it is impossible to obtain all potential Pareto optima points as there is an infinite number of points that satisfy the problem criteria and constraints. Even if it is theoretically possible to determine all efficient solutions, there are some challenges in achieving that. The computational time and cost, and numerical complexity are the main challenges in obtaining the complete set of optimal solutions. However, presenting a complete or partial set of Pareto optimal points can be prepared graphically, analytically as a formula, numerically as a set of points, or even in a mixed form consists of a parametrized set of points (Ruzika and Wiecek, 2005).

An efficient way to present Pareto optima points to the decision makers is by generating what is called the trade-off curve in the objectives space. In the case of bi-objective optimisation problems, this way of mapping Pareto front is practical as it provides full information on both objective values. Also, it gives the decision maker the ability to observe how improving one objective comes at the cost of weakening the second objective when moving along the trade-offs curve. However, when the number of objectives increases beyond two, it becomes impractical to represent the solution space for visualisation reasons (Parsons and Scott, 2004).

When the number of objectives is relatively small, it is common to map the Pareto front in a series of bi-objective slices of the entire Pareto front. The method of displaying was introduced by (Zeleny and Cochrane, 1973) to map a three-criteria problem. Figure 6.3 shows an example of a Pareto surface for a three-criteria problem presented in (Parsons and Scott, 2004) study. All the obtained solutions fall on this three-dimensional surface which is bounded by the three optimum solutions $f_1^0, f_2^0,$ and f_3^0 which are determined by solving the three objective functions individually taking into account the problem's constraints. This surface is not easy to fully understand and to be used to gain all the required information to be provided to the decision maker. Therefore, three bi-objective projections of the surface are used to demonstrate the solutions space. Figure 6.4 shows a two-dimensional projection of Pareto surface for both transportation cost and light ship where the locations of $f_1^0, f_2^0,$ and f_3^0 can be seen and identified as well as the locations of the min-max and the nearest to utopian points.

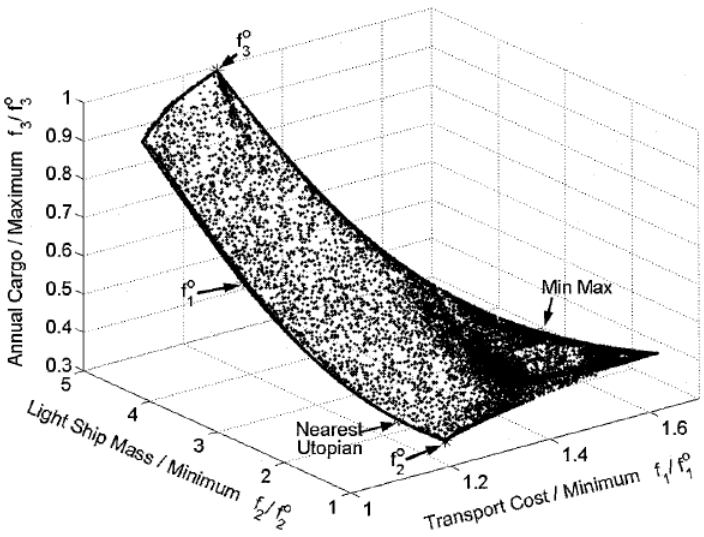

Figure 6.3 The Pareto surface in 3D space

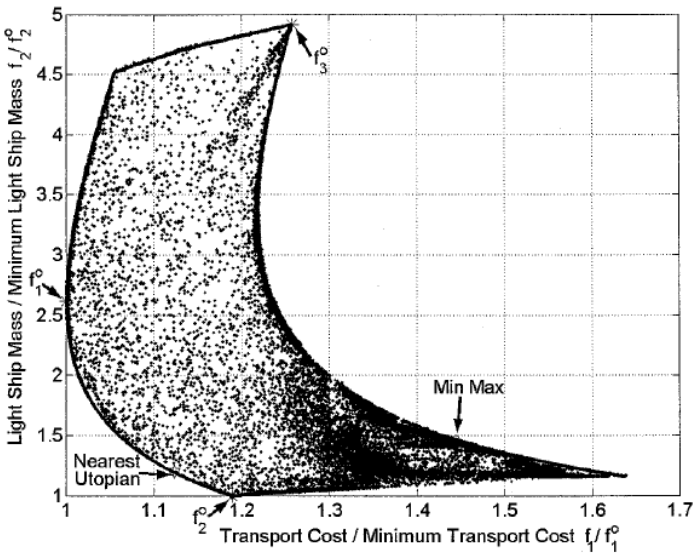

Figure 6.4 Two-dimensional projection of Pareto surface

A number of methods are available to generate and map Pareto front. That includes:

- Exhaustive search of the parameter space: several sets of the independent variables of the problem are selected randomly while retaining all sets which satisfy the inequality and equality constraints. Then the objective functions are solved for these feasible variable sets individually. The solutions define the boundary and the corresponding region of the feasible optimal solutions space as in Figure 6.5 for a simple example of an optimisation problem with two objective functions. In the case of complex problems with many objective functions, this approach can be time consuming.

- Repeated weighted-sum solutions: the user can systematically generate varied sets of weights for which weight sum solutions can be obtained as illustrated in Figure 6.6. This approach is applicable if the feasible object function space has a convex shape. The weights for a normed scalar function can be obtained using the Analytical Hierarchy Process AHP. APH is a structured technique that is used to assist decision makers in organising and analysing complex problems depending on the importance of the criteria. A preference rating scheme is used among the criteria using pairwise comparisons. There is a wide range of software programs utilising the AHP method but the majority of them are commercial and expensive. However, Microsoft Excel has an add-in tool called DAME (Decision Analysis Module for Excel). It can be used for all types of

evaluations and comparisons of designs, strategies, products, etc. (Perzina and Ramík, 2014).

- Repeated weighted min-max solutions: as in the previous approach, weighted min-max solutions can be obtained for several systematically varied weights. This approach can be applied if the feasible object function space, as in Figure 6.7, does not have a slope that exceeds w_1/w_2.

- GA applications: in the recent years many applications have been developed based on utilising genetic algorithms GAs to perform the scalar preference function of multi-object optimisation problems and to map the Pareto front (Parsons and Scott, 2004). In this way, no weights are needed to pre-determine the relative importance of the problem objectives. Mainly this type of methods generates and operates in a pool of candidate solutions. The initial population is generated in a random manner, and then a specific ranking scheme is applied to determine the rank of the candidate solutions individually. The initial population is evolved based on the rank to produce more generations until a pre-specified termination criterion or criteria are satisfied. The final population of solutions corresponds to the Pareto front, and any of these solutions can be selected and implemented depending on the decision maker's preference (Hu *et al.*, 2013).

An efficient approach has been developed by (Hu *et al.*, 2013) aiming to produce a complete exact Pareto front as the previous approaches do not guarantee a complete Pareto front neither an accurate one but only approximations of the real Pareto front. In Hu *et al.* (2013) study, the new deterministic approach to solve discrete problems is capable of computing the *k* best solutions to each of the given objectives. This approach consists of a deterministic search technique and a ripple-spreading algorithm that is designed to calculate the full exact Pareto front for multi-objective route optimization.

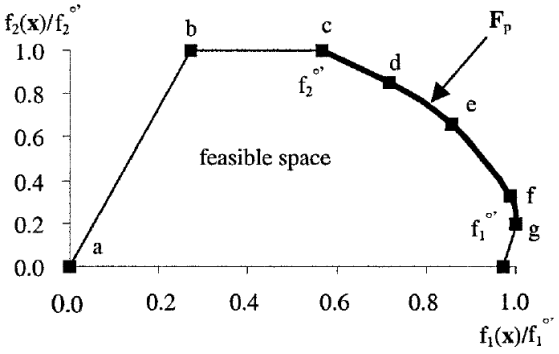

Figure 6.5 Feasible function space

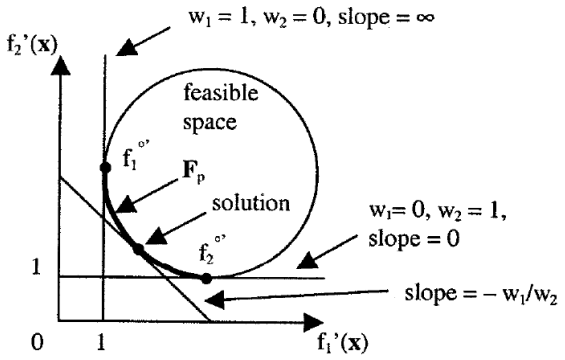

Figure 6.6 Solutions using weighted-sum optimum

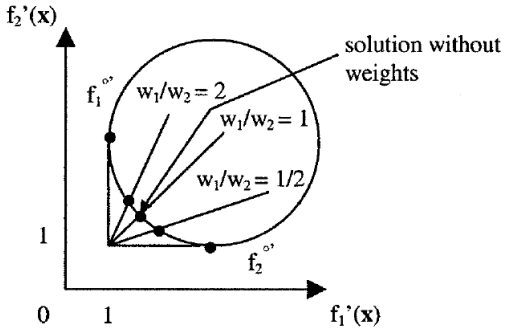

Figure 6.7 Solutions using weighted-minmax optimum

6.7 Optimisation Methodology for the case study

An optimisation framework has been developed based on the concept of Pareto optimality to assess decision making and to determine robust designs as well as operational profiles based on results from the three models. The framework includes a macro model that is developed to carry out the optimisation process, and it is written in Visual Basic for Applications (VBA) in Microsoft Excel which is a subset of the powerful Visual Basic programming language. A five-parameter, four-criteria, eight-scenario, 14- to 17-constraint optimisation case study will be presented and discussed in the following sections showing the trade space between improving the energy efficiency of ships and maximising the economic performance.

In a problem like what the thesis is covering where there are more than one objective function to be minimised, it is impossible to locate a single global solution in the design space. Instead, a set of design solutions can be found as none of these solutions can be improved for one objective without degrading another. Those design points define what is called Pareto front which represent a trade space between the conflicting objects.

First of all, the independent design variables and the associated lower and upper limits that shape the design space and form the constraints set are shown in Table 6.1. In addition, to take

into account EEDI future phases, the required reduction in the EEDI value is considered in the model as an additional constraints.

Table 6.1 Design variables and constraints

Variable		Upper Limit	Lower Limit
Length L_{BP}	x_1	222.75	182.25
Breadth to Draught Ratio B/T	x_2	2.913	2.383
Block Coefficient C_B	x_3	0.8749	0.7759
Longitudinal Center of Buoyancy $LCB\%L$	x_4	0.01	-0.01
Speed V	x_5	17	5
Breadth B		33.824	30.595
Draught T		12.839	11.913
$EEDI_A/EEDI_{Ref}$: Phase 0		≤ 1.0	
$EEDI_A/EEDI_{Ref}$: Phase 1		≤ 0.9	
$EEDI_A/EEDI_{Ref}$: Phase 2		≤ 0.8	
$EEDI_A/EEDI_{Ref}$: Phase 3		≤ 0.7	

The input data that defines the market conditions and the trip characteristics are the route distance between the charging and discharging ports, freight rates, fuel prices for bunker fuel and MDO. Eight different scenarios will be covered in the optimisation model, and they are shown in Table 6.2:

Table 6.2 Market scenarios

		Freight Rate ($/ton cargo)	380 CST ($/ton fuel)	MDO ($/ton fuel)
Rout One 2000 n.mile	Scenario 1	9.0	500	700
	Scenario 2	15.0	500	700
	Scenario 3	9.0	800	1000
	Scenario 4	15.0	800	1000
Rout Two 7000 n.mile	Scenario 1	26.0	500	700
	Scenario 2	40.0	500	700
	Scenario 3	26.0	800	1000
	Scenario 4	40.0	800	1000

The objective functions that the optimisation model is handling are:

- Minimise the delivered power to displacement ratio $f_1 = P_D/Dis$,
- Minimise the attained EEDI to EEDI reference ratio $f_2 = EEDI_A/EEDI_{Ref}$,
- Maximise the annual profit per tonne.mile $f_3 = Profit/tonne.mile$ as an alternative of the annual profit per tonne which was used in the economic model. That is mainly to demonstrate the options this study offers,
- Maximise the Net Present Value $f_4 = \text{NPV}$.

The values of the objective functions are calculated using the regression formulas found and used in the previous chapters as well as other submodels' equations to estimate all the performance parameters. Mainly, that includes:

- regression equations (3.11) to estimate P_D/Dis,
- regression equations (4.18) to estimate $EEDI_A/EEDI_{Ref}$,
- the cost and revenue equations in addition to the assumptions in Chapter 5 to estimate the profit per deadweight and the net present value.

As discussed before, there are several approaches and theories to solve multi-criteria optimisation problems, and hence to develop Pareto-optimal front. For the purpose of this study, a multi-objective evolutionary method and Generalized Reduced Gradient GRG method are examined before adopting an appropriate method to solve this particular multi-objective optimisation problem of a tanker ship. These two optimisation algorithms and the Simplex LP method for linear functions are available for use in the Solver tool in Microsoft Excel (2013) and the previous editions.

In reality, these algorithms have both strengths and weaknesses compared to classical optimization methods. The GRG method assumes that the objective function and the problem constraints are smooth nonlinear functions of the decision variables with no sharp corners or breaks. The Evolutionary algorithm is suitable to solve nonlinear and non-smooth problems. It is more suitable to solve problems with functions such as IF, CHOOSE, and LOOKUP where graphs might contain breaks and functions that has sharp corners such as ABS.

The GRG method is quiet accurate, and it yields local optimum solutions with a high probability to find global solutions. The Evolutionary algorithms can often find better solutions than the

GRG algorithms and even global optimum solutions. The GRG method is 10 to 20 times faster than an evolutionary algorithm.

Both algorithms have been tested to solve a few optimisation cases regarding the tanker ship case study. For this particular case study, it was found that the solutions found by both methods generate similar Pareto front. However, the computational time for GRG method was relatively less than when using the Evolutionary method. Therefore, the design solutions will be obtained using the Generalized Reduced Gradient GRG method in the Solver tool. The complete VBA code for both algorithms is presented in the Appendix section Appendix I).

The Solver tool in Microsoft Excel gives the ability to choose the optimisation engine as in Figure 6.8 in addition to advanced options for the Solver model as in Figure 6.9. That mainly includes determining:

- the maximum time Solver will spend solving the problem,
- the maximum number of iterations Solver will use in solving the problem. The default option is Zero which means no limit is set,
- the precision with which the constraints must be satisfied,
- the convergence tolerance when searching for the optimum solutions to tell the Solver to stop,
- the population size of candidate solutions that Solver selects randomly when searching for the best solutions,
- the mutation-rate that specifies the rate at which the Evolutionary Solving method will make mutations to existing population members, and it has the value between zero and one.

The GRG and the Evolutionary algorithms in the Macro Codes are used with the options as following:

```
SolverOptions MaxTime:=0, Iterations:=0, Precision:=0.000001, Convergence:= _
    0.0000001, StepThru:=False, Scaling:=True, AssumeNonNeg:=True, Derivatives:=1
SolverOptions PopulationSize:=50, RandomSeed:=0, MutationRate:=0.075, Multistart _
    :=False, RequireBounds:=True, MaxSubproblems:=0, MaxIntegerSols:=0, _
    IntTolerance:=1, SolveWithout:=False, MaxTimeNoImp:=30
```

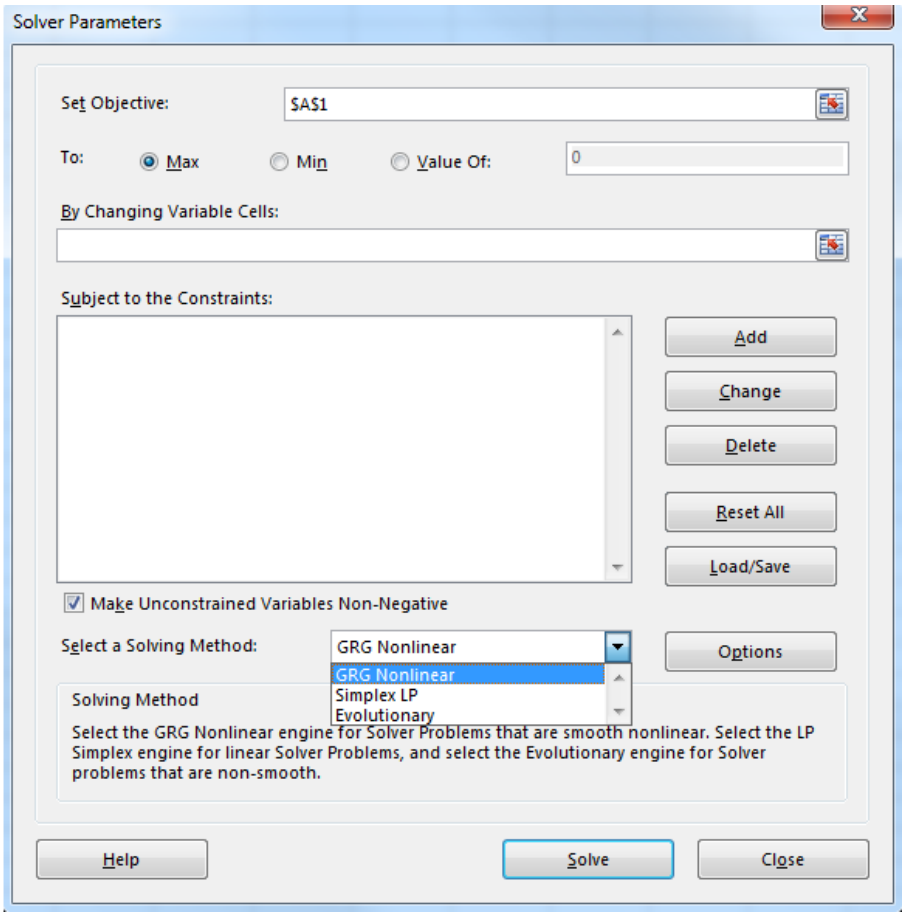

Figure 6.8 Solver interface

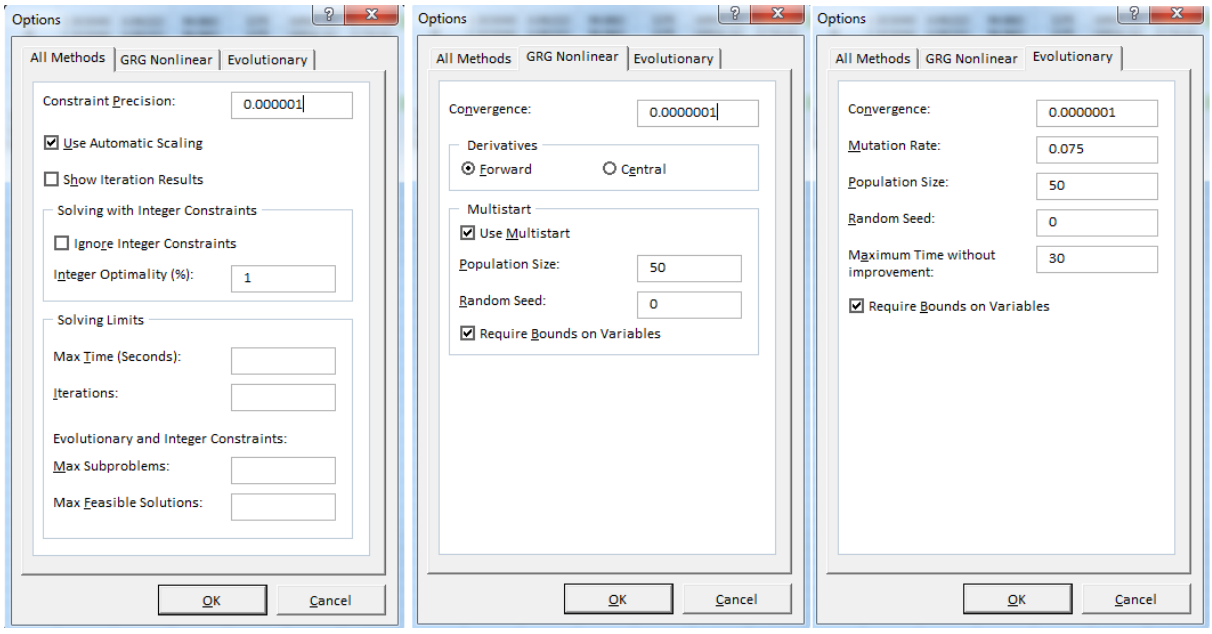

Figure 6.9 Solver engines options

Five different approaches have been selected to formulate the single scalar function to perform the multi-objective optimisation. Basically, this single function aggregate the four objective functions that are of concern covered in this study. These five approaches that used in this study to transform the objective function vector are:

- The weighted sum optimum
- The min-max optimum
- Global criterion optima
- Global criterion optima in the L_2-norm
- The nearest to the utopian optimum

The Optimisation code gives the ability to optimise any problem for individual objective function or solve multi-objectives problems using one or more of these five different formulation methods. It should be noted that these formulation methods might give different solutions, and hence, form a relatively different Pareto front. Therefore, several optimisation studies apply more than one methods aiming to obtain a better Pareto optima where solutions are scattered along Pareto front because it might happen that the solutions are not scattered evenly.

Finally, the set of Pareto efficient allocations that form The Pareto frontier are obtained for any formulation approach by randomly altering the weights for the four objective functions in the weighted scalar function for any of the five selected multi-criteria formulation methods.

The optimisation model runs for two different cases which are: firstly searching for the optimum hull parameters at the design speed, and secondly over the speed range. The results are obtained for the same scenarios of routes and market conditions as been seen in Table 6.2.

6.8 Results for the Multi-objective Design Optimisation Case Study

6.8.1 Optimisation Solutions at the Design Speed

The first set of solutions are obtained by running the VBA code at a constant speed (15 knots) while varying the hull parameters, and for the four different market conditions (fuel price and freight rates) in the case of short-distance route as well as the long-distance route.

Initially, the results for the four criteria considered one at a time f_k^* are obtained by running the VBA code while assigning a weight factor of 1 to the particular objective function that is of interest, and a weight factor of 0 to the remaining objective functions.

The results for the low fuel price and low fright rates scenario (Scenario One) will be discussed in detail to highlight the main findings from the optimisation model and the possible explanations of the diverse solutions along Pareto front. However, the remaining results and Pareto fronts figures are presented in the Appendices section.

Results for the single objective functions solutions at the design speed are shown in **bold** in Table 6.3 for Route One - Scenario One. They are: $f_1^* = 0.10969\, kW/ton,\ f_2^* = 0.81358$, $f_3^* = 0.45084\ \$/tonn.mile$, $f_4^* = \$ - 23.2554\, m.$

Solving the optimisation problem to minimise the power to displacement ratio and to minimise the attained EEDI to the reference EEDI ratio prompts the same hull design. It is a design with the longest hull within the dimensions' boundaries, the lowest breadth to draught ratio, the lowest block coefficient value, and the furthest backward position for LCB. These results validate what has been found earlier in both the hydrodynamic and the environmental impact models that long hulls with fine bodies are the most efficient designs and they show the greatest performance in terms of energy efficiency.

When maximising the profit per tonne of transported goods per mile and maximising the net present value of the whole investment individually, that leads to the same alternative design. This vessel has the biggest hull and the highest carrying capacity because the length, breadth, draught, and block coefficient values are the maximum in the design space. That is a kind of advantages of economies of scale which give rise to lower per-unit costs.

Both design solutions have an $EEDI_A/EEDI_{ref}$ ratio less than one which means both vessels comply with the International Maritime Organisation IMO regulations and meet the reference level for Phase 0 which was applicable between January 2013 and December 2014. However, taking into account the introduction of further CO_2 emissions reduction targets of 10%, 20%, and 30% between 2015 and 2025, then only the first vessel obtained by minimising the consumed energy will be able to comply with IMO requirements for Phase 1 (1st Jan 2015 – 31st Dec 2019). None of these two optimum designs would pass the IMO requirements for Phase 2 and 3 as the attained EEDI values are higher than the reference EEDI unless some technical

and operational measures are taken such as fitting some energy saving devices which implies extra cost. Another efficient measure can be adopting slow steaming whose implications will be discussed later.

The conflict among the hydrodynamic and economic criteria is clearly noticeable by comparing the solutions. For example, the capital cost for the second vessel obtained by running the optimisation code considering the economic objective functions alone is estimated around ($40.8 million) which is ($2.34 million) more than the capital cost to acquire the first vessel which has a better hydrodynamic performance. However, this additional cost comes with benefits in the long term as the net present value NPV of the whole business and investment is higher by over ($9.0 million). That is resulted mainly because of the lower annual cost per one tonne of oil carried onboard associated with carrying more products per trip. The cost and profit per dwt for both designs are (181.9 $/dwt, 7.67 $/dwt) and (170.1 $/dwt, 19.5 $/dwt), respectively.

Table 6.3 Single Criterion results for Route One, Scenario One at the design speed

	Minimum P_D/Dis	Minimum $EEDI_A/EEDI_{Ref}$	Maximum *Profit/tonne.mile*	Maximum *NPV*
Criteria				
P_D/Dis	**0.11**	0.11	0.13	0.13
$EEDI_A/EEDI_{Ref}$	0.81	**0.81**	0.99	0.99
$Profit/tonne.mile \times 10^{-3}$	0.18	0.18	**0.45**	0.45
NPV	-32.34	-32.34	-23.26	**-23.26**
Independent Variables				
Length	222.75	222.75	222.75	222.75
Breadth	30.60	30.60	33.82	33.82
Draught	12.84	12.84	12.84	12.84
Breadth/Draught	2.38	2.38	2.63	2.63
Block Coefficient	0.78	0.78	0.87	0.87
Long Centre of Buoyancy %L	-0.01	-0.01	-0.01	-0.01
Speed	15.00	15.00	15.00	15.00
Other Characteristics				
Deadweight [ton]	54900.31	54900.31	70472.14	70472.14
Lightweight [ton]	14683.93	14683.93	16276.77	16276.77
Capital Cost [$ m]	38.47	38.47	40.81	40.81

Annual Fuel Cost [$]	3602444.55	3602444.55	4866796.12	4866796.12
Annual Operating cost [$]	2963476.16	2963476.16	3014061.24	3014061.24
Total annual cost [$]	9984856.44	9984856.44	11984768.40	11984768.40
Profit per DWT [$/dwt]	7.67	7.67	19.48	19.48
Annual Bunker Cons [ton]	5754.97	5754.97	7918.57	7918.57
Annual MDO Cons [ton]	1035.66	1035.66	1296.45	1296.45

The entire Pareto front for the case study problem at the design speed is shown in Figure 6.10 for the short route and scenario one (low fuel cost price and low freight rate). It is obtained using the VBA code to solve the optimisation problem for each individual set of the weight factors for the different formulation approaches. Those curves consist of thousands of solutions, and they represent the trade-offs between the conflicting objective functions. Those solutions are constrained in speed as the optimisation problem is solved with constant speed (15 knots).

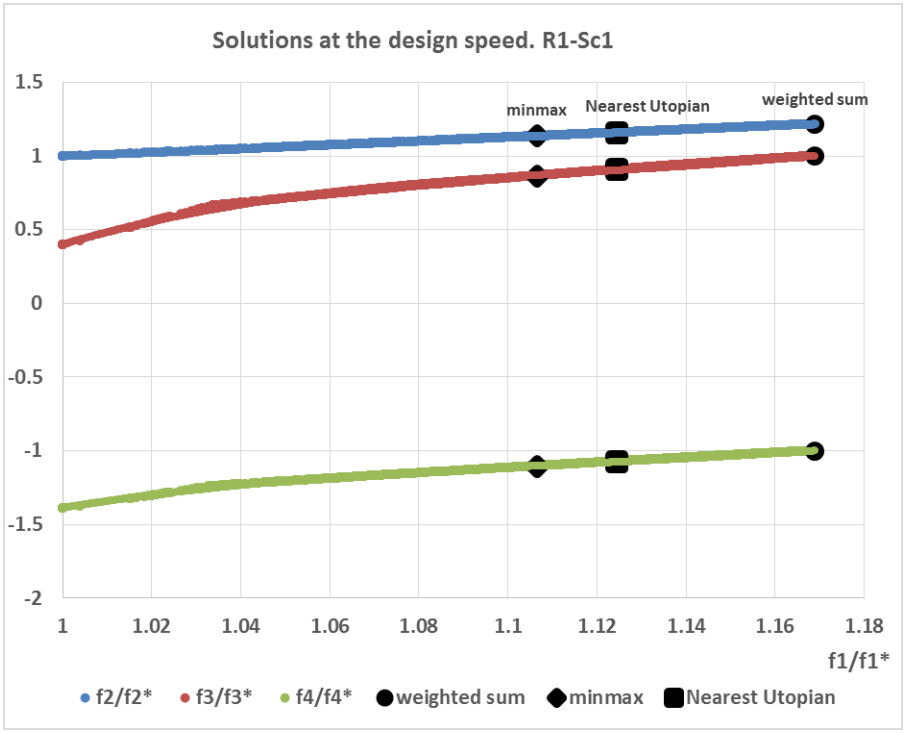

Figure 6.10 Pareto front at the design speed. Route One, Scenario One

Since the four criteria have vastly different units and scales, it is necessary to normalise them in a way that makes it easier to visualise Pareto front. They are normalised by a reference value which is the optimum solution obtained considering the objective functions at once f_k^*. The primary horizontal axis is chosen to be f_1/f_1^* while the values for the other three criteria (f_2/f_2^*, f_3/f_3^*, f_4/f_4^*) are presented on the vertical axis.

Moreover, the solutions obtained for equal weights using the sum-weighted, minmax, and the nearest to utopian methods are shown in Figure 6.10. It is clear that those solutions yield different designs because the formulation approaches address different preference levels to the different conflicting criteria. However, in this specific case study, the three methods tend to favour big and full hulls with higher carrying capacity. In this case, the three solutions lead to the maximum length, breadth and draught. The three optimum solutions' details are shown in Table 6.4:

Table 6.4 Multicriterion results for Route One, Scenario One at the design speed

	Weighted Sum Design	*Minmax Design*	*The Nearest to Utopian Design*
Criteria			
P_D/Dis	0.13	0.12	0.12
$EEDI_A/EEDI_{Ref}$	0.99	0.92	0.94
$Profit/tonne.mile \times 10^{-3}$	0.45	0.39	0.41
NPV	-23.26	-25.67	-24.95
Independent Variables			
Length	222.75	222.75	222.75
Breadth	33.82	33.82	33.82
Draught	12.84	12.84	12.84
Breadth/Draught	2.63	2.63	2.63
Block Coefficient	0.87	0.83	0.84
Long Centre of Buoyancy %L	-0.01	-0.01	-0.01
Speed	15.00	15.00	15.00
Other Characteristics			
Deadweight [ton]	70472.14	65993.45	67281.45
Lightweight [ton]	16276.77	16206.82	16226.84
Capital Cost [$ m]	40.81	40.13	40.33
Annual Fuel Cost [$]	4866796.12	4456889.07	4572479.32
Annual Operating cost [$]	3014061.24	2999512.23	3003696.29
Total annual cost [$]	11984768.40	11395669.26	11562792.25
Profit per DWT [$/dwt]	19.48	16.86	17.68
Annual Bunker Cons [ton]	7918.57	7207.69	7408.15
Annual MDO Cons [ton]	1296.45	1218.64	1240.58

Applying the EEDI reduction factors, and setting the new EEDI targets as constraints in the optimisation code will produce different solutions. The optimisation process is carried out for the four reduction factors: [0%, 10%, 20%, and 30%].

Since all the solutions obtained for the unconstrained case have an $EEDI_A/EEDI_{ref}$ ratio less than one, then for the 0% reduction factor case, the optimisation algorithm will lead to the same solutions that have been obtained before and shown in Figure 6.10.

Pareto front for Phase One (10% reduction factor) is presented in Figure 6.11. It can be seen that the efficient solutions that form Pareto fronts have lower values for the first two normalised objective functions (f_1/f_1^* and f_2/f_2^*) as a result of the need to lower the energy consumption to reduce CO_2 emissions to meet the EEDI requirements. All the individual designs operating at the design speed (15 knots) have an attained EEDI value that meet the EEDI requirements for Phase One (1st January 2015- 31st December 2019).

On the other hand, Pareto efficient solutions have worse economic performance as they prioritise f_1 and f_2 because of the EEDI reduction factor constraint. The designs in this case have hulls with lower block coefficient values and narrower hulls. That leads, as already mentioned, to reduce the annual profit and the net present value. The most optimum design that still meets the EEDI requirements for Phase One and has the best economic performance is the one that is found by the weighted sum, mimmax, and the nearest to the utopian methods for equal weights as shown in Figure 6.11. The parameters and results from the optimisation model for this solution are shown in Table 6.5.

Running the optimisation model in the case of adding the EEDI reduction factors (20% and 30%) as constraints for Phase Two and Phase Three respectively yields one single solution in both cases. This solution is the most optimum design to satisfy the reduction factor constraint and as it has the most efficient hull when operating at the design speed. However, it is worth mentioning that neither Phase Two requirements nor Phase Three requirements regarding EEDI value are met as the attained EEDI value for this design is greater than the EEDI values for future phases by 1.7% and 16% for Phase two and Three, respectively. The parameters and results from the optimisation model for this solution are shown in Table 6.5.

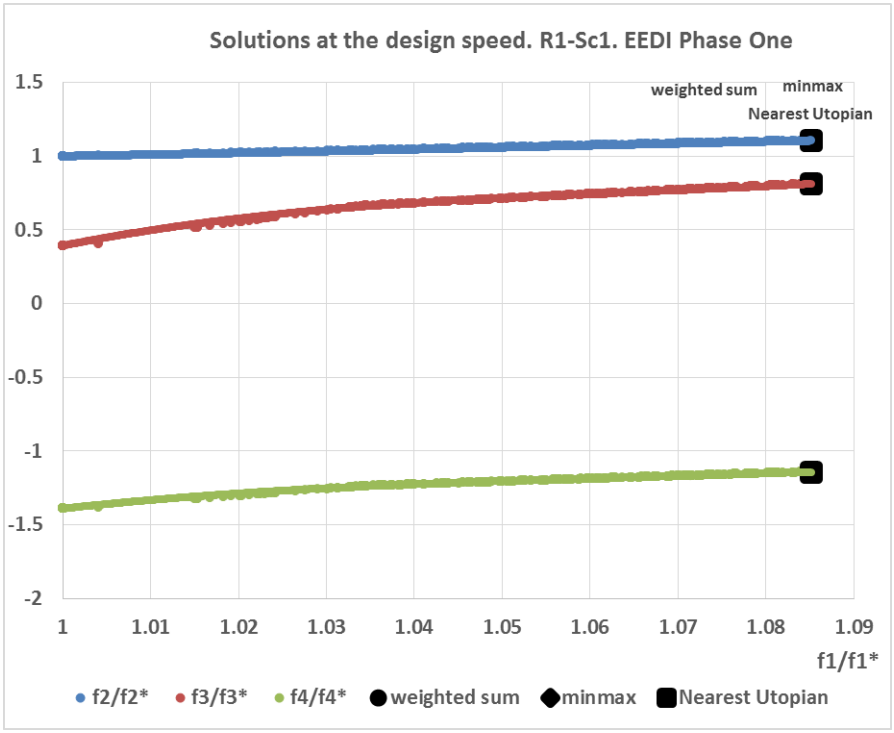

Figure 6.11 Pareto front at the design speed. Route One, Scenario One. EEDI Phase One

Table 6.5 Optimum solutions with the added EEDI reduction factor constraint. Route One, Scenario One

	Phase One reduction factor constraint	*Phase Two and Three reduction factors constraint*
Criteria		
P_D/Dis	0.12	0.11
$EEDI_A/EEDI_{Ref}$	0.90	0.81
$Profit/tonne.mile \times 10^{-3}$	0.37	0.18
NPV	-26.56	-32.34
Independent Variables		
Length	222.75	222.75
Breadth	33.82	30.60
Draught	12.84	12.84
Breadth/Draught	2.63	2.38
Block Coefficient	0.81	0.78
Long Centre of Buoyancy %L	-0.01	-0.01
Speed	15.00	15.00
Other Characteristics		
Deadweight [ton]	64467.35	54900.31

Lightweight [ton]	16183.20	14683.93
Capital Cost [$ m]	39.91	38.47
Annual Fuel Cost [$]	4322326.00	3602445.00
Annual Operating cost [$]	2994555.00	2963476.00
Total annual cost [$]	11200047.00	9984856.00
Profit per DWT [$/dwt]	15.81	7.67
Annual Bunker Cons [ton]	6974.32	5754.97
Annual MDO Cons [ton]	1193.10	1035.66
$EEDI_A/EEDI_{Ref\text{-}Phase\ One}$	1.00 (satisfied)	0.91
$EEDI_A/EEDI_{Ref\text{-}Phase\ Two}$	1.13	1.02 (not satisfied)
$EEDI_A/EEDI_{Ref\text{-}PhaseThree}$	1.29	1.16 (not satisfied)

A summary of the optimisation model results for the oil tanker case study obtained by running the VBA code for the different scenarios in the case of the short and long routes is presented in Appendix J.

6.8.2 Optimisation Solutions over Speed Range

Similarly, as presented in the previous section, the results for the low fuel price and low fright rates scenario (Scenario One) will be discussed in detail to highlight the main findings from the optimisation model and the possible explanations of the diverse solutions along Pareto front. The optimisation model in this case is extended to include speed as an independent variable and it varies between 5 and 17 knots. The results and Pareto front figures for the remaining scenarios are presented in the Appendices section.

Initially, the optimum values' results for the four criteria considered one at a time f_k^* are obtained yet again after the speed variable is added. The VBA code is run while assigning a weight factor of 1 to the particular objective function that is of interest, and a weight factor of 0 to the remaining objective functions.

These solutions for the single objective functions in a five-parameter design space (L, B/T, CB, LCB%L, V) are shown in **bold** in Table 6.6 for Route One -Scenario One case. They are:

$f_1^* = 0.00325\ kW/ton$ at speed 5 knots,

$f_2^* = 0.27434$ at speed 5.55 knots,

$f_3^* = 0.73899\ \$/tonn.mile$ at speed 12.05 knots,

$f_4^* = \$ - 15.91411\ m$ at speed 13.0 knots.

As it was anticipated, all the energy efficiency and economic performance indicators have improved when considering the speed as a variable in the optimisation problem. Based on the results, the hull designs obtained from solving the optimisation problem have a satisfied low attained EEDI values that meet the current IMO requirements and the future targets for the three phases including Phase Three (1st January 2015 and onwards).

It is interesting to note that even the fuel consumption and hence the fuel bill are very low in the first two solutions sailing at super slow speeds (columns two and three in Table 6.6) obtained considering the power to displacement ration and the EEDI ratio objective functions one at a time, the annual profit margins turn negative as the costs exceed the total annual revenue. The low generated revenue is a result of the low number of trips made per year because of the super slow operating speed at the laden and ballast legs. The negative net present values ($ -50.37 m and -$51.12 m) indicate the enormous financial loss comparing with the situation when sailing at the design speed as seen in Table 6.3 where NPV values are higher by around ($18.0 m).

The other two solutions (columns four and five in Table 6.6) give the priority to the economic performance while still meeting the IMO regulations regarding greenhouse gas emissions ($EEDI_A < EEDI_{Ref}$). However, even though these two designs comply with IMO regulations but the fuel consumption is relatively greater than the first two solutions that priories the energy efficiency performance. That can be seen in the last two rows in Table 6.6, and estimating CO_2 emissions show a hefty increase when sailing at higher speeds. For instance, CO_2 emissions per tonne.mile when sailing at 12 knots is 3.56 g/tonne.mile while it is 1.56 g/tonne.mile when sailing at 5 knots. That yields to around 3262 tonnes of CO_2 emissions per year comparing with 497 tonnes of CO_2 for the third hull and first hull, respectively.

As previously discussed, bigger ships with longer and fuller hulls show a better performance because of the higher carrying capacity where the additional revenue would compensate the extra capital and fuel costs over long terms. It is found that sailing at a speed around 12-13

knots would benefit the ship owner and charterer. Operating at a speed lower by around 3 knots from the design speed would increase the profit per deadweight by around $8 which, in the case of low freight rates condition, would yield in a considerable increase of around ($ 8.3 million) in the net present value of the investment over 25 years. These long-term benefits come at no additional capital cost but as a result of adopting slow steaming.

Table 6.6 Single Criterion results for Route One, Scenario One over the speeds range

	Minimum P_D/Dis	Minimum $EEDI_A/EEDI_{Ref}$	Maximum *Profit/tonne.mile*	Maximum *NPV*
Criteria				
P_D/Dis	**0.00325**	0.00528	0.05378	0.06830
$EEDI_A/EEDI_{Ref}$	0.30	**0.27**	0.57	0.65
Profit/tonne.mile $\times 10^{-3}$	-0.89	-1.10	**0.74**	0.73
NPV	-50.37	-51.12	-16.91	**-15.91**
Independent Variables				
Length	222.75	222.75	222.75	222.75
Breadth	30.60	30.60	33.82	33.82
Draught	12.84	12.84	12.84	12.84
Breadth/Draught	2.38	2.38	2.63	2.63
Block Coefficient	0.87	0.78	0.87	0.87
Long Centre of Buoyancy %L	-0.01	-0.01	-0.01	-0.01
Speed	5.00	5.55	12.05	13.00
Other Characteristics				
Deadweight [ton]	63643.08	54900.31	70472.14	70472.14
Lightweight [ton]	14824.26	14683.93	16276.77	16276.77
Capital Cost [$ m]	39.78	38.47	40.81	40.81
Annual Fuel Cost [$]	1091510.82	1051530.68	2850714.64	3260197.53
Annual Operating cost [$]	2991877.05	2963476.16	3014061.24	3014061.24
Total annual cost [$]	5871195.28	5781718.06	9414981.76	10008883.80
Profit per DWT [$/dwt]	-15.53	-21.15	27.06	28.25
Annual Bunker Cons [ton]	706.75	821.87	3944.29	4743.98
Annual MDO Cons [ton]	1054.48	915.14	1255.10	1268.87

The entire Pareto front is shown in Figure 6.12 for the short route and scenario one (low fuel price and low freight rate) when the speed variable is considered in the optimisation model. Those Pareto fronts represent the trade-offs between the conflicting objective functions. The

optimum operating speed for all the solutions allocate in the design space varies between 5 and 13 knots where a better economic performance occurs close to 13 knots as already seen.

One interesting observation is that any increase in speed in the range between 9 and 13 knots does not yield a noticeable improvement in the profit per tonne.mile or the net present value. One the other hand, these extra knots lead to a numerous increase in the required power because of the cubic law of speed and power. Hence, the increase in fuel consumption and CO_2 emissions overcome the trivial gain in revenue and profit. Facing the serious danger of climate changes, ship owners and charters should be willing to offer such financial sacrifice when it comes to fight climate change. Figure 6.13 shows the normalised objective functions as a function of the speed variable on the horizontal axes where f_1/f_1^* is on the right vertical axes and the others on the right vertical axes (f_2/f_2^*, f_3/f_3^*, f_4/f_4^*).

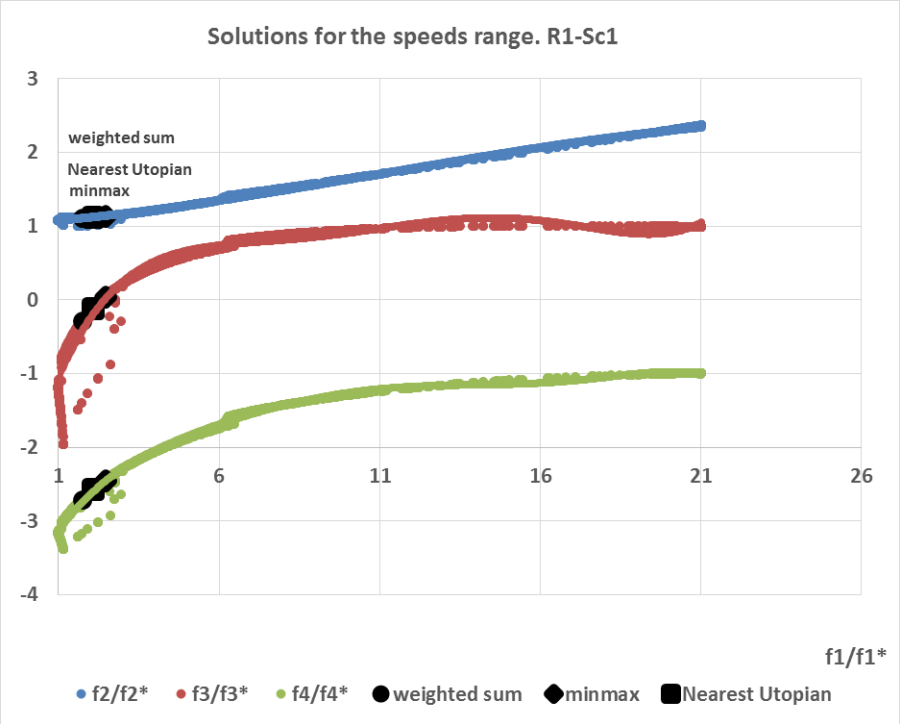

Figure 6.12 Pareto front over the speeds range. Route One, Scenario One

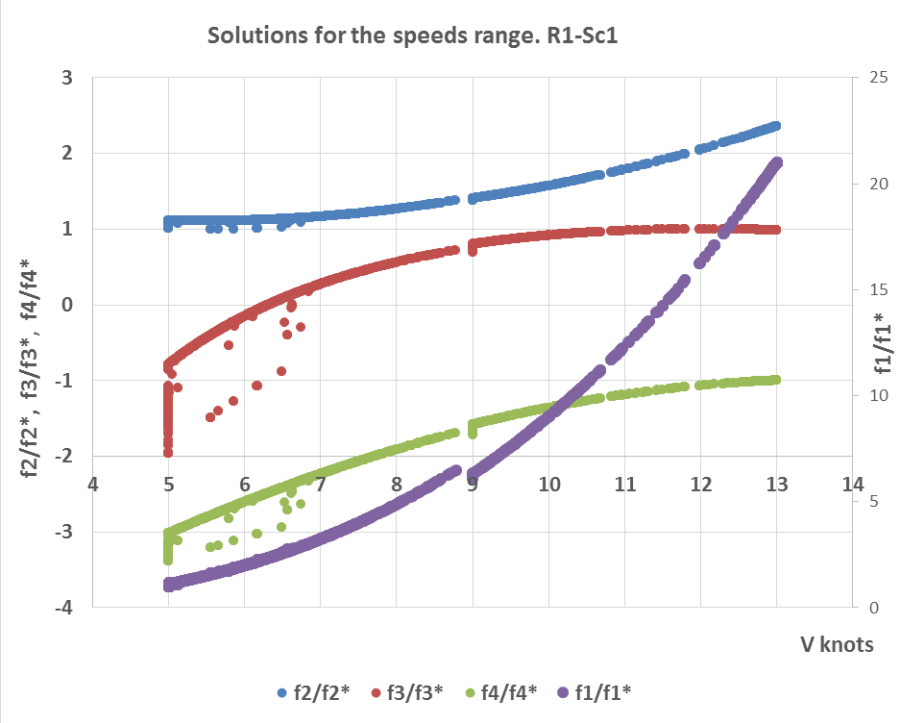

Figure 6.13 Normalised objective functions over the speeds range

Applying the EEDI reduction factors [10%, 20%, and 30%], and setting the new EEDI targets as constraints in the optimisation code yield the exact same Pareto efficiency solutions. The only reason is that all the solutions obtained in the first run with no EEDI reduction factor constraints meet the IMO requirements for all phases as a result of the energy saving gained by reducing speed.

A summary of the optimisation model's results for the oil tanker case study obtained by running the VBA code for the different scenarios in the case of the short and long routes while considering the speed as an additional independent variable is presented in Appendix K. The solutions are presented in the case of imposing EEDI reduction factors for phases Zero, One, Two and Three just whenever the optimisation model yield different designs to meet the EEDI targets. Since the optimum speed range where the ship is more efficient in terms of the energy saving and financial performance needs to be determined, all Pareto front figures are also presented as a function of speed. That helps in providing additional information for decision makers.

The optimisation framework with the three built-in models have provided a large array of input parameter values and calculated output values and also a large number of solution sets which offer a means for determining parameters sensitivity and understanding the relations within the

model through different techniques. That would help for the decision making in determining the designs' robustness and its ability to resist changes in the design variables. In the previous chapters we conduct a sensitivity analysis to determine each parameter's contribution to the variability present in the model outputs and overall performance by varying model parameter values one-at-a-time and building response surfaces. However, the overall performance and robustness of a design or product depends not only on the importance of individual parameters but also on how they interact and influence each other. Therefore, the complex relationship and combined influence of the design variables on the different objective functions were examined as well.

Reviewing the performance results from previous chapters and examining Pareto front plots obtained from the optimisation framework for both routes and the different scenarios show that none of the four hull variables (L, B/T, CB, LCB) can be addressed as insignificant to be eliminated from the model. However, they show a different degree of importance and correlation with the response parameters along the speed range and when considering all the independent factors. Therefore, it is somehow challenging to determine which of the selected parameters is most influential on the response parameters and the overall performance.

Generally speaking, the results obtained from the optimisation model showed that in order to offer a more robust design(s) that has the ability to remain effective and efficient under different conditions, then the choice should fall for bigger hulls with high carrying capacity operating at slower speeds than the design speed. Slow steaming in the region of 10-13 knots would offer a significant potential for emissions mitigation and profit maximisation in the short-term and long-term.

It can be seen that the optimisation framework described in this research thesis has been to be efficient when applied to a complex case study for optimising the hull design and operation profile of the tanker ship. It has offered robust designs and trade-off solutions that can operate efficiently regardless the fluctuating market conditions and operating conditions. Considering all the Pareto-optimal solutions that are presented in this section and in the Appendices, the designers or decision makers will have the ability to experience the improvements in the performance across all the objective functions as a result of implementing the multi-objective optimisation.

6.9 Conclusions

In the chapter, an optimisation framework using a VBA macro code has been developed based on the concept of Pareto optimality. The objective functions that the optimisation framework is handling are: hydrodynamic performance (P_D/Dis), environmental impact ($EEDI_A/EEDI_{Ref}$), and economic performance (Net Present Value and Profit per tonne.mile).

The optimisation process was carried out for a Panamax tanker case study using 5 parameters and a set of constraints for the hull parameters and speed. Five approaches were selected to formulate the single scalar function to perform the multi-objective optimisation. Moreover, the Generalized Reduced Gradient GRR in the Solver tool built within EXCEL was chosen to obtain the design solutions as the running time is less than in case of using the Evolutionary algorithms. The outcome of the optimisation framework are presented graphically to form what is known as Pareto front which determines the design space and the trade-offs between the different competing objective functions.

The VBA code was used to solve the optimisation problem to generate the entire Pareto front for both routes across the 4 different scenarios for each individual set of the weight factors for the different for the different formulation approaches. Results obtained by solving the optimisation problem at the design speed for Scenario One have validated what has been found earlier in the case of minimising the energy consumption. It was found that the best solutions were obtained for long hulls, low breadth to draught ratio, low block coefficient and with backward LCB position. Moreover, results obtained by solving the optimisation problem at the design speed while considering profit maximisation have shown that the ship economic performance tends to improve for bigger hulls with high carrying capacity. That is mainly an advantage of economies of scale which promote lower per-unit costs. The results showed that for equal weights, the optimisation methods tend to favour big and full hulls with higher carrying capacity.

However, the EEDI analysis showed that none of the optimum alternative designs would pass the IMO requirements for Phase 2 and 3 as the attained EEDI values are higher than the reference EEDI. Therefore, the speed optimisation was introduced into the optimisation process to show the importance of slow steaming. The results for Scenario one (low fuel price and low freight rates) across the speed range were presented. The energy efficiency and economic

performance were improved, and the obtained hull designs have a satisfied low attained EEDI values that meet IMO future targets regarding CO_2 emissions.

It was found that for bigger ships, sailing at a speed around 12-13 knots would benefit both the ship owner and charterer. The annual profit per deadweight would increase by around $8, and that would yield in a considerable increase in the NPV of around ($ 8.3 million). These long-term benefits in reducing the emissions and boosting the economic performance come at no additional capital cost but as a result of adopting slow steaming.

The results of this study further support the idea that sailing at slower speeds between 9 and 13 knots, simultaneously, improve the energy efficiency and reduce fuel consumption on one hand and, on the other hand, increase the profitability regardless the fluctuating shipping market conditions. This optimisation model could assist decisions making where it is possible to choose a robust design or designs that offer a near-optimum performance regardless any fluctuations in the market and or the operation profile, and eliminate any significant sub-optimal designs.

Chapter 7. Conclusions, Further Work and Recommendations

7.1 Introduction

The purpose of Chapter Seven is to wrap together all the main findings of the thesis, and to present the major achievements and conclusions from this research study. A review of the research is presented in conjunction with a summary of the significance of the research. This is followed by the recommendations for future research on the subject based on the potential improvements and limitations of the study.

7.2 Summary and Conclusions

The motivation of the study conducted in this thesis is originated from the author's passion for undertaking an extended search to determine the potentials to improve the ship's performance at different scopes including the hydrodynamic and economic aspects through adopting slow steaming concept and hull optimization.

A framework has been developed consisting of a number of models that take into account the hydrodynamic performance, energy efficiency, and the economic performance through a ship's life span. The developed framework deals with complex and conflicting multi-objective problems starting at the early design stage of a ship through her entire operating life and ending with the scrapping stage. The framework will help in choosing a robust deign(s) which are able to operate efficiently and response to any changes in the unstable maritime market, to comply at the same time with the international regulations regarding the environmental impact, and to generate the most for shipowners and charterers.

7.2.1 Development of the Hydrodynamic Model

The hull optimization concept was described in Chapter Three along with presenting the main elements and characteristics including geometry manipulation tool and an optimization method.

A thorough study has been carried out to develop and test the hydrodynamic model as following:

- A bare-hull of a 54,000 DWT Tanker ship was selected as a case study for this project to demonstrate the potential resistance reduction and energy saving that can be achieved by adopting the slow steaming concept and hull optimization process.

- AVEVA Marine 12.1 has been adopted in the thesis to generate the base body, and as a tool for the hull parametric scaling and distortion, and also to perform basic and complex naval architectural analyses and evaluations such as the hydrostatics calculations and power estimations.

- Four hull parameters have been chosen for the parametric analysis in addition to the operating speed. In order to determine the effect of the hull parameters on the hydrodynamic performance, the distortion process is done in three stages where the performance sensitivity is investigated when parameters are changes individually and simultaneously.

- The general hydrodynamic performance of the generated hulls and the powering characteristics were compared with those of the initial design.

- AVEVA output from Stage Three hulls was used to obtain a set of regression formulas to estimate the delivered power to displacement ratio P_D/Dis as a function of speed and the design variables using Minitab17 and the Regression Tool built in Excel.

- Taguchi statistical and experimental technique has been used to search for the most favourable form(s) and insensitive designs depending on the common naval architect knowledge and skills, and on a trial and error procedure.

7.2.2 Development of the Environmental Impact Model

The latest international and national procedures and codes that regulate shipping activities and control harmful pollutants from ships were presented in Chapter 2. That is followed by describing some methods to estimate fuel consumption on board ships and emissions during the different journey phases including cruising, manoeuvring, and hoteling. Then, the speed optimisation as an efficient way to mitigate CO_2 emissions from ships was discussed along with

a number of other technical and operational measures to reduce shipping emissions promote by IMO were introduced.

In Chapter 4, the environmental model is built upon the EEDI formula and carried out taking into account the following:

- Assumptions regarding emission factors, energy consumption, engine loads, cargo capacity, etc. to calculate the reference EEDI and attained EEDI values for the environmental model were presented.

- Amedia method to estimate the lightship weight and hence to calculate the ship deadweight to be used in the EEDI formula was discussed.

- EEDI values for the base hull and the alternative hulls were calculated over the speed range using the hydrodynamic model results.

- EEDI results from the three stages were compared with the base hull results at the design speed as well as at other speeds.

- The attained EEDI to EEDI reference ratio $\left(EEDI_A/EEDI_{Ref}\right)$ was chosen as the objective function (response parameter) in the environmental model. It was used as an indicator while exploring the design space to choose alternative designs that demonstrate a better energy efficiency performance in order to meet the IMO requirements.

- Mimitab17 and the Regression Tool built in EXCEL were used to run the regression analysis. A set of regression equations were obtained to estimate the attained EEDI to EEDI reference ratio.

- A sensitivity analysis was carried out to gain a better 'cause and effect' understanding of how changes in hull parameters and how operating speed affects the $(\mathrm{EEDI_A}/\mathrm{EEDI_{Ref}})$ value.

7.2.3 Development of the Economic Model

The main and important aspects of the economics of ships were covered in Chapter Five. It focused on the key criteria that affect decisions making when it comes to design and build a

new ship, and also on all the considerations that ship charterers and operators should take into account to maximize the economic performance of a ship within the life span taking into account all the fluctuations in the shipping market.

An economic model was developed to evaluate the economic performance of all ships and in order to determine the sensitivity of a ship performance and profitability to changes in the market conditions. The economic model in this study was developed by considering the following:

- Two different tanker routes (2000 n.mile and 7000 n.mile) were chosen to carry out the calculations to estimate the voyage and annual revenue using the average freight rates from year 2012 using the Worldscale index.

- Low and high fright rates for both routes were determined to be used in the revenue calculations in order to investigate the market fluctuations on a ship financial performance and optimum operating speed.

- High and low fuel prices for both bunker and diesel fuels were used in the calculations to determine the influence of oil prices on the optimum operating speed.

- Four different scenarios of combinations of fuel price and freight rates were set for each maritime route. The economic model was conducted for the base hull and all the other alternative designs in order to investigate the implications of changes in all the previous elements of the ship finance.
  - Low fuel prices, Low freights,
  - Low fuel prices, High freights,
  - High fuel prices, Low freights,
  - High fuel prices, High freights.

- Simplified approximation regression formulas were obtained as a function of the deadweight to estimate the operating costs and also dry-docking costs for tanker ships using commercial data from OpCst annual report 212.

- Information regarding port tariffs and dues for different ports around the world were collected for the purpose of determining a straightforward way to estimate costs a tanker ship pays at both the lading and discharging ports.

- A linear regression formula to calculate a ship gross tonnage GT was derived using collected data for 908 tanker ships from Seaweb website to be used in estimating the port costs while waiting at the berth.

- Fuel cost per round trip and per annum was calculated by estimating fuel consumption by all consumers onboard (main and auxiliary engines and boilers) during journey phases (cruising, manoeuvring and hoteling).

- In specific, the main purpose of developing the economic model is to evaluate the impact of speed optimisation on fuel consumption and emissions reductions as well as shipping economics and the benefits for owners and charterers and also the cost of adopting this measure.

- An approximation formula for estimating the newbuilding price was derived using real data of 218 crude oil and product tankers from Sea-web Ships database. The newbuilding price was estimated as a function of the ship deadweight and length, and the producer price index was included to allow for inflation adjustments.

- The scrapping value was also taken into account in the model as it is an important item in the balance sheet and the cashflow statement.

- The profit per tonne.mile and the net present value NPV are calculated in the economic analysis to be used as indicators to compare alternative designs for different routes and market conditions scenarios.

7.2.4 Development of the Optimisation Framework

Chapter 6 focused on how to improve, simultaneously, the design and the operational profile of ships by balancing the conflicting performance indicators which have been addressed in the previous chapters. A brief explanation of optimisation was introduced covering single and multi-objective optimisation problems in engineering, economy, and other disciplines. The structure of the this chapter can be summarised as following:

- A robust and comprehensive optimisation framework was developed based on the concept of Pareto optimality to assess decision making and to determine robust designs

as well as operational profiles based on results from the hydrodynamic model, environmental impact model, and the economic model.

- VBA macro was developed to carry out the optimisation process for the case study. It is written in Visual Basic for Applications (VBA) in Microsoft Excel which is a subset of the powerful Visual Basic programming language.

- The Generalized Reduced Gradient GRG method in the Solver tool built in EXCEL was utilised to search the design space and obtain the design solutions.

- Five different approaches have been selected to formulate the single scalar function to perform the multi-objective optimisation. These five approaches are:

  - The weighted sum optimum
  - The min-max optimum
  - Global criterion optima
  - Global criterion optima in the L2-norm
  - The nearest to the utopian optimum

- The Optimisation code gives the ability to optimise any problem for individual objective function or solve multi-objectives problems using one or more of these five different formulation methods.

- The set of Pareto efficient allocations that form The Pareto frontier are obtained for any formulation approach by randomly altering the weights for the four objective functions in the weighted scalar function for any of the five selected multi-criteria formulation methods.

- The objective functions which were considered in this multi-criterion problem consist of:

  - Minimise the delivered power to displacement ratio $f_1 = P_D/Dis$,
  - Minimise the attained EEDI to EEDI reference ratio $f_2 = EEDI_A/EEDI_{Ref}$,
  - Maximise the annual profit per tonne.mile $f_3 = Profit/tonne.mile$,
  - Maximise the Net Present Value $f_4 = \text{NPV}$.

- A five-parameter, four-criteria, eight-scenario, 14- to 17-constraint optimisation case study was presented and discussed showing the trade space between improving the energy efficiency of ships and maximising the economic performance.
- The results were obtained for the same scenarios of routes and market conditions as had been seen in the previous chapter.
- The optimisation code runs for two different cases which are: firstly searching for the optimum hull parameters at the design speed and secondly over the speeds range.
- The solutions were presented graphically to form what is known as Pareto front which determines the design space and the trade-off between the different competing objective functions.

7.2.5 Key Findings and Conclusions

The research conducted for this thesis extends the state of the art with several noteworthy contributions to the subject of multi-objective optimisation in the shipping industry. Overall, the conclusions drawn in this thesis have shed contemporary light on the complex issues of trade-offs in the goal for making ships more efficient and greener while reducing the costs and increasing the profitability for all stakeholders especially owners and operators.

Some crucial conclusions have been derived from carrying out the optimisation framework for the tanker ship case study can be listed as follows:

- The study demonstrated the significant gain in both the hydrodynamic and economic performance through the successful application of parametric modification and slow steaming to tanker ships.
- The author developed a robust framework combining three models that estimate and evaluate the ship performance.
- The hydrodynamic model results suggested that modifications in the hull parameters and optimising the sailing speed can improve the energy saving and required power by up to 15%.

- A significant reduction in the delivered power P_D can be gained at high speeds above 13 knots for ships with hulls longer and slimmer than the basic hull while keeping the displacement constant.

- For a constant displacement, the P_D results showed that a reasonable reduction of about 4.5% in the required power can be achieved across all the speed range for designs with deeper hulls and smaller beam while keeping the length constant.

- The results showed that any increase in the block coefficient introduces a significant increase in the required propulsion power per ton displacement which could reach 24% at the design speed for a 6% increase in C_B at the design speed. This undesirable impact on the required power as a result of increasing the block coefficient drops in value for slower speeds till it has a positive impact in reducing the required power at lower speeds.

- Moving the LCB position backward would lead to a reasonable reduction in the required power up to 3.5% for high speeds and 1.8% for the $[-1\%L, LCB]$ for instance.

- The signal to noise ratio analysis showed that longer hulls with a minimum breadth to draught ratio and a slim shape (low block coefficient) and a backward LCB have generally a better hydrodynamic performance.

- A closer look at the results from Stage Three revealed that some individual designs show a great energy saving potential such as design no.61 with long hull, low breadth to draught ratio, high block coefficient and backward LCB position which shows the best performance among all other alternative hulls at slow speeds up to speed 13 knots.

- Results from the EEDI and emissions model demonstrated that the improvement of power saving and emissions reductions a significant gain in energy saving on-board up to 20% a ship can be achieved by reducing speed by 1 knot and for the favour of longer and finer hulls.

- The results of the attained EEDI values for the base ship over the speed range (5-17 knots) showed that the EEDI is predominantly sensitive to the operating speed. Reducing the speed by 1 knot from the design speed reduces the EEDI by 18%, whereas increasing the speed by 1 knot increases the EEDI by 25%.

- The base ship at her design speed fails to meet the required EEDI minimum values for the future reduction phases. Therefore, to comply with IMO regulations, the base ships needs to reduce the operating speed at least by 1 knot to meet the required minimum EEDI for phase 1 and phase 2 and by 2 knots to avoid the EEDI penalty for phase 3 (January 2025).

- All the four design variables (L, B/t, CB, LCB) have a significant influence on the EEDI value.

- Analysing the individual influence of the design parameters showed that none of the new generated hulls in Stage One would meet Phase I EEDI baseline at the design speed but hulls $-4\%\ C_B$ and $-6\%\ C_B$.

- The results obtained from the model indicated that the new designs in Stage One need to sail at speed 13 knots and below in order to meet Phase III (January 2025) EEDI targets.

- The combined influence of speed and variations in the controllable primary and secondary design variable on the energy efficiency and attained EEDI has been analysed using the set of the derived regression formulas to estimate the attained EEDI to EEDI reference ratio $\left(EEDI_A/EEDI_{Ref}\right)$.

- It was found that the maximum reduction of (-18.20%) in EEDI is achieved for Hull 55 (L_3, B/T_1, C_{B1}, $LCB\%L_1$) while Hull 27 (L_1, B/T_3, C_{B3}, $LCB\%L_3$) demonstrated the poorest practice among all hulls as the increase in the EEDI is around (+31.22%).

- The signal to noise ratio analysis showed that longer hulls with a minimum breadth to draught ratio and a slim shape (low block coefficient) and a backward LCB have generally a better energy efficiency performance and hence less emissions.

- Reducing the service speed by 5 knots would reduce the bunker fuel consumption significantly by around 70%. However, the results showed that the annual fuel saving and CO_2 emissions for the base ship is higher for the long distance route than the short distance route. This saving was found to be up to 43% at speed 5 knots.

- The annual loss is reduced by 83% for scenario one when sailing at speed 11 knots compared with the loss at the design speed, and by 72% for scenario three at speed 8 knots. The ship generates a greater profit at higher speeds for the high fright rate scenarios (Scenarios 2&4). The optimum operating speeds are 13 knots for Scenario Two with low fuel price, and 11 knots for Scenario Four with high fuel price.

- The study showed that sailing on the long distance route would benefit the ship and reduce the loss in the case of low fright rate scenarios when high port dues and cargo handling charges are assumed. That is mainly because of the reduction in the number of port visits per year. On the other hand, the results showed that the bunker fuel consumption per year at the design speed for the short distance trip is less by 13%.

- Running the model for the other speeds (5-17 knots) highlighted the importance of speed and routing optimisation on the revenue and cost items. A positive profit was generated for Scenario One (low freight rate and low fuel price) at speeds between 8 knots and 14 knots while a negative profit occurred when operating at the design speed and speeds in the range (5-7) and (16-17) knots.

- NPV results showed that at the design speed, the base ship has a negative net present value across all the scenarios expect Scenario Two where fright rates are high and fuel prices are low. However, reducing the speed by a few knots would offer a superior value of the investment over time for both routes; i.e. the short and long ones.

- The results revealed that length and block coefficient have the greatest effect on the newbuilding price to deadweight ratio NB/DWT.

- Hull no. 61 (L_3, B/T_1, CB_3, $LCB\%L_1$) has showed the best economic performance across all speeds and scenarios. Moreover, the results for both routes and across the four scenarios showed that profit per deadweight for all alternative hulls regardless market conditions has been improved for low speeds between 10 and 13 knots.

- The solutions obtained from the developed optimisation framework were presented graphically to form what is known Pareto front which determines the design space and the trade-off between the different competing objective functions.

- The results of this study further support the idea that sailing at slower speeds between 9 and 13 knots improves the energy efficiency and reduces fuel consumption on one hand and, on the other hand, increases the profitability regardless the fluctuating shipping market conditions.

- The results and findings of this work showed great potential for the improvement in the energy efficiency of ships and the reduction of CO_2 emissions from optimising the hull design parameters in the range of low speeds while taking into account the economic performance to keep the ship a profitable investment from the day of her first trip till the day she ends in a scrapping yard.

- This optimisation model could assist decisions making where it is possible to choose a robust design or designs that offer a near-optimum performance regardless any fluctuations in the market and or the operation profile, and eliminate any significant sub-optimal designs.

In summary, the primary purpose of this research study was to clarify some central issues as regards hull optimisation and ship speed optimization at the technological and operational levels. The study's main contribution is the incorporation of fundamental hydrostatics and hydrodynamics parameters as well as other considerations that account for the financial aspects that weigh heavily in a ship owner's or charterer's decision regarding initial capital investment, cargo capacity, routing, and speed.

7.3 Challenges, Limitations, and Recommendations for Future Work

It is the author's belief that this thesis has provided insight into the further application of multi-objective optimisation for complex made-to-order products. The scope of the studies and analysis was enormous in terms of the data collected and the scenarios and factors considered in this study. The developed optimisation framework with its three hydrodynamic, environmental, and economic models has a number of distinct advantages as a tool to assist decision makers in balancing conflicting objective functions in the shipping industry.

The main challenges the author faced while conducting this study can be summarised as following:

- Generating the bare hull on AVEVA and carrying out the parametric distortion and the lines smoothing.

- Time consumption to generate new hulls and to run the Hydrostatic & Hydrodynamic calculations on AVEVA for all the alternative hulls in order to increase the accuracy of the regression formulas.

- Choosing the right variables to derive the regression formulas to estimate the objective functions is challenging. Many attempts were carried out in order to derive these regression formulas with minimum number of variables where an acceptable level of accuracy is achieved.

- The data generated by running the three individual models and from the optimisation framework is enormous. Different complex statistical techniques were tested to choose the most effective method to digest and analyse these data in order to obtain useful information.

- Gaining accurate and real data about building costs from shipyards is difficult and near impossible as such data is confidential and all information regarding cost details especially during building stages is kept between the shipowner and the shipyard.

- Up-to-date and continuous database in the shipping market is limited and not available for the research purposes. Therefore, it was challenging to gather the required data for this study through contacting several shipping companies and port authorities worldwide, and through compiling data published on annual reports.

- Minimizing the computing time to run the optimisation code in order to obtain a converging solution is a significant challenge because of the conflicting criteria among the three models.

However, there are still some improvements that can be added and limitations that need to be tackled for future work. The author believes that:

- More hull parameters and propulsion factors to be included in the study in order to stretch the design space in the aim to allocate better and more efficient hulls.

- The hydrodynamic and economic models in this study considers the ballast leg and assumes in the solved case study that the ship operates at the same speed on the laden and ballast legs. However, more scenarios that assume different speeds for both legs are worth investigated.

- A shipping market prediction tool is needed to be a part of the framework. Such tool can be constructed on the basis of historical data analysis, data collected from shipping companies, ship yards and brokers, bunker prices from suppliers and Oil refineries, tariff data from worldwide port authorities, etc.

- This research focused on tanker ships sector and mainly on Panamax class. More vessels types and classes need to be included in the optimisation framework in order to cover a wider spectrum of the shipping market and industry. Further validation case studies for the three models and the optimisation framework worth investigated.

- The developed economic model in this research work does not take into account the change in the fright rates as a function of speed and delay in the delivery time as a result of slow steaming. Therefore, more realistic results that represent the actual behaviour in the fright market can be achieved by introducing a point system that estimates the change in the fright rates as a function of changes in speed away from the design speed. A general practise that can be included in the model suggests a 0.5 point premium in the agreed worldscale for each additional 0.5 knot increase and a 0.5 point discount for each 0.5 knots decrease.

- The framework is built using Excel and VBA macro. However, it does not offer a user-friendly interface which makes it not easy to be used with users who are not familiar with EXCEL and Visual Basic environment. Therefore, it is suggested for future work that the three models and codes to be wrapped and presented in a way that is stress-free.

References

1. *ABS (2013) Ship Energy Efficiency Measures: Status and Guidance. [Online]. Available at: https://www.eagle.org/eagleExternalPortalWEB/ShowProperty/BEA%20Repository/References/Capability%20Brochures/ShipEnergyEfficiency.*

2. *ACCESS: Arctic Climate Change - Economy and Society (2014) Calculation of fuel consumption per mile for various ship types and ice conditions in past, present and in future. [Online]. Available at: http://www.access-eu.org/modules/resources/download/access/Deliverables/D2-42-HSVA_Report_CE_CS_NR_rev02_submitted.pdf.*

3. *Acomi, N. and Acomi, O.C. (2014) 'Improving the Voyage Energy Efficiency by Using EEOI', Procedia - Social and Behavioral Sciences, 138, pp. 531-536.*

4. *Alderton, P.M. (2008) Port management and operations. 3rd edn. London: Informa.*

5. *Alvarez, N.J., Walker, L.M. and Anna, S.L. (2009) 'A non-gradient based algorithm for the determination of surface tension from a pendant drop: Application to low Bond number drop shapes', Journal of Colloid and Interface Science, 333(2), pp. 557-562.*

6. *Anaxagorou, P.G., Pappas, A., Giraud, I., Stratigis, D., Papadopoulos, E., Pongolini, L., Ballini, F., Treichel, P., Martínez de Osés, X. and Velásquez Correa, S. (2015) Economic impact to shipping industry: Economic impact to shipping industry considering Maritime Spatial Planning and green routes in pilot case studies. Available at: http://commons.wmu.se/cgi/viewcontent.cgi?article=1001&context=monalisa2.*

7. *Anderson, K. and Bows, A. (2011) 'Beyond 'dangerous' climate change: Emission scenarios for a new world', Philosophical Transactions of the Royal Society A: Mathematical, Physical and Engineering Sciences, 369(1934), pp. 20-44.*

8. *Andersson, J. (2000) 'A survey of multiobjective optimization in engineering design', Department of Mechanical Engineering, Linktjping University. Sweden.*

9. *Andersson, J. (2001) Multiobjective optimization in engineering design: applications to fluid power systems. Linköpings universitet.*

10. *Anink, D. and Krikke, M. (2009) The IMO Energy Efficiency Design Index A Netherlands Trend Study (3064). Netherlands.*

11. *Anyanwu, J.O. (2013) 'Analysis of the Interrelationships between the Various Shipping Markets', Analysis, 3(10).*

12. Apostolidis, A., Kokarakis, J. and Merikas, A. (2012) 'Modeling the Dry-Docking Cost - The Case of Tankers', Journal of Ship Production and Design, 28(3), pp. 134-143.

13. Armstrong, V.N. (2013) 'Vessel optimisation for low carbon shipping', Ocean Engineering, 73(0), pp. 195-207.

14. Arora, J.S., Elwakeil, O.A., Chahande, A.I. and Hsieh, C.C. (1995) 'Global optimization methods for engineering applications: A review', Structural optimization, 9(3), pp. 137-159.

15. Athenian Shipbrokers S.A. [Online]. Available at: http://www.atheniansa.gr/.

16. AVEVA MARINE (2011) Initial Design - User Guide.

17. Ballou, P., Chen, H. and Horner, J.D. (2008) 'Advanced methods of optimizing ship operations to reduce emissions detrimental to climate change', OCEANS 2008. Quebec City, QC, 15-18 Sept. 2008. pp. 1-12.

18. Barbahan, M.Y. (2008) Ships Hydrodynamics I. Syria - Latakia: Tishreen University.

19. Barker, T.B. (1990) Engineering quality by design: interpreting the Taguchi approach.

20. Bendell, A. (1989) Taguchi methods : proceedings of the 1988 European conference. London: Elsevier.

21. Bertram, V. (2012) Practical ship hydrodynamics. 2nd edn. Amsterdam;London: Elsevier/Butterworth-Heinemann.

22. Bertram, V. and Schneekluth, H. (1998) Ship design for efficiency and economy. Butterworth-Heinemann.

23. Bialystocki, N. and Konovessis, D. (2016) 'On the estimation of ship's fuel consumption and speed curve: A statistical approach', Journal of Ocean Engineering and Science, 1(2), pp. 157-166.

24. Bijwaard, G.E. and Knapp, S. (2009) 'Analysis of ship life cycles—The impact of economic cycles and ship inspections', Marine Policy, 33(2), pp. 350-369.

25. Birk, L. (2009) 'Application of Constrained Multi-Objective Optimization to the Design of Offshore Structure Hulls', Journal of Offshore Mechanics and Arctic Engineering, 131(1), pp. 011301-011301-9.

26. Birk, L., Clauss, G.n.F. and Lee, J.Y. (2004) 'Practical Application of Global Optimization to the Design of Offshore Structures', (37459), pp. 567-579.

27. Blendermann, W. (1996) Wind loading of ships: Collected data from wind tunnel tests in uniform flow. Inst. für Schiffbau, Germany.

28. Bodansky, D. (2016) 'Regulating Greenhouse Gas Emissions from Ships: The Role of the International Maritime Organization'.

29. Borup, L. and Parkinson, A. (1992) Proceedings of the 18th Annual ASME Design Automation Conference.

30. Bose, N., Zhu, D.-X., Mewis, F., Insel, M., Toki, N., Steen, S., Hwangbo, S.-M. and Anzböck, R. (2005) The Specialist Committee on Powering Performance Prediction - Final Report and Recommendations to the 24th ITTC. Paper presented at the Proceedings of the 24th ITTC - Edinburgh.

31. Box, M.J. (1965) 'A New Method of Constrained Optimization and a Comparison With Other Methods', The Computer Journal, 8(1), pp. 42-52.

32. Branch, A.E. (1988a) 'Economics of ship operation', in Economics of Shipping Practice and Management. Dordrecht: Springer Netherlands, pp. 101-132.

33. Branch, A.E. (1988b) Economics of shipping practice and management. 2nd edn. London ; New York: London ; New York : Chapman and Hall.

34. Brizzolara, S. (2004) 'Parametric optimization of SWAT-hull forms by a viscous-inviscid free surface method driven by a differential evolution algorithm', Proceedings 25th Symposium on Naval Hydrodynamics, St. John's, Newfoundland and Labrador. pp. 47-64.

35. Buhaug, Ø., Corbett, J.J., Endresen, Ø., Eyring, V., Faber, J., Hanayama, S., Lee, D.S., Lee, D., Lindstad, H. and Markowska, A.Z. (2009) 'Second IMO GHG Study 2009', International Maritime Organization (IMO) London, UK.

36. Buxton, I.L. (1987) Engineering economics and ship design. 3rd edn. Wallsend: British Maritime Technology Limited.

37. Cariou, P. (2011) 'Is slow steaming a sustainable means of reducing CO2 emissions from container shipping?', Transportation Research Part D: Transport and Environment, 16(3), pp. 260-264.

38. Cariou, P. and Cheaitou, A. (2012) 'The effectiveness of a European speed limit versus an international bunker-levy to reduce CO 2 emissions from container shipping', Transportation Research Part D: Transport and Environment, 17(2), pp. 116-123.

39. Chang, C.C. (2012) 'Marine energy consumption, national economic activity, and greenhouse gas emissions from international shipping', Energy Policy, 41, pp. 843-848.

40. Choi, J.E., Min, K.S., Kim, J.H., Lee, S.B. and Seo, H.W. (2010) 'Resistance and propulsion characteristics of various commercial ships based on CFD results', Ocean Engineering, 37(7), pp. 549-566.

41. Chun, H.-H. (2010) 'Hull Form Parameterization Technique With Local and Global Optimization Algorithms', The International Conference on Marine Technology MARTEC. Dhaka, Bangladesh.

42. Clarkson Research Services. [Online]. Available at: http://www.crsl.com/.

43. Clarkson Research Services Limited (2014) 'Sources and Methods for the Shipping intelligence weekly'.

44. Claudepierre, M., Klanac, A. and Aleström, B. (2012) Green Ship Technology Conference. Available at: http://www.transportportal.se/ShipDocs/2014-01-21rec162250.pdf.

45. Clerc, M. (2006) 'Particle Swarm Optimization, ISTE, London'.

46. Connor, A.M. and Tilley, D.G. (1998) 'A tabu search method for the optimization of fluid power circuits', Proceedings of the Institution of Mechanical Engineers, Part I: Journal of Systems and Control Engineering, 212(5), pp. 373-381.

47. Corbett, J.J. and Fischbeck, P. (1997) 'Emissions from ships', Science, 278(5339), pp. 823-824.

48. Corbett, J.J., Fischbeck, P.S. and Pandis, S.N. (1999) 'Global nitrogen and sulfur inventories for oceangoing ships', Journal of Geophysical Research Atmospheres, 104(D3), pp. 3457-3470.

49. Cui, Y., Geng, Z., Zhu, Q. and Han, Y. (2017) 'Review: Multi-objective optimization methods and application in energy saving', Energy, 125, pp. 681-704.

50. Date, J. and Turnock, S.R. (2000) 'CFD estimation of skin friction experienced by a plane moving through water', RINA Transactions Part B, 142, pp. 116-135.

51. David Cooper (2002) 'Representative emission factors for use in quantification of emissions from ships associated with ship movements between port in the European Community', IVL Swedish Environmental Research Institute Ltd (ENV. C. 1/ETU/2001/0090), Final Report.

52. Davis, L. (1991) 'Handbook of genetic algorithms'.

53. Deb, K. (2005) 'Multi-Objective Optimization', in Burke, E.K. and Kendall, G. (eds.) Search Methodologies: Introductory Tutorials in Optimization and Decision Support Techniques. Boston, MA: Springer US, pp. 273-316.

54. Deb, K. and Deb, K. (2014) 'Multi-objective Optimization', in Burke, E.K. and Kendall, G. (eds.) Search Methodologies: Introductory Tutorials in Optimization and Decision Support Techniques. Boston, MA: Springer US, pp. 403-449.

55. Devanney, J. (2010) 'The impact of bunker price on VLCC spot rates', Proceedings of the 3rd International Symposium on Ship Operations, Management and Economics. pp. 7-8.

56. Devanney, J. (2011a) 'The impact of the energy efficiency design index on very large crude carrier design and CO2 emissions', Ships and Offshore Structures, 6(4), pp. 355-368.

57. Devanney, J. (2011b) Speed Limits versus Slow Steaming. Center for Tankship Excellence. USA.

58. Devanney, J. and Beach, S. (2010) 'EEDI–a case study in indirect regulation of CO2 pollution', Center for Tankship Excellence, Version, 1.

59. Dinwoodie, J. and Morris, J. (2003) 'Tanker forward freight agreements: the future for freight futures?', Maritime Policy & Management, 30(1), pp. 45-58.

60. DNV -Det Norske Veritas (2014) Rules for ships (Pt 3, Ch1). [Online]. Available at: https://rules.dnvgl.com/servicedocuments/dnv.

61. DNV GL EEDI and EEOI. Available at: https://www.dnvgl.com/.

62. Dolphin, M.J. and Melcer, M. (2008) 'Estimation of ship dry air emissions', Naval Engineers Journal, 120(3), pp. 27-36.

63. Du, K.-L. and Swamy, M.N.S. (2016) 'Simulated Annealing', in Search and Optimization by Metaheuristics: Techniques and Algorithms Inspired by Nature. Cham: Springer International Publishing, pp. 29-36.

64. Dylan W. Temple and Matthew Collette (2012) 'Multi-objective hull form optimization to compare cost and lifetime fuel consumption', IMDC2012. Galsgow, United Kingdom. pp. 391-403.

65. Energy and Environmental Analysis Inc and EPA (2000) Analysis of Commercial Marine Vessels Emissions and Fuel Consumption Data. United States Environmental Protection Agency EPA. [Online]. Available at: https://permanent.access.gpo.gov/gpo14294/r00002.pdf.

66. Eschenauer, H., Koski, J. and Osyczka, A. (2012) Multicriteria design optimization: procedures and applications. Springer Science & Business Media.

67. Eyring, V., Isaksen, I.S.A., Berntsen, T., Collins, W.J., Corbett, J.J., Endresen, O., Grainger, R.G., Moldanova, J., Schlager, H. and Stevenson, D.S. (2010) 'Transport impacts on atmosphere and climate: Shipping', Atmospheric Environment, 44(37), pp. 4735-4771.

68. *Faber, J., Freund, M., Köpke, M. and Nelissen, D. (2010) Going Slow to reduce Emissions: Can the current surplus of maritime transport capacity be turned into an opportunity to reduce GHG emissions? (10.7115.21). Seas At Risk. [Online]. Available at: http://www.seas-at-risk.org/pdfs/speed%20study_Final%20version_SS.pdf.*

69. *Faber, J., Markowska, A., Nelissen, D., Davidson, M., Eyring, V., Cionni, I., Selstad, E., Kågeson, P., Lee, D. and Buhaug, Ø. (2009) Technical support for European action to reducing Greenhouse Gas Emissions from international maritime transport. Available at: https://ec.europa.eu/clima/sites/clima/files/transport/shipping/docs/ghg_ships_report_en.pdf.*

70. *Faber, J., Nelissen, D., Hon, G., Wang, H. and Tsimplis, M. (2012) Regulated slow steaming in maritime transport: An assessment of options, costs and benefits. CE Delft. Delft, N.*

71. *Fearnleys. [Online]. Available at: https://www.fearnleys.no/.*

72. *Fletcher, R. (1987) Practical methods of optimization. 2nd edn. John Wiley & Sons.*

73. *Fowlkes, W.Y. and Creveling, C.M. (1995) Engineering methods for robust product design : using Taguchi methods in technology and product development. Reading, Mass.: Addison-Wesley Pub. Co.*

74. *Froude, W. (1868) 'Observations and Suggestions of determining by experiments the resistance of ships - Correspondence with the Admirality, Reprinted in "The papers of William Froude (1810-1879)"', The Institiution of Naval Architects, London, 1955.*

75. *Garzon, I.E., University of Newcastle upon Tyne. Dept. of Mechanical Materials and Manufacturing Engineering. and University of Newcastle upon Tyne. (2000) Optimisation for product and process improvement : investigation of Taguchi tools and genetic algorithms. University of Newcastle upon Tyne [Online]. Available at: http://hdl.handle.net/10443/471.*

76. *Gazi, V. and Passino, K.M. (2011) 'Particle Swarm Optimization', in Swarm Stability and Optimization. Berlin, Heidelberg: Springer Berlin Heidelberg, pp. 251-279.*

77. *Gentle, N.F. and Perkins, R.J. (1982) 'An Estimate of Operating Costs for Bulk, Ro-ro and Container Ships', Bureau of Transport Economics*

78. *Gkonis, K.G. and Psaraftis, H.N. (2012) 'Modeling tankers' optimal speed and emissions', Society of Naval Architects and Marine Engineers. Transactions, 120, pp. 90-115.*

79. *Glover, F. (1989) 'Tabu search—part I', ORSA Journal on computing, 1(3), pp. 190-206.*

80. *Glover, F. (1990) 'Tabu search—part II', ORSA Journal on computing, 2(1), pp. 4-32.*

81. Glover, F., Laguna, M., Taillard, E. and De Werra, D. (1993) 'Tabu search', Annals of Operations Research, 41(1), pp. 3-28.

82. Glover, F. and Marti, R. (2006) 'Tabu Search', in Alba, E. and Martí, R. (eds.) Metaheuristic Procedures for Training Neutral Networks. Boston, MA: Springer US, pp. 53-69.

83. Goldberg, D.E. and Holland, J.H. (1988) 'Genetic Algorithms and Machine Learning', Machine Learning, 3(2), pp. 95-99.

84. Guin, J.A. (1968) 'Modification of the complex method of constrained optimization', The Computer Journal, 10(4), pp. 416-417.

85. Guldhammer, H.E. and Harvald, S.A. (1974) Ship resistance : Effect of Form and Principal Dimensions. Cph.: Akademisk Forlag.

86. Haakenstad, K. (2012) Analysis and correction of sea trials. Master thesis [Online]. Available at: http://www.diva-portal.org/smash/get/diva2:566119/FULLTEXT01.pdf (Accessed: August 2015).

87. Hajela, P. (1999) 'Nongradient methods in multidisciplinary design optimization-status and potential', Journal of aircraft, 36(1), pp. 255-265.

88. Harvald, S.A. (1983) Resistance and propulsion of ships. New York: Wiley.

89. Harvald, S.A. (1992) Resistance and propulsion of ships. Malabar, Fla: Krieger Pub.

90. Hellenic Shipping News. [Online]. Available at: http://www.hellenicshippingnews.com.

91. Hernández-Domínguez, J.S., Toscano-Pulido, G. and Coello Coello, C.A. (2012) Berlin, Heidelberg. Springer Berlin Heidelberg.

92. Hill, N., Watson, R. and James, K. (2016) Government GHG conversion factors for company reporting: methodology paper for emission factors. Department for Business, Energy & Industrial Strategy (BEIS). [Online]. Available at: https://www.gov.uk/government/uploads/system/uploads/attachment_data/file/553488/2016_methodology_paper_Final_V01-00.pdf.

93. Hirdaris, S. and Cheng, F. (2012) 'Keynote Paper - The Role of Technology in Green Ship Design', IMDC2012. Galsgow, United Kingdom. pp. 21-40.

94. A History of the Baltic indices. Poslovni.hr. [Online]. Available at: http://www.poslovni.hr/media/PostAttachments/312464/Indeksi%20i%20velicina%20brodova.pdf.

95. *Hochkirch, K. and Bertram, V. (2010) 'Engineering options for more fuel efficient ships', Proceedings of first international symposium on fishing vessel energy efficiency. Vigo, Spain.*

96. *Holland, J. (1975) 'Adaptation in natural and artificial systems: an introductory analysis with application to biology', Control and artificial intelligence.*

97. *Holland, J.H. (1992) Adaptation in Natural and Artificial Systems: An Introductory Analysis with Applications to Biology, Control and Artificial Intelligence. MIT press.*

98. *Holtrop, J. (1977) 'A statistical analysis of performance test results', International Shipbuilding Progress, 24(270), pp. 23-28.*

99. *Holtrop, J. (1984) 'A statistical re-analysis of resistance and propulsion data', International Shipbuilding Progress, 31(363), pp. 272-276.*

100. *Holtrop, J. and Mennen, G.G. (1982) 'An approximate power prediction method', International Shipbuilding Progress, 29(335), pp. 166-170.*

101. *Hu, X., Wang, M. and Paolo, E.D. (2013) 'Calculating Complete and Exact Pareto Front for Multiobjective Optimization: A New Deterministic Approach for Discrete Problems', IEEE Transactions on Cybernetics, 43(3), pp. 1088-1101.*

102. *Hughes, G. (1954) 'Friction and form resistance in turbulent flow, and a proposed formulation for use in model and ship correlation', Trans. RINA, 96.*

103. *Hwang, C.L., Paidy, S.R., Yoon, K. and Masud, A.S.M. (1980) 'Mathematical programming with multiple objectives: A tutorial', Computers & Operations Research, 7(1), pp. 5-31.*

104. *IMO (1993) Interim Standards for Ship Manoeuvrability. IMO Resolution A. 751(18) adopted on 4 November 1993.*

105. *IMO (2016) IMO Train the Trainer (TTT) Course on Energy Efficient Ship Operation. Module 2 – Ship Energy Efficiency Regulations and Related Guidelines. London: International Maritime Organisation.*

106. *IMO (2017) Low carbon shipping and air pollution control. Available at: www.IMO.org.*

107. *IMO MEPC 57/4/5 (2007) 'Prevention of air pollution from ships: Report of the Intersessional Correspondence Group on Greenhouse Gas Related Issues'.*

108. *IMO MEPC 60/4/34 (2010) 'Prevention of air pollution from ships: Influence of Design Parameters on the Energy Efficiency Design Index for Tankers, Containerships, and LNG Carriers'. Available at: http://www.rina.org.uk/c2/uploads/mepc%2060_4_34.pdf.*

109. IMO MEPC 63/23 Annex 9. (2012) '2012 Guidelines for the Development of a Ship Energy Efficiency Management Plan (SEEMP)'. Available at: http://www.imo.org/en/KnowledgeCentre/IndexofIMOResolutions/Documents/MEPC%20-%20Marine%20Environment%20Protection/213(63).pdf.

110. IMO MEPC 68/6/4 (2011) 'Consideration and adoption of amendments to mandatory instruments - Calculation of parameters for determination of EEDI reference values'. Available at: http://www1.veristar.com/veristar/dps_info.nsf/0/ec849aeef0cc79c6c1257957003cbc9a/$FILE/MEPC_62-6-4.pdf.

111. IMO MEPC.1/CIrc.683. (17 August 2009) 'GUIDANCE FOR THE DEVELOPMENT OF A SHIP ENERGY EFFICIENCY MANAGEMENT PLAN (SEEMP) '. Available at: https://www.register-iri.com/forms/upload/MEPC.1-Circ.683.pdf.

112. Inkpen, A.C. and Moffett, M.H. (2011) The global oil & gas industry management, strategy & finance. PennWell,. Available at: http://app.knovel.com.libproxy.ncl.ac.uk/web/toc.v/cid:kpGOGIMSF1.

113. Intergovernmental Panel on Climate Change (2006) IPCC guidelines for national greenhouse gas inventories. [Online]. Available at: http://www.ipcc-nggip.iges.or.jp./public/2006gl/index.html.

114. Intermodal. [Online]. Available at: http://www.intermodal.gr/.

115. International Organization for Standardization ISO (2015) ISO 15016:2015 (The 2nd revised edition of ISO 15016:2002): Ships and marine technology -- Guidelines for the assessment of speed and power performance by analysis of speed trial data.http://www.iso.org/iso/home/store/catalogue_tc/catalogue_detail.htm?csnumber=61902.

116. ITTC (1957) 'Report of the skin friction and turbulence simulation committe', Proceedings of the 8th International Towing Tank Conference, Madrid.

117. ITTC (1979) '1978 ITTC Performance Prediction Method', International Towing Tank Conference.

118. J. Falls and Mayer, R. (2012) Principles of Ship Performance. United States Naval Academy USNA. Available at: http://www.usna.edu/NAOE/academics/en400.php#catalog (Accessed: September 2015).

119. Jalkanen, J.P., Brink, A., Kalli, J., Pettersson, H., Kukkonen, J. and Stipa, T. (2009) 'A modelling system for the exhaust emissions of marine traffic and its application in the Baltic Sea area', Atmospheric Chemistry and Physics, 9(23), pp. 9209-9223.

120. Jalkanen, J.P., Johansson, L., Kukkonen, J., Brink, A., Kalli, J. and Stipa, T. (2012) 'Extension of an assessment model of ship traffic exhaust emissions for particulate matter and carbon monoxide', Atmos. Chem. Phys., 12(5), pp. 2641-2659.

121. *Janet Porter - Lloyd's list (2009) BV chief rejects rival's view on slow steaming.*

122. *Jansson, A. (1994) 'Fluid power system design-a simulation approach'.*

123. *Jensen, G. (1994) 'Moderne Schiffslinien', Handbuch der Werften, XXII, p. 93.*

124. *Jinfeng, H. (2012) 'Hull form hydrodynamic optimization based on parametric modeling', Systems and Informatics (ICSAI), 2012 International Conference on. 19-20 May 2012. pp. 1196-1200. Available at: http://ieeexplore.ieee.org/xpls/abs_all.jsp?arnumber=6223249.*

125. *Jon Rysst and Eirik Nyhus (2009) 'Climate change regulations - consequences for ship design in a challenging business environment', 10th International Marine Design Conference (IMDC 2009), Trondheim, Norway. Trondheim, Norway. Tapir Academic Press, pp. 36-46.*

126. *Jorge d' Almeida (2009) Arquitectura Naval - O Dimensionamento do Navio. Tipografia Lousanense.*

127. *Justin Stares - Lloyd's list (2008a) IMO sulphur limits deal could see more freight hit the road.*

128. *Kennedy, J. and Eberhart, R. (1995) Neural Networks, 1995. Proceedings., IEEE International Conference on. Nov/Dec 1995.*

129. *Kim, H. (2009) 'Multi-Objective Optimization for ship hull form design'.*

130. *Kirkpatrick, S., Gelatt Jr, C.D. and Vecchi, M.P. (1983) 'Optimization by simulated annealing', Science, 220(4598), pp. 671-680.*

131. *Klanac, A., Nikolić, P., Kovac, M. and McGregor, J. (2010) 'Economics and environmental impact of ship speed reduction for AFRAMAX tankers', Proceedings of XIX SORTA Conference.*

132. *Knapp, S., Kumar, S.N. and Remijn, A.B. (2008) 'Econometric analysis of the ship demolition market', Marine Policy, 32(6), pp. 1023-1036.*

133. *Konak, A., Coit, D.W. and Smith, A.E. (2006) 'Multi-objective optimization using genetic algorithms: A tutorial', Reliability Engineering & System Safety, 91(9), pp. 992-1007.*

134. *Kristenen, H.O. and Psaraftis, H. (2015) Energy demand and exhaust gas emissions of marine engines. HOK Marineconsult ApS and The Technical University of Denmark.*

135. *Kristensen, H.O. (2012) Prediction of Ship Resistance and Propulsion Power (ULYSSES). Technical University of Denmark (DTU) (Accessed: 2012).*

136. Lackenby, H. (1950) 'On the systematic geometrical variation of ship forms', Trans. INA, 92, pp. 289-315.

137. Lackenby, H. and Milton, D. (1972) 'DTMB STANDARD SERIES 60. A NEW PRESENTATION OF THE RESISTANCE DATA FOR BLOCK COEFFICIENT, LCB, BREADTH-DRAUGHT RATIO, AND LENGTH-BREADTH RATIO VARIATIONS', Publication of: ASSOCIATION OF AMERICAN RAILROADS, 114.

138. Lamb, T. and Society of Naval Architects and Marine Engineers (U.S.) (2003) Ship design and construction. Society of Naval Architects and Marine Engineers,. Available at: http://app.knovel.com.libproxy.ncl.ac.uk/web/toc.v/cid:kpSDCV0001.

139. Li, S. and Zhao, F. (2012) 'An Innovative Hullform Design Technique for Low Carbon Shipping', Journal of Shipping and Ocean Engineering, 2(1), pp. 28-35.

140. Lin, C. and Feng, Q. (2007) 'The Standard Particle Swarm Optimization Algorithm Convergence Analysis and Parameter Selection', Natural Computation, 2007. ICNC 2007. Third International Conference on. 24-27 Aug. 2007. pp. 823-826.

141. Lindstad, H., Asbjørnslett, B.E. and Strømman, A.H. (2011) 'Reductions in greenhouse gas emissions and cost by shipping at lower speeds', Energy Policy, 39(6), pp. 3456-3464.

142. Lloyd's Register (2012a) Implementing a ship energy efficiency management plan (SEEMP): Guidance for shipowners and operators - June 2012 (version 2.0). London.

143. Lloyd's Register (2012b) Implementing the Energy Efficiency Design Index (EEDI): Guidance for owners, operators, shipyards and tank test organisations- December 2012 (version 3.0). London.

144. Lloyd's Register (2013) Rules and Regulations for the Classification of Ships (Pt 3, Ch5).

145. Lochner, R.H. and Matar, J.E. (1990) Designing for quality : an introduction to the best of Taguchi and western methods of statistical experimental design. ASQC Quality Press.

146. Logothetis, N. and Wynn, H.P. (1989) Quality through design: experimental design, off-line quality control, and Taguchi's contributions. Oxford England

147.

148. Lun, Y.H.V., Hilmola, O.-P., Goulielmos, A.M., Lai, K.-h. and Cheng, T.C.E. (2012) Oil transport management. Springer Science & Business Media.

149. Maggs, J. (2011) Speed Limits for Ships. European Climate Change Programme (EECP). [Online]. Available at: https://ec.europa.eu/clima/sites/clima/files/docs/0036/steaming_en.pdf.

150. MAN B&W (2001) Basic Principles of Ship Propulsion. MAN B&W Diesel A/S.

151. MAN Diesel & Turbo (2010) SFOC Optimisation Methods – For MAN B&W Two-stroke IMO Tier II Engines.

152. MAN Diesel & Turbo (2013) Marine Engine IMO Tier ll - Programme 2013.

153. MARPOL Annex VI (2013) EEDI & SEEMP. Available at: https://www.marpol-annex-vi.com/.

154. McQuilling Services LLC. [Online]. Available at: https://www.mcquilling.com/.

155. MEPC - IMO (2012) 'GUIDELINES ON SURVEY AND CERTIFICATION OF THE ENERGY EFFICIENCY DESIGN INDEX (EEDI) - RESOLUTION MEPC.214(63) - Adopted on 2 March 2012 '. IMO. Available at: http://www.imo.org/en/KnowledgeCentre/IndexofIMOResolutions/Documents/MEPC%20-%20Marine%20Environment%20Protection/214(63).pdf.

156. Michalski, J.P. (2004a) 'Parametric method of prediction of the ship operating costs', Polish Maritime Research, (S 1), pp. 20-23.

157. Michalski, J.P. (2004b) 'Parametric method of preliminary prediction of the ship building costs', Polish Maritime Research, (S 1), pp. 16-19.

158. Miola, A. and Ciuffo, B. (2011) 'Estimating air emissions from ships: Meta-analysis of modelling approaches and available data sources', Atmospheric Environment, 45(13), pp. 2242-2251.

159. Miola, A., Ciuffo, B., Giovine, E. and Marra, M. (2010) 'Regulating air emissions from ships: the state of the art on methodologies, technologies and policy options', Regulating Air Emissions from Ships: The State of the Art on Methodologies, Technologies and Policy Options.

160. Molland, A.F., Turnock, S.R. and Houdson, D.A. (2009) 'Design Metrics for Evaluating the Propulsive Efficiency of future Ships', 10th International Marine Design Conference. Trondheim, Norway. Tapir Academic Press, pp. 209-225.

161. Molland, A.F., Turnock, S.R. and Hudson, D.A. (2011) Ship resistance and propulsion : practical estimation of ship propulsive power. New York: Cambridge University Press.

162. Mongeau, M., Karsenty, H., Rouzé, V. and Hiriart-Urruty, J.B. (2000) 'Comparison of public-domain software for black box global optimization', Optimization Methods and Software, 13(3), pp. 203-226.

163. Moore Stephens LLP. (2013) 'OpCost 2013 : Benchmarking vessel running costs'. London: Moore Stephens LLP.

164. Mori, T. (2011) Taguchi methods : benefits, impacts, mathematics, statistics, and applications. New York: ASME Press.

165. Mulligan, R.F. (2008) 'A Simple Model for Estimating Newbuilding Costs', Maritime Econ Logistics, 10(3), pp. 310-321.

166. Murphy, A.J., Landamore, M., Pazouki, K. and Gibson, M. (2013) 'Modelling ship emission factors and emission indices', Low Carboon Shipping Conference, London.

167. OCIMF (2011a) Energy Efficiency Design Index (EEDI). [Online]. Available at: https://www.ocimf.org/.

168. OCIMF (2011b) GHG Emission-Mitigating Measures for Oil Tankers - Part A: Review of Reduction Potential. London. [Online]. Available at: http://www.ocimf.org/library/information-papers/ (Accessed: January 2014).

169. OECD (2010) Globalisation, Transport and the Environment. OECD Publishing.

170. Olesen, H.R., Winther, M., Ellermann, T., Christensen, J. and Plejdrup, M. (2009) 'Ship Emissions and air pollution in Denmark. Present situation and future scenarios', Danish Ministry of the Environment.

171. Osiadacz, A.J. (1989) 'Multiple criteria optimization; theory, computation, and application, Ralph E. Steuer, Wiley Series in Probability and Mathematical Statistics-Applied, Wiley, 1986, No. of pages 546, Price f5 1.40, $77.10', Optimal Control Applications and Methods, 10(1), pp. 89-90.

172. Osyczka, A. (1984) Multicriterion optimization in engineering with FORTRAN programs. Chichester.

173. Pacheco, J. and Martí, R. (2006) 'Tabu search for a multi-objective routing problem', Journal of the operational research society, 57(1), pp. 29-37.

174. Papanikolaou, A. (2014) Ship design: methodologies of preliminary design. Springer.

175. Parsons, M.G. and Scott, R.L. (2004) 'Formulation of Multicriterion Design Optimization Problems for Solution With Scalar Numerical Optimization Methods', Journal of Ship Research, 48(1), pp. 61-76.

176. Paxian, A., Eyring, V., Beer, W., Sausen, R. and Wright, C. (2010) 'Present-day and future global bottom-up ship emission inventories including polar routes', Environmental Science and Technology, 44(4), pp. 1333-1339.

177. Peace, G.S. (1993) Taguchi methods : a hands-on approach. Reading, Mass.: Addison-Wesley.

178. *Pedersen, B.P. and Larsen, J. (2009) 'Modeling of ship propulsion performance', World Maritime Technology Conference WMTC2009, Jan. 21. Available at: http://www.dcmt.dk/fpublic/dcmt/dokumenter/maga%20dokumenter/Papers/Benjamin/Modeling%20of%20Ship%20Propulsion%20Performance.pdf (Accessed: 14-08-2014).*

179. *Percival, S., Hendrix, D. and Noblesse, F. (2001) 'Hydrodynamic optimization of ship hull forms', Applied Ocean Research, 23(6), pp. 337-355.*

180. *Peri, D., Rossetti, M. and Campana, E.F. (2001) 'Design Optimization of Ship Hulls via CFD Techniques', Journal of Ship Research, 45(2), pp. 140-149.*

181. *Perzina, R. and Ramík, J. (2014) 'Microsoft Excel as a Tool for Solving Multicriteria Decision Problems', Procedia Computer Science, 35, pp. 1455-1463.*

182. *Philippe Crist (2009) Greenhouse Gas Emissions Reduction Potential from International Shipping (2009/11). Joint Transport Research Centre of the OECD and the International Transport Forum Publishing, O. [Online]. Available at: http://www.oecd-ilibrary.org/transport/greenhouse-gas-emissions-reduction-potential-from-international-shipping_223743322616.*

183. *Počuča, M. (2006) 'Methodology of day-to-day ship costs assessment', PROMET-Traffic&Transportation, 18(5), pp. 337-345.*

184. *Prohaska, C.W. (1966) 'A simple method for the evaluation of the form factor and low speed wave resistance', Proceedings 11th ITTC.*

185. *Psaraftis, H.N. and Kontovas, C.A. (2008) Ship emissions study. Prepared for Hellenic Chamber of Shipping. [Online]. Available at: http://nee.gr/downloads/66ship.emissions.study.pdf.*

186. *Psaraftis, H.N. and Kontovas, C.A. (2009) 'Ship Emissions: Logistics and Other Tradeoffs', 10th International Marine Design Conference (IMDC 2009), Trondheim, Norway. Trondheim, Norway. Tapir Academic Press, pp. 904-921.*

187. *Psaraftis, H.N. and Kontovas, C.A. (2010) 'Balancing the economic and environmental performance of maritime transportation', Transportation Research Part D: Transport and Environment, 15(8), pp. 458-462.*

188. *Psaraftis, H.N. and Kontovas, C.A. (2013) 'Speed models for energy-efficient maritime transportation: A taxonomy and survey', Transportation Research Part C: Emerging Technologies, 26(0), pp. 331-351.*

189. *Psaraftis, H.N., Lyridis, D.V. and Kontovas, C.A. (2012) 'The economics of ships', The Blackwell Companion to Maritime Economics, 11, p. 373.*

190. Ragab, S.A. (2001) 'An Adjoint Formulation for Shape Optimization in Free-Surface Potential Flow', Journal of Ship Research, 45(4), pp. 269-278.

191. Rechenberg, E. (1973) 'Optimierung technischer Systeme nach Prinzipien der biologischen Evolution. 1973', Frommann-Holzboog Verlag, Stuttgart.

192. Review of Maritime Transport (2011, 2012, 2013).

193. Rigo, P. (2001) 'Least-cost structural optimization oriented preliminary design', Journal of Ship Production, 17(4), pp. 202-215.

194. Robert, F.M. (2008) 'A Simple Model for Estimating Newbuilding Costs', Maritime Economics & Logistics, 10(3), pp. 310-321.

195. Ronen, D. (1982) 'The Effect of Oil Price on the Optimal Speed of Ships', The Journal of the Operational Research Society, 33(11), pp. 1035-1040.

196. Ross, J. (2005) 'Weight-based cost estimating during initial design', COMPIT'05.

197. Ross, J.M. (2004) COMPIT.

198. Ross, P.J. (1988) Taguchi techniques for quality engineering : loss function, orthogonal experiments, parameter and tolerance design. New York: McGraw-Hill.

199. Ross, P.J. (1996) Taguchi techniques for quality engineering : loss function, orthogonal experiments, parameter and tolerance design. 2nd edn. New York: McGraw-Hill.

200. Ruzika, S. and Wiecek, M.M. (2005) 'Approximation Methods in Multiobjective Programming', Journal of Optimization Theory and Applications, 126(3), pp. 473-501.

201. S&P Global - Platts. [Online]. Available at: https://www.platts.com/.

202. Schittkowski, K. (2003) NLPJOB Version 2.0: A Fortran Code for Multicriteria Optimization- User's Guide. [Online]. Available at: https://tomopt.com/docs/NLPJOB.pdf.

203. Schrooten, L., De Vlieger, I., Panis, L.I., Chiffi, C. and Pastori, E. (2009) 'Emissions of maritime transport: A European reference system', Science of the Total Environment, 408(2), pp. 318-323.

204. Shetelig, H. (2013) Shipbuilding Cost Estimation: Parametric Approach. Institutt for marin teknikk.

205. Simpson Spence & Young Ltd Tanker forward freight agreements.

206. Skjølsvik, K.O., Andersen, A.B., Corbett, J.J. and Skjelvik, J.M. (2000) 'Study of greenhouse gas emissions from ships (report to International Maritime Organization on the outcome of the IMO Study on Greenhouse Gas Emissions from Ships)', Study of Greenhouse Gas Emissions from Ships.

207. Smith, T.W.P., Parker, S. and Rehmatulla, N. (2011) International Conference on Technologies, Operations, Logistics and Modelling for Low Carbon Shipping, LCS2011. University of Strathclyde, Glasgow, UK.

208. Sophia Parker, Carlo Raucci, Tristan Smith and Ludovic Laffineur (2015) Understanding the Energy Efficiency Operational Indicator: an empirical analysis of ships from the Belgian Shipowners' Association UCL Energy Institute, Royal Belgian Shipowners' Association. [Online]. Available at: http://www.lowcarbonshipping.co.uk/files/Ben_Howett/RBSA_final_main.pdf.

209. Spendley, W., Hext, G.R. and Himsworth, F.R. (1962) 'Sequential application of simplex designs in optimisation and evolutionary operation', Technometrics, 4(4), pp. 441-461.

210. Spillers, W.R. and MacBain, K.M. (2009) 'Multicriteria Optimization', in Structural Optimization. Boston, MA: Springer US, pp. 175-178.

211. Stopford, M. (2009) Maritime economics. 3rd edn. London: Routledge.

212. Stuer-Lauridsen, F., Husum, H., Jensen, M.P., Odgaard, T. and Winther, K.M. (2004) 'Oil tanker phase-out and the ship scrapping industry: a study on the implications of the accelerated phase out scheme of single hull tankers proposed by the EU for the world ship scrapping and recycling industry', Final Report, Brussels.

213. Sullivan, W.G., Wicks, E.M. and Luxhoj, J.T. (2006) Engineering economy. 13th edn. Upper Saddle River, N.J.: Pearson/Prentice Hall.

214. Swann, W.H. (1969) 'A survey of non-linear optimization techniques', FEBS letters, 2(S1), pp. S39-S55.

215. Szelangiewicz, T. and Żelazny, K. 14 (2007) 'Calculation of the mean long-term service speed of transport ship: Part III Influence of shipping route and ship parameters on its service speed' Polish Maritime Research. p. 27 2. Available at: //www.degruyter.com/view/j/pomr.2007.14.issue-2/v10012-007-0010-4/v10012-007-0010-4.xml (Accessed: 2015-09-29t02:37:58.097+02:00).

216. Szelangiewicz, T. and Żelazny, K. (2012) 'The influence of chosen parameters on the Energy Efficiency Design Index', Zeszyty Naukowe/Akademia Morska w Szczecinie, (32 (104) z. 1), pp. 102-107.

217. Taguchi, G. and Phadke, M.S. (1989) 'Quality Engineering through Design Optimization', in Dehnad, K. (ed.) Quality Control, Robust Design, and the Taguchi Method. Boston, MA: Springer US, pp. 77-96.

218. Taguchi, G.B. (1993) Taguchi on robust technology development : bringing quality engineering upstream. New York: ASME Press.

219. Taguchi, G.B. and Wu, Y.-i. (1985) Introduction to off-line quality control. Nagaya, Japan: Central Japan Quality Control Assoc.

220. Teukolsky, S.A., Flannery, B.P., Press, W.H. and Vetterling, W.T. (1992) 'Numerical recipes in C', SMR, 693(1).

221. Third IMO GHG Study (2014). [Online]. Available at: http://www.imo.org/en/OurWork/Environment/PollutionPrevention/AirPollution/Documents/Third%20Greenhouse%20Gas%20Study/GHG3%20Executive%20Summary%20and%20Report.pdf.

222. Tien Anh, T. (2016) 'Calculation and Assessing the EEDI Index in the Field of Ship Energy', Journal of Marine Science: Research & Development, 6(6).

223. Todd, F.H. (1953) 'Some further experiments on single screw merchant ship forms-series 60', Transactions of the Society of Naval Architects and Marine Engineers, 61, pp. 516-589.

224. Todd, F.H., Stuntz, G.R. and Pien, P.C. (1957) 'Series 60—The Effect upon Resistance and Power of Variation in Ship Proportions', Trans. SNAME, 65, pp. 445-589.

225. Townsin, R.L. and Kwon, Y.J. (1983) 'Approximate formulae for the speed loss due to added resistance in wind and waves', Transactions RINA, 125.

226. Tran, T.A. (2017) 'A research on the energy efficiency operational indicator EEOI calculation tool on M/V NSU JUSTICE of VINIC transportation company, Vietnam', Journal of Ocean Engineering and Science, 2(1), pp. 55-60.

227. Trodden, D.G. (2014) Optimal Propeller Selection when Accounting for a Ship's Manoeuvring Response due to Environmental Loading. Newcastle University.

228. Trozzi, C. (2010) 'Emission estimate methodology for maritime navigation. ', 19th Annual International Emission Inventory Conference. Rome.

229. Tzannatos, E. (2010) 'Ship emissions and their externalities for the port of Piraeus - Greece', Atmospheric Environment, 44(3), pp. 400-407.

230. ULYSSES (2011) (Proposal number: 266030).

231. Van Den Boom, H., Van Der Hout, I. and Flikkema, M. (2008) 'Speed-power performance of ships during trials and in service', 2nd International Symposium on Ship Operations, Management and Economics 2008. pp. 22-28. Available at: http://www.scopus.com/inward/record.url?eid=2-s2.0-77956324338&partnerID=40&md5=4bb8220ab8e825b8385084d59a6ded52.

232. Vladimir, N., Ančić, I. and Šestan, A. (2017) 'Effect of ship size on EEDI requirements for large container ships', Journal of Marine Science and Technology.

233. Wang, C. and Corbett, J.J. (2007) 'The costs and benefits of reducing SO2 emissions from ships in the US West Coastal waters', Transportation Research Part D: Transport and Environment, 12(8), pp. 577-588.

234. Wang, C., Corbett, J.J. and Firestone, J. (2007) 'Modeling energy use and emissions from North American shipping: Application of the ship traffic, energy, and environment model', Environmental Science and Technology, 41(9), pp. 3226-3232.

235. Wang, D., Tan, D. and Liu, L. (2018) 'Particle swarm optimization algorithm: an overview', Soft Computing, 22(2), pp. 387-408.

236. Wang, H., Wang, C. and Zhang, L. (2010) 'Evaluating the economic reasons of China's stance on ship-based GHG reduction negotiations', Proceedings of the 89th TRB Annual Meeting. Washington DC.

237. Watson, D.G.M. (1998) Practical ship design. 1st edn. Amsterdam: Elsevier.

238. Weber Tanker Report / Week 10 - March 2013. [Online]. Available at: http://cdn.capitallink.com/files/docs/shipping_industry_reports/WeberWeekly10-13.pdf.

239. Whitley, D. (1994) 'A genetic algorithm tutorial', Statistics and computing, 4(2), pp. 65-85.

240. Wijnolst, N. and Wergeland, T. (2009) Shipping innovation. IOS Press.

241. Wilson, R.V., Carrica, P.M. and Stern, F. (2007) 'Simulation of ship breaking bow waves and induced vortices and scars', International journal for numerical methods in fluids, 54(4), pp. 419-451.

242. Worldscale Association (London) and Worldscale Association (NYC) 'New worldwide tanker nominal freight scale : applying to the carriage of oil in bulk : effective 1st January'. London

243. New York: Worldscale Association (London) Ltd. ;

244. Worldscale Association (NYC) Inc. Available at: http://www.worldscale.co.uk/Worldscale/home%5Fstart.asp.

245. Wright, P., Hutchinson, K., White, G. and Applegarth, I. (2012) AVEVA Initial Design 12.1, Undergraduate Student User Notes. Newcastle University.

246. Wu, Y. and Wu, A. (2000) Taguchi Methods for robust design. New York: ASME Press.

247. Xiujuan, L. and Zhongke, S. (2004) 'Overview of multi-objective optimization methods', Journal of Systems Engineering and Electronics, 15(2), pp. 142-146.

248. Xu, J.J., Yip, T.L. and Liu, L. (2011) 'A directional relationship between freight and newbuilding markets: A panel analysis', Maritime Econ Logistics, 13(1), pp. 44-60.

249. Zakaria, N.M.G. and Baree, M.S. (2008) 'Alternative Methods on Added Resistance of Ships in Regular Head Waves', The Institution of Engineers, Malaysia, 69(4), pp. 15-22.

250. Zeleny, M. and Cochrane, J.L. (1973) Multiple criteria decision making. University of South Carolina Press.

251. Zitzler, E., Laumanns, M. and Bleuler, S. (2004) 'A tutorial on evolutionary multiobjective optimization', in Metaheuristics for multiobjective optimisation. Springer, pp. 3-37.

Appendices

Appendix A

A1 - Runs layout for Stage Three:

StdOrder	L	B/T	CB	LCB
1	1	1	1	1
2	1	1	1	2
3	1	1	1	3
4	1	1	2	1
5	1	1	2	2
6	1	1	2	3
7	1	1	3	1
8	1	1	3	2
9	1	1	3	3
10	1	2	1	1
11	1	2	1	2
12	1	2	1	3
13	1	2	2	1
14	1	2	2	2
15	1	2	2	3
16	1	2	3	1
17	1	2	3	2
18	1	2	3	3
19	1	3	1	1
20	1	3	1	2
21	1	3	1	3
22	1	3	2	1
23	1	3	2	2
24	1	3	2	3
25	1	3	3	1
26	1	3	3	2
27	1	3	3	3
28	2	1	1	1
29	2	1	1	2

30	2	1	1	3
31	2	1	2	1
32	2	1	2	2
33	2	1	2	3
34	2	1	3	1
35	2	1	3	2
36	2	1	3	3
37	2	2	1	1
38	2	2	1	2
39	2	2	1	3
40	2	2	2	1
41	2	2	2	2
42	2	2	2	3
43	2	2	3	1
44	2	2	3	2
45	2	2	3	3
46	2	3	1	1
47	2	3	1	2
48	2	3	1	3
49	2	3	2	1
50	2	3	2	2
51	2	3	2	3
52	2	3	3	1
53	2	3	3	2
54	2	3	3	3
55	3	1	1	1
56	3	1	1	2
57	3	1	1	3
58	3	1	2	1
59	3	1	2	2
60	3	1	2	3
61	3	1	3	1
62	3	1	3	2
63	3	1	3	3
64	3	2	1	1
65	3	2	1	2

66	3	2	1	3
67	3	2	2	1
68	3	2	2	2
69	3	2	2	3
70	3	2	3	1
71	3	2	3	2
72	3	2	3	3
73	3	3	1	1
74	3	3	1	2
75	3	3	1	3
76	3	3	2	1
77	3	3	2	2
78	3	3	2	3
79	3	3	3	1
80	3	3	3	2
81	3	3	3	3

A2– Design parameters for Stage Three:

StdOrder	L	B/T	CB	LCB
1	186.3	2.383	0.776	95.984
2	186.3	2.383	0.776	97.847
3	186.3	2.383	0.776	99.710
4	186.3	2.383	0.817	95.984
5	186.3	2.383	0.817	97.847
6	186.3	2.383	0.817	99.710
7	186.3	2.383	0.858	95.984
8	186.3	2.383	0.858	97.847
9	186.3	2.383	0.858	99.710
10	186.3	2.621	0.776	95.984
11	186.3	2.621	0.776	97.847
12	186.3	2.621	0.776	99.710
13	186.3	2.621	0.817	95.984
14	186.3	2.621	0.817	97.847
15	186.3	2.621	0.817	99.710
16	186.3	2.621	0.858	95.984

17	186.3	2.621	0.858	97.847
18	186.3	2.621	0.858	99.710
19	186.3	2.86	0.776	95.984
20	186.3	2.86	0.776	97.847
21	186.3	2.86	0.776	99.710
22	186.3	2.86	0.817	95.984
23	186.3	2.86	0.817	97.847
24	186.3	2.86	0.817	99.710
25	186.3	2.86	0.858	95.984
26	186.3	2.86	0.858	97.847
27	186.3	2.86	0.858	99.710
28	204.525	2.383	0.776	105.374
29	204.525	2.383	0.776	107.419
30	204.525	2.383	0.776	109.464
31	204.525	2.383	0.817	105.374
32	204.525	2.383	0.817	107.419
33	204.525	2.383	0.817	109.464
34	204.525	2.383	0.858	105.374
35	204.525	2.383	0.858	107.419
36	204.525	2.383	0.858	109.464
37	204.525	2.621	0.776	105.374
38	204.525	2.621	0.776	107.419
39	204.525	2.621	0.776	109.464
40	204.525	2.621	0.817	105.374
41	204.525	2.621	0.817	107.419
42	204.525	2.621	0.817	109.464
43	204.525	2.621	0.858	105.374
44	204.525	2.621	0.858	107.419
45	204.525	2.621	0.858	109.464
46	204.525	2.86	0.776	105.374
47	204.525	2.86	0.776	107.419
48	204.525	2.86	0.776	109.464
49	204.525	2.86	0.817	105.374
50	204.525	2.86	0.817	107.419
51	204.525	2.86	0.817	109.464
52	204.525	2.86	0.858	105.374

53	204.525	2.86	0.858	107.419
54	204.525	2.86	0.858	109.464
55	222.75	2.383	0.776	114.764
56	222.75	2.383	0.776	116.991
57	222.75	2.383	0.776	119.219
58	222.75	2.383	0.817	114.764
59	222.75	2.383	0.817	116.991
60	222.75	2.383	0.817	119.219
61	222.75	2.383	0.858	114.764
62	222.75	2.383	0.858	116.991
63	222.75	2.383	0.858	119.219
64	222.75	2.621	0.776	114.764
65	222.75	2.621	0.776	116.991
66	222.75	2.621	0.776	119.219
67	222.75	2.621	0.817	114.764
68	222.75	2.621	0.817	116.991
69	222.75	2.621	0.817	119.219
70	222.75	2.621	0.858	114.764
71	222.75	2.621	0.858	116.991
72	222.75	2.621	0.858	119.219
73	222.75	2.86	0.776	114.764
74	222.75	2.86	0.776	116.991
75	222.75	2.86	0.776	119.219
76	222.75	2.86	0.817	114.764
77	222.75	2.86	0.817	116.991
78	222.75	2.86	0.817	119.219
79	222.75	2.86	0.858	114.764
80	222.75	2.86	0.858	116.991
81	222.75	2.86	0.858	119.219

Appendix B

The average (P_D/Dis) and the mean S/N ratio:

StdOrder	Average y (P_D/Dis)	S/N
Original	0.0704	20.0018
1	0.0664	20.7273
2	0.0676	20.5356
3	0.0691	20.3144
4	0.0692	20.1317
5	0.0717	19.7601
6	0.0748	19.3056
7	0.0768	18.7839
8	0.0834	17.9324
9	0.0930	16.7672
10	0.0684	20.4657
11	0.0697	20.2685
12	0.0712	20.0412
13	0.0717	19.8044
14	0.0743	19.4236
15	0.0777	18.9539
16	0.0805	18.3448
17	0.0875	17.4708
18	0.0981	16.2585
19	0.0705	20.1960
20	0.0719	19.9955
21	0.0735	19.7638
22	0.0742	19.4927
23	0.0770	19.1075
24	0.0805	18.6343
25	0.0839	17.9673
26	0.0913	17.0879
27	0.1025	15.8577
28	0.0620	21.4585
29	0.0630	21.2989
30	0.0641	21.1168
31	0.0636	21.0510
32	0.0655	20.7393
33	0.0679	20.3637
34	0.0685	20.0409
35	0.0733	19.3522
36	0.0803	18.3783
37	0.0640	21.1773
38	0.0650	21.0122

39	0.0662	20.8249
40	0.0660	20.7077
41	0.0692	20.1938
42	0.0722	19.7397
43	0.0744	19.2162
44	0.0808	18.3439
45	0.0915	16.9977
46	0.0661	20.8918
47	0.0672	20.7230
48	0.0684	20.5280
49	0.0685	20.3654
50	0.0707	20.0393
51	0.0734	19.6364
52	0.0753	19.1586
53	0.0810	18.3986
54	0.0894	17.3429
55	0.0588	22.0255
56	0.0596	21.8895
57	0.0605	21.7371
58	0.0595	21.7619
59	0.0611	21.4958
60	0.0630	21.1812
61	0.0627	21.0186
62	0.0666	20.3976
63	0.0721	19.5584
64	0.0607	21.7336
65	0.0615	21.5917
66	0.0625	21.4338
67	0.0594	21.8810
68	0.0635	21.1333
69	0.0655	20.8060
70	0.0658	20.5532
71	0.0701	19.9099
72	0.0761	19.0323
73	0.0627	21.4361
74	0.0637	21.2898
75	0.0647	21.1252
76	0.0643	21.0495
77	0.0661	20.7685
78	0.0683	20.4320
79	0.0691	20.1082
80	0.0736	19.4567
81	0.0800	18.5585

Appendix C

Energy Efficiency Design Index EEDI:

The final formula to calculate EEDI was stated in Resolution MEPC.212 (63) adopted in March 2012 as following:

$$\frac{\left(\prod_{j=1}^{n} f_j\right)\left(\sum_{i=1}^{nME} P_{ME(i)} \cdot C_{FME(i)} \cdot SFC_{ME(i)}\right) + \left(P_{AE} \cdot C_{FAE} \cdot SFC_{AE}*\right) + \left(\left(\prod_{j=1}^{n} f_j \cdot \sum_{i=1}^{nPTI} P_{PTI(i)} - \sum_{i=1}^{neff} f_{eff(i)} \cdot P_{AEeff(i)}\right) C_{FAE} \cdot SFC_{AE}\right) - \left(\sum_{i=1}^{neff} f_{eff(i)} \cdot P_{eff(i)} \cdot C_{FME} \cdot SFC_{ME}**\right)}{f_i \cdot f_c \cdot Capacity \cdot f_w \cdot V_{ref}}$$

* If part of the Normal maximum Seal Load is provided by shaft generators, SFC_{ME} and C_{FME} may – for the part of the power – be used instead of SFC_{AE} and C_{FAE}.

** In case of $P_{PTI(i)} > 0$, the average weighted value of $(SFC_{ME} \,.\, C_{FME})$ and $(SFC_{AE} \,.\, C_{FAE})$ and to be used for calculation of P_{eff}.

The details of the EEDI equation as stated in the MEPC.212 (63) resolution are:

1. C_F is a non-dimensional conversion factor between fuel consumption measured in g and CO_2 emission also measured in g based on carbon content. C_F corresponds to the fuel used when determining SFC listed in the applicable test report included in a Technical File. The value of C_F is as follows:

Type of fuel	Reference	Carbon content	$C_F\ (t - CO_2/t - fuel)$
Diesel/Gas Oil	ISO 8217 Grades DMX through DMB	0.8744	3.206
Light Fuel Oil (LFO)	ISO 8217 Grades DMX through DMB	0.8594	3.151
Heavy Fuel Oil (HFO)	ISO 8217 Grades DMX through DMB	0.8493	3.1144
Liquified Petroleum Gas (LPG)	Propane Butane	0.8182 0.8264	3.0 3.03
Liquified Natural Gas (LNG)		0.75	2.75

2. V_{ref} is the ship speed, measured in nautical miles per hour (knot), on deep water in the condition corresponding to the $Capacity$ as defined later (in case of passenger ships and ro-ro passenger ships, this condition should be summer load draught) at the shaft power of the engine(s) and assuming the weather is calm with no wind and no waves. The maximum design load condition shall be defined by the deepest draught with its

associated trim, at which the ship is allowed to operate. This condition is obtained from the stability booklet approved by the Administration.

3. $Capacity$ is defined as follows:

- For bulk carriers, tankers, gas tankers, ro-ro cargo ships, general cargo ships, refrigerated cargo carrier and combination carriers, deadweight should be used as $Capacity$.
- For passenger ships and ro-ro passenger ships, gross tonnage in accordance with the International Convention of Tonnage Measurement of Ships 1969, Annex I, regulation 3 should be used as $Capacity$.
- For containerships, 70 per cent of the deadweight (DWT) should be used as $Capacity$. EEDI values for containerships are calculated as follows:
  - attained EEDI is calculated in accordance with the EEDI formula using 70 per cent deadweight for $Capacity$.
  - estimated index value in the Guidelines for calculation of the reference line is calculated using 70 per cent deadweight as:

$$Estimated\ Index\ Value = 3.1144.\frac{190.\sum_{i=1}^{NME} P_{MEi} + 215.P_{AE}}{70\%DWT.V_{ref}}$$

  - parameters a and c for containerships in Table 2 of regulation 21 of MARPOL Annex VI are determined by plotting the estimated index value against 100 per cent deadweight i.e. $a = 174.22$ and $c = 0.201$ were determined.
  - required EEDI for a new containership is calculated using 100 per cent deadweight as:

$$Required\ EEDI = (1 - X/100).a.100\%\ DWT^{-c}$$

    where X is the reduction factor (in percentage) in accordance with Table 1 in regulation 21 of MARPOL Annex VI relating to the applicable phase and size of new containership.

4. $Deadweight$ means the difference in tonnes between the displacement of a ship in water of relative density of (1,025 kg/m3) at the summer load draught and the lightweight of the ship. The summer load draught should be taken as the maximum summer draught as certified in the stability booklet approved by the Administration or an organization recognized by it.

5. P is the power of the main and auxiliary engines, measured in kW. The subscripts ($_{ME}$) and ($_{AE}$) refer to the main and auxiliary engine(s), respectively. The summation on i is for all engines with the number of engines (^{nME}).

- $P_{ME(i)}$ is 75% of the rated installed power (MCR) for each main engine (i) after having deducted any installed shaft generator(s):

$$P_{ME(i)} = 0.75 \,.\, (MCR_{MEi} - P_{PTOi})$$

The following figure gives guidance for determination of $P_{ME(i)}$:

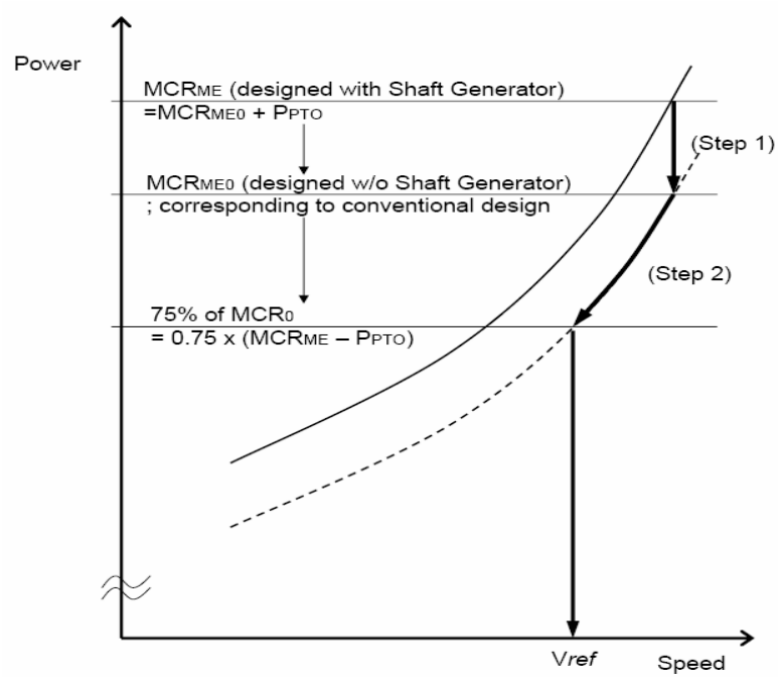

- $P_{PTO(i)}$ is 75% output of each shaft generator installed divided by the relevant efficiency of that shaft generator.
- $P_{PTI(i)}$ is 75% of the rated power consumption of each shaft motor divided by the weighted averaged efficiency of the generator(s).
  In case of combined PTI/PTO, the normal operational mode at sea will determine which of these to be used in the calculation.
- $P_{eff(i)}$ is 75% of the main engine power reduction due to innovative mechanical energy efficient technology. Mechanical recovered waste energy directly coupled to shafts need not be measured.
- $P_{AEeff(i)}$ is the auxiliary power reduction due to innovative electrical energy efficient technology measured at $P_{ME(i)}$.

- P_{AE} is the required auxiliary engine power to supply normal maximum sea load including necessary power for propulsion machinery/systems and accommodation, e.g., main engine pumps, navigational systems and equipment and living on board, but excluding the power not for propulsion machinery/systems, e.g., thrusters, cargo pumps, cargo gear, ballast pumps, maintaining cargo, e.g., reefers and cargo hold fans, in the condition where the ship engaged in voyage at the speed (V_{ref}) under the design loading condition of Capacity.
  - For ships with a main engine power of 10000 kW or above, P_{AE} is defined as:

$$P_{AE(MCRME>1000kW)} = \left(0.025 \times \left(\sum_{i=1}^{nME} MCR_{MEi} + \frac{\sum_{i=1}^{nPTI} P_{PTI(i)}}{0.75}\right)\right) + 250$$

  - For ships with a main engine power below 10000 kW, P_{AE} is defined as:

$$P_{AE(MCRME<1000kW)} = 0.05 \times \left(\sum_{i=1}^{nME} MCR_{MEi} + \frac{\sum_{i=1}^{nPTI} P_{PTI(i)}}{0.75}\right)$$

  - For ship types where the P_{AE} value calculated by the previous two equations above is significantly different from the total power used at normal seagoing, e.g., in cases of passenger ships, the P_{AE} value should be estimated by the consumed electric power (excluding propulsion) in conditions when the ship is engaged in a voyage at reference speed (V_{ref}) as given in the electric power table, divided by the weighted average efficiency of the generator(s).

6. $V_{ref}, Capacit,$ and P should be consistent with each other.

7. SFC is the certified specific fuel consumption, measured in g/kWh, of the engines. The subscripts $_{ME(i)}$ and $_{AE(i)}$ refer to the main and auxiliary engine(s), respectively. For engines certified to the E2 or E3 duty cycles of the NOx Technical Code 2008, the engine Specific Fuel Consumption $(SFC_{ME(i)})$ is that recorded on the EIAPP Certificate(s) at the engine(s) 75% of MCR power or torque rating. For engines certified to the D2 or C1 duty cycles of the NO_x Technical Code 2008, the engine Specific Fuel Consumption $(SFC_{AE(i)})$ is that recorded on the EIAPP Certificate(s) at the engine(s) 50% of MCR power or torque rating.

SFC $_{AE}$ is the power-weighted average among SFC $_{AE(i)}$ of the respective engines i.

8. f_j is a correction factor to account for ship specific design elements. The f_j for ice-classed ships should be taken as the greater value of f_{j0} and $f_{j,min}$ as tabulated in the table below but not greater than $f_{j,max} = 1.0$. For other ship types, f_j should be taken as 1.0.

Correction factor for power f_j for ice-classed ships

Ship Type	f_{j0}	$f_{j,min}$ depending on the Ice Class			
		IA Super	IA	IB	IC
Tanker	$\frac{0.308{L_{PP}}^{1.920}}{\sum_{i=1}^{nME} P_{MEi}}$	$0.15{L_{PP}}^{0.30}$	$0.27{L_{PP}}^{0.21}$	$0.45{L_{PP}}^{0.13}$	$0.70{L_{PP}}^{0.06}$
Bulk Carrier	$\frac{0.639{L_{PP}}^{1.754}}{\sum_{i=1}^{nME} P_{MEi}}$	$0.47{L_{PP}}^{0.09}$	$0.58{L_{PP}}^{0.07}$	$0.73{L_{PP}}^{0.04}$	$0.7287^{0.02}$
General Cargo Ship	$\frac{0.0227{L_{PP}}^{2.483}}{\sum_{i=1}^{nME} P_{MEi}}$	$0.31{L_{PP}}^{0.16}$	$0.43{L_{PP}}^{0.12}$	$0.56{L_{PP}}^{0.09}$	$0.67{L_{PP}}^{0.07}$

9. f_w is a non is a non-dimensional coefficient indicating the decrease of speed in representative sea conditions of wave height, wave frequency and wind speed (e.g., Beaufort Scale 6), and should be determined as follows:

- for attained EEDI calculated under regulations 20 and 21 of MARPOL Annex VI, f_w is 1.0;
- when f_w is calculated according to the subparagraph below, the value for attained EEDI calculated by EEDI formula using the obtained f_w should be referred to as "attained $EEDI_{weather}$";

  - f_w can be determined by conducting the ship specific simulation on its performance at representative sea conditions. The simulation methodology should be based on the Guidelines developed by the Organization and the method and outcome for an individual ship should be verified by the Administration or an organization recognized by the Administration; and

  - in cases where a simulation is not conducted, f_w should be taken from the "Standard f_w" table/curve. A "Standard f_w" table/curve is provided in the Guidelines for each ship type, and expressed as a function of Capacity (e.g. deadweight). The "Standard f_w" table/curve is based on data of actual

speed reduction of as many existing ships as possible under the representative sea condition.

10. $f_{eff(i)}$ is the availability factor of each innovative energy efficiency technology. $f_{eff(i)}$ for waste energy recovery system should be one (1.0).

11. f_i is the capacity factor for any technical/regulatory limitation on capacity, and can be assumed one (1.0) if no necessity of the factor is granted. f_i for ice-classed ships is determined by the standard f_i in the following table.

Capacity correction factor f_i for ice-classed ships

Ship Type	f_{i0}	$f_{i,max}$ depending on the Ice Class			
		IA Super	IA	IB	IC
Tanker	$\frac{0.00138{L_{PP}}^{3.331}}{capacity}$	$2.10{L_{PP}}^{-0.11}$	$1.71{L_{PP}}^{-0.08}$	$1.47{L_{PP}}^{-0.06}$	$1.27{L_{PP}}^{-0.04}$
Bulk Carrier	$\frac{0.00403{L_{PP}}^{3.3123}}{capacity}$	$2.10{L_{PP}}^{-0.11}$	$1.80{L_{PP}}^{-0.09}$	$1.54{L_{PP}}^{-0.07}$	$1.31{L_{PP}}^{-0.05}$
General Cargo Ship	$\frac{0.0377{L_{PP}}^{2.625}}{capacity}$	$2.18{L_{PP}}^{-0.11}$	$1.77{L_{PP}}^{-0.08}$	$1.51{L_{PP}}^{-0.06}$	$1.28{L_{PP}}^{-0.04}$
Containership	$\frac{0.1033{L_{PP}}^{2.329}}{capacity}$	$2.10{L_{PP}}^{-0.11}$	$1.77{L_{PP}}^{-0.08}$	$1.47{L_{PP}}^{-0.06}$	$1.27{L_{PP}}^{-0.04}$
Gas Carrier	$\frac{0.0474{L_{PP}}^{2.590}}{capacity}$	1.25	$2.10{L_{PP}}^{-0.12}$	$1.60{L_{PP}}^{-0.08}$	$1.25{L_{PP}}^{-0.04}$

12. f_c is the cubic capacity correction factor and should be assumed to be one (1.0) if no necessity of the factor is granted.

13. $Length\ between\ perpendiculars$, L_{PP} means 96% of the total length on a waterline at 85% of the least moulded depth measured from the top of the keel, or the length from the foreside of the stem to the axis of the rudder stock on that waterline, if that were greater. In ships designed with a rake of keel the waterline on which this length is measured shall be parallel to the designed waterline. The length between perpendiculars (L_{PP}) shall be measured in metres.

Appendix D

D1: Attained EEDI at speeds (5 to 17 knots) for Stage One Hulls:

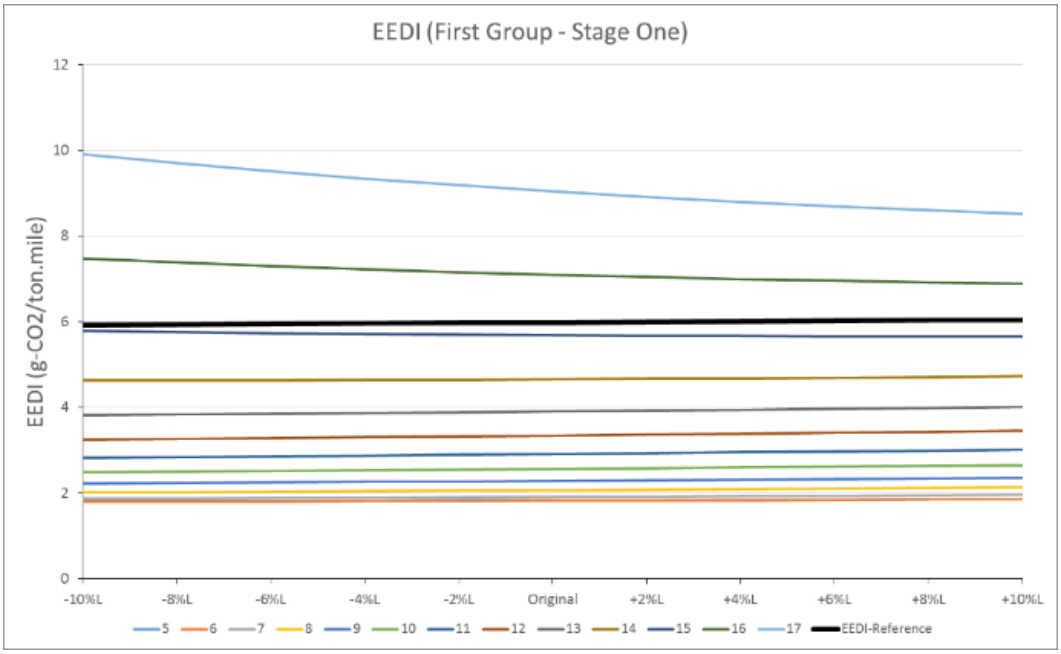

(a)

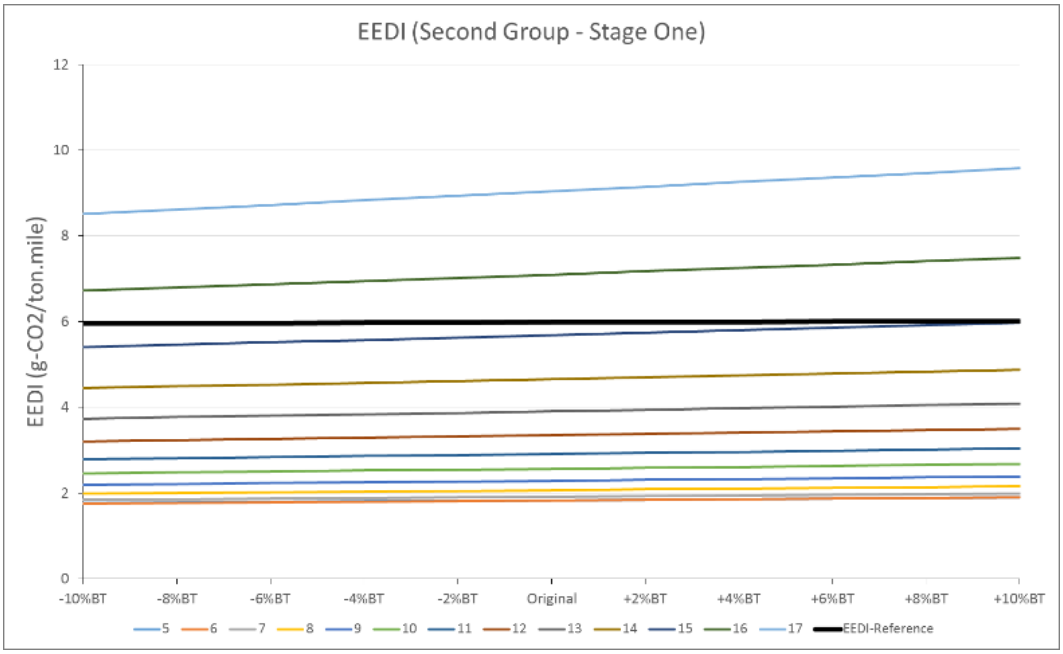

(b)

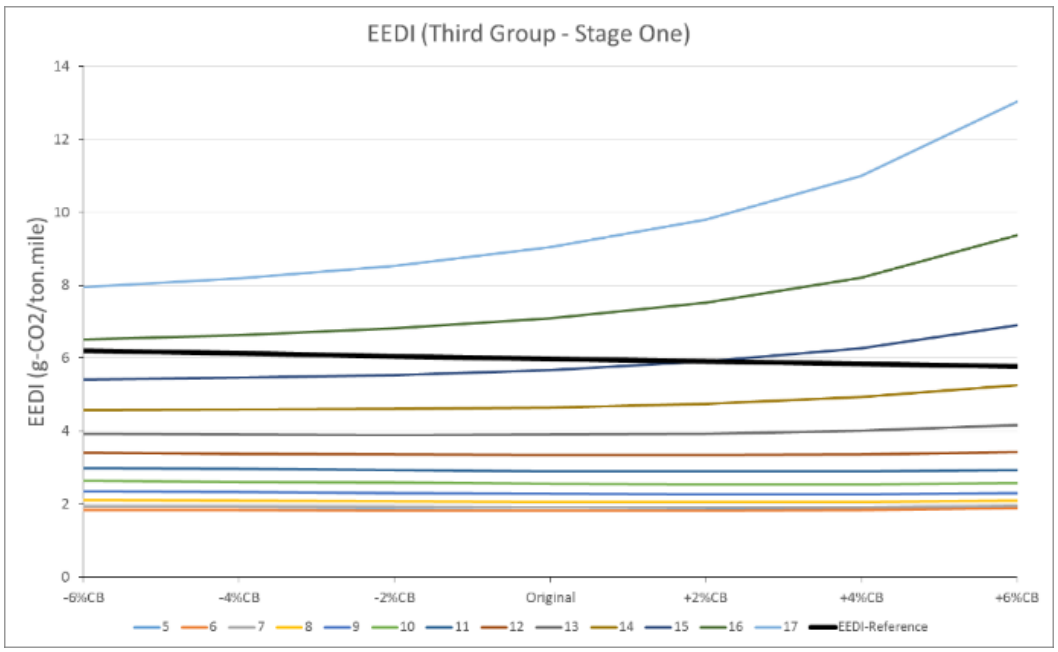
EEDI (Third Group - Stage One)
EEDI (g-CO2/ton.mile)
14
12
10
8
6
4
2
0
-6%CB
-4%CB
-2%CB
Original
+2%CB
+4%CB
+6%CB
5 6 7 8 9 10 11 12 13 14 15 16 17 EEDI-Reference

(c)

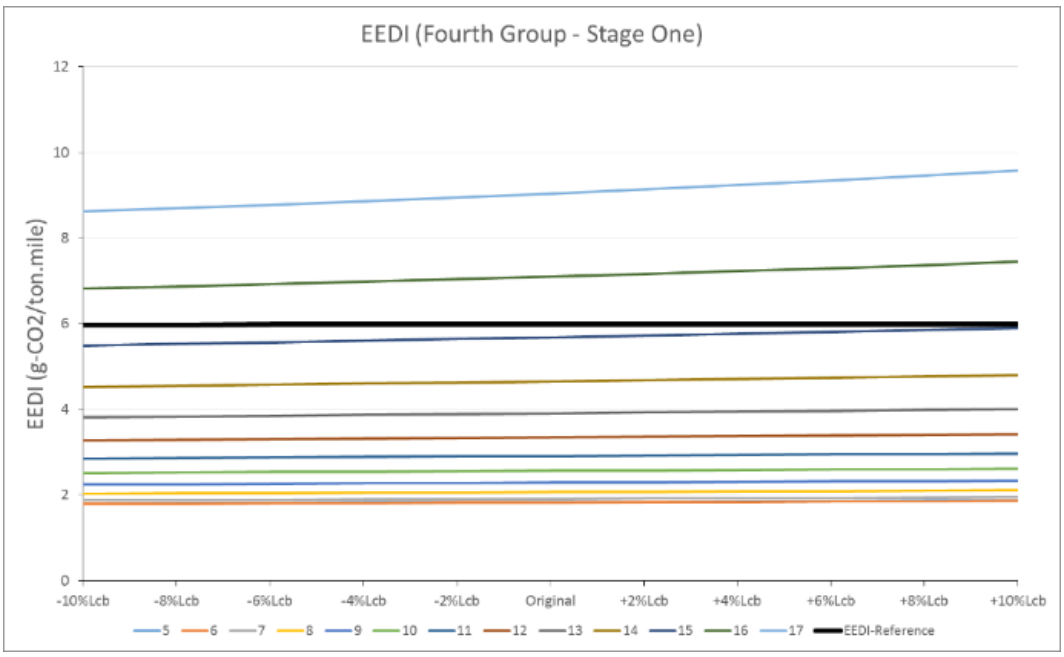
EEDI (Fourth Group - Stage One)
EEDI (g-CO2/ton.mile)
12
10
8
6
4
2
0
-10%Lcb
-8%Lcb
-6%Lcb
-4%Lcb
-2%Lcb
Original
+2%Lcb
+4%Lcb
+6%Lcb
+8%Lcb
+10%Lcb
5 6 7 8 9 10 11 12 13 14 15 16 17 EEDI-Reference

(d)

D2: %EEDI Difference at speeds (17, 15, 12, 10, 7 knots) for Stage Two Hulls:

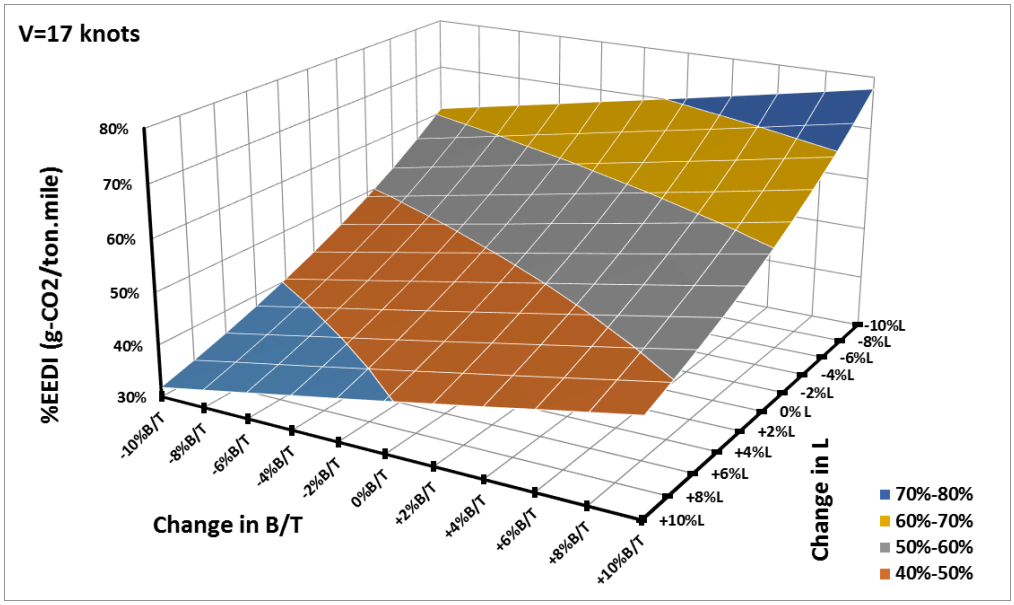

(a)

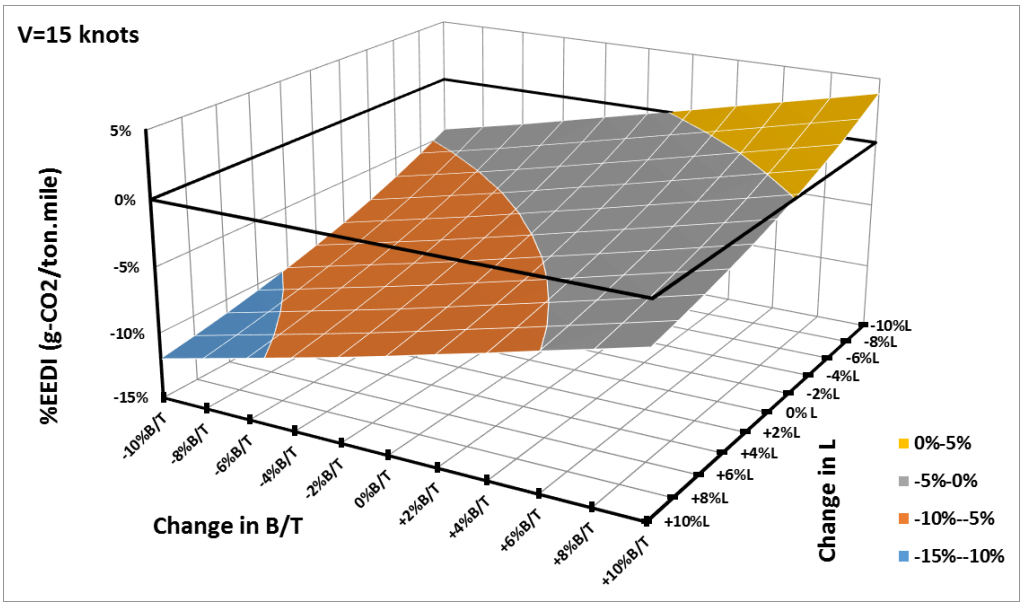

(b)

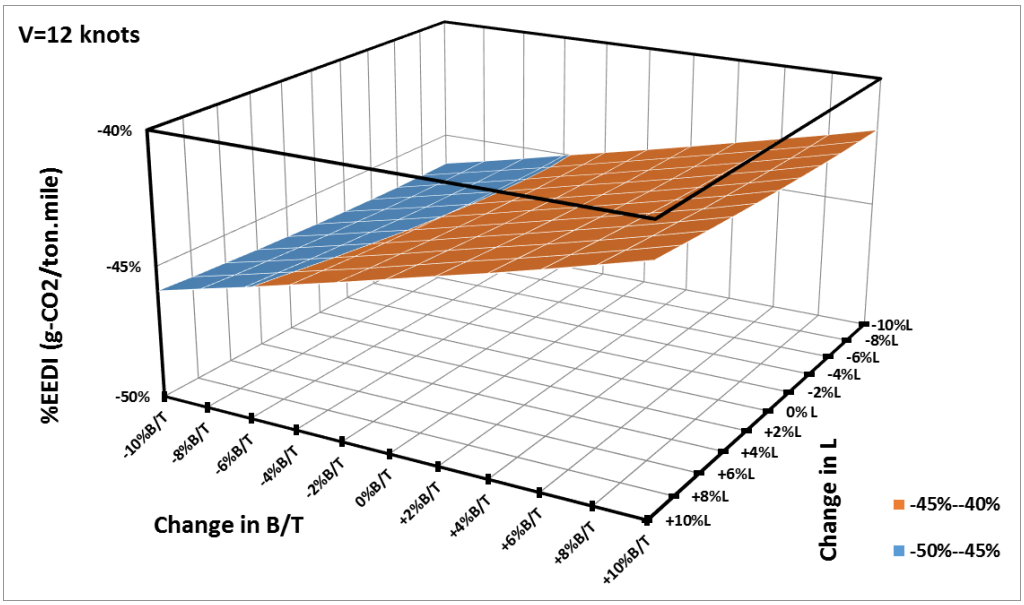
V=12 knots
%EEDI (g-CO2/ton.mile)
-40%
-45%
-50%
-10%B/T
-8%B/T
-6%B/T
-4%B/T
-2%B/T
0%B/T
+2%B/T
+4%B/T
+6%B/T
+8%B/T
+10%B/T
Change in B/T
-10%L
-8%L
-6%L
-4%L
-2%L
0% L
+2%L
+4%L
+6%L
+8%L
+10%L
Change in L
-45%--40%
-50%--45%

(c)

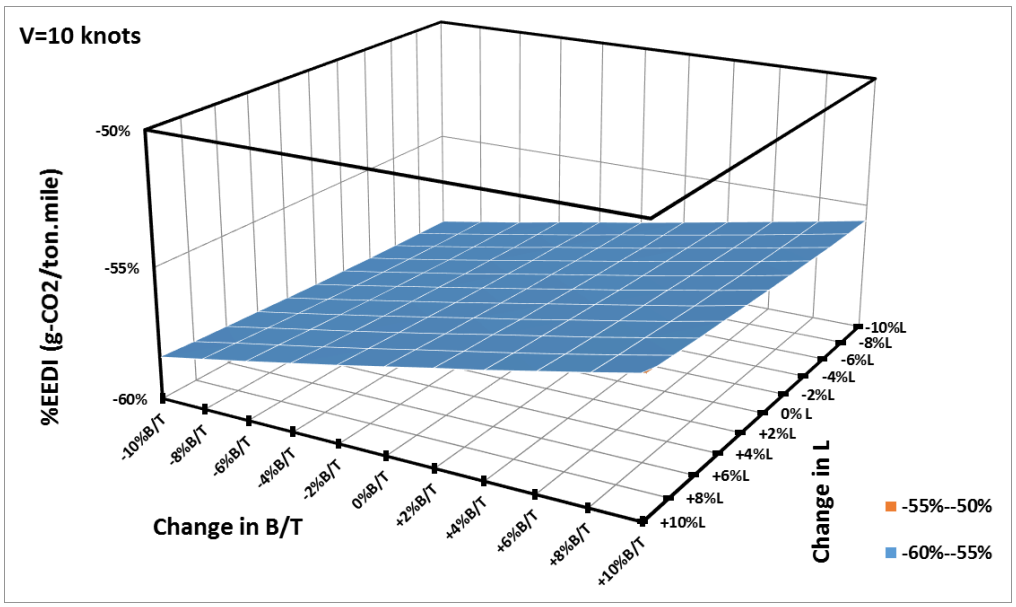
V=10 knots
%EEDI (g-CO2/ton.mile)
-50%
-55%
-60%
-10%B/T
-8%B/T
-6%B/T
-4%B/T
-2%B/T
0%B/T
+2%B/T
+4%B/T
+6%B/T
+8%B/T
+10%B/T
Change in B/T
-10%L
-8%L
-6%L
-4%L
-2%L
0% L
+2%L
+4%L
+6%L
+8%L
+10%L
Change in L
-55%--50%
-60%--55%

(d)

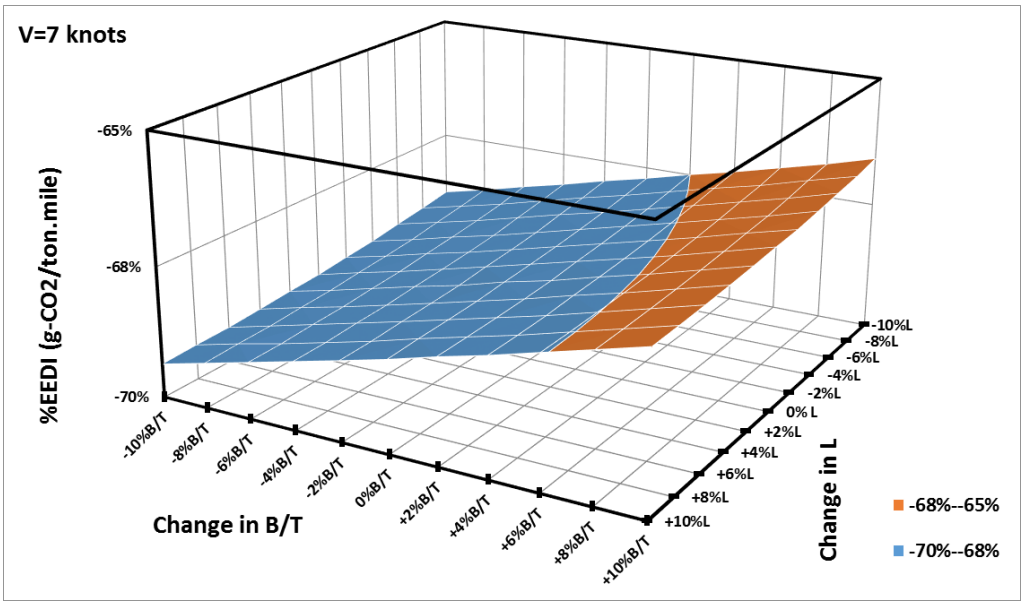
V=7 knots
%EEDI (g-CO2/ton.mile)
-65%
-68%
-70%
-10%B/T
-8%B/T
-6%B/T
-4%B/T
-2%B/T
0%B/T
+2%B/T
+4%B/T
+6%B/T
+8%B/T
+10%B/T
Change in B/T
-10%L
-8%L
-6%L
-4%L
-2%L
0% L
+2%L
+4%L
+6%L
+8%L
+10%L
Change in L
-68%--65%
-70%--68%

(e)

D3: EEDI Attained, EEDI reference, and %EEDI for Stage Three Hulls

Hulls	5	6	8	10	13	14	15	17	EEDI-Ref	%EEDI @ 15 knots
Original	1.829	1.821	2.068	2.566	3.905	4.655	5.681	9.041	5.98	-5.05%
1	1.814	1.811	2.066	2.568	3.838	4.499	5.369	8.063	6.41	-16.29%
2	1.845	1.838	2.094	2.600	3.892	4.572	5.469	8.281	6.41	-14.73%
3	1.877	1.869	2.122	2.632	3.949	4.652	5.584	8.546	6.42	-12.95%
4	1.828	1.809	2.031	2.500	3.790	4.522	5.524	8.831	6.22	-11.19%
5	1.871	1.849	2.073	2.550	3.884	4.654	5.722	9.288	6.22	-8.03%
6	1.909	1.885	2.109	2.594	3.982	4.804	5.959	9.885	6.22	-4.23%
7	1.837	1.801	1.989	2.428	3.817	4.711	6.019	10.711	6.05	-0.44%
8	1.917	1.875	2.067	2.523	4.022	5.025	6.517	11.966	6.05	7.75%
9	2.021	1.972	2.159	2.630	4.284	5.450	7.233	13.943	6.05	19.52%
10	1.883	1.879	2.143	2.664	3.977	4.663	5.567	8.389	6.44	-13.54%
11	1.913	1.908	2.173	2.697	4.032	4.738	5.674	8.624	6.44	-11.88%
12	1.949	1.940	2.203	2.731	4.092	4.821	5.796	8.909	6.44	-9.99%
13	1.893	1.874	2.107	2.596	3.936	4.698	5.751	9.266	6.24	-7.88%
14	1.926	1.907	2.145	2.643	4.030	4.834	5.954	9.755	6.24	-4.65%
15	1.967	1.945	2.184	2.691	4.135	4.994	6.208	10.405	6.25	-0.61%
16	1.904	1.869	2.070	2.532	3.985	4.927	6.327	11.389	6.07	4.29%
17	1.987	1.948	2.153	2.632	4.204	5.263	6.852	12.764	6.07	12.88%
18	2.102	2.052	2.251	2.744	4.484	5.724	7.632	14.965	6.07	25.65%
19	1.956	1.952	2.228	2.768	4.127	4.838	5.775	8.733	6.46	-10.63%
20	1.988	1.983	2.258	2.803	4.186	4.917	5.889	8.981	6.46	-8.88%
21	2.025	2.016	2.291	2.839	4.249	5.005	6.018	9.282	6.46	-6.89%
22	1.950	1.935	2.183	2.696	4.090	4.884	5.985	9.680	6.26	-4.46%
23	1.985	1.970	2.223	2.746	4.186	5.024	6.199	10.199	6.27	-1.08%
24	2.027	2.009	2.264	2.795	4.295	5.188	6.462	10.886	6.27	3.10%
25	1.970	1.939	2.157	2.644	4.163	5.152	6.619	12.002	6.09	8.73%
26	2.058	2.023	2.244	2.750	4.388	5.496	7.175	13.458	6.09	17.80%
27	2.180	2.133	2.349	2.870	4.683	5.977	7.998	15.819	6.09	31.22%
28	1.734	1.739	1.999	2.497	3.707	4.306	5.068	7.305	6.15	-17.65%
29	1.757	1.760	2.022	2.524	3.753	4.367	5.149	7.469	6.15	-16.35%
30	1.783	1.785	2.047	2.551	3.801	4.432	5.240	7.666	6.16	-14.88%
31	1.725	1.718	1.951	2.418	3.632	4.279	5.134	7.795	5.97	-13.96%
32	1.754	1.747	1.983	2.458	3.709	4.386	5.288	8.131	5.97	-11.39%
33	1.785	1.775	2.013	2.496	3.790	4.505	5.471	8.568	5.97	-8.33%
34	1.707	1.687	1.891	2.331	3.610	4.372	5.442	9.062	5.80	-6.12%

35	1.769	1.747	1.957	2.414	3.777	4.616	5.809	9.917	5.80	0.19%
36	1.848	1.820	2.030	2.500	3.982	4.938	6.339	11.304	5.80	9.26%
37	1.801	1.806	2.077	2.592	3.848	4.473	5.268	7.626	6.18	-14.75%
38	1.828	1.831	2.102	2.621	3.896	4.535	5.355	7.805	6.18	-13.35%
39	1.856	1.856	2.128	2.650	3.945	4.603	5.453	8.018	6.18	-11.78%
40	1.780	1.775	2.021	2.510	3.776	4.453	5.353	8.199	5.99	-10.63%
41	1.821	1.814	2.062	2.560	3.883	4.615	5.604	8.818	5.99	-6.46%
42	1.857	1.849	2.097	2.602	3.978	4.760	5.835	9.398	5.99	-2.63%
43	1.799	1.779	1.998	2.466	3.851	4.702	5.917	10.165	5.82	1.68%
44	1.875	1.851	2.071	2.553	4.049	5.008	6.407	11.421	5.82	10.05%
45	1.991	1.954	2.167	2.663	4.332	5.480	7.211	13.674	5.83	23.78%
46	1.874	1.880	2.160	2.696	3.999	4.649	5.479	7.959	6.20	-11.68%
47	1.902	1.905	2.187	2.727	4.050	4.716	5.572	8.148	6.20	-10.20%
48	1.920	1.924	2.207	2.752	4.099	4.785	5.673	8.377	6.21	-8.58%
49	1.838	1.836	2.097	2.609	3.931	4.642	5.591	8.607	6.01	-7.00%
50	1.869	1.866	2.130	2.651	4.013	4.757	5.762	9.002	6.01	-4.18%
51	1.901	1.898	2.166	2.695	4.105	4.893	5.973	9.524	6.01	-0.69%
52	1.835	1.822	2.055	2.542	3.953	4.809	6.028	10.254	5.84	3.25%
53	1.908	1.891	2.130	2.635	4.145	5.089	6.466	11.340	5.84	10.70%
54	2.002	1.979	2.216	2.734	4.385	5.473	7.098	13.067	5.84	21.45%
55	1.673	1.684	1.948	2.441	3.607	4.163	4.850	6.781	5.93	-18.20%
56	1.693	1.704	1.968	2.466	3.647	4.214	4.916	6.910	5.93	-17.08%
57	1.716	1.723	1.989	2.490	3.688	4.269	4.991	7.062	5.93	-15.83%
58	1.641	1.644	1.885	2.351	3.511	4.099	4.850	7.078	5.75	-15.59%
59	1.664	1.667	1.912	2.386	3.577	4.187	4.976	7.339	5.75	-13.42%
60	1.689	1.691	1.938	2.419	3.645	4.286	5.122	7.671	5.75	-10.88%
61	1.607	1.601	1.818	2.257	3.456	4.127	5.034	7.939	5.58	-9.79%
62	1.658	1.651	1.874	2.329	3.600	4.332	5.339	8.624	5.58	-4.35%
63	1.723	1.712	1.937	2.404	3.772	4.595	5.759	9.674	5.58	3.13%
64	1.742	1.753	2.026	2.537	3.750	4.331	5.050	7.093	5.95	-15.19%
65	1.763	1.774	2.048	2.563	3.791	4.384	5.123	7.236	5.96	-13.97%
66	1.780	1.789	2.065	2.585	3.831	4.439	5.200	7.399	5.96	-12.68%
67	1.667	1.676	1.934	2.421	3.589	4.158	4.871	6.931	5.77	-15.56%
68	1.717	1.724	1.982	2.477	3.723	4.366	5.202	7.747	5.77	-9.86%
69	1.744	1.749	2.010	2.514	3.797	4.474	5.361	8.113	5.77	-7.10%
70	1.666	1.663	1.893	2.357	3.620	4.333	5.307	8.489	5.60	-5.27%
71	1.725	1.718	1.955	2.433	3.776	4.558	5.642	9.252	5.60	0.68%
72	1.795	1.784	2.022	2.512	3.961	4.847	6.106	10.432	5.61	8.91%
73	1.803	1.817	2.103	2.636	3.898	4.505	5.259	7.416	5.98	-12.05%

74	1.818	1.831	2.120	2.659	3.939	4.559	5.334	7.567	5.98	-10.81%
75	1.834	1.846	2.138	2.681	3.981	4.617	5.417	7.745	5.98	-9.43%
76	1.750	1.759	2.029	2.540	3.809	4.460	5.302	7.856	5.79	-8.47%
77	1.777	1.785	2.059	2.578	3.880	4.558	5.444	8.166	5.79	-6.02%
78	1.803	1.811	2.089	2.616	3.959	4.671	5.613	8.564	5.79	-3.12%
79	1.733	1.732	1.978	2.466	3.798	4.557	5.601	9.030	5.62	-0.40%
80	1.792	1.789	2.042	2.547	3.960	4.788	5.950	9.857	5.62	5.77%
81	1.867	1.860	2.114	2.632	4.159	5.098	6.444	11.146	5.63	14.51%

D4: The average $(\mathrm{EEDI_A}/\mathrm{EEDI_{Ref}})$ and the mean S/N ratio:

StdOrder	Average z $(\mathbf{EEDI_A}/\mathbf{EEDI_{Ref}})$	S/N
Original	0.6315	2.7444
1	0.5634	3.9144
2	0.5734	3.7407
3	0.5848	3.5438
4	0.5929	3.3018
5	0.6121	2.9744
6	0.6344	2.5875
7	0.6520	2.0958
8	0.7001	1.3393
9	0.7692	0.3046
10	0.5824	3.6225
11	0.5929	3.4447
12	0.6050	3.2423
13	0.6152	2.9626
14	0.6347	2.6349
15	0.6585	2.2341
16	0.6822	1.6610
17	0.7338	0.8832
18	0.8092	-0.1966
19	0.6027	3.3224
20	0.6139	3.1414
21	0.6266	2.9351
22	0.6375	2.6399
23	0.6579	2.3080
24	0.6828	1.9038
25	0.7115	1.2754
26	0.7657	0.4910
27	0.8457	-0.6070
28	0.5563	4.1170
29	0.5647	3.9718
30	0.5741	3.8091
31	0.5769	3.6712
32	0.5924	3.4018
33	0.6103	3.0844
34	0.6183	2.7727
35	0.6555	2.1652
36	0.7084	1.3163
37	0.5761	3.8061
38	0.5851	3.6562
39	0.5950	3.4893
40	0.5989	3.3236

41	0.6234	2.8924
42	0.6458	2.5090
43	0.6670	2.0073
44	0.7160	1.2423
45	0.7961	0.0576
46	0.5972	3.4899
47	0.6067	3.3366
48	0.6165	3.1717
49	0.6221	2.9743
50	0.6392	2.6943
51	0.6599	2.3527
52	0.6781	1.8981
53	0.7227	1.2271
54	0.7862	0.2998
55	0.5542	4.2126
56	0.5615	4.0882
57	0.5695	3.9510
58	0.5678	3.9004
59	0.5807	3.6719
60	0.5956	3.4066
61	0.5970	3.2329
62	0.6291	2.6915
63	0.6726	1.9683
64	0.5748	3.8897
65	0.5825	3.7607
66	0.5904	3.6261
67	0.5709	3.9169
68	0.6037	3.3082
69	0.6199	3.0313
70	0.6260	2.7785
71	0.6609	2.2151
72	0.7087	1.4560
73	0.5956	3.5701
74	0.6032	3.4446
75	0.6115	3.3056
76	0.6136	3.1807
77	0.6283	2.9391
78	0.6455	2.6541
79	0.6565	2.3340
80	0.6934	1.7635
81	0.7449	0.9840

Appendix E

Resistance Results – Ballast Condition

Speed	Fn	Rn	Cf	Cf x k	Cr	Ca	Ct	CircC
kts		/10^9	*10^3	*10^3	*10^3	*10^3	*10^3	
5.000	0.058	0.438	1.700	0.440	0.000	0.420	2.560	0.719
6.000	0.069	0.526	1.660	0.430	0.000	0.420	2.510	0.705
7.000	0.081	0.614	1.628	0.421	0.000	0.420	2.470	0.694
8.000	0.092	0.701	1.600	0.414	0.002	0.420	2.437	0.684
9.000	0.104	0.789	1.577	0.408	0.007	0.420	2.412	0.678
10.000	0.115	0.877	1.556	0.403	0.021	0.420	2.400	0.674
11.000	0.127	0.964	1.538	0.398	0.049	0.420	2.405	0.675
12.000	0.139	1.052	1.521	0.394	0.099	0.420	2.434	0.684
13.000	0.150	1.140	1.506	0.390	0.178	0.420	2.494	0.701
14.000	0.162	1.227	1.492	0.386	0.292	0.420	2.591	0.728
15.000	0.173	1.315	1.480	0.383	0.446	0.420	2.730	0.767
16.000	0.185	1.403	1.468	0.380	0.644	0.420	2.913	0.818
17.000	0.196	1.490	1.458	0.377	0.885	0.420	3.140	0.882

Speed-Power Results – Ballast Condition

Speed	Pe	THDF	WFT	ETAR	ETA0	QPC	Pd	RPM
kts	(kW)						(kW)	
5.000	172	0.182	0.454	1.019	0.565	0.862	200	23.83
6.000	293	0.182	0.452	1.019	0.569	0.864	339	28.45
7.000	457	0.182	0.450	1.019	0.572	0.866	528	33.05
8.000	674	0.182	0.449	1.019	0.574	0.867	777	37.65
9.000	950	0.182	0.447	1.019	0.576	0.868	1094	42.27
10.000	1297	0.182	0.446	1.019	0.577	0.868	1494	46.93
11.000	1729	0.182	0.445	1.019	0.577	0.867	1995	51.69
12.000	2273	0.182	0.444	1.019	0.576	0.864	2631	56.62
13.000	2961	0.182	0.444	1.019	0.573	0.859	3448	61.83
14.000	3842	0.182	0.443	1.019	0.569	0.851	4516	67.43
15.000	4979	0.182	0.442	1.019	0.562	0.840	5928	73.55
16.000	6447	0.182	0.442	1.019	0.554	0.826	7803	80.20
17.000	8337	0.182	0.441	1.019	0.544	0.811	10286	87.41

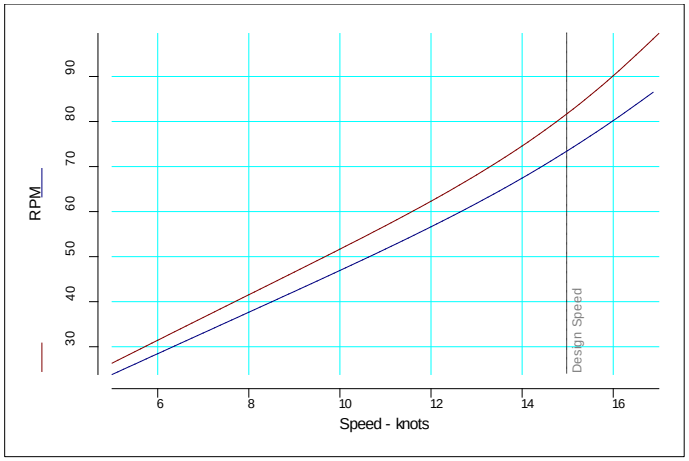
RPM
90
80
70
60
50
40
30
Design Speed
6
8
10
12
14
16
Speed - knots

Appendix F

Main trade routes for the dirty tanker (TD) sector and the clean product (TC) sector:

Information about Tankers maritime routes are collected from different resources and reports. Similarly, the Flat Rates for some popular routes in 2012 are collected from different reports of shipping companies and marine transport services such as:

(*Review of Maritime Transport*, 2011, 2012, 2013)

(McQuilling Services LLC)

(Hellenic Shipping News)

(Clarkson Research Services)

(Fearnleys)

(Intermodal)

(S&P Global - Platts)

(*A History of the Baltic indices*)

(Simpson Spence & Young Ltd)

(Worldscale Association (London) and Worldscale Association (NYC))

Moreover, no accurate data is available regarding routes distance between ports. Therefore, average ranges for the distance between ports are collected from these websites:

http://www.portworld.com/map/

http://ports.com/sea-route/

https://sea-distances.org/

Route index	Vessel size	Route description	Distance (Nautical mile)	WS100 in 2012 ($/MT)
TD1 / VLCC	280,000 mt	Middle East Gulf to US Gulf	9509 – 10891	46.31
TD2 / VLCC	260,000 mt	Middle East Gulf to Singapore	3663 – 4226	15.24
TD3 / VLCC	250,000 mt	Middle East Gulf to Japan	6568 – 8003	26.95
TD4 / VLCC	260,000 mt	West Africa to US Gulf	5888 – 6812	23.2
TD5 / Suezmax	130,000 mt	West Africa to USAC	5178 – 6548	21.05
TD6 / Suezmax	130,000 mt	Cross Mediterranean (Novorossiysk* to Augusta)	1248 – 1626	9.57
TD7 / Aframax	80,000 mt	North Sea to Continental Europe	560 – 695	7.11
TD8 / Aframax	80,000 mt	Kuwait to Singapore	3806 – 4413	15.9
TD9 / Aframax	70,000 mt	Caribbean to US Gulf	2130 – 2788	10.76
TD10 / Panamax	50,000 mt	Caribbean to USAC	1750 – 2026	9.21
TD11 / Aframax	80,000 mt	Cross Mediterranean	1656 – 1885	9.58
TD12 / Panamax	55,000 mt	Amsterdam-Rotterdam-Antwerp to US Gulf	5004 – 6093	22.08
TD14 / Aframax	80,000 mt	South East Asia to east coast Australia	3687 – 4431	18.83
TD15 / VLCC	260,000	West Africa to China		39.42
TD16	30,000	Odessa - Augusta		10.32
TD17	100,000 mt	Baltic to UK-Continental Europe (UKC)	1078 – 1860	9.51
TD18	30,000 mt	Baltic to UKC		
TD19	80,000	Cross Mediterranean		10.96
TD20		West Africa to Continental Europe		
TD21		Caribbean to US Gulf		

TC1, LR2	75,000 mt	Ras Tanura, Saudi Arabia, to Yokohama, Japan	6547 – 7991	26.65
TC2, MR	33,000 mt	Rotterdam to New York	3308 – 3918	14.98
TC3, MR	30,000 mt	Caribbean to US Atlantic coast	1750 – 2026	9.21
TC4, MR	30,000 mt	Singapore to Japan	2907 – 3772	
TC5, LR1	55,000 mt	Ras Tanura to Yokohama	6547 – 7991	26.65
TC6	30,000	Skikda, Algeria, to Marseilles, France		
TC7, MR	30,000 mt	Singapore to Sydney		
TC8, LR1	65,000 mt	Jubail, Saudi Arabia, to Rotterdam	6383 – 7344	
TC9	22,000 mt	Baltic to UK/Cont		26.84
TC10		Yeosu, South Korea, to Los Angeles		
TC11		Yeosu to Singapore		
TC12		Sikka, India, to Chiba, Japan		
TC14		Houston to Amsterdam		

Appendix G

Newbuilding cost per deadweight ton (NB/DWT) values in [$/dwt ton] and the mean S/N ratio for all the 81 hulls generated in Stage Three.

StdOrder	Average q (NB/DWT)	S/N
Original	702.34	-56.93
1	779.04	-57.83
2	779.17	-57.83
3	779.31	-57.83
4	740.78	-57.39
5	741.01	-57.40
6	741.29	-57.40
7	707.29	-56.99
8	707.81	-57.00
9	708.53	-57.01
10	784.03	-57.89
11	784.16	-57.89
12	784.31	-57.89
13	745.22	-57.45
14	745.46	-57.45
15	745.75	-57.45
16	711.33	-57.04
17	711.87	-57.05
18	712.64	-57.06
19	788.84	-57.94
20	788.98	-57.94
21	789.14	-57.94
22	749.50	-57.50
23	749.75	-57.50
24	750.05	-57.50
25	715.19	-57.09
26	715.76	-57.10
27	716.57	-57.11
28	736.18	-57.34
29	736.27	-57.34
30	736.38	-57.34
31	700.11	-56.90
32	700.28	-56.91
33	700.48	-56.91
34	668.48	-56.50
35	668.84	-56.51
36	669.34	-56.51
37	741.13	-57.40
38	741.23	-57.40

39	741.34	-57.40
40	704.50	-56.96
41	704.77	-56.96
42	705.02	-56.96
43	672.63	-56.56
44	673.10	-56.56
45	673.83	-56.57
46	745.90	-57.45
47	746.01	-57.45
48	746.13	-57.46
49	708.75	-57.01
50	708.93	-57.01
51	709.15	-57.01
52	676.27	-56.60
53	676.69	-56.61
54	677.28	-56.62
55	700.58	-56.91
56	700.65	-56.91
57	700.73	-56.91
58	666.34	-56.47
59	666.47	-56.48
60	666.62	-56.48
61	636.28	-56.07
62	636.56	-56.08
63	636.94	-56.08
64	705.50	-56.97
65	705.58	-56.97
66	705.67	-56.97
67	670.50	-56.53
68	670.84	-56.53
69	671.00	-56.53
70	640.20	-56.13
71	640.51	-56.13
72	640.92	-56.14
73	710.26	-57.03
74	710.34	-57.03
75	710.44	-57.03
76	674.92	-56.58
77	675.06	-56.59
78	675.23	-56.59
79	644.00	-56.18
80	644.31	-56.18
81	644.74	-56.19

Appendix H

Profit per Deadweight for Routes One and Two.

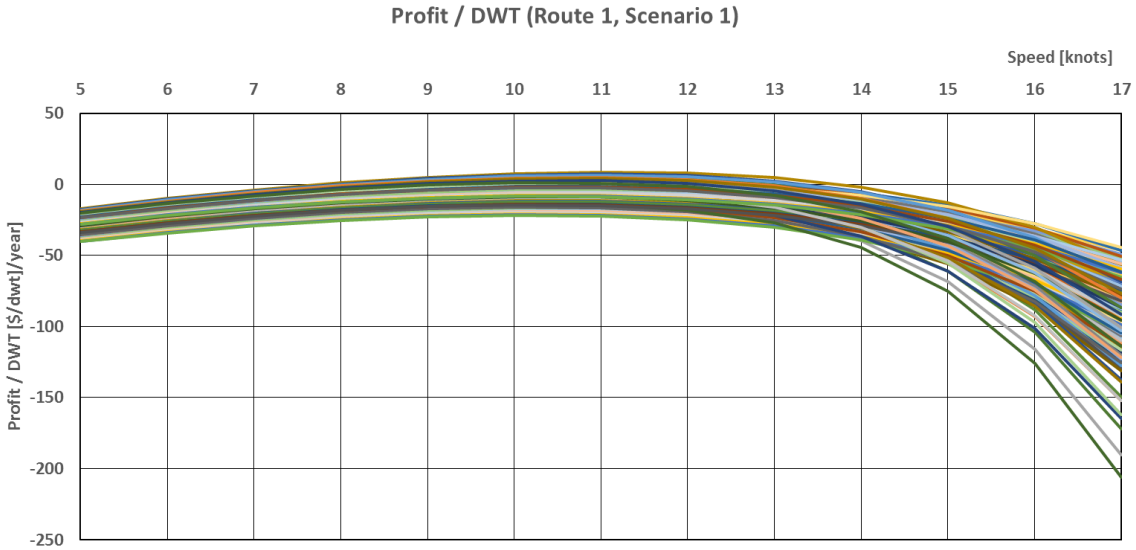

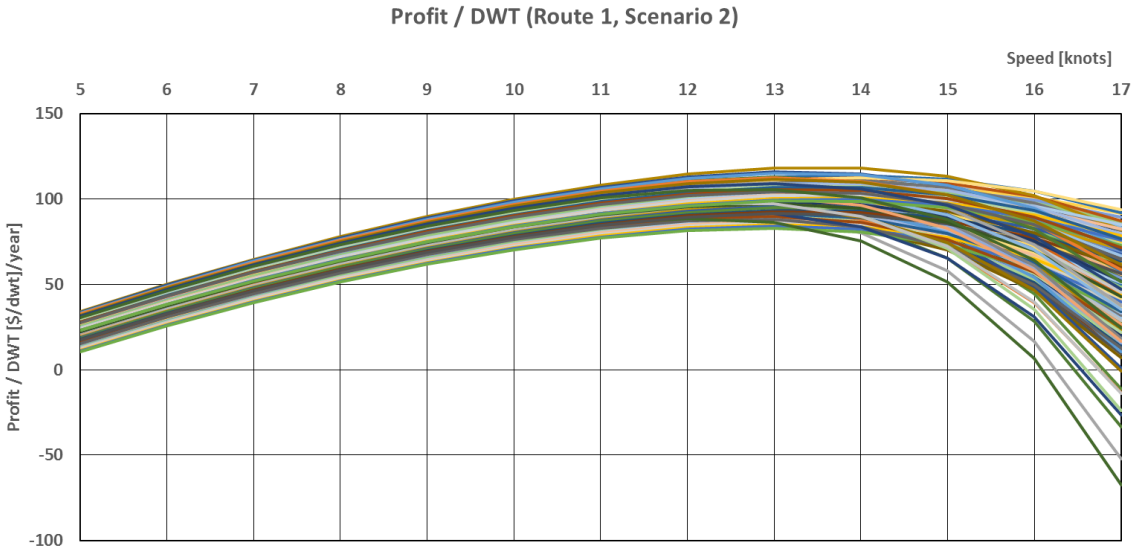

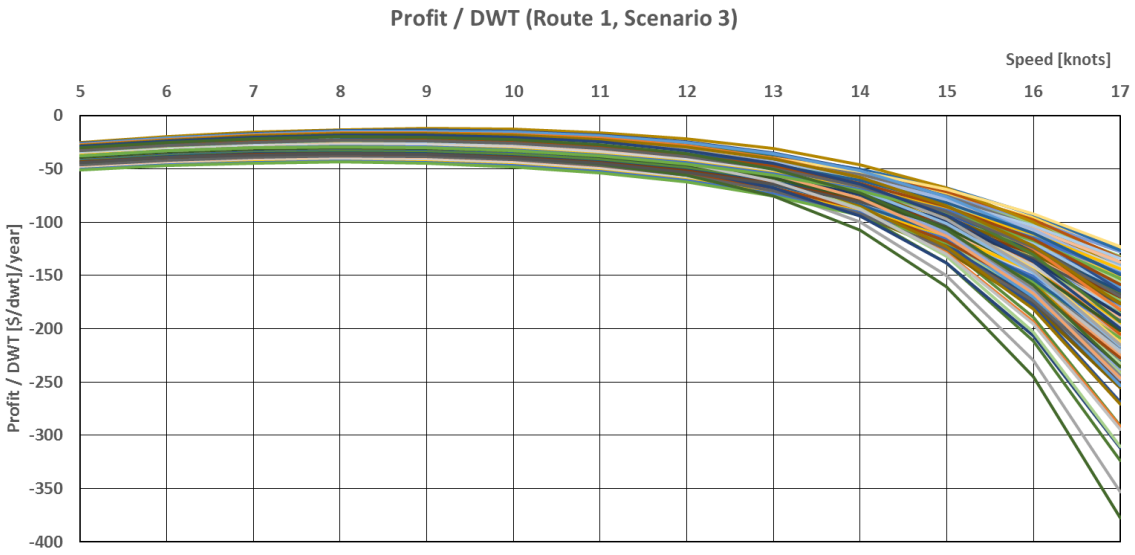
Profit / DWT (Route 1, Scenario 3)
Speed [knots]
5 6 7 8 9 10 11 12 13 14 15 16 17
0 -50 -100 -150 -200 -250 -300 -350 -400
Profit / DWT [$/dwt]/year]

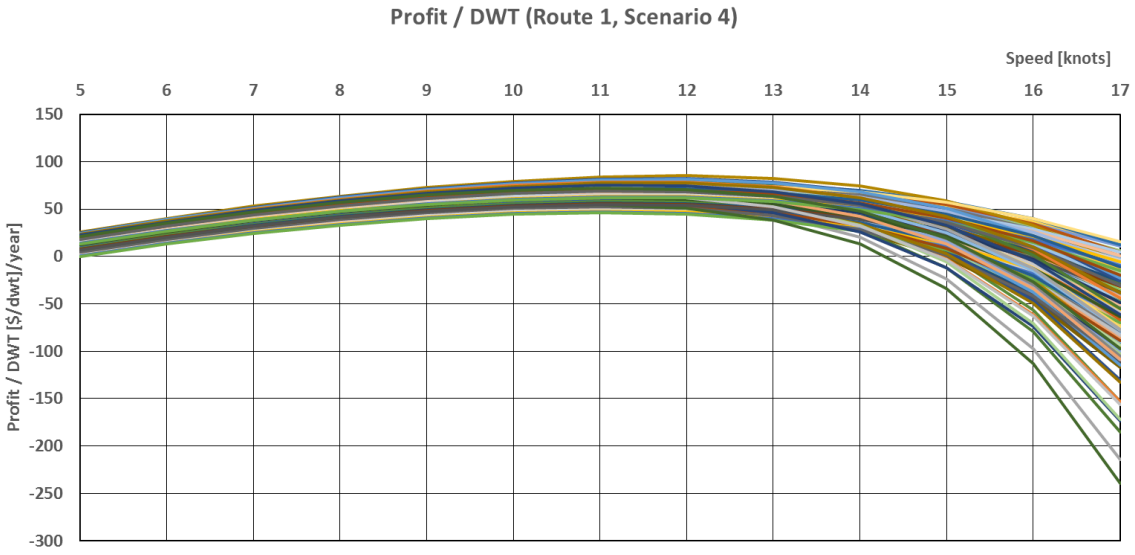
Profit / DWT (Route 1, Scenario 4)
Speed [knots]
5 6 7 8 9 10 11 12 13 14 15 16 17
150 100 50 0 -50 -100 -150 -200 -250 -300
Profit / DWT [$/dwt]/year]

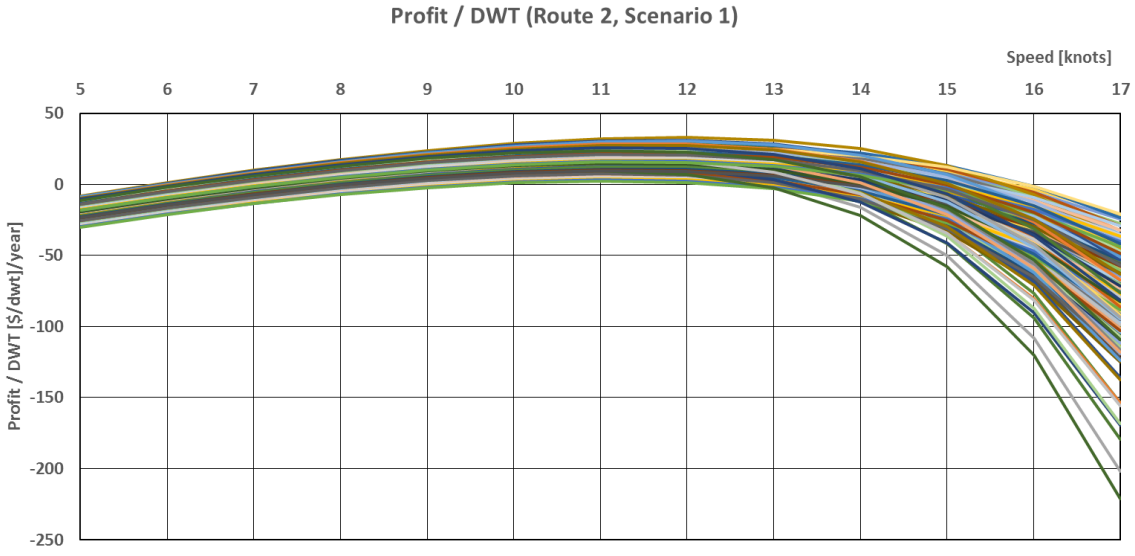
Profit / DWT (Route 2, Scenario 1)
Speed [knots]
5 6 7 8 9 10 11 12 13 14 15 16 17
50 0 -50 -100 -150 -200 -250
Profit / DWT [$/dwt]/year]

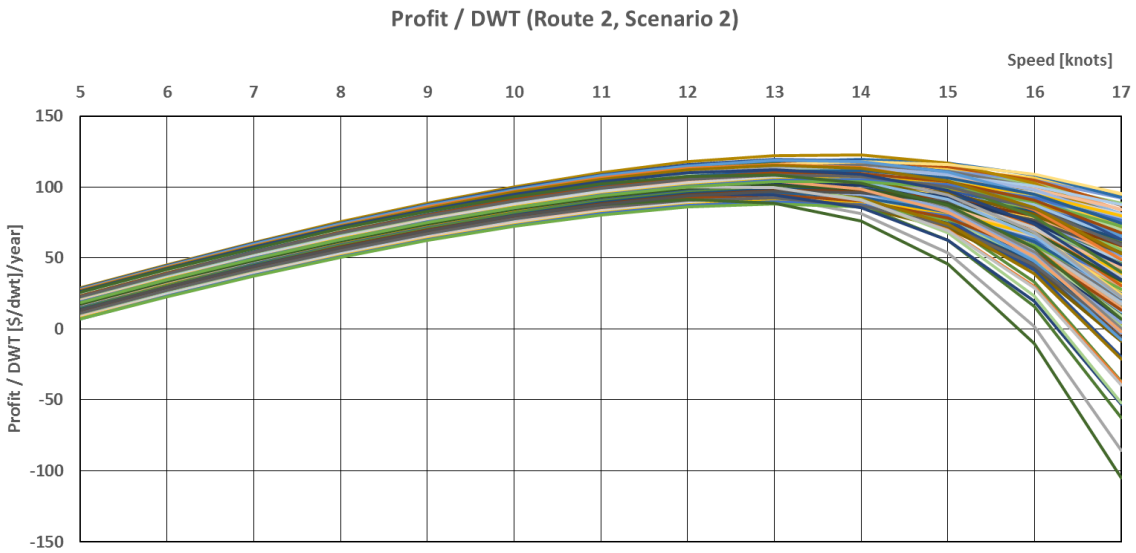
Profit / DWT (Route 2, Scenario 2)
Speed [knots]
5 6 7 8 9 10 11 12 13 14 15 16 17
150 100 50 0 -50 -100 -150
Profit / DWT [$/dwt]/year]

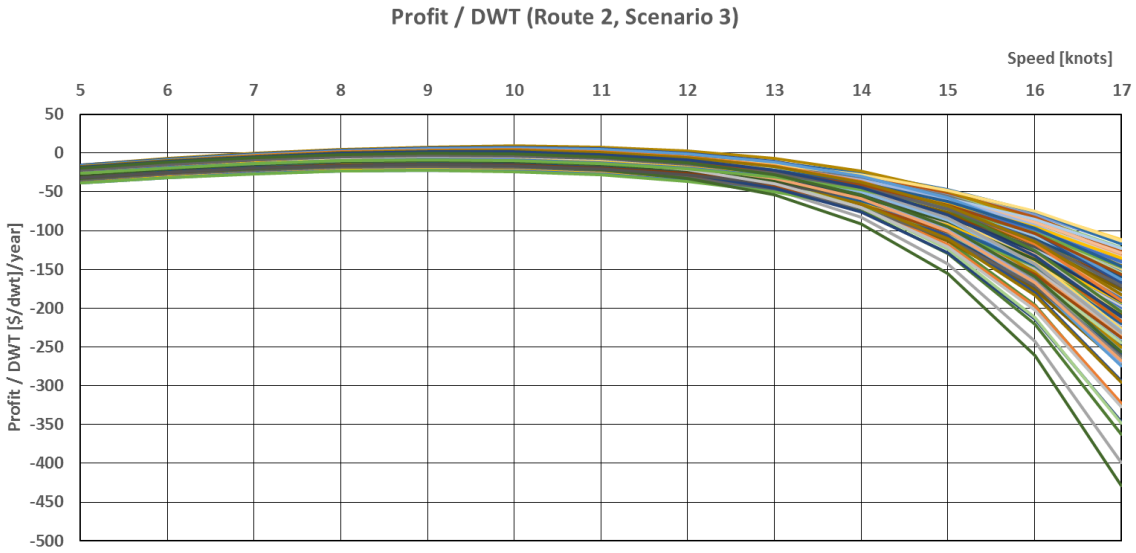
Profit / DWT (Route 2, Scenario 3)
Speed [knots]
5 6 7 8 9 10 11 12 13 14 15 16 17
50 0 -50 -100 -150 -200 -250 -300 -350 -400 -450 -500
Profit / DWT [$/dwt]/year]

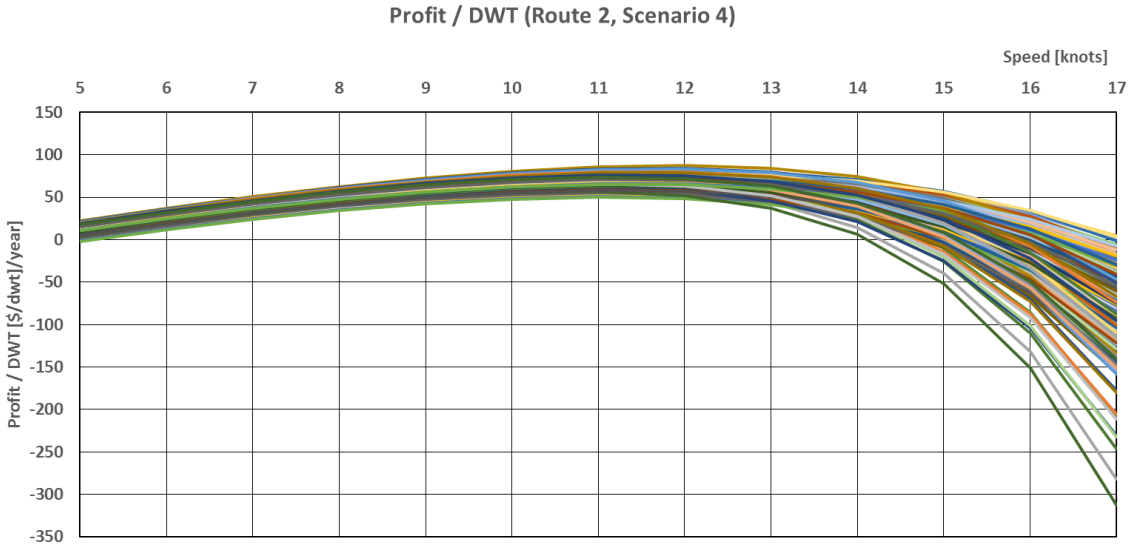
Profit / DWT (Route 2, Scenario 4)
Speed [knots]
5 6 7 8 9 10 11 12 13 14 15 16 17
150 100 50 0 -50 -100 -150 -200 -250 -300 -350
Profit / DWT [$/dwt]/year]

Appendix I

1- VBA Code to solve the optimisation problem for single criterion considered one at a time in the case of constant design speed and for the speed range case.

```
Sub f0()

'

' Pick up Route details

Range("$E$15").Value = Range("$DX$2").Value
Range("$E$16").Value = Range("$DX$3").Value
Range("$E$17").Value = Range("$DX$4").Value
Range("$E$18").Value = Range("$DX$5").Value


' f_0 at design speed

Dim j As Integer
For j = 0 To 3

Range("$BJ$3").Value = Range("$BJ$19").Offset(0, j)
Range("$BJ$4").Value = Range("$BJ$20").Offset(0, j)
Range("$BJ$5").Value = Range("$BJ$21").Offset(0, j)
Range("$BJ$6").Value = Range("$BJ$22").Offset(0, j)


SolverReset

    SolverOk    SetCell:=Range("$BH$19").Offset(j,    0),    MaxMinVal:=2,
ValueOf:=0, ByChange:= _
        "$J$3,$K$3,$L$3,$M$3,$N$3", Engine:=1, EngineDesc:="GRG Nonlinear"

    SolverAdd CellRef:="$J$3", Relation:=1, FormulaText:="$J$5"
    SolverAdd CellRef:="$J$3", Relation:=3, FormulaText:="$J$4"
    SolverAdd CellRef:="$K$3", Relation:=1, FormulaText:="$K$5"
    SolverAdd CellRef:="$K$3", Relation:=3, FormulaText:="$K$4"
    SolverAdd CellRef:="$L$3", Relation:=1, FormulaText:="$L$5"
    SolverAdd CellRef:="$L$3", Relation:=3, FormulaText:="$L$4"
    SolverAdd CellRef:="$M$3", Relation:=1, FormulaText:="$M$5"
    SolverAdd CellRef:="$M$3", Relation:=3, FormulaText:="$M$4"
    SolverAdd CellRef:="$N$3", Relation:=1, FormulaText:="$N$5"
    SolverAdd CellRef:="$N$3", Relation:=3, FormulaText:="$N$4"
    SolverAdd CellRef:="$O$3", Relation:=1, FormulaText:="$O$5"
    SolverAdd CellRef:="$O$3", Relation:=3, FormulaText:="$O$4"
    SolverAdd CellRef:="$P$3", Relation:=1, FormulaText:="$P$5"
    SolverAdd CellRef:="$P$3", Relation:=3, FormulaText:="$P$4"

    Range("$O$3").Value = 15

    SolverOptions    MaxTime:=0,    Iterations:=0,    Precision:=0.000001,
Convergence:= _
        0.0000001,  StepThru:=False,  Scaling:=True,  AssumeNonNeg:=False,
Derivatives:=1
    SolverOptions PopulationSize:=100, RandomSeed:=0, MutationRate:=0.075,
Multistart _
```

```
        :=True, RequireBounds:=True, MaxSubproblems:=0, MaxIntegerSols:=0,

        IntTolerance:=1, SolveWithout:=False, MaxTimeNoImp:=30


    SolverSolve True


Dim n As Integer
For n = 0 To 43

    Range("$BS$5").Offset(j, n).Value = Range("$BS$3").Offset(0, n).Value
Next n

    Next j


' f_0 at speed range

Dim i As Integer
For i = 0 To 3


Range("$BJ$3").Value = Range("$BJ$19").Offset(0, i)
Range("$BJ$4").Value = Range("$BJ$20").Offset(0, i)
Range("$BJ$5").Value = Range("$BJ$21").Offset(0, i)
Range("$BJ$6").Value = Range("$BJ$22").Offset(0, i)


SolverReset

    SolverOk    SetCell:=Range("$BI$19").Offset(i,    0),    MaxMinVal:=2,
ValueOf:=0, ByChange:= _
        "$J$3,$K$3,$L$3,$M$3,$N$3,$O$3",    Engine:=1,    EngineDesc:="GRG
Nonlinear"

    SolverAdd CellRef:="$J$3", Relation:=1, FormulaText:="$J$5"
    SolverAdd CellRef:="$J$3", Relation:=3, FormulaText:="$J$4"
    SolverAdd CellRef:="$K$3", Relation:=1, FormulaText:="$K$5"
    SolverAdd CellRef:="$K$3", Relation:=3, FormulaText:="$K$4"
    SolverAdd CellRef:="$L$3", Relation:=1, FormulaText:="$L$5"
    SolverAdd CellRef:="$L$3", Relation:=3, FormulaText:="$L$4"
    SolverAdd CellRef:="$M$3", Relation:=1, FormulaText:="$M$5"
    SolverAdd CellRef:="$M$3", Relation:=3, FormulaText:="$M$4"
    SolverAdd CellRef:="$N$3", Relation:=1, FormulaText:="$N$5"
    SolverAdd CellRef:="$N$3", Relation:=3, FormulaText:="$N$4"
    SolverAdd CellRef:="$O$3", Relation:=1, FormulaText:="$O$5"
    SolverAdd CellRef:="$O$3", Relation:=3, FormulaText:="$O$4"
    SolverAdd CellRef:="$P$3", Relation:=1, FormulaText:="$P$5"
    SolverAdd CellRef:="$P$3", Relation:=3, FormulaText:="$P$4"


    SolverOptions    MaxTime:=0,    Iterations:=0,    Precision:=0.000001,
Convergence:= _
        0.0000001,  StepThru:=False,  Scaling:=True,  AssumeNonNeg:=False,
Derivatives:=1
    SolverOptions PopulationSize:=100, RandomSeed:=0, MutationRate:=0.075,
Multistart _
        :=True, RequireBounds:=True, MaxSubproblems:=0, MaxIntegerSols:=0,
_
        IntTolerance:=1, SolveWithout:=False, MaxTimeNoImp:=30
```

```
    SolverSolve True


Dim q As Integer
For q = 0 To 43

    Range("$BS$11").Offset(i, q).Value = Range("$BS$3").Offset(0, q).Value
Next q

    Next i

End Sub
```

2- VBA Code to solve the multi-objective functions optimisation problem at the design speed:

```
Sub Design_Speed()

'

' Pick up Route deatails

Range("$E$15").Value = Range("$DX$2").Value
Range("$E$16").Value = Range("$DX$3").Value
Range("$E$17").Value = Range("$DX$4").Value
Range("$E$18").Value = Range("$DX$5").Value


' f_0 at design speed

Dim j As Integer
For j = 0 To 3

Range("$BJ$3").Value = Range("$BJ$19").Offset(0, j)
Range("$BJ$4").Value = Range("$BJ$20").Offset(0, j)
Range("$BJ$5").Value = Range("$BJ$21").Offset(0, j)
Range("$BJ$6").Value = Range("$BJ$22").Offset(0, j)


SolverReset

    SolverOk SetCell:=Range("$BH$19").Offset(j, 0), MaxMinVal:=2,
ValueOf:=0, ByChange:= _
        "$J$3,$K$3,$L$3,$M$3,$N$3", Engine:=1, EngineDesc:="GRG
Nonlinear"

    SolverAdd CellRef:="$J$3", Relation:=1, FormulaText:="$J$5"
    SolverAdd CellRef:="$J$3", Relation:=3, FormulaText:="$J$4"
    SolverAdd CellRef:="$K$3", Relation:=1, FormulaText:="$K$5"
    SolverAdd CellRef:="$K$3", Relation:=3, FormulaText:="$K$4"
    SolverAdd CellRef:="$L$3", Relation:=1, FormulaText:="$L$5"
    SolverAdd CellRef:="$L$3", Relation:=3, FormulaText:="$L$4"
    SolverAdd CellRef:="$M$3", Relation:=1, FormulaText:="$M$5"
    SolverAdd CellRef:="$M$3", Relation:=3, FormulaText:="$M$4"
    SolverAdd CellRef:="$N$3", Relation:=1, FormulaText:="$N$5"
    SolverAdd CellRef:="$N$3", Relation:=3, FormulaText:="$N$4"
    SolverAdd CellRef:="$O$3", Relation:=1, FormulaText:="$O$5"
    SolverAdd CellRef:="$O$3", Relation:=3, FormulaText:="$O$4"
    SolverAdd CellRef:="$P$3", Relation:=1, FormulaText:="$P$5"
    SolverAdd CellRef:="$P$3", Relation:=3, FormulaText:="$P$4"

    Range("$O$3").Value = 15

    SolverOptions MaxTime:=0, Iterations:=0, Precision:=0.000001,
Convergence:= _
        0.0000001, StepThru:=False, Scaling:=True, AssumeNonNeg:=False,
Derivatives:=1
    SolverOptions PopulationSize:=100, RandomSeed:=0,
MutationRate:=0.075, Multistart _
        :=True, RequireBounds:=True, MaxSubproblems:=0,
MaxIntegerSols:=0, _
        IntTolerance:=1, SolveWithout:=False, MaxTimeNoImp:=30
```

```
    SolverSolve True


Dim n As Integer
For n = 0 To 43

    Range("$BS$5").Offset(j, n).Value = Range("$BS$3").Offset(0, n).Value
Next n

    Next j


' f_0 at speed range

Dim i As Integer
For i = 0 To 3


Range("$BJ$3").Value = Range("$BJ$19").Offset(0, i)
Range("$BJ$4").Value = Range("$BJ$20").Offset(0, i)
Range("$BJ$5").Value = Range("$BJ$21").Offset(0, i)
Range("$BJ$6").Value = Range("$BJ$22").Offset(0, i)


SolverReset

    SolverOk SetCell:=Range("$BI$19").Offset(i, 0), MaxMinVal:=2,
ValueOf:=0, ByChange:= _
        "$J$3,$K$3,$L$3,$M$3,$N$3,$O$3", Engine:=1, EngineDesc:="GRG
Nonlinear"

    SolverAdd CellRef:="$J$3", Relation:=1, FormulaText:="$J$5"
    SolverAdd CellRef:="$J$3", Relation:=3, FormulaText:="$J$4"
    SolverAdd CellRef:="$K$3", Relation:=1, FormulaText:="$K$5"
    SolverAdd CellRef:="$K$3", Relation:=3, FormulaText:="$K$4"
    SolverAdd CellRef:="$L$3", Relation:=1, FormulaText:="$L$5"
    SolverAdd CellRef:="$L$3", Relation:=3, FormulaText:="$L$4"
    SolverAdd CellRef:="$M$3", Relation:=1, FormulaText:="$M$5"
    SolverAdd CellRef:="$M$3", Relation:=3, FormulaText:="$M$4"
    SolverAdd CellRef:="$N$3", Relation:=1, FormulaText:="$N$5"
    SolverAdd CellRef:="$N$3", Relation:=3, FormulaText:="$N$4"
    SolverAdd CellRef:="$O$3", Relation:=1, FormulaText:="$O$5"
    SolverAdd CellRef:="$O$3", Relation:=3, FormulaText:="$O$4"
    SolverAdd CellRef:="$P$3", Relation:=1, FormulaText:="$P$5"
    SolverAdd CellRef:="$P$3", Relation:=3, FormulaText:="$P$4"


    SolverOptions MaxTime:=0, Iterations:=0, Precision:=0.000001,
Convergence:= _
        0.0000001, StepThru:=False, Scaling:=True, AssumeNonNeg:=False,
Derivatives:=1
    SolverOptions PopulationSize:=100, RandomSeed:=0,
MutationRate:=0.075, Multistart _
        :=True, RequireBounds:=True, MaxSubproblems:=0,
MaxIntegerSols:=0, _
        IntTolerance:=1, SolveWithout:=False, MaxTimeNoImp:=30


    SolverSolve True
```

```
Dim q As Integer
For q = 0 To 43

    Range("$BS$11").Offset(i, q).Value = Range("$BS$3").Offset(0,
q).Value
Next q

    Next i


' All Calculations

' change constraint for EEDI
Dim g As Integer
For g = 0 To 4

' change optimisation method
Dim h As Integer
For h = 0 To 4


' Run the macro at the Design Speed for different weights


Dim m As Integer
For m = 0 To 485

Range("$BJ$3").Value = Range("$DR$2").Offset(m, 0)
Range("$BJ$4").Value = Range("$DS$2").Offset(m, 0)
Range("$BJ$5").Value = Range("$DT$2").Offset(m, 0)
Range("$BJ$6").Value = Range("$DU$2").Offset(m, 0)


'
    SolverReset

    SolverOk SetCell:=Range("$BK$7").Offset(0, h), MaxMinVal:=2,
ValueOf:=0, ByChange:= _
        "$J$3,$K$3,$L$3,$M$3,$N$3", Engine:=1, EngineDesc:="GRG
Nonlinear"

    SolverAdd CellRef:="$BG$4", Relation:=1,
FormulaText:=Range("$BO$19").Offset(g, 0)
    SolverAdd CellRef:="$J$3", Relation:=1, FormulaText:="$J$5"
    SolverAdd CellRef:="$J$3", Relation:=3, FormulaText:="$J$4"
    SolverAdd CellRef:="$K$3", Relation:=1, FormulaText:="$K$5"
    SolverAdd CellRef:="$K$3", Relation:=3, FormulaText:="$K$4"
    SolverAdd CellRef:="$L$3", Relation:=1, FormulaText:="$L$5"
    SolverAdd CellRef:="$L$3", Relation:=3, FormulaText:="$L$4"
    SolverAdd CellRef:="$M$3", Relation:=1, FormulaText:="$M$5"
    SolverAdd CellRef:="$M$3", Relation:=3, FormulaText:="$M$4"
    SolverAdd CellRef:="$N$3", Relation:=1, FormulaText:="$N$5"
    SolverAdd CellRef:="$N$3", Relation:=3, FormulaText:="$N$4"
    SolverAdd CellRef:="$O$3", Relation:=1, FormulaText:="$O$5"
    SolverAdd CellRef:="$O$3", Relation:=3, FormulaText:="$O$4"
    SolverAdd CellRef:="$P$3", Relation:=1, FormulaText:="$P$5"
    SolverAdd CellRef:="$P$3", Relation:=3, FormulaText:="$P$4"

    Range("$O$3").Value = 15
```

```
    SolverOptions MaxTime:=0, Iterations:=0, Precision:=0.000001,
Convergence:= _
        0.0000001, StepThru:=False, Scaling:=True, AssumeNonNeg:=False,
Derivatives:=1
    SolverOptions PopulationSize:=50, RandomSeed:=0, MutationRate:=0.075,
Multistart _
        :=True, RequireBounds:=True, MaxSubproblems:=0,
MaxIntegerSols:=0, _
        IntTolerance:=1, SolveWithout:=False, MaxTimeNoImp:=30


    SolverSolve True


Dim p As Integer
For p = 0 To 61

    Range("$EA$5").Offset(m + (h * 486), p + (g * 62)).Value =
Range("$EA$3").Offset(0, p).Value
Next p

    Range("$DY$5").Offset(h * 486, 0).Value = Range("$DX$55").Offset(h,
0).Value
    Range("$DY$5").Offset(h * 486, 0).Interior.Color = vbYellow

    Next m
    Next h
    Next g


End Sub
```

3- VBA Code to solve the multi-objective functions optimisation problem at the speed range:

```
Sub All_Speeds ()


' All Calculations

' change constraint for EEDI
Dim g As Integer
For g = 0 To 4

' change optimisation method
Dim h As Integer
For h = 0 To 4


' Run the macro at the Design Speed for different weights


Dim m As Integer
For m = 0 To 485

Range("$BJ$11").Value = Range("$DR$2").Offset(m, 0)
Range("$BJ$12").Value = Range("$DS$2").Offset(m, 0)
Range("$BJ$13").Value = Range("$DT$2").Offset(m, 0)
Range("$BJ$14").Value = Range("$DU$2").Offset(m, 0)


'
    SolverReset

    SolverOk    SetCell:=Range("$BK$15").Offset(0,    h),    MaxMinVal:=2,
ValueOf:=0, ByChange:= _
        "$J$3,$K$3,$L$3,$M$3,$N$3,$O$3",    Engine:=1,    EngineDesc:="GRG
Nonlinear"

    SolverAdd                CellRef:="$BG$12",                Relation:=1,
FormulaText:=Range("$BO$19").Offset(g, 0)
    SolverAdd CellRef:="$J$3", Relation:=1, FormulaText:="$J$5"
    SolverAdd CellRef:="$J$3", Relation:=3, FormulaText:="$J$4"
    SolverAdd CellRef:="$K$3", Relation:=1, FormulaText:="$K$5"
    SolverAdd CellRef:="$K$3", Relation:=3, FormulaText:="$K$4"
    SolverAdd CellRef:="$L$3", Relation:=1, FormulaText:="$L$5"
    SolverAdd CellRef:="$L$3", Relation:=3, FormulaText:="$L$4"
    SolverAdd CellRef:="$M$3", Relation:=1, FormulaText:="$M$5"
    SolverAdd CellRef:="$M$3", Relation:=3, FormulaText:="$M$4"
    SolverAdd CellRef:="$N$3", Relation:=1, FormulaText:="$N$5"
    SolverAdd CellRef:="$N$3", Relation:=3, FormulaText:="$N$4"
    SolverAdd CellRef:="$O$3", Relation:=1, FormulaText:="$O$5"
    SolverAdd CellRef:="$O$3", Relation:=3, FormulaText:="$O$4"
    SolverAdd CellRef:="$P$3", Relation:=1, FormulaText:="$P$5"
    SolverAdd CellRef:="$P$3", Relation:=3, FormulaText:="$P$4"



    SolverOptions    MaxTime:=0,    Iterations:=0,    Precision:=0.000001,
Convergence:= _
        0.0000001,  StepThru:=False,  Scaling:=True,  AssumeNonNeg:=False,
Derivatives:=1
```

```
    SolverOptions PopulationSize:=50, RandomSeed:=0, MutationRate:=0.075,
Multistart
        :=True, RequireBounds:=True, MaxSubproblems:=0, MaxIntegerSols:=0,
_
        IntTolerance:=1, SolveWithout:=False, MaxTimeNoImp:=30


    SolverSolve True


Dim p As Integer
For p = 0 To 61

    Range("$EA$5").Offset(m + (h * 486), p + (g * 62)).Value =
Range("$EA$3").Offset(0, p).Value
Next p

    Range("$DY$5").Offset(h * 486, 0).Value = Range("$DX$55").Offset(h,
0).Value
    Range("$DY$5").Offset(h * 486, 0).Interior.Color = vbYellow

    Next m
    Next h
    Next g


End Sub
```

Appendix J

- **Optimisation model's solutions at the design speed for Route One, Scenario Two (low fuel price and high fright rates):**

Single Criterion results for Route One, Scenario Two at the design speed

	Minimum P_D/Dis	Minimum $EEDI_A/EEDI_{Ref}$	Maximum *Profit/tonne.mile*	Maximum *NPV*
Criteria				
P_D/Dis	**0.10969**	0.10969	0.12822	0.12822
$EEDI_A/EEDI_{Ref}$	0.81358	**0.81358**	0.98976	0.98976
Profit/tonne.mile $\times 10^{-3}$	3.10249	3.10249	**3.37584**	3.37584
NPV	50.01310	50.01310	82.45227	**82.45227**
Independent Variables				
Length	222.75	222.75	222.75	222.75
Breadth	30.5950	30.5950	33.8241	33.8241
Draught	12.8388	12.8388	12.8388	12.8388
Breadth/Draught	2.3830	2.3830	2.6345	2.6345
Block Coefficient	0.7759	0.7759	0.8749	0.8749
Long Centre of Buoyancy %L	-0.01	-0.01	-0.01	-0.01
Speed	15	15	15	15
Other Characteristics				
Deadweight [ton]	54900.3106	54900.3106	70472.1370	70472.1370
Lightweight [ton]	14683.9319	14683.9319	16276.7683	16276.7683
Capital Cost [$ m]	38.4690	38.4690	40.8065	40.8065
Annual Fuel Cost [$]	3602444.55	3602444.55	4866796.12	4866796.12
Annual Operating cost [$]	2963476.16	2963476.16	3014061.24	3014061.24
Total annual cost [$]	9984856.44	9984856.44	11984768.40	11984768.40
Profit per DWT [$/dwt]	134.02751	134.02751	145.83607	145.83607
Annual Bunker Cons [ton]	5754.97	5754.97	7918.57	7918.57
Annual MDO Cons [ton]	1035.66	1035.66	1296.45	1296.45

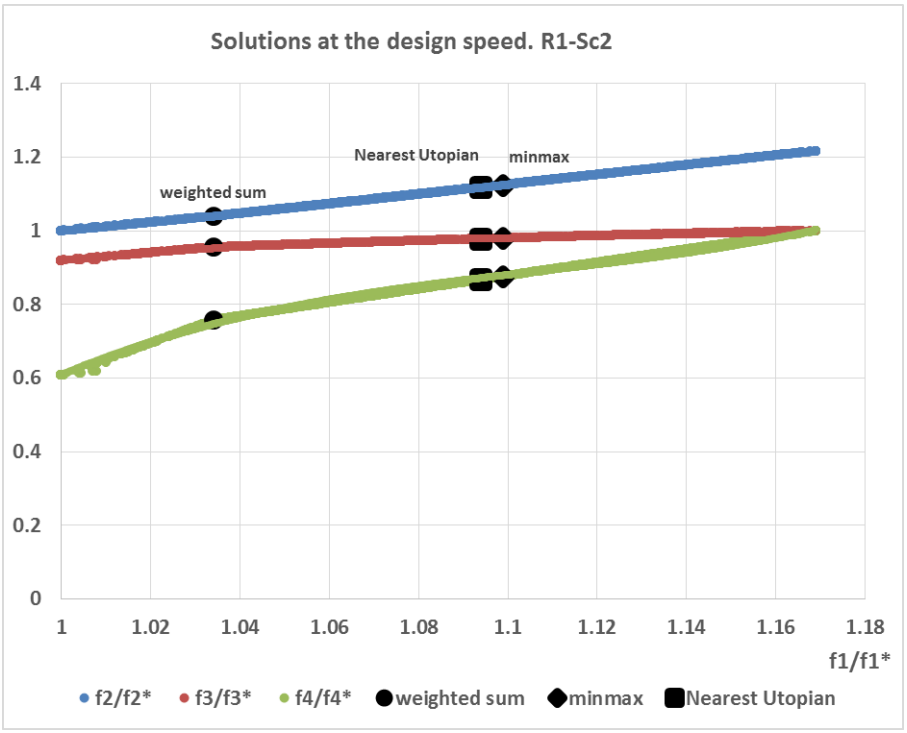

Pareto front at the design speed. Route One, Scenario Two

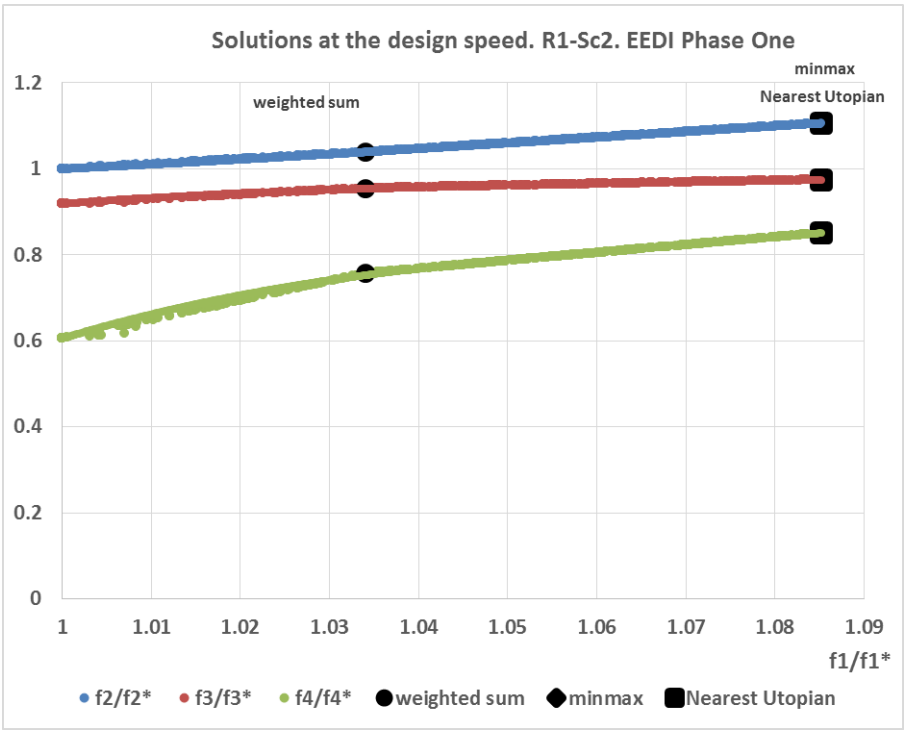

Pareto front at the design speed. Route One, Scenario Two. EEDI Phase One

Optimum solutions with the added EEDI reduction factor constraint. Route One, Scenario Two

	Phase One reduction factor constraint	*Phase Two and Three reduction factors constraint*
Criteria		
P_D/Dis	0.11903	0.1099
$EEDI_A/EEDI_{Ref}$	0.9	0.81357
$Profit/tonne.mile \times 10^{-3}$	3.290924	3.102489
NPV	70.14386	50.0131
Independent Variables		
Length	222.75	222.75
Breadth	33.8241	30.5950
Draught	12.8388	12.8388
Breadth/Draught	2.6345	2.3830
Block Coefficient	0.8134	0.7759
Long Centre of Buoyancy %L	-0.01	-0.01
Speed	15	15
Other Characteristics		
Deadweight [ton]	64467.35	54900.31
Lightweight [ton]	16183.2	14683.93
Capital Cost [$ m]	39.905	38.46902
Annual Fuel Cost [$]	4322326	3602445
Annual Operating cost [$]	2994555	2963476
Total annual cost [$]	11200047	9984856
Profit per DWT [$/dwt]	142.1679	134.0275
Annual Bunker Cons [ton]	6974.32	5754.967
Annual MDO Cons [ton]	1193.1	1035.658
$EEDI_A/EEDI_{Ref\text{-}Phase\ One}$	1 (satisfied)	0.903977
$EEDI_A/EEDI_{Ref\text{-}Phase\ Two}$	1.125	1.016974 (not satisfied)
$EEDI_A/EEDI_{Ref\text{-}PhaseThree}$	1.285714	1.162256 (not satisfied)

- **Optimisation model's solutions at the design speed for Route One, Scenario Three (high fuel price and low fright rates):**

Single Criterion results for Route One, Scenario Three at the design speed

	Minimum P_D/Dis	Minimum $EEDI_A/EEDI_{Ref}$	Maximum *Profit/tonne.mile*	Maximum *NPV*
Criteria				
P_D/Dis	**0.10969**	0.10969	0.12822	0.11838
$EEDI_A/EEDI_{Ref}$	0.81358	**0.81358**	0.98976	0.89368
Profit/tonne.mile $\times 10^{-3}$	-0.68147	-0.68147	**-0.45723**	-0.51913
NPV	-56.52001	-56.52001	-56.07228	**-55.64095**
Independent Variables				
Length	222.75	222.75	222.75	222.75
Breadth	30.5950	30.5950	33.8241	33.8241
Draught	12.8388	12.8388	12.8388	12.8388
Breadth/Draught	2.3830	2.3830	2.6345	2.6345
Block Coefficient	0.7759	0.7759	0.8749	0.8091
Long Centre of Buoyancy %L	-0.01	-0.01	-0.01	-0.01
Speed	15	15	15	15
Other Characteristics				
Deadweight [ton]	54900.3106	54900.3106	70472.1370	64044.4879
Lightweight [ton]	14683.9319	14683.9319	16276.7683	16176.6748
Capital Cost [$ m]	38.4690	38.4690	40.8065	39.8417
Annual Fuel Cost [$]	5639632.28	5639632.28	7631300.36	6714466.39
Annual Operating cost [$]	2963476.16	2963476.16	3014061.24	2993181.02
Total annual cost [$]	12022044.17	12022044.17	14749272.65	13575268.56
Profit per DWT [$/dwt]	-29.43953	-29.43953	-19.75226	-22.42623
Annual Bunker Cons [ton]	5754.97	5754.97	7918.57	6910.45
Annual MDO Cons [ton]	1035.66	1035.66	1296.45	1186.10

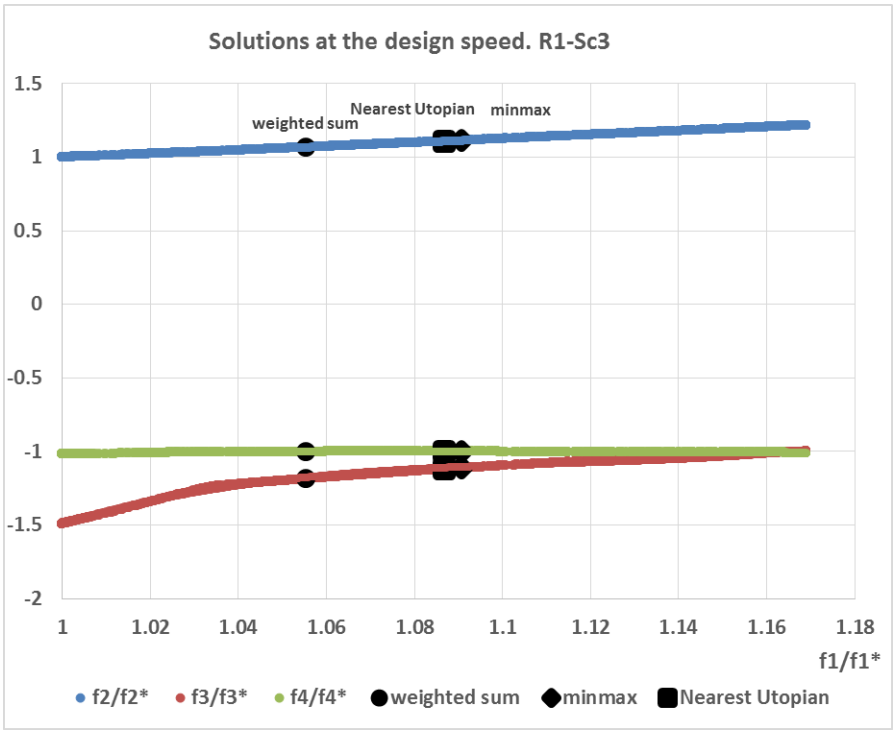

Pareto front at the design speed. Route One, Scenario Three

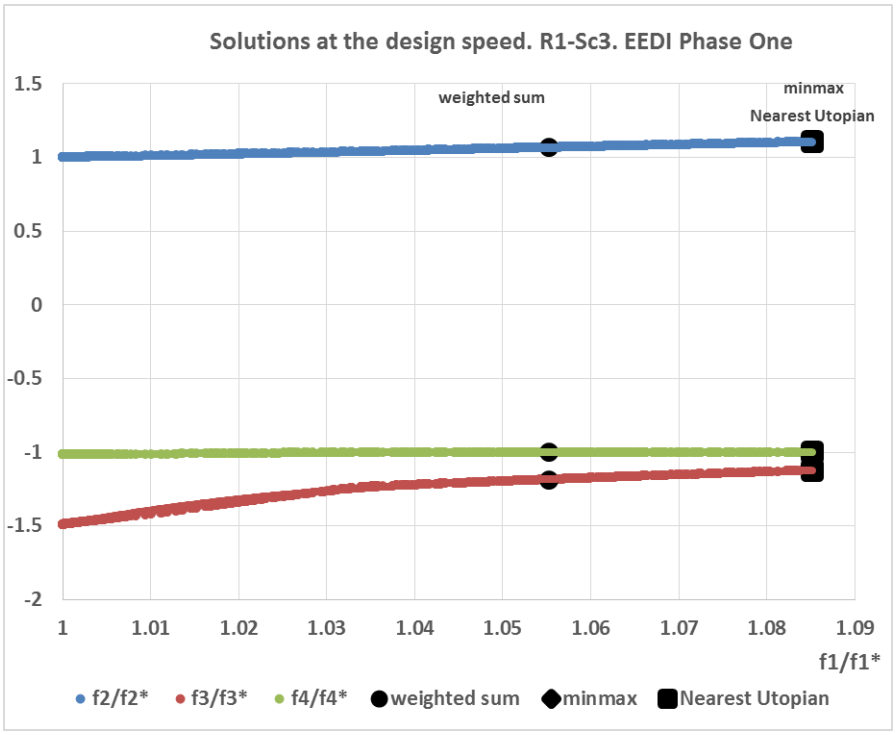

Pareto front at the design speed. Route One, Scenario Three. EEDI Phase One

Optimum solutions with the added EEDI reduction factor constraint. Route One, Scenario Three

	Phase One reduction factor constraint	*Phase Two and Three reduction factors constraint*
Criteria		
P_D/Dis	0.11903	0.1099
$EEDI_A/EEDI_{Ref}$	0.9	0.81357
$Profit/tonne.mile \times 10^{-3}$	-0.51387	-0.68147
NPV	-55.6428	-56.52
Independent Variables		
Length	222.75	222.75
Breadth	33.8241	30.5950
Draught	12.8388	12.8388
Breadth/Draught	2.6345	2.3830
Block Coefficient	0.8134	0.7759
Long Centre of Buoyancy %L	-0.01	-0.01
Speed	15	15
Other Characteristics		
Deadweight [ton]	64467.35	54900.31
Lightweight [ton]	16183.2	14683.93
Capital Cost [$ m]	39.905	38.46902
Annual Fuel Cost [$]	6772550	5639632
Annual Operating cost [$]	2994555	2963476
Total annual cost [$]	13650271.03	12022044
Profit per DWT [$/dwt]	-22.1993	-29.4395
Annual Bunker Cons [ton]	6974.32	5754.967
Annual MDO Cons [ton]	1193.1	1035.658
$EEDI_A/EEDI_{Ref\text{-}Phase\ One}$	1 (satisfied)	0.903977
$EEDI_A/EEDI_{Ref\text{-}Phase\ Two}$	1.125	1.016974 (not satisfied)
$EEDI_A/EEDI_{Ref\text{-}PhaseThree}$	1.285714	1.162256 (not satisfied)

- **Optimisation model's solutions at the design speed for Route One, Scenario Four (high fuel price and high fright rates):**

Single Criterion results for Route One, Scenario Four at the design speed

	Minimum P_D/Dis	Minimum $EEDI_A/EEDI_{Ref}$	Maximum *Profit/tonne.mile*	Maximum *NPV*
Criteria				
P_D/Dis	**0.10969**	0.10969	0.12822	0.12822
$EEDI_A/EEDI_{Ref}$	0.81358	**0.81358**	0.98976	0.98976
Profit/tonne.mile × 10^{-3}	2.24353	2.24353	**2.46777**	2.46777
NPV	25.83007	25.83007	49.63543	**49.63543**
Independent Variables				
Length	222.75	222.75	222.75	222.75
Breadth	30.5950	30.5950	33.8241	33.8241
Draught	12.8388	12.8388	12.8388	12.8388
Breadth/Draught	2.3830	2.3830	2.6345	2.6345
Block Coefficient	0.7759	0.7759	0.8749	0.8749
Long Centre of Buoyancy %L	-0.01	-0.01	-0.01	-0.01
Speed	15	15	15	15
Other Characteristics				
Deadweight [ton]	54900.3106	54900.3106	70472.1370	70472.1370
Lightweight [ton]	14683.9319	14683.9319	16276.7683	16276.7683
Capital Cost [$ m]	38.4690	38.4690	40.8065	40.8065
Annual Fuel Cost [$]	5639632.28	5639632.28	7631300.36	7631300.36
Annual Operating cost [$]	2963476.16	2963476.16	3014061.24	3014061.24
Total annual cost [$]	12022044.17	12022044.17	14749272.65	14749272.65
Profit per DWT [$/dwt]	96.92047	96.92047	106.60774	106.60774
Annual Bunker Cons [ton]	5754.97	5754.97	7918.57	7918.57
Annual MDO Cons [ton]	1035.66	1035.66	1296.45	1296.45

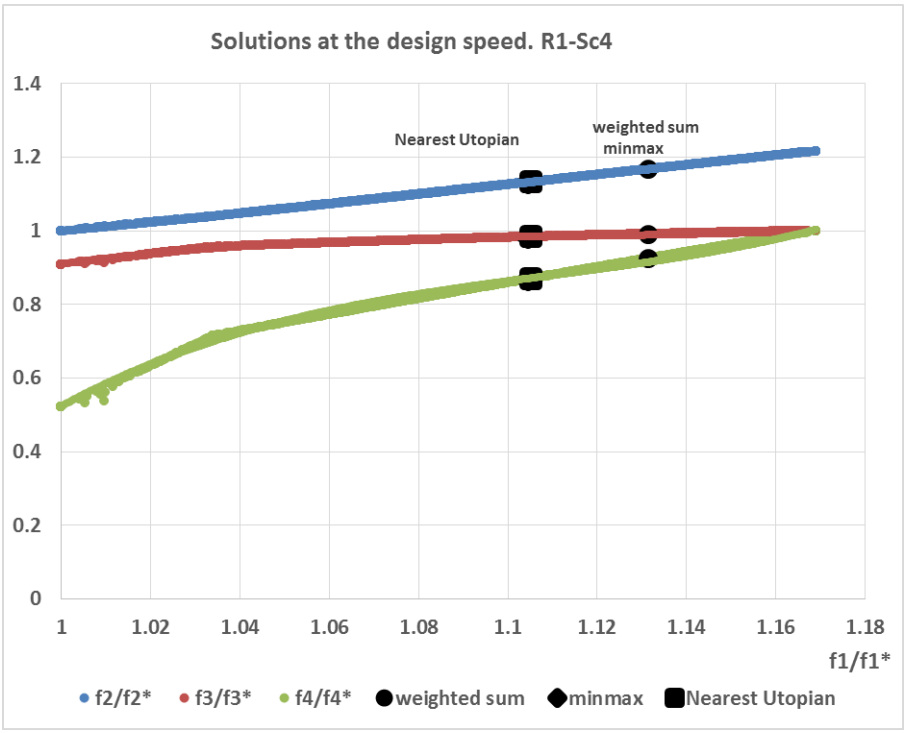

Pareto front at the design speed. Route One, Scenario Four

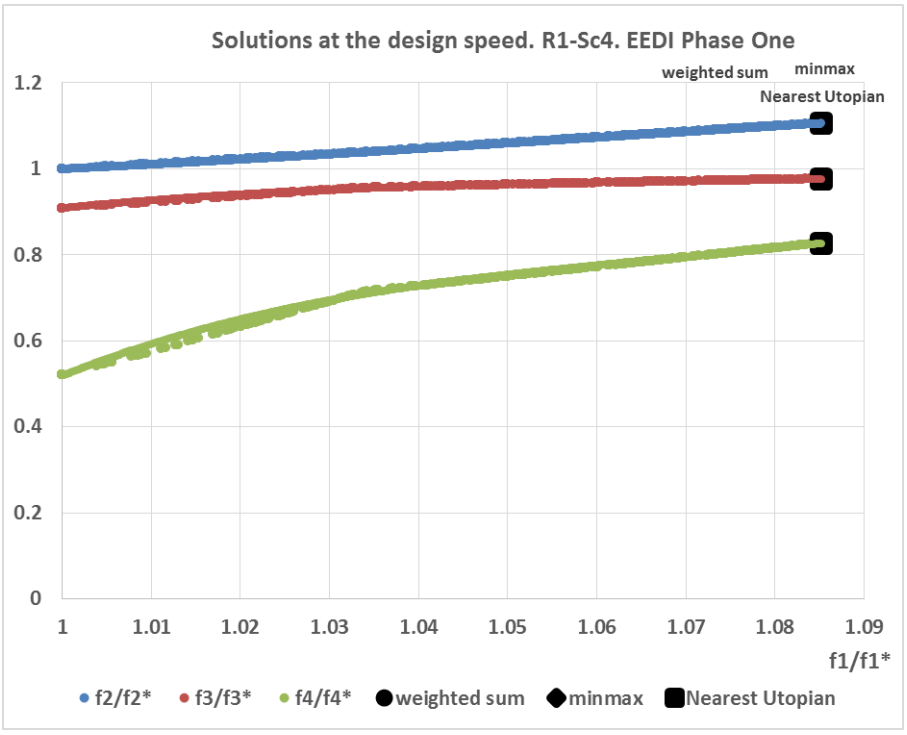

Pareto front at the design speed. Route One, Scenario Four. EEDI Phase One

Optimum solutions with the added EEDI reduction factor constraint. Route One, Scenario Four

	Phase One reduction factor constraint	*Phase Two and Three reduction factors constraint*
Criteria		
P_D/Dis	0.11903	0.1099
$EEDI_A/EEDI_{Ref}$	0.9	0.81357
$Profit/tonne.mile \times 10^{-3}$	2.411128	2.243529
NPV	41.05776	25.83007
Independent Variables		
Length	222.75	222.75
Breadth	33.8241	30.5950
Draught	12.8388	12.8388
Breadth/Draught	2.6345	2.3830
Block Coefficient	0.8134	0.7759
Long Centre of Buoyancy %L	-0.01	-0.01
Speed	15	15
Other Characteristics		
Deadweight [ton]	64467.35	54900.31
Lightweight [ton]	16183.2	14683.93
Capital Cost [$ m]	39.905	38.46902
Annual Fuel Cost [$]	6772550	5639632
Annual Operating cost [$]	2994555	2963476
Total annual cost [$]	13650271.03	12022044
Profit per DWT [$/dwt]	104.1607	96.92047
Annual Bunker Cons [ton]	6974.32	5754.967
Annual MDO Cons [ton]	1193.1	1035.658
$EEDI_A/EEDI_{Ref\text{-}Phase\ One}$	1 (satisfied)	0.903977
$EEDI_A/EEDI_{Ref\text{-}Phase\ Two}$	1.125	1.016974 (not satisfied)
$EEDI_A/EEDI_{Ref\text{-}PhaseThree}$	1.285714	1.162256 (not satisfied)

- **Optimisation model's solutions at the design speed for Route Two, Scenario One (low fuel price and low fright rates):**

Single Criterion results for Route Two, Scenario One at the design speed

	Minimum P_D/Dis	Minimum $EEDI_A/EEDI_{Ref}$	Maximum *Profit/tonne.mile*	Maximum *NPV*
Criteria				
P_D/Dis	**0.10969**	0.10969	0.12822	0.12822
$EEDI_A/EEDI_{Ref}$	0.81358	**0.81358**	0.98976	0.98976
Profit/tonne.mile × 10^{-3}	0.80524	0.80524	**0.94843**	0.94843
NPV	-9.37739	-9.37739	2.71916	**2.71916**
Independent Variables				
Length	222.75	222.75	222.75	222.75
Breadth	30.5950	30.5950	33.8241	33.8241
Draught	12.8388	12.8388	12.8388	12.8388
Breadth/Draught	2.3830	2.3830	2.6345	2.6345
Block Coefficient	0.7759	0.7759	0.8749	0.8749
Long Centre of Buoyancy %L	-0.01	-0.01	-0.01	-0.01
Speed	15	15	15	15
Other Characteristics				
Deadweight [ton]	54900.3106	54900.3106	70472.1370	70472.1370
Lightweight [ton]	14683.9319	14683.9319	16276.7683	16276.7683
Capital Cost [$ m]	38.4690	38.4690	40.8065	40.8065
Annual Fuel Cost [$]	3778712.78	3778712.78	5270551.37	5270551.37
Annual Operating cost [$]	2963476.16	2963476.16	3014061.24	3014061.24
Total annual cost [$]	8236442.15	8236442.15	10035043.90	10035043.90
Profit per DWT [$/dwt]	42.89727	42.89727	50.52537	50.52537
Annual Bunker Cons [ton]	6304.05	6304.05	8972.12	8972.12
Annual MDO Cons [ton]	895.27	895.27	1120.70	1120.70

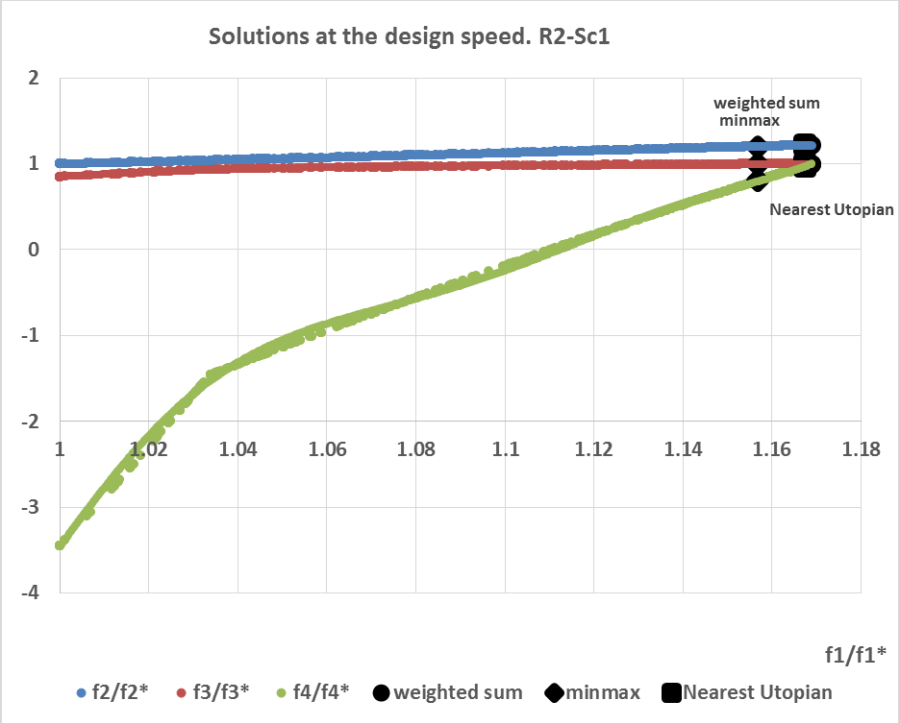

Pareto front at the design speed. Route Two, Scenario one

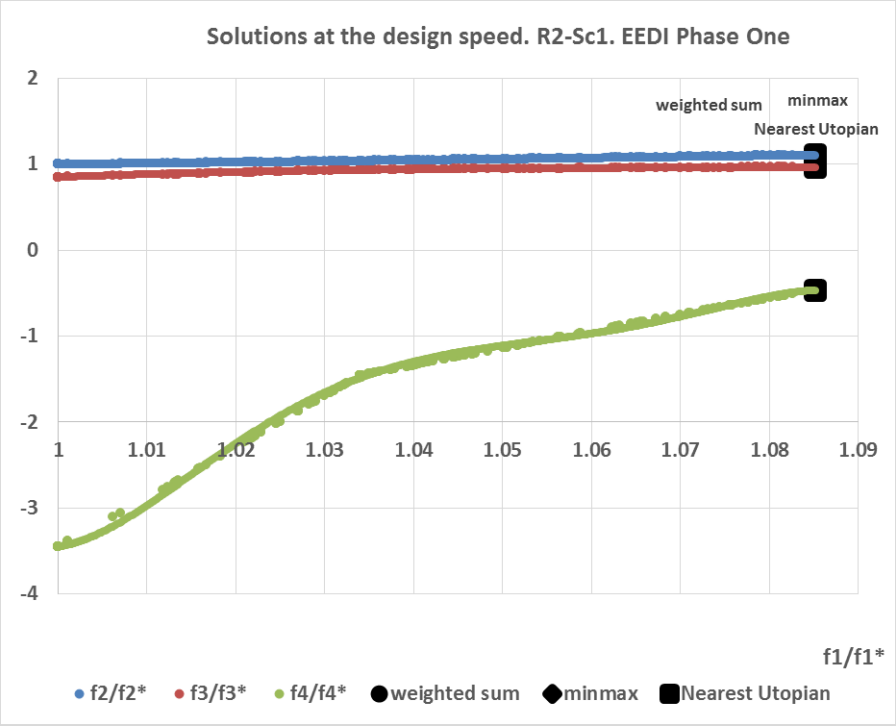

Pareto front at the design speed. Route Two, Scenario One. EEDI Phase One

Optimum solutions with the added EEDI reduction factor constraint. Route Two, Scenario One

	Phase One reduction factor constraint	*Phase Two and Three reduction factors constraint*
Criteria		
P_D/Dis	0.11903	0.1099
$EEDI_A/EEDI_{Ref}$	0.9	0.81357
$Profit/tonne.mile \times 10^{-3}$	3.290924	0.805242
NPV	70.14386	-9.37739
Independent Variables		
Length	222.75	222.75
Breadth	33.8241	30.5950
Draught	12.8388	12.8388
Breadth/Draught	2.6345	2.3830
Block Coefficient	0.8134	0.7759
Long Centre of Buoyancy %L	-0.01	-0.01
Speed	15	15
Other Characteristics		
Deadweight [ton]	64467.35	54900.31
Lightweight [ton]	16183.2	14683.93
Capital Cost [$ m]	39.905	38.46902
Annual Fuel Cost [$]	4625807	3778713
Annual Operating cost [$]	2994555	2963476
Total annual cost [$]	9287295.696	8236442
Profit per DWT [$/dwt]	48.86069824	42.89727
Annual Bunker Cons [ton]	7807.712	6304.053
Annual MDO Cons [ton]	1031.359	895.2661
$EEDI_A/EEDI_{Ref\text{-}Phase\ One}$	1 (satisfied)	0.903977
$EEDI_A/EEDI_{Ref\text{-}Phase\ Two}$	1.125	1.016974 (not satisfied)
$EEDI_A/EEDI_{Ref\text{-}PhaseThree}$	1.285714	1.162256 (not satisfied)

- **Optimisation model's solutions at the design speed for Route Two, Scenario Two (low fuel price and high fright rates):**

Single Criterion results for Route Two, Scenario Two at the design speed

	Minimum P_D/Dis	Minimum $EEDI_A/EEDI_{Ref}$	Maximum *Profit/tonne.mile*	Maximum *NPV*
Criteria				
P_D/Dis	**0.10969**	0.10969	0.12822	0.12822
$EEDI_A/EEDI_{Ref}$	0.81358	**0.81358**	0.98976	0.98976
Profit/tonne.mile × 10^{-3}	2.75524	2.75524	**2.89843**	2.89843
NPV	58.32319	58.32319	89.62222	**89.62222**
Independent Variables				
Length	222.75	222.75	222.75	222.75
Breadth	30.5950	30.5950	33.8241	33.8241
Draught	12.8388	12.8388	12.8388	12.8388
Breadth/Draught	2.3830	2.3830	2.6345	2.6345
Block Coefficient	0.7759	0.7759	0.8749	0.8749
Long Centre of Buoyancy %L	-0.01	-0.01	-0.01	-0.01
Speed	15	15	15	15
Other Characteristics				
Deadweight [ton]	54900.3106	54900.3106	70472.1370	70472.1370
Lightweight [ton]	14683.9319	14683.9319	16276.7683	16276.7683
Capital Cost [$ m]	38.4690	38.4690	40.8065	40.8065
Annual Fuel Cost [$]	3778712.78	3778712.78	5270551.37	5270551.37
Annual Operating cost [$]	2963476.16	2963476.16	3014061.24	3014061.24
Total annual cost [$]	8236442.15	8236442.15	10035043.90	10035043.90
Profit per DWT [$/dwt]	146.77873	146.77873	154.40682	154.40682
Annual Bunker Cons [ton]	6304.05	6304.05	8972.12	8972.12
Annual MDO Cons [ton]	895.27	895.27	1120.70	1120.70

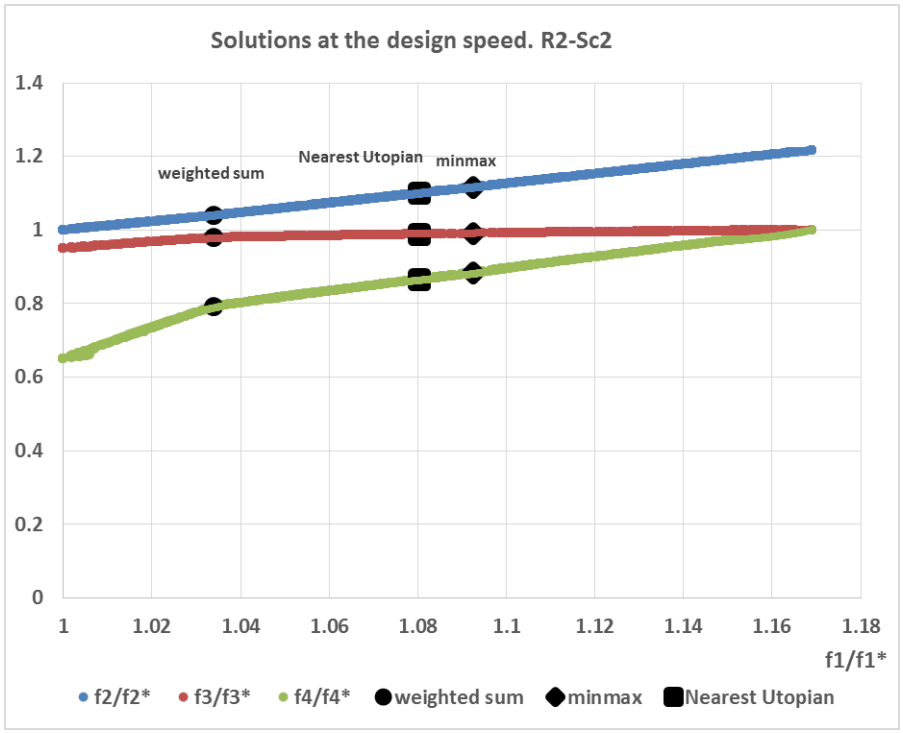

Pareto front at the design speed. Route Two, Scenario Two

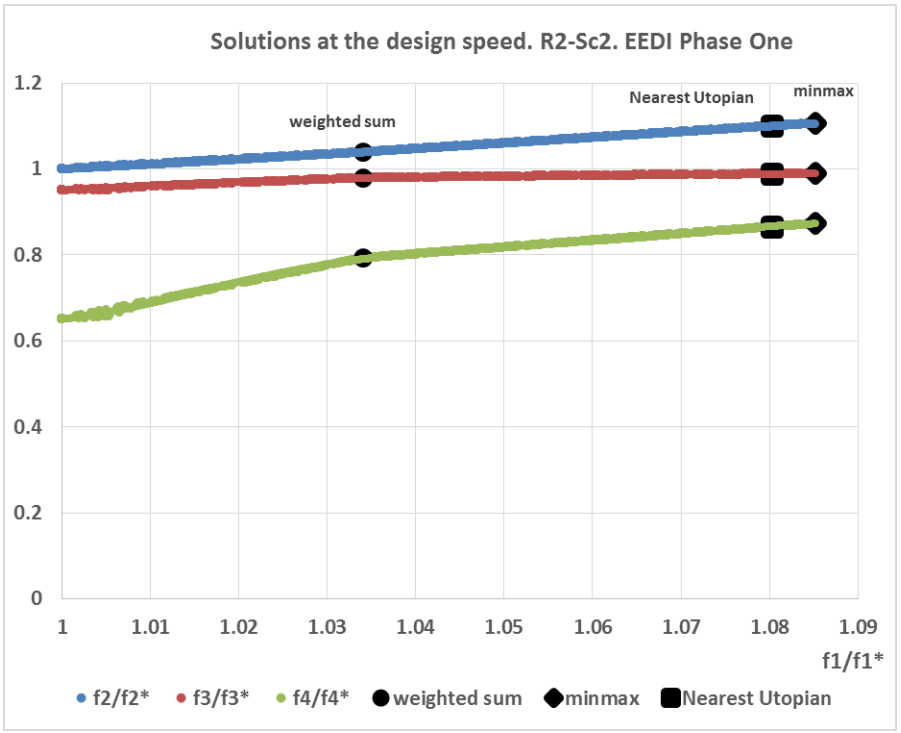

Pareto front at the design speed. Route Two, Scenario Two. EEDI Phase One

Optimum solutions with the added EEDI reduction factor constraint. Route Two, Scenario Two

	Phase One reduction factor constraint	*Phase Two and Three reduction factors constraint*
Criteria		
P_D/Dis	0.11903	0.1099
$EEDI_A/EEDI_{Ref}$	0.9	0.81357
$Profit/tonne.mile \times 10^{-3}$	3.290924	2.755242
NPV	70.14386	58.32319
Independent Variables		
Length	222.75	222.75
Breadth	33.8241	30.5950
Draught	12.8388	12.8388
Breadth/Draught	2.6345	2.3830
Block Coefficient	0.8134	0.7759
Long Centre of Buoyancy %L	-0.01	-0.01
Speed	15	15
Other Characteristics		
Deadweight [ton]	64467.35	54900.31
Lightweight [ton]	16183.2	14683.93
Capital Cost [$ m]	39.905	38.46902
Annual Fuel Cost [$]	4625807	3778713
Annual Operating cost [$]	2994555	2963476
Total annual cost [$]	9287295.696	8236442
Profit per DWT [$/dwt]	152.742149	146.7787
Annual Bunker Cons [ton]	7807.712	6304.053
Annual MDO Cons [ton]	1031.359	895.2661
$EEDI_A/EEDI_{Ref\text{-}Phase\ One}$	1 (satisfied)	0.903977
$EEDI_A/EEDI_{Ref\text{-}Phase\ Two}$	1.125	1.016974 (not satisfied)
$EEDI_A/EEDI_{Ref\text{-}PhaseThree}$	1.285714	1.162256 (not satisfied)

- **Optimisation model's solutions at the design speed for Route Two, Scenario Three (high fuel price and low fright rates):**

Single Criterion results for Route Two, Scenario Three at the design speed

	Minimum P_D/Dis	Minimum $EEDI_A/EEDI_{Ref}$	Maximum *Profit/tonne.mile*	Maximum *NPV*
Criteria				
P_D/Dis	**0.10969**	0.10969	0.12213	0.11866
$EEDI_A/EEDI_{Ref}$	0.81358	**0.81358**	0.93034	0.89638
Profit/tonne.mile $\times 10^{-3}$	0.06677	0.06677	**0.14632**	0.14474
NPV	-35.01587	-35.01587	-32.80348	**-32.73945**
Independent Variables				
Length	222.75	222.75	222.75	222.75
Breadth	30.5950	30.5950	33.8241	33.8241
Draught	12.8388	12.8388	12.8388	12.8388
Breadth/Draught	2.3830	2.3830	2.6345	2.6345
Block Coefficient	0.7759	0.7759	0.8342	0.8109
Long Centre of Buoyancy %L	-0.01	-0.01	-0.01	-0.01
Speed	15	15	15	15
Other Characteristics				
Deadweight [ton]	54900.3106	54900.3106	66496.9116	64225.4316
Lightweight [ton]	14683.9319	14683.9319	16214.6369	16179.4659
Capital Cost [$ m]	38.4690	38.4690	40.2098	39.8688
Annual Fuel Cost [$]	5938508.53	5938508.53	7614135.17	7237980.12
Annual Operating cost [$]	2963476.16	2963476.16	3001147.72	2993768.81
Total annual cost [$]	10396237.89	10396237.89	12310437.83	11895318.47
Profit per DWT [$/dwt]	3.55696	3.55696	7.79473	7.71073
Annual Bunker Cons [ton]	6304.05	6304.05	8191.65	7762.60
Annual MDO Cons [ton]	895.27	895.27	1060.82	1027.90

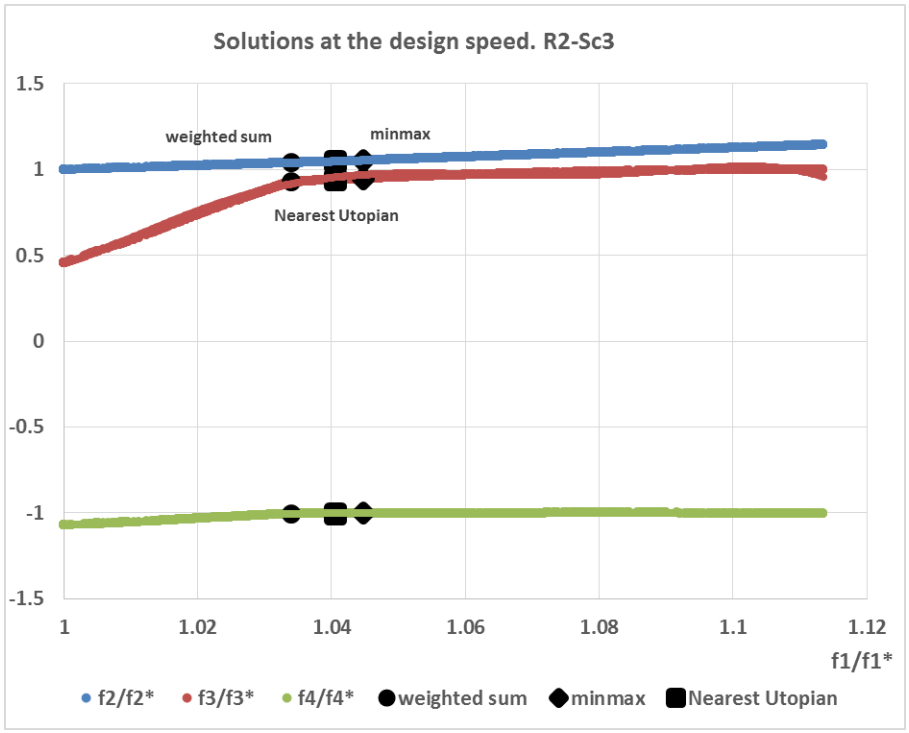

Pareto front at the design speed. Route Two, Scenario Three

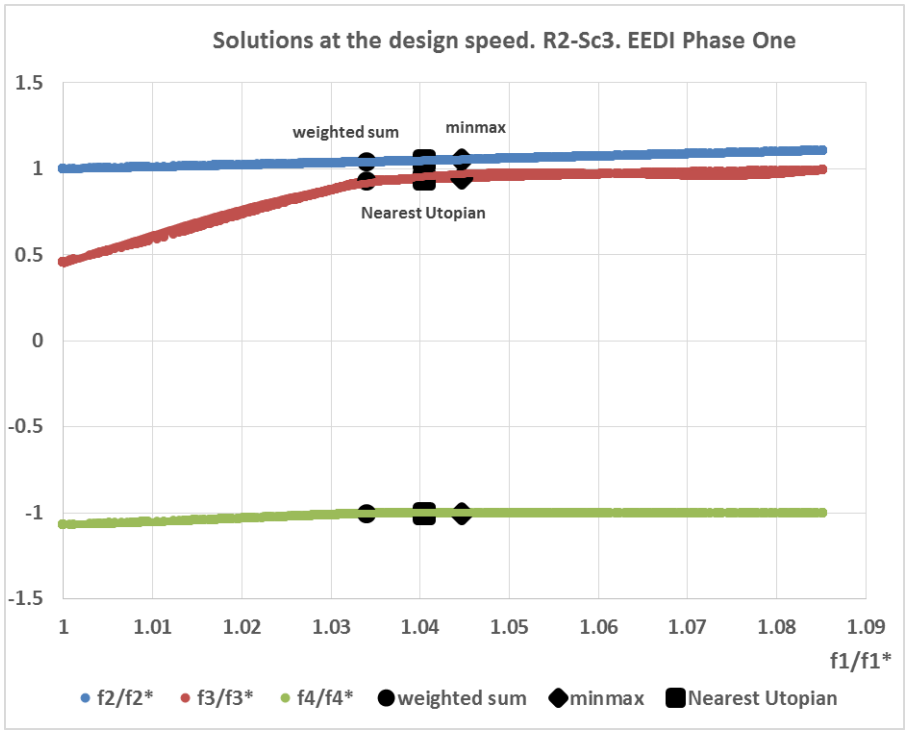

Pareto front at the design speed. Route Two, Scenario Three. EEDI Phase One

Optimum solutions with the added EEDI reduction factor constraint. Route Two, Scenario Three

	Phase One reduction factor constraint	*Phase Two and Three reduction factors constraint*
Criteria		
P_D/Dis	0.11903	0.1099
$EEDI_A/EEDI_{Ref}$	0.9	0.81357
$Profit/tonne.mile \times 10^{-3}$	0.145064	0.066769
NPV	-32.7402	-35.0159
Independent Variables		
Length	222.75	222.75
Breadth	33.8241	30.5950
Draught	12.8388	12.8388
Breadth/Draught	2.6345	2.3830
Block Coefficient	0.8134	0.7759
Long Centre of Buoyancy %L	-0.01	-0.01
Speed	15	15
Other Characteristics		
Deadweight [ton]	64467.35	54900.31
Lightweight [ton]	16183.2	14683.93
Capital Cost [$ m]	39.905	38.46902
Annual Fuel Cost [$]	7277529	5938509
Annual Operating cost [$]	2994555	2963476
Total annual cost [$]	11939017.09	10396238
Profit per DWT [$/dwt]	7.727919682	3.556955
Annual Bunker Cons [ton]	7807.712	6304.053
Annual MDO Cons [ton]	1031.359	895.2661
$EEDI_A/EEDI_{Ref\text{-}Phase\ One}$	1 (satisfied)	0.903977
$EEDI_A/EEDI_{Ref\text{-}Phase\ Two}$	1.125	1.016974 (not satisfied)
$EEDI_A/EEDI_{Ref\text{-}PhaseThree}$	1.285714	1.162256 (not satisfied)

- **Optimisation model's solutions at the design speed for Route Two, Scenario Four (high fuel price and high fright rates):**

Single Criterion results for Route Two, Scenario Four at the design speed

	Minimum P_D/Dis	Minimum $EEDI_A/EEDI_{Ref}$	Maximum *Profit/tonne.mile*	Maximum *NPV*
Criteria				
P_D/Dis	**0.10969**	0.10969	0.12213	0.12822
$EEDI_A/EEDI_{Ref}$	0.81358	**0.81358**	0.93034	0.98976
Profit/tonne.mile × 10^{-3}	2.01677	2.01677	**2.09632**	2.09192
NPV	32.68471	32.68471	49.19750	**53.67929**
Independent Variables				
Length	222.75	222.75	222.75	222.75
Breadth	30.5950	30.5950	33.8241	33.8241
Draught	12.8388	12.8388	12.8388	12.8388
Breadth/Draught	2.3830	2.3830	2.6345	2.6345
Block Coefficient	0.7759	0.7759	0.8342	0.8749
Long Centre of Buoyancy %L	-0.01	-0.01	-0.01	-0.01
Speed	15	15	15	15
Other Characteristics				
Deadweight [ton]	54900.3106	54900.3106	66496.9115	70472.1370
Lightweight [ton]	14683.9319	14683.9319	16214.6369	16276.7683
Capital Cost [$ m]	38.4690	38.4690	40.2098	40.8065
Annual Fuel Cost [$]	5938508.53	5938508.53	7614135.17	8298398.07
Annual Operating cost [$]	2963476.16	2963476.16	3001147.72	3014061.24
Total annual cost [$]	10396237.89	10396237.89	12310437.83	13062890.60
Profit per DWT [$/dwt]	107.43841	107.43841	111.67618	111.44166
Annual Bunker Cons [ton]	6304.05	6304.05	8191.65	8972.12
Annual MDO Cons [ton]	895.27	895.27	1060.82	1120.70

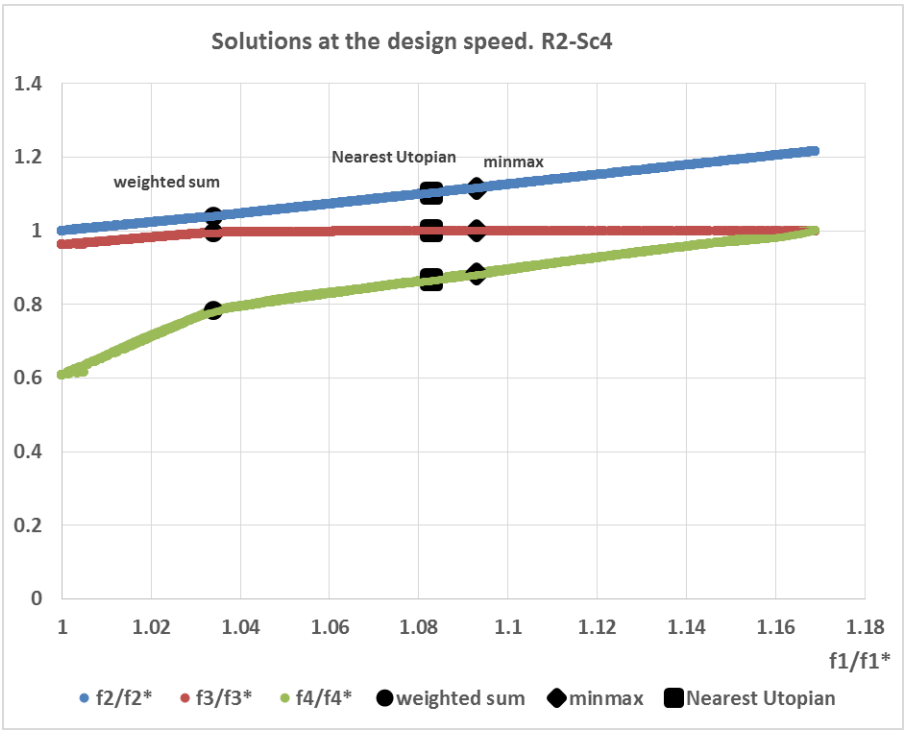

Pareto front at the design speed. Route Two, Scenario Four

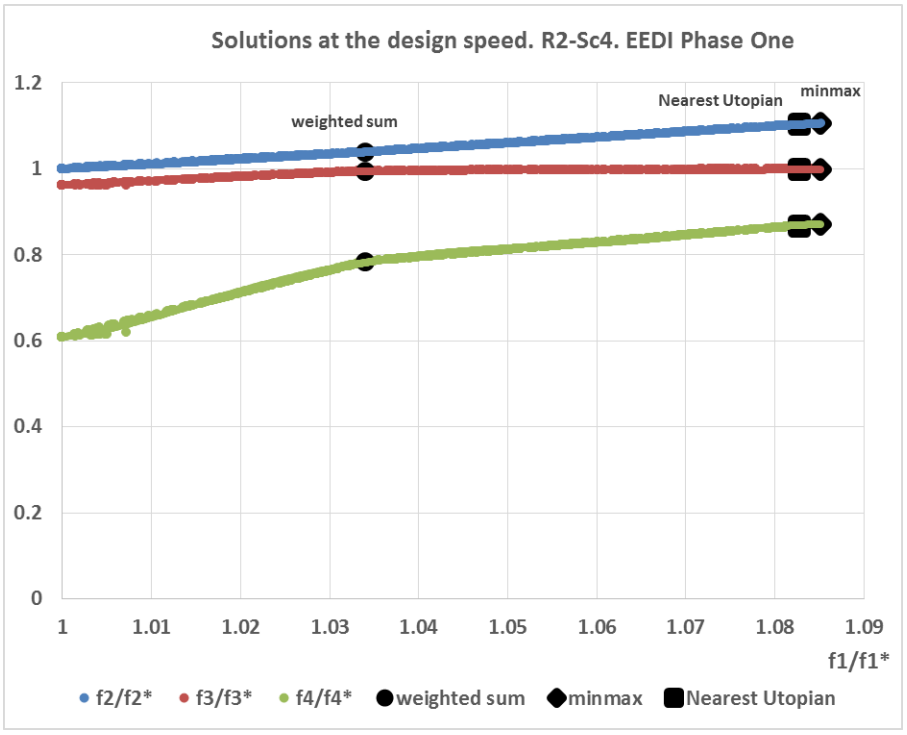

Pareto front at the design speed. Route Two, Scenario Four. EEDI Phase One

Optimum solutions with the added EEDI reduction factor constraint. Route Two, Scenario Four

	Phase One reduction factor constraint	*Phase Two and Three reduction factors constraint*
Criteria		
P_D/Dis	0.11903	0.1099
$EEDI_A/EEDI_{Ref}$	0.9	0.81357
$Profit/tonne.mile \times 10^{-3}$	2.095064	2.016769
NPV	46.75805	32.68471
Independent Variables		
Length	222.75	222.75
Breadth	33.8241	30.5950
Draught	12.8388	12.8388
Breadth/Draught	2.6345	2.3830
Block Coefficient	0.8134	0.7759
Long Centre of Buoyancy %L	-0.01	-0.01
Speed	15	15
Other Characteristics		
Deadweight [ton]	64467.35	54900.31
Lightweight [ton]	16183.2	14683.93
Capital Cost [$ m]	39.905	38.46902
Annual Fuel Cost [$]	7277529	5938509
Annual Operating cost [$]	2994555	2963476
Total annual cost [$]	11939017.09	10396238
Profit per DWT [$/dwt]	111.6093705	107.4384
Annual Bunker Cons [ton]	7807.712	6304.053
Annual MDO Cons [ton]	1031.359	895.2661
$EEDI_A/EEDI_{Ref\text{-}Phase\ One}$	1 (satisfied)	0.903977
$EEDI_A/EEDI_{Ref\text{-}Phase\ Two}$	1.125	1.016974 (not satisfied)
$EEDI_A/EEDI_{Ref\text{-}PhaseThree}$	1.285714	1.162256 (not satisfied)

Appendix K

- **Optimisation model's solutions over the speeds range for Route One, Scenario Two (low fuel price and high fright rates):**

Single Criterion results for Route One, Scenario Two over the speeds range

	Minimum P_D/Dis	Minimum $EEDI_A/EEDI_{Ref}$	Maximum *Profit/tonne.mile*	Maximum *NPV*
Criteria				
P_D/Dis	**0.00325**	0.00528	0.05378	0.14131
$EEDI_A/EEDI_{Ref}$	0.29624	**0.27437**	0.56652	1.06917
Profit/tonne.mile × 10^{-3}	2.03666	1.82215	**3.66399**	3.31700
NPV	-11.73057	-14.55575	72.68898	**82.55786**
Independent Variables				
Length	222.75	222.75	222.75	222.75
Breadth	30.5950	30.5950	33.8241	33.8241
Draught	12.8388	12.8388	12.8388	12.8388
Breadth/Draught	2.3830	2.3830	2.6345	2.6345
Block Coefficient	0.8749	0.7759	0.8749	0.8749
Long Centre of Buoyancy %L	-0.01	-0.01	-0.01	-0.01
Speed	5	5.545	12.053	15.38
Other Characteristics				
Deadweight [ton]	63643.0820	54900.3106	70472.1370	70472.1370
Lightweight [ton]	14824.2552	14683.9319	16276.7683	16276.7683
Capital Cost [$ m]	39.7814	38.4690	40.8065	40.8065
Annual Fuel Cost [$]	1091510.82	1051530.67	2850714.62	5204733.44
Annual Operating cost [$]	2991877.05	2963476.16	3014061.24	3014061.24
Total annual cost [$]	5871195.28	5781718.04	9414981.74	12390361.01
Profit per DWT [$/dwt]	35.61239	34.95147	134.16531	145.96229
Annual Bunker Cons [ton]	706.75	821.87	3944.29	8587.37
Annual MDO Cons [ton]	1054.48	915.14	1255.10	1301.50

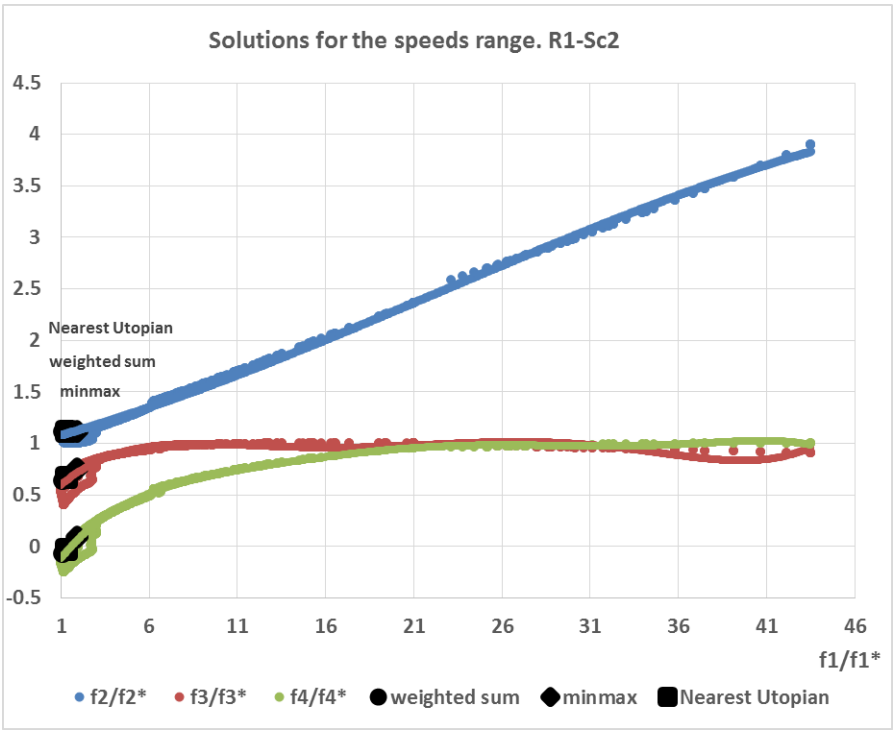

Pareto front over the speeds range. Route One, Scenario Two

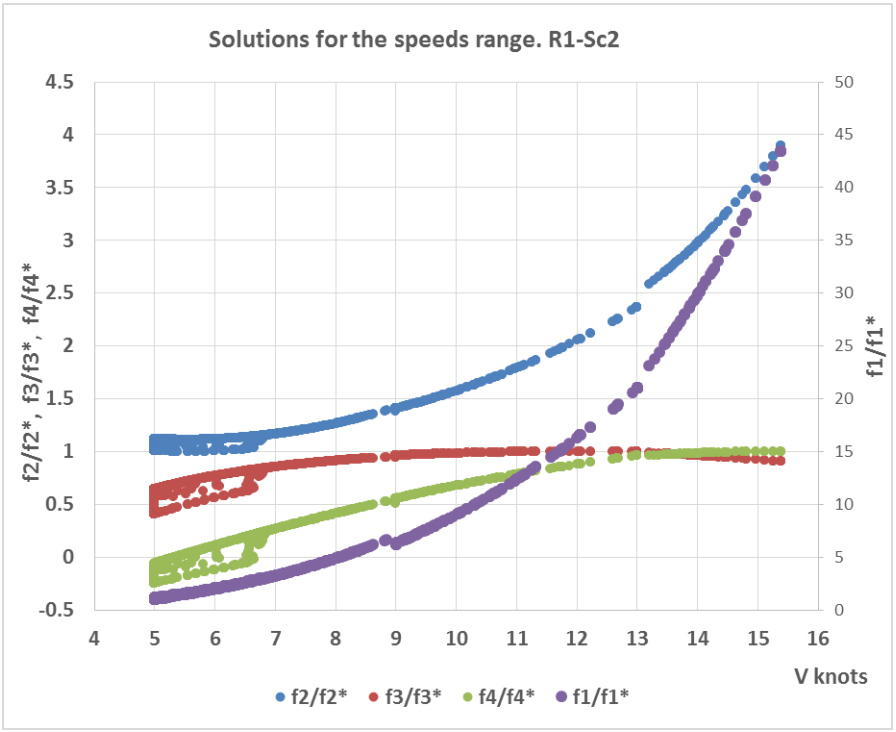

Normalised objective functions over the speeds range

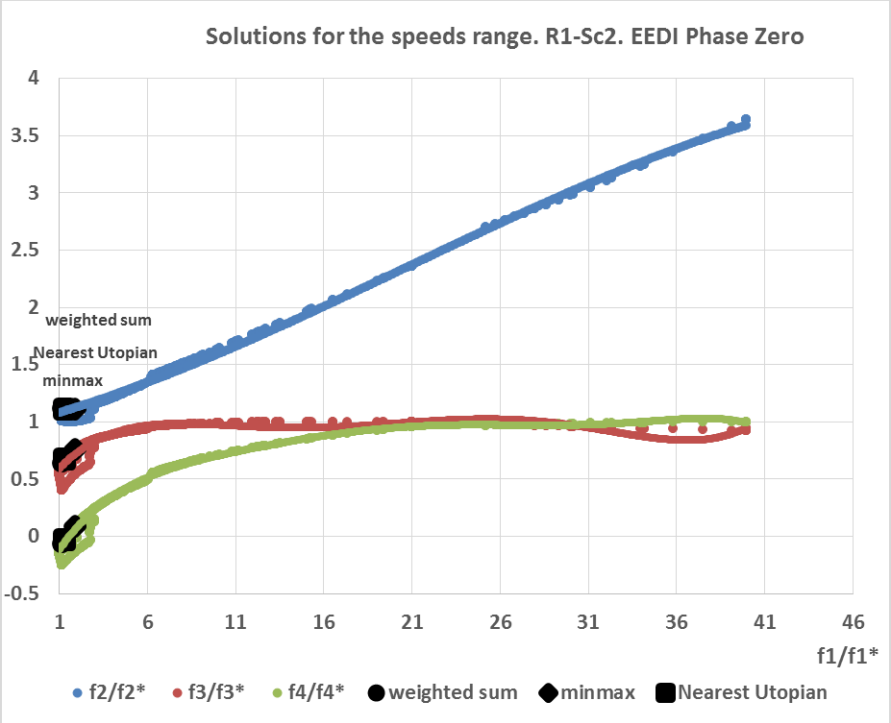

Pareto front over the speeds range. Route One, Scenario Two. EEDI Phase Zero

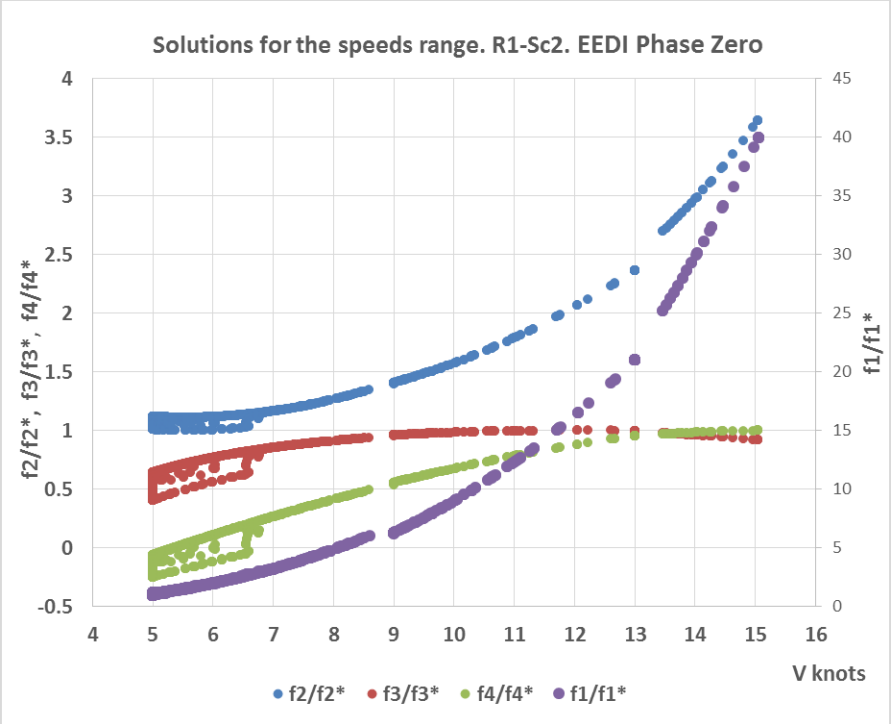

Normalised objective functions over the speeds range. EEDI Phase Zero

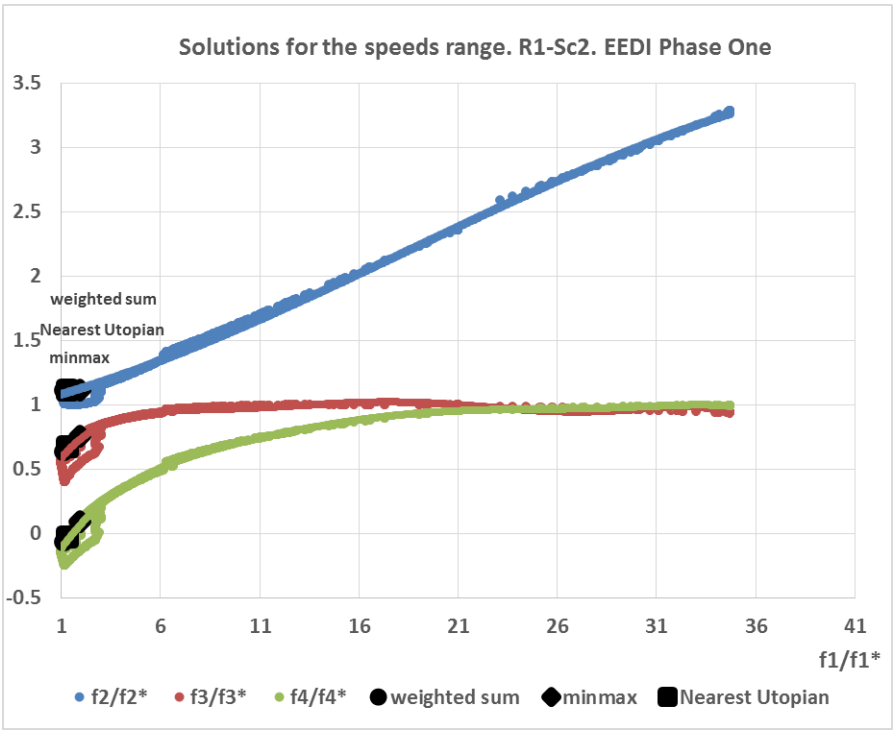

Pareto front over the speeds range. Route One, Scenario Two. EEDI Phase One

Normalised objective functions over the speeds range. EEDI Phase One

Pareto front over the speeds range. Route One, Scenario Two. EEDI Phase Two

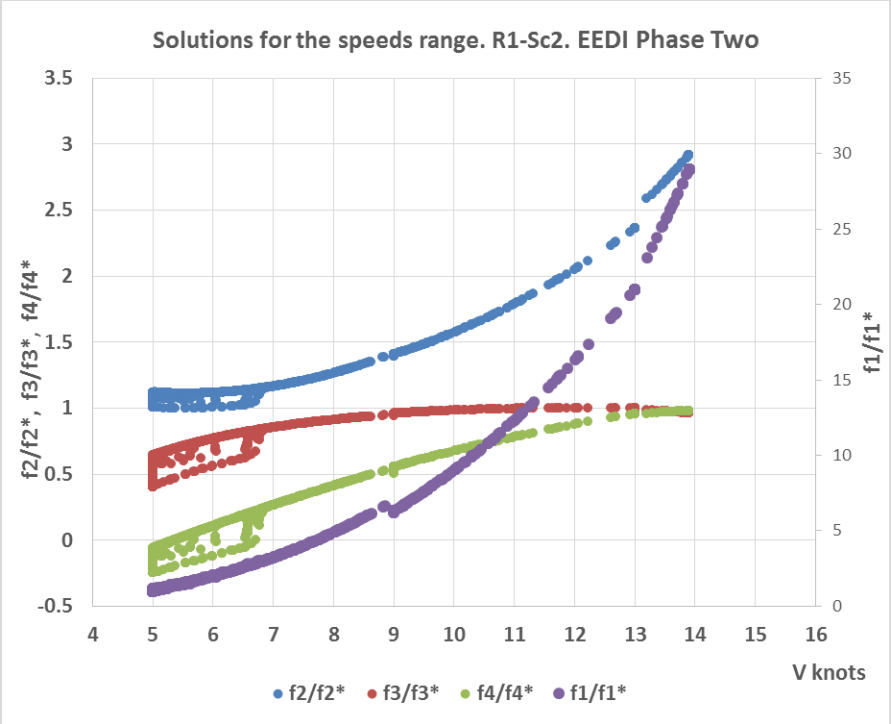

Normalised objective functions over the speeds range. EEDI Phase Two

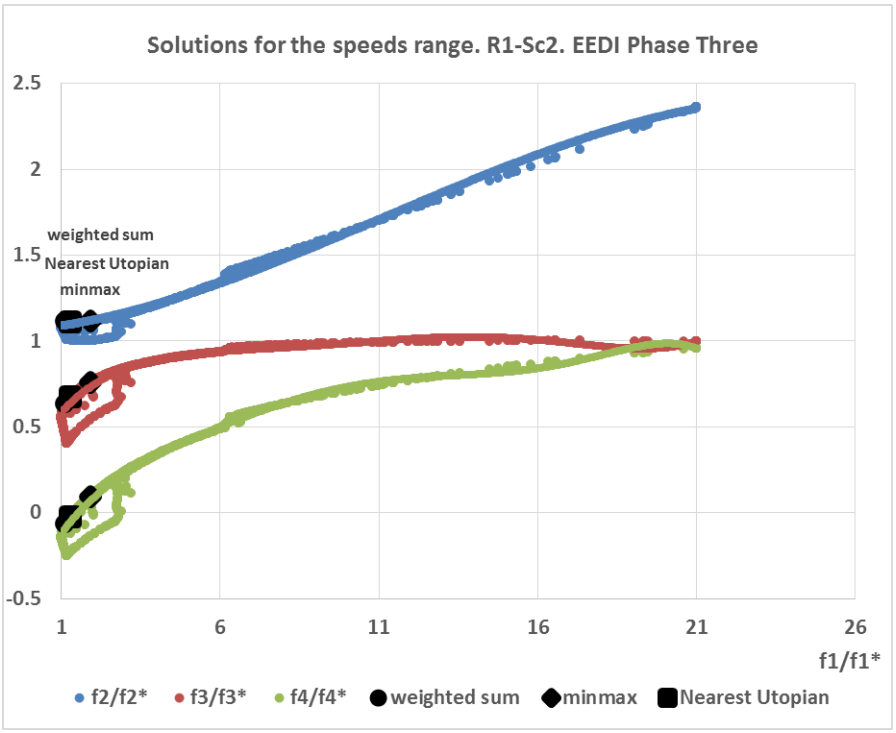

Pareto front over the speeds range. Route One, Scenario Two. EEDI Phase Three

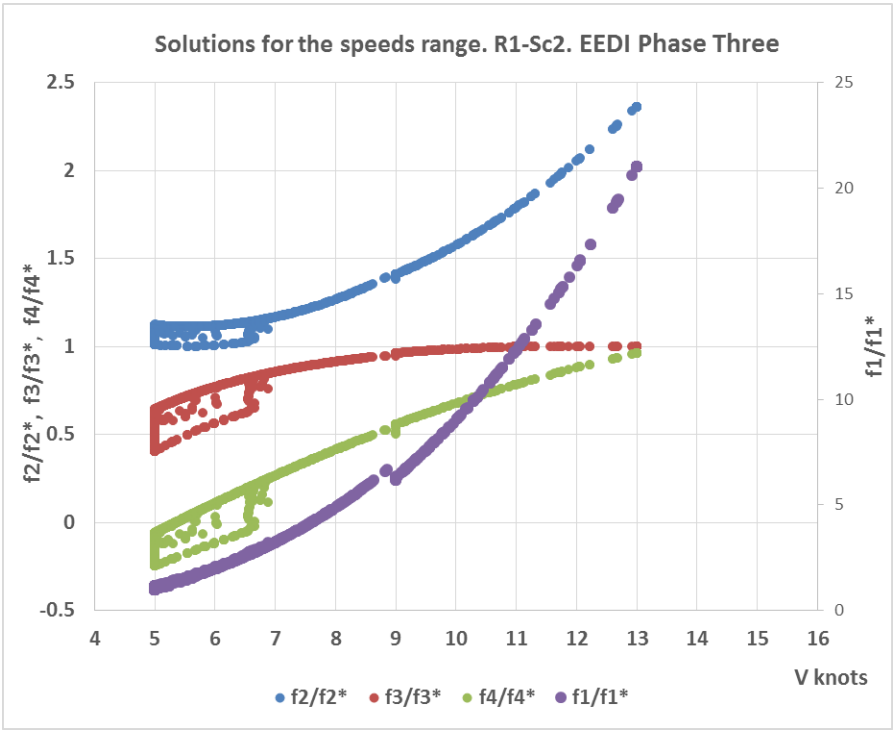

Normalised objective functions over the speeds range. EEDI Phase Three

- **Optimisation model's solutions over the speeds range for Route One, Scenario Three (high fuel price and low fright rates):**

Single Criterion results for Route One, Scenario Three over the speeds range

	Minimum P_D/Dis	Minimum $EEDI_A/EEDI_{Ref}$	Maximum *Profit/tonne.mile*	Maximum *NPV*
Criteria				
P_D/Dis	**0.00325**	0.00528	0.03487	0.03844
$EEDI_A/EEDI_{Ref}$	0.29624	**0.27437**	0.46137	0.48105
Profit/tonne.mile × 10^{-3}	-1.36314	-1.59769	**0.17811**	0.17604
NPV	-56.64299	-57.30635	-34.64003	**-34.58042**
Independent Variables				
Length	222.75	222.75	222.75	222.75
Breadth	30.5950	30.5950	33.8241	33.8241
Draught	12.8388	12.8388	12.8388	12.8388
Breadth/Draught	2.3830	2.3830	2.6345	2.6345
Block Coefficient	0.8749	0.7759	0.8749	0.8749
Long Centre of Buoyancy %L	-0.01	-0.01	-0.01	-0.01
Speed	5	5.5495	10.537	10.8577
Other Characteristics				
Deadweight [ton]	63643.0820	54900.3106	70472.1370	70472.1370
Lightweight [ton]	14824.2552	14683.9319	16276.7683	16276.7683
Capital Cost [$ m]	39.7814	38.4690	40.8065	40.8065
Annual Fuel Cost [$]	1619879.91	1572632.29	3516714.24	3690348.20
Annual Operating cost [$]	2991877.05	2963476.16	3014061.24	3014061.24
Total annual cost [$]	6399564.36	6302819.68	9771743.95	10012143.22
Profit per DWT [$/dwt]	-23.83540	-30.64611	5.86724	5.93850
Annual Bunker Cons [ton]	706.75	821.87	2855.89	3066.70
Annual MDO Cons [ton]	1054.48	915.14	1232.01	1236.99

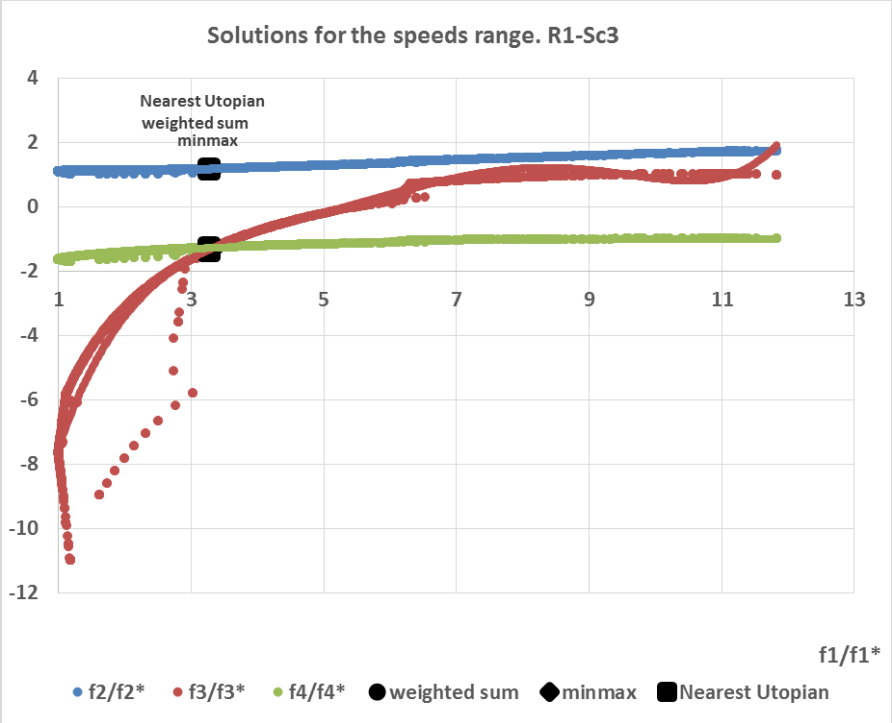

Pareto front over the speeds range. Route One, Scenario Three

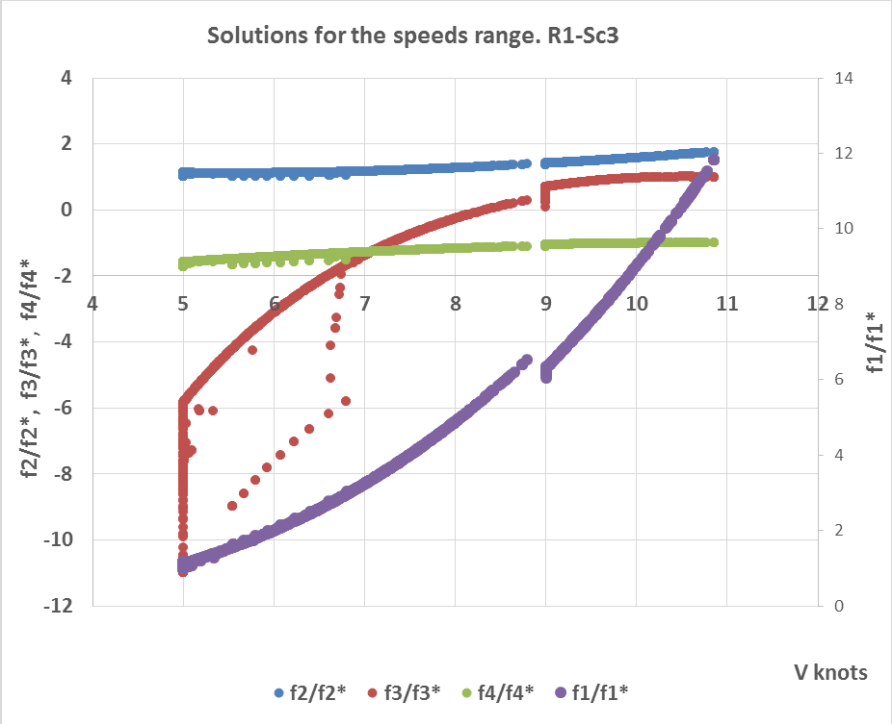

Normalised objective functions over the speeds range

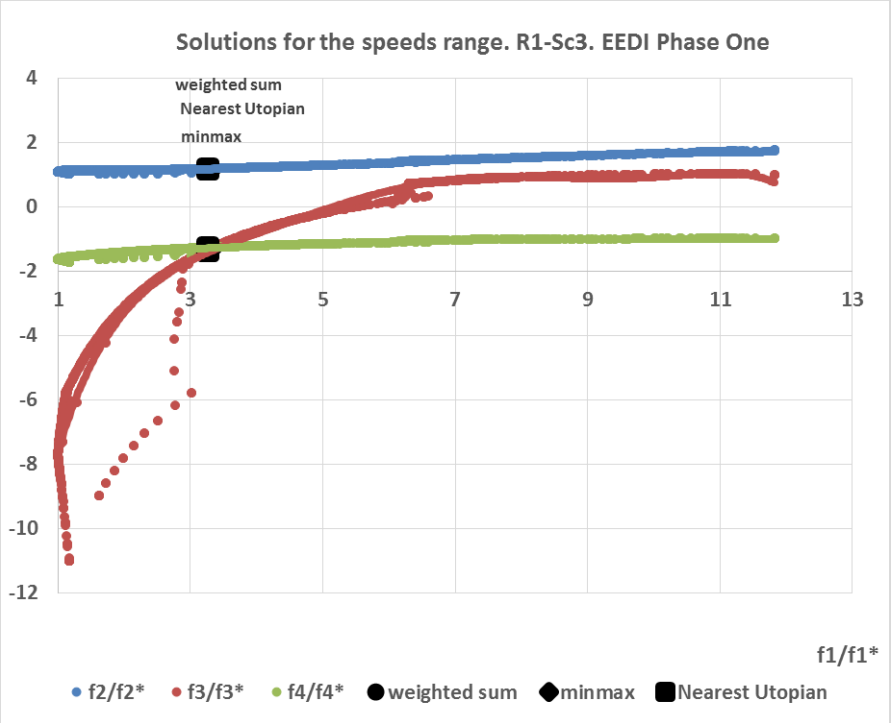

Pareto front over the speeds range. Route One, Scenario Three. EEDI Phase One

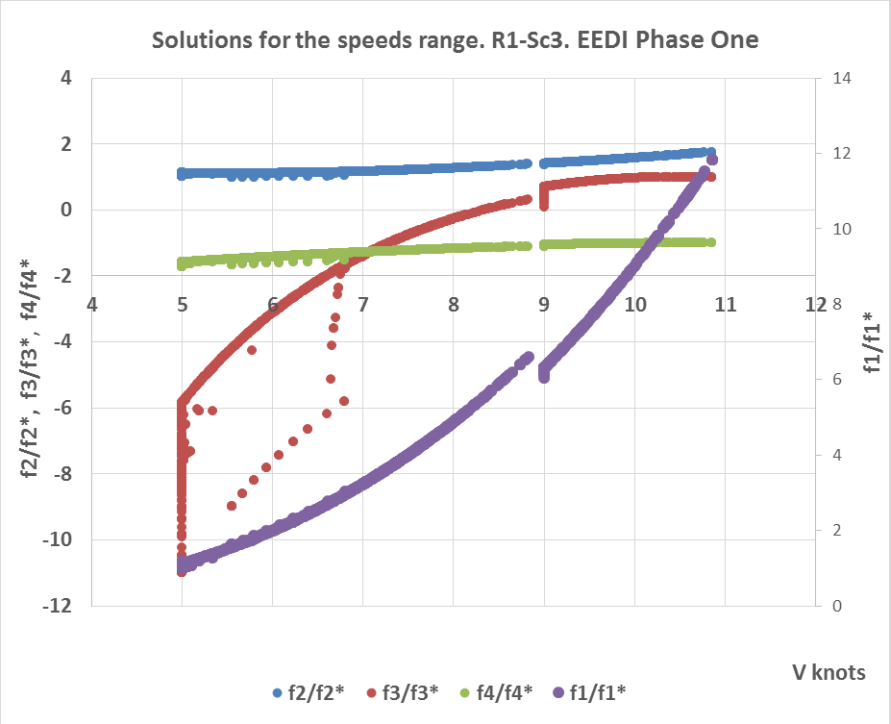

Normalised objective functions over the speeds range. EEDI Phase One

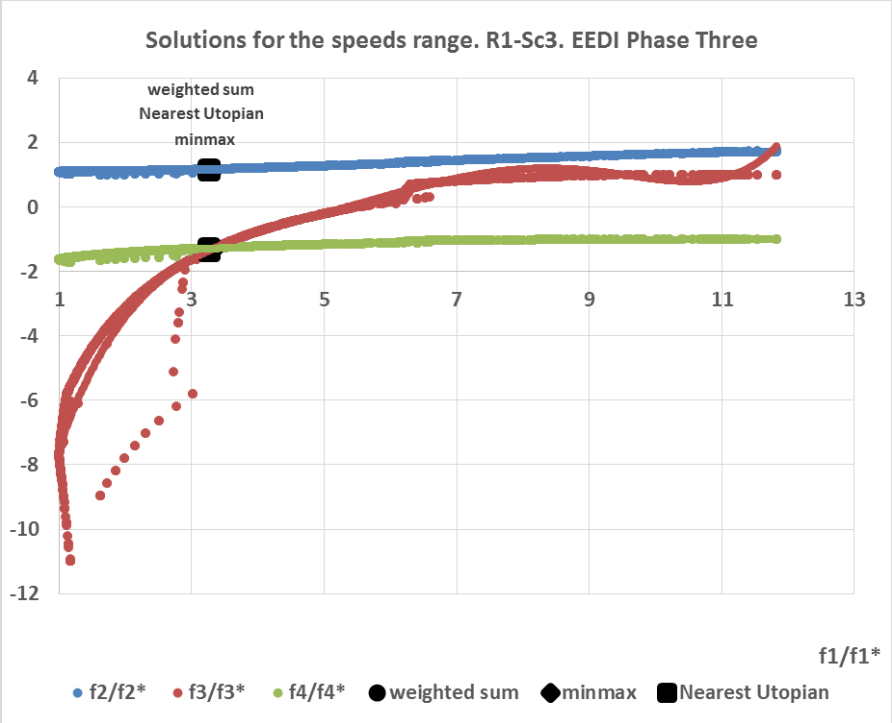

Pareto front over the speeds range. Route One, Scenario Three. EEDI Phase Three

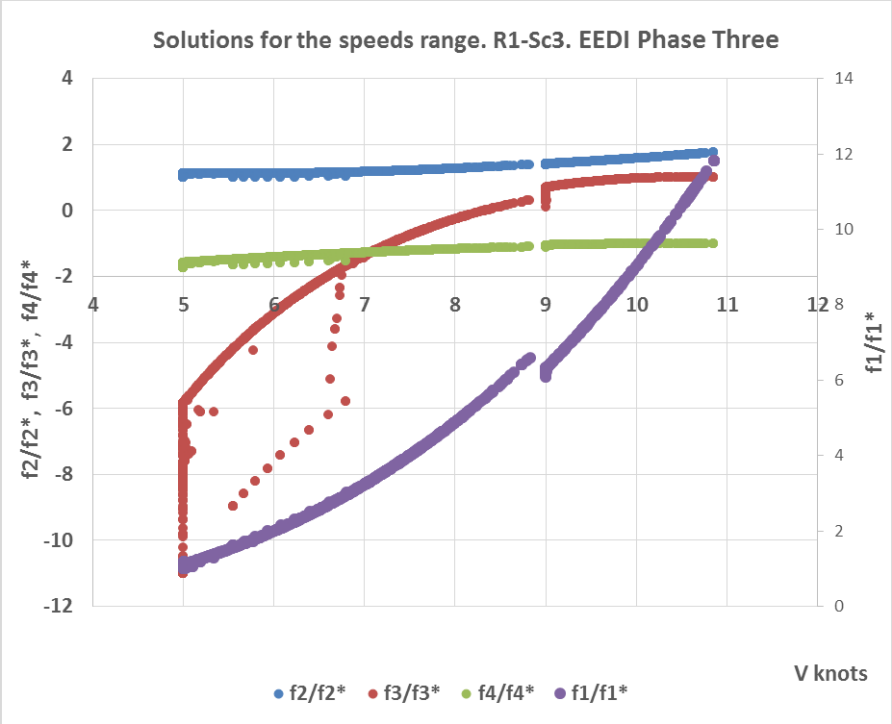

Normalised objective functions over the speeds range. EEDI Phase Three

- **Optimisation model's solutions over the speeds range for Route One, Scenario Four (high fuel price and high fright rates):**

Single Criterion results for Route One, Scenario Four over the speeds range

	Minimum P_D/Dis	Minimum $EEDI_A/EEDI_{Ref}$	Maximum *Profit/tonne.mile*	Maximum *NPV*
Criteria				
P_D/Dis	**0.00325**	0.00528	0.03487	0.06830
$EEDI_A/EEDI_{Ref}$	0.29624	**0.27437**	0.46137	0.64753
Profit/tonne.mile $\times 10^{-3}$	1.56186	1.32731	**3.10311**	2.99341
NPV	-18.00273	-20.74163	45.96438	**57.63777**
Independent Variables				
Length	222.75	222.75	222.75	222.75
Breadth	30.5950	30.5950	33.8241	33.8241
Draught	12.8388	12.8388	12.8388	12.8388
Breadth/Draught	2.3830	2.3830	2.6345	2.6345
Block Coefficient	0.8749	0.7759	0.8749	0.8749
Long Centre of Buoyancy %L	-0.01	-0.01	-0.01	-0.01
Speed	5	5.5495	10.537	12.99
Other Characteristics				
Deadweight [ton]	63643.0820	54900.3106	70472.1370	70472.1370
Lightweight [ton]	14824.2552	14683.9319	16276.7683	16276.7683
Capital Cost [$ m]	39.7814	38.4690	40.8065	40.8065
Annual Fuel Cost [$]	1619879.91	1572632.28	3516714.22	5064051.69
Annual Operating cost [$]	2991877.05	2963476.16	3014061.24	3014061.24
Total annual cost [$]	6399564.36	6302819.64	9771743.92	11812737.95
Profit per DWT [$/dwt]	27.31032	25.45970	102.21947	116.17351
Annual Bunker Cons [ton]	706.75	821.87	2855.89	4743.98
Annual MDO Cons [ton]	1054.48	915.14	1232.01	1268.87

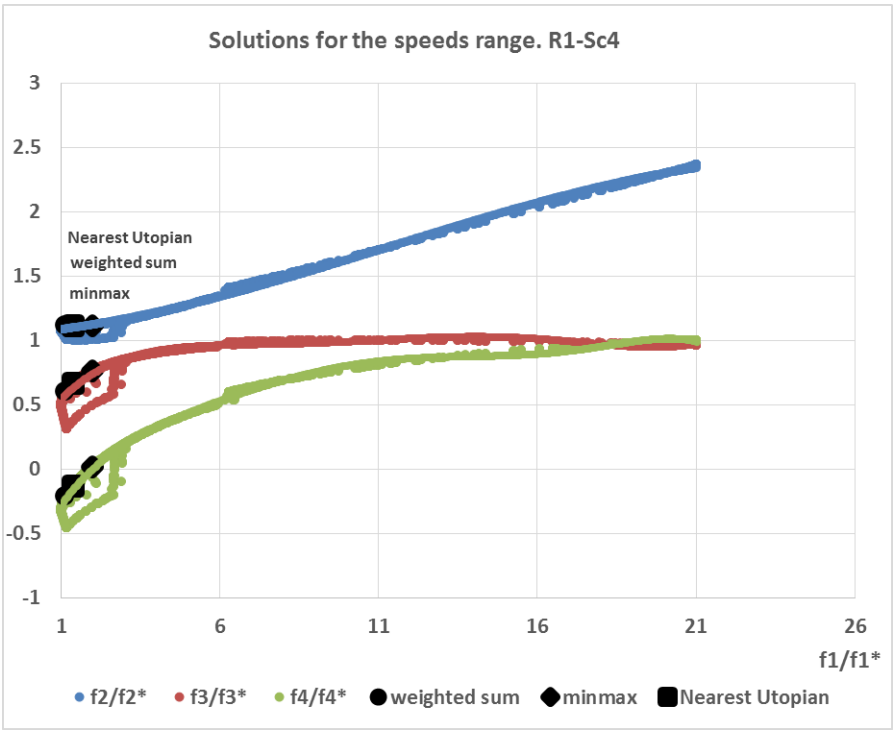

Pareto front over the speeds range. Route One, Scenario Four

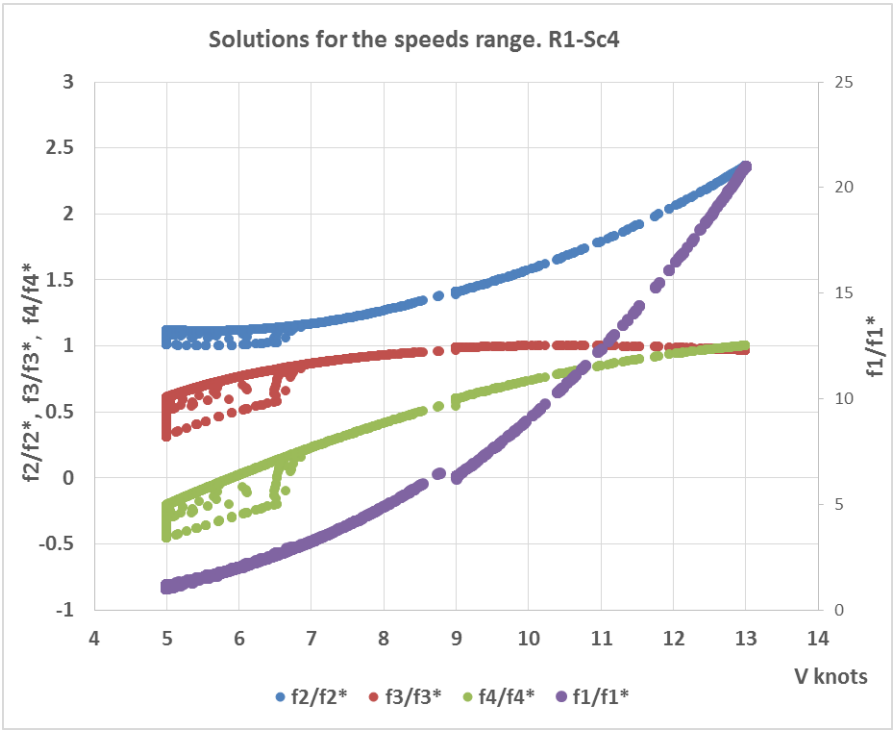

Normalised objective functions over the speeds range

- **Optimisation model's solutions over the speeds range for Route Two, Scenario One (low fuel price and low fright rates):**

Single Criterion results for Route Two, Scenario One over the speeds range

	Minimum P_D/Dis	Minimum $EEDI_A/EEDI_{Ref}$	Maximum *Profit/tonne.mile*	Maximum *NPV*
Criteria				
P_D/Dis	**0.00325**	0.00528	0.05378	0.06830
$EEDI_A/EEDI_{Ref}$	0.29624	**0.27437**	0.56652	0.64753
Profit/tonne.mile × 10^{-3}	-0.35621	-0.47510	**1.23658**	1.22555
NPV	-43.73116	-43.81737	5.56082	**8.38282**
Independent Variables				
Length	222.75	222.75	222.75	222.75
Breadth	30.5950	30.5950	33.8241	33.8241
Draught	12.8388	12.8388	12.8388	12.8388
Breadth/Draught	2.3830	2.3830	2.6345	2.6345
Block Coefficient	0.8749	0.7759	0.8749	0.8749
Long Centre of Buoyancy %L	-0.01	-0.01	-0.01	-0.01
Speed	5	5.5495	12.053	12.999
Other Characteristics				
Deadweight [ton]	63643.0820	54900.3106	70472.1370	70472.1370
Lightweight [ton]	14824.2552	14683.9319	16276.7683	16276.7683
Capital Cost [$ m]	39.7814	38.4690	40.8065	40.8065
Annual Fuel Cost [$]	930580.37	887032.69	2796432.52	3285787.66
Annual Operating cost [$]	2991877.05	2963476.16	3014061.24	3014061.24
Total annual cost [$]	4793332.94	4709280.89	7328604.39	7893546.12
Profit per DWT [$/dwt]	-6.74480	-9.94828	53.92220	57.29555
Annual Bunker Cons [ton]	483.55	585.59	4048.17	5018.98
Annual MDO Cons [ton]	984.00	848.91	1103.35	1109.00

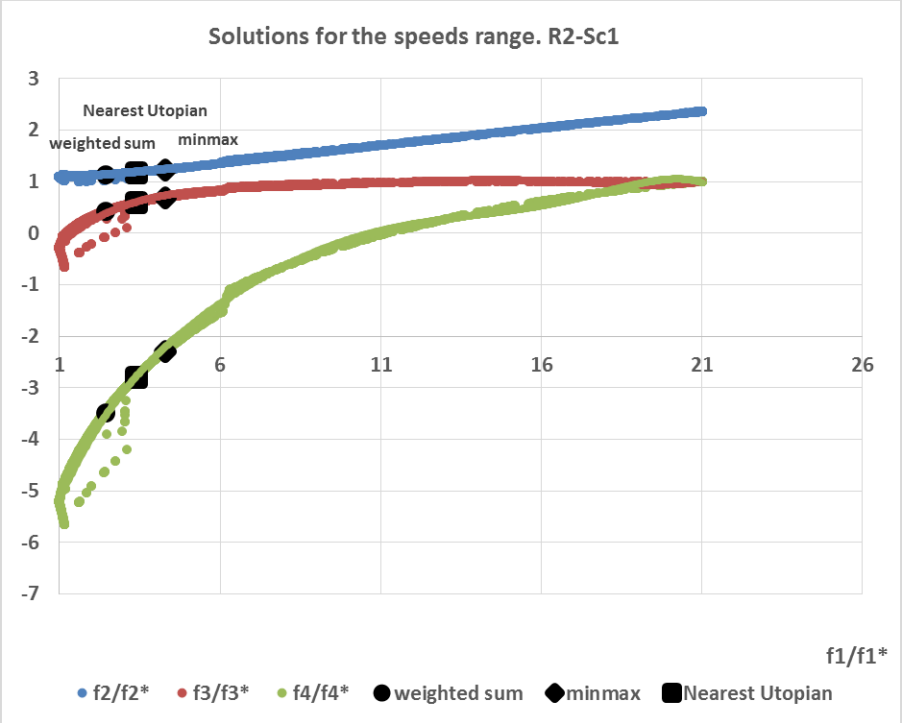

Pareto front over the speeds range. Route Two, Scenario One

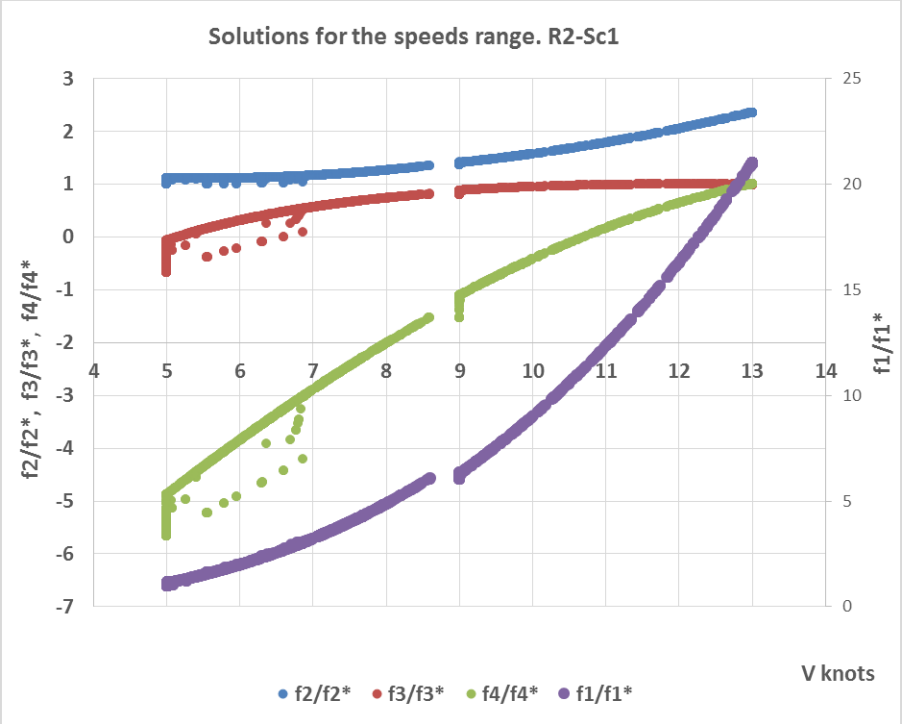

Normalised objective functions over the speeds range

- **Optimisation model's solutions over the speeds range for Route Two, Scenario Two (low fuel price and high fright rates):**

Single Criterion results for Route Two, Scenario Two over the speeds range

	Minimum P_D/Dis	Minimum $EEDI_A/EEDI_{Ref}$	Maximum *Profit/tonne.mile*	Maximum *NPV*
Criteria				
P_D/Dis	**0.00325**	0.00528	0.05378	0.14985
$EEDI_A/EEDI_{Ref}$	0.29624	**0.27437**	0.56652	1.12246
Profit/tonne.mile $\times 10^{-3}$	1.59379	1.47490	**3.18658**	2.80133
NPV	-15.83616	-17.20687	76.69454	**89.97026**
Independent Variables				
Length	222.75	222.75	222.75	222.75
Breadth	30.5950	30.5950	33.8241	33.8241
Draught	12.8388	12.8388	12.8388	12.8388
Breadth/Draught	2.3830	2.3830	2.6345	2.6345
Block Coefficient	0.8749	0.7759	0.8749	0.8749
Long Centre of Buoyancy %L	-0.01	-0.01	-0.01	-0.01
Speed	5	5.5495	12.0532	15.622
Other Characteristics				
Deadweight [ton]	63643.0820	54900.3106	70472.1370	70472.1370
Lightweight [ton]	14824.2552	14683.9319	16276.7683	16276.7683
Capital Cost [$ m]	39.7814	38.4690	40.8065	40.8065
Annual Fuel Cost [$]	930580.37	887032.69	2796432.59	5976609.89
Annual Operating cost [$]	2991877.05	2963476.16	3014061.24	3014061.24
Total annual cost [$]	4793332.94	4709280.89	7328604.47	10789049.72
Profit per DWT [$/dwt]	30.17807	30.88352	138.95343	154.82286
Annual Bunker Cons [ton]	483.55	585.59	4048.17	10379.23
Annual MDO Cons [ton]	984.00	848.91	1103.35	1124.28

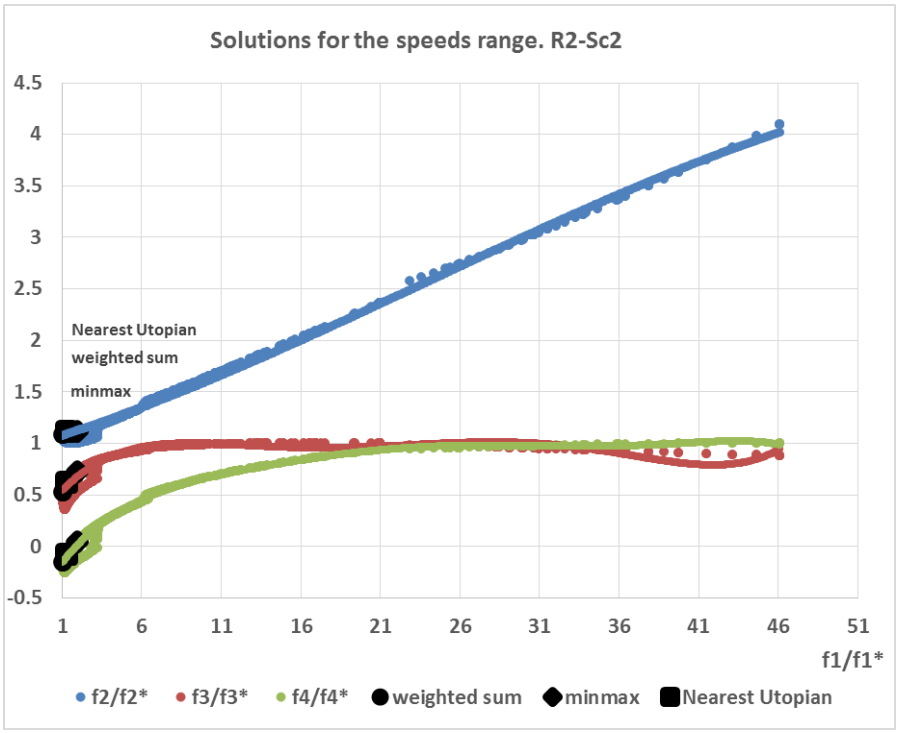

Pareto front over the speeds range. Route One, Scenario Two

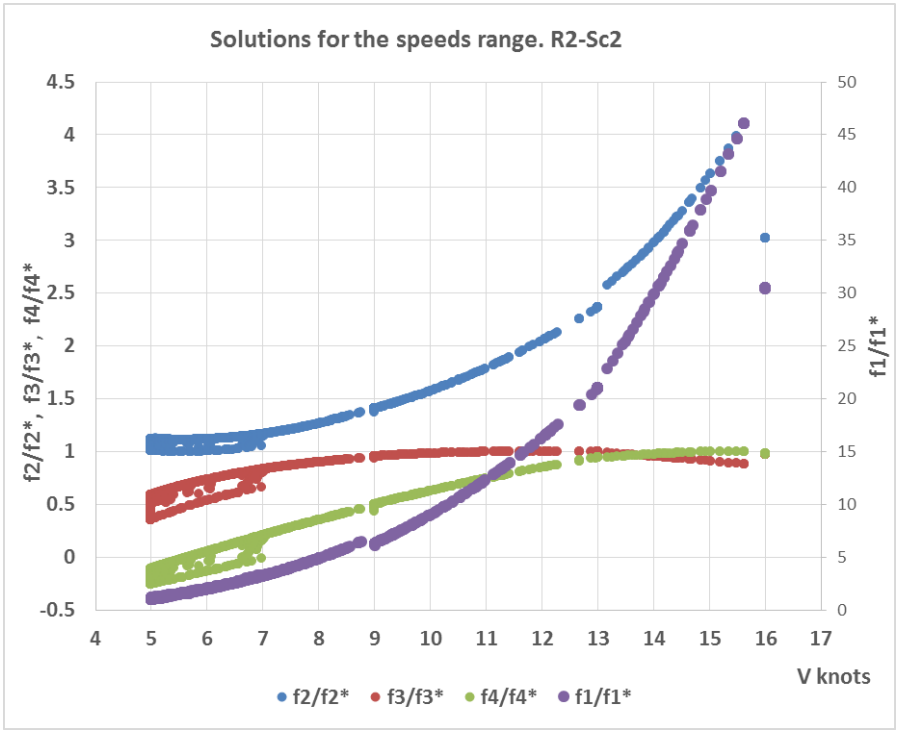

Normalised objective functions over the speeds range

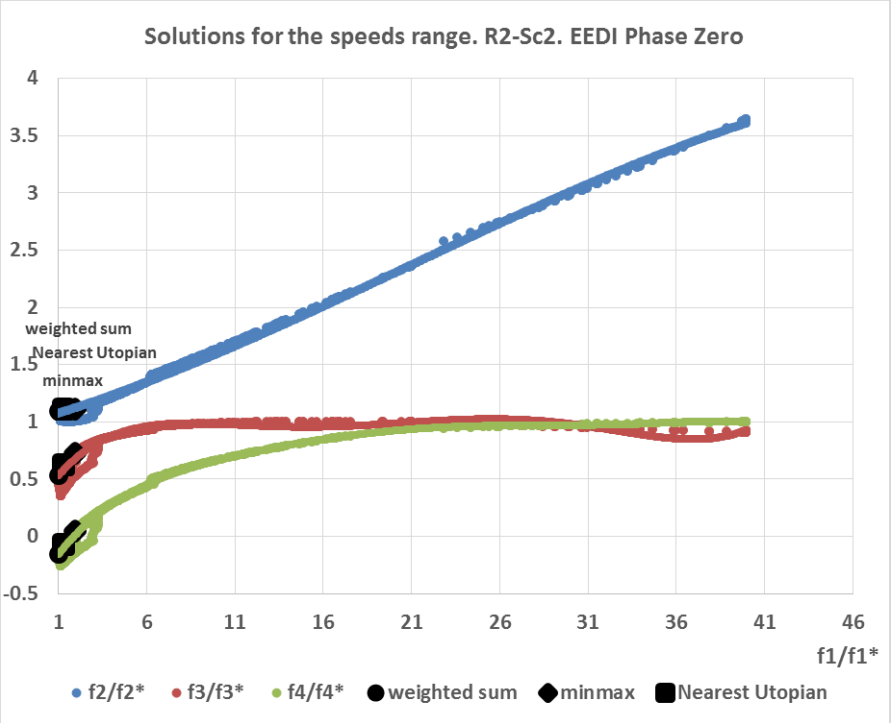

Pareto front over the speeds range. Route One, Scenario Two. EEDI Phase Zero

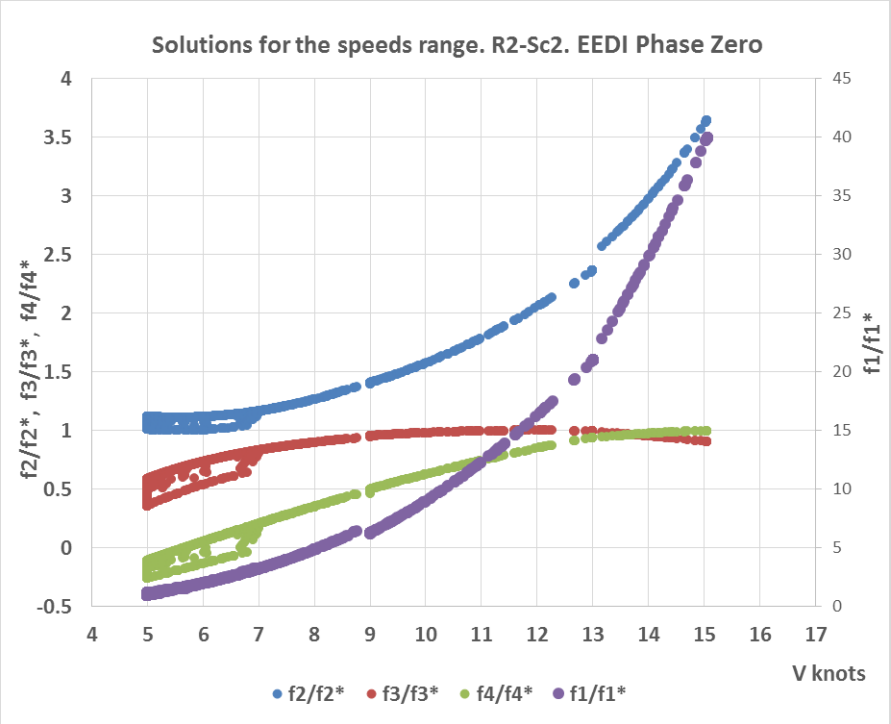

Normalised objective functions over the speeds range. EEDI Phase Zero

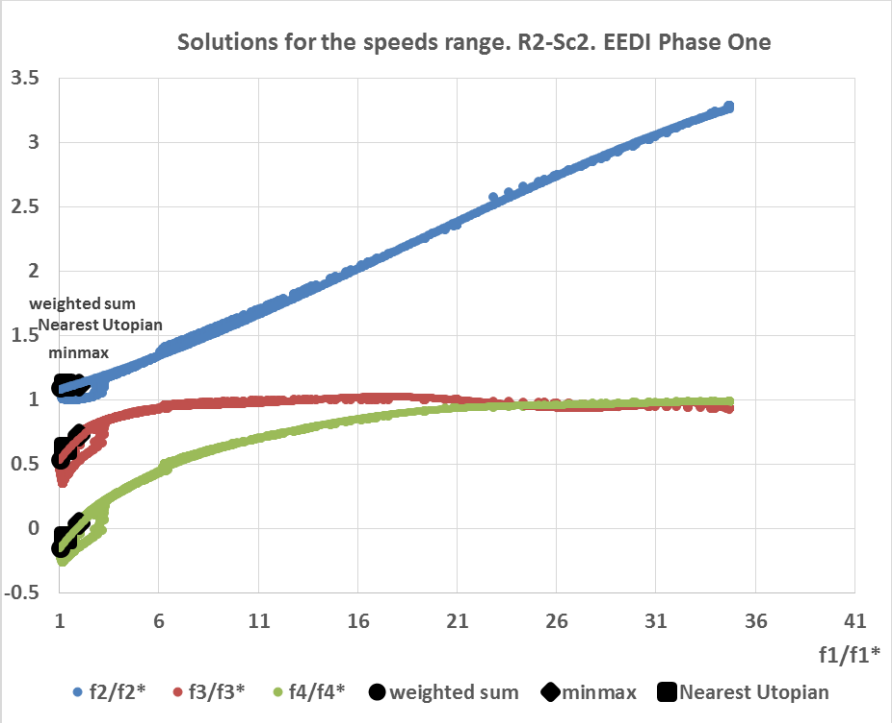

Pareto front over the speeds range. Route One, Scenario Two. EEDI Phase One

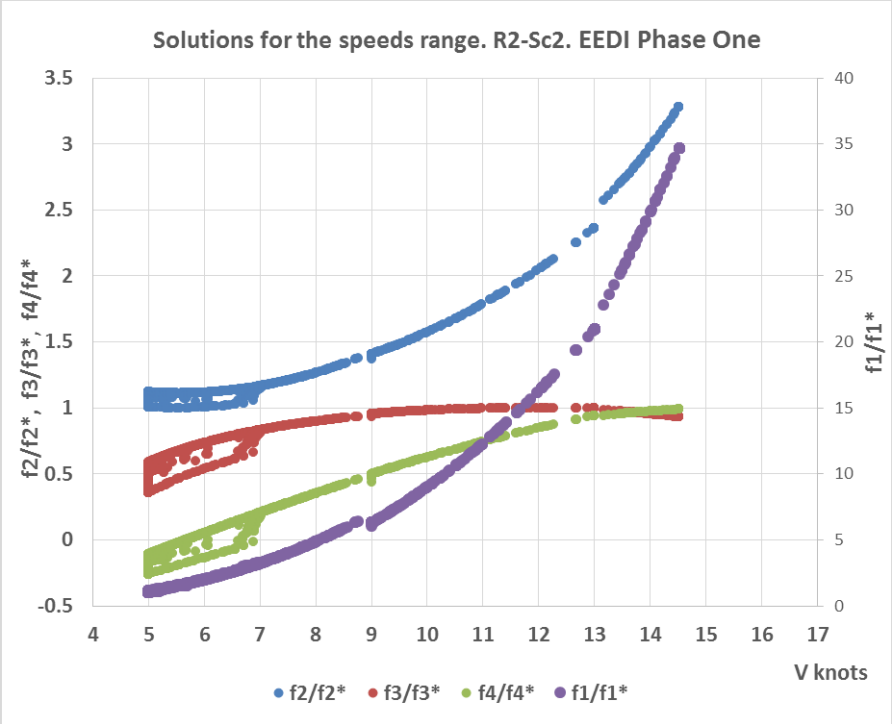

Normalised objective functions over the speeds range. EEDI Phase One

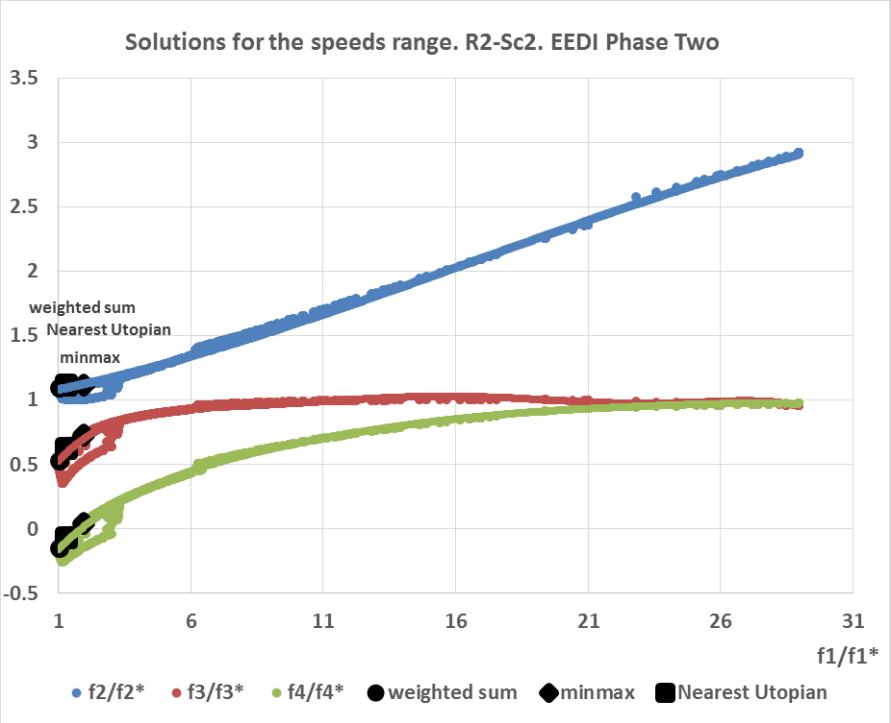

Pareto front over the speeds range. Route One, Scenario Two. EEDI Phase Two

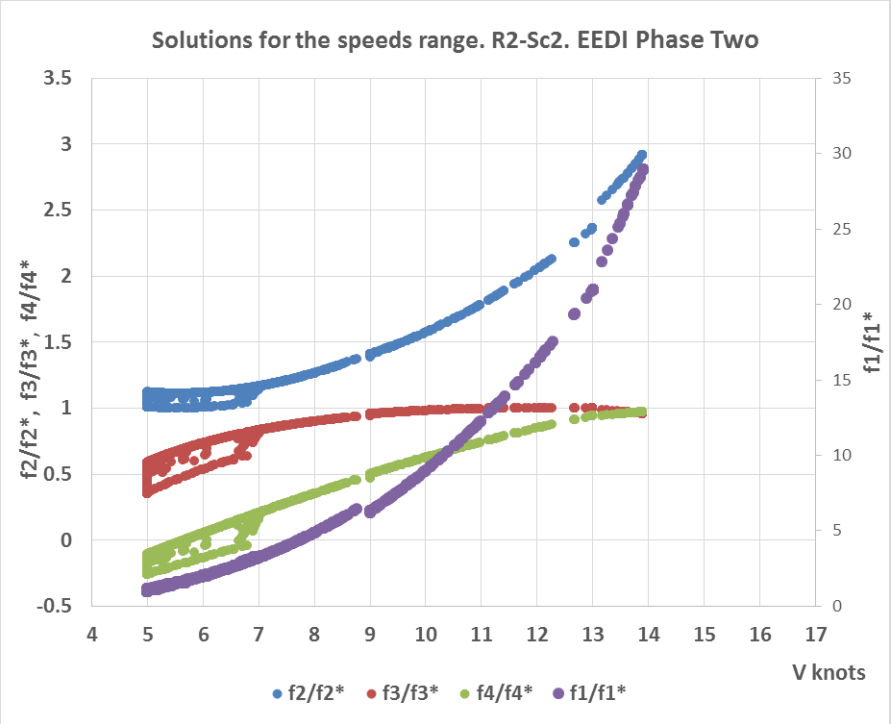

Normalised objective functions over the speeds range. EEDI Phase Two

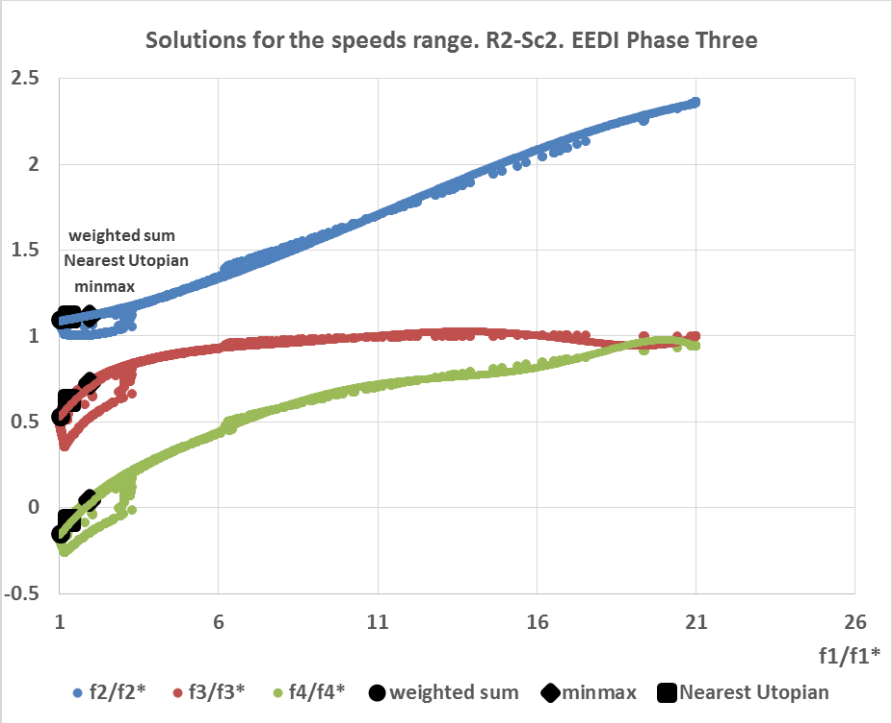

Pareto front over the speeds range. Route One, Scenario Two. EEDI Phase Three

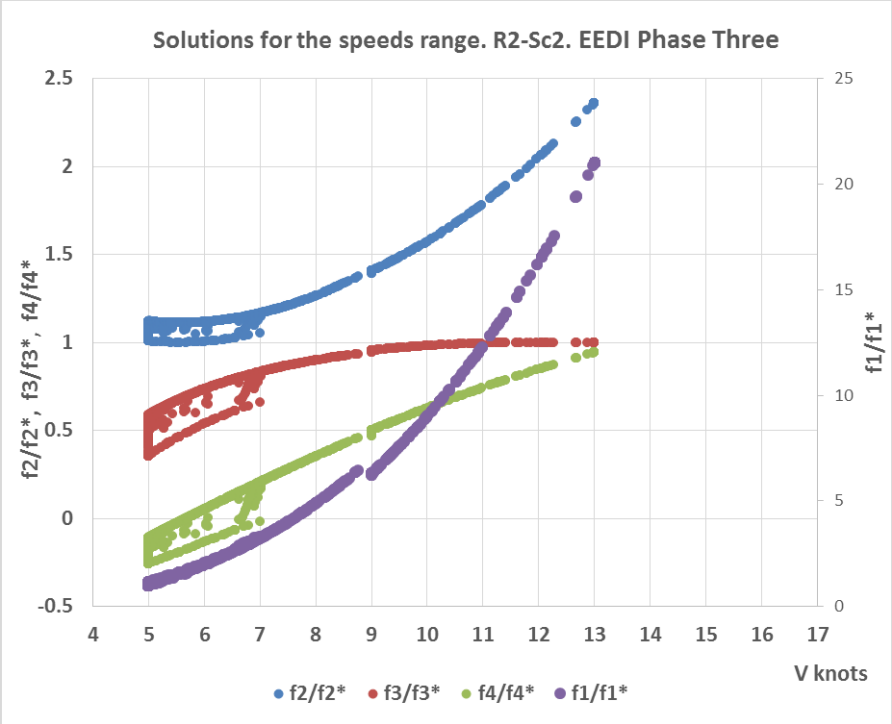

Normalised objective functions over the speeds range. EEDI Phase Three

- **Optimisation model's solutions over the speeds range for Route Two, Scenario Three (high fuel price and low fright rates):**

Single Criterion results for Route Two, Scenario Three over the speeds range

	Minimum P_D/Dis	Minimum $EEDI_A/EEDI_{Ref}$	Maximum *Profit/tonne.mile*	Maximum *NPV*
Criteria				
P_D/Dis	**0.00325**	0.00528	0.03487	0.05413
$EEDI_A/EEDI_{Ref}$	0.29624	**0.27437**	0.46137	0.56848
Profit/tonne.mile $\times 10^{-3}$	-0.72156	-0.84945	**0.77726**	0.73230
NPV	-48.95748	-48.92596	-14.52111	**-12.78452**
Independent Variables				
Length	222.75	222.75	222.75	222.75
Breadth	30.5950	30.5950	33.8241	33.8241
Draught	12.8388	12.8388	12.8388	12.8388
Breadth/Draught	2.3830	2.3830	2.6345	2.6345
Block Coefficient	0.8749	0.7759	0.8749	0.8749
Long Centre of Buoyancy %L	-0.01	-0.01	-0.01	-0.01
Speed	5	5.55	10.537	12.078
Other Characteristics				
Deadweight [ton]	63643.0820	54900.3106	70472.1370	70472.1370
Lightweight [ton]	14824.2552	14683.9319	16276.7683	16276.7683
Capital Cost [$ m]	39.7814	38.4690	40.8065	40.8065
Annual Fuel Cost [$]	1370848.06	1317382.85	3305550.50	4360917.87
Annual Operating cost [$]	2991877.05	2963476.16	3014061.24	3014061.24
Total annual cost [$]	5233600.63	5139631.05	7714781.51	8895071.92
Profit per DWT [$/dwt]	-13.66256	-17.78704	29.91684	31.99271
Annual Bunker Cons [ton]	483.55	585.59	2764.22	4071.77
Annual MDO Cons [ton]	984.00	848.91	1094.17	1103.50

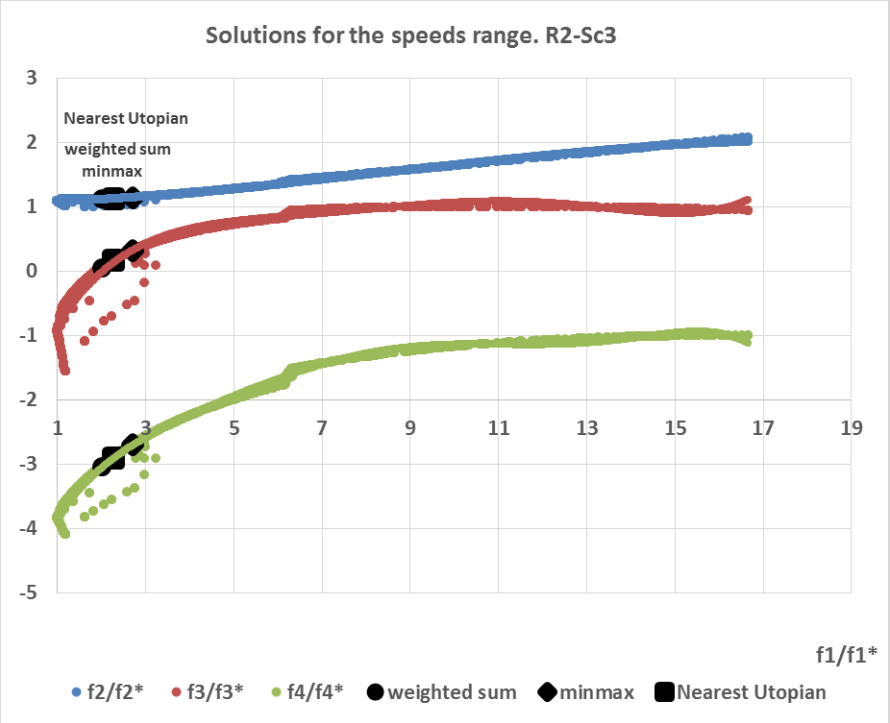

Pareto front over the speeds range. Route One, Scenario Three

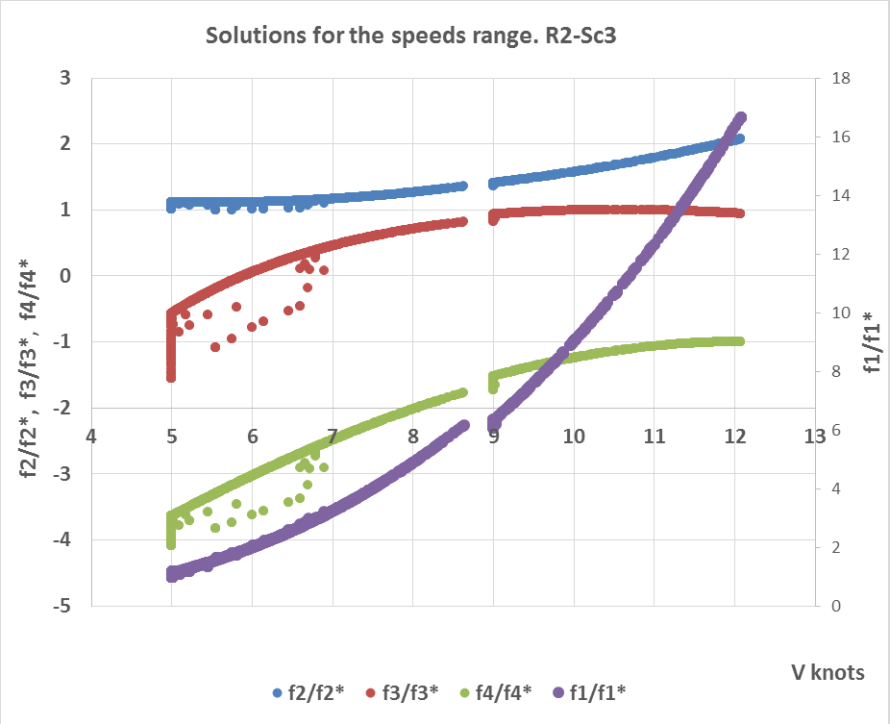

Normalised objective functions over the speeds range

- **Optimisation model's solutions over the speeds range for Route Two, Scenario Four (high fuel price and high fright rates):**

Single Criterion results for Route Two, Scenario Four over the speeds range

	Minimum P_D/Dis	Minimum $EEDI_A/EEDI_{Ref}$	Maximum *Profit/tonne.mile*	Maximum *NPV*
Criteria				
P_D/Dis	**0.00325**	0.00528	0.03487	0.06830
$EEDI_A/EEDI_{Ref}$	0.29624	**0.27437**	0.46137	0.64753
Profit/tonne.mile $\times 10^{-3}$	1.22844	1.10055	**2.72726**	2.61755
NPV	-21.06249	-22.31547	48.26769	**62.82399**
Independent Variables				
Length	222.75	222.75	222.75	222.75
Breadth	30.5950	30.5950	33.8241	33.8241
Draught	12.8388	12.8388	12.8388	12.8388
Breadth/Draught	2.3830	2.3830	2.6345	2.6345
Block Coefficient	0.8749	0.7759	0.8749	0.8749
Long Centre of Buoyancy %L	-0.01	-0.01	-0.01	-0.01
Speed	5	5.5495	10.537	12.99
Other Characteristics				
Deadweight [ton]	63643.0820	54900.3106	70472.1370	70472.1370
Lightweight [ton]	14824.2552	14683.9319	16276.7683	16276.7683
Capital Cost [$ m]	39.7814	38.4690	40.8065	40.8065
Annual Fuel Cost [$]	1370848.06	1317382.85	3305550.55	5124180.69
Annual Operating cost [$]	2991877.05	2963476.16	3014061.24	3014061.24
Total annual cost [$]	5233600.63	5139631.05	7714781.57	9731939.17
Profit per DWT [$/dwt]	23.26031	23.04476	104.97279	122.37298
Annual Bunker Cons [ton]	483.55	585.59	2764.22	5018.98
Annual MDO Cons [ton]	984.00	848.91	1094.17	1109.00

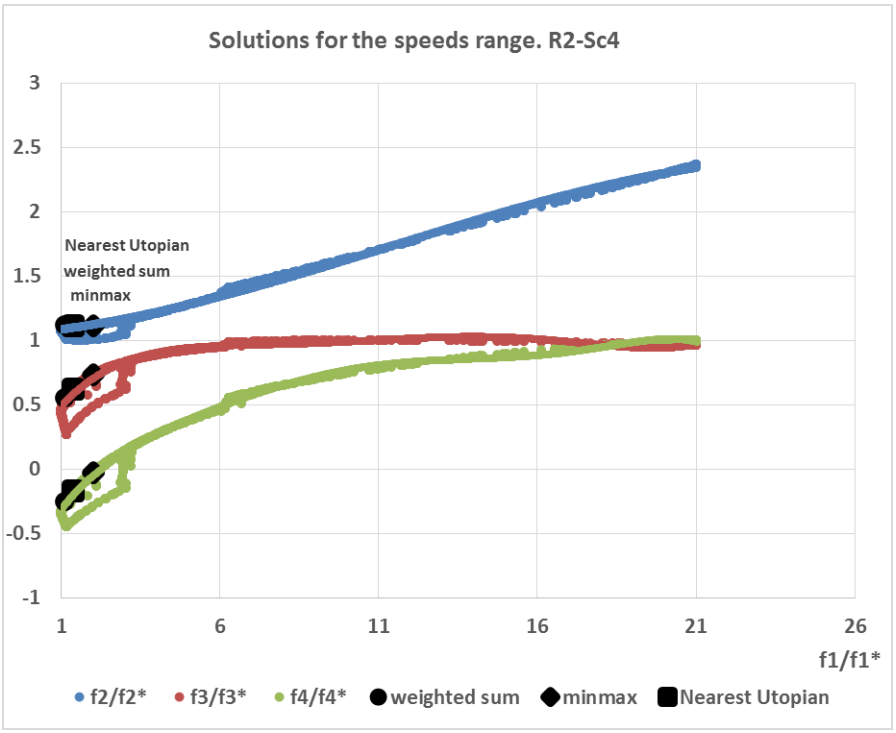

Pareto front over the speeds range. Route One, Scenario Four

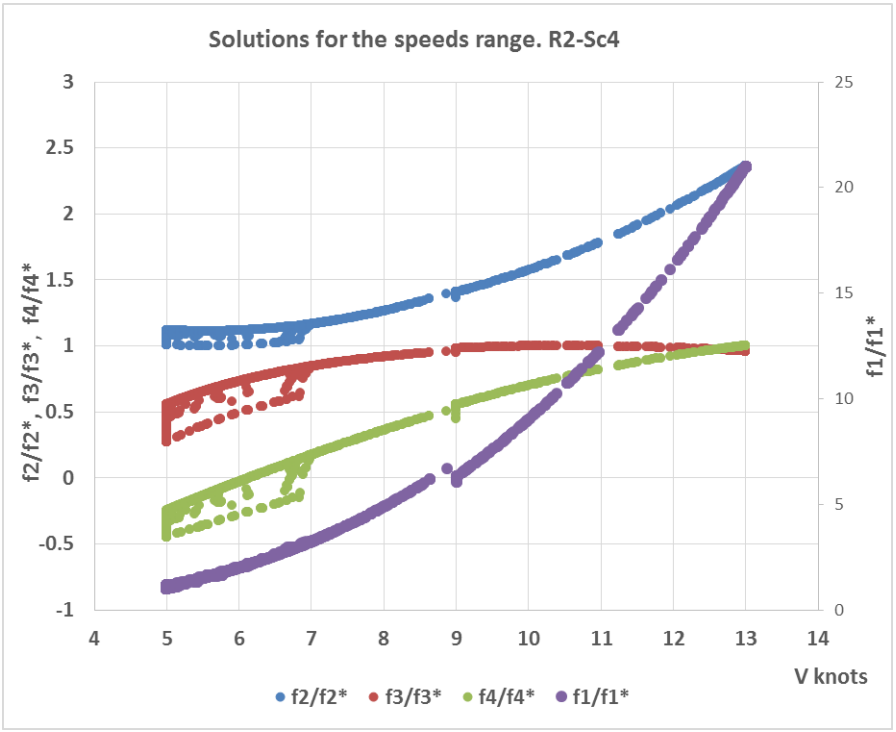

Normalised objective functions over the speeds range